UNITED STATES DEPARTMENT OF THE INTERIOR

GEOLOGICAL SURVEY

NATIONAL EARTHQUAKE HAZARDS REDUCTION PROGRAM, SUMMARIES OF TECHNICAL REPORTS VOLUME XXV

Prepared by Participants in

NATIONAL EARTHQUAKE HAZARDS REDUCTION PROGRAM

October 1987

March 3, 1849

OPEN-FILE REPORT 88-16

Menlo Park, California

1988

UNITED STATES
DEPARTMENT OF THE INTERIOR
GEOLOGICAL SURVEY

NATIONAL EARTHQUAKE HAZARDS REDUCTION PROGRAM, SUMMARIES OF TECHNICAL REPORTS VOLUME XXV

Prepared by Participants in

NATIONAL EARTHQUAKE HAZARDS REDUCTION PROGRAM

Compiled by

Muriel L. Jacobson

Thelma R. Rodriguez

The research results described in the following summaries were submitted by the investigators on October 1, 1987 and cover the period from May 1, 1987 through October 1, 1987. These reports include both work performed under contracts administered by the Geological Survey and work by members of the Geological Survey. The report summaries are grouped into the five major elements of the National Earthquake Hazards Reduction Program.

Open File Report No. 88-16

The data and interpretations in these progress reports may be reevaluated by the investigators upon completion of the research. Readers who wish to cite findings described herein should confirm their accuracy with the author.

CONTENTS

Earthquake Hazards Reduction Program

Page

ELEMENT I - Recent Tectonics and Earthquake Potential

Determine the tectonic framework and earthquake potential of U.S. seismogenic zones with significant hazard potential

Page

ELEMENT II. Earthquake Prediction Research

Collect observational data and develop the instrumentation, methodologies, and physical understanding needed to predict damaging earthquakes.

Objective (II-1): Prediction Methodology and Evaluation

Develop methods to provide a rational basis for estimates of increased earthquake potential. Evaluate the relevance of various geophysical, geochemical, and hydrological data for earthquake prediction.

1. Develop, operate and evaluate instrumentation for monitoring potential earthquake precursors.
2. Analyze and evaluate seismicity data collected prior to medium and large earthquakes.
3. Obtain and analyze data from seismically active regions of foreign countries through cooperative projects with the host countries.
4. Systematically evaluate data and develop statistics that relate observations of specific phenomena to earthquake occurrence.
5. Develop, study and test prediction methods that can be used to proceed from estimates of long-range earthquake potential to specific short-term predictions...203

Objective (II-2): Earthquake Prediction Experiments

Conduct data collection and analysis experiments in areas of California capable of great earthquakes, where large populations are at risk. The experiments will emphasize improved coordination of data collection, data reporting, review and analysis according to set schedules and standards.

1. Collect and analyze data for an earthquake prediction experiment in southern California, concentrating on the southern San Andreas fault from Parkfield, California to the Salton Sea.
2. Collect and analyze data for an earthquake prediction experiment in central California, concentrating on the San Andreas fault north of Parkfield, California..315

Page

Objective (II-3): Theoretical, Laboratory and Fault Zone Studies

Improve our understanding of the physics of earthquake processes through theoretical and laboratory studies to guide and test earthquake prediction observations and data analysis. Measure physical properties of those zones selected for earthquake experiments, including stress, temperature, elastic and anelastic characteristics, pore pressure, and material properties.

1. Conduct theoretical investigations of failure and pre-failure processes and the nature of large-scale earthquake instability.
2. Conduct experimental studies of the dynamics of faulting and the constitutive properties of fault zone materials.
3. Through the use of drilled holes and appropriate down hole instruments, determine the physical state of the fault zone in regions of earthquake prediction experiments................................407

Objective (II-4): Induced Seismicity Studies

Determine the physical mechanism responsible for reservoir-induced seismicity and develop techniques for predicting and mitigating this phenomena.

1. Develop, test, and evaluate theories on the physics of induced seismicity.
2. Develop techniques for predicting the character and severity of induced seismicity.
3. Devise hazard assessment and mitigation strategies at sites of induced seismicity.......................466

ELEMENT III Evaluation of Regional and Urban Earthquake Hazards

Delineate, evaluate, and document earthquake hazards and risk in urban regions at seismic risk. Regions of interest, in order of priority, are:

1) The Wasatch Front
2) Southern California
3) Northern California

ELEMENT IV Earthquake Data and Information Services

ELEMENT V: Engineering Seismology

Objective (V-1): Strong Motion Data Acquisition and Management

Objective (V-2): Strong Ground Motion Analysis and Theory

Southern California Seismic Arrays

Cooperative Agreement No. 14-08-0001-A0257

Clarence R. Allen and Robert W. Clayton
Seismological Laboratory, California Institute of Technology
Pasadena, California 91125 (818-356-6912)

Investigations

This semi-annual Technical Report Summary covers the six-month period from 1 April 1987 to 30 September 1987. The Cooperative Agreement's purpose is the partial support of the joint USGS-Caltech Southern California Seismographic Network, which is also supported by other groups, as well as by direct USGS funding to its own employees at Caltech. According to the Agreement, the primary visible product will be a joint Caltech-USGS catalog of earthquakes in the southern California region; quarterly epicenter maps and preliminary catalogs have been submitted as due during the Agreement period. About 250 preliminary catalogs are routinely distributed to interested parties.

Results

Figure 1 shows the epicenters of all cataloged shocks that were located during the six-month recording period. This was an extremely quiet period, and the preliminary data processing is virtually complete. Some of the seismic highlights of this period were:

Number of earthquakes fully or partially processed: 4682
Number of earthquakes of $M = 3.0$ and greater: 82
Number of earthquakes of $M = 4.0$ and greater: 0
Number of earthquakes of $M = 5.0$ and greater: 0
Largest event within network area: $M_L = 3.9$ on May 11 in Lucerne Valley area, north of Big Bear Lake, felt in Palm Springs, Big Bear and San Bernardino
Smallest events felt: both $M_L = 2.6$, one on May 12 in the San Bernardino area and one on July 19 in the Carpenteria area
Number of earthquakes reported felt: 51
Number of earthquakes for which systematic telephone notification to emergency-response agencies was made: 1

In addition to the smallest felt earthquakes of M_L 2.6, many residents felt and heard the explosion of a fireworks plant in Rialto on 25 September. This event was well recorded by our network and had a magnitude of $M_{CA} = 1.6$.

Figure 1 shows the activity during the reporting period. This activity was very typical of long-term southern California seismicity.

On the day following the close of this reporting period, metropolitan Los Angeles experienced an $M_L = 6.0$ earthquake located in the Whittier

Narrows Recreation Area, near Whittier, Rosemead, and San Gabriel. Damage occurred in these cities and also in Pasadena, South Pasadena and Los Angeles. A question has arisen as to whether the unusually low level of seismicity in the preceding months might be viewed as a precursory quiescence to the October 1 earthquake. The last event with M_L of 5.0 or greater within our regular reporting area occurred on 29 October 1986. The question of precursory quiescence remains unresolved.

Data processing efforts continued throughout the reporting period in an effort to finish the backlogs created by the installation of a new VAX-750 in late 1985 and by the 1986 North Palm Springs, Oceanside and Chalfant Valley sequences. Just before the end of September this effort bore fruit; the first stage of data processing is complete from 1983 to the present. (The backlog created by the Coalinga sequence in 1983 remains to be processed.) This first stage of routine analysis includes interactive timing of phases and location of hypocenters using the CUSP analysis system.

1 April 1987 - 30 September 1987

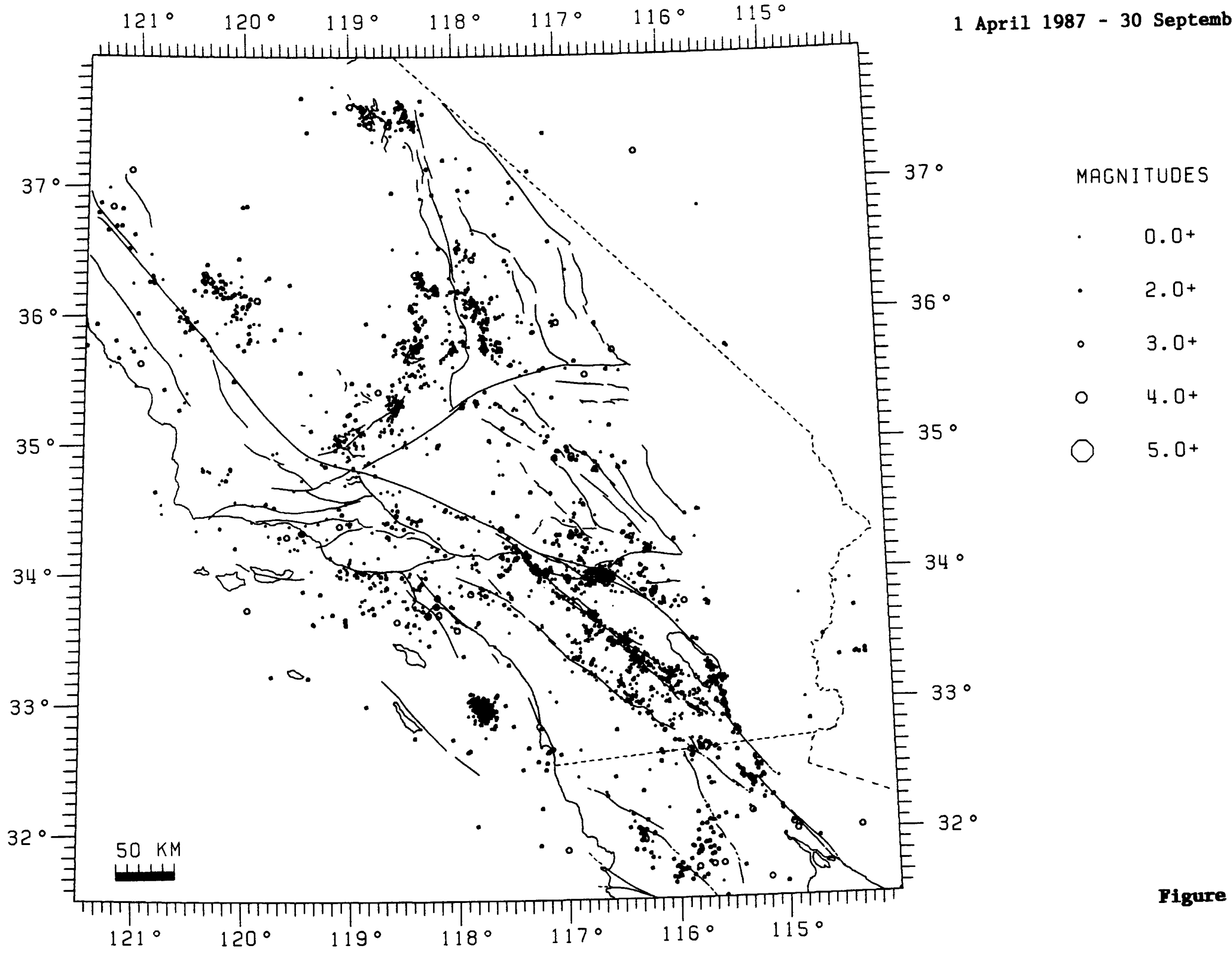

Figure 1

Regional Seismic Monitoring Along The Wasatch Front Urban Corridor And Adjacent Intermountain Seismic Belt

14-08-0001-A0265

W. J. Arabasz, R.B. Smith, J.C. Pechmann, and E.D. Brown
Department of Geology and Geophysics
University of Utah
Salt Lake City, Utah 84112
(801) 581-6274

Investigations

This cooperative agreement supports "network operations" (including a computerized central recording laboratory) associated with the University of Utah 85-station regional seismic telemetry network. USGS support focuses on the seismically hazardous Wasatch Front urban corridor of north-central Utah but also encompasses neighboring areas of the Intermountain seismic belt. Primary products for this USGS support are quarterly earthquake catalogs and a semi-annual data submission, in magnetic-tape form, to the USGS Data Archive.

During the report period, significant efforts were made in: (1) further development of a system for *in-situ* calibration of remote telemetry stations, (2) conversion of the northern part of the Wasatch Front seismic network from leased telephone-line telemetry to microwave telemetry (using a new junction in the state of Utah's microwave system), and operation of up to 6 movable telemetry stations in three different target areas (Salt Lake Valley, Utah-Idaho border area, Great Salt Lake Desert).

Results

1. Network Seismicity

Figure 1 shows the epicenters of 228 earthquakes ($M_L \leq 4.8$) located in part of the University of Utah study area designated the "Utah region" (lat. 36.75°-42.5°N, long. 108.75°-114.25°W) during the six-month period April 1, to September 30, 1987. The seismicity sample includes thirteen shocks of magnitude 3.0 or greater and four felt earthquakes.

The largest earthquake during the six-month report period was a shock of M_L4.8 (4.7, U of U; 4.9 USGS) on September 25 (GMT), located west of the Great Salt Lake (A, fig. 1). The earthquake was felt from Wendover (on the Utah-Nevada border) to the Salt Lake Valley and was the largest earthquake to occur in the Utah region since the 1975 Pocatello Valley earthquake of M_L6.0. Other felt earthquakes, identified in figure 1, include: (B) an M_L3.6 earthquake on April 1, felt in Tremonton, Utah, and other parts of Box Elder County; (C) an M_L3.1 earthquake on April 3, strongly felt in Cedar City; and (D) a small shock of M_L1.7 on September 10, felt locally in the NE part of Salt Lake City.

2. *Lakeside Earthquake Sequence*

The M_L4.8 earthquake of September 25 (04:27 GMT) in the Great Salt Lake Desert occurred 16 miles west of Lakeside, Utah, beneath the middle of a broad saline mud flat between the Newfoundland and Lakeside Mountains (fig. 2a). The earthquake and its associated sequence attracted attention because of its proximity to a $60-million pumping facility that began operation in the spring of 1987 to lower the level of the Great Salt Lake by pumping into the western desert. Earthquake activity has occurred episodically since at least 1965 within 30 km of the September 25 earthquake, including an M_L4.0 event in 1967.

A magnitude-time plot for the earthquake sequence through October 26 (fig. 2b), for events recorded by our network, shows that the M_L4.8 shock on September 25 was preceded by three foreshocks (M_L3.9, 2.0, 4.1) and was followed by an M_L4.3 aftershock within one hour and numerous smaller aftershocks of $M_L \leq 3.9$. Shocks of M_L4.3 and 4.8 followed respectively on October 23 and 26. Portable seismographs were deployed within 20 hrs of the M_L4.8 earthquake on September 25, and four temporary telemetry stations were subsequently installed (fig. 2a). Detailed analysis of this sequence, including investigation into any possible connection (e.g. pore pressure diffusion) with the pumping, is currently underway.

Reports and Publications

Brown, E.D., Utah earthquake activity, *Wasatch Front Forum*, v. 3, no. 2, p. 7, 1986.

Brown, E.D., Utah earthquake activity, January through June, 1987, *Survey Notes (Utah Geological and Mineral Survey)*, v. 21, no. 1, p. 8, 1987.

[For other reports and publications, see technical summary for companion research award—R.B. Smith, W.J. Arabasz, J.C. Pechmann, and E.D. Brown, University of Utah, this volume.]

UTAH EARTHQUAKES

April 1 - September 30, 1987

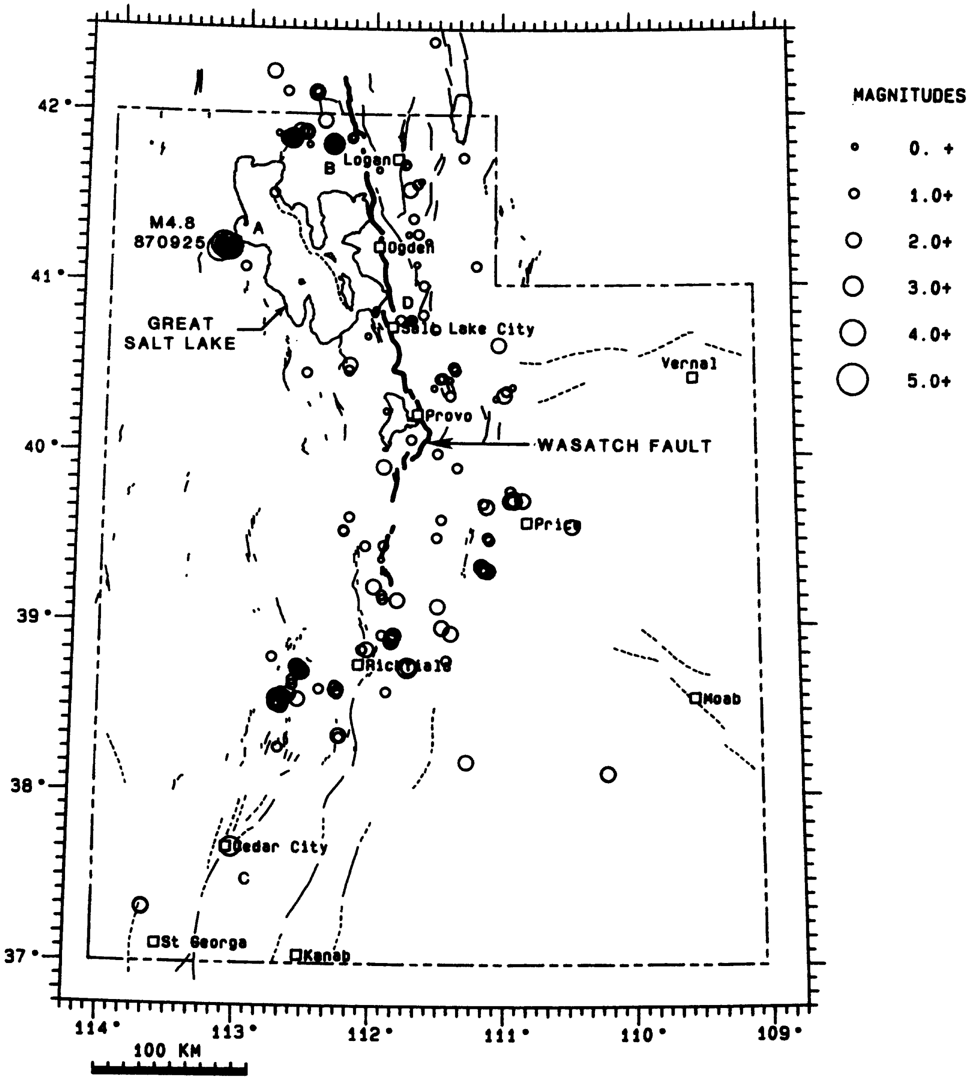

Figure 1.

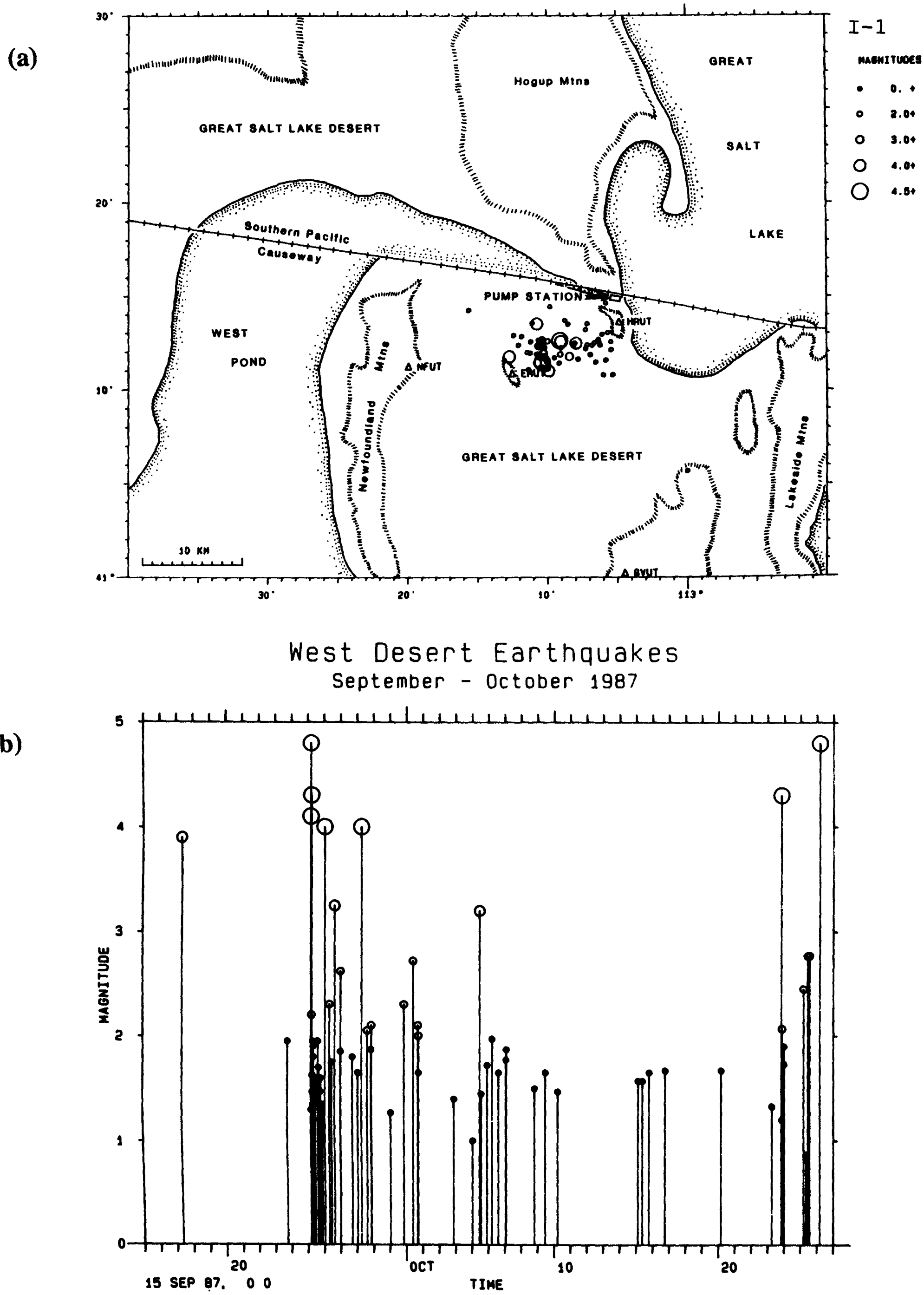

Figure 2. (a) Epicenter map and (b) magnitude-time plot for the September-October 1987 Lakeside earthquake sequence ($M_L \leq 4.8$). (See text.)

Central Aleutian Islands Seismic Network

Agreement No. 14-08-0001-A0259

Selena Billington and Carl Kisslinger
Cooperative Institute for Research in Environmental Sciences
Campus Box 449, University of Colorado
Boulder, Colorado 80309

(303) 492-6042

Brief Description of Instrumentation and Data Reduction Methods

The Adak seismic network consists of 13 high-gain, high-frequency, two-component seismic systems and one six-component system (ADK) located at the Adak Naval Base. Station ADK has been in operation since the mid-1960s; nine of the additional stations were installed in 1974, three in 1975, and one each in 1976 and 1977.

Data from the stations are FM-telemetered to recording sites near the Naval Base, and are then transferred by cable to the Observatory on the Base. Data were originally recorded by Develocorder on 16 mm film; since 1980 the film recordings are back-up and the primary form of data recording has been on analog magnetic tape. The tapes are mailed to CIRES once a week.

At CIRES the analog tapes are played back at four-times the speed at which they were recorded into a computer which digitizes the data, automatically detects events, and writes an initial digital event tape. This tape is edited to eliminate spurious triggers, and a demultiplexed tape containing only seismic events is created. All subsequent processing is done on this tape. Times of arrival and wave amplitudes are read from an interactive graphics display terminal. The earthquakes are located using a program developed for this project by E. R. Engdahl, which uses corrections to the arrival times which are a function of the station and the source region of the earthquake.

Data Annotations

A major earthquake (M_S 7.6) occurred immediately to the east of the network coverage area on May 7, 1986 (at 22:47). Thousands of aftershocks of that earthquake occurred within the network coverage area. At the time of this writing, the local catalog of hypocenters is still incomplete for the immediate time period following the mainshock. A discussion of research on that earthquake and its aftershocks is published under the report of Grant. No. G1368 (Kisslinger) elsewhere in this volume.

The network was serviced from mid-July through September, 1986. Due to major logistic problems, two of the westernmost stations could not be reached at that time, and we were also unable to make a needed return trip to one other far-west station. Of the 28 short-period vertical and horizontal components, 21 were operating for most of the time period of May through July, 1986. By the end of the 1986 summer field trip to Adak, 23 of the 28 components were operating (AK2z, AK5h, AD3 and AD5 having been brought back up).

During the time period of August 1986 through August of 1987, AK2z, AK3, and AK4 were not operating. In addition, there were some periods of time during this year when AD6 and ADK were intermittently down. Maintenance was performed on the network between mid-August and mid-October of 1987. By the end of the 1987 summer field trip to Adak, 23 of the 28 components were operating (AD6 and ADK having been brought back up). Again, due to logistic problems, AK2z, AK3, and AK4 could not be reached.

Current Observations

So far, 581 earthquakes have been located with data from the network for the period between the time (20:43) of the M_S 6.0 foreshock of the May 7 mainshock and 24:00 on May 13. During the past six months, project personnel have located 123 aftershocks: 49 aftershocks which occurred throughout May 11, 41 aftershocks occurring on May 12, and 33 aftershocks occurring on May 13. We have also skipped ahead in time and located 52 events which occurred in July, 1986. Epicenters of *all* the events for the time period May 11 through May 13, as well as events occurring within the time periods in July of 9 - 13, and 17 and 18, are shown in Figures 1a and 1b and vertical cross-sections are given in Figures 2a and 2b.

14 of the events located with data from the Adak network for May 11 through May 13 were large enough to be located teleseismically (USGS PDEs), of which 5 occurred on May 11, 7 on May 12, and 2 on May 13. A number of other teleseismically located aftershocks within the network region are difficult for us to locate due to their arrivals being masked by the codas of other aftershocks. Also, 3 of the events located with data from the Adak network for the specified dates in July, 1986, were large enough to be located teleseismically (USGS PDEs). No attempt is being made to locate aftershocks with duration magnitudes (m_d) of less than 2.3. More detailed information about the network status and a catalog of the hypocenters determined for the time period reported here are included in our semi-annual data report to the U.S.G.S. Recent research using these data is reported in the Technical Summary for U.S.G.S. Grant No. G1368.

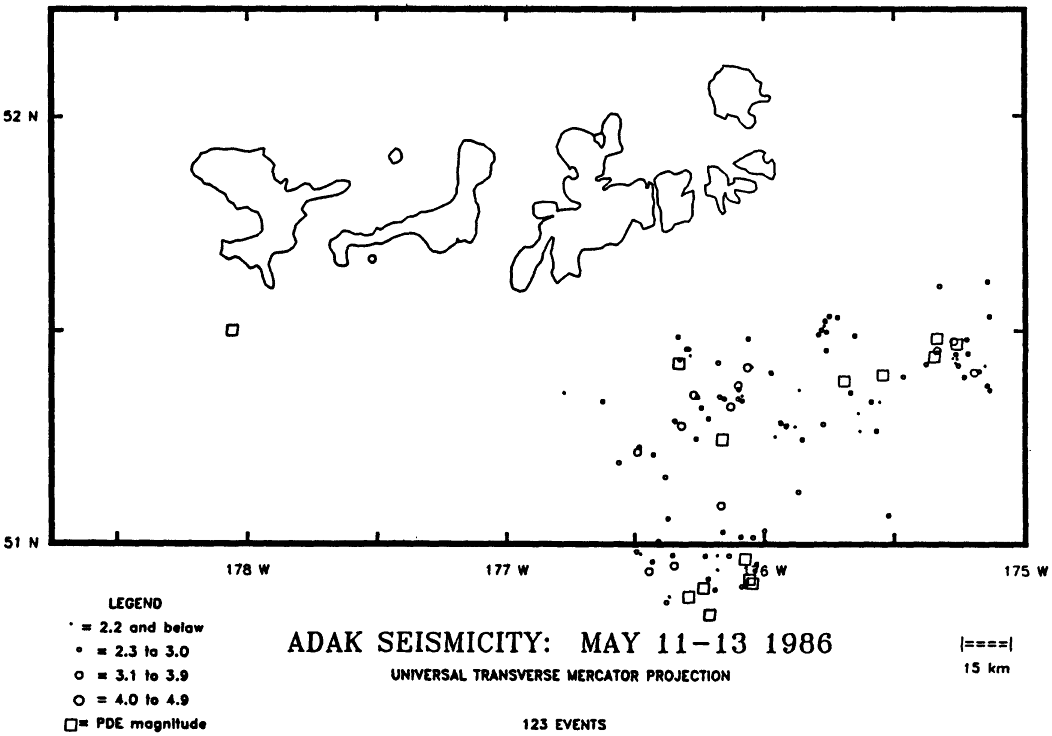

Figure 1a: Map of seismicity which occurred for the time period May 11 through May 13, 1986. All epicenters were determined from Adak network data. Events marked with squares are those for which a teleseismic body-wave magnitude has been determined by the USGS; all other events are shown by symbols which indicate the duration magnitude determined from Adak network data. The islands mapped (from Tanaga on the west to Great Sitkin on the east) indicate the geographic extent of the Adak seismic network.

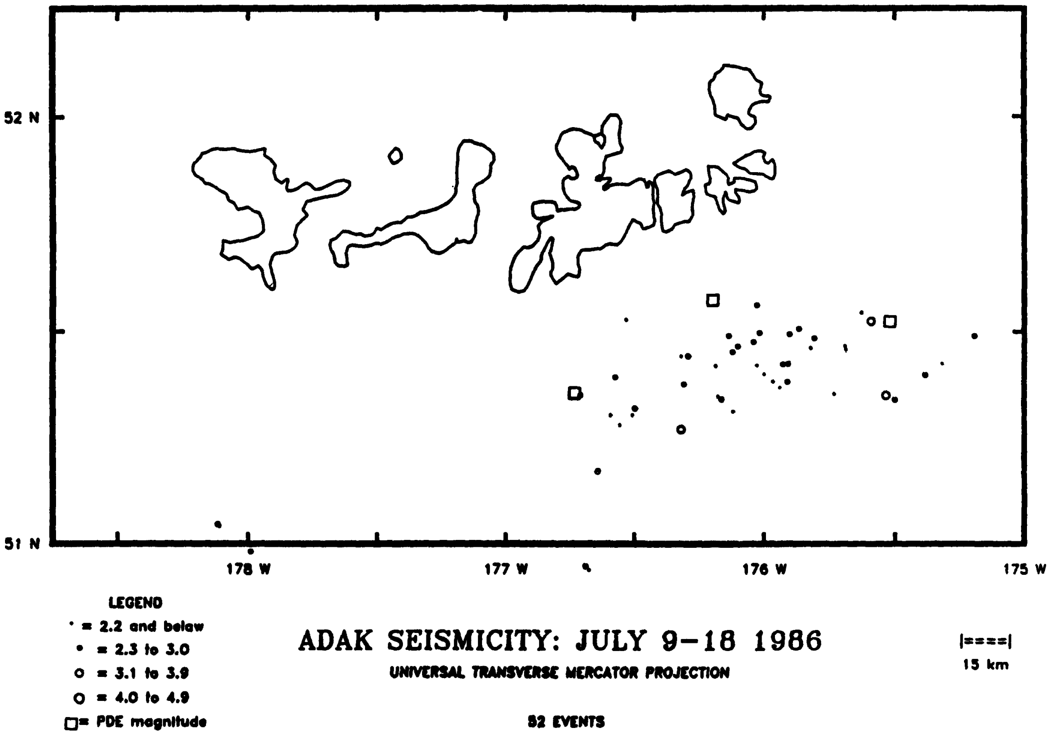

Figure 1b: Map of seismicity which occurred for the time periods in July of 9–13, and 17 and 18, 1986. Symbols as in Figure 1a.

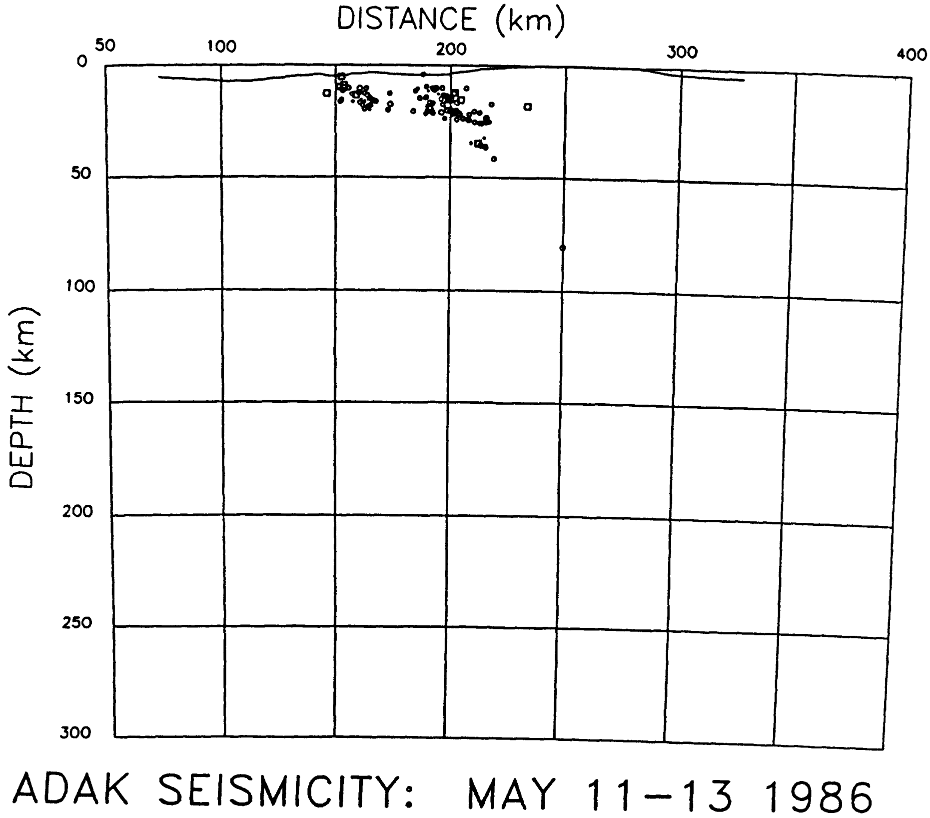

Figure 2a: Vertical cross section of seismicity which occurred for the time period May 11 through May 13, 1986. Events are projected according to their depth (corresponding roughly to vertical on the plot) and distance from the pole of the Aleutian volcanic line. The zero-point for the distance scale marked on the roughly-horizontal axis of the plot is arbitrary. Events marked with squares are those for which a teleseismic body-wave magnitude has been determined by the USGS; all other events are shown by symbols which indicate the duration magnitude determined from Adak network data. The irregular curve near the top of the section is bathymetry.

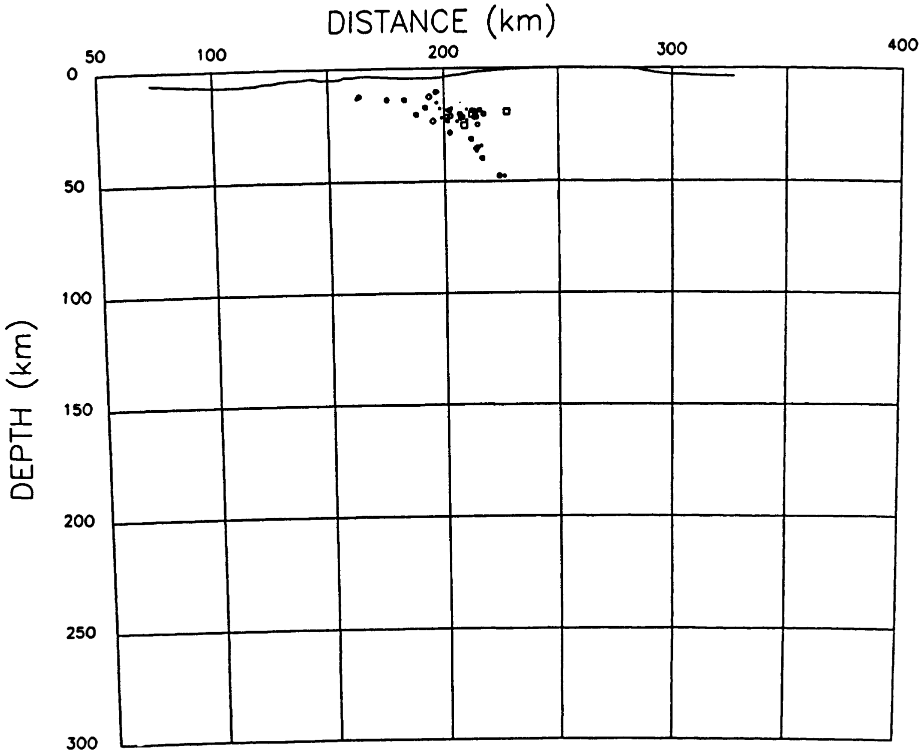

ADAK SEISMICITY: JULY 9–18 1986

Figure 2b: Vertical cross section of seismicity which occurred for the time periods in July of 9 - 13, and 17 and 18, 1986. Projection and symbols as in Figure 2a.

Regional Seismic Monitoring in Western Washington

14-08-0001-A0266

R.S. Crosson and S.D. Malone
Geophysics Program
University of Washington
Seattle, WA 98195
(202) 543-8020

Investigations

Operation of the western Washington regional seismograph network and routine preliminary analysis of earthquakes in western Washington are carried out under this contract. Quarterly catalogs of seismic activity in Washington and Northern Oregon are available for 1984 through 1986, and the first three quarters of 1987. These catalogs are funded jointly by this contract and others. The University of Washington operates approximately 80 stations west of 120.5°W. Twenty eight are funded under this contract.

Data are provided for USGS contract 14-08-0001-G1390 and other research programs. Efforts under this contract are closely related to and overlap objectives under contract G1390, also summarized in this volume. Publications are listed in the G1390 summary. This summary covers a six month period from April 1, 1987 through September 30, 1987.

Excluding blasts, probable blasts, and earthquakes outside the U. W. network, 412 earthquakes west of 120.5°W were located during this period. Thirty of these were located at Mount St. Helens, which was quiet during this interval and which last erupted in October of 1986. The 382 earthquakes outside of Mt. St. Helens and west of 120.5°W indicate a slight increase in activity over the two preceding six-month periods, which were seismically quiet, and which had counts (excluding Mt. St. Helens) of 280 (11/86 - 3/87) and 288 (4/87 - 10/87). The current increase represents a return to a more average level of seismicity.

The largest earthquake located in western Washington or northern Oregon between April 1 and Sept. 30 was a M_c 3.9, which occurred offshore on June 19th, about 20 km southwest of the mouth of Grays Harbor. This is the largest offshore earthquake yet located near the coast of southern Washington. A depth of 35 km was computed for this earthquake, however the lack of stations to the west of the event makes accurate depth determination difficult.

Central California Network Operations

9930-01891

Wes Hall
Branch of Seismology
U.S. geological Survey
345 Middlefield Road - Mail Stop 977
Menlo Park, California 94025
(415) 329-4713

Investigations

Maintenance and and recording of 329 seismograph stations (433 components) located in Northern and Central California. Also recording 60 components from other agencies. The area covered is from the Oregon border south to Santa Maria.

Results

1. Seismic VCO/AMP replacements for maintenance or upgrade
   J302ML - 84 ea
   J402H - 63 ea
   J404L - 4 ea
   J502 - 21 ea

2. Assembled and tuned additional forty (40) J502 VCO/AMPs for HVO (total requirement was 80 ea.) This completes this order.

3. Installed and began recording Froelich dilatometer (PFRQ, PFRS).

4. Installation and recording of new seismic components
   LRRN (Red Rock Mountain Horz.)
   LRRV (Red Rock Mountain Vert.)

5. Removed following seismic stations
   PTFE, PTFN, PTFV, PPFV, LRDN

6. Installed power modification to all microwave sites so back-up batteries would be on trickle charge

7. Halliburton House installation for Parkfield experiment
   a. Installed 50 foot antenna tower to recieve telemetry data.
   b. Installed telephone type cable from Haliburton House to KAR microwave site.

8. New tower installations
   a. Reason Peak
   b. Hog Canyon
   c. Geyser Peak
   d. Tassajara

9. Installed second parabolic antenna at Mt. Tamalpais microwave site for space diversity reception to Monument Peak.

10. Realign Cal Tech microwave system

11. Installed Black Mountain microwave site.

Alaska Seismic Studies

9930-01162

John C. Lahr, Christopher D. Stephens, Robert A. Page, Kent A. Fogleman
Branch of Seismology
U. S. Geological Survey
345 Middlefield Road, MS 977
Menlo Park, California 94025
(415) 329-4744

Investigations

1) Continued collection and analysis of data from the high-gain short-period seismograph network extending across southern Alaska from the volcanic arc west of Cook Inlet to Yakutat Bay, and inland across the Chugach mountains. This region spans the Yakataga seismic gap, and a special effort is made to note changes of activity within the gap that might change our assessment of the imminence of a gap-filling event.

2) Cooperated with the Branch of Engineering Seismology and Geology in operating 17 strong-motion accelerographs in southern Alaska, including 12 between Icy Bay and Cordova in the area of the Yakataga seismic gap.

3) Responsibility for monitoring of the region around the proposed Bradley Lake hydroelectric project on the Kenai Peninsula has been assumed by the University of Alaska.

Results

1) During the past six months preliminary hypocenters have been determined for 1,357 earthquakes that occured between February and July 1987 (Figure 1). The coda-duration magnitudes (M_D) of the events ranged from -0.2 to 4.7, and 99 were M_D 3 or larger. All 99 were located west of longitude 145°W, and all but 4 had calculated depths deeper than 30 km. The three largest events with magnitudes $M_D \geq 4$ were located at depths between 68 and 200 km within the Aleutian Wadati-Benioff (W-B) zone west of about longitude 150.5° W. On April 18, a M_D 4.4 (5.6 m_b, NEIC) earthquake occurred at a depth of 68 km about 50 km northwest of Anchorage. Felt reports (NEIC) included MM intensity V at Anchorage, Eagle River, Palmer and Skwentna, and intensity IV at Chugiak, Cooper Landing, Fort Richardson, Seward, Sterling, Sutton, Talkeetna, Tyonek, Whittier and Willow. The mainshock was followed 12 minutes later by a M_D 3.6 (4.4 m_b) aftershock which was felt with intensity III at Palmer and Anchorage. The April 18 earthquake is the largest Aleutian W-B zone shock in the upper Cook Inlet region since the mid-1970's when a magnitude 6.1 m_b shock occurred on January 1, 1975 at 51 km depth about 100 km northeast of Anchorage. Single event focal mechanism solutions for the mainshock and largest aftershock and a composite solution for 20 smaller aftershocks all are characterized by down-dip tension axes. A M_D 4.0 earthquake occurred on June 20 at 200 km depth near latitude 58.5°N., longitude 156.25°W. (just outside the southwest corner of Figure 1). On July 20, a

M_D 4.7 (5.0 m_b) shock occurred approximately 20 km west of Iliamna volcano at 154 km depth. This event was felt strongly on the Kenai Peninsula, and reported intensities include MM V at Anchor Point and IV at Ninilchik (NEIC). The focal mechanism indicates down-dip tension and north-south horizontal compression which agrees with the focal mechanisms reported by Pulpan and Frohlich (1985) for Aleutian W-B zone earthquakes with depths greater than 50 km between latitudes 59°N and 60.5°N.

Within the aftershock zone of the 1979 St. Elias earthquake, which abuts the eastern edge of the Yakataga seismic gap, over 350 shocks were located during the recent six-month period. This number represents a decrease relative to the previous six-month period and returns the rate of activity back to the level of February - July 1986. A swarm of 15 earthquakes with magnitudes ranging up to M_D 2.4 occurred in March about 25 km northwest of Yakutat Bay. In May, the same area experienced a swarm of 12 earthquakes with magnitudes up to 1.8 M_D. The location of these two swarms is identical to a cluster of events that occurred within six months prior to the 1979 mainshock and just south of a prominent swarm that occurred in December 1986.

In and around the Yakataga seismic gap the pattern of shallow seismicity during the last six months was comparable to that observed for at least the past nine years. The largest earthquake to occur in the persistent, diffuse concentration of shallow (depth < 30 km) seismicity beneath Waxell Ridge near the middle of the gap was a M_D 2.7 shock on March 2. A M_D 2.8 event occurred on May 8 approximately 40 km northwest of Kayak Island near the mouth of the Copper River and was located at a depth of 35 km. This is the largest shock near the inferred western edge of the gap since a M_D 2.8 event occurred in March 1986, about 20 km north of Kayak Island.

2) Beneath Prince William Sound, significant levels of microseismicity are observed that tend to be concentrated in persistent clusters. The nature of this seismicity, whether it occurs along the buried megathrust or within the subducted and overthrust plates, is at present uncertain. In order to obtain improved locations and focal mechanisms for some of these events, five digital event-triggered seismic recorders (ELOG's) were deployed from July 9 to August 9 in a 60-km diameter array around Knight Island. Three permanent telemetered seismic stations (two on Knight Island and one on the Kenai Peninsula) were situated inside the array. The ELOG recorders incorporate a new software algorithm that employs the Walsh transform to reject non-seismic triggers. A total of 825 individual waveforms of 12s duration were recorded by the ELOG's. Approximately 88 percent of these waveforms are from earthquakes; the rest are noise from glaciers, aircraft, human, or unknown sources. Of the 355 earthquakes recorded by one or more ELOG's, about one-third have at least one S-P time interval of less than 8s (corresponding to an epicentral distance of less than 64 km). For one conspicuous cluster of events located beneath northern Knight Island the preliminary depths determined using phases timed from ELOG recordings plus phases from the regional network range from 18 to 24 km. For events from this cluster, single-event and composite focal mechnism solutions were determined from

intial P-wave polarities. Most of these mechanisms have nearly horizontal T-axes oriented east-west, but a few shocks have first-motion patterns which are clearly different from the main trend. Although these results are preliminary, they tend to favor the interpretation that the cluster of seismicity beneath Knight Island is occurring within the subducted Pacific plate in response to down-dip tension from either bending of the plate or body forces.

3) We have continued to relocate earthquakes recorded by the southern Alaska regional seismograph network with velocity models based on seismic refraction surveys conducted as part of the Trans-Alaska Crustal Transect. Recent investigations have focused on earthquakes in the Wrangell W-B zone and the northeast end of the Aleutian zone. We adopted a simple two-gradient velocity model for the crust based on seismic-refraction profiles along and across the Chugach Mountains east and northeast of Valdez. Velocity increases rapidly with depth from 5.9 km/s at the surface to 7.1 km/s at 15 km and then slowly to 7.3 km/s at the Moho at 60 km. Using well located earthquakes as calibration events, we adopted station corrections appropriate for this model. Finally, we relocated more than 7000 events from the region 59.5°N-63°N and 142°-148°W for the interval 1971-1986. The relocated hypocenters provide a clearer picture of the relationship between the Aleutian and Wrangell (W-B) zones and of the tectonic setting of recent seismicity in the Prince William Sound region. We divided the study area into three regions (Figure 2). Region A--the most active--includes the northeastern end of the Aleutian W-B zone, which dips to the north-northwest in the region northwest of the study area; region B--the least active--encompasses the NNE-dipping Wrangell W-B zone. The divergence of dip between the two zones and the marked difference in levels of seismicity previously led us to speculate that there may be a discontinuity between the two zones (Stephens and others, 1984). The relocated hypocenters, however, exhibit no vertical offset in the distribution of hypocenters between the two zones; rather, the two zones appear to be continuous (Figure 3). The relocated hypocenters (Figure 3) also suggest that little of the recent seismicity in the Prince William sound region originated within the shallow-crust (at depths less than 15 km). Further, the recent activity does not appear to be concentrated on a gently dipping surface suggestive of a megathrust. We infer that since 1971, most of the Prince William Sound seismicity has occurred within the subducting plate. We are currently testing this inference (see item Knight Island).

4) Several modifications were made to existing computer programs within the CUSP data processing system to facilitate analysis of Alaska seismic data. Among the more significant additions is the ability to measured amplitudes and periods on the seismograms in order to compute magnitudes. Other programs were developed to integrate seismogram data from ELOG and PC-based event detectors into the CUSP data base. Currently, comparisons between measurements made on CUSP and equivalent measurements from Develocorder records are being made to identify possible differences between the two processing systems that must be corrected to ensure compatability.

5) In addition to routine station servicing, two new pieces of hardware were installed in Alaska, as follows:
a) PCELOG - A Compaq computer with special data acquition hardware and software written in TurboPascal was set up in Yakutat to gather seismic data. This approach allows the recovery of seismic data from this region without a costly leased phone line.
b) ATI (Analog Telemetry Interface) - A third generation telemetry interface, previously called a "Filter Bridge", was also installed in Yakutat. In addition to filtering unwanted noise the new unit has the ability to translate VCO channels, thus allowing optimum utilization of the few available phone line channels.

References cited

Pulpan, Hans and Frolich, Cliff, 1985, Geometry of the subducted plate near Kodiak Island and lower Cook Inlet, Alaska, determined from relocated earthquake hypocenters, Bulletin of the Seismological Society of America, v. 75, n. 3, p. 791-810.

Stephens, C. D., Fogleman, K. A., Lahr, J. C., and Page, R. A., 1984, Wrangell Benioff zone, southern Alaska; Geology, v. 12, p. 373-376.

Reports

Lahr, J. C., Page, R. A., and Stephens, C. D., 1987, Seismic sources in the Cook Inlet region of Alaska, (abs.), 1987 Geologic Hazards Symposium - Alaska Geological Society Symposium Agenda and Abstracts.

Page, R. A., 1987, Seismicity in southern Alaska, 1987, Geologic hazards Symposium-Alaska Geological Society Symposium Agenda and Abstracts.

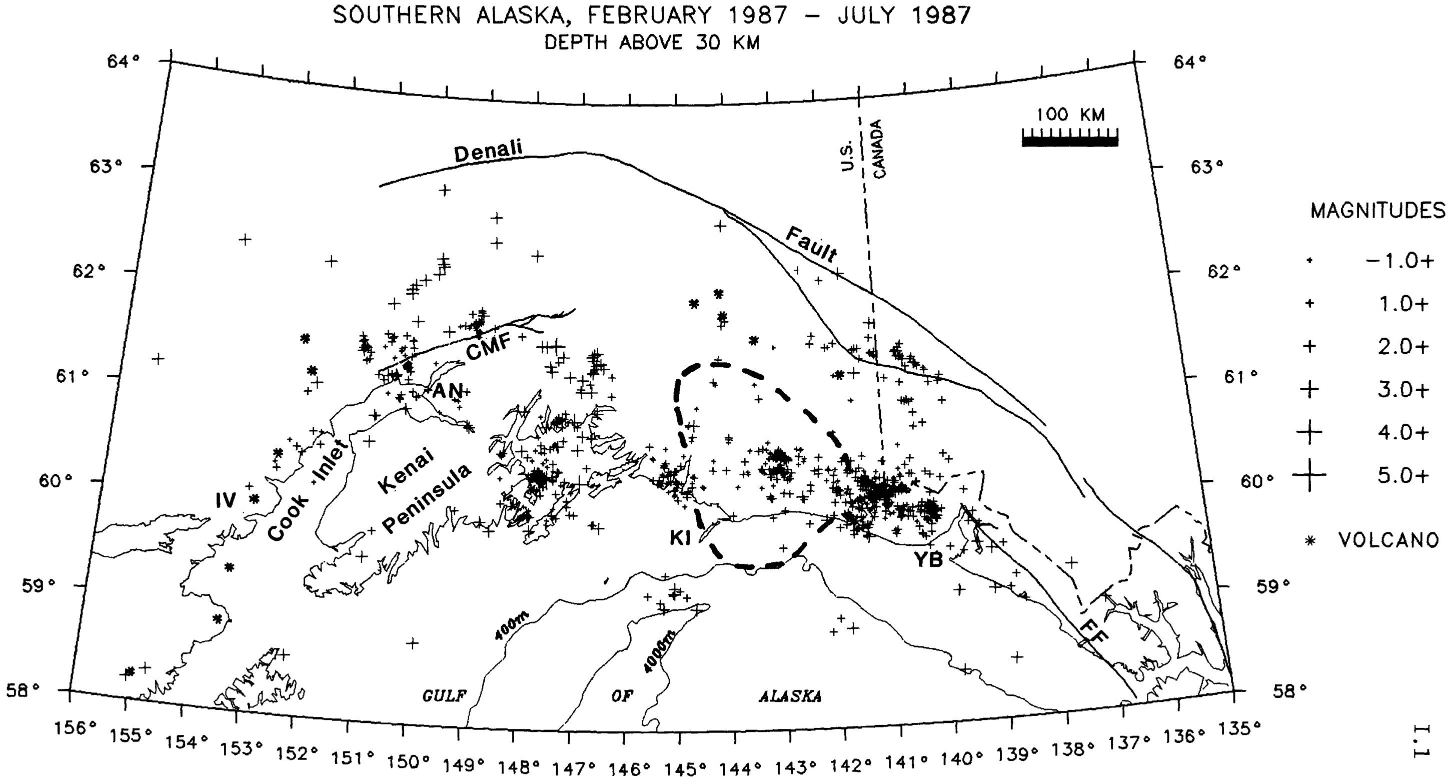

Figure 1a. Epicenters of 931 earthquakes located using the USGS southern Alaska seismograph network for the period February-July 1987. Magnitudes are determined from coda duration or maximum amplitude, and events of magnitude 3 or larger can be as much as one unit smaller than the corresponding m_b magnitude. The lowest magnitude level to which data is processed varies across the network due to uneven station spacing and changes in processing criteria. Heavy dashed contour indicates inferred extent of Yakataga seismic gap. Abbreviations are: AN - Anchorage; CMF - Castle Mountain fault; FF - Fairweather fault; IV - Iliamna Volcano; KI - Kayak Island; YB - Yakutat Bay.

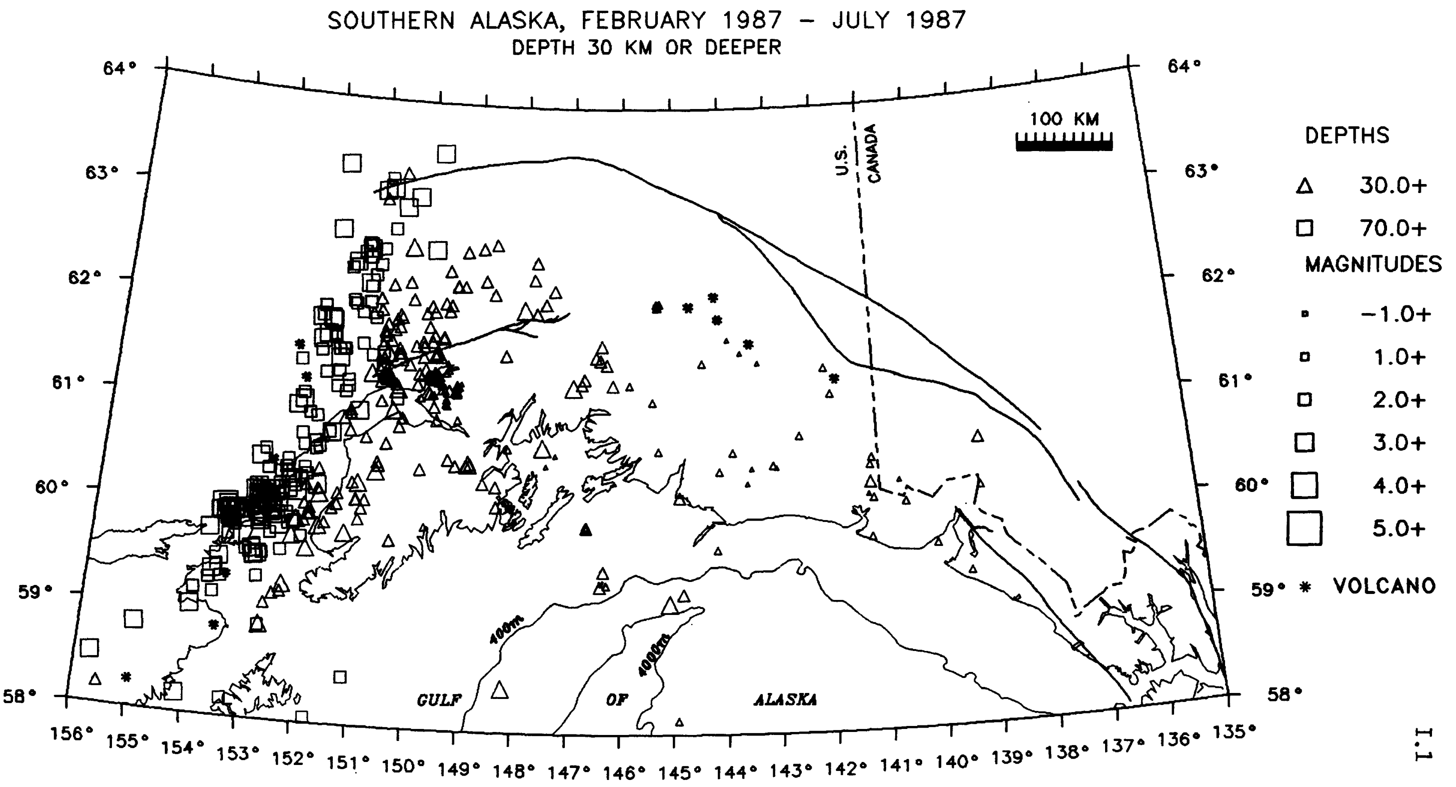

Figure 1b. Epicenters of 426 earthquakes with depths of 30 km or deeper located using the USGS seismograph network for the period February-July 1987. See Figure 1a for details about magnitudes and for identification of map features.

Seismic Data Library

9930-01501

W. H. K. Lee
U.S. Geological Survey
Branch of Seismology
345 Middlefield Road, Mail Stop 977
Menlo Park, California 94025
(415) 323-8111, Ext. 2630

This is a non-research project and its main objective is to provide access of seismic data to the seismological community. Ths Seismic Data Library was started by Jack Pfluke at the Earthquake Mechanism Laboratory before it was merged with the Geological Survey. Over the past ten years, we have built up one of the world's largest collections of seismograms (almost all of them on microfilm) and related materials. Our collection includes approximately 4.5 million WWNSS seismograms (1962 - present), 1 million USGS local earthquake seismograms (1966-1979), 0.5 million historical seismograms (1900-1962), 20,000 earthquake bulletins, reports and reprints, and a collection of several thousand magnetic tapes containing (1) a complete set of digital waveform data of the Global Digital Seismic Network (Data Tapes), and (2) a complete set of digital archive data of Calnet (CUSP archive tapes).

Northern and Central California Seismic Network Processing

9930-01160

Fredrick W. Lester
Branch of Seismology
U.S. Geological Survey
345 Middlefield Road M/S 977
Menlo Park, California 94025
(415) 329-4747

Investigations

1. In 1966 a seismographic network was established by the USGS to monitor earthquakes in central California. In the following years the network was expanded to monitor earthquakes in most of northern and central California, particularly along the San Andreas Fault, from the Oregon border to Santa Maria. In its present configuration there are over 350 single and multiple component stations in the network. There is a similar network in southern California. From about 1969 to 1984 the primary responsibility of this project was to manually monitor, process, analyze, and catalog the data recorded from this network. In 1984 a more efficient and automatic computer-based monitoring and processing system (CUSP) began online operation, gradually replacing most of the manual operations previously performed by this project. For a more complete description of the CUSP system see the project description "Consolidated Digital Recording and Analysis" by S. W. Stewart.

   Since the introduction of the CUSP system the responsibilities of this project have changed considerably. The main focus of the project now is that of finalizing and publishing preliminary network data from the years 1978 through 1984. We also continue to manually scan network seismograms as back-up event detection for the CUSP system. We then supplement the CUSP data base with data that were detected only visually or by the other automatic detection system (Real-Time Processor, RTP) and digitized from the continuously recording analog magnetic tapes. Project personnel also act as back-up for the processing staff in the CUSP project. As time permits some research projects are underway on some of the more interesting or unusual events or sequences of earthquakes that have occurred within the network.

   This project continues to maintain a data base for the years 1969 - present on both a computer and magnetic tapes for those interested in research on the network seismic data. As soon as the older data are finalized they are exchanged for preliminary data in the data base.

Results

1. Figure 1 illustrates nearly 6500 earthquakes located by this office for northern and central California during the time period April through September 1987. The largest earthquake to occur was a M5.5 shock that occurred on July 31 near Cape Mendocino, approximately 75 km south of Eureka. It was accompanied by a northeast-southwest trending, 30-35 kilometer long zone of aftershocks. To date there have been more than 260 aftershocks. There were no other earthquakes that were magnitude 5 or larger for this time period and there were no other large or significant sequences of earthquakes.

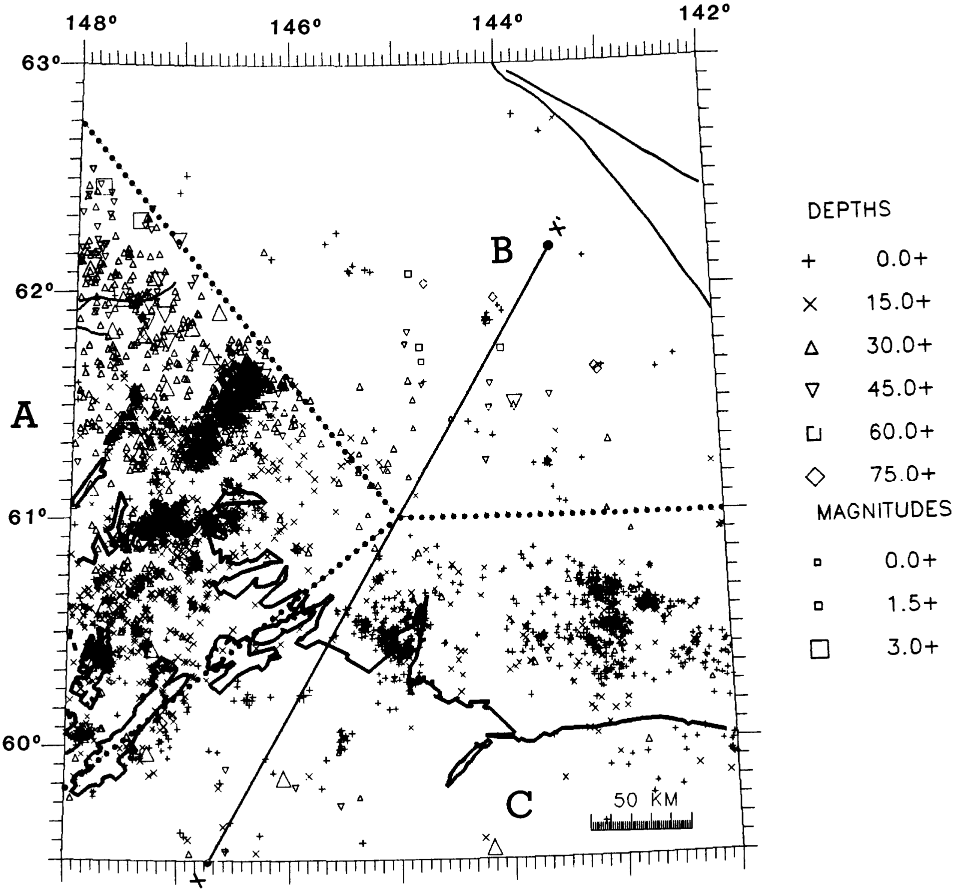

Figure 2. Epicenter for 3,882 selected relocated earthquakes from 1971-1986. Selection criteria: RMS<0.5s, lengths of horiontal axes of 68 percent joint confidence ellipsoid < 5km, length of vertical axis < 10 km, total number of phases $\geq$ 8, and number of S phases $\geq$ 3. Symbol type indicates depth; symbol size indicates magnitude. A,B, and C indicate regions. Heavy line XX' is projection plane in Fig. 3.

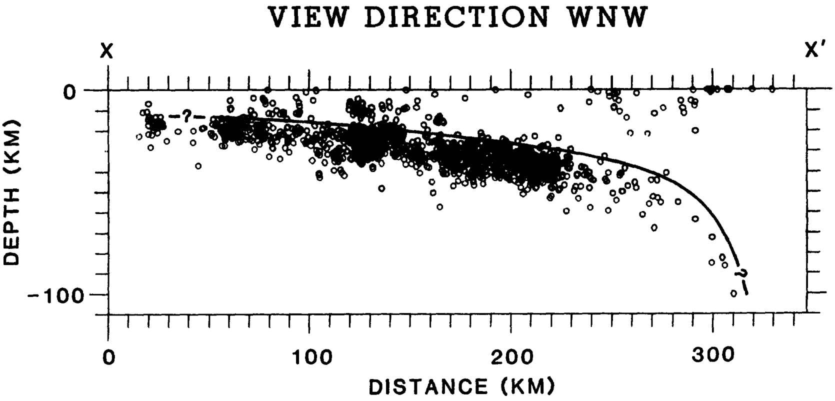

Figure 3. Hypocenters for 1,546 selected relocated earthquakes from regions A and B projected on to NNE-SSW vertical plane (XX', Fig. 2). For region B, the data are those included in Fig. 2. For region A, the data are a subset of those in Fig. 2 selected by the criteria: RMS<0.3s, lengths of horizontal axes of 68 percent confidence ellipsoid < 3 km, length of vertical axis < 5 km, total number of phases ≥ 10, and number of S phases ≥ 4. Curved line indicates inferred upper boundary to seismogenic zone within the subducting plate.

2. Final processing of data for the second half of the calendar year 1982 is complete and those data are ready for publication, as are the data from the Lake Shasta area for 1981-1984.

3. Since June 1986 this project has been involved in a combined effort with personnel from many different projects. The first purpose of this group endeavor is to collect all available seismic data pertaining to the more than 150,000 earthquakes that the USGS has located in northern and central California, mainly from 1969 to the present. Those data will then be combined, checked for errors and omissions, reprocessed as necessary, and finalized for publication. It is estimated that this job will take at least one year, which is much less time than would be necessary for this project alone. Personnel in this project will be responsible for coordinating much of this group effort. To date all but a small portion of the data have been collected, had gross errors corrected, and have been rerun through the location program.

4. For the time period April- September there were from 0 to 6 events per day missed by the CUSP automatic detection system, with an average of 2.6 missed each day. These were added to the existing CUSP data base from the back-up magnetic tape and processed using standard CUSP processing techniques. Most of the earthquakes that were missed occurred in northern California, north of latitude 39 degrees. This is a particular problem in the north because of telemetry noise that exists on those circuits. To avoid producing an abnormally large number of false triggers in the detection system the trigger thresholds are often set higher than normal and therefore some of the real events are missed.

5. Quarterly reports were prepared on seismic activity around Monticello Dam, Warm Springs Dam, the Auburn Dam site and, New Melones Dam for the appropriate funding agencies.

6. For the past 2 or 3 years Mari Kauffmann has been involved in the development of an automatic system to pick p-phases off magnetic tapes from portable 3-component seismographs. The system is now operational and is being utilized with Mari as the chief operator. There are several other people involved and they have made improvements so that digital seismograms can also be produced on magnetic tape. These seismograms can then be processed and analyzed using CUSP software. To date Mari has processed a large volume of data from numerous California earthquake sequences from areas that include Long Valley, Coalinga, Kettleman Hills, Morgan Hill, Chalfant Valley, and Palm Springs.

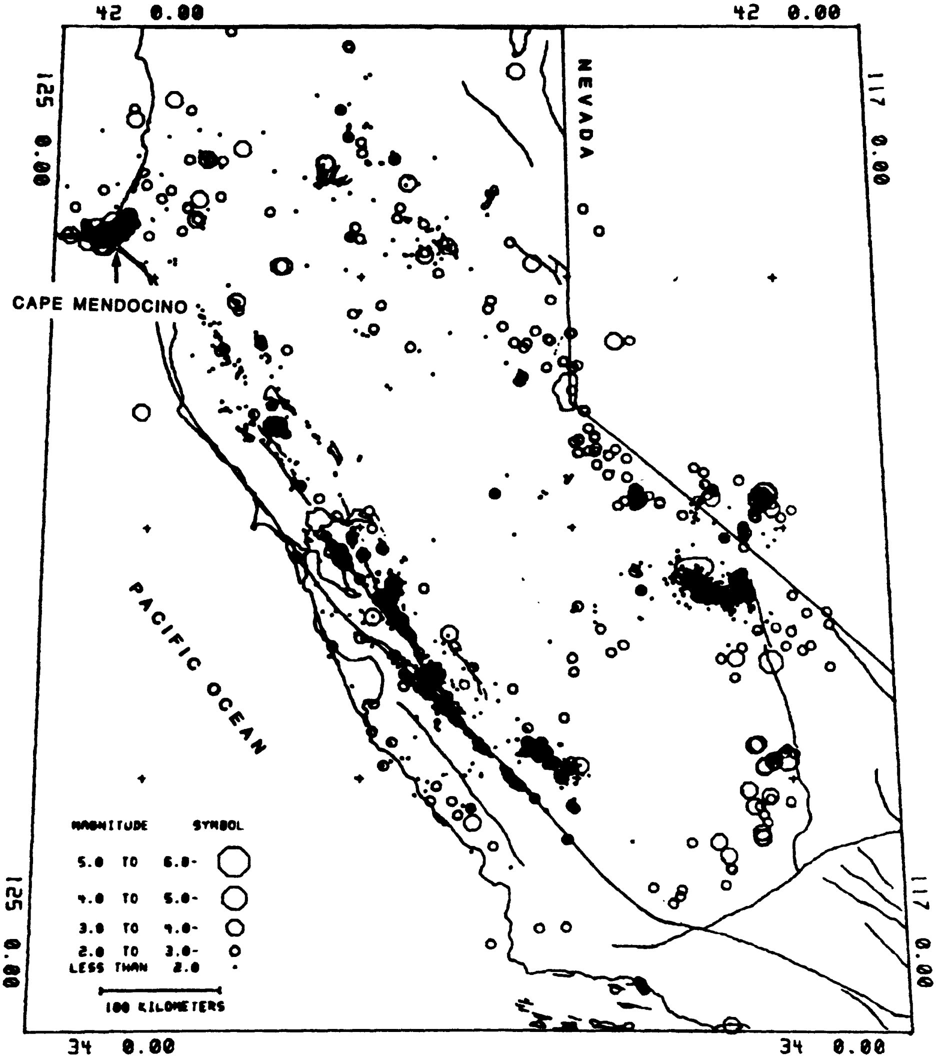

Figure 1. Northern and central California seismicity
April - September 1987

Earthquake Hazard Studies in the Northeast United States

14-08-0001-A0261

L. Seeber
J.G. Armbruster
D. Johnson
Lamont-Doherty Geological Observatory
of Columbia University
Palisades, New York 10964
(914) 359-2900

Investigations:

1. Monitor seismic activity in New York State and vicinity

2. Record locally the aftershocks of the July 13, 1987 Asutabula, Ohio earthquake. Study the implications of this probably induced earthquake.

Results:

The 13 July 1987 Ashtabula earthquake in Ohio is the best candidate yet for a macroseismic event in the eastern U.S. which has been induced by fluid injection in a deep waste disposal well.

This event generated relatively abundant aftershocks which were locally monitored with analog and digital seismic recorders beginning two days after the main shock. All 36 well-determined hypocenters are clustered in a narrow E-W striking vertical plane about 1.5 km long, 2 km in depth and 1/4 km wide. First-motions fit a well constrained composite fault-plane solution characterized by a vertical east-west plane with horizontal left-lateral slip (Figures 1 & 2). No evidence for such a fault has been reported in the Paleozoic sediments. The Appalachian Plateau in northeastern Ohio is characterized by subhorizontal Paleozoic sediments (4.5 km/sec) above Precambrian basement (6.0 km/sec). The depth of the unconformity in the epicentral area is 1.8 km. The July 1987 hypocenters are scattered at and below the unconformity. Considering location uncertainties, all earthquakes could be generated in the basement.

The July 1987 Ashtabula event is near an injection well; the zone of injection is less than a km from the July 1987 hypocenters (Figure 2). Except for one event in 1857, no other earthquakes are known to have occurred within 30 km of Ashtabula. Thus, there are good grounds to suspect that the earthquake was induced by injection activity. The Ashtabula well has been active for about one year at a nearly uniform flow rate of 30 gal/min and a head pressure of 10 MPa. In 1986 an $M_S = 5$ earthquake occurred near Chardon 45 km southwest of Ashtabula. A causal relation between that event and several injection wells located 10 km north of the epicenter is also considered possible. These and other disposal wells in Ohio inject waste fluid into the Mt. Simon sandstone which lies immediately above the unconformity. High-permeability paths may include brittle faults in the basement, as suggested by the seismicity.

Stress data from the Appalachian Plateau indicate that the Paleozoic sediments are subjected to differential stresses which are close to failure levels and suggest that the stress perturbation caused by waste disposal could cause failure. No stress data are available for the basement.

Given the increasing reliance on deep wells to dispose of fluid waste, the mechanical effect of injection in the seismogenic upper crust and the potential for induced damaging earthquakes need to be considered.

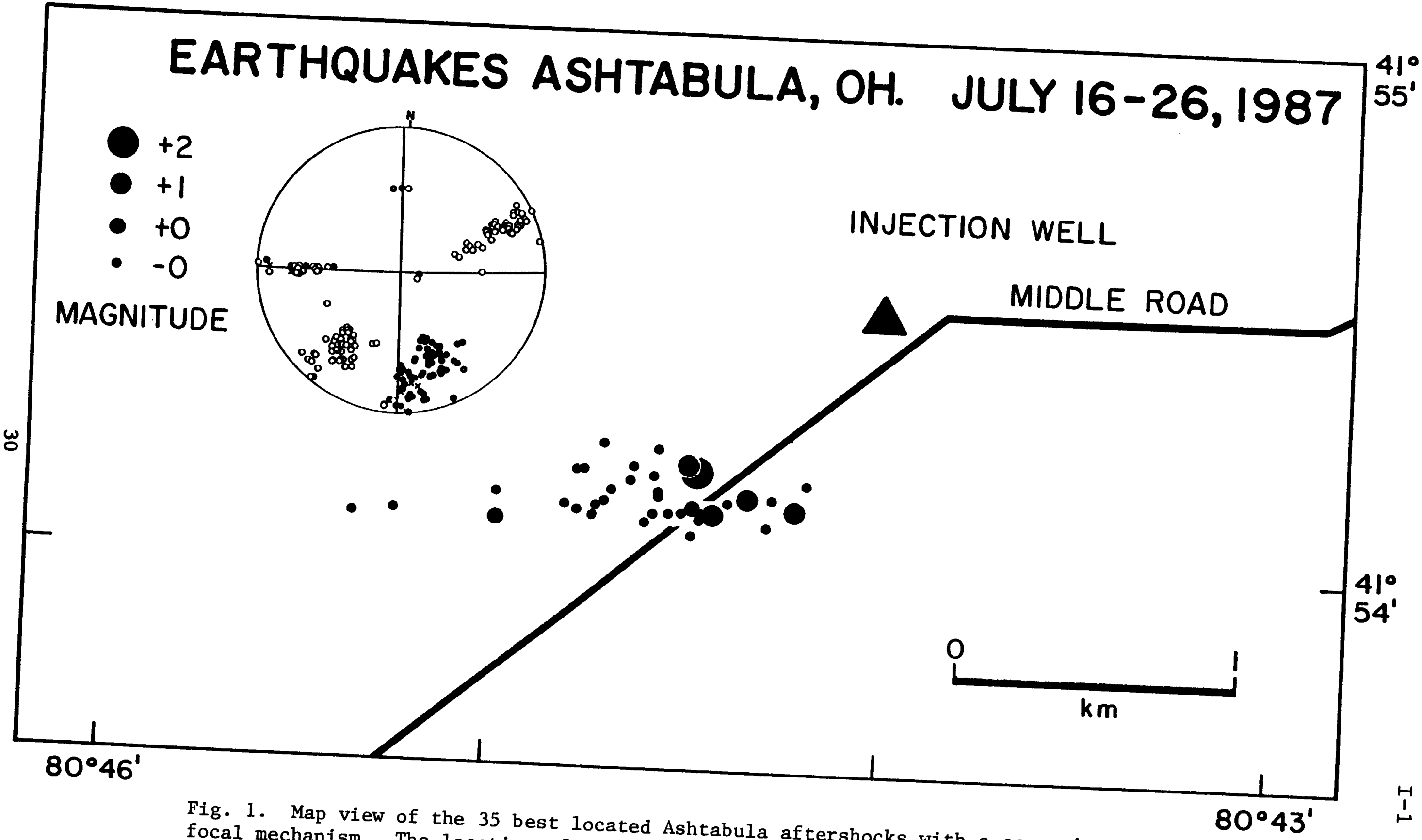

Fig. 1. Map view of the 35 best located Ashtabula aftershocks with a composite focal mechanism. The location of a waste fluid injection well is indicated.

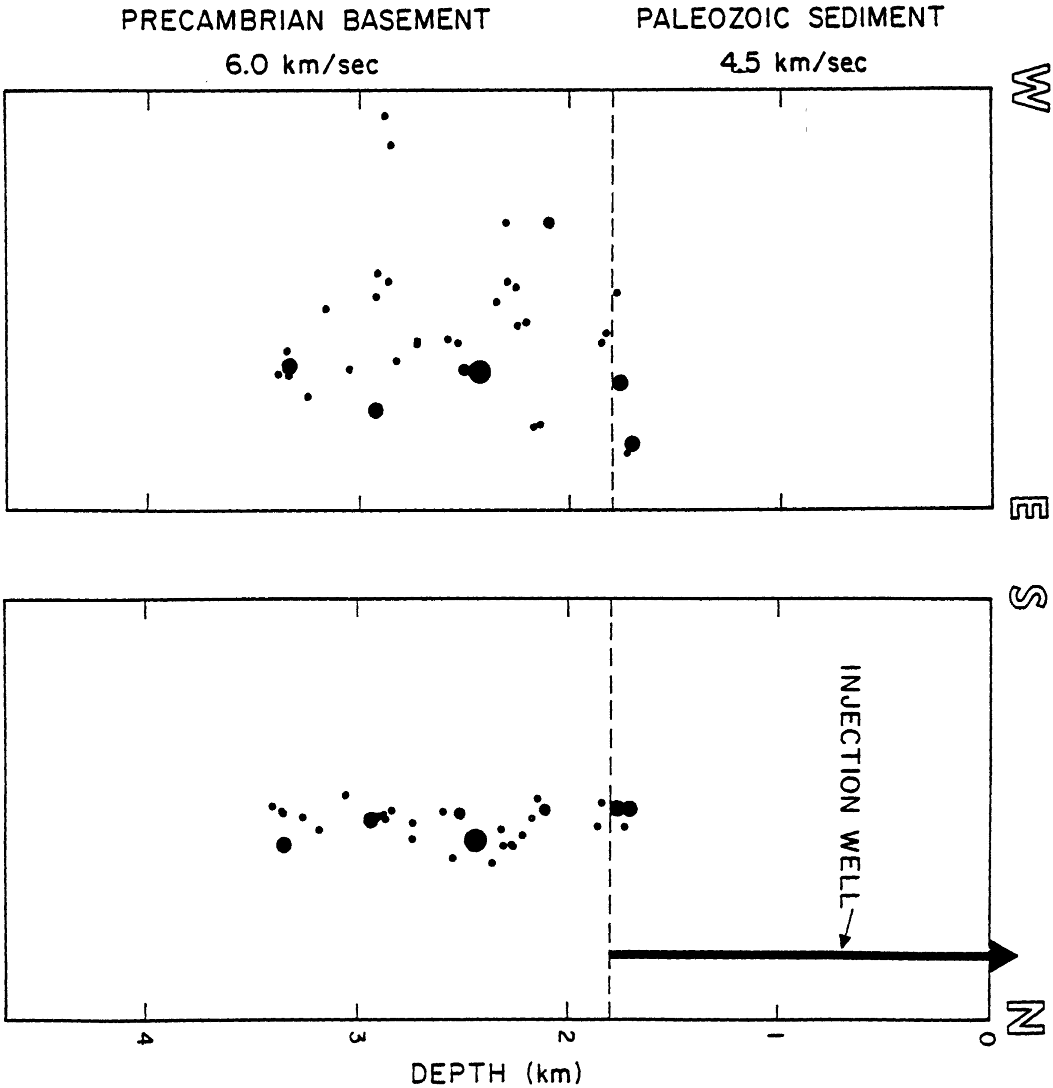

Fig. 2. Two cross sectional views of 35 aftershocks. Note the well defined fault plane in or very near the basement and the proximity of the bottom of the well to the hypocenters.

Regional Microearthquake Network in the Central Mississippi Valley

14-08-0001-A0263

William V. Stauder and Robert B. Herrmann
Department of Earth and Atmospheric Sciences
Saint Louis University
P.O. Box 8099 Laclede Station
St. Louis, MO 63156-8099
(314) 658-3131

Investigations

The purpose of the network is to monitor seismic activity in the Central Mississippi Valley Seismic zone, in which the large 1811-1812 New Madrid earthquakes occurred. The following section gives a summary of network observations during the first six months of the year 1987.

Results

In the first six months of 1987, 154 earthquakes were located and 52 other nonlocatable earthquakes were detected by the 42 station regional telemetered microearthquake network operated by Saint Louis University for the U. S. Geological Survey and the Nuclear Regulatory Commission. Figure 1 shows 140 earthquakes located within a 4° x 5° region centered on 36.5°N and 89.5°W. Seismograph stations are denoted by triangles and are labeled by the station code. The magnitudes are indicated by the size of the open symbols. Figure 2 shows the locations and magnitudes of 112 earthquakes located within a 1.5° x 1.5° region centered at 36.25°N and 89.75°W. Figures 3 and 4 are similar to Figures 1 and 2, but the epicenter symbols (squares) are scaled to focal depth.

In the first six months of 1987, 103 teleseisms were recorded by the PDP 11/34 microcomputer. Epicentral coordinates were determined by assuming a plane wave front propagating across the network and using travel-time curves to determine back azimuth and slowness, and by assuming a focal depth of 15 kilometers using spherical geometry. Arrival-time information for teleseismic P and PkP phases has been published in the quarterly earthquake bulletin.

The significant earthquakes occurring in the first six months of 1987 include the following:

1. 16 January 1987, UTC 0325, 35.86°N, 89.97°W: felt (III) at Blytheville and Dell, Arkansas. m_{Lg}(10Hz)=2.7 (SLM), m_{bLg}=3.0 (NEIS).

2. 27 March 1987, UTC 0729, 35.57°N,84.21°W: slight damage (VI) at Friendsville, Greenback, Louisville and Tallassee. Felt (V) at Benton, Delano, Harriman, Jacksboro, Philadelphia, Sweetwater, Tellico Plains, Turtletown and Vonore. Also felt (V) at Epworth and Mineral Bluff, Georgia. Felt in much of eastern Tennessee and in parts of Georgia and North Carolina. m_{Lg}=(10Hz)=4.2 (SLM), m_{bLg}=4.2 (NEIS), m_b=4.3 (PDE), m_d=4.3 (TEIC).

3. 10 June 1987, UTC 2348, 38.71°N, 87.95°W: minor damage in parts of Illinois, Indiana and Kentucky. Felt in parts of 21 states and Canada. m_{Lg}(10Hz)=5.2 (SLM), m_b=4.9 (PDE), M_{sz}=4.4 (PDE).

4. 13 June 1987, UTC 2117, 36.54°N, 89.69°W: felt in the Kennett-Portageville-New Madrid area. m_{Lg}(10Hz)=4.1 (SLM), m_{bLg}=4.1 (NEIS), m_d=4.1 (TEIC).

5. An absence of seismic activity has been noted on the southwest extension of the New Madrid fault zone at approximately 36°N and extending about 15 km to the southwest. The last event in this zone occurred in the first quarter of 1985.

Acknowledgements

The cooperation of the Tennessee Earthquake Information Center, National Earthquake Information Service, and the University of Kentucky is gratefully acknowledged for providing station readings, magnitude data, and felt information. The results reported were supported by the Department of the Interior, U. S. Geological Survey, under Contract 14-08-0001-A0263 and the U.S. Nuclear Regulatory Commission under Contract NRC-04-86-121.

References

Central Mississippi Valley Earthquake Bulletin, Department of Earth and Atmospheric Sciences, Saint Louis University. 1987 Nos. 51 and 52.

PDE Preliminary Determination of Epicenters, Monthly Listings, U.S. Geological Survey, 1987

TEIC Quarterly Seismological Bulletin, Tennessee Earthquake Information Center, Memphis State University. 1987, Vol. 7, No. 1.

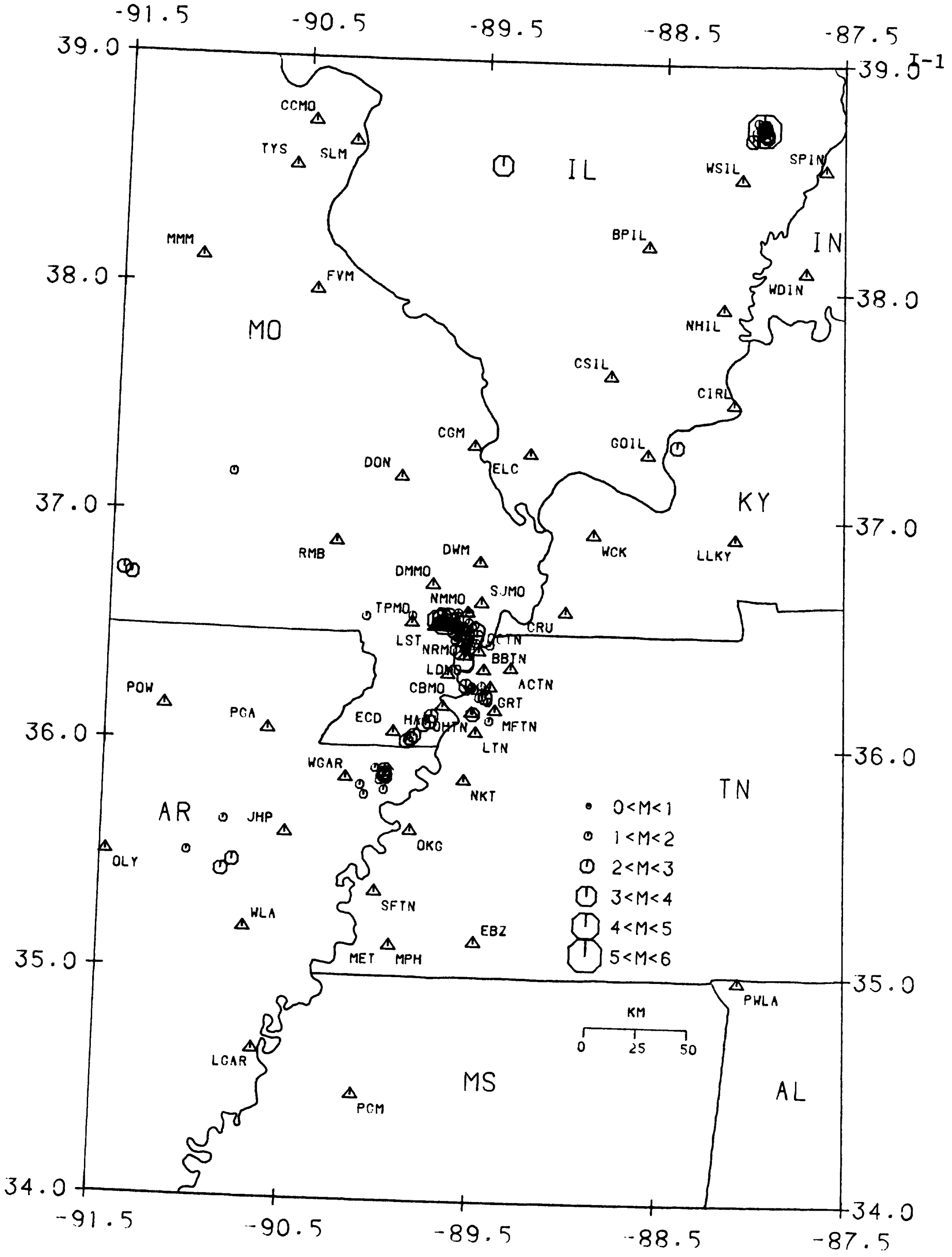

FIGURE 1
CUMULATIVE EVENTS 01 JAN 1987 TO 30 JUN 1987
LEGEND ▲ STATION ⊙ EPICENTER

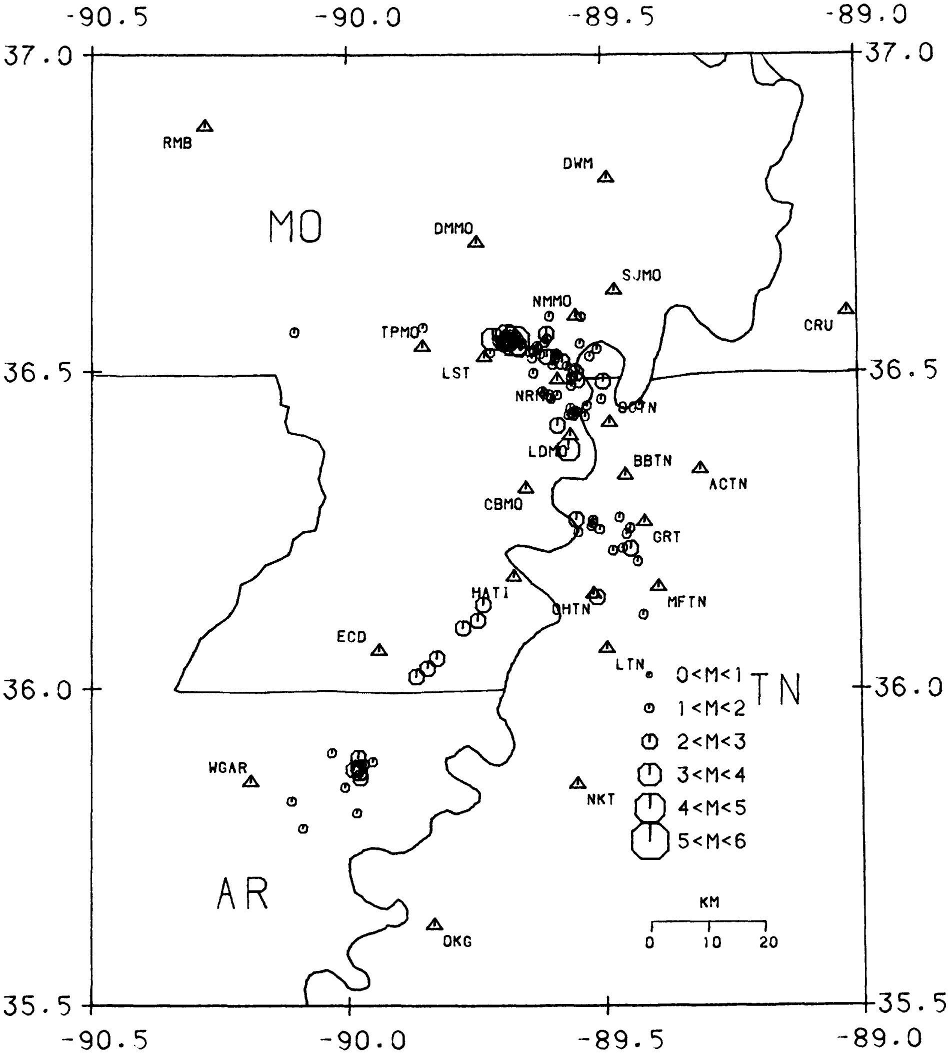

FIGURE 2
CUMULATIVE EVENTS 01 JAN 1987 TO 30 JUN 1987
LEGEND . ⚠ STATION ⊕ EPICENTER

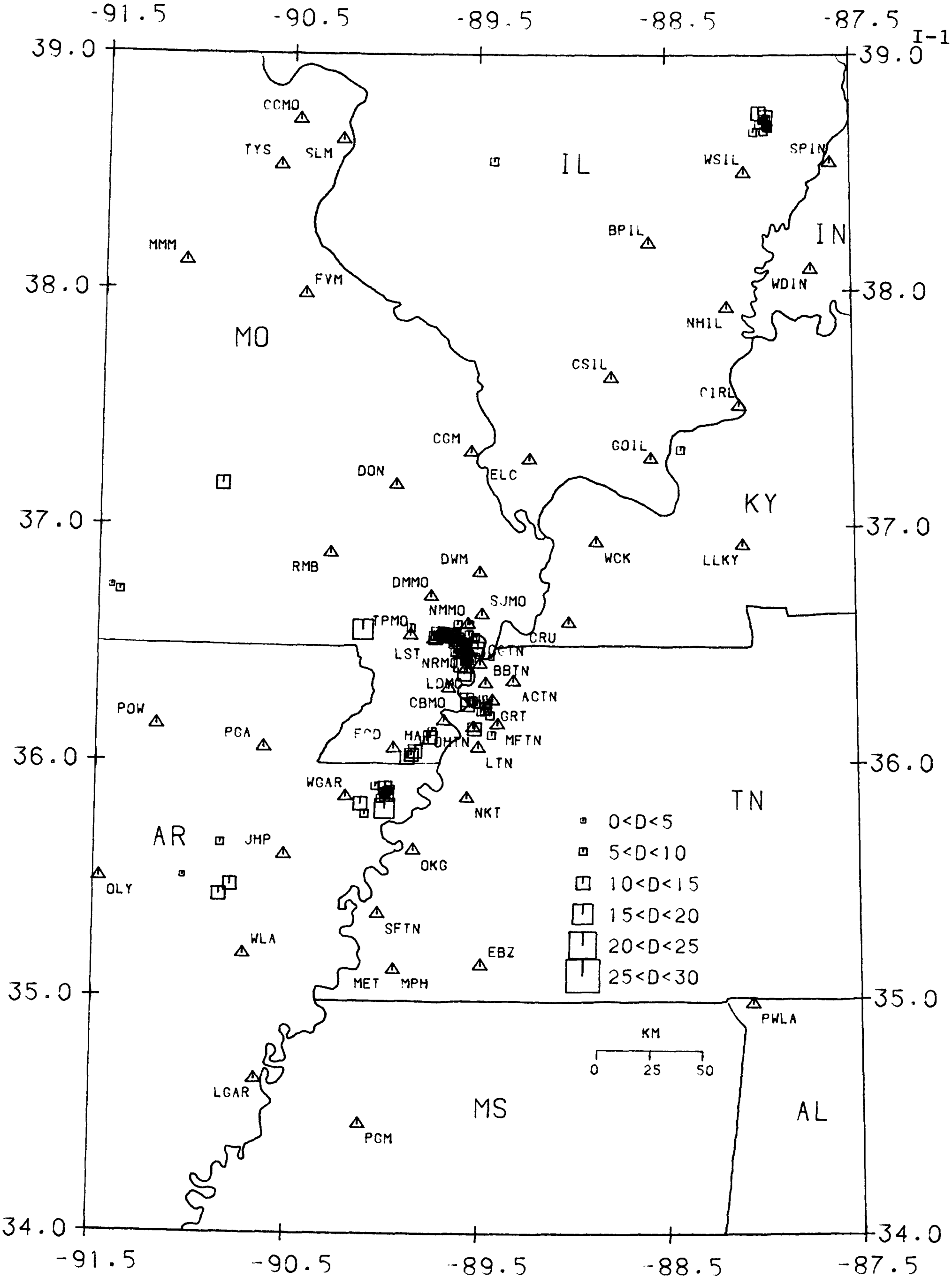

FIGURE 3
CUMULATIVE EVENTS 01 JAN 1987 TO 30 JUN 1987
LEGEND ▲ STATION □ EPICENTER

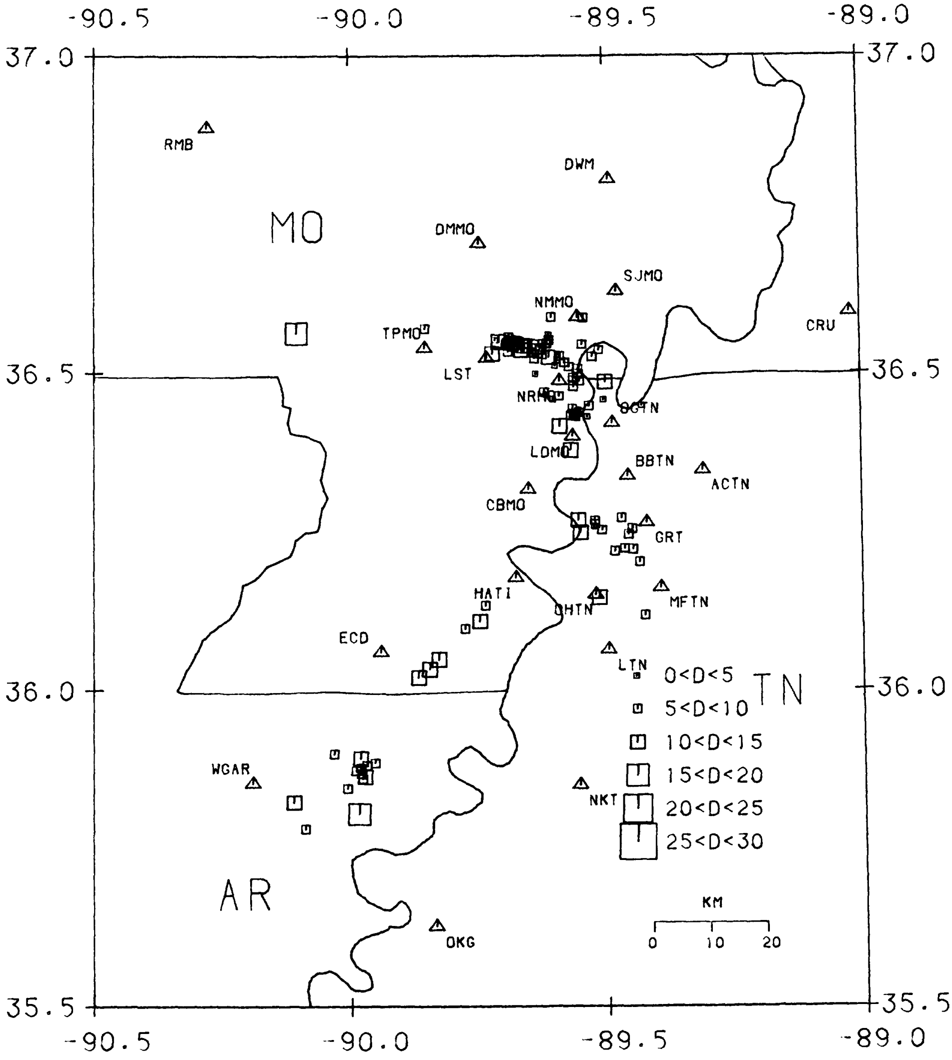

FIGURE 4

CUMULATIVE EVENTS 01 JAN 1987 TO 30 JUN 1987

LEGEND . △ STATION ◻ EPICENTER

Consolidated Digital Recording and Analysis

9930-03412

Sam Stewart
Branch of Seismology
U. S. Geological Survey
345 Middlefield Road, Mail Stop 977
Menlo Park, California 94025
(415) 329-4772

Investigations

This project is responsible (1) for operating, on a routine and reliable basis, a computer-automated system that will detect and process earthquakes occurring within the USGS Central California Earthquake Network (also known as CALNET), (2) for maintaining and developing software relevant to automated processing techniques, including analog-to-digital conversion and processing of events from analog magnetic tapes, and (3) for making the data available for research purposes on a timely basis. Presently, the signals from about 490 seismic instruments (including hi-gain vertical seismometers, lo-gain 3-component seismometers, force balance accelerometers and dilatometers) are telemetered to a central recording point in Menlo Park. One PDP 11/44 computer system is dedicated to online, realtime detection of earthquakes and storing of the digitized waveforms for later analysis. A second PDP 11/44 computer is dedicated to offline timing, processing and archiving of the waveform data. The DEC VAX/750 operated by the Branch of Seismology is used for final processing and archiving of the earthquake data. This computer is used by the research staff to obtain our data for research purposes. The total processing hardware/software systems used by the three DEC computers is known generically as the 'CUSP' system. The system was conceived of, designed and developed by Carl Johnson while in Pasadena. It has been modified considerably by Peter Johnson, Bob Dollar and Sam Stewart to meet the specific needs of Menlo Park.

Results

1. The CUSP system processed approximately 5406 earthquakes detected online during the period April thru September. Of these, 5171 were classified as 'local' events, and 235 were classified as 'regional' or 'teleseismic'. The usual few thousand non-seismic noise events that were detected had to be examined and deleted from the system as well. In addition, we are reviewing and cleaning up older data, using programs and techniques that were not available to us when the system first started in January 1984.

2. Major progress was made in reducing the transient noise introduced into the online analog-to-digital converter by noise sources within the computer room and telemetry instrumentation room. By introducing a new grounding rod and re-arranging sources of line power in the telemetry room, digitizing noise was reduced from a high range of about 500 mv to about 50 mv. By adding a .33 micro-farad capacitor to the input of each of the 16 channels on one of the digitizer multiplexor cards, noise was reduced from a high range of about 50 mv to about 5 mv. This modification remains to be done to all of the other multiplexor cards.

3. Digitizing of earthquakes recorded on the 'daily' analog telemetry tapes, and insertion of these events into the CUSP processing flow, is now happening on a routine basis. Bob Dollar and Peter Johnson developed software that allows digitizing at a rate of 128,000 bytes/sec on the VAX/750. This allows 40 analog channels to be digitized at a rate of 100 samples/second, using a tape speed-up factor of 16x. In addition, they developed a Command Line Interpreter and associated data base system that simplifies and organizes entry of digitizing requests into the system, optimizes the selection of events to be digitized, and keeps track of the status of each digitizing request.

4. The CUSP timing system on the VAX/750 was modified by Chris Stephens (Alaska Seismic Studies project) to allow amplitudes and periods of waveforms to be measured by the analyst while the waveform is being routinely timed. A 'weight' and phase-identifying remark can also be entered. This is a significant improvement, in that this provides the fundamental data to calculate earthquake magnitudes from amplitude and period measurements.

5. A Megatape 'streaming' tape drive was added to the VAX/750 and to the Parkfield Microvax-II data acquisition system by Bob Dollar. The 750 megabyte capacity (formatted) is equivalent to about 6 or 7 of the standard 2400 foot tapes recorded at 6250 BPI density. Use of this system results in the following advantages: (1)disk-to-tape backup operations on the 750 can be done more efficiently while at the same time the tri-density tape drive is freed up for other uses; (2) at Parkfield, the Microvax-II can function as a very high-data-capacity field recording system, reducing to a large extent the possibility of running out of tape during an active seismic sequence; (3) at Parkfield, the online data acquisition system can run as a diskless system, using only the CPU, memory and the Megatape drive--thus very strong ground motion that might cause disk heads to crash should not affect this configuration of the Parkfield Microvax II.

6. Peter Johnson developed some very useful Block I/O data transfer subroutines for the VAX/VMS system. These routines are the backbone of any largescale data acquisition or processing operations, are Fortran callable, and the user need not understand the details of VMS system service calls to use these routines.

7. A Texas Instruments 2115 Laser printer was installed on the VAX/750. The CUSP graphic programs TROUT and PLOTALL were modified by Peter Johnson to plot to this device. Although the plots are much cleaner than those from the Versatec 1200 plotter, the increased plot time and disk space that are required limit the usefulness of the Laser printer, so far.

Reports

Lee, W.H.K., and S.W. Stewart (1988). Large Scale Processing and Analysis of Digital Waveform Data from the USGS Central California Microearthquake Network. Proc. of the Centennial Symposium of the University of California Seismographic Stations, May 28-29, 1987.

Seismic Monitoring of the Shumagin Seismic Gap, Alaska

USGS 14-08-0001-A0260

John Taber
Lamont-Doherty Geological Observatory of Columbia University
Palisades, New York 10964
(914) 359-2900

Investigations

Seismic data from the Shumagin seismic network were processed to obtain origin times, hypocenters, and magnitudes for local and regional events. The processing resulted in files of hypocenter solutions and phase data, and archive tapes of digital data. These files are used for the analysis of possible earthquake precursors, seismic hazard evaluation, and studies of regional tectonics and volcanicity (see Analysis Report, this volume). Yearly bulletins are available starting in 1984.

Results

The Shumagin network was used to locate 642 earthquakes from January through August 1987. The seismicity of the Shumagin Islands region for this time period is shown in map view and cross section in figure 1. The largest event in this period in the region occurred on 6/21/87, had a M_s of 6.2, and was located south of the network at 54.04N, 162.46W (obvious cluster on seismicity map). The event was felt up to 300 km away. 139 aftershocks have been located through August, the largest having an m_b of 5.5. Not including the aftershock sequence of the June event there were 14 events over magnitude 4. The largest of these earthquakes was an m_b 5.1 event on 5/2/87 that was felt (intensity V) in Sand Point. Otherwise the overall pattern over this time period is similar to the long term seismicity. Concentrations of events occur at the base of the main thrust zone and in the shallow crust directly above it. The continuation of the thrust zone towards the trench is poorly defined. West of the network (which ends at 163°) and the June sequence, the seismicity is more diffuse in map view and extends closer to the trench. Eight of the 14 located events larger than magnitude 4 that were not aftershocks of the June event occurred in this western region. Below the base of the main thrust zone (~45 km) the dip of the Benioff zone steepens. Part of the double plane of the lower Benioff zone is evident near 100 km depth.

Servicing of the network was successfully completed in June and July. All stations were visited and all were still operational as of 10/31/87. The network is capable of digitally recording and locating events as small as M_l=0.4 with uniform coverage at the 2.0 level. Events are picked and located automatically at the central recording site in Sand Point, Alaska and the results, along with subsets of the digital data, can be accessed via telephone modem. Onscale recording is possible to ~M_s=6.5 on a telemetered 3 component force-balance accelerometer. Larger events are recorded by one digitally recording accelerometer and on photographic film by 12 strong-motion accelerometers.

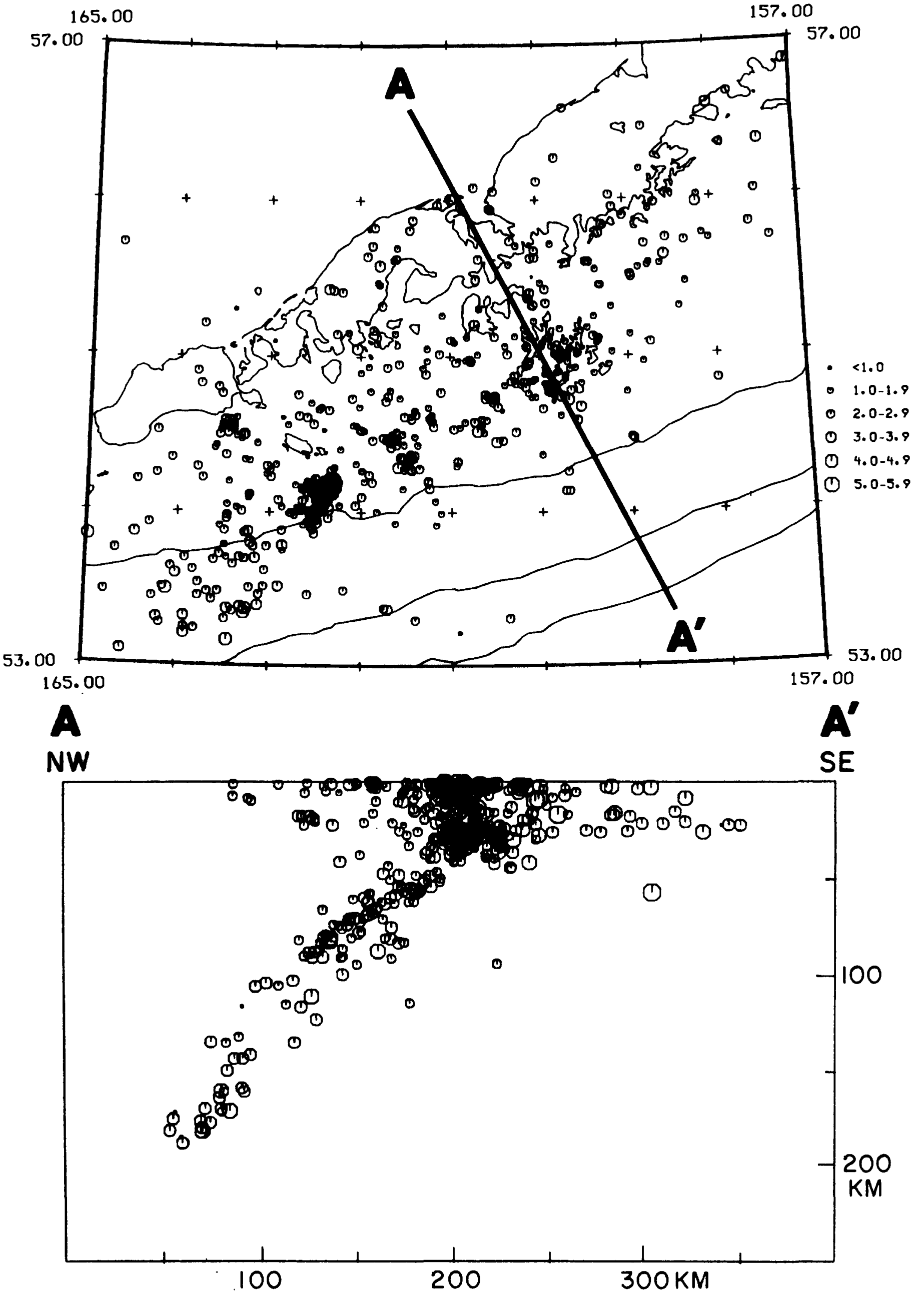

Figure 1. Top: Seismicity recorded by the Shumagin seismic network from January though August 1987. Bottom: Cross section of seismicity projected along the line A-A' in the upper figure.

Earthquake Hazard Research in the Greater Los Angeles Basin and Its Offshore Area

#14-08-0001-A0264

Ta-liang Teng
Thomas L. Henyey
Egill Hauksson

Center for Earth Sciences
University of Southern California
Los Angeles, CA 90089-0741
(213) 743-6124

INVESTIGATIONS

(1) Monitor earthquake activity in the Los Angeles Basin and the adjacent offshore area.

(2) Upgrade data acquisition system for the USC LA Basin network.

(3) Upgrade of telemetry electronics used by remote field stations. A new version of the microprocessor-based Optimum Telemetry System has been deployed for field testing at one seismic station.

RESULTS

(1) The earthquake activity that occurred in the Los Angeles basin from January 1 to October 15, 1987 is shown in Figure 1. The seismicity rate during 1987 is similar to the rate that was recorded during the previous three years. The earthquake activity in the Los Angeles basin is characterized by single shocks that are scattered throughout the region. Several spatial clusters are observed in the monitoring region. Clusters of seismicity are observed at the northern segments of both the Newport-Inglewood fault as well as the Palos Verdes fault during 1987. The adjacent offshore area in Santa Monica Bay is also characterized by a moderate level of seismic activity. A cluster of earthquakes is observed near the aftershock zone of the 1973 Point Mugu earthquake. The Whittier Narrows (M_L=5.9) main shock-aftershock sequence is also shown in Figure 1. Over 250 aftershocks were recorded by the USC Los Angeles basin seismic network from October 1-15, 1987.

(2) We have installed a new 16 bit Tustin A/D and a MicroVAX II workstation to record the Los Angeles Basin network data. In Figure 2 we show a schematic diagram of the hardware configuration. We currently digitize 48 channels at 100 sps. To the right in Figure 2 we indicate how much of the system resources are used during periods of background activity. During the October 1987 Whittier Narrows main shock-aftershock sequence this new system performed very well and recorded over 250 aftershocks.

The online and offline software that we run on the MicroVAX II workstation to collect and analyze earthquake data is shown in Figure 3. The different computer programs are indicated by square boxes and hardware parts are indicated with round edge boxes. The programs used for data acquisition were initially written by Carl Johnson and later modified by Bob Dollar (both of USGS). The None-CUSP programs used for offline processing were either developed at USC or are standard USGS data analysis programs such as HYPOINVERSE by Fred Klein. This software package allows us to collect and analyze data on the same MicroVAX. In the future when CUSP has been adopted for MicroVAX we plan to standardize our offline data processing software.

(3) A second generation of the Optimum Telemetry System (OTS) has been designed and deployed in the field. The front-end anti-aliasing filters have been upgraded to 7 poles. To minimize electronic noise the microprocessor has been placed on a separate circuit board. The design goals are to achieve a background noise level of 1 mV or less. Field testing of the new OTS began one week before the October 1, 1987 Whittier Narrows earthquakes.

The OTS was installed at station GFP, located on granitic bedrock 25 km away from the Whittier Narrows main shock. In Figure 4 we show gain ranged, vertical component, seismograms from the (M_L=5.9) main shock, (M_L=5.3) largest aftershock and a small (M_L=3.4) aftershock. The main shock seismogram is similar to the (USGS) vertical component strong motion records from the Whittier Narrows Dam, located a few km away from the main shock epicenter. These on-scale seismograms will be used to study source parameters of the Whittier Narrows sequence and to establish local scaling relationships. Furthermore, these seismograms can be used for studying weak motion site effects in the Los Angeles basin.

REPORTS

Hauksson, E., Seismotectonics of the Newport-Inglewood Fault Zone in the Los Angeles Basin, Southern California, Bull. Seism. Soc. Amer. 77, 539-561.

Hauksson, E., T. L. Teng and T. L. Henyey, Near-Surface Attenuation of Waveforms of Local Earthquakes: Results from a 1500 m Deep Downhole Seismometer Array, to appear in Bull. Seism. Soc. Amer., December, 1987.

Hauksson, E., Seismotectonics of the Newport-Inglewood Fault Zone and the 1933 Long Beach Earthquake (M_L = 6.3) in the Los Angeles Basin, Southern California, presented at S.S.A. Meeting Santa Barbara, March, 1987.

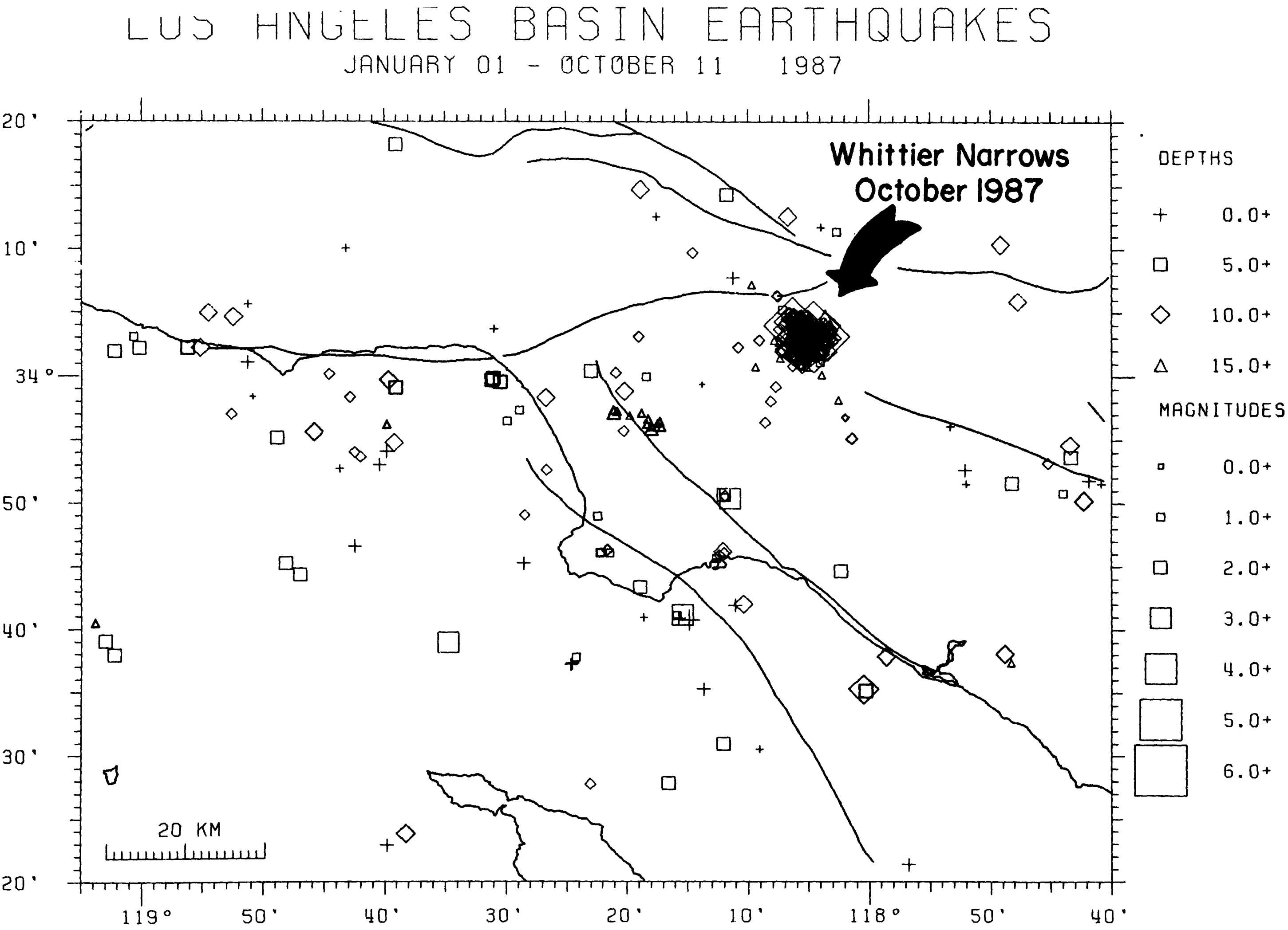

Figure 1. Seismicity January 1 to October 11, 1987, recorded by the USC Los Angeles basin seismic network.

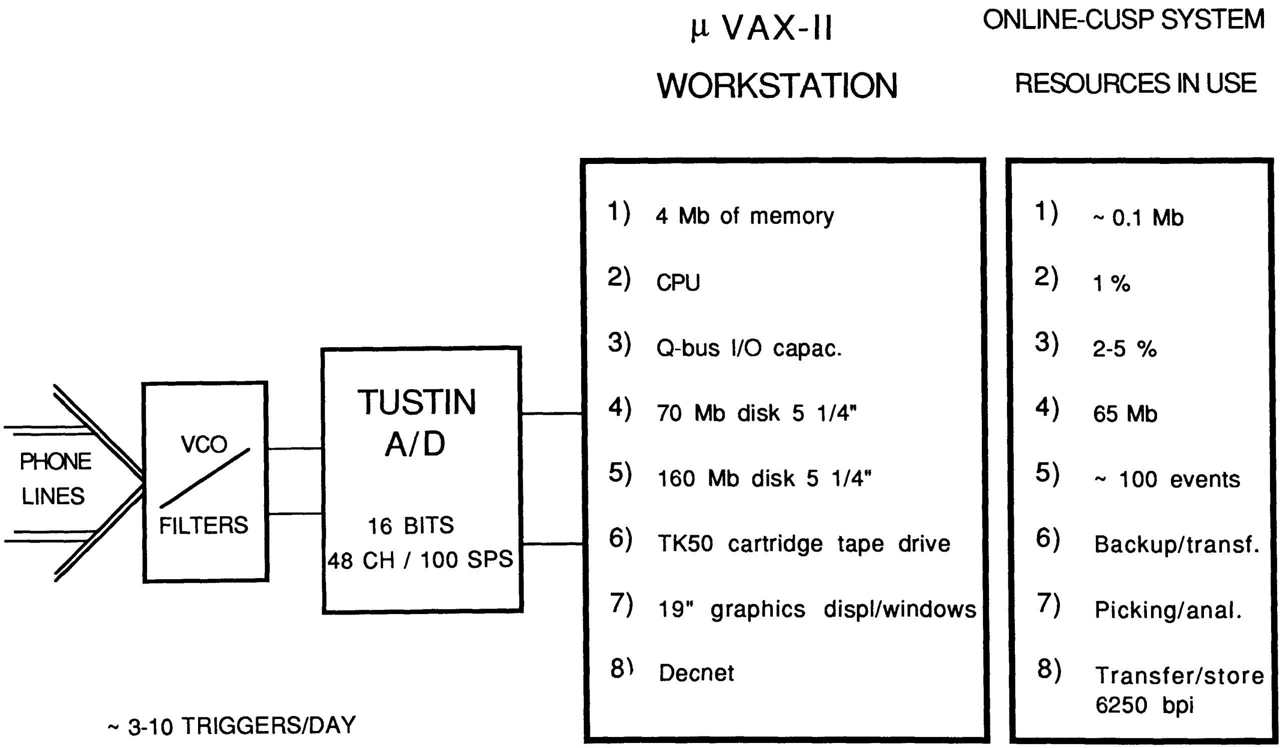

Figure 2. USC Los Angeles basin network:
seismic data acquisition system.
Hardware configuration.

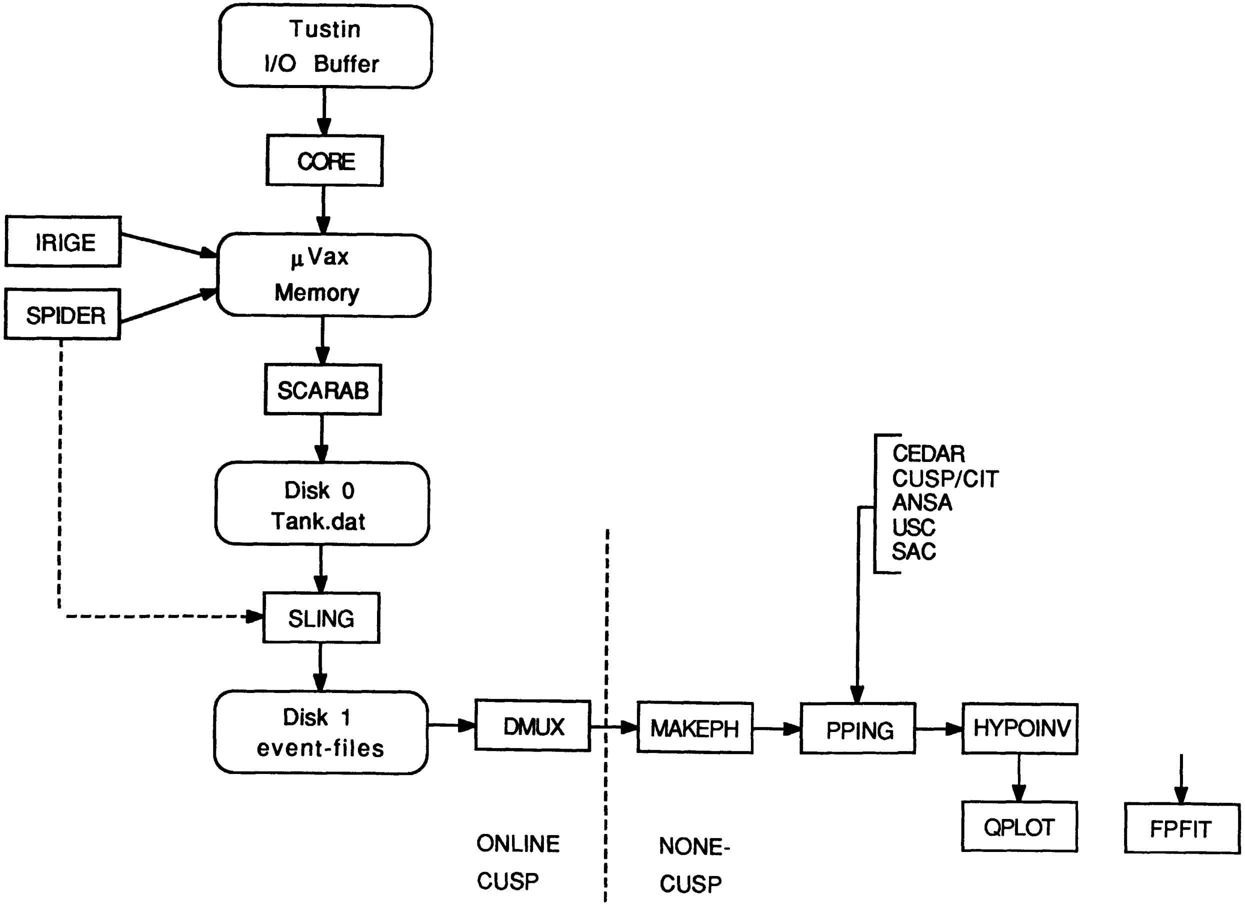

Figure 3. USC Los Angeles basin network: seismic data acquisition system. Software and data flow diagram.

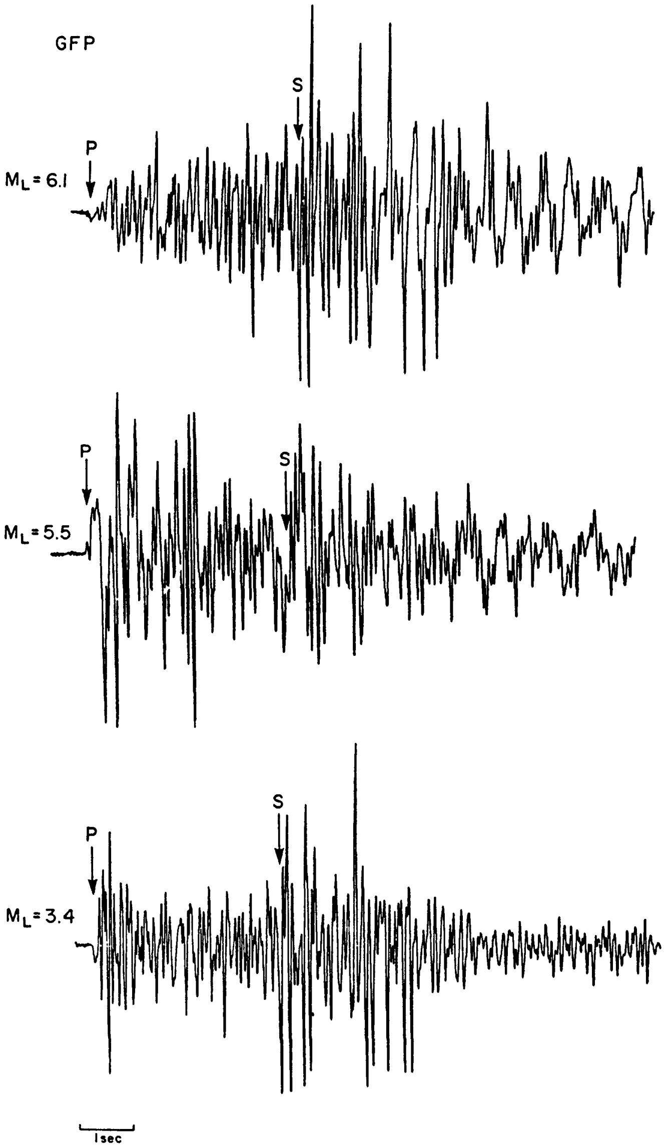

Figure 4. On scale seismograms of the (M_L=6.1) mainshock, largest aftershock (M_L=5.5) and a small aftershock, (M_L=3.4) recorded at a station 23 km away from the epicentral zone using OTS.

Field Experiment Operations

9930-01170

John Van Schaack
Branch of Seismology
U. S. Geological Survey
345 Middlefield Road MS-977
Menlo Park. California 94025
(415) 329-4780

Investigations

This project performs a broad range of management. maintenance. field operation, and record keeping tasks in support of seismology and tectonophysics networks and field experiments. Seismic field systems that it maintains in a state of readiness and deploiys and operates in the field (in cooperation with user projects) include:

a. 5-day recorder portable seismic systems.
b. "Cassette" seismic refraction systems.
c. Portable digital event recorders.
d. Smoked paper recorder portable seismic systems

This project is responsible for obtaining the required permits from private landowners and public agencies for installation and operation of network sensors and for the conduct of a variety of field experiments including seismic refraction profiling, aftershock recording, teleseism P-delay studies. volcano monitoring. etc.

This project also has the responsibility for managing all radio telemetry frequency authorizations for the Office of Earthquakes, Volcanoes. and Engineering and its contractors.

With the consolidation of projects personnel of this project are now responsible for maintaining the seismic networks data tape library. This includes processing daily telemetry tapes to dub the appropriate seismic events and making playbacks of requested network events and events recorded on the 5-day recorders.

Results

Seismic Refraction

One hundred twenty seismic cassette recorders were used in two seperate experiments. The first experiment was carried out in Arizona and was part of the PACE Experiment. The profile on this reflection/refraction experiment extended from Parker to Prescott. Arizona and consisted 240 recording sites and about 24 shots. The recording instruments were spaced at 1Km intervals. The second experiment was part of the TACT Experiment in Alaska. This experiment consisted of two deployments of 120 instruments along a profile extending from near Glen Allen to the Yukon River along the Alaskan Pipe Line. Approximately 30 shots were fired along the profile. Data quality was good from both experiments.

Telemetry Networks

We have completed the installation of telemetered Force Balance Accelerometers in the Parkfield area. We have made numerous modifications to the Microwave Network to improve coverage and reliability.

Portable Networks

Six 5-day recorders were deployed in a special cluster near Mammoth Lakes CA. This experiment was carried out in conjunction with personnel of the University of Nevada. The experiment lasted about 6 weeks.

Geothermal Seismotectonic Studies

9930-02097

Craig S. Weaver
Branch of Seismology
U. S. Geological Survey
at Geophysics Program AK-50
University of Washington
Seattle, Washington 98195
(206) 442-0627

Investigations

1. Continued analysis of the seismicity and volcanism patterns of the Pacific Northwest in an effort to develop an improved tectonic model that will be useful in updating earthquake hazards in the region. (Weaver, with Guffanti of IGP branch)

2. Continued acquisition of seismicity data along the Washington coast, directly above the interface between the North American plate and the subducting Juan de Fuca plate. (Weaver, Zollweg, UW contract)

3. Continued seismic monitoring of the Mount St. Helens area, including Spirit Lake (where the stability of the debris dam formed on May 18, 1980 is an issue), Elk Lake, and the southern Washington-Oregon Cascade Range (north of Three Sisters). The data from this monitoring is being used in the development of seismotectonic models for southwestern Washington. (Weaver, Zollweg, Grant, Yelin, UW contract)

4. Study of Washington seismicity, 1960-1969. Efforts are underway to determine magnitudes based on a revised, empirical Wood-Anderson-coda duration relation. Earthquakes with magnitudes greater than 4.5 are being re-read from original records and will be re-located using master event techniques. Focal mechanism studies are being attempted for all events above magnitude 5.0. (Yelin, Weaver)

5. Detailed analysis of the seismicity sequence accompanying the May 18, 1980 eruption of Mount St. Helens. Earthquakes are being located in the ten hours immediately following the onset of the eruption, and the seismic sequence is being compared with the detailed geologic observations made on May 18. Re-examination of the earthquake swarms that followed the explosive eruptions of May 25 and June 13, 1980, utilizing additional playbacks of 5-day recorder data. (Weaver, Zollweg, Norris, UW contract)

6. Study of earthquake catalogs for the greater Parkfield, California region for the period 1932-1969. Catalogs from the University of California (UCB) and CalTech (CIT) are being compared, duplicate entries noted, and the phase data used by each reporting institution are being collected. The study is emphasizing events greater than 3.5, and most events will be relocated using station corrections determined from a set of master events located by the modern networks. (Meagher, Weaver, with Lindh, Ellsworth)

7. Analysis of a swarm of over 500 sub-edificial (depths 3 - 14 km) earthquakes that occurred at Mt. St. Helens prior to the 1980 eruption. Sub-edifical earthquakes have recently been found to be useful in mapping the overall geometry of the magma feeder system, and the pre-May 18 data set is probably the best available to us in terms of numbers of events, numbers and distribution of stations recording them, and background noise level. (Zollweg, Norris, UW contract)

Results

1. Mount St. Helens lies along the western front of the Cascade Range between Mount Rainier, Washington and Mount Hood, Oregon. This is an area of transition, both geologically and geophysically. North of Mount Rainier, late Cenozoic volcanism is limited to the major stratovolcanoes, whereas south of Mount Hood the volcanic cover from both stratovolcanoes and monogenetic vents is nearly continuous for 300 km. The dominant stratovolcanoes in the southern Washington Cascade Range are physiographically similar to those in the North Cascades, but the volcanic cover is similar to the Oregon Cascades. A saddle occurs in the Bouguer gravity data over the Columbia River, interrupting a west-east gravity gradient observed along the rest of the Oregon Cascade Range. Heat flow values are intermediate, being lower than those observed in Oregon but higher than those observed north of Mount Rainier. Seismicity is mostly concentrated along the St. Helens zone (SHZ), and all crustal earthquakes greater than magnitude 5 since 1960 in Washington and northern Oregon have ocurred between Mount Rainier and Mount Hood. Little seismicity is known within the Cascade Range south of Mount Hood, and few earthquakes occur within the North Cascades of Washington. Magnetotelluric studies indicate a conductor within the area bounded by Mount Rainier, Mount Adams, and Mount St. Helens, and the conductor is interpreted as an east-dipping, compressed marine terrain in the upper plate. Mount St. Helens is located at a dextral offset in the SHZ where the SHZ intersects a set of older, mapped fractures that are preferrentially aligned with the contemporary regional principal stress direction. Aeromagnetic and gravity data suggest the presence of an intrusive body beneath the volcano; petrogenesis studies favor multiple intrusions of small batches of magma into the shallow volcanic system.

2. An earthquake catalog for Washington and northern Oregon complete to M_D,M_L = 3.5 (duration and local magnitude, respectively) for the years 1960-1984 has been compiled. Earthquakes associated with the eruptions of Mount St. Helens are not included. The 1960-1969 section of the catalog is based upon examination of ten years worth of seismograms from the hightest gain, continually operating station in the region. The catalog from 1970-1984 is based upon the University of Washington network catalog, but contains newly determined M_L for the earthquakes, to achieve maximum consistency with the 1960-1969 part of the catalog. This study revealed a number of errors in magnitude determination in previously published studies of seismicity in the region. Important features and patterns of seismicity were both revealed and verified. The 1965 Seattle earthquake, a normal faulting event within the subducted Juan de Fuca plate, had no foreshocks at the $M_D \geq 2.0$ level in 1965, and, beginning about eight minutes after it's initial rupture (when the LON record went back on scale), it had no aftershocks at the $M_D \geq 3.0$ level except for one possible aftershock six months after the main shock. A significant difference between pre-1969 seismicity and post-1968 seismicity is the lack of earthquakes at the $M_D \geq 3.5$ level in northwestern Oregon in the latter time period. The 1965 Seattle earthquake released about 91% of the total moment released from 1960-1984 by earthquakes in this catalog. About 630×10^{22} dyne-cm of moment was released by earthquakes within the overthrust North America plate from 1960-1984. About 5% of this was released in the backarc, 28% in the forearc and 67% in the Cascade volcanic arc. The 1961 and 1981 earthquake sequences on the Saint Helens seismic zone in the southern Washington Cascades released about 50% of the combined moment released in the arc and forearc from 1960-1984. If the 1962 Portland earthquake and the two Goat Rocks earthquakes of 1981 southeast of Mount Rainier are included, 75% of the total moment released in the arc and forearc is accounted for.

3. Five new seismic stations were installed in the central Oregon Cascade Range in the vicinity of Bend. These stations provide seismic monitoring of Mount Jefferson, Newberry Volcano, and the Three Sisters area. Discussions have started with the Bonneville Power Administration to move existing microwave drops to serve an expanded Oregon network that is planned for installation during the summer of 1988.

Reports

Grant, W. C. and Weaver, C. S., Seismicity of the Spirit Lake area: Estimates of possible earthquake magnitudes for engineering design, in *The formation and significance of major lakes impounded during the 1980 eruption of Mount St. Helens, Washington, U. S. Geological Survey Professional Paper,* edited by R. L Shuster and W. Meyer, (still in press).

Weaver, C. S. and G. E. Baker, Geometry of the Juan de Fuca plate beneath Washington: Evidence from seismicity and the 1949 South Puget Sound earthquake, *Bulletin of the Seismological Society of America, 77,* (in press), 1987.

Baker, G. E. and C. A. Langston, Source parameters of the magnitude 7.1 South Puget Sound, Washington, earthquake as determined from long-period body waves and strong ground motions, *Bulletin of the Seismolgical Society of America, 77,* 1530-1557, 1987.

Weaver, C. S., W. C. Grant, and J. E. Shemeta, Local crustal extension at Mount St. Helens, Washington, *J. Geophys. Res., 92,* 10,170-10,178, 1987.

Weaver, C. S. and S. D. Malone, Overview of the tectonic setting and recent studies of eruptions of Mount St. Helens, Washington, *J. Geophys. Res., 92,* 10,149-10,154, 1987.

Guffanti, M. and C. S. Weaver, Distribution of late Cenozoic volcanic vents in the Cascade Range (USA): Volcanic arc segmentation and regional tectonic considerationsr, *submitted to J. Geophys. Res..*

Weaver, C. S. and J. E. Zollweg, Seismological studies at Mount St. Helens, USA: Implications for forecasting other volcanic events, (abs), *Proceedings, 1987 IUGG meeting, vol. 1,* (in press), 1987.

Weaver, C. S., Seismological constraints on the geometry of the Juan de Fuca plate, *Proceedings, 1987 IUGG meeting, vol. 1,* in press, 1987.

Meagher, K.L., C. S. Weaver, A. G. Lindh, and W. L. Ellsworth, Seismicity in Central California, 1932-1969: Initial results of a catalog study, (abs), *EOS, Trans. Am. Geophys. U., 68,* 362, 1987.

Grant, W. C., and D. D. McLaren, Evidence for Holocene subduction earthquakes along the northern Oregon coast, (abs), *EOS, Trans. Am. Geophys. U., 68,* (in press), 1987.

Guffanti, M. and C. S. Weaver, Late Cenozoic volcanism in the Pacific Northwest: Cascade Arc segmentation, subducting-plate geometry, and basin-range extension, (abs), *Geothermal Resources Council,* (in press), 1987.

Strong Ground Motion Data Analysis

9910-02676

J. Boatwright, M. Andrews, J. Fletcher, and A. McGarr
Branch of Engineering Seismology and Geology
U. S. Geological Survey
345 Middlefield Road, MS 977
Menlo Park, California 94025
(415) 329-5609, 329-5607, 329-5628, 329-5645

Investigations

1. Theoretical investigation of the earthquake rupture process.

2. High-frequency acceleration radiated by extended seismic sources.

3. Analysis of seismograms from borehole and array instruments at Anza, CA with regard to the discrimination of nuclear explosions from earthquakes.

Results

1. The earthquake rupture process is decomposed into the rupture of a set of discrete sub-events, S_i, which rupture at times t_i. The slip associated with the stress release on S_i is calculated by modeling the sub-event as an asperity with the dynamic stress drop s_i and setting the stress drop on the complement of the sub-event area $S(t) - S_i$ equal to zero. The sub-event failure produces slip on both the sub-event area and the complement area. The moment release of a sub-event is proportional to $Ws_i \cdot S_i \cdot S(B)^{1/2}$, while the radiated acceleration spectrum is proportional to $Ws_i \cdot S_i^{1/2}$. Because the model parameters are reduced to the set of sub-event stress drops and rupture times, the decomposition yields a convenient basis for inverting seismograms to obtain the space-time distribution of stress release. To model the sub-event radiation, aftershock recordings are causally filtered to enhance the low frequeny content by the factor $(S(B)/S_i)^{1/2}$. The inversion process was performed for a $M_L = 5.5$ aftershock of the 1983 Coalinga, using a 3.6 M_L aftershock as a Green's function. A rupture process comprised of twelve sub-events was obtained, with a generally updip rupture direction and stress drops ranging from 2 to 9 times the stress drop of the 3.6 M_L aftershock.

2. The theory derived by Boatwright (1982) was extended to analyze the expected acceleration radiated by extended faults. In contrast to kinematic treatments, where the source excitation is obtained from the distribution of the slip velocity multiplied by the radiation pattern, in the high-frequency analysis, the source excitation is obtained from the distribution of the dynamic stress drop multiplied by a high-frequency radiation pattern which incorporates directivity and crack diffraction effects. By specifying the approximate rupture history, the high-frequency analysis yields an envelope for the radiated acceleration. Inversion of this envelope to obtain the distribution of stress drop and the approximate rupture history is being implemented using a tomographic inversion procedure.

3. The *Hardin* nuclear explosion ($M_b = 5.3$) was recorded by the borehole seismometers at Keenwild, CA. The seismograms from these instruments are not similar to earthquakes in that no S-wave is observable on these traces whereas earthquakes observed at distances beyond a few hundred kilometers have large emergent S-wave trains that apprear to be made up of S_g, S_n, and L_g. The seismometers used in the borehole systems are 2 Hz geophones and do not have a good low-frequency response, but nevertheless these systems recorded considerably less S-wave energy for the explosion than for earthquakes observed at roughly the same distance range. The largest signals on the records are associated with the P-wave.

   The signal-to-noise ratio is about 1 at 10 Hz for the data from the downholes which suggests that the path to NTS is fairly heavily attenuating in that recent seismograms from the array inside Russia where waves propagates through much older terrane also has much higher frequency content.

   Jim Brune and William Walters are pursuing the discrimination problem by analyzing the amplitudes of 30 Hz energy from a number of earthquakes including those from Anza. The principal question is whether or not the high frequency amplitudes could discriminate an explosion from an earthquake based on a model drevied by Archambeau (1968, 1972), and discussed by Evernden *et al.* (1986) as a basis for discrimination. Amplitudes of 30 Hz energy do not support the Archambeau model and are more in agreement with the ω^{-2} model. In fact, many explosions have smaller amplitudes than predicted by the Sharpe (1942) model and some earthquakes have larger amplitudes than the Sharpe model. Thus it appears that further research into the effects of the propagation path both in stable shield areas and in areas marked by recent tectonism as well as into source excitation is needed before amplitudes at 10 Hz and above can be reliably used for discrimination and yield issues.

References

Archambeau, C.B., 1968, General theory of elastidynamic source fields: *Reviews of Geophysics*, v. 6, p. 241-288.

Archambeau, C.B., 1972, The theory of stress wavae radiation from explosions in prestressed media: *Journal of Geophysics*, v. 29, p. 329-366.

Evernden, J.F., Archambiea, C.B., and Cranswick, E., 1986, An evaluation of seismic decoupling and underground nuclear test monitoring high frequency seismic data: *Reviews of Geophysics*, v. 7, p. 143-216.

Sharpe, J.A., 1942, The production of elastic waves by explosion pressures, 1, Theory and empirical field observations: *Geophysics*, v.. 7, p. 144-154.

Publications

Walter, W.R., Brune, J.N., Priestly, K., and Fletcher, J., 1987, Observations of high-frequency P-wave earthquake and explosion spectra compared with ω^{-2} and ω^{-3} and Sharpe source models: submitted August 1987.

Strong Ground Motion of Large Intraplate Earthquakes Estimated from Teleseismic Recordings

9910-04186

John Boatwright
Branch of Engineering Seismology and Geology
U.S. Geological Survey
345 Middlefield Road, MS 977
Menlo Park, California 94025
(415) 329-5609

George L. Choy
Branch of Global Seismicity
U.S. Geological Survey, Box 25046, MS 967
DDenver Federal Center, CO 80225
FTS 776-1506

Investigations

We have analyzed the teleseismic P-waves radiated by ten shallow thrust intraplate earthquakes in the frequency domain. The method of spectral analysis used to analyze these events is derived in detail by Boatwright and Choy (1987a). The set of earthquakes were chosen as analogs for possible large earthquakes in North Eastern North America, where the focal mechanisms are predominately thrust and reverse, and the source depths are shallow. The earthquakes range in size from an aftershock ($m_{blg} = 5.4$) of the 1982 Miramichi earthquake to the 1978 Tabas, Iran, earthquake ($M_S = 7.4$).

Results

The shapes of the corrected P-wave spectra have a consistent intermediate trend, where the acceleration spectra is linearly proportional to frequency. Above this trend, the spectra are approximately flat. This spectral shape is significantly different from the Brune-type spectral shape of subduction zone earthquakes analyzed by Boatwright and Choy (1987a). The high frequency source spectral levels $R\ddot{u}_{\alpha}|$ for the 10 earthquakes are plotted below as a function of the seismic moments. The corrected acceleration spectral levels for five subduction zone earthquakes are also plotted.

Reports

Boatwright, J., 1987, The seismic radiation from composite models of faulting, *Bulletin of the Seismological Society of America*, v. 77, in press.

Boatwright, J., and G.L. Choy, 1987a, The acceleration spectra of large, shallow, subduction zone, earthquakes, submitted to *Journal of Geophysical Research*, v. 92.

Choy G.L., and Boatwright, J., 1987b, Teleseismic analysis of the Nahanni earthquakes in Northwest Territories, Canada, submitted to *Bulletin of the Seismological Society of America*, v. 77.

Boatwright, J. and G.L. Choy, 1978, Acceleration source spectra for large earthquakes in North Eastern North America, abs. submitted to EOS, v. 97.

Figure Caption. Acceleration spectral levels plotted against seismic moment for intraplate and subduction zone earthquakes.

10/87

ACCELERATION SPECTRAL LEVEL vs SEISMIC MOMENT

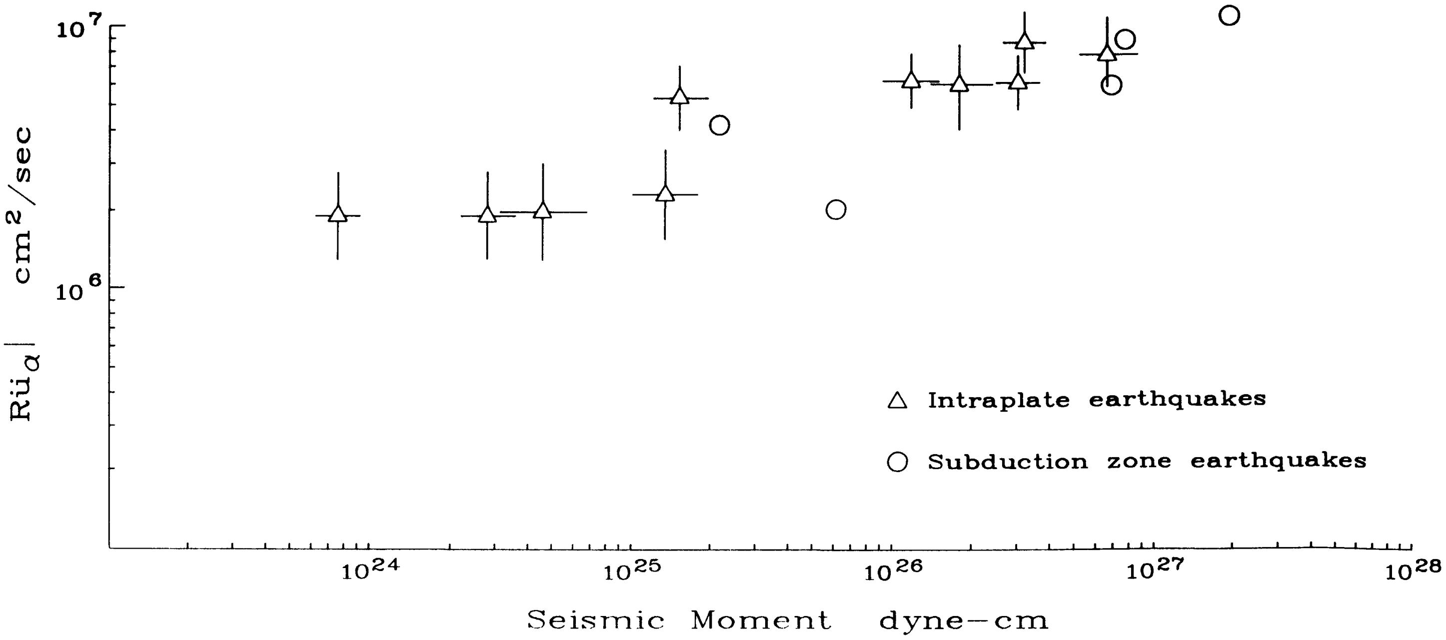

Intensive Studies of Source Zone and Crustal Structure of the Arkansas Swarm Region using a 40-station Three-Component, Telemetry, Portable, Digital Array

Contract Number : 14-08-0001-G1327

Jer-Ming Chiu, Jose Pujol, and Arch Johnston

Memphis State University
Center for Earthquake Research and Information
Memphis, TN 38152
Tel: 901-454-2007

The PANDA (Portable Array for Numerical Data Acquisition) array has been deployed and is fully operational in the Arkansas earthquake swarm region (Figure 1) from early January to late April, 1987. Totally, 12 swarm earthquakes and 4 blasts are recorded by the array during the experiment period. Although seismicity during the experiment period was very low, the high resolution three-component digital data recorded by PANDA (40 stations) provide us the best data bank for studies of the Arkansas swarm region. On-going research topics and preliminary results are outlined in the following.

(1). 3-Dimensional Velocity Inversion Studies

An iterative joint inversion method (Roecker, 1982) which uses local P and S travel times have been used to simultaneously compute three-dimensional velocity structure and relocate hypocenters. The method of parameter separation is employed to enable the inversion tractable with the large joint hypocenter data set (Pavlis and Booker, 1980). An approximate ray tracing technique (Thurber and Ellsworth, 1980) provides fast and reasonable estimates of both path geometry and travel times within the block structure. Synthetic data sets are first constructed to test the convergence of velocity inversion technique with a given velocity model and hypocenters. Test results show that inversion solutions can be unique (or converge very well) at ±20% of velocity perturbation.

Results of P and S wave inversion are presented in three layers as shown in Figure 2. Both P and S velocity inversion indicate that a fault may exist near the northern edge of the swarm striking east-west which is spatially consistent with a normal fault in the area identified from industrial seismic profiles. A high velocity region with about +15% velocity anomaly is found at shallow depth from surface to about 1.22 km and a low velocity region with about -13% velocity anomaly is found at deeper depth from 1.22 km to 6.23 km. This observation of high velocity zone above a low velocity region is similar to the observations in other geothermal areas and suggest that the origin of Arkansas swarm may be associated with the geothermal activities in the immediate region. In addition, Vp/Vs ratio in the swarm hypocentral region show dramatic changes from about 1.78 near surface to 1.53 at deeper depth of about 6.23 km which may indicate a highly fractured region in the swarm region and also supports the observation of low velocity zone in depth.

(2). Study of Three Secondary Arrivals between the P and S Arrivals.

An outstanding feature of the digital seismograms collected in the Arkansas swarm region is the abundant of secondary arrivals (at least three) between the P and S as shown in Figure 3. Detailed study of these secondary arrivals will provide three-dimensional image of the major discontinuities where conversion or reflection took place. Method of particle motions analysis, polarization filter analysis, and ray tracing technique will be used to study these arrivals. This study is in progress.

(3). Study of Digital Seismograms from Four Blasts

During the field work period in the Arkansas swarm region, four blasts associated with the dismantling of Titan Missile Site were successfully recorded. Characteristic features of these seismograms include (1) large amplitude surface waves after the P waves which show very large moveout in time as the station distance from the source increases, and (2) air-coupling surface and body waves. Analyses of apparent velocity, particle motion, polarization direction, travel time moveout, and theoretical modeling of these seismograms are in progress.

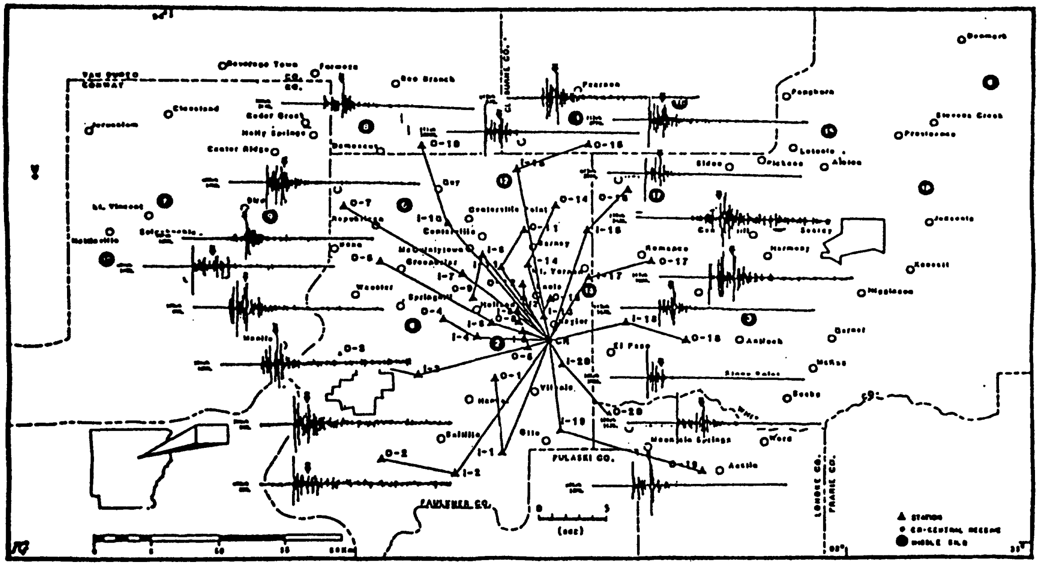

Figure 1. The PANDA array and some displays of the vertical component seismograms from an earthquake occurred in February 7, 1987. Epicenter is marked by the solid star. Radio links from outer stations ("0") to inner stations ("I") and to central recording site ("CR") are drawn. Seismograms are displayed roughly in correspondent to the azimuth of the stations from the epicenter. The S arrival time is picked up from the two horizontal components and is marked by the arrow above each trace. Complicated waveforms between the P and S arrivals are apparent in all the seismograms shown here.

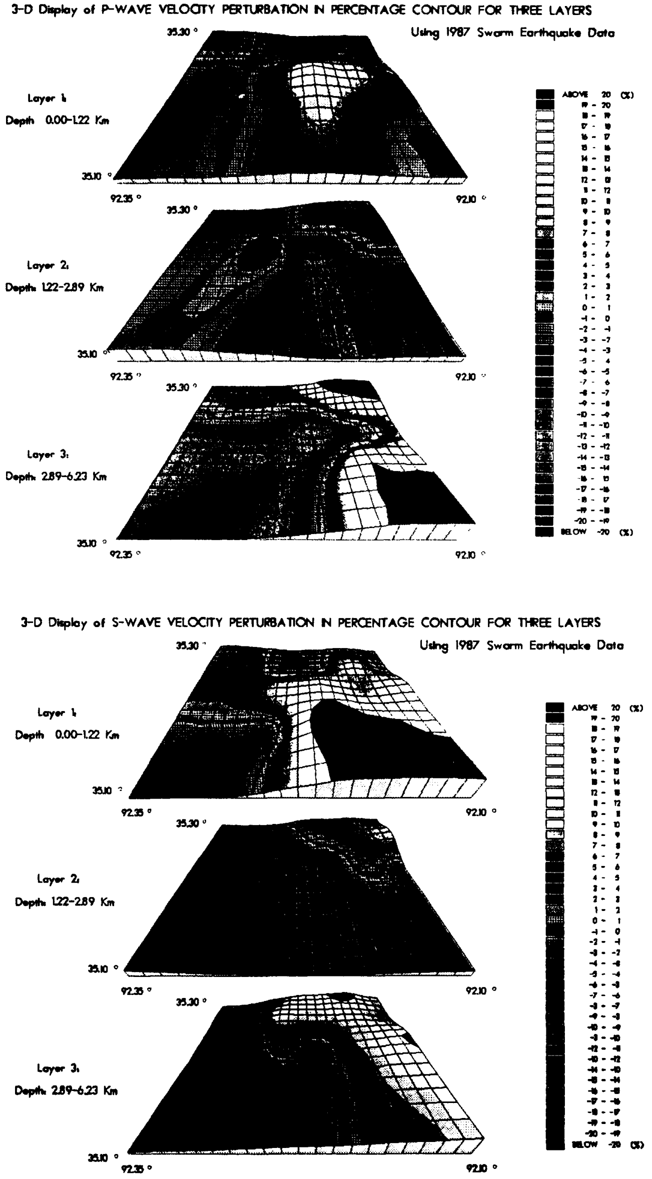

3-D Display of P-WAVE VELOCITY PERTURBATION IN PERCENTAGE CONTOUR FOR THREE LAYERS

Using 1987 Swarm Earthquake Data

3-D Display of S-WAVE VELOCITY PERTURBATION IN PERCENTAGE CONTOUR FOR THREE LAYERS

Using 1987 Swarm Earthquake Data

Figure 2. The three-dimensional shaded contour map shows the percentage perturbation of P (above) and S (below) for the upper three layers. The hight correlates to the percentage perturbation, i.e. -20% to the minimum height and +20% to the maximum height.

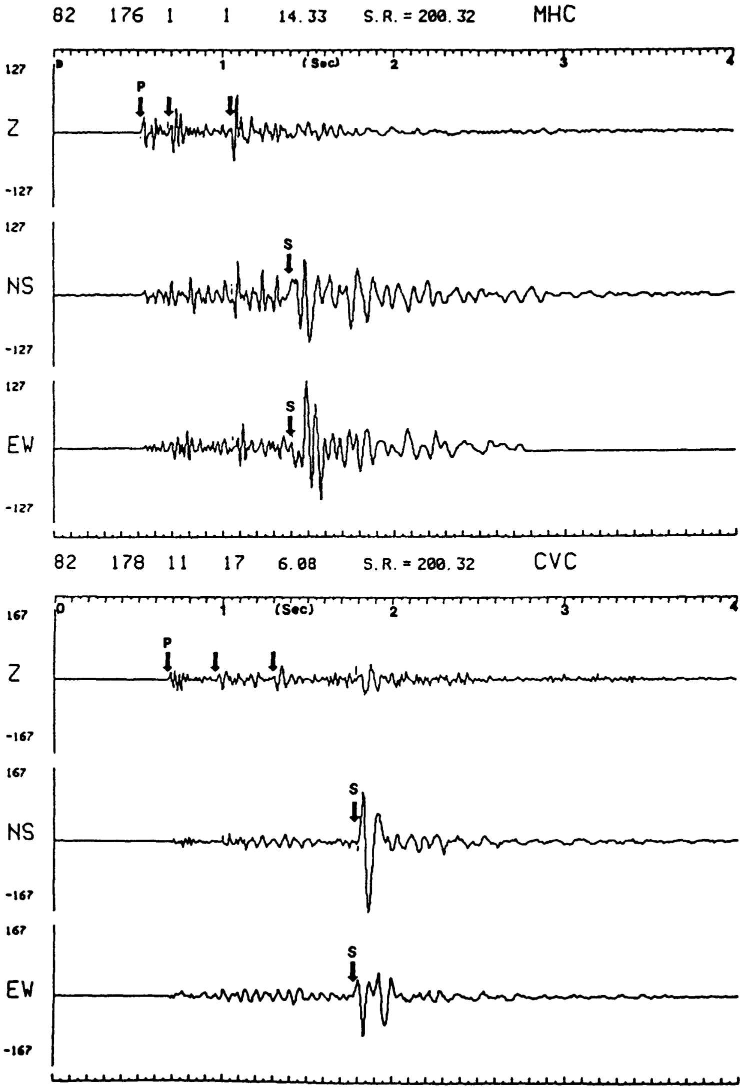

Figure 3. Examples of three-component digital seismograms recorded at stations MHC and CVC in 1982 experiment. The P and S arrivals are marked by arrows. Two strong secondary arrivals between the direct P and S can be seen clearly on the vertical component seismograms. The numbers from upper left to right are the year, day, hour, minute, and seconds of the first digitized point on the seismograms. Sampling rate is 200.32 points/sec. All seismograms are scaled to their maximum amplitude (in digital counts) as shown on the left above and beneath the component code (Z, NS, EW).

Comparative Earthquake and Tsunami Potential for Zones in the Circum-Pacific Region

9600-98700

George L. Choy
Stuart P. Nishenko
William Spence
Branch of Global Seismology and Geomagnetism
U.S. Geological Survey
Denver Federal Center
Box 25046, Mail Stop 967
Denver, Colorado 80225
(303) 236-1506

Investigations

1. Prepare detailed maps and text of comparative earthquake potential for west coasts of Mexico, Central America and South America.

2. Develop a working model for the interaction between forces that drive plate motions and the occurrence of great subduction zone earthquakes.

3. Develop methods for the rapid estimation of the source properties of significant earthquakes.

4. Conduct investigations of the historic repeat-time data for great earthquakes in the northern Pacific Ocean margin.

5. Compile tsunami data for the circum-Pacific and the corresponding seismic source zones.

Results

1. The probabilistic work for northern Mexico has been completed and published in three papers by Nishenko and Singh in 1987. Two regions have the highest probabilities for the recurrence of large earthquakes within the next two decades: the central Oaxaca gap and the Acapulco-Marco gap. With the occurrence of the catastrophic earthquake of September 19, 1985, the Michoacan seismic gap now has a very low probability for recurrence of a great earthquake within 20 years. However, plate motions related to this earthquake could cause stress to transfer to the seismic gap at Acapulco and trigger a great earthquake there within the next few years. A study of aftershocks of the great 1979 Colombia earthquake has been accepted for publication (Mendoza, 1987). The study of this event in the context of the great 1906 and 1958 earthquakes will help the probabilistic assessment for the recurrence of great earthquakes in this region. The probablistic work for the west coast of Chile has already been done. Choy and Dewey (1987) have studied earthquake characteristics and seismotectonics using the extended earthquake sequence associated with the great thrust earthquake of March 1985 near Valparaiso. The study of this earthquake sequence is particularly important because Nishenko has concluded that the moment

released since the turn of the century in this area is only about one-third of the moment of the great 1906 earthquake. The southern third of the Valparaiso zone is still at high risk.

2. An evaluation of the ridge-push and slab-pull forces in the context of stresses that lead to great subduction zone earthquakes has been completed (Spence, 1987). An important conclusion is that specific parts of a subducting plate may be monitored for precursors to seismic gap-filling earthquakes.

3. We have been integrating techniques of analyzing broadband data in the data flow of the NEIC. Broadband data are now used routinely to increase the accuracy of some reported parameters such as depth. We have implemented a semi-automated package to compute radiated energy from digitally recorded broadband data for all earthquakes with $m_b > 5.8$. The algorithm used is a great improvement over past approximate methods.

4. Data on the occurrence of great earthquakes and tsunamis from the Queen Charlotte Islands to the Aleutian Islands have been collected and the evaluation of probabilistic recurrence is being conducted by Drs. Nishenko and Jacob.

5. Several tsunami catalogs have been gathered prior to compilation of a comprehensive tsunami catalog. Dr. Nishenko has designed a form for systematically gathering and analyzing tsunami data. Currently, there is no uniform approach to this data acquisition.

Reports

Choy, G. L., and Dewey, J. W., 1987, Rupture process of an extended earthquake sequence: Teleseismic analysis of the Chilean earthquake sequence of 3 March 1985: Journal of Geophysical Research, (submitted).

Choy, G. L., and Engdahl, E. R., 1987, Analysis of broadband seismograms from selected IASPEI events: Physics of the Earth and Planetary Interiors, v. 47, p. 80-92.

Langer, C. J., and Spence, W., Deformation of the Nazca Plate related to the gap-filling earthquake series of October-November 1974: Journal of Geophysical Research (submitted).

Mendoza, C., 1987, Source mechanisms of Colombia aftershocks using digital surface-wave data: Bulletin of the Seismological Society of America, v. 76, p. 1597-1613.

Nishenko, S. P., 1987, A questionnaire for rapid tsunami damage assessment, in Bernard, E., ed., Proceedings 1987 Tsunami Symposium, Vancouver, B.C.: Pacific Marine Environmental Lab, NOAA.

Nishenko, S. P., 1987, Paleoseismology and earthquake hazards forecasting--A consumer's perspective, in Crone, T., ed., Proceedings of symposium on paleoseismology: U.S. Geological Survey Open-File Report.

Nishenko, S. P., and Buland, R. P., 1987, A generic recurrence interval distribution for earthquake forecasting: Bulletin of the Seismological Society of America, v. 77, p. 1382-1399.

Nishenko, S. P., and Singh, S. K., 1987, Relocation of the great Mexican earthquake of 17 January 1903: Bulletin of the Seismological Society of America, v. 77, p. 256-259.

Nishenko, S. P., and Singh, S. K., 1987, The Acapulco-Ometepec, Mexico earthquakes of 1907-1982--Evidence for a variable recurrence history: Bulletin of the Seismological Society of America, v. 77, p. 1359-1367.

Nishenko, Stuart P., and Singh, S. K., Conditional probabilities for the recurrence of large and great interplate earthquakes along the Mexican subduction zone: Bulletin of the Seismological Society of America (submitted).

Spence, William, 1987, Slab pull and the seismotectonics of subducting lithosphere: Reviews of Geophysics, v. 25, p. 55-69.

Investigation of Seismic-Wave Propagation for Determination of Crustal Structure

9950-01896

Samuel T. Harding
Branch of Geologic Risk Assessment
U.S. Geological Survey
Box 25046, MS 966, Denver Federal Center
Denver, Colorado 80225
(303) 236-1572

Investigations

1. Collection and processing of multichannel marine seismic-reflection data in Puget Sound, Wash., and in the Strait of Juan de Fuca.

   During the month of May 1987, 461 km of multichannel seismic-reflection data were obtained in Puget Sound and in the Strait of Juan de Fuca. The track lines for this data set are shown in figure 1. The data were shot with a 15 in^3 water gun, 24 channel and samples at 1ms. The shot spacing for most of the lines was every 6 m--some at 3-m spacing.

Results

1. About one third of the data is in various stages of processing. Several abrupt steps in the water-bottom interface have been identified. Profile segments containing these conspicuous steps are targeted for detailed analysis because they mark sites of geologically young (possibly Holocene) sea-bottom faulting. One is a west-facing, 115-m-high feature directly west of Alki Point, Seattle, Wash. (location shown in fig. 1; seismic-reflection profile shown in fig. 2). Unfortunately, the strike and extent of the feature are not known. Preliminary interpretation of sub-bottom reflections along the east-west profile west of Alki Point indicates the step is at a surface projection of 50° and is an east-dipping reverse fault. A second step is west-facing, is a 74-m-high feature that is 37 km west of Seattle in Hood Canal. This feature lies above a steep-reflection discontinuity and coincides with the trace of a fault reported by Gower and others (1985) along Hood Canal.

References

None.

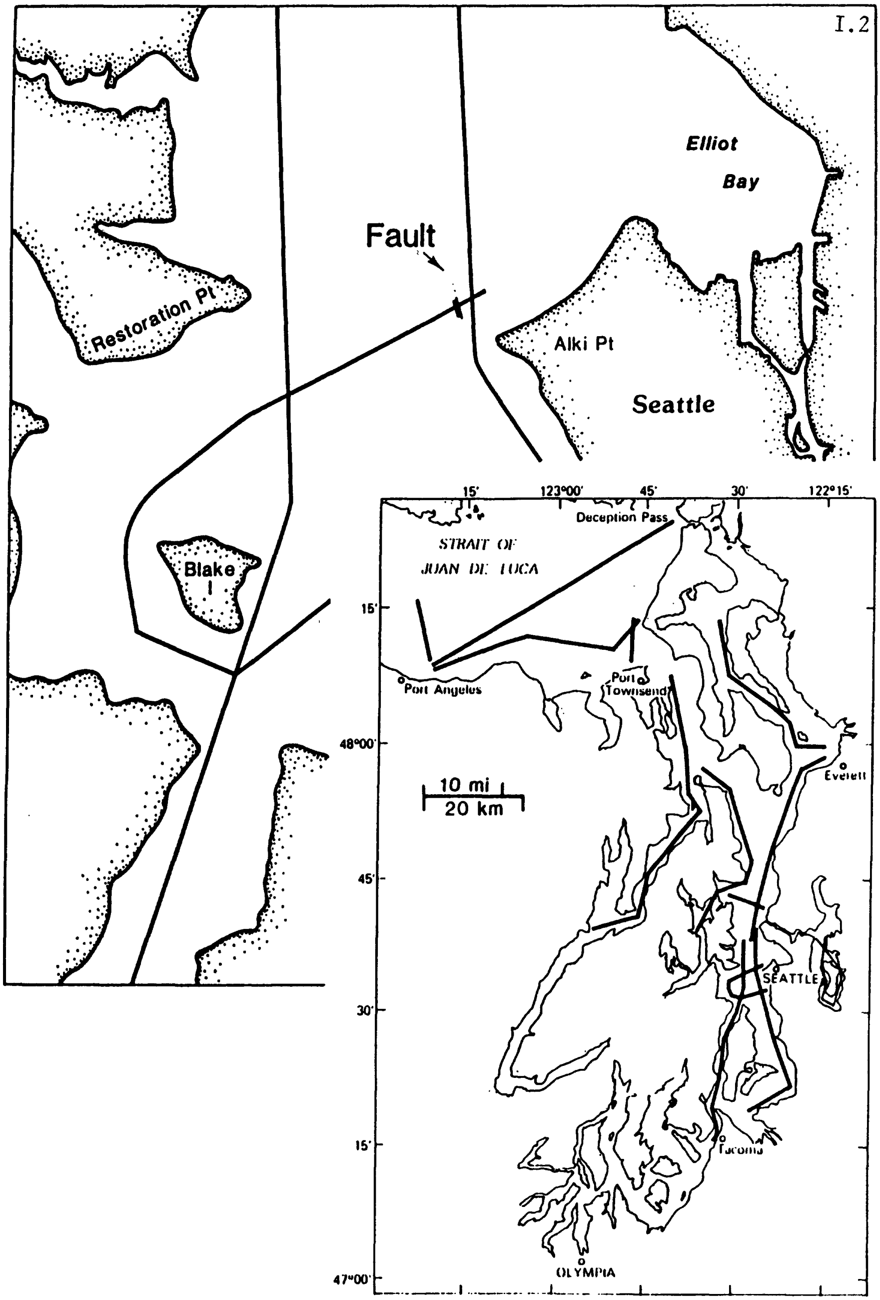

FIGURE 1.--Map showing location of 461 km of multichannel seismic-reflection lines surveyed on Puget Sound, Washington. Magnified area of Seattle shows location of possible fault.

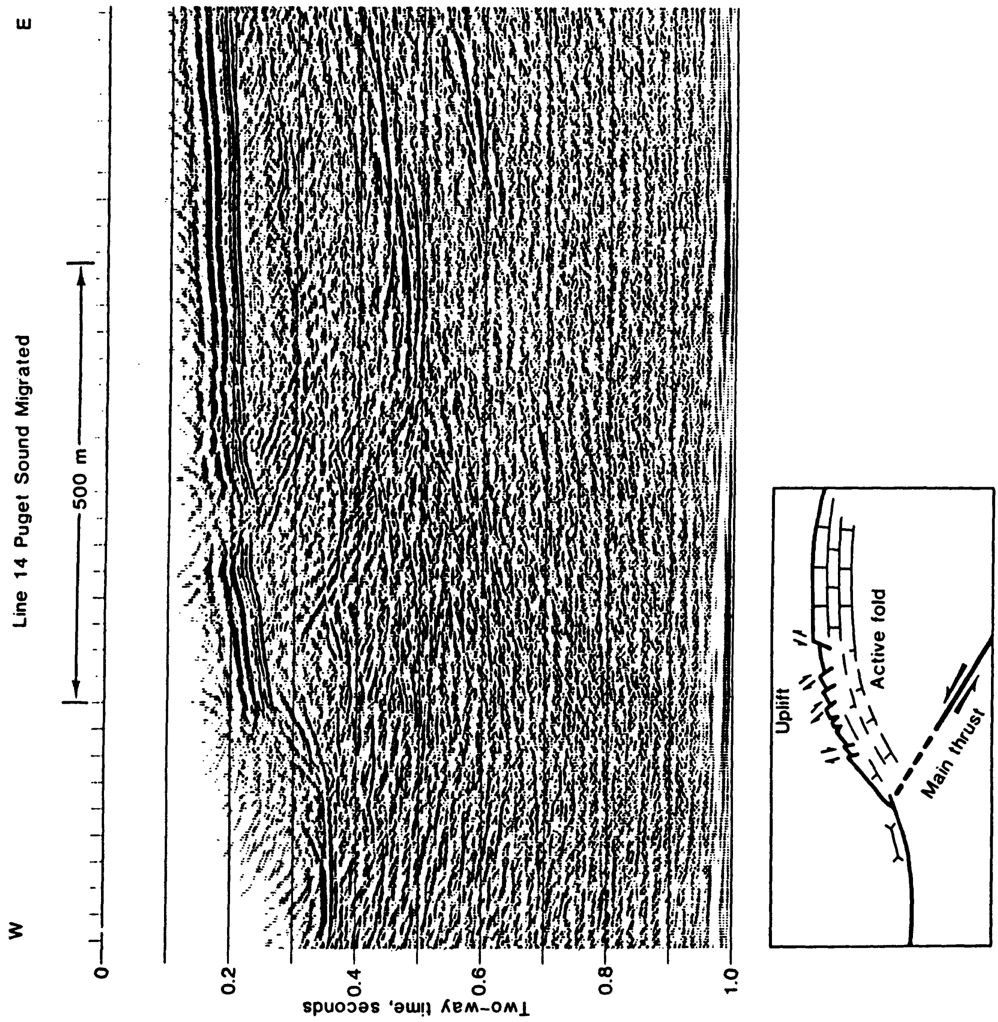

FIGURE 2.--Interpreted migrated section of line near the scarp at Alki Point, Seattle, Washington.

Analysis of Earthquake Data from the Greater Los Angeles Basin and Adjacent Offshore Area, Southern California

#14-08-0001-G1328

Egill Hauksson
Ta-liang Teng
Center for Earth Sciences
University of Southern California
Los Angeles, CA 90089-0741
(213) 743-7007

INVESTIGATIONS

Analyze earthquake data recorded by the USC and CIT/USGS networks during the last 12 years in the Los Angeles basin to improve earthquake locations including depth and to determine the detailed patterns of faulting in the study region.

RESULTS

The Oceanside 1986 earthquake sequence.

A mainshock of M_L=5.3 occurred 55 km offshore at 32° 58.1'N and 117° 52.2'W, southwest of Oceanside in San Diego County on July 13th, 13h 47m (UT). The mainshock was followed by an extensive aftershock sequence, with 55 events of M_L>3.0 during July 1986. The preliminary epicenters of the mainshock and aftershocks are located at the northern end of the San Diego Trough - Bahia Soledad fault zone (SDT-BS) (Figure 1). The north-northwest striking SDT-BS is one of three strike-slip fault systems that constitute the Agua Blanca fault system. The spatial distribution of aftershock epicenters indicates a unilateral 5-10 km long rupture to the east away from the epicenter of the mainshock. The focal mechanism of the mainshock also has a steeply dipping east-striking plane with mostly left-lateral strike slip movement. Focal mechanisms of the larger aftershocks (M_L>3.0) however, show a mixture of strike-slip and reverse faulting on west to northwest striking planes. Hence this sequence may have occurred on a small fault that provides for a left step in the San Diego Trough fault as it curves toward the west around the Santa Cruz - Catalina escarpment.

The 1987 Whittier Narrows earthquake sequence.

The moderate-sized (M_L=5.9, revised magnitude) Whittier Narrows main shock that occurred in the east Los Angeles metropolitan area at 7:42 (PDT) on October 1, 1987 caused fatalities and substantial damage in many communities in Los Angeles and Orange Counties. The main shock (34° 3.0'N, 118° 4.8'W) is located 3 km (2 mi) north of the Whittier Narrows Dam, at the northwestern end of the Puente Hills, at a depth of approximately 14±1 km (9 mi). The aftershocks are located on an approximately circular surface that dips gently to the north, centered at the epicenter of the main shock, with a radius of 4 to 5 km (3 mi) (Figure 2). The focal mechanism of the main shock, derived from first motion polarities recorded at local seismograph stations, shows that the motion during the main shock was vertical slip ("thrust faulting") on a fault striking east-west and dipping 25° to the north. Hence, the spatial distribution of the main shock and aftershocks as well as the focal mechanism of the main shock indicate that the causative fault is a gently dipping thrust fault with an east-west strike, located at depths from 11 to 16 km. Because the Whittier fault is a northwest-striking, steeply dipping fault, these seismologic data imply that the Whittier Narrows earthquake did not occur on the Whittier fault. Instead, it appears that the earthquake originated on a thrust fault buried beneath the sediments of the San Gabriel Valley.

The largest aftershock (M_L=5.3, revised magnitude), which occurred at 3:59 (PDT) October 4, 1987 is located 2.5 km (1.6 mi) to the northwest of the epicenter of the main shock. Unlike the main shock, the largest aftershock occurred from horizontal motion ("strike-slip faulting") on a steeply dipping, north-northwest striking fault. The largest aftershock originated at a depth of 12±1 km (8 mi) within the hanging wall, 2-3 km (1.2-1.8 mi) above the rupture surface of the main shock. The north-northwest striking vertical fault defined by the largest aftershock forms the western edge of the aftershock distribution of the main shock and may have terminated the main shock rupture.

The main shock occurred on a previously unrecognized thrust fault with no obvious surface expression. If this fault were to extend farther to the west, it could pose a serious earthquake risk to the city of Los Angeles. The seismologic data available at present cannot resolve the spatial extent of this fault. The occurrence of small earthquakes (M_L<3.5) in the northwestern Los Angeles basin with focal mechanisms showing thrust faulting are consistent with thrust faults under Los Angeles, but are not definitive proof of the existence of such a fault. If such a fault exists, further research will be needed to estimate the largest earthquake that could realistically occur on it.

PUBLICATIONS AND REPORTS

Hauksson, E., Seismotectonics of the Newport-Inglewood Fault Zone in the Los Angeles Basin, Southern California, Bull. Seism. Soc. Amer. 77, 539-561, 1987.

Hauksson, E., T. L. Teng and T. L. Henyey, Near-Surface Attenuation of Waveforms of Local Earthquakes: Results from a 1500 m Deep Downhole Seismometer Array, to appear in Bull. Seism. Soc. Amer., December, 1987.

Saldivar, G. V., E. Hauksson and T. L. Teng, Seismotectonics of the Santa Monica and Palos Verdes Fault Systems in the Santa Monica Bay, Southern California, to be submitted to BSSA, 1987.

Hauksson, E., Seismotectonics of the Newport-Inglewood Fault Zone and the 1933 Long Beach Earthquake ($M_L = 6.3$) in the Los Angeles Basin, Southern California, presented at S.S.A. Meeting Santa Barbara, March, 1987.

Hauksson, E., and L. M. Jones, The July 1986 Oceanside Earthquake Sequence (M_L=5.3) in the Continental Borderland, Southern California, to be presented at AGU 1987 Fall Meeting.

Jones, L. M. and E. Hauksson, The Size and Location of the Next Great Southern California Earthquake: Implication of Constant Stress Drops, to be presented at AGU 1987 Fall Meeting.

Hutton, K. L., L. M. Jones, E. Hauksson and D. G. Given, Seismotectonics of Southern California, submitted to Decade of North American Geology Neotectonics of North America, Geol. Soc. Amer. Ser.

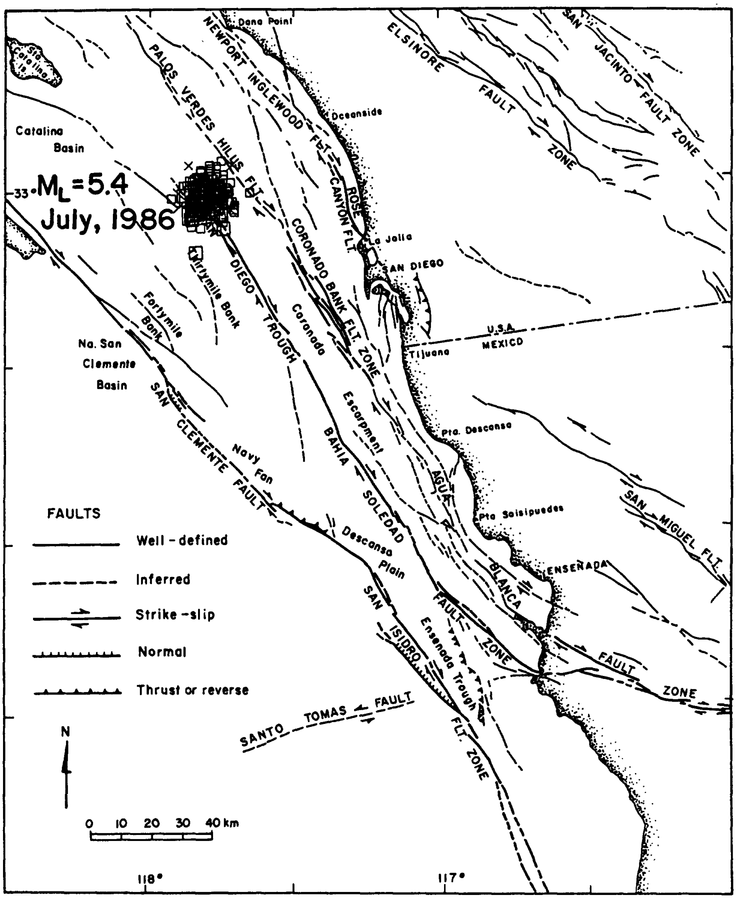

Figure 1 Offshore faults from Legg (1985) and the Oceanside mainshock aftershock sequence of July, 1986.

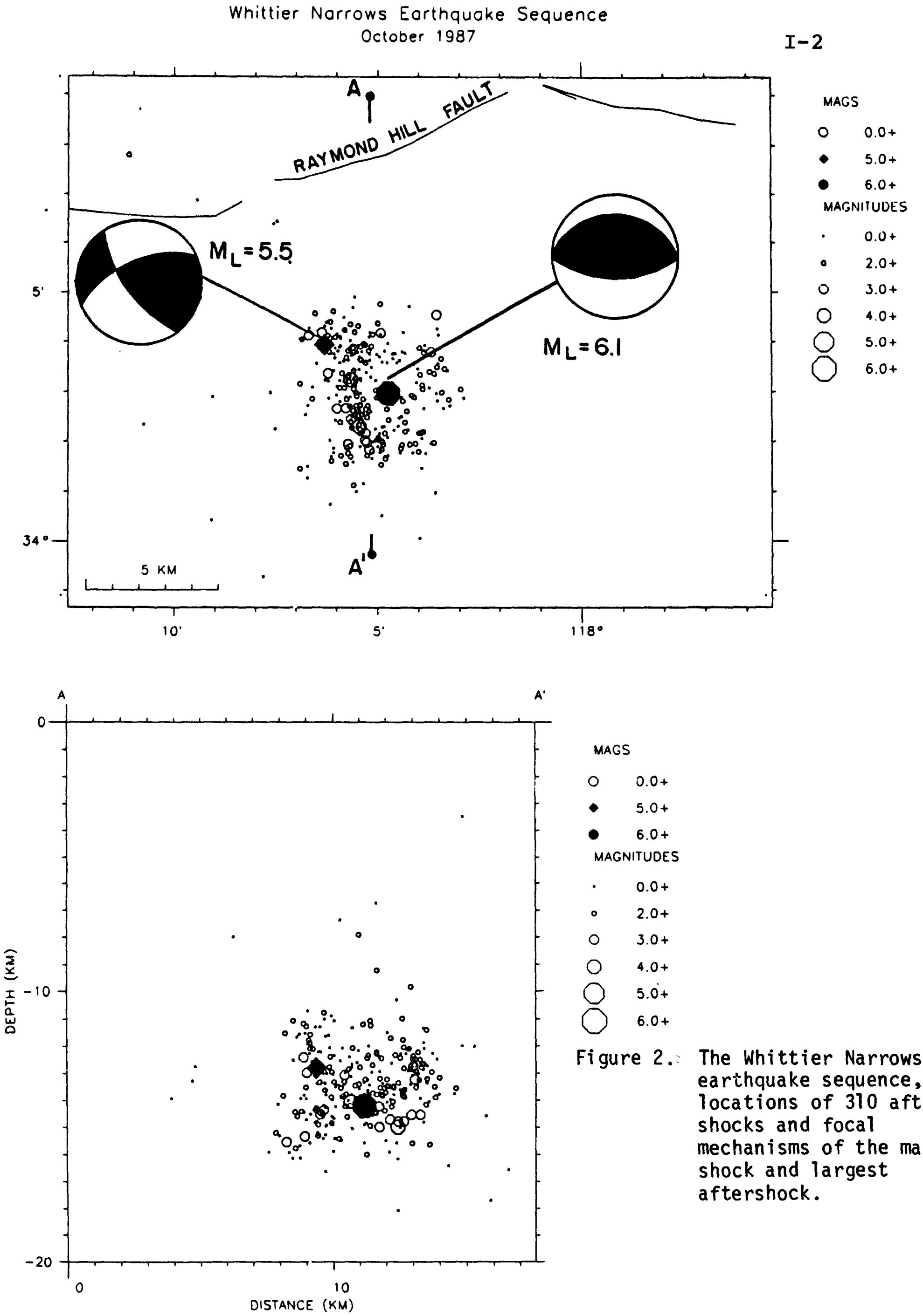

Figure 2. The Whittier Narrows earthquake sequence, locations of 310 aftershocks and focal mechanisms of the main shock and largest aftershock.

Seismic Source Characteristics of Western States Earthquakes

Contract No. 14-08-0001-21912

Donald V. Helmberger

Seismological Laboratory
California Institute of Technology
Pasadena, California 91125
(818) 356-6998

Investigation: This study addresses the characteristics of pre and post 1962 Western U.S. earthquakes. The four major tasks are:

1. Extended analysis of low-gain recordings of earthquakes occurring in the Imperial Valley and Northern Baja; to fix the depths of main energy release (asperity concentration).

2. Analysis of body waves at all ranges using direct inversion for fixed earth models, application of the intercorrelation method to measure differences between events and develop master events per region.

3. Analysis of historic events (pre-1962) using the same methods (masters) but on a more regional basis.

4. Reassessment of events with sparsely recorded strong motions using more accurate Green's functions computed from laterally varying earth models.

Results: Most of the more important post 1962 events have been studied with respect to the WWSS network including the 1 October 1987 Whittier Narrows event, with publications by Bent and Helmberger to follow shortly. These events, as recorded on the local assorted instruments, have proven the most difficult to understand. But, since only these type of records exist for many pre 1962 events, we are forced to address their meaning.

Figure 1 displays some theoretical Green's function appropriate for a profile along a path from Imperial Valley to Pasadena assuming a source depth of 7km. Corresponding synthetics for the three main types of observations available at PAS are displayed in Figure 2 assuming the strike-slip orientation. Long period records (30, 90) are generally on scale for events less than $M_L = 5$ at distances greater about 200 kms. These responses are relatively easy to model and have been discussed in previous reports, see Ho and Helmberger (1987). The long-period torsions operated at various times from 1940 through 1960. Their response appears to be nearly ideal for studying regional phases, as pointed out by Thatcher and Hanks (1973). The short period torsions (Wood-Anderson) has been in operation for the past 50 years with a low gain version (100x) operating at PAS for much of this time. Examples of observed data after rotation into SH (tangential component) is displayed in Figures 3 and 4. Events occurring along this particular profile at various depths and magnitudes can be explained quite nicely by our present set of Green's functions.

Recordings of small events on the long period torsions, aftershocks in particular, play a key role in deriving these responses, as in the empirical Green's function approach, see Figure 5. Because the magnitude of the events are generally quite different, it becomes nearly impossible to obtain the response from the same instrument of both large and small events. Thus, we routinely record the mainevent on the 100X sp.torsion while the aftershock is only visible on the 2800X sp.torsion or preferred lp.torsion. The most suitable mainevent-aftershock comparison is equalizing the differences in source duration by recording the aftershock on the lp.torsion, as displayed in Figure 5. In the upper comparison we used the 1954 Borrego aftershock since these instruments were, unfortunately, no longer in operation in 1969. The bottom two traces as well as the other component (no verticals exist for this instrument) are nearly identical indicating the complete trade-off of the instrumental response. The intermediate periods provided in the long period torsion records can be used to link the long period (30, 90) derived structures to modifications required to explain higher frequency propagation.

In conclusion, we have attempted to display the types of waveform data available at the Seismological Laboratory and have indicated how it might be used to more fully assess historic events. To date, we have concentrated our efforts almost exclusively on the tangential motions since they appear easier to understand. Clearly, all three components need to be analyzed to obtain the most complete information from the waveform data.

References:

Bent, A. L. and D. V. Helmberger, 1987, Some characteristics of earthquakes in the Big Bend Region of California, Seismol. Soc. of Am., Bull., **87**, Santa Barbara, in preparation.

Hartzell, S. T. and T. H. Heaton (1983), Inversion of strong ground motion and teleseismic waveform data for the fault rupture history of the 1979 Imperial Valley, California, earthquake, Seismol. Soc. Am., Bull., **73**, 1553-1583.

Helmberger, D. V. and J. Vidale, 1987, Modeling strong motions produced by earthquakes with 2-D numerical codes, submitted to Seismol. Soc. Am., Bull.

Ho-Liu, P. and D. V. Helmberger, 1987, Broad-band modeling of regional earthquakes; Imperial Valley to Pasadena, in preparation.

Ho-Liu, P. and D. V. Helmberger, 1987, Source retrieval from regional long period records, Seismol. Soc. Am., Bull., **87**, Santa Barbara.

Thatcher, W. and T. C. Hanks, 1973, Source parameters of southern California earthquakes, J. Geophys. Res., **78**, 8547-8576.

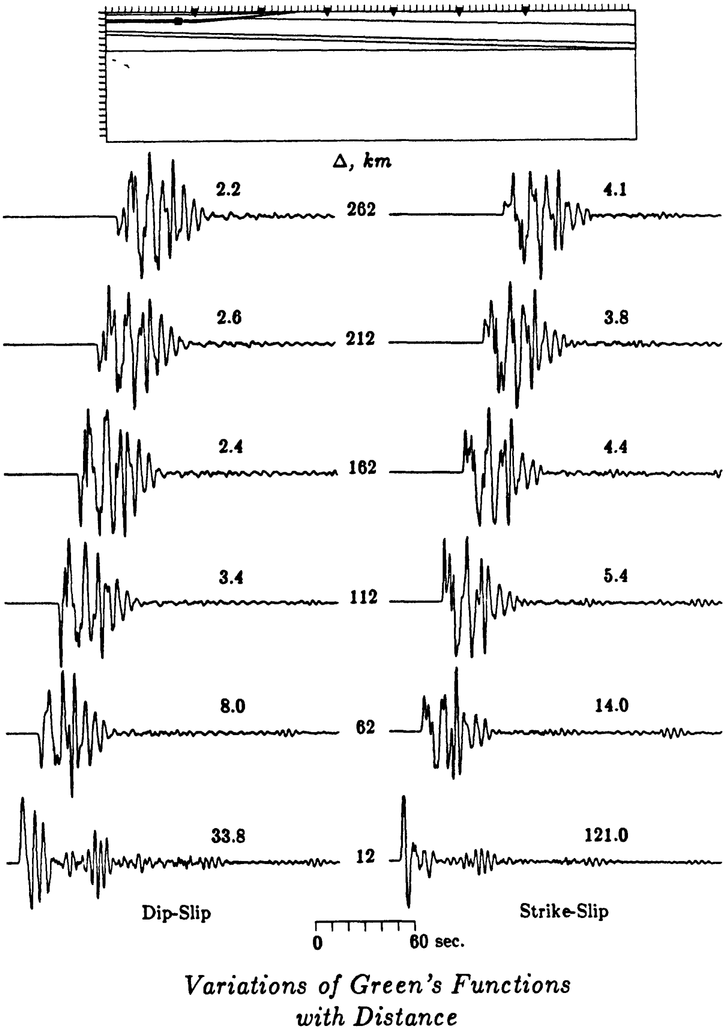

Figure 1. Delta-function responses (smoothed) or Green's functions for events at a depth of 7 km in Imperial Valley along a profile to Pasadena. Note the rapid development of surface waves in the first 50 kms and slow changes at larger distances, see references.

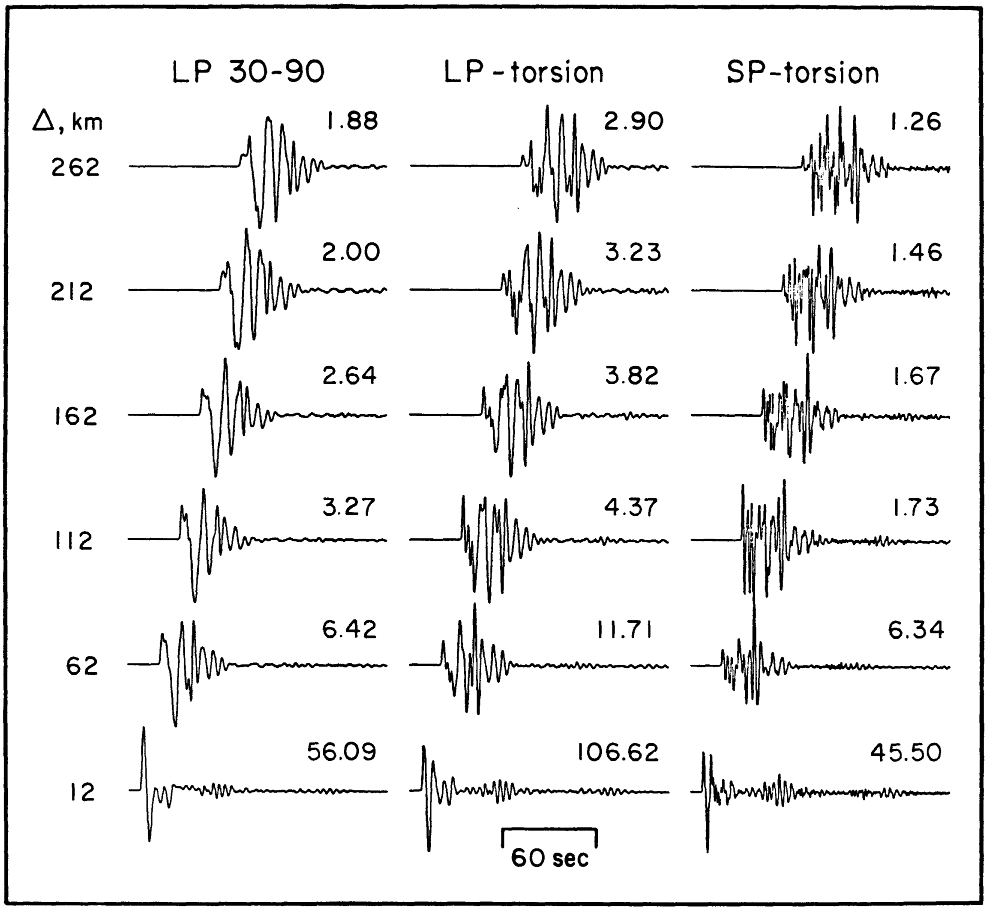

Figure 2. Synthetics appropriate for the strike-slip case displayed in Figure 1 and PAS instruments.

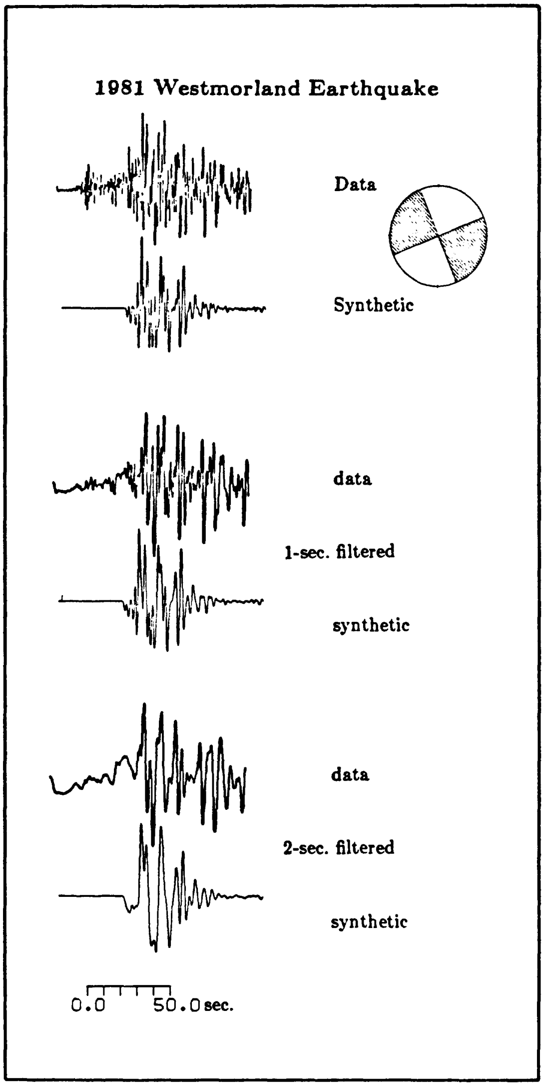

Figure 3. WA (100x) recording from the Westmoreland earthquake. Two sources were used in generating the synthetics, one with an m_o of 2.5 x 10^{24} dyne-cm at a depth of 7 km and the second one with an m_o of 4.5 x 10^{24} dyne-cm at a depth of 10.5 km, delayed by about 2.5 secs. This 2.5 sec. delay is also observed in local strong motion accelerograms.

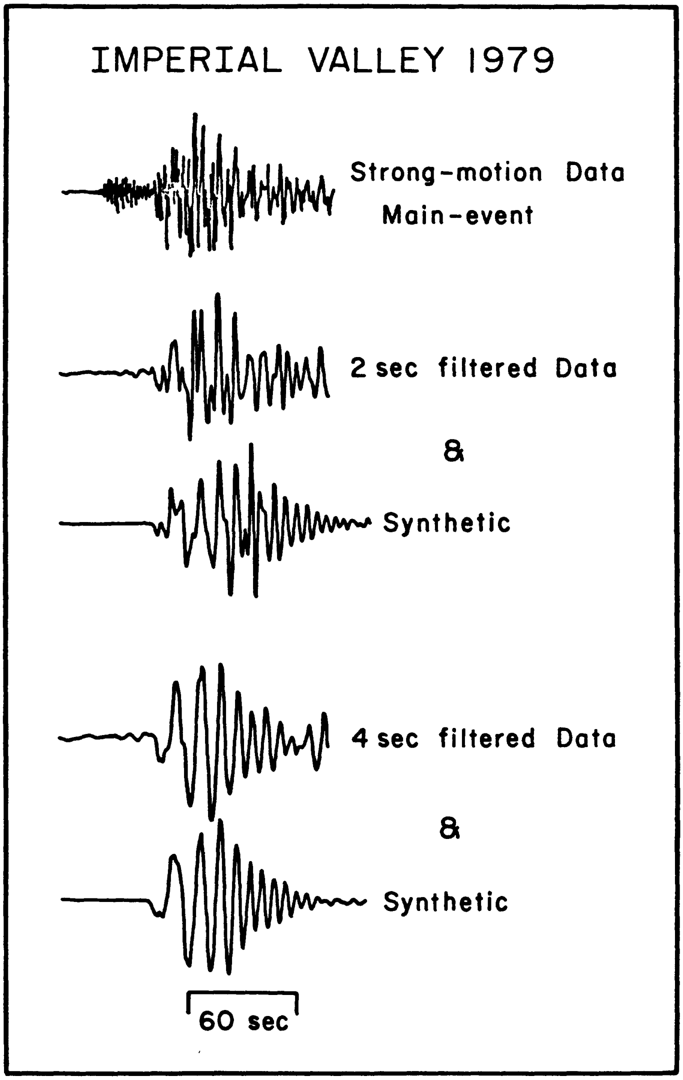

Figure 4. Unfiltered data on the 100x WA for the 1979 Imperial Valley earthquake as recorded in PAS along with filtered versions. Synthetics are appropriate for the distributed faulting parameters of Hartzell and Heaton (1983).

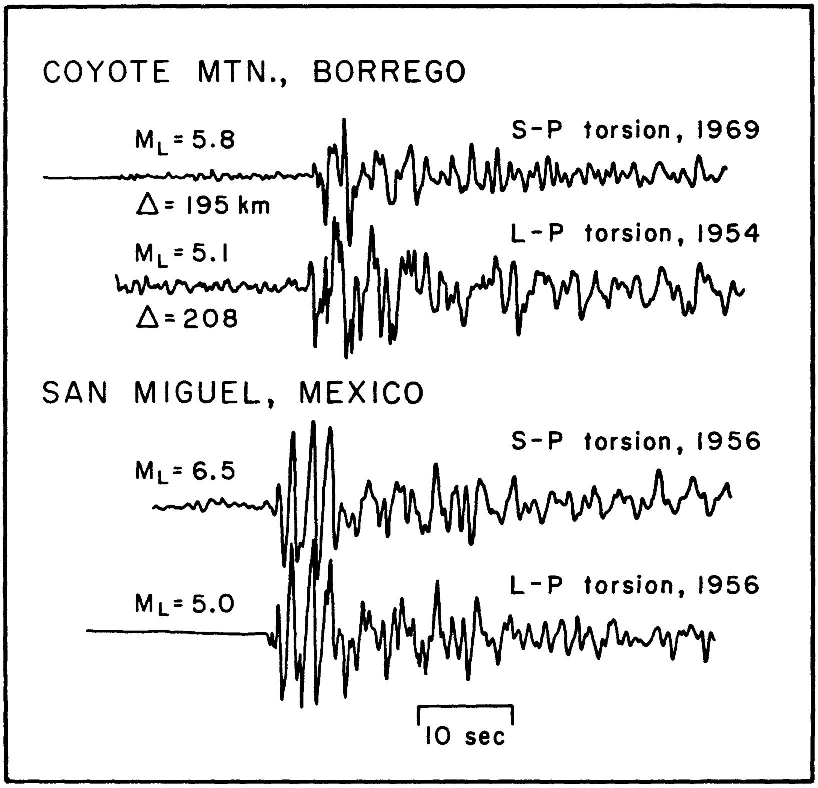

Figure 5. Comparison of mainshock-aftershock pair of earthquakes where the main events are recorded on a short-period 100x WA while the aftershocks were recorded on the long period torsion.

Earthquake Source Parameters Using Regional Seismic Network Data: Application to California and Eastern United States

14-08-0001-G1391

Robert B. Herrmann
Department of Earth and Atmospheric Sciences
Saint Louis University
P.O. Box 8099 Laclede Station
St. Louis, MO 63156
(314) 658-3131

Goals

1. Perform research on the earthquake process in the New Madrid Seismic Zone to delineate the active tectonic processes.

2. Perform more general research relating to the problems of the eastern U. S. earthquake process and of the nature of eastern U. S. earthquakes compared to western U. S. earthquakes.

Investigations

1. A magnitude 5.2 earthquake occurred in southeastern Illinois on 10 June 1987. A surface-wave focal mechanism was obtained. The surface-wave solution consistent with P-wave first motion data has nodal planes striking N40°E dipping 84°SE and striking N50°W and dipping 76°SW. The seismic moment and source depth are estimated to be 4.1 x 10^{23} dyne-cm and 11 km, respectively. The focal depth of the main event is compatible with aftershock locations. The focal mechanism is presented in the attached figure.

2. The Lg spectral analysis of eastern U.S. earthquakes has been completed and a paper submitted to the Bulletin, Seismological Society of America. The conclusions are that Lg data can be used to estimate the seismic moment and corner frequency of the source if Q corrections are applied. The results are compatible with short distance S-wave and teleseismic P-wave estimates for the region.

Papers Presented

Taylor, R. B. and Herrmann, R. B., Source parameters if the southern Illinois earthquake of 10 June 1987, presented Eastern Section SSA meeting, Fall 1987, St. Louis.

Taylor, K. B., Battlo, J., Herrmann, R. B., O'Sullivan, C., Johnston, A, and Langer, C., Aftershock monitoring of the southern Illinois earthquake of 10 June 1987, presented Eastern Section SSA meeting, Fall 1987, St. Louis.

Publications

O'Sullivan, C., R. B. Herrmann, C. Finn, M. Lydon and R. L Street (1988). Source parameter determination using the Lg wave with application to the eastern United States, *Bull Seism. Soc. Am.* **78**, (in review).

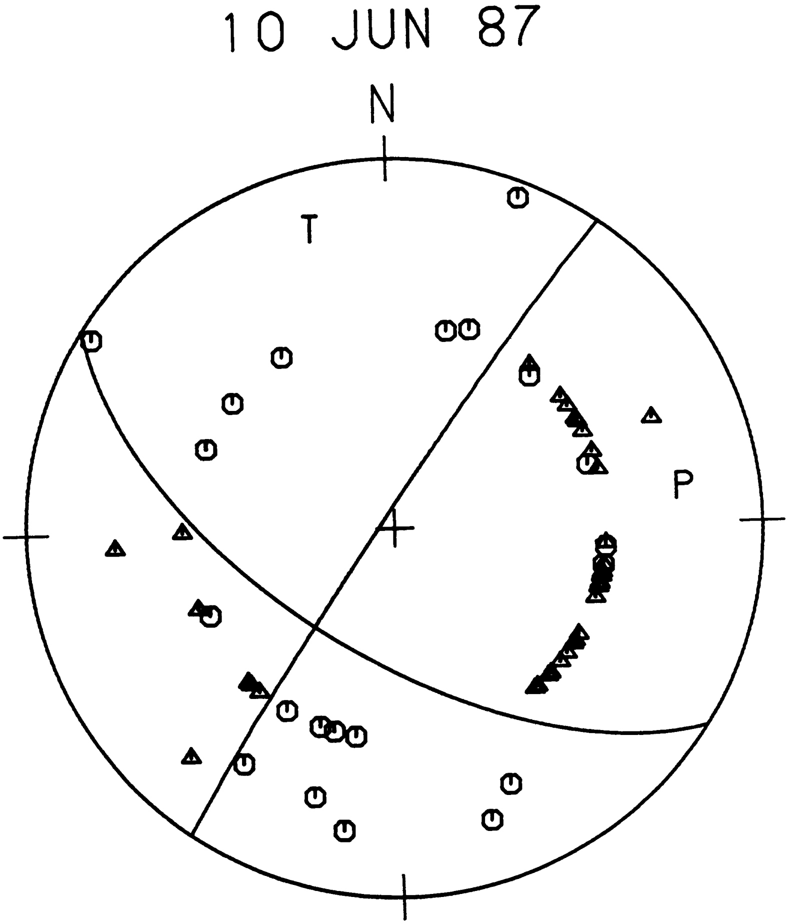
10 JUN 87
N
T
P

Tectonics of Central and Northern California

9910-01290

William P. Irwin
Branch of Engineering Seismology and Geology
U. S. Geological Survey
345 Middlewfield Road
Menlo Park, CA 94025
(415) 329-5908

Investigations

1. Preparation of a geologic map of the Klamath Mountains and adjacent areas in northwestern California and southwestern Oregon for purposes of tectonic analysis.

2. Study of distribution of radiolarian-bearing chert deposits in the California Coast Ranges as a possible means of determining regional tectonic dislocations.

3. Preparation and revision of manuscripts.

Results

1. Compilation of the geology of the various source maps of the Klamath Mountains has been completed (scale 1:500,000), although problems of correlation of some of the major units remain. A preliminary draft of the explanatory material also has been completed.

2. Samples of radiolarian chert have been collected from the main exposures of Franciscan rocks in the central and southern coast ranges for the purpose of extending and refining the known distribution of the Lower Jurassic chert. The Lower Jurassic chert, which is the oldest paleontologically dated rock of the Franciscan assemblage, has previously been paid scant attention, but its pattern of distribution may possibly provide important information relating to large tectonic dislocations of the Franciscan rocks on either side of the Salinian block. The study is in collaboration C. D. Blome and M. J. Rymer. Progress has been slowed this report period by a delay in processing of the chert samples.

3. Several manuscripts were in revision during this report period following Branch review. These include: a report on the geology and plate tectonics of the San Andreas fault, prepared as a chapter for a multi-authored bulletin on the San Andreas fault, R. E. Wallace, ed.; a summary report on the paleomagnetism of the Eastern Klamath terrane and its implications for the tectonic history of the region, in collaboration with E. A. Mankinen and C. S. Gromme; and a speculative paper, in collaboration with R.A. Schweickert, describing evidence for extensional tectonics in the southern

Klamath Mountains and the similarity of the Trinity ultramafic sheet to metamorphic core complexes. Two additional reports were completed and received Director's approval (see below).

Reports

Fraticelli, L. A., Albers, J. P., Irwin, W. P., and Blake, M. C., Jr., 1987, Geologic map of the Redding 1 X 2-degree quadrangle, Shasta, Tehama, Humboldt, and Trinity Counties, California: *U. S. Geological Survey Open-File Report 87-257*, map scale 1:250,000, with 15-page text.

Mankinen, E. A., Irwin, W. P., and Gromme, C. S., 1987, Paleomagnetic results from the Shasta Bally plutonic belt in the Klamath Mountains province, northern California: Submitted to *Geology*.

Seismicity Patterns and the Stress State in Subduction-Type Seismogenic Zones

Grant Number 14-08-0001-G1368

Carl Kisslinger
Cooperative Institute for Research in Environmental Sciences
Campus Box 449, University of Colorado
Boulder, Colorado 80309-0449
(303) 492-6089

Research during the six months, May - October, 1987, was focused on two main topics: 1) the temporal and spatial properties of the aftershocks of the May 7, 1986 Andreanof Islands earthquake and a comparison of the temporal behavior of this aftershock sequence and some others from earthquakes of similar magnitude (near M8) in other subduction zones; 2) analysis of seismograms from microearthquakes before and after the main shock in a search for evidence of changes in fault zone properties and earthquake characteristics produced by this major event.

Aftershock Studies

1. Aftershocks of the May 7, 1986 earthquake

The teleseismic catalogue of aftershocks, provided by the Monthly Listing, PDE, has been analyzed to determine the aftershock decay rate by fitting the sequence to the Modified Omori relation. For data through February, 1987, the p-value has been found to stabilize at about 0.93, for the lower magnitude cuts of both $m_b4.6$ and m_b5. No evidence of a relative quiescence within the sequence that could be interpreted as a precursor to any of the strong aftershocks has been found.

The catalogue of the aftershocks as recorded by the local Adak network is compiled at the $M_D \geqslant 2.3$ level only through May 13, 1986. (It has been necessary to jump ahead in the sequence in order to acquire the data for other studies, and the intervening interval is gradually being filled in.) For 449 events at this magnitude level, through six days, the p-value is 0.78. It is important to know if this slower rate of decay, compared to the teleseismic events, is real, or if the sequence down to small magnitudes will eventually approach a value similar to the moderate and strong aftershocks.

The spatial distribution of the aftershocks as determined from the local network data, lower part of Figure 1, and for the teleseismic events, relocated by E.R. Engdahl (not shown here), show a very strong concentration of aftershocks within the part of the seismic zone that exhibited the highest rate of microearthquake activity before September, 1982, the sharpest and prolonged quiescence before the May 7 earthquake (upper part of Figure 1), and the site of the strongest moment release during the earthquake. This observation demonstrates a clear physical relation between the quiescence and the subsequent rupture process and should be a useful constraint on future studies of the physical basis of quiescence.

2. Michoacan, Mexico and Santiago, Chile Earthquakes, 1985

Two other subduction-zone earthquakes with similar magnitudes to the May 7, 1986 event have been selected for study. The selection was based on results for moment release distributions by H. Kanamori that showed distinct differences in the properties of the three rupture zones. The Michoacan fault (19 September 1985) was marked by two separate and distinct asperities that

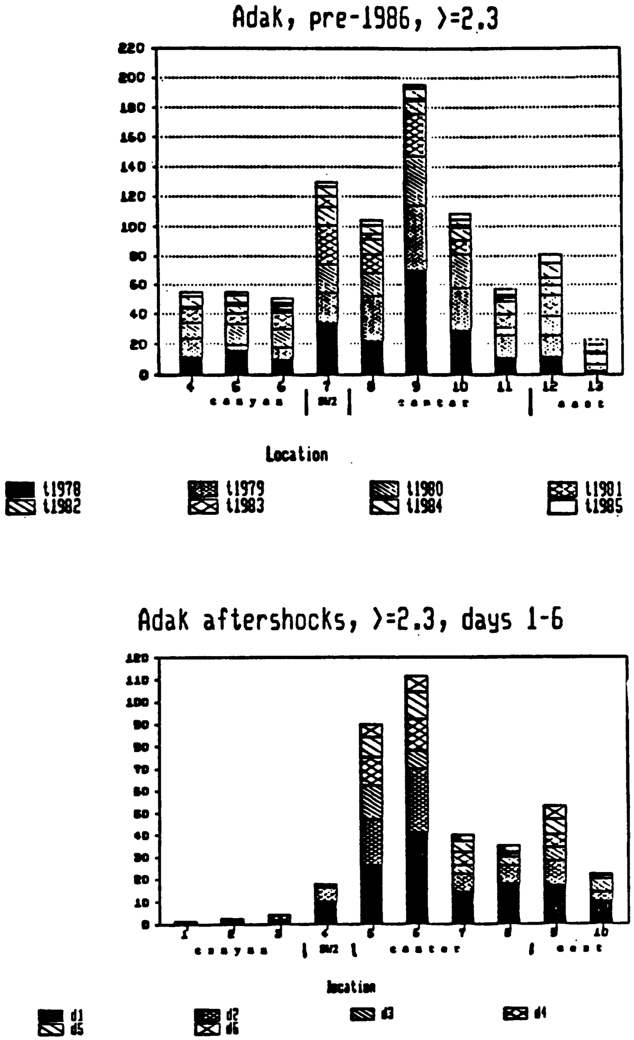

FIGURE 1

Seismicity distribution, local data, before and after the May 7, 1986 earthquake. Number of events in 20 km wide north-south strips across the main thrust zone.
Top: Activity by years, 1978-1985. The high rate prior to 1982 in SW2 and the Center subregions is seen, as well as the pronounced quiescence in Center after 1982.
Bottom: Aftershocks by days, for first six days. The concentration of in the places of greatest activity in the Center subregion prior to 1982 and most pronounced quiescence, as well as near the epicenter, East subregion, is seen.

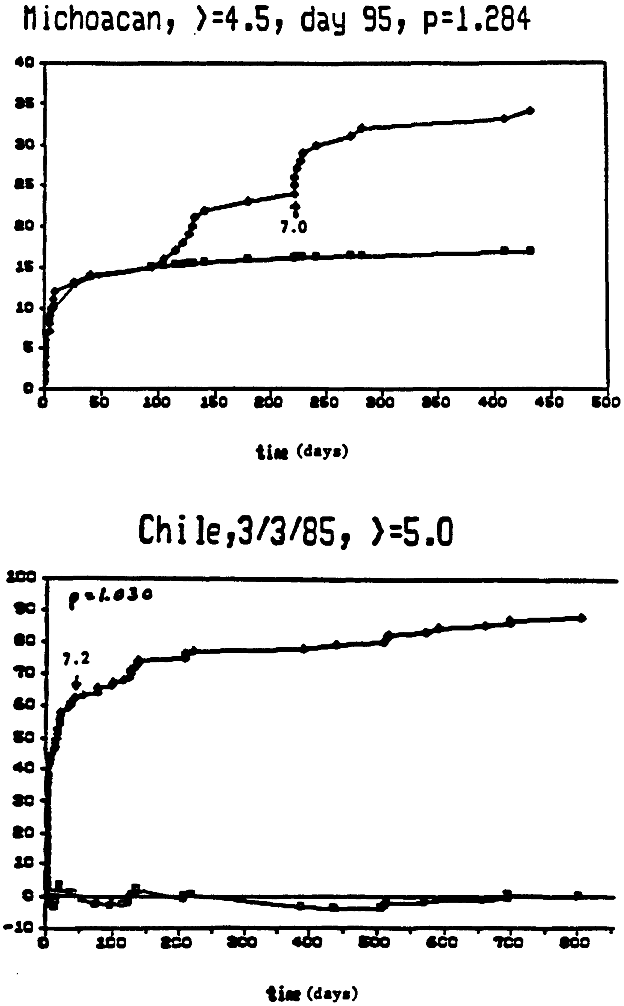

FIGURE 2

Aftershock sequences of major subduction-zone earthquakes, cumulative number vs. time.
Top: Michoacan, Mexico, September 19, 1985, $M_s 8.1$. The modified Omori fit to the data for the first 95 days is given by the smooth curve marked by squares. The sequence has a small number of events and, overall, is not described well by the Modified Omori relation.
Bottom: Santiago, Chile, March 3, 1985, $M_s 7.8$. This sequence is described well by the Modified Omori relation, with p = 1.030. Departures (actual number - calculated number) are shown in the lower part of the figure.

broke about 25 sec apart, the Santiago event (3 March 1985) exhibited a much more uniform distribution of asperities of various strengths over the rupture (i.e., was inherently a more heterogeneous fault than Michoacan), and the Andreanof Islands rupture was somewhere in between. These events provide an excellent set for examining the relationship of fault-zone heterogeneity to aftershock decay rate and investigating the potential usefulness of the p-value as a measure of interesting fault zone properties.

The Santiago earthquake aftershocks, lower part of Figure 2, fit the Modified Omori relation very well, with the p-value close to the canonical value 1, here 1.03, for $m_b \geqslant 5$. The p-value after 220 days (77 events) was 1.038, essentially the same as after 802 days (88 events). This earthquake is, thus, almost a textbook example of the original Omori relation.

The Michoacan event, upper part of Figure 2, on the other hand, is not well described by the Modified Omori relation. The total number of aftershocks is remarkably few for an earthquake with M_s8.1, evidence that the overall rupture surface was quite homogeneous, outside of the two major asperities. For the first 95 days (15 events, $m_b \geqslant 4.5$), the sequence is fit well with $p = 1.28$, a value at the high end of the range reported in other studies of sequences. An event on 30 April 1986, M_s7, in the northwest part of the original aftershock zone, appears to have generated its own sequence of a few aftershocks. Only 34 events at the selected magnitude level occurred during the first 465 days. The small number of aftershocks and the fast rate of decay of the sequence are in accord with a more homogeneous rupture surface, outside of the two prominent asperities.

These first results, $p = 0.93$ for Andreanof Islands, 1.03 for Santiago, and 1.28 for Michoacan, suggest that the p-value is a valid indicator of relative heterogeneity of rupture surfaces of large events. Many questions remain about the sensitivity of this parameter to other variables, especially the low magnitude cutoff chosen (teleseismic vs. microearthquake data) and the magnitude of the main shock, and the possible inherent variability of p itself with time.

Effects of the Major Earthquake on Local Earthquake and Fault Zone Properties

Further experiments with synthetic seismograms have confirmed that converted phases, usually P-to-S conversions, are present on many of the seismograms recorded by the Adak network. These converted waves often arrive so close to the arrival of the true direct S wave that they mask it. The resulting contamination of the S-wave spectra is the source of much of the scatter in calculated stress drops and apparent stresses. For this reason, alternate approaches have been sought for detecting changes in waveform properties that are diagnostic of changes in the fault zone caused by the occurrence of the May 7, 1986 earthquake.

A very promising approach is based on the availability in the Adak database of numerous clusters of earthquakes with almost identical waveforms. These events have almost identical hypocenters and occur at various times, before and after May 7, 1986. Pairs of these events, called "doublets" are analyzed by the technique suggest by Poupinet, in 1984, and applied by others. The cross-spectrum of a doublet pair should have a phase that is linearly related to the time difference between the two events. Time differences detected in this way can be related to small differences in event location, and when this effect is removed, to changes in wave velocity along the hypocenter-station path during the interval between the two events.

A computer program to apply doublet analysis to Adak data has been written. The inherent accuracy of the technique has been tested by applying it to seismograms from one station, AD5, from a doublet separated by about one hour, Figure 3. It is assumed that no physical changes in the fault zone or along the propagation path occurred in this short time. The strikingly similar seismograms are shown in the upper section of the figure. The delay times for the doublet appear just below the seismograms. These were calculated for a window of 2 sec (about 150 data points), a smoothing of 20 samples, and a high-frequency cutoff of 15 Hz. The delay

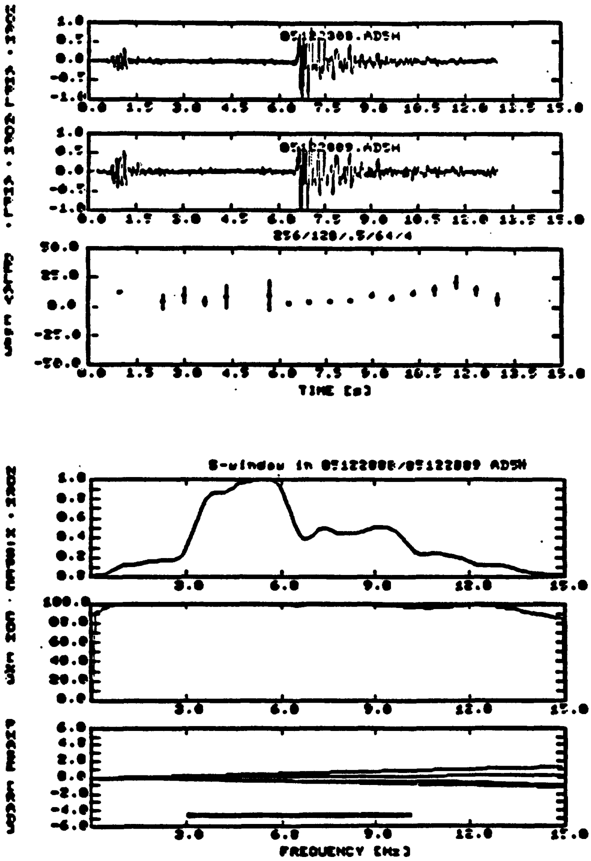

FIGURE 3

Doublet analysis, two events at same location, one hour apart. From top to bottom: the seismograms (AD5H), the calculated time delays, the normalized cross-spectrum, the coherence, the phase of the cross spectrum.

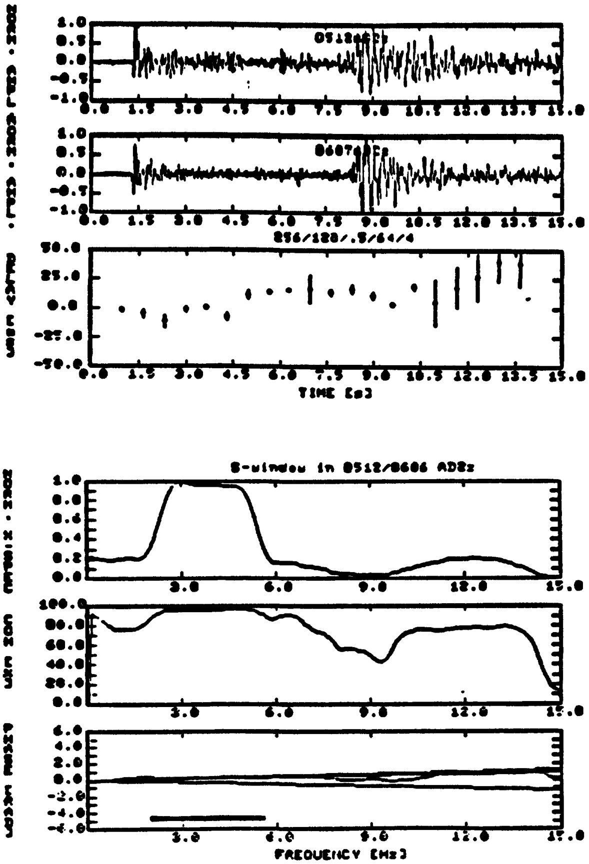

FIGURE 4

Same as Figure 3, for a doublet, one event in December, 1985, the other in July, 1986, after the May 7, 1986 major earthquake.

times are small and stable until well past the S-wave coda. The cross-=spectrum, the coherence, and the phase of the cross spectrum for the window containing the S arrival are given in the lower part of the figure. The high degree of coherence within the frequency band of interest confirms the apparent similarity of the two seismograms. The phase is linear with frequency, as required by the theory. The bottom part of the figure shows the fit to the phase from which the time delays were calculated. This case provided a test of the software, the general applicability of the method, and a measure of the calculated time delays to be expected when no changes in velocity were likely to be involved.

Next, a doublet pairing one event before the May 7 main shock (December, 1985) and one after (July, 1986) was processed. The results are shown in Figure 4. The seismograms from one station, AD2Z, top of the figure, are again very similar by visual inspection, suggesting a common source location. The delay times for the doublet are given below the seismograms. The differences in behavior from Figure 3 are clear. The coherence is high over most of the frequency band.

These first tests confirm the validity of the method for detecting changes along the paths from hypocenter to station. The large number of suitable doublets in the Adak database provide an excellent opportunity to apply this method to the investigation of physical changes related to the occurrence of a major earthquake.

Publications

Kisslinger, C., Evaluation of the Central Aleutian Islands Prediction Experiment, 1983-1986, *Inter. Assoc. Seismo. and Physics Earth's Int., General Assembly, August 9-22, 1987, Abstracts*, p. 262.

Engdahl, E.R., Billington, S., and C. Kisslinger, Assessment of Teleseismically Recorded Seismicity before and after the May 7, 1986 Andreanof Islands Earthquake, *Inter. Assoc. Seismo. Physics Earth's Int., General Assembly, August 9-22, 1987, Abstracts*, p. 276.

Seismological Field Investigations

9950-01539

C. J. Langer
Branch of Geologic Risk Assessment
U.S. Geological Survey
Box 25046, MS 966, Denver Federal Center
Denver, CO 80225
(303) 236-1593

Investigation

Illinois postearthquake study--local investigation of aftershocks resulting from the M_{blg} 5.1 earthquake of 10 June 1987.

Results

Within 1-1/2 days following the magnitude 5.1 main shock on 10 June 1987 near Olney, Illinois, the installaion of a portable network of analog and digital seismographs was in progress. Network operation continued for about four days and included several additional analog stations operated by personnel from the Tennessee Earthquake Information Center.

Approximately 100 aftershocks were recorded of which about half (55) have been located thus far using HYPOELLIPSE. Most solution Quality measures are A/A, average GAP $\approx$ 68 deg and average DMIN $\approx$ 3 km. In fact, there were usually about ten stations whose epicentral distances were less than the computed focal depths. These parameters attest to the high quality of the computed hypocentral locations. The velocity model utilized was the St. Louis University Uplands Model with a V_P/V_S of 1.77.

The average standard error measures associated with the hypocentral locations are: ERH = 0.4 km and ERZ = 1.0 km. The hypocentral zone is very small and occupies a volume somewhat elongate to the northeast: the zone is about 1.5 km long, 1.0 km wide, with some 4 km of vertical extent between about 8 and 12 km in depth. Explanation of this unusual, but not rare, nearly cylindrical aftershock distribution will be a primary objective in our ongoing studies of this important shock.

Focal mechanism solutions for the aftershocks are being developed. Some very preliminary single-event solutions and a cursory examination of the P-wave first motion patterns in general seem to indicate either reverse displacement on north- to northeasterly striking planes, right-lateral strike-slip motion on planes striking northeast to east-northeast, or a combination thereof. The main shock focal mechanism solution determined from 59 short-period P-wave polarity readings show near-vertical nodal planes. The indicated mode of faulting is either right-lateral strike-slip to the northeast or left lateral strike-slip to the northwest.

Hayward Fault

9910-04191

J.J. Lienkaemper
Branch of Engineering Seismology and Geology
U.S. Geological Survey
345 Middlefield Road, MS 977
Menlo Park, California 94025
(415) 329-5642

Investigations

Determine slip rates and earthquake recurrence intervals on the Hayward fault. Compare geologic surface slip rate to historic creep rates and geodetically determined deep slip rate. Analyze the effect of geometric complexity and segmentation of faulting upon how recurrence may be inferred from slip rates.

Results

We began trenching near Fremont Civic Center in September 1986, and continued in May-June 1987. We analyzed the trench logs to reconstruct the original shape of the northern margin of a gravelly sand deposit that has been offset by the fault. The apparent offset is about 32 m (Borchardt, *et al.*, 1987), but total offset is 44.5 ± 4.1 m when the effects of horizontal and vertical warping and subsidiary faulting are removed. Detrital charcoal sampled from immediately below the marker unit yielded a ^{14}C-date of 7990 ± 160 yr BP. An independent check of age came from detrital charcoal taken from deposits immediately above the marker unit (8260 ± 190 yr BP). The slight inversion in the age of the upper sample (within 2 standard deviations) confirms the lower sample as a good indicator of the time of deposition. Furthermore, the charcoal at the horizon of the lower sample was abundant and not abraded, suggesting it came from a nearby fresh burn.

Thus slip rate during the last 8040 years has been 5.5 ± 0.5 mm/yr at this site. A curb located 0.4 km to the southeast has been creeping 5.4 ± 0.4 mm/yr since 1968. A railroad guardrail located 2.4 km to the northwest has been creeping at about 5.3 mm/yr since 1954. Thus the Holocene rate of slip appears to equal the historic rate. However, all of these rates are in a 400-m rightward jog in the fault that extends across the Niles alluvial cone from the Niles to the Irvington Districts of Fremont. In the Irvington District and southeastward for 3 km we have determined that the creep rate has been about 9 mm/yr since 1920. Continuing investigations will attempt to explain what happens to the 3-4 mm/yr of additional slip observed in Irvington but not where the fault jogs right across Niles Cone, and to find data on recurrence of major earthquakes.

Reports

Borchardt, G., Lienkaemper, J.J., and Schwartz, D.P., 1987, Holocene slip rate for the Fremont segment of the Hayward fault, Fremont City Hall, California: *EOS*, ____, p. ____.

San Andreas Fault Slip History Near Cholame, California

9910-04192

J.J. Lienkaemper
Branch of Engineering Seismology and Geology
U.S. Geological Survey
345 Middlefield Road, MS 977
Menlo Park, California 94025
(415) 329-5642

Investigations

1. Slip histories of Parkfield segment.

2. Slip history of Cholame segment.

Results

1. The manuscript on Parkfield Slip History is nearly ready for Branch review. Results are essentially the same as Lienkaemper *et al.* (1985, *EOS 66*, 985) except: we include Highway 46 results (about same creep rate and slip per event as at Water Tank), we determine Parkfield bridge slip history from offset at ground level, and we remove the slow down in creep following the 1983 Coalinga earthquake from the slip model. The average event slip at the bridge is 31 ± 3 cm and the creep rate is 10-12 mm/yr. The estimate of post-1857 slip deficit at Parkfield remains about 0.25 m.

2. I mapped all fault traces on the 30-km Cholame segment at 1:2400-scale on the 1986 low sun-angle aerial photographs and have measured and tabulated all stream offsets visible on these. Offsets range from 0 to 600 m. Of a total of 93 offsets, 44 are less than 20 m. Most (25) of these smaller offsets range from 4-8 m and presumably reflect slip associated with the great 1857 earthquake. Reconstruction of channel geometry to account for degradation since 1857 can be difficult even for the simplest drainages (*e.g.* Lienkaemper and Sturm, in review) and permit ambiguous measurement of slip. These data are not accurate enough to define the 1857 slip curve on the Cholame segment, but indicate that slip was distinctly less than the 9 m of Carrizo Plain, and probably much larger than the 3-4 m estimates by Sieh (1978, *Bull. Seism. Soc. Am.*). The 1857 slip seems to be 6 ± 2 m. Given this greater value of slip and uncertainty in its value, the probability of the next Parkfield earthquake to trigger major slip on the Cholame segment (Sieh and Jahns, 1984, *Geol. Soc. Am. Bull.*) should not be considered large or distinct. Future work will involve trenching and other detailed investigations to resolve ambiguous slip measurements.

Reports

Lienkaemper, J.J., 1987, 1857 slip on the San Andreas fault southeast of Cholame, California: *EOS*, ____, p. ___.

Lienkaemper, J.J., and Sturm, T.A., 198_, Reconstruction of a channel offset in 1857(?) by the San Andreas fault near Cholame, California: *Bulletin of the Seismological Society of America*, ___, ___-___.

10/87

Array Studies of Seismicity

9930-02106

David H. Oppenheimer
Branch of Seismology
United States Geological Survey
345 Middlefield Road - MS 977
Menlo Park, California 94025
415-329-4792

Investigations

1. Analyze fault-plane solutions of aftershocks of the M6.2 Morgan Hill earthquake which occurred on April 24, 1984 to gain understanding of regional stress field.
2. Continue consolidation and clean-up of phase data of central California Seismic Network (CALNET) from 1969 through present.
3. Analyze digitized seismograms of characteristic earthquake sets in the Stone Canyon–Bear Valley region of the San Andreas fault to determine the stability of their source processes.

Results

1. This research effort is the result of a collaboration between myself, Paul Reasenberg and Robert Simpson. We have completed our studies and have submitted a manuscript describing our findings to J.G.R. We computed fault-plane solutions for 946 aftershocks of the April 24, 1984 Morgan Hill, California M6.2 earthquake which reveal a pattern of complex faulting within a 10-km-wide zone surrounding the Calaveras fault. The fault-plane solutions fall naturally into three groups: strike-slip mechanisms with vertical, north-northwest-striking dextral slip planes located along the Calaveras fault; strike-slip mechanisms with vertical, north-striking dextral slip planes located northeast of the Calaveras fault; and northwest-striking reverse mechanisms located southwest of the Calaveras fault.

The average azimuth of P-axes for aftershocks located on the Calaveras fault is N10 ± 8°E. In contrast, the average orientations of P-axes for aftershocks northeast and southwest of the Calaveras fault are horizontal with azimuths N49 ± 13°E and N37 ± 11°E, respectively. By assuming that the earthquakes occur on pre-existing cracks, and that the stress field is uniform over the region, we infer from the observed slip directions that the direction of maximum horizontal compression is oriented approximately 80° from the local strike of the Calaveras fault.

The combination of this inferred ambient stress field and the changes in static stress field calculated for the 1984 mainshock offset successfully explains observed patterns in the spatial distribution of the aftershocks and orientation of their fault-plane solutions. Areas in which the Coulomb failure function increased by only a few tenths MPa correspond well to areas of intense aftershock activity. The calculated stress orientations agree with aftershock fault-plane solutions, except for the reverse mechanisms near Anderson Lake. Addition to the model of the static stress field change inferred for the 1979 Coyote Lake offset predicts these mechanisms as well.

A conceptual model to explain how fault-normal stress may arise near the Pacific-North American plate boundary consists of a vertical fault locked above the base of the seismogenic zone and slipping freely below in response to uniform right-lateral shear stress imposed on it. Slip on the lower fault surface effectively cancels the applied shear stress over most of the halfspace, but imposes large crack-tip shear stresses on the base of the seismogenic zone. When the applied shear is oblique to the fault, the resulting three-dimensional stress field includes fault-normal compression at seismogenic depth. This compressive stress may, in turn, contribute to the development of deformational features such as folds, reverse faults, and perhaps, the Coast Ranges.

2. Substantial effort was again devoted to the collection, organization, relocation, archiving, and documentation all the CALNET earthquake data since 1969. Programs which detect gross errors in the phase data and programs to merge phase data from separate networks into a common set were enhanced as unforeseen problems arose. Recognized errors in the data from 1969 through 1983 have been corrected, the station

names have been changed in accordance with a unique naming convention, and the earthquakes have been relocated with velocity models specific to the epicentral region. Discrete data sets for this time period are to be merged into a common catalog in the near future. Post 1983 CUSP and RTP data are currently being processed as described above and also will be merged. We expect this phase of the network reprocessing to be completed by the end of 1987.

3. Broad-band seismograms were digitized from FM tapes recorded at U. C. Berkeley Seismographic Station for 2 event pairs in the Stone Canyon region. Using cross-spectral analysis methods, we have determined that the earthquakes of one pair have identical spectra at frequencies at least as high as the system pass-band (7-8 Hz), although the events differ in moment by 16%. The cross-spectral coherence exceeds 0.95 throughout the measurement band for this pair, suggesting that they share a common source process. The second pair of events studied are also highly coherent. However, their spectra exhibit a small yet significant difference corresponding to a slope of roughly 2-3 dB/octave in the amplitude ratio spectrum. Current efforts are directed toward understanding the origin of this apparent difference in the source process and toward collecting seismograms for additional characteristic pairs in this region.

Reports

Oppenheimer, D. H., P. Reasenberg, and R. W. Simpson, Fault-plane solutions for the 1984 Morgan Hill, California earthquake sequence: Evidence for the state of stress on the Calaveras Fault, *submitted to* J. Geophys. Res., 64 pp.

Oppenheimer, D. H., and P. Reasenberg, 1987, Analysis of fault plane solutions for aftershocks of the M6.2 Morgan Hill, California earthquake, EOS, Tran. Am. Geophys. Union, 68, p. 362.

Detailed Geologic Studies, Central San Andreas Fault Zone

9910-01294

James A. Perkins
John D. Sims
Branch of Engineering Seismology and Geology
U.S. Geological Survey
345 Middlefield Road, MS 977
Menlo Park, California 94025
(415) 329-5647 or (415) 329-5653

Investigations

1. Continued studies of late Quaternary movement along the Calaveras and Paicines faults (Perkins, Barclay, Sims).
2. Calibrate fault scarp degradation dating techniques to alluvial deposits (Perkins, Barclay).
3. Detailed mapping of active faults and alluvial deposits along a 60-km-long reach of the San Benito River.

Results

1. Continuing investigations of the Calaveras and Paicines faults concentrate on two study sites: the Windfield Ranch along the Calaveras fault and the Roberts Ranch along the Paicines fault. Previous trenching and geomorphic studies at Windfield Ranch suggest that the Calaveras fault here has averaged about 9 mm/yr during the last 14 ka. Three additional charcoal samples have been submitted to the University of Arizona for radiocarbon analysis. During this reporting period we began new field investigation of the Oa_5 alluvial deposit of the San Benito River that is displaced about 125 m along the Paicines fault at Roberts Ranch. Trenching of the Qa_5 deposit revealed a thick (>4m) sequence of dominantly fine-grained alluvium that contains small pieces of disseminate charcoal. Insufficient charcoal for age determination of the Qa_5 deposit was recovered during the preliminary trenching. The fluvial character of the Qa_5 deposit exposed in the trenches suggests that additional trenching may yield sufficient material for radiometrically dating this deposit.

2. Numerous alluvial deposits along the San Benito River are displaced by the Calaveras or Paicines faults, but the age of the deposits is unknown. Calibration and application of fault scarp degradation dating techniques to these displaced alluvial deposits may provide multiple slip rates for the Calaveras and Paicines faults. During this reporting period we have recalculated the ages of four deposits on the basis of their riser morphology. Age determinations vary significantly as a result of uncertainty in diffusivities. Seven additional radiometric age determinations may allow us to calculate a diffusivity that is widely applicable to San Benito River alluvium.

3. Field work on detailed mapping of active faults and alluvial deposits along the San Benito River between the towns of Tres Pinos and San Benito is complete. Final map compilation is 80 percent complete. Work has begun on text and figure to accompany the final report.

Reports

Perkins, J.A., 1987, Provenance of the upper Miocene and Pliocene Etchegoin Formation: Implications for the paleogeography of the late Miocene of central California: *U.S. Geologial Survey Open-File Report 87-167*, 86 p.

10/87

INTEGRATED ANALYSIS OF SOURCE PARAMETERS FOR A BASIN AND RANGE EARTHQUAKE SEQUENCE

14-08-0007-G1326

Keith F. Priestley and Kenneth D.Smith
Seismological Laboratory, Mackay School of Mines
University of Nevada, Reno, Nevada 89557
(702)-784-4975

INVESTIGATIONS:

Our objective is to determine source parameters for the main shock and many of the aftershocks of the 1984 Round Valley, California earthquake sequence, and interpret this with respect to the details of the aftershock development. We have determined the source paramters of 26 aftershocks, $M_L>2.7$, using a pulse width technique (Frankel and Kanamori; 1983) and the short period clipped records. Source parameters for the Round Valley mainshock have been determined incorporating local strong motion records, region surface waves, teleseismic body waves, and short period first motion data. We have completed a study of the foreshock sequence of the 1986 Chalfant, California earthquake, and a detailed analysis of cluster of earthquakes, including several above M_L 4, near the town of Mina, Nevada that occurred during July and August 1987 in the proposed White Mountains 'seismic gap' (Hill et al, 1982), Also, we have persued a method for the calculation of radiated energy, during fault rupture, that involves integration of composite velocity squared spectra.

RESULTS:

The 1984 Round Valley earthquake has been one in a series of moderate size $M_L \approx 6$ earthquakes to have occurred in the Mammoth Lakes-Bishop, California area since 1978. The most recent of this series, the 1986 Chalfant, California sequence, took place 15 km to the northeast of the Round Valley epicentral area and included 5 events over M_L 5. These sequences have occurred within the U.S. Geological Survey-University of Nevada local short period network, which has provided an excellent data set for determining the character of earthquake activity in this area.

Source Parameters of Aftershocks (Pulse Width Technique)

We have selected the pulse technique of Frankel and Kanamori (1983) and O'Neill and Healy (1973) to determine source parameters of a number of aftershocks between $M_L \approx 3$ and 4. This technique is applied to the clipped velocity records of the local short period network. Although first pulses are generally clipped for this magnitude range and distance (≈10 km), pulse widths are preserved (Ellis and Lindh, 1976). The technique involves substracting the pulse width of small events ($< M_L$ 2) from that of the larger events, effectively deconvolving the path and instrument effects. The corrected pulse width is then assumed to represent the source process time, and the source radius can then be calculated directley (Boatwright, 1980). To apply this technique, assumptions must also be made about the source geometry and the rupture velocity. The stress drop is then calculated by scaling the source radius measurement to the seismic moment.

Initially we applied a moment magnitude scale (Chavez and Priestley, 1985), and magnitudes had been determined from the short period records using a duration magnitude scale or from regional broadband recordings converted to Wood-Anderson equivalents. This has been somewhat of a problem. Duration magnitudes are not consistent with regional magnitude determinations. In fact the duration magnitude has been systematiclly .4 M_L higher than the Wood-Anderson equivalents. Duration magnitudes have been calibrated to the California Richter magnitude and this difference is apparently due to different attenuation properties in the Basin and Range. We have accumulated the region recordings of many of the M_L 3-4 events from the UNR and Livermore broadband digital networks are in the process of fitting the surface wave ampiltudes to determine the seismic moment directly. Focal mechanims for the bulk of the sequence are unusually well contrained allowing use to correct for radiation pattern very precisely. Our moment calculations from the regional stations should solve the magnitude problem as it applies to this study.

Frankel and Kanamori (1983), subtracted the pulse widths of small events located as near as possible to larger in order to make the proper path correction. We have found that corrections for individual events is insignificant compared to a general station pulse width correction for this earthquake sequence. We feel that this is because the sequence is confined to a relatively small zone and that station coverage is at all azimuths and small epicentral distances which was not the case for the Frankel and Kanamori (1983) study Since the last report, we have recalculated stress drops using individual stations corrections instead of individual event corrections with little change in the stress drop value. As reported previouly, there is a tendency for a increased stress drop with depth, but in applying the new correction there is less scatter in the stress drop values (more of a constancy of stress drop).

Clustering of Small Earthquakes in the Mina, Nevada Region

Three M_L 4 and several M_L 3.5+ earthquakes occurred within a shallow localized cluster of activity during July and August 1987 near the small town of Mina, Nevada. The larger earthquakes were strongly felt by residents of Mina. This area is of particular interest because it is within the proposed White Mountains 'seismic gap' (Hill et al, 1985), and also, Savage and Cockerham (1987) have developed a statistical model for the reccurance of moderate earthquakes in the region. The White Mountions 'seismic gap' is defined to the south by the northern exent of the 1872 M_L 8 Owens Valley earthquake and to the north by the 1932 M_L 7.1 Ceder Mountains earthquake.

Shallow clustering of small earthquakes has preceeded several of the $M_L \approx 6$ events of the Bishop-Mammoth Lakes, California earthquake sequence, 150 km to the southwest of Mina along the eastern front the of Sierra Nevada (Ryall and Ryall, 1981; Smith and Priestly, 1987). The tectonics of Bishop California area is somewhat similar to the Mina region in that we see significant range front faults with obvious Holcene vertical displacements but only strike slip faulting. Also, periods of localized clustering are not unusual to either area.

In this study we have analyzes the 1987 Mina activity, attempted to isolate the causitive faults and discussed recent seismicity patterns in the region with respect to localized clustering and active faulting.

Between July 28 and August 31, 1987, 140 events were located by Univeristy of Nevada Seismological Laboratory (UNSL) in the Mina area. Of these, 13 were M_L 3 or greater, 3 were greater than M_L 4 (Table 1), and 45 were in the M_L 2.5-3.0 range (duration magnitudes in all cases). The activity occurred to the east of the UNSL short period network. Srengnether DR100's with three component L4-C 1 Hz seismometers were in operation from July 29 through August 4 to supplement network phase data and acquire near source digital waveforms. Portable recorders provided eastern station coverage, significantly improving hypocentral control, and near in first motion data for focal mechanism constraints. One instrument was placed several hundred feet within a mine tunnel, 12 km epicentral distance to obtain digital waveform data not contaminated by surface effects.

July and August 1987 Mina earthquake activity was confined to a small shallow volume of the crust. Focal mechanisms show little variation and indicate nearly pure strike slip motion, right lateral on a NNE striking fault or left lateral on a WNW striking plane. This is precisely the local where left lateral trending faults of the Excelcior Mountains region meet the right lateral offsets of the Walker Lane, so a combination of both left lateral and right lateral strike slip motion cannot be ruled out. Recent earthquake sequences in the Bishop, California include both right lateral and left lateral strike motion in near conjugate planes of faulting. (Smith and Priestley, 1987; Priestley and Smith, 1986). The seismicity locates above the trace of the range front fault of the Pilot Mountains, 7 km to the east. A dip of less than 45 degrees would be required for the seismicity to have taken place on the range front fault. The locations and focal mechanisms conform to a set of faults near Sodaville that are oblique to the range front fault and apparently intersect the range front very near this particular activity.

The two most recent moderate size earthquakes in the region, the 1984 M_L 5.7 Round Valley and 1986 M_L 6.4 Chalfant, California events, occurred on faults with a similar geometry with respect to a range front as those apparently responsible for the 1987 Mina activity (Figure ??). These particular events, both with strike slip mechansims, took place within a few kilometers of their respective range front faults, the Round Valley Fault and White Mountains Fault. Aftershock patterns define fault planes for the Round Valley and Chalfant events that are oblique to the range fronts.

Radiated Energy of Fault Rupture

We have integrated velocity squared spectra in order to determine the seismic energy radiated during fault rupture. The high frequency spectral fall-off and the shape of the spectrum at the corner frequency are critical to the energy calculation. High frequency sprectal fall-offs of ω^{-2} beyond the corner frequency, in a Brune (1970) source model, return radiated energies approximately equal to that of an Orowan (1960) type fault failure, where the final stress level is equal to the dynamic frictional stress. Any spectra with an extended intermediate slope of ω^{-1} would therefore result in higher radiated energies. Savage and Wood (1971) proposed a model in which the final stress level was less than the dynamic stress level and that this was the result of "overshoot". They based their model on the observation that the ratio of twice the apparent stress to the stress drop was typically around .3. We have determined that for such a ratio to exist high frequency spectral fall-offs of $\approx\omega^{-3}$ would be required. Composite spectra have been constructed for several moderate to large earthquakes, these spectra have been compared to that predicted by the Haskell (1966) model and velocity squared spectra have been integrated to determine the radiated energy. In all cases this ratio, twice the apparent stress to the stress drop, is greater than or equal to one, violating the Savage and Wood (1971) inequality, and provides evidence against "overshoot" as a source model.

Reports

Priestley, K.F. and K.D. Smith (1987). The 1984 Round Valley, California earthquake earthquake, submitted to *G.J.R.A.*

Smith, K.D., J.N. Brune, and K.F. Priestley (1987) Seismic energy, spectrum and the Savage and Wood Inequality for complex earthquakes, submitted to the *Proceedings of the 100th Aniversary of the Berkeley Seismological Laboratory.*

Smith K.D. and K.F. Priestley (1986). Rupture duration and stress drop for aftershocks of the November 23, 1984 Round Valley California earthquake, abstract *Earthquakes Notes 57*, 23.

Smith, K.D., K.F. Priestley, and R.S. Cockerham (1987). Spatial and temporal variations in the 1984 Round Valley, California earthquake sequence, submitted to *Geology.*

Smith, K.D. and K.F. Priestley (1987). Foreshock sequence of the 1986 Chalfant, California sequence, submitted to *Bull. Seism. Soc. Am.*

Smith, K.D., U.R. Vetter, and K.F. Priestley (1986). Focal mechanisms of the July 1986 Chalfant, Claifornia earthquake sequence, abstract *EOS Trans. 44*, 1106.

Smith, K.D. and K.F. Priestley (1987). Foreshock sequence of the 1986 Chalfant, California earthquake, abstract *Seism. Res. Lett. 58*, 20.

References

Boatwright, J. (1980). A spectral theory for circular seismic sources: simple estimates of source dimension, dynamic stress drop and radiated energy, Bull. Seism. Soc. Am. 70, 1-28.

Brune, J.N. (1970). Tectonic stress and the spectra of seismic shear waves from earthquakes, J. Geophys. Res. 75, 4997-5009.

Chavez, D.E. and K.F. Priestley (1985). M_L observations in the Great Basin and M_o of the 1980 Mammoth Lakes, California, earthquake sequence, Bull. Seism. Soc. Am. 75, 1583-1598.

Ellis, J. and A. Lindh (1976). Linearity of VCO-discriminator system with respect to zero crossing times, U.S. Geol. Survey Open-File Rept. 76-873.

Frankel, A. and H. Kanamori (1983). Determination of rupture duration and stress drop for earthquakes in southern California, Bull.Seism Soc. Am. 73, 1527-1551.

Hill, D.P., R.A. Bailey, and A.S. Ryall (1985). Active tectonic and magmatic processes beneath Long Valley caldera, eastern California: an overview, *J. Geophys. Res. 90*, 11,111- 11,120.

Hill, D.P., R.E. Wallace, R.S. Cockerham (1985). Review of evidence on the potential for major earthquakes and volcanism in the Long Valley-Mono Craters-White Mountains regions of eastern California, *Earthquake Predict. Res. 3*, 571.

Haskell, N.A. (1966). Total energy spectral density of elastic wave radiation from propagating faults: Part II. A statistical source model, *Bull. Seism. Soc. Am. 56*, 125-140.

O'Neill, M.E. and J.H. Healy (1973). Determination of source parameters of small earthquakes from P-wave rise time, Bull. Seism. Soc. Am. 63, 599-614.

Orowan, E. (1960). Mechanism of seismic faulting, *Geol. Soc. Am. Mem. 79*, 323-345.

Ryall, A.S. and F. Ryall (1981). Spatial-temporal variations in seismicity preceding the May 1980, Mammoth Lakes, California, *Bull. Seism. Soc. Am. 71*, 747-760.

Savage, J.C. and R.S. Cockerham (1987). Quasiperiodic occurrence of earthquakes in the 1978-1986 Bishop-Mammoth Lakes sequence, Eastern California, (submitted to *Bull. Seism. Soc. Am.*)

Savage, J.C. and M.D. Wood (1971). The relation between apparent stress and stress drop, *Bull. Seism. Soc. Am. 61*, 1381-1386.

Basement Tectonic Framework Studies
Southern Sierra Nevada, California

9910-01291

Donald C. Ross
Branch of Engineering Seismology and Geology
345 Middlefield Road, MS 977
Menlo Park, California 94025
(415) 329-5650

Investigations

1. Filed investigations in the Woody area of the southern Sierra, near the west margin of batholithic exposures.

2. Determination of specific gravity on more than 600 samples of granitic rocks of the southern Sierra Nevada by Howard Oliver and his associates of the Geophysics Branch.

3. Modal analysis of more than 100 samples of granitic rock collected in 1987 from the southern Sierra Nevada.

4. Preparation of report summarizing specific gravity data on some 1500 granitic samples from the southern Sierra Nevada.

5. Compiling data for a report on the chemical character of the southern Sierra Nevada.

Results

1. Field investigations in the spring of 1987 revealed large bodies south of Woody of previously unidentified mafic rocks, now largely amphibolite, but containing remnants of gabbro and gabbronorite and probably related to the gabbronorite of Quedow Mountain extensively exposed southeast of Porterville.

2. These 1987 field investigations also resulted in the "dissolution" of the previously named "tonalite of Woody", and its replacement by several areas of fine- to medium-grained dikes and small masses ranging in composition from granite to quartz diorite. Some of the tonalitic rocks of this suite in the Cedar Creek area are mineralogically and chemically (based on calculations from modes) somewhat "trondhjemitic". Essentially, they are biotite tonalites with relatively felsic (about AN_{30}) plagioclase. No other "trondhjemitic" rocks have been found on the west side of the southern Sierra Nevada, though some are present, but not common, in the central and northern Sierra Nevada.

3. Specific gravities have now been determined on more than 1500 modally analyzed granitic samples from the southern Sierra Nevada. Much discussion has centered on whether specific gravity data are valuable, or not, in classifying and separating granitic rock masses. My general experience

has suggested that if a rock has a good mode, nothing is gained by a specific gravity measurement, as far as classifying the rock, and differentiating it from some other rock. However, specific gravity does measure a classifying feature of a whole rock of whatever size you choose, whereas a mode only samples a finite surface of a specimen and heterogeneities of granitic rock limit its value in characterizing large masses. Also specific gravity is much faster to determine than is slabbing, staining, and modally analyzing a granitic sample. Therefore, for a quick determination of color index, silica content, and rock type, a specific gravity figure has value and it would be particularly valuable in the rapid study of an area where modes were not available.

Reports

Ross, D.C. 1987, Mafic plutonic rocks of the southern Sierra Nevada, California: *U.S. Geological Survey Open-File report 87-275*, 42 p.

Ross, D.C., 1987, Generalized geologic map of the basement rocks of the southern Sierra Nevada, California: *U.S. Geological Survey Open-File Report 87-276*, scale 1:250,000, 28 p.

Ross, D.C., 1987, Granitic rock modal data from the southern Sierra Nevada, California: *U.S. Geological Survey Open-File Report 87-375*, 276 p.

Salton Trough Tectonics and Quaternary Faulting

9910-01292

Robert V. Sharp
Branch of Engineering Seismology and Geology
U.S. Geological Survey
345 Middlefield Road, MS 977
Menlo Park, California 94025
(415) 329-5652

Investigations

1. Geologic and geomorphic features of the Clark and other closely related fault strands of the San Jacinto zone in the region of the 1954 Arroyo Salada earthquake (M_L6.2).
2. Neotectonic investigation of the Tanlu fault, Shandong Province, Peoples Republic of China (with John Sims).

Results

1. The Clark fault is especially well delineated and nearly straight between Clark Valley and Smoke Tree Wash near the 1954 main shock epicenter, as recently relocated by Sanders *et al.* (1986). The fault strike on the ground surface is nearly identical to their strike slip focal mechanism. Aftershocks of the 1954 event that exceeded M 3.9, as well as a preshock cluster, were confined to a diffuse region east and eastsoutheast of the main shock. The distributions of the pre- and post-shocks match a zone of multiple stranded splaying, *en echelon* segmentation, and convergence with widespread normal faulting with strikes in the northeast quadrant. Field examination of the surface expression of the Clark fault 9 years after the event and reexamination during this report period confirms that this strand of the San Jacinto zone is indeed a youthful appearing feature, but no unequivocal evidence of new surface movement in 1954 was found. Right lateral surface displacement smaller than that of the 1968 Borrego Mountain event (<0.4m) might have accompanied the 1954 earthquake , but its recognition even 9 years after the fact might have been impossible. ASCS airphotos taken in 1953 show very subtle subsidiary fault traces on alluvial surfaces, and their photographic end points coincide with those that can now be identified in the field. Although this proves their creation before the 1954 earthquake, small-scale enhancement of these topographic features during 1954 is not ruled out. Albeit unlikely, continuity of the Clark fault (or an *en echelon* strand) is possible beyond the southeasternmost identified surface expression. The location of such a hypothetic extension is constrained to the alluvium-covered swath between Arroyo Salada and Tule Wash in western Imperial County. The latest surface faulting movement along such a path would have preceded the last filling of Lake Cahuilla (about 300 years ago) but could have been much earlier.

2. Our trip to China in April and May 1987 was made to assess the present understanding of the Ouaternary history of movement on the Tanlu fault in Shandong Province and particularly to be able to see the field evidence in support of this understanding. Geologic and geomorphic relations along the Tanlu fault are being comprehensively documented by the Shandong Seismological Bureau, and this agency plans to publish the documentation in the form of a "Tanlu Fault Atlas". Field sites visited during our trip lay along various strands of the fault between Juxian and Tancheng, the segment of the zone thought to have been activated during the $M>8$ earthquake of 1668.

   The involvement of late Quaternary sediments is abundantly clear at many sites along the Tanlu fault. However, Holocene and even historic surface faulting remains to be demonstrated. Because of the intensity of agricultural and clay mining activities, sites undisturbed by man along the fault traces are very rare. Evidence of surface effects within the 1668 epicentral region at present is restricted to sand-filled subsurface fissures south of Tancheng probably caused by lateral spreading at a time of strong shaking. Although this fissured material remains undated, quite likely it represents the 1668 event.

   Geomorphic evidence in support of lateral displacement on the Tanlu fault is complicated by the fact that severe gullying and local badland formation along the margins of uplands have occurred within the past century. Stream courses showing lateral meanders at or near some fault traces in most cases are better ascribed to recent gullying than to fault displacement in 1668 or earlier.

Reports

Sharp, R.V., and Magistrale, H., Seismicity and tectonics in the region of the 1954 Arroyo Salada earthquake, San Jacinto fault zone, southern California, *Bulletin of the Seismological Society of America*, in preparation.

Seismotectonic Framework and Earthquake Source Characterization (Continued)— Wasatch Front, Utah, and Adjacent Intermountain Seismic Belt

14-08-0001-G1349

R.B. Smith, W.J Arabasz, and J.C. Pechmann*
Department of Geology and Geophysics
University of Utah
Salt Lake City, Utah 84112
(801) 581-6274

Investigations

1. Synthesis of seismological observations relevant to the evaluation of earthquake hazards and risk in the Wasatch Front area.
2. Slip rate and earthquake potential of the East Great Salt Lake fault.
3. Source mechanism of the 1962 M_L5.7 Logan earthquake.

Results

1. We have completed a paper (Arabasz et al., 1987) that presents and considers in a systematic way up-to-date information from observational seismology that is basic to evaluating earthquake hazards and risk in the Wasatch Front area. We present fundamental information relating to (1) the earthquake data base, (2) the seismotectonic framework, (3) seismic source zones and seismicity parameters, (4) ground-shaking hazard, and (5) current seismicity and the Wasatch fault.

Important features of the seismotectonic framework of the Wasatch Front include (1) a threshold magnitude for surface faulting of M_L6.0 to 6.5, (2) a maximum magnitude of M_S7.5 to 7.7, (3) the absence of any large surface faulting earthquakes and the notable paucity of smaller earthquakes on the Wasatch fault during historic time, and (4) the problematic correlation of background seismicity with mapped Cenozoic faulting. In light of this framework, we consider seismic hazards in the Wasatch Front region to arise from two fundamental sources: first, the occurrence of infrequent large (M_S 6.5 to 7.5±0.2) surface-faulting earthquakes on identifiable faults having evidence of late Quaternary displacement; and, second, small- to moderate-size (up to M_L 6.5) earthquakes that are not constrained in location to mapped faults and may occur anywhere throughout the region. The small to moderate earthquakes dominate the historical earthquake record, and at most localities are the largest contributor to probabilistic ground-shaking hazard for exposure periods of 50 years or less (Figure 1). Recurrence modeling using independent mainshocks from the 25-year instrumental catalog predicts an average return period of 24±10 years for potentially damaging earthquakes of magnitude 5.5 or greater along the Wasatch Front.

---

*E.D. Brown, W.P. Nash, K.J. Quigley, and J.E. Shemeta also contributed significantly to this project during the report period.

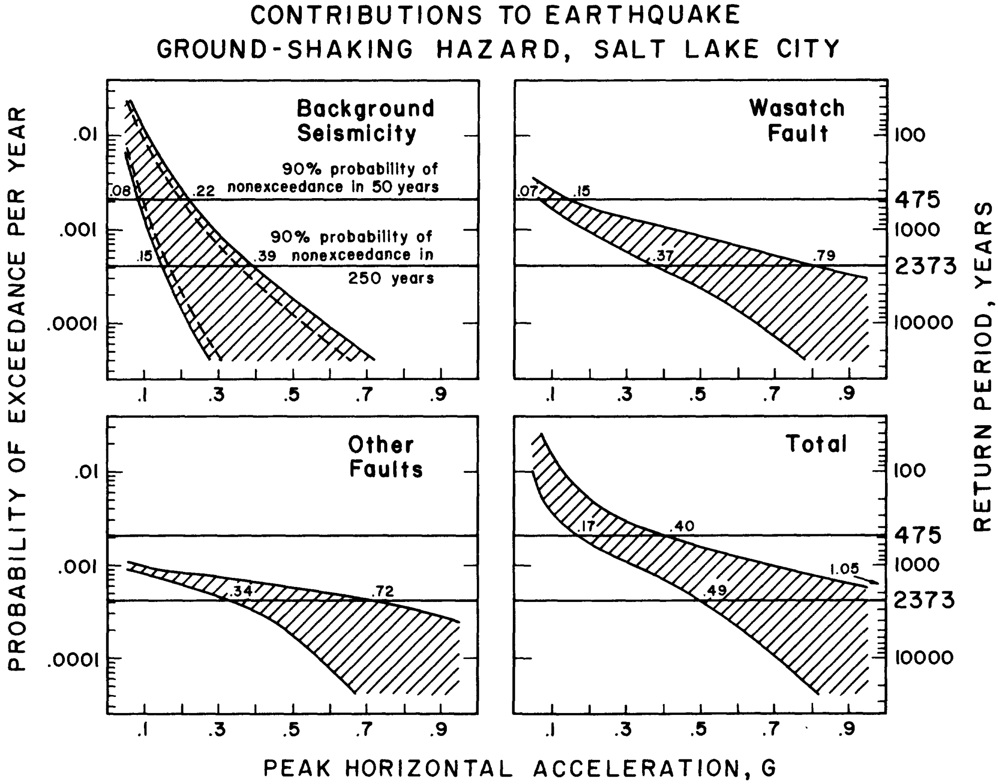

Figure 1. Graphs showing the probability of exceedance per year for peak horizontal ground accelerations on soil at the intersection of I-15 and I-80 in South Salt Lake at approximately 40°43.1'N, 111°54.2'W. The shaded zones represent the range of values calculated using the range of median attenuation curves for peak horizontal acceleration presented by Campbell (1987). The results of separate calculations for the background seismicity, the Wasatch fault, other faults (the West Valley, East Great Salt Lake, and North Oquirrh Mountains faults), and all of these sources together are shown. On the graph for the background seismicity, the dashed curves bound the range of values obtained using a preferred b- value of 0.71 obtained from recurrence modeling. The lower solid curve was calculated using our upper-bound b-value of 0.80 and Campbell's lower-bound acceleration estimates, whereas the upper solid curve was calculated using our lower-bound b-value of 0.62 and Campbell's upper-bound acceleration estimates. The vertical axes at the right show the average return period in years (the inverse of the annual probability).

2. Gravity and seismic reflection data indicate a major NNW-striking fault concealed beneath the Great Salt Lake that we conclude is of first-order importance for regional seismic hazard. This west-dipping fault, named the East Great Salt Lake fault by Cook et al. (1980), follows the west boundary of a linear topographic high formed by the Promontory Mts. and Fremont and Antelope Islands. This fault and related faults cut late Quaternary sediments, and must therefore be considered active despite the lack of associated seismicity. The East Great Salt Lake fault appears to be separated by a left-stepping offset into two segments, each about 50 km long. These segment lengths are comparable to those proposed for the Wasatch fault, suggesting that the East Great Salt Lake fault could generate earthquakes of up to the maximum M_S of 7.5±0.2 estimated for the Wasatch fault.

We have determined the slip rate on the East Great Salt Lake fault from a combined interpretation of seismic reflection data (released by Amoco) and published depths of Pliocene and Quaternary time markers found in wells. The time markers include volcanic ashes, a basalt, and stratigraphic horizons identified from palynology. Results indicate vertical subsidence rates of 0.3 to 0.5 mm/yr near the fault. Taking subsurface fault dip into account, these rates translate into fault slip rates of 0.4 to 0.7 mm/yr, assuming that the sedimentation rates are controlled by subsidence along the fault. These slip rates are about half of those measured for the central segments of the Wasatch fault, which have average recurrence intervals for maximum earthquakes of about 2,000 years. This comparison suggests that each segment of the East Great Salt Lake fault has a recurrence interval of about 4,000 years. Coseismic displacement of the lake floor could generate large, damaging water waves in the Great Salt Lake.

3. We are evaluating the source properties of moderate-size earthquakes in Utah that have been well recorded at regional distances on the WWSSN and LRSM networks. The first event analyzed was the M_L 5.7 Logan earthquake of August 30, 1962. This earthquake is particularly important to understanding earthquake hazards of the Wasatch Front region because it is the only earthquake in Utah for which a strong ground motion record has been recorded. At our request, J. Dewey of the U.S. Geological Survey recently relocated this earthquake relative to the M_L 6.0 Pocatello Valley earthquake near the Utah-Idaho border. The epicenter he calculated is at 41°55.3'N, 111°38.0'W, in the Bear River Range and 14 km east of the East Cache fault, a major west-dipping normal fault in northern Utah.

Using the generalized inverse method of Nabelek, the source parameters obtained for the Logan event (primarily from long-period records), in cooperation with R. Westaway, Liverpool University, are as follows: (1) focal depth of 8±1 km, (2) strike of 12° to 15°, (3) dip of 45°, (4) rake of -80° to -90°, (5) seismic moment of 3×10^{17} N-M, and (6) source time function of 5 sec duration with a peak at 1 sec followed by a secondary peak at 3.5 sec. The focal mechanism is similar to the one obtained by Smith and Sbar (1974) from P-wave first motion data. The east-dipping nodal plane is the preferred fault plane based on the 50° to 60° eastward dip of the aftershock zone. This interpretation suggests anomalous downward movement of the Bear River Range block relative to Cache Valley on the west.

Reports and Publications

Arabasz, W.J., J.C. Pechmann, and E.D. Brown (1987). Observational seismology and the evaluation of earthquake hazards and risk in the Wasatch Front area, Utah, submitted to Assessment of Regional Earthquake Hazards and Risk Along the Wasatch Front, Utah, W.W. Hays and P.L. Gori, Editors, *U.S. Geol. Surv. Prof. Pap.*

Benz, H.M., and R.B. Smith (1987). Kinematic source modelling of normal-faulting earthquakes using the finite element method, *Geophys. J. R. Astr. Soc., 90,* 305-325.

Bjarnason, I.T., and J.C. Pechmann (1987). Contemporary tectonics of the Wasatch Front region, Utah, from earthquake focal mechanisms, submitted to *Bull. Seism. Soc. Am.*

Richins, W.D., J.C. Pechmann, R.B. Smith, C.J. Langer, S.K. Goter, J.E. Zollweg, and J.J. King (1987). The 1983 Borah Peak, Idaho, earthquake and its aftershocks, *Bull. Seism. Soc. Am., 77,* 694-723.

Thorbjarnardottir, B.S., and J.C. Pechmann (1987). Constraints on relative earthquake locations from cross correlation of waveforms, *Bull. Seism. Soc. Am., 77,* 1626-1634.

Great Earthquakes and Great Asperities, Southern California: A Program of Data Analysis

14-08-0001-G-1096

Lynn R. Sykes and Leonardo Seeber
Lamont-Doherty Geological Observatory of Columbia University
Palisades, New York 10964
(914) 359-2900

Investigations

During the period of this grant the principal investigators and their colleagues have carried out a number of major studies of earthquakes and tectonics of southern California. This work has resulted in three papers being published, one in press that will soon be published, one in preprint form that is nearly ready for journal submission and the final study "Fault mechanisms associated with the southern San Andreas fault: Seismicity of the eastern Transverse Ranges" by Williams, Sykes, Nicholson and Seeber is also in preprint form.

Results

The paper "Great earthquakes and great asperities, San Andreas fault, southern California" by Sykes and Seeber was published in *Geology* in December 1985. They find that the big bend region of the southern San Andreas fault consists of two great asperities that rupture infrequently in great earthquakes. The eastern knot near San Gorgonio Pass, which has not ruptured historically in a great event, is the main locus of plate motion, appears to break in great events every few hundred years and is more advanced in the cycle of strain accumulation than the western knot. The large size of these asperities results in the properties of these earthquakes being nearly invariant over many cycles of great shocks. An unusual sequence of moderate-size shocks within the eastern knot from 1940 to 1948 is an example of the type of precursory phenomena that might precede a great earthquake.

The paper "Seismicity and fault kinematics through the eastern Transverse Ranges, California : block rotation, strike-slip faulting and shallow-angle thrusts" by Nicholson, Seeber, Williams and Sykes, was published in the *Journal of Geophysical Research* in April 1986. This paper uses data from the southern California seismic network to study focal mechanisms and detailed distribution of earthquakes in the major tectonic knot in southern California near San Gorgonio Pass. Surprisingly, little seismic activity can be directly associated with major throughgoing faults. Seismicity is generally absent in the upper 5 km. This pattern of behavior appears to be typical of the inter-seismic period between great earthquakes. Great earthquakes in this area, which appear to have a repeat time of 300 to 500 years, are thought to mainly rupture the throughgoing faults. The predominant style of faulting above 10 to 12 km is oblique slip with a large reverse (thrust) component. The spatial distribution of relocated hypocenters and first-motion data suggest the presence of left-slip faults striking northeast. The pattern of faults in conjunction with an unusual set of normal and reverse focal mechanisms is interpreted as the clockwise rotation of the small set of crustal blocks subjected to regional right-lateral shear. At depths of greater than about 10 km seismicity defines a wedge-shaped volume undergoing pervasive internal deformation and a combination of strike-slip and low-angle thrust faults. A low-velocity seismic zone beneath the San Bernardino Mountains and the transition between block rotation and the deeper style of deformation may correspond to a major detachment under much of the region and would imply that the overthrust San Bernardino

Mountains are allochthonous. The present pattern of seismic deformation may change systematically as a region prepares to accommodate large right-lateral displacements in an eventual future great earthquake.

The paper "Seismic evidence for conjugate slip and block rotation within the San Andreas fault system, southern California" by Nicholson, Seeber, Williams and Sykes was published in *Tectonics* in August 1986. This paper expands a number of the ideas developed in the previous paper for the region near San Gorgonio Pass to other areas of southern California. Again, the pattern of seismicity for small to moderate size earthquakes of the past ten years indicates that much of that activity is presently occurring on secondary structures, several of which are oriented nearly orthogonal to the strikes of major throughgoing faults. Slip along these secondary transverse features is predominantly left-lateral and is consistent with the reactivation of conjugate faults by the current regional stress field. A number of small to moderate size crustal blocks are defined which are undergoing contemporary rotation in response to the regional stress field. A rotational block model accounts for a number of structural styles characteristic of strike-slip deformation in California including; variable slip rates and alternating transtensional and transpressional features observed along strike of major wrench faults; domains of evenly-spaced antithetic faults that terminate against major fault boundaries; continued development of bends and faults with large lateral displacements; anomalous focal mechanisms; and differential uplift in areas otherwise expected to experience extension and subsidence. Low-angle structures like detachments may be involved in the contemporary tectonics of southern California. Changes in the translation of small crustal blocks and their relative rotation parts could represent important premonitory changes prior to large to great earthquakes along major throughgoing faults.

The paper "Block rotation along the San Andres fault system in California: long-term structural signature and short-term effects in the earthquake cycle" by Seeber and Nicholson, which is in preprint form, describes the rotation of small crustal blocks located between closely spaced subparallel strike-slip faults. Block rotation can allow one of these strands to grow at the expense of the other. Not only structural and paleomagnetic data, but also recent small earthquakes provide evidence for block rotation of this type. Associated seismicity often occurs on left-lateral secondary faults that strike northeast and are symptomatic of block rotation. Examples of this phenomena are illustrated for Coyote ridge, which is located between branches of the San Jacinto fault zone of southern California and the complex rupture involved in the Coyote Lake earthquake of 1979 along the Calaveras fault of northern California.

Bogen and Seeber (preprint) in their paper "Late Quaternary block rotation within the San Jacinto fault zone, southern California" report abundant structural and seismological evidence for block rotation during the past 0.94 million years or less in the region between two major branches of the San Jacinto fault zone between Anza and Borrego in southern California.

Williams, Sykes, Nicholson and Seeber (in preparation) examined fault mechanisms and seismicity in the vicinity of the southernmost San Andreas fault and the eastern Transverse Ranges of southern California. Data from the southern California seismic network for the period 1977 to 1985 were used to study precise locations of small earthquakes, focal mechanisms and the state of stress. The southernmost San Andreas fault in the Coachella Valley is essentially quiescent at the microearthquake level. Relocation of earthquakes using only stations northeast of the San Andreas fault, proximal to the activity but outside the Salton trough does not seriously effect epicentral locations, suggesting the observed offset of epicenters from the San Andreas fault is not an artifact of the velocity models used. Many of the earthquakes in the broad region to the northeast of the San Andreas fault occur along steeply dipping, left-lateral faults striking northeasterly. Focal mechanisms involve strike-slip, normal fault or a combination of the two mechanisms. In contrast, reverse and strike-slip faulting characterize San Gorgonio Pass and the region to the west within the big bend region of southern California. These observations imply that relatively high normal stresses of tectonic origin are present across the San Andreas fault in San Gorgonio Pass, while lower normal stresses are found across the southernmost San Andreas fault from Palm Springs to the Salton Sea. One stress regime appears to be associated with long repeat times for great earthquakes within the two major tectonic knots in southern California whereas shorter repeat times are indicated for the other stress regimes near the southernmost San Andreas fault.

The paper "Secondary faults associated with the 7 July 1986 Palm Springs earthquake rupture on the San Andreas fault" (in preparation) by Seeber, Armbruster, and Tuttle discusses a well defined aftershock zone that delineates the 10 km long NW rupture of the 1986 Palm Springs earthquake. Fault plane solutions in the main zone of aftershocks show consistently oblique right-lateral and reverse slip on a NW plane dipping northeasterly, and reflect the geometry of slip in the main shock. The sharp boundaries of the aftershock zone appear to coincide with the intersection between the main strand and secondary faults. Several secondary reverse and left-lateral faults were recognized primarily from seismicity during the aftershock sequence. They observed that the lower limit of the Palm Springs earthquake, about 13 km deep, coincides with the upper limit of a widespread zone of midcrustal seismicity in the San Gorgonio Pass area and is bounded by the Palm Spring earthquake, locally, and the Mission Creek fault, regionally. This zone may be associated with a detachment as observed on fault plane solutions.

Pacheco and Nabelek (preprint) studied the source processes of three moderate California earthquakes which occurred in July 1986. They determined that the July 8, 1986 M_L=5.9 Palm Springs earthquake had a simple rupture with most of the seismic moment released in the first three seconds by a single pulse. The faulting mechanism is right-lateral strike-slip with a sizable reverse component consistent with uplift of the Banning fault. The M_L=5.3 earthquake offshore of Oceanside on July 13, 1986 consists of 2 pulses that released most of the moment in the first 3 sec. The source mechanism indicates reverse faulting and is consistent with the missing component of plate convergence not taken up by the onshore strike-slip systems. The source function of the M_L=6.2 Chalfant Valley earthquake which occurred on July 21, 1968 indicates that in a 4 sec time window three asperities were broken. The average parameters for this rupture indicate right-lateral strike-slip motion, with a sizable normal component.

The paper "Importance of Transverse features along the southern San Jacinto fault zone, California" (in preparation) by Petersen, Seeber and Hudnut uses a teleseismic long period P and SH body wave inversion technique to analyze the waveforms of the April 28, 1969 Coyote Mountain earthquake M_L = 5.8 and reanalyze the April 9, 1968 Borrego Mountain earthquake M_L = 6.5 It was found that some of the energy of these earthquakes may have been released on secondary structures. In addition, they found that velocities tend to be higher on the western side of the Coyote Creek fault than to the east in the vicinity of Borrego Mountain. Recent seismicity (1981-86) has been analyzed which suggests that earthquake activity has been occurring on secondary faults and that seismicity on one fault may directly influence seismicity patterns on an adjacent fault.

Continuing Studies

Continuing work on earthquakes and tectonics of southern California includes the following studies: examination of regional time-space patterns of seismicity for the period 1932 to 1986 (Seeber, Armbruster, Williams and Sykes); analysis of teleseismic source mechanisms of July 1986 earthquake (M_L>5) (Pacheco and Nabelek); documentation of triggered slip on the southern San Andreas after the July 8, 1986 North Palm Springs earthquake (Williams, Fagerson, and Sieh); secondary faults and the 1986 North Palm Springs rupture on the main strand of the San Andreas (Seeber and Armbruster); relationships between seismicity patterns on adjacent faults (Petersen and Seeber).

Publications

Bogen, N., and L. Seeber, Late Quaternary block rotation within the San Jacinto fault zone, southern California, submitted for publication, 1987.

Nicholson, C., L. Seeber, P. Williams, and L. R. Sykes, Seismicity and fault kinematics through the eastern Transverse Ranges, California: Block rotation, strike-slip faulting and shallow-angle thrusts, *J. Geophys. Res., 91*, 4891-4908, 1986.

Nicholson, C., L. Seeber, P. L. Williams, and L. R. Sykes, Seismic deformation along the southern San Andreas fault, California: Implications for conjugate slip and rotational block tectonics, *Tectonics, 5*, 629-649.

Pacheco, J., and J. Nabelek, Source mechanisms of three moderate southern California earthquakes of July 1986 (abstract), *EOS, Trans. AGU, 67*, 1091, 1986.

Petersen, M.D., L. Seeber, K. Hudnut, Importance of transverse features along the southern San Jacinto fault zone, California (abstract), submitted *EOS*, 1987.

Seeber, L., and C. Nicholson, Block rotation along the San Andreas fault system in California: Long term structural signature and short term effects in the earthquake cycle, prerprint, 1987.

Seeber, L., J. G. Armbruster, P. Williams, and L. R. Sykes, Faults antithetic to the San Andreas delineated by seismicity in the San Gorgonio Pass of southern California (abstract), *EOS, Trans. AGU, 67*, 1200, 1986.

Seeber, L., J. G. Armbruster, M. Tuttle, Secondary faults associated with the 7 July 1986 Palm Springs earthquake rupture on the San Andreas fault (abstract), *Seismol. Soc. Am. Abstracts with Programs*, pp. 20, 1987.

Seeber, L., and J. Armbruster, Secondary faults as agents for segmentation of the master strands in southern California (abstract), *IUGG Conference* , Vancouver, Canada, Aug. 17-22, 1987.

Sykes, L. R., and L. Seeber, Great earthquakes and great asperities, San Andreas fault, southern California, *Geology, 113*, 835-838, 1985.

Williams, P., S. Fagerson, and K. Sieh, Triggered slip of the San Andreas fault after the July 8, 1986 North Palm Springs earthquake (abstract), *EOS, Trans. AGU, 67*, 1090, 1986.

Williams, P. L., L. R. Sykes, C. Nicholson, and L. Seeber, Seismicity and state of stress in the eastern Transverse Ranges: Implications of seismic potential of the southern San Andreas fault, California, in preparation.

Seismic Reflection Investigations of Mesozoic Basins, Eastern U.S.

9950-03869

John D. Unger
Branch of Geologic Risk Assessment
U.S. Geological Survey
922 National Center
Reston, VA 22092
(703) 648-6790

ONGOING INVESTIGATIONS

1. To consolidate and synthesize the available seismic reflection information that pertains to the internal and external structure of Mesozoic basins, with special emphasis on the hypocentral area of the present seismicity of Charleston, South Carolina and the Ramapo fault zone in New Jersey and Pennsylvania.

2. To use 2-D synthetic seismic reflection models of the basement structure along selected seismic reflection traverses in the Charleston and Ramapo regions as an aid to processing and interpretation of the seismic reflection data and to allow the use of ray-tracing algorithms to be used for earthquake relocation.

3. To use 2- and 3- dimensional GIS (Geographical Information System) techniques to display, analyze, and interpret geological and geophysical data collected in and around Mesozoic basins and other seismogenic structures in the Eastern U.S.

4. To investigate the role of Mesozoic basins as seismogenic tectonic features in the Eastern U.S.

RESULTS

1. The seismic data I have acquired are being analyzed for their quality and suitability for further study. Jean Krespi, a post doctoral structural geologist working with Al Froelich, has utilized some of these data in her study of the internal structure and geologic history of eastern Mesozoic basins. She also used my ray migration program to determine the true dips of the reflectors in the sections. I have been using the data as input to Dynamic Graphics' Interactive Surface Modelling program to attempt to construct 3-dimensional models of some of the basins where good seismic reflection, gravity, and magnetic data exist. This aspect of my project shows good promise for future research related to using GIS techniques to unravel geological and geophysical problems.

REPORTS

Unger, J. D., 1986, A microcomputer program to migrate line drawings of seismic reflection profiles, U.S.G.S. Open-File Report 86-296, 31 pages.

Unger, J. D., 1986, A simple technique for analysis and migration of seismic reflection profiles from the Mesozoic basins of The Eastern United States, U.S.G.S. Bulletin 1776, in press.

DEVELOPMENT OF A PREDICTION MODEL FOR A POSSIBLE 1994 ± 1.5 KAOIKI MAINSHOCK

14-08-0001-G1325

Max Wyss
CIRES/Dept. of Geological Sciences
University of Colorado
Boulder, CO 80309-0449
(303) 492-5642

Investigations

(1) Macroseismic location of historic Kaoiki earthquakes.
(2) Moment-magnitude relation for Hawaii.
(3) A proposed model for the 1868 great Kau earthquake.
(4) The source model of the November 1975 Kalapana ($Ms = 7.2$) earthquake.

Results

(1) In collaboration with personnel of the Hawaii Volcano Observatory we are compiling a catalog of macroseismic maps for historic mainshocks in Hawaii. The purposes are to evaluate whether any of the historic earthquakes before 1941 could have occurred in the Kaoiki source volume, and to evaluate the seismic hazard in general in Hawaii. We have been able to find data for drawing macroseismic maps for approximately 30 shocks which occurred in the period 1868-1983. Based on the felt reports for recent events with known location and magnitude we developed relationships between magnitude and epicentral distance to given intensities. Based on these relationships we will estimate the magnitudes of earlier historic mainshocks It appears that some historic earthquakes may be attributed to the Kaoiki fault zone, but for others the data are not detailed enough to allow a choice between Kaoiki, Hilea, Kilauea and Mauna Loa as source areas. The catalog of macroseismic maps for historic earthquakes in Hawaii will be finished at the end of the grant period.

(2) Based on seismic spectra of 960 Hawaiian earthquakes we propose relationships relating the seismic moment (M_o) to the local (M_L) and the duration magnitude (M_D). The data consisted of two sets, one covering the range $0.7 \leqslant M_L \leqslant 2.5$ and the period December 1976 to October 1983, the other covered the range $2.8 \leqslant M_L \leqslant 3.9$ and the period March 1963 to December 1981.

The proposed relationships are

$$\log M_o = 16.59 + 1.1 M_L$$

and

$$\log M_o = 17.3 + 0.84 M_D$$

These relationships are similar to those found for other tectonic areas.

(3) On April 2, 1868 a destructive earthquake occurred in southern Hawaii which was felt at 600 km distance, and for which ground shaking of intensity VIII reached 200 km distance. Its rupture area probably included the Kaoiki source volume. Based on the felt area size and on the very strong destruction in the epicentral area it is estimated that the magnitude of this earthquake must have been at least 8. One fore- and one aftershock probably exceeded magnitude 6.5.

The foreshock sequence lasted 5 days, the aftershocks lasted for years to perhaps a decade. It appears that this earthquake was one of the very few largest events in historic time in the United States, excluding Alaska, but its return period is unknown.

It is proposed that the source of this earthquake was slip of the upper crust by about 8 m towards the SE along a near horizontal plane at 9±2 km depth. The rupture plane must have had dimensions of at least 50x80 km. It is proposed that its eastern edge extended from near Mauna Loa's summit to the south along the volcano's southwest rift. In this model magma intrusions into Mauna Loa and its southwest rift provide the stresses which act perpendicular to the rift and which push the volcano's southwest flank away from the edifice of the island of Hawaii. The oceanic sediment layer upon which this edifice is deposited acts as a layer of weakness containing the fault plane. This model explains the eruptive pattern of Mauna Loa and its southwest rift, as well as the growing separation between the southwest rift zones of the two volcanos Kilauea and Mauna Loa.

Geodetic monitoring of southern Hawaii, particularly of the area between the two active volcano's southwest rifts, could test the above hypothesis, and lead to an estimate of the recurrence time.

(4) In a recent paper in J. Geophys. Research (92, 4827, 1987) Eissler and Kanamori propose that the tectonic event of 29 November 1975 on the south coast of Hawaii was a landslide not an earthquake. In their paper they omitted many tectonic facts which strongly suggest that this event was indeed an earthquake. Because the understanding of the 1975 Kalapana earthquake is important to the understanding of seismic hazard in Hawaii we submitted a comment to J. Geophys. Research in which we point out the facts supporting the generally accepted model for the Kalapana 1975 earthquake (Wyss and Kovach, 1988).

Publications

Zuniga, F.R., M. Wyss and F. Scherbaum, A moment-magnitude relation for Hawaii, *Bull. Seis. Soc. Am.*, in press, 1987.

Wyss, M., A proposed source model for the great Kau, Hawaii, earthquake of 1868, *Bull. Seis. Soc. Am.*, submitted, 1988.

Wyss, M. and R. L. Kovach, Comments on "A single force model for the 1975 Kalapana, Hawaii, earthquake" by H.K. Eissler and H. Kanamori, *J. Geophys. Res.*, submitted, 1988.

Wyss, M. and R. Koyanagi, Macroseismic maps for earthquakes in Hawaii, 1868 to 1983, in preparation, 1988.

Geologic studies for seismic zonation of the Puget lowland

Brian F. Atwater
Branch of Western Regional Geology
University of Washington AJ-20
Seattle, Washington 98195
(206) 442-2927 FTS 399-2927

INVESTIGATIONS

Field description and radiocarbon dating of buried Holocene wetlands exposed at low tide in southwestern Washington. Chief goal: to test the possibility that the burial of these wetlands resulted from subsidence of great areal extent, as should have been the case if the subsidence accompanied earthquakes of magnitude 8 or 9

RESULTS

Buried lowland soils suggest that much of coastal southwestern Washington underwent many decimeters of rapid subsidence at eight or more times in the past 5000 years. The buried soils, each typically overlain by upward-fining intertidal mud, crop out widely between the Copalis and Columbia Rivers (Tables 1, 2). They are especially well exposed at Grays Harbor and northern Willapa Bay, where the youngest five soils (1-5, Table 2) form an apparently regional sequence in which the uppermost, middle, and lowermost soils are distinct and the other two are faint (Table 2). Two features seen in outcrop suggest that the last five episodes of subsidence recurred at dissimilar intervals. (1) Stumps rooted in the soils record a more advanced stage of vegetational succession for the distinct than for the faint soils. (2) Only the upper two distinct soils (soils 1 and 3, Table 2) developed conspicuous, organic-poor (E?) horizons in which the A or O horizon of the underlying soil has been mostly digested. Dissimilar recurrence intervals are also indicated by a suite of about 100 ^{14}C ages obtained chiefly from spruce roots in the soils, from sticks and rhizomes just above the soils, and from the peaty uppermost parts of the soils themselves (Table 3). These ages, though departing as much as 250 ^{14}C years from means for individual episodes of subsidence, imply that rapid subsidence occurred widely in SW Washington about 300, 1600(?), 1700, 2700, and 3100 sidereal years ago.

Vented sand, containing clasts of the mud through which it rose, buried a wooded wetland along the Copalis River about 1000 sidereal years ago (Fig. 1). The venting, probably due to strong shaking, does not seem have been accompanied by rapid subsidence along the Copalis River, at Grays Harbor, or at northern Willapa Bay. Rapid subsidence did occur about 1000 sidereal years ago, however, in northwesternmost Washington (Waatch River estuary, Tables 2 and 3) and, perhaps, near the Columbia River (Willapa Bay locality Be-1 and Columbia River locality De-1, Tables 2 and 3). In a recently published abstract (Atwater and others, 1987), I misinterpreted the sand along the Copalis River as having been vented during the subsidence episode of about 300 sidereal years ago (caption, Fig. 1).

REPORTS

Atwater, B. F., 1987, Evidence for great Holocene earthquakes along the outer coast of Washington state: Science, v. 236, p. 942-944.

Atwater, B. F., Hull, A. G., and Bevis, K. A., 1987, Aperiodic Holocene recurrence of widespread, probably coseismic subsidence in southwestern Washington: EOS [Transactions, American Geophysical Union], v. 68, issue of 3 November 1987.

Hull, A. G., 1987, Buried lowland soils from Willapa Bay, southwest Washington: Further evidence for recurrence of large earthquakes during the last 5000 years: EOS [Transactions, American Geophysical Union], v. 68, issue of 3 November 1987.

ADDITIONAL REFERENCE CITED

Obermeier, S. F., Gohn, G. S., Weems, R. E., Gelinas, R. L., and Rubin, Meyer, 1985, Geologic evidence for recurrent moderate to large earthquakes near Charleston, South Carolina: Science, v. 227, p. 408-411.

Table 1. Radiocarbon localities for buried Holocene wetlands in westernmost Washington
[Localities listed from north to south]

ACRONYM	NAME	LATITUDE (degrees and minutes)	LONGITUDE (degrees and minutes)	TOWNSHIP/ RANGE- 16TH SECTION [a]	7.5-MINUTE QUADRANGLE	LEVEL OF EFFORT	
						Person days [b]	C-14 ages
			WAATCH RIVER ESTUARY				
Wa-u	upper Waatch River	48 21.405	124 37.955	33N/15W-15M	Makah Bay	2	3
Wa-m	middle Waatch River	48 21.160	124 39.995	33N/15W-15N	Makah Bay	2	5
Wa-l	lower Waatch River	48 21.075	124 38.700	33N/15W-16Q	Makah Bay	1	1
			COPALIS RIVER ESTUARY				
Co-u	upper Copalis River	47 07.225	124 09.655	19N/12W-22K	Copalis Beach	2	3
Co-m	middle Copalis River	47 07.170	124 09.700	19N/12W-22K	Copalis Beach	2	5
Co-l	lower Copalis River	47 07.030	124 10.060	19N/12W-22N	Copalis Beach	1	2
			GRAYS HARBOR				
CC	Chenois Creek	47 02.38	124 01.85	18N/11W-22B	Copalis Crossing	1	1
Bl	Blue Slough	46 56.85	123 43.42	17N/08W-19G	Central Park	2	8
CR	Chehalis River	46 56.73	123 43.91	17N/08W-19F	Central Park	1	4
Jo-l	lower Johns River	46 54.41	124 00.04	16N/11W-02A	Westport	1	1
Jo-m	middle Johns River	46 54.095	123 59.105	16N/11W-01K	Hoquiam	1	2
Jo-u	upper Johns River	46 53.55	123 59.175	16N/11W-12C	Hoquiam	2	5
			WILLAPA BAY				
Wi	Willapa River	46 41.37	123 49.02	14N/09W-21D	South Bend	1	1
Wi-S	South Fork Willapa River	46 40.34	123 44.01	14N/08W-30E	Raymond	10	14
BC	Bay Center beach	46 37.82	123 57.42	13N/10W-37	Bay Center	1	1
Ni-l	lower Niawiakum River	46 37.77	123 54.53	13N/10W-10G	Bay Center	8	20
Ni-u	upper Niawiakum River	46 36.899	123 53.955	13N/10W-14E	Nemah	1	4
NO	north of Oysterville	46 34.970	124 01.35	13N/11W-27L	Oysterville	1	2
Ta	Tarlatt Slough	46 22.24	124 00.79	10N/11W-11E	Cape Disappointment	1	6
Be-l	lower Bear River	46 21.245	123 59.560	10N/10W-18G	Chinook	1	5
Be-u	upper Bear River	46 21.210	123 57.505	10N/10W-18G	Chinook	1	3
			COLUMBIA RIVER ESTUARY				
De-u	upper Deep River	46 20.07	123 41.95	10N/08W/20P	Rosburg	1	3
De-l	lower Deep River	46 19.86	123 41.77	10N/08W/20L	Rosburg	2	7
Gr	Grays River	46 19.37	123 39.83	10N/08W/28H	Rosburg	1	4

---

[a] Subdivision of sections:

D	C	B	A
E	F	G	H
M	L	K	J
N	P	Q	R

[b] Field work; excludes initial reconnaissance

Table 2. Soils of buried Holocene wetlands in westernmost Washington [Top line for each locality describes modern wetland]

LO-CAL-ITY (Ta-ble 1)	SOIL (local se-quence)	TYP-ICAL DEPTH (dm) [a]	KNOWN EXTENT (m) [b]		--------UPPERMOST 30 CM OF SOIL--------			--------LOWERMOST 20 CM OF OVERLYING DEPOSITS--------			
			K	I	A or O horizon [c]	Roots and rhizomes (excludes roots from overlying deposits) [d]	Estimated grain size [e]	Estimated grain size (excludes any basal sand) [e]	Laminae visible to naked eye [e]	Woody or leafy detritus [f]	Rhizomes [d]
							WAATCH RIVER ESTUARY				
Wa-u	Marsh; used for pasture										
	1	9	15	30	Silty peat	Triglochin	Silt	VF-F sand	None	Little	None
Wa-m	Marsh with few spruce trees; used for pasture										
	1	9	5	40	Peaty mud	Triglochin (many)	M-C silt	VF-F sand	None	Little	None
							COPALIS RIVER ESTUARY				
Co-u	Marsh with unidentified coastal (beach and dune?) grass										
	1	5	3	50	Peat	Spruce?	VF sand	Mud	VF sand	Much?	None
	x	9	3	20	Peat	Spruce	Clayey silt	VF sand with clasts of mud and peat			None
Co-m	Marsh with Potentilla and minor Juncus										
	1	8	3	250	Peat	Spruce	Clayey silt	Clayey silt	Basal VF sand	None?	Triglochin
	2	12	2	10	Peaty mud	Carex?	Clayey silt	Clayey silt	None	None	None?
	3	17	0	3c	Peat	n.d.	Clayey silt	Silt	Basal VF-F sand	Little	Carex?
Co-l	Marsh with Potentilla, Juncus, Jaumea, and Atriplex										
	1	16	3	15	Peat	Deschampsia	Clayey silt	Silt	Basal VF-F sand	None	Triglochin
							GRAYS HARBOR				
CC	Marsh with few spruce trees										
	1	5	10	10	Peat	Spruce	Mud	Mud	C silt partings	Much	n.d.

Table 2. Soils of buried Holocene wetlands in westernmost Washington--Continued

LO-CAL-ITY (Ta-ble 1)	SOIL (local se-quence)	TYP-ICAL DEPTH (dm) [a]	KNOWN EXTENT (m) [b]		--------UPPERMOST 30 CM OF SOIL--------			--------LOWERMOST 20 CM OF OVERLYING DEPOSITS--------			
			K	I	A or O horizon [c]	Roots and rhizomes (excludes roots from overlying deposits) [d]	Estimated grain size [e]	Estimated grain size (excludes any basal sand) [e]	Laminae visible to naked eye [e]	Woody or leafy detritus [f]	Rhizomes [d]
Bl	Natural levee with alder, crabapple, salal, and spruce										
	1	8	9	20	Mud, peaty mud	Spruce	Clayey silt	Clayey silt	C silt partings	Little	None
	2	14	15	20	Mud	One spruce stump	Clayey silt	Clayey silt	None	Little	None
	3	20	12	60	Peaty mud	Spruce	Clayey silt	Clayey silt	C silt partings	Much	None?
	4	23	20	20	Mud	None	Clayey silt	Clayey silt	None	Little	None
	5	29	30	30	Peaty mud	Spruce	Clayey silt	Clayey silt	C silt partings	None?	Carex
CR	Natural levee with salmonberry, spruce, Oenothera, Deschampsia, Carex obnupta										
	1	8	15	15	Peaty mud	Spruce	Mud	Mud	C silt parting	Much	Carex
	2	14	2	8	Peaty mud	Unidentified herbs	Mud	Mud	None	None?	None
	3	18	15	15	Peat	Spruce?	Mud	Mud	None	Much	Carex
	4	25	1	1	Mud	None	Mud	Mud	None	None	Carex?
Jo-l	Marsh with Deschampsia and Triglochin										
	1	10	10	120	Peaty mud	Triglochin (many)	Mud	Muddy VF sand	Sand and mud	None	None
Jo-m	Marsh with Deschampsia										
	1	15	100	300	Peaty mud	Potentilla	Mud	VF sandy mud	Sand and mud	None?	None
Jo-u	Marsh with Potentilla and Atriplex atop bank; mostly diked										
	1	9	10	30	Peat	Potentilla; moss?	Clayey silt	M-C silt	C silt partings	Much	None
	2	14	10	30	Mud	None	Clayey silt	M silt	Few; silty	None	None
	3	18	15	50	Peat	Spruce	Clayey silt	M silt	C silt partings	Much	None
	4	22	15	30	Mud	None	Clayey silt	M silt	C silt partings	None	None
	5	30	15	60	Peat	Potentilla, Descham.	Clayey silt	M silt	C silt partings	None	Triglochin

Table 2. Soils of buried Holocene wetlands in westernmost Washington--Continued

					--------UPPERMOST 30 CM OF SOIL--------			--------LOWERMOST 20 CM OF OVERLYING DEPOSITS--------			
LO-CAL-ITY (Ta-ble 1)	SOIL (local se-quence)	TYP-ICAL DEPTH (dm) [a]	KNOWN EXTENT (m) [b] K	I	A or O horizon [c]	Roots and rhizomes (excludes roots from overlying deposits) [d]	Estimated grain size [e]	Estimated grain size (excludes any basal sand) [e]	Laminae visible to naked eye [e]	Woody or leafy detritus [f]	Rhizomes [d]
							WILLAPA BAY				
Wi	Marsh										
	1	6	10	30	Peat	n.d.	Clayey silt	Clayey silt	Silt partings	Little	None
Wi-S	Marsh with Potentilla and Carex lyngbyei atop bank										
	1	10	10	100	Peaty mud	Spruce	Mud	Mud	Few; silty	Much	Carex
	2	15	2	3	Mud	None	Mud	Mud	None	Little	Carex
	3	18	7	100	Peaty mud	Spruce	Mud	Mud	Few; silty	Much	Carex
	4	22	3	40	Peaty mud	None	Mud	Mud	n.d.	n.d.	n.d.
	5	28	3	40	Peaty mud	Spruce	Mud	Mud	n.d.	Much	Carex
	6	32	3	40c	Peaty mud	Spruce	Mud	Mud	n.d.	Much	Carex?
	7	45	0	20c	Peaty mud	n.d.	Mud	Mud	n.d.	n.d.	Carex?
	8	55	0	20c	Peaty mud	n.d.	Clayey silt	Silt	n.d.	n.d.	Carex?
BC	Beach face with fossil stumps that are submerged at high tide										
	1	20	2	60	Peat	Spruce	Clayey silt	Clayey silt	C silt parting	Little	Triglochin
Ni-1	Marsh with Deschampsia										
	1	9	10	50	Peat	Spruce	Clayey silt	Clayey silt	Basal VF sand	Little	None
	2	12	2	50	Mud	None	Clayey silt	Clayey silt	M silt partings	None	None
	3	16	25	60	Peat	Spruce	Clayey silt	Clayey silt	None	Much	None
	4	21	3	50	Peaty mud	Unidentified rhizomes	Clayey silt	Clayey silt	C silt partings	Little	None
	5	26	20	50	Peat	Spruce	Clayey silt	Clayey silt	None	Little	None
	6	34	20	50	Peaty mud	None woody	Clayey silt	Clayey silt	None	Little	Triglochin

Table 2. Soils of buried Holocene wetlands in westernmost Washington--Continued

LOCALITY (Table 1)	SOIL (local sequence)	TYPICAL DEPTH (dm) [a]	KNOWN EXTENT (m) [b]		----------------UPPERMOST 30 CM OF SOIL-------------			--------LOWERMOST 20 CM OF OVERLYING DEPOSITS--------			
			K	I	A or O horizon [c]	Roots and rhizomes (excludes roots from overlying deposits) [d]	Estimated grain size [e]	Estimated grain size (excludes any basal sand) [e]	Laminae visible to naked eye [e]	Woody or leafy detritus [f]	Rhizomes [d]
Ni-u	Marsh with Deschampsia, Agrostis, Potentilla, Juncus										
	1	12	3	100	Peaty mud	Spruce	Clayey silt	Clayey silt	None	Little	Triglochin
	2	18	1	5c	Mud, peaty mud	None woody	Clayey silt	Clayey silt	None	None	None
	3	22	3	100	Peat	Spruce	Clayey silt	Clayey silt	None	Little	Triglochin
NO	Beach face with fossil stumps rooted near lower limit of live Distichlis										
	1	20	5	200	Peat	Spruce	Clayey silt	Silt	n.d.	Much	None
Ta	Marsh with Deschampsia, Agrostis, Potentilla, Achillea, Rumex										
	1	7	10	10	Peat	Western hemlock?	Clayey silt	Clayey silt	Basal VF sand	Little	Carex?
	2	10	2	10	Peaty mud	None	Clayey silt	Clayey silt	None	None	None
	3	15	2	10c	Peat	Western hemlock?	n.d.	Clayey silt	None	Much	None
Be-l	Shrubby marsh a few meters wide, between upland and channel; road metal in uppermost 20 cm of soil										
	1	10	1	7	Mud; spruce root system occupies most of soil site			Mud	Silt partings	Little	None
	2	14	5	5	Mud, peaty mud	Spruce	Mud	Mud	None	None	None
	3	20	6	6	Mud, firm	None	Mud	Mud	None	None	Triglochin
	4	24	6	6	Peaty mud	None	Mud	Mud	None	Little	Triglochin
Be-u	Diked(?) marsh with Potentilla and spruce										
	1	12	1	8	Peat; 2 spruce root systems occupy most of soil site			Mud	None	n.d.	None
	2(?)	This part of section exposed too poorly to indicate whether or not a faint soil is present between soils 1 and 3(?)									
	3(?)	20	5	8	Peat	Spruce and moss	Mud	Mud	None?	Much	None?

Table 2. Soils of buried Holocene wetlands in westernmost Washington--Continued

LOCALITY (Table 1)	SOIL (local sequence)	TYPICAL DEPTH (dm) [a]	KNOWN EXTENT (m) [b]		UPPERMOST 30 CM OF SOIL			LOWERMOST 20 CM OF OVERLYING DEPOSITS			
			K	I	A or O horizon [c]	Roots and rhizomes (excludes roots from overlying deposits) [d]	Estimated grain size [e]	Estimated grain size (excludes any basal sand) [e]	Laminae visible to naked eye [e]	Woody or leafy detritus [f]	Rhizomes [d]
							COLUMBIA RIVER ESTUARY				
De-u	Diked wetland; outcrop directly beneath dike										
	1	15	5	15	Peaty mud	Spruce	Clayey silt	Silt	None?	Much	None?
	2	19	3	15	Peaty mud	None?	Clayey silt	Clayey silt	None	None?	None
	3	21	3	15	Peat	None woody	Clayey silt	Silt	Plant fragments	Little	Carex
De-l	Diked wetland; outcrop directly beneath dike										
	1	16	17	22	Peaty mud	Spruce, 3 systems	Clayey silt	Silt	Plant fragments	Much	n.d.
	2	22	1	19	Mud, peaty mud	Willow?	Clayey silt	Clayey silt	None	Little	None
	3	29	19	19	Peaty mud	None	Clayey silt	Silt	C silt	Little	Carex
Gr	Natural levee with spruce, alder, and cedar; logged for first time in 1987										
	n+1	21	1	1	Peat	Spruce	Clayey silt	Silt	None	Little	None
	n+2	25	15	15	Peat	None woody	Clayey silt	Silt	None?	Much	None
	n+3	30	1	15c	Peat	None woody	Mud	Mud	n.d.	n.d.	Phragmites

Table 2. Soils of buried Holocene wetlands in westernmost Washington--Continued

[a] Datum is broadest surface of modern wetland except at Deep River (De-1, De-2), where datum is highest foliage made muddy by tidal water; such foliage is typically close to the level of broad, modern wetland at the other localities

[b] K, known from continuous exposure, as seen in natural outcrop or in excavation. I, inferred from discontinuous exposure or from cores (c), at least four of which penetrated the soil

[c] Muddy A horizons of buried soils 2 and 4 are typically darker (browner or blacker) but scarcely if any more organic than the mud above and below them

[d] Plant fossils: Carex, Carex lyngbyei; Deschampsia, Deschampsia caespitosa; Phragmites, Phragmites australis; Potentilla, Potentilla pacifica; spruce, Picea sitchensis; Triglochin, Triglochin maritima; western hemlock, Tsuga heterophylla

[e] VF, very fine; F, fine; M, medium; C, coarse. Mud denotes clayey silt or silty clay. Basal denotes lowermost few centimeters

[f] In lowermost few centimeters

Table 3. Radiocarbon ages on the burial of Holocene wetland soils in westernmost Washington

LOCALITY (acronym; Table 1)	AGE AND ERROR (C-14 yr B.P.) [a]		EVENT (local buried soil) [b]	MATERIAL [c], [d]	SAMPLE NUMBER		COLLECTOR [f]
					Field	Lab [e]	
WAATCH RIVER ESTUARY							
Wa-u	1,750	120	1	Stick	SL86-22A	RIDDL-366	A
Wa-u	1,220	110	1	Leaf base on rhizome in peat	SL86-22G	RIDDL-367	A
Wa-u	1,305	40	1	Peat; stored wet at room temperature	SL86-22C	USGS-2,369	A
Wa-m	1,100	110	1	Cone (8 seeds) ¦ (from same	SL86-32B1	RIDDL-369	A
Wa-m	850	130	1	Cone (scale) ¦ cone)	SL86-32B2	RIDDL-370	A
Wa-m	550	340	1	Rhizomes high in soil 1	SL86-32A2	USGS-2,373	A
Wa-m	1,080	80	1	Leaf bases on rhizomes high in soil 1	SL86-32A1	USGS-2,372	A
Wa-m	1,170	130	1	Leaf base on rhizome high in soil 1	SL86-32A	RIDDL-368	A
Wa-l	740	290	post-1	Rhizomes below terrace inset into soil 1	SL86-25A	USGS-2,370	A
COPALIS RIVER ESTUARY							
Co-u	700	50	post-2, pre-1	Root, detrital?; dropped onto vented sand?	A-40D	Beta-22,897	A
Co-u	1,050	100	post-2, pre-1	Roots, spruce; in peat below vented sand	A-40A	Beta-22,895	A
Co-u	1,210	80	post-2, pre-1	Stick in peat below vented sand	A-40C	Beta-22,896	A
Co-m	230	45	1	Root, spruce? ¦ (in big system;	SL86-66E	USGS-2,427	A+G
Co-m	235	40	1	Root, spruce ¦ from same tree?)	SL86-66D	USGS-2,428	A+G
Co-m	1,640	100	3	Stick	SL86-66C2	RIDDL-683	A+G
Co-m	1,673	80	3	Stick in peat	SL86-66B	RIDDL-682	A+G
Co-m	1,800	40	3	Peat; stored wet at room temperature	SL86-66A	USGS-2,429	A+G
Co-l	-1,310s		1	Rhizomes	SL86-65B	USGS-2,430	A+G
Co-l	12,080s	60	1	Peat; stored wet at room temperature	SL86-65A	USGS-2,431	A+G
GRAYS HARBOR							
CC	370	70	1	Root, spruce; in big system	JP-2A	Beta-22,898	P
Bl	240	80	1	Root, spruce; small	A-37N	Beta-22,385	A
Bl	1,820	50	2	Root, spruce; on stump with >87 rings	A-37K	Beta-22,384	A
Bl	1,820	100	3	Sticks and cones	A-37I	Beta-22,383	A
Bl	1,790	60	3	Root, spruce; in big system	A-37G	Beta-22,381	A
Bl	1,540	90	3	Peat, 260	A-37H	Beta-22,382	A
Bl	2,500	70	5	Root, spruce; in big system	A-37A	Beta-22,378	A
Bl	2,810	80	5	Root, spruce; small	A-37B	Beta-22,379	A
Bl	3,220	80	5	Peat, 200	A-37C	Beta-22,380	A
CR	80	50	1	Root, spruce; on stump 30-40 cm diameter	A-19F	Beta-22,003	A
CR	1,640	80	2	Peat, 340	KB-21A	Beta-22,009	B
CR	1,600	60	3	Sticks and cones	A-19D	Beta-22,002	A
CR	1,700	70	3	Peat, 400	A-19C	Beta-22,001	A
Jo-l	310	70	1	Rhizomes	KB-25A	Beta-22,012	B
Jo-m	330	50	1	Peat, 290	KB-23A	Beta-22,010	B
Jo-m	650	60	post-2, pre-1	Rhizomes below soil 1	KB-23B	Beta-22,011	B
Jo-u	310	60	1	Peat, 345	A-20M	Beta-22,008	A
Jo-u	1,500	70	3	Sticks and cones	A-20J	Beta-22,007	A
Jo-u	1,490	70	3	Root, spruce; in big system	A-20G	Beta-22,005	A
Jo-u	1,930	70	3	Peat, 360; largely sticks and needles	A-20H	Beta-22,006	A
Jo-u	3,070	80	5	Peat, 350	A-20B	Beta-22,004	A

Table 3. Radiocarbon ages on the burial of Holocene wetland soils in westernmost Washington--Continued

LOCALITY (acronym; Table 1)	AGE AND ERROR (C-14 yr B.P.) [a]		EVENT (local buried soil) [b]	MATERIAL [c], [d]	SAMPLE NUMBER		COLLECTOR [f]
					Field	Lab [e]	
				WILLAPA BAY			
Wi	720	70	post-2, pre-1	Rhizomes below soil 1	KB-92B	Beta-22,899	B
Wi-S	110	50	1	Root, spruce; in big system	A-15K	Beta-21,836	A
Wi-S	160	60	1	Root, spruce; in big system	A-15L	Beta-21,837	A
Wi-S	1,690	60	3	Cones	A-15J	Beta-21,835	A
Wi-S	1,740	50	3	Root, spruce; in big system	A-15H	Beta-21,833	A
Wi-S	1,870	80	3	Peat, 360	A-15I	Beta-21,834	A
Wi-S	2,460	70	4	Peat	A-15G	Beta-21,832	A
Wi-S	3,030	80	5	Sticks	A-15F	Beta-22,369	A
Wi-S	2,630	70	5	Root, spruce; small	A-15D	Beta-21,830	A
Wi-S	3,160	80	5	Peat	A-15E	Beta-21,831	A
Wi-S	3,090	60	6	Sticks	A-15C	Beta-21,829	A
Wi-S	3,300	70	6	Root, spruce; in big system	A-15A	Beta-21,827	A
Wi-S	3,050	70	6	Peat	A-15B	Beta-21,828	A
Wi-S	3,760	80	7	Peat	H1-A	Beta-21,838	H+B
Wi-S	4,290	80	8	Peat	H1-B	Beta-21,839	H+B
BC	330	20	1	Root, spruce; on stump	W-1	QL-4,148	W+M
Ni-l	230	70	1	Root, spruce ¦ (in big system;	SL86-106O	Beta-19,839	A
Ni-l	250	60	1	Root, spruce? ¦ from same tree?)	SL86-106P	Beta-19,840	A
Ni-l	360	70	1	Root, spruce; in big system	A-1F	Beta-22,368	A
Ni-l	1,800	70	3	Stick (or root?)	SL86-106K1	Beta-19,837	A
Ni-l	1,740	70	3	Root (or stick?)	SL86-106L	Beta-19,838	A
Ni-l	2,590	80	4	Stick	SL86-106H	Beta-19,836	A
Ni-l	2,530	100	4	Sticks and cones	A-2A+B	Beta-21,826	A
Ni-l	2,590	60	4	Stick	A-1N1	Beta-22,370	A
Ni-l	2,510	80	4	Stick	A-1N2	Beta-22,371	A
Ni-l	2,258	75	4	Stick in peat	SL86-106I	RIDDL-686	A
Ni-l	2,800P		4	Peat; stored wet at room temperature	SL86-106J	USGS-2,539	A
Ni-l	3,190	110	5	Root, spruce; small	SL86-106F	Beta-19,834	A
Ni-l	2,840	70	5	Root, spruce; small	SL86-106G	Beta-19,835	A
Ni-l	2,920P		5	Peat; stored wet at room temperature	SL86-106E	USGS-2,538	A
Ni-l	2,790	120	5	Peat, 400	A-1D	Beta-21,824	A
Ni-l	3,320	80	6	Rhizomes	A-1C	Beta-21,823	A+S
Ni-l	3,063	80	6	Stick	SL86-106B	RIDDL-684	A
Ni-l	3,230	60	6	Stick	A-1B	Beta-21,822	A
Ni-l	3,262	80	6	Stick in peat	SL86-106C	RIDDL-685	A
Ni-l	3,570	70	post-7, pre-6	Rhizomes below soil 6	A-1E	Beta-21,825	A
Ni-u	330	40	1	Rhizomes	SL86-45F	USGS-2,396	A
Ni-u	35	45	1	Stick	SL86-45E	USGS-2,394	A
Ni-u	1,930	90	3	Sticks (2)	SL86-45B	USGS-2,393	A
Ni-u	1,590	90	3	Stick	SL86-45B3	USGS-2,395	A
NO	70	120	1	Sticks	A-33D1+2	Beta-22,893	A
NO	70	70	1	Root, spruce; on stump with about 100 rings	A-33E	Beta-22,894	A
Ta	90	70	1	Sticks (2)	A-21K	Beta-22,175	A
Ta	180	60	1	Root, western hemlock?	A-21J	Beta-22,174	A
Ta	430	60	1	Peat, 385	A-21G	Beta-22,173	A
Ta	1,720	100	3	Sticks	A-21C	Beta-22,172	A

Table 3. Radiocarbon ages on the burial of Holocene wetland soils in westernmost Washington--Continued.

LOCALITY (acronym; Table 1)	AGE AND ERROR (C-14 yr B.P.) [a]		EVENT (local buried soil) [b]	MATERIAL [c], [d]	SAMPLE NUMBER		COLLECTOR [f]
					Field	Lab [e]	
Ta	1,750	80	3	Roots, western hemlock?	A-21A	Beta-22,170	A
Ta	2,060	70	3	Peat, 420	A-21B	Beta-22,171	A
Be-l	500	60	1	Root, spruce; in big system	A-17E	Beta-21,997	A
Be-l	1,130	60	2	Root, spruce; in big root system	A-17D	Beta-21,996	A
Be-l	1,910	80	3	Rhizomes	A-17C	Beta-21,995	A
Be-l	2,390	70	4	Rhizomes	A-17B	Beta-21,994	A
Be-l	2,640	90	4	Peat, 335	A-17A	Beta-21,993	A
Be-u	470	60	1	Root, spruce; on stump about 1.5 m diameter	A-18C	Beta-22,000	A
Be-u	1,840	70	3(?)	Peat, 350-400; largely moss	A-18B	Beta-21,999	A
Be-u	2,290	80	pre-3(?)	Rhizomes below soil 3	A-18A	Beta-21,998	A
				COLUMBIA RIVER ESTUARY			
De-l	180	70	1	Root, spruce ¦ (in big systems but	A-22J	Beta-22,178	A
De-l	570	50	1	Root, spruce ¦ from different trees)	A-22R	Beta-22,373	A
De-l	870	60	2	Stick	A-22Q	Beta-22,372	A
De-l	1,080	90	2	Root, willow?	A-22G	Beta-22,177	A
De-l	1,250	70	3	Sticks	A-22N	Beta-22,892	A
De-l	1,400	75	3	Sticks in peat	A-22M	Beta-22,891	A
De-l	1,620	60	3	Peat, 340	A-22B	Beta-22,176	A
De-u	150	50	1	Cones	KB-52H	Beta-22,181	A
De-u	490	70	1	Root, spruce; on stump about 1 m diameter	KB-52G	Beta-22,180	A
De-u	1,350	70	3	Peat, 450-500	KB-52F	Beta-22,179	A
Gr	850	100	n+1	Roots (s), spruce; small	A-36G1	Beta-22,376	A
Gr	1,560	60	n+1	Peat, 450	A-36G2	Beta-22,377	A
Gr	1,560	70	n+2	Peat, 435	A-36D	Beta-22,375	A
Gr	1,720	70	n+3	Peat, 400	A-36A	Beta-22,374	A

Table 3. Radiocarbon ages on the burial of Holocene wetland soils in westernmost Washington--Continued

[a] B.P., before A.D. 1950. Delta C-13 assumed to equal -25 parts per thousand. P, preliminary age; s, age probably spurious, being too modern (USGS-2430) or too ancient (USGS-2431).

[b] Buried soils numbered from uppermost (1) to lowermost (higher numbers) in the local sequence (Table 2). Use of the same number does not necessarily imply correlation among localities. Limiting ages: "post-" means that the dated material probably accumulated long after burial of the indicated soil; "pre-" means that the material should significantly predate burial of the soil. Along Copalis River, at locality Co-u, soil x is buried only by vented sand. For Grays River (Gr) soils, n equals 1, 2, or 3

[c] Stratigraphic setting of dated material with respect to top of dated soil (unless noted otherwise):
rhizomes--10-30 cm above;
sticks and cones--0-3 cm above;
peat--0-1 cm below;
root--0-20 cm below.
Rhizomes, all of Triglochin maritima, include leaf bases that were attached to them. Cones and spruce roots are Picea sitchensis (Sitka spruce). Dated parts of woody roots come from outermost 10-30 rings and exclude bark. Spruce roots:
on stump--traced to stump that seems rooted solely in the buried soil;
in big system--though stump not observed, dated root is part of system of large (>20 cm diameter) roots that seem anchored solely in the buried soil;
small--chiefly <3 cm diameter; source tree probably lived on the buried soil but conceivably could have lived on a younger soil.
"Peat" signifies muddy peat and peaty mud in the O or A1 horizon of the buried soil. Three-digit number following "peat" gives moisture content as 100(w/d), where w is wet weight and d is dry weight

[d] Unless noted otherwise, samples were frozen within 24 hours of collection, then dried at 50-100 degrees Celsius. For samples stored wet at room temperature, such storage lasted no more than 10 weeks

[e] Counting methods: Beta, liquid scintillation; QL and USGS, proportional gas; RIDDL, tandem accelerator and mass spectrometer

[f] A, Brian F. Atwater; B, Kenneth A. Bevis; G, Wendy C. Grant; H, Alan G. Hull; M, Dennis R. McCrumb; P, James R. Phipps; S, Steven R. McMullen; W, Donald O. West

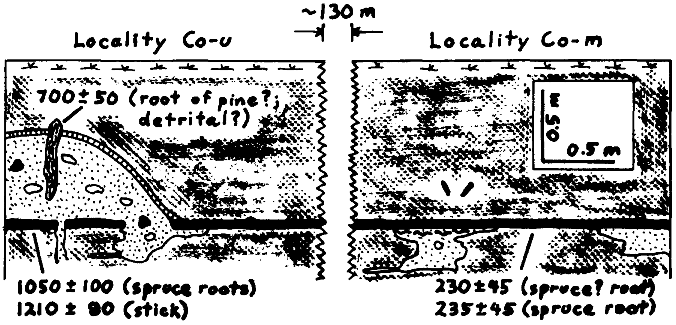

EXPLANATION

- ⊥ ⊥ MODERN A HORIZON--At surface of modern marsh
- \ / RHIZOMES--Of Triglochin maritima
- ▨ BLACK PEAT--Contains much decomposed wood; grades laterally into brown peat
- ▬ BROWN PEAT--Contains few to many spruce roots
- ⋯ MUD--Sandy in uppermost 50 cm of section
- ░ SAND--Very fine to fine, well sorted
- ○ ● INCLUSIONS--Clasts of peat (shaded) and of mud (unshaded)
- ∼∼ LAMINAE--Of peaty mud in uppermost part of sand body at locality Co-u; perhaps the incipient fill of a 1000-year-old sand blow (if so, analogous to layer 4 of Obermeier and others, 1985)

Figure 1. Simplified sketch of injected and vented sand along the Copalis River. After obtaining radiocarbon ages from locality Co-m, but before obtaining radiocarbon ages from locality Co-u, I interpreted the black peat at Co-u as degraded forest litter on a sand volcano that erupted onto a wooded wetland about 300 years ago (Atwater and others, 1987). The ages from Co-u, however, indicate that the volcano erupted about 1000 years ago. I now believe that the black peat represents the wetland surface of about 300 years ago where the 300-year-old surface climbs onto the volcano. I further believe that organic matter of the wetland surface of about 1000 years ago is abundantly preserved only beneath sand volcanoes; elsewhere this organic matter was probably digested in the soil of the 300-year-old surface, which lies at the same altitude as the 1000-year-old surface.
Probable sequence of events:

* Before about 1000 years ago--construction of spruce-dotted wetland;
* About 1000 years ago--injection and venting of sand onto this wetland, with little or no accompanying subsidence;
* About 300-1000 years ago--maintenance of wooded wetland, perhaps including the filling of a shallow sand-blow crater at locality Co-m;
* About 300 years ago--rapid lowering of this wetland into the intertidal zone, with little or no reactivation of 1000-year-old sand blows at localities Co-u and Co-m;
* Since 300 years ago--construction of high-level intertidal marsh, beginning with deposition on a Triglochin maritima mudflat

Frequency and Magnitude of Late Quaternary Faulting, Sierra Nevada, California

14-08-0001-G1334

Peter W. Birkeland and Margaret E. Berry
Department of Geological Sciences
University of Colorado
Boulder, Colorado, 80309
(303) 492-6985

Investigation

The project is designed to study the history of late Quaternary faulting along a portion of the eastern escarpment of the Sierra Nevada, California. The work is being conducted in the area between Bishop and McGee (N) Creeks, and entails the study of 1) the glacial stratigraphic sequences in valleys where deposits have been offset by faulting, and 2) the fault scarps which cut these deposits. The main objectives of this work are to determine a time frame for faulting, and to gain some understanding about rates of offset, frequency of faulting, and amounts of offset associated with the displacement events. Work on the project during the past five months has included the excavation and detailed field study of two trenches, and the laboratory analyses of soil and sediment samples collected in the trenches.

Results

1) One trench was located in the McGee (N) Creek valley, on a scarp cutting a Tioga recessional moraine. The other trench was located in the Bishop Creek area, on a scarp cutting a Tahoe or pre-Tahoe moraine. Both trenches were mapped at a scale of 1:20. Three soil profiles were described and sampled in each trench. In addition, 14C and thermoluminescence (TL) samples were collected from the trench in McGee (N) Creek. Analysis of these samples should provide some age control for the timing of fault generated colluvium deposition. Weathering characteristics of the scarp-colluvium in the Bishop Creek trench suggest that much of the fault displacement occurred prior to extensive grussification of boulders. To help understand the history of scarp-colluvium deposition in this trench, samples were also collected for petrographic analysis of the weathering features.

2) Fourty-two soil samples collected in the McGee (N) Creek trench have been analyzed for particle-size and organic carbon distributions. Results of these analyses show that in the <2-mm size fraction, the colluvial sediments have a uniform distribution of grain size, and a pachic distribution of organics. No clear-cut buried soils (easily recognized pedologic features) have been identified. Twenty-one samples from the Bishop Creek trench have been analyzed thus far for particle-size distribution. Additional analyses are currently in progress.

Surface Faulting Studies

9910-02677

M.G. Bonilla
Branch of Engineering Seismology and Geology
U.S. Geological Survey
345 Middlefield Road, MS 977
Menlo Park, CA 94025
(415) 329-5615

Investigations

Preparation of reports.

Results

Revisions were made in a report on the minimum magnitude associated with reported surface faulting, and in "Faulting and seismic activity," a report for Geological Society of America Centennial Volume CSV-3. The galley proofs of this report were corrected. Major revisions were made in the input data, figures, and text of a manuscript on the appearance of active faults exposed in exploratory trenches.

Reports

Bonilla, M.G., *in press*, Minimum earthquake magnitude associated with coseismic surface faulting: *Association of Engineering Geologists Bulletin*.

Bonilla, M.G., *in press*, Faulting and seismic activity, Chapter 10 in Kiersch, G.A., ed., The heritage of engineering geology--the first hundred years: *Geological Society of America Centennial Special Volume CSV-3*.

Crone, A.J., Machette, M.N., Bonilla, M.G., Lienkaemper, J.J., Pierce, K.L., Scott, W.E., and Bucknam, R.C., 1987, Surface faulting accompanying the Borah Peak earthquake and segmentation of the Lost River fault, central Idaho: *Seismological Society of America Bulletin*, v. 77, no. 3, p. 739-770.

Langer, C.J., Bonilla, M.G., and Bollinger, G.A., 1987, Aftershocks and surface faulting associated with the intraplate Guinea, west Africa, earthquake of 22 December 1983: *Seismological Society of America Bulletin*, v. 77, no. 5, p. 1579-1601.

10/87

Northern San Andreas Fault System

9910-03831

Robert D. Brown
Branch of Engineering Seismology and Geology
U.S. Geological Survey
345 Middlefield Road, MS 977
Menlo Park, California 94025
(415) 329-5620

Investigations

1. Continuing research and compilation of data on Quaternary deformation in the San Andreas fault system, for a planned volume summarizing current geologic and geophysical knowledge of the fault system.

2. Research and review of work by others on the tectonic setting and earthquake potential at Diablo Canyon Power Plant (DCPP), near San Luis Obispo, California. Activities are in an advisory capacity to the Nuclear Regulatory Commission (NRC) and are chiefly to review and evaluate data and interpretations obtained by Pacific Gas and Electric Company (PG&E) through its long-term seismic program.

3. Serve as vice-chairman on Policy Advisory Board, Bay Area Earthquake Preparedness Project (BAREPP). A joint project of the State of California and the Federal Emergency Management Agency, BAREPP seeks to further public awareness of earthquake hazards and to improve mitigative and response measures used by local government, businesses, and private citizens.

Results

1. Completed first draft of paper entitled Quaternary deformation of the San Andreas fault system in form for internal (USGS) review.

2. Participated in several field and workshop reviews related to DCPP and provided oral and written review comments to NRC. Coordinated USGS review and data acquisition efforts related to DCPP.

3. Provided informal oral and written data, analysis, and recommendations to BAREPP and other Policy Advisory Board members on geologic, seismologic, and management issues relating to earthquake hazard mitigation in California.

Reports

None.

10/87

Characteristics of Active Faults

9950-03870

Robert C. Bucknam
Branch of Geologic Risk Assessment
U.S. Geological Survey
Box 25046, MS 966, Denver Federal Center
Denver, Colorado 80225
(303) 236-1604

Investigations

1. Mapped three trenches dug across a fault scarp along the eastern foot of the Fish Springs Range, western Utah.

2. Continued photogrammetric monitoring of erosion of the fault scarp formed during the 1983 Borah Peak, Idaho, earthquake.

3. Continued compilation of data on active faults in the Great Basin for the Decade of North American Geology (DNAG) Neotectonic Map.

4. Coordinated compilation of data for International Geological Correlation Program (IGCP) Project 206 atlas on active faults.

Results

1. The prominent fault scarp along the eastern foot of the Fish Springs Range in Juab County, western Utah, has provided a high-quality set of data on the morphology of the scarp based on more than 40 profiles. A qualitative comparison of these data with similar data from the Bonneville shoreline scarp, the lack of a free face on the scarp and the geomorphic youthfulness of offset features across the scarp, suggest that the probable age of the scarp is several thousand years or less. Geologic relations along the scarp also indicate that it is the result of a single faulting event. The data provide a basis for estimating ages of other youthful fault scarps, but the data would be of greater value as a calibration point if there were independent evidence for the age of the scarp.

   M.N. Machette, A.J. Crone, and R.C. Bucknam mapped relations exposed in the walls of three trenches dug across the scarp in September 1987 in cooperation with the U.S. Fish and Wildlife Service. We collected datable material in stratigraphic positions that will more closely constrain the age of faulting. A second objective of the study was to make certain that the scarp is the result of a single faulting event.

   The length of the scarp between the northern and southern ends is about 17 km. The scarp has a 3.5-km-long northern section with a maximum throw of about 1.2 m and a 10-km-long southern section with a maximum throw of 3.3 m. There is a 4-km gap in the surface faulting that coincides with a prominent left-stepping en echelon offset and major transverse structure in the range.

A trench dug across the northern section of faulting exposed fine-grained sediments ranging from silty sands to clayey silts. The site is on a mudflat of Lake Bonneville sediments beyond the bajada but adjacent to the northern part of the Fish Springs Range. At this site, the fault is expressed at the surface as a distinct scarp with 0.4 m of surface relief and as a monocline in the near subsurface. No datable materials were exposed in this trench.

Two trenches were dug across the scarp on the bajada to the south in alluvial-fan and lacustrine gravels of Lake Bonneville. Relationships exposed in the trenches showed evidence only of a single faulting event. Charcoal and gastropods associated with the faulted deposits and the colluvial wedge were collected and will be submitted for radiocarbon dating using the TAMS facility. Ages derived from these samples will provide constraints on the time of faulting independent of the broad estimate of several thousand years before present derived from the surface morphology of the scarp.

2. Documentation of the erosion of scarps formed by the 1983 Borah Peak, Idaho, earthquake has been carried out since 1985 using close-range photogrammetric methods in collaboration with Sherman Wu, Branch of Astrogeology, Flagstaff. The procedures are briefly described under this project in the previous report in this series (Summaries of Technical Reports, Volume XXIII, U.S. Geological Survey Open-File Report 87-63, p. 49-50).

   An isobase map of changes in the scarp between October 1985 and May 1986 (fig. 1) was prepared from contour maps of the scarp, drawn on a vertical datum and 2-cm contour interval. The isobase map shows most of the scarp has retreated about 5 cm with local areas showing more than 15 cm of retreat. The 5-cm value is associated with raveling of the sandy gravel matrix of the alluvium exposed in the scarp. The larger values are closely associated with the dislodgment of cobbles and boulders from the scarp face.

   Preliminary evaluation of data from a June 1987 survey shows much less retreat occurred during the 1986-87 winter than during the preceding winter. The 1986-87 winter was generally very dry in contrast to the preceding winter. Several more seasons of monitoring may permit semiquantitative associations of the rate of retreat with precipitation and temperature, particularly precipitation during periods with freeze-thaw cycles.

3. Compilation of a map of faults in the Great Basin with evidence of late-Quaternary through historic movement for the DNAG neotectonic map was about 90 percent complete at the end of September 1987. Data have been digitized to allow easy editing and plotting.

4. A major objective of IGCP Project 206 (A Worldwide Comparison of the Characteristics of Major Active Faults) is the compilation of maps and other data on selected active faults. The data, much of which is previously unpublished, are being prepared for publication in an atlas

format. The final project meeting is to be held June 18-July 7, 1989, in the United States, immediately preceding the International Geological Congress.

Reports

Andrews, D.J., and Bucknam, R.C., 1987, Fitting degradation of shoreline scarps by a model with nonlinear diffusion: Journal of Geophysical Research (in press).

Barnhard, T.P., and Dodge, R.L., 1987, Map of fault scarps formed in unconsolidated sediments, Tooele 1°X1° quadrangle, Utah: U.S. Geological Survey Miscellaneous Field Studies Map, scale 1:250,000 (in press).

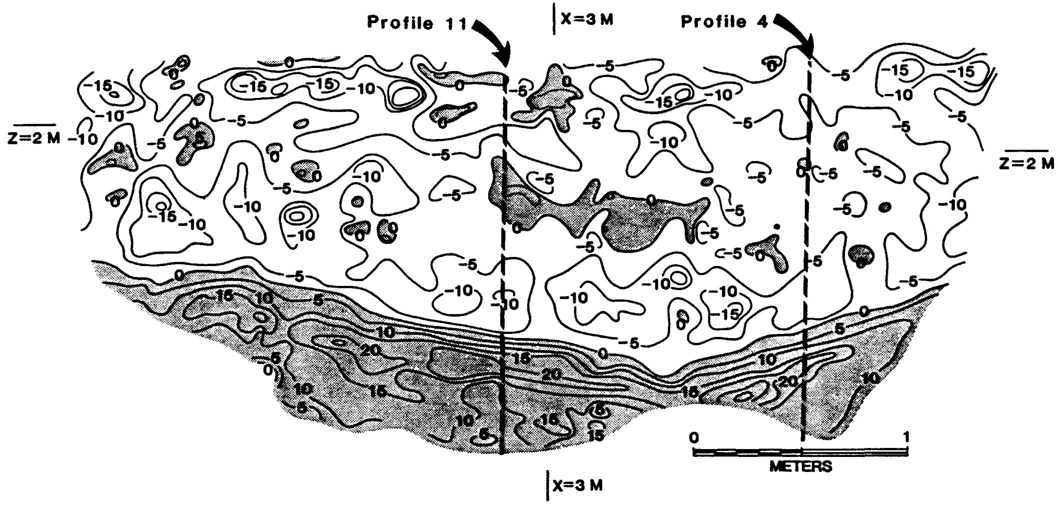

FIGURE 1.--Isobase map, contours in centimeters, drawn relative to a vertical datum plane showing changes along a section of 1983 fault scarp at Borah Peak, Idaho, area. Z is a horizontal axis parallel to the scarp, X is a vertical axis. Negative numbers reflect loss of material relative to vertical datum plane. Gray pattern shows areas of gain of material. Profiles 4 and 11 are shown in the open-file report referenced in the text.

Late Quaternary Slip Rates on Active Faults of California

9910-03554

Malcolm M. Clark
Branch of Engineering Seismology and Geology
345 Middlefield Road, MS 77
Menlo Park, CA 94025
(415) 329-5624, FTS 459-5624

Investigations

Recently active traces of Calaveras fault at San Felipe Creek (K.K. Harms, J.W. Harden, M.M. Clark). *See also J.W. Harden, this volume.*

Results

The drainage pattern of San Felipe Creek upstream from Anderson Reservoir has been controlled by lateral and vertical movement along the Calaveras fault. During late Quaternary time, the fault displaced several terraces of San Felipe Creek, and the place where the creek crosses the fault shifted abruptly southeastward by more than 1 km. We have described 24 soils on 6 of the displaced terraces. We will use the Harden soil index to help constrain the ages of these surfaces.

The oldest terrace southwest of the fault that is related to the present stream course dates the time that a gap in the NE block lined up with a gap on the SW block to allow the abrupt shift in location of the channel. These gaps have since moved a maximum of 550 m relative to each other. A charcoal sample collected at a 235 cm depth on this oldest terrace yielded a radiocarbon age of 38,400 ± 1800 y. Assuming that this is a minimum age and using the maximum offset results in a maximum slip rate of 15 mm/yr at this site.

Reports:

Lubetkin, L.K.C., and Clark, M.M., 1987, Late Quaternary fault scarp at Lone Pine, California; location of oblique slip during the great 1872 and earlier earthquakes: *Cordilleran Section of the Geological Society of America Centennial Field Guide*, v. 19 p. 151-156.

10/87

Subsurface Study of the Late Cenozoic Structural Geology of the Los Angeles Basin

14-08-0001-G1371

THOMAS L. DAVIS
GEOLOGICAL CONSULTANT
3937 RODERICK ROAD
LOS ANGELES, CA 90065
213-259-3086

I.Objectives:

A.Detection or postulation of concealed late Cenozoic faults in the basin.

B.Determine subsurface geometry, sense of slip, displacement history for faults within the basin. Estimate overall convergence rate for basin and slip rates of individual faults during last 3 Ma.

C.Principal format for this study is the construction of retrodeformable cross sections across the basin using subsurface data from oil wells and surface geologic mapping(Figure 1). Limited subsurface mapping is being completed between the cross sections to better understand the three dimensional geometry of the basin and to assist projections of well data into the lines of section.

II. Results:

A.Central Los Angeles Basin cross section(A-A')now complete. Original section completed at 1:24,000 scale and restoration completed at 1:48,000(Figures 2 and 3).

B.Tentative Whittier Narrows cross section completed at 1:62,500 scale(Figure 4).

C.Well data collected and stratigraphic correlations made for a West Los Angeles cross section at 1:24,000 scale.

D.I am supervising Kurt Hayden's masters thesis(Cal State Univ. Long Beach) on the subsurface structural geology of a portion of the Elysian Park antiform.

III. Discussion of central Los Angeles Basin cross section and restoration(Figures 2 and 3):

A.Important geologic relationships and assumptions used for cross section construction:

1.Major compression started in the Los Angeles Basin during latest Repetto time or about 3.0 Ma. This is well documented by the angular discordance between Repetto age strata(Tpr) and upper Pliocene(Tpu) along the south flank of the Elysian Park antiform(EPA).

2)The cross section is an integrated structural solution that attempts to explain the origin and geometry of the major geologic relationships such as folds and angular unconformities. In addition the solution is quantitatively consistent with the observed structural relief across the major structures and the solution is restorable. The cross section is highly interpretive below drilling depths. It is assumed that folding is due to ramps in thrust faults and that the fold models and equations of Suppe(1985) give a first order approximation of the relationship between fault shape and fold shape. This assumption is based on a number of studies of late Cenozoic folds and thrust faults in the Coast Ranges and western Transverse Ranges of California (Davis, 1983; Davis and Namson,1986,1987; Namson, et al., in press; Namson and Davis, in press; Medwedeff, 1988).

3)No significant amounts of strike-slip offsets are well documented for the last 3 Ma along any of the major faults intersected by the cross section line. This allows a straightforward restoration perpendicular to the trend of major fold axes. A number of studies using subsurface well data show that the Newport-Inglewood fault(NIF) has had only 2-4 km of right-lateral offset since late Miocene time and probably not more than 1.5 km of right lateral displacment during the last 2 Ma(Yerkes, et al, 1965; Hill, 1971; Castle and Yerkes,1976; Woodward and Clyde, 1979). Published subsurface mapping and subsurface mapping completed during this study along the NIF show that the structural geometry changes very gradually along strike and thus the small amount of strike-slip offset documented along the NIF will have a negligible impact on the cross section restoration. In cross section A-A' and the restoration the NIF is interpreted to be a significant Miocene and early Pliocene normal fault with only a small amount of late Pliocene and Quaternary strike-slip offset. The Las Cienegas fault(LCF) does not offset Repetto age strata(lower Pliocene) and thus has no impact on the restoration. No significant amount of strike-slip offset has been documented along the Raymond Hill fault(RHF) for the last 3 Ma. Major left-lateral offset amounting to 53-55 km has been proposed for the combined Malibu Coast-Santa Monica-Raymond Hill fault zone(Yeats,1973; Campbell and Yerkes, 1976; Truex,1976); however, it is believed that most of this offset occurred during middle Miocene time. Preliminary subsurface mapping along the eastern end of the Santa Monica fault(SMF) seems to require little or no strike slip offset along the SMF since latest Miocene time. In addition the large antiformal trend of the eastern Santa Monica Mountains merges with the western end of the Elysian Park antiform(EPA) without any apparent lateral offset by the Santa Monica fault(Figure 1). No strike-slip offset has been documented for the York Blvd.(YBF), Eagle Rock(ERF), Tujunga(TF), and Sierra Madre(SMDF) faults. The San Gabriel fault(SGF) probably had right-lateral offset of 60 km(Crowell,1975) but most if not all of this fault movement occurred from 7-3 Ma and thus does not impact the restoration.

4)It is assumed that the edges of the Los Angeles Basin were controlled by normal faulting from middle Miocene through early Pliocene time. The positions and geometries of these extensional faults are best viewed in the restoration(Figure 3). Some of faults such as the York Blvd. fault have syntectonic scarp breccia of middle to late Miocene age(Lamar,1970).

5)The cross section intersects two major deformational zones that have undergone significant crustal shortening during the last 3 Ma (Figure 1). Both zones are east-west trending and are defined by numerous compressional earthquakes, late Pliocene and Quaternary age antiforms or mountain ranges with strata that have moderate-to steeply-dipping southern flanks coinciding with major topographic breaks, and in a few places late Pliocene and Quaternary age thrust faults that break through to the surface or are known in the shallow subsurface. The southernmost zone consist of the Santa Monica Mountains(SMMA), Elysian Park antiform(EPA), and the Puente Hills(PH). This zone continues to the west, partly offshore, probably as far as the eastern end of Santa Cruz Island. The northern zone include the south flank of the San Gabriel Mountains and the Verdugo-San Rafael Hills(SRH). In cross section A-A' these two zones nearly overlap between the Raymond Hill fault(RHF) and the Eagle Rock fault(ERF). It should be noted that despite the proximity of these two faults they are shown on the cross section as rooting into fundamentally different zones.

6)Major fault-propagation folds such as that under the Palos Verdes Hill(PVH) and the Elysian Park antiform(EPA) allow depth to detachment calculations. The depth to detachment is from 11-13 km which is consistent with the base of significant seismic activity within the Los Angeles Basin(Hauksson,1987).

B. Convergence rates, fault displacements, and slip rates on thrust faults for the last 3 Ma:

Cross section A-A' is 100 km long and the restoration is 136 km long. Thus there has been 36 km of north-south linear convergence during the last 3 Ma. This yields a convergence rate of 12 mm/yr.

Fault displacements can be measured directly from cross section A-A' and mean slip rates calculated using 3 Ma as the initiation of significant compression.

	Total dip-slip	Slip rate
Fault A(FA):	3.7 km	1.2 mm/yr
Fault B(FB):	3.7 km	1.2 mm/yr
Fault C(RHF is part of this system)	13.5 km	4.5 mm/yr
Eagle Rock(ERF)-Tujunga fault(TF) system	9.6 km	3.2 mm/yr
Minor thrusts between PVH and NIF	3.7 km	1.2 mm/yr
Slip continuing offshore	2.1 km	0.7 mm/yr
TOTALS	36.3 km	12.0 mm/yr

IV. Discussion of Whittier Narrows cross section B-B'(Figure 4):

A. Cross section B-B' was constructed after the October 1,1987 earthquake(M=6.1). The shallow portion of the section is constrained by limited well data, surface mapping, and a top of the basement profile(large dots) provided by B.Yerkes of the USGS. Presently more subsurface and surface data are being gathered so the present section is subject to change. The deep level structural interpretation was constrained by the hypocenter location and the focal plane solution of the October 1 earthquake. Focal plane solutions for the smaller pre-October 1 events were plotted on after the section was constructed. This cross section crosses the Elysian Park antiform(EPA) about 12 km east of cross section A-A' and structural interpretations shown on both sections are consistent on at least a first-order level.

B. The cross section presents a structural solution that places the origin of the October 1 earthquake on a deep level blind thrust fault. This fault is unnamed and is not related to the Whitter fault(WF). The WF is shown projected into cross section B-B'; however, this is conjectural and further study of the subsurface data will have to be made to determine if the WF continues this far to the northwest. The basis for accepting the blind thrust over the WF for the cause of the earthquake consist of the following:

1. The first motion was pure dip-slip. The focal plane solution indicates either a reverse fault dipping steeply to the south or a low-angle thrust dipping to the north and the distribution of aftershocks favors the thrust fault solution(L. Jones,USGS,

personal communication). The **WF** is considered to be a reverse right-oblique fault(Yerkes, 1985) and abundant well data and surface mapping show the **WF** has a steep north dip in the upper 2-3 kms of the crust. The thrust model is consistent with the seismic charateristics of the October 1 earthquake.

2. Although much of the damage associated with the earthquake occurred adjacent to the **WF** no tectonic surface rupture was reported along the **WF** or at any location(P.Williams, CAL TECH, personal communication). In the thrust model surface rupture associated with the causative fault would not be expected. A large enough earthquake might produce flexural slip or reactivation of the shallow-level thrust faults shown in cross section B-B', however, this was not observed. Intense damage reported along the Whittier fault in the city of Whittier may be due to its structural position directly above the steep limb of the growing antiform. This is an area of the fold that would be subjected to high strain during movement of the blind thrust.

3. The location of the hypocenter is some distance from the Whittier fault(Figure 4). For the **WF** to accomodate the focal mechanism of the October 1 earthquake and its shallow crustal geometry a strongly listric-shaped(flattening with depth) fault surface would be required. This fault geometry would require a distinctive fold shape in the upper plate of the **WF** but this fold shape is not observed at upper crustal levels. Furthermore,the western portion of the Whittier fault is located near the crest of the eastern continuation of the Elysian Park antiform as it merges with the antiformal structure of the Puente Hills. This position does not allow the **WF** to be the causative structure for this young antiformal trend. The size and extent of the antiformal structure indicates there is a deeper and more fundamental fault under the **WF**. The thrust model explains both the origin of the earthquake and shallow-level fold geometry.

4. The Whittier fault has had a complex history that starts back in the middle Miocene under a radically different tectonic setting(Yerkes,1972). Documented late Pliocene and Quaternary deformation along the **WF** may be the result of reactivation of this fault by deformation associated with the postulated deeper and more fundamental thrust fault under the **WF**.

V. SUMMARY: The high north-south convergence rate of 12.0 mm/yr for the last 3.0 Ma in the Los Angeles Basin combined with the presence of blind thrusts capable of generating at least moderate-sized earthquakes such as the October 1, 1987 Whittier Narrows event suggest that seismic potential of the basin has probably been underestimated. Furthermore, geologic maps based solely on surface studies and showing active or potentially active faults probably do a reasonable job of showing areas of potential surface rupture during a modeate to large earthquake; however, these maps probably give an abbreviated picture of the possible sources for future damaging earthquakes in the Los Angeles Basin.

VI. REFERENCES:

Campbell,R.H.,and Yerkes,R.F.,1976,Cenozoic evolution of the Los Angeles basin area-relation to plate tectonics, in Howell,D.G.,ed.,Aspects of the geologic history of the California continental borderland:Pacific Section AAPG.,Misc. Pub.24,p.541-558.

Castle,R.O.and Yerkes,R.F.,1976, Recent surface movements in the Baldwin Hills, Los Angeles County, California: U.S.Geological Survey Professional Paper 882, 125 p.

Crowell,J.C.,1975, San Andreas fault in southern California,in Crowell,J.C.,ed.,San Andreas fault in southern California: California Division of Mines and Geology Special Report 118,p.1-7.

Davis,T.L.,1983,Late Cenozoic structure and tectonic history of the western "big bend" of the San Andreas fault and adjacent San Emigdio Mountains: PhD dissertation Department of Geological Sciences University of California Santa Barbara, 579 p.

Davis,T.L.and Namson,J.S.,eds.,1986 and 1987,Geologic transect across the western Transverse Ranges: Pacific Section SEPM guidebooks 48(74p.) and 48A(156p.).

Hauksson,E.,1987, Seismotectonics of the Newport-Inglewood fault zone in the Los Angeles Basin, southern California: Bulletin of the Seismological Society of America, v.77, no.2, p. 539-561.

Hill,M.L.,1971, Newport-Inglewood zone and Mesozoic subduction, California: Geological Society of America Bulletin, v.82, p.2957-2962.

Lamar,D.L.,1970, Geology of the Elysian Park-Repetto Hills area, Los Angeles County, California: California Division of Mines and Geology Special Report 101, 45p.

Medwedeff,D.A.,1988, Strucutral analysis and tectonic significance of late Tertiary and Quaternary compressive-growth folding, San Joaquin Valley, California: PhD dissertation Department of Geological and Geophysical Sciences Princeton University, 184p.

Namson, J.S. and Davis,T.L.,in press, Seismically active fold and thrust belt in the San Joaquin Valley, Central California: Geological Society of America Bulletin.

Namson,J.S., Davis,T.L., Lagoe,M.B.,in press, Tectonic history and thrust-fold deformation style of seismically active structures near Coalinga: U.S.Geological Survey Professional Paper, Coalinga Earthquake, California.

Suppe,J.,1985, Principles of Structural Geology, Prentice-Hall, Englewood Cliffs, New Jersey, 537p.

Truex,J.N.,1976, Santa Monica and Santa Ana Mountains-relation to Oligocene Santa Barbara basin: American Association of Petroleum Geologists Bulletin, v.60, no.1, p.65-86.

Woodward and Clyde Consultants,1979, Report of the evaluation of maximum earthquake and site ground motion parameters associated with the offshore zone of deformation San Onofre Nuchlear Generating Station: unpublished study prepared for Southern California Edison,P.O.Box 800, Rosemead, CA 91770.

Yeats,R.S.,1973, Newport-Inglewood fault zone, Los Angeles basin, California: American Association of Petroleum Geologists Bulletin, v.57, p.117-135.

Yerkes,R.F.,1972, Geology and oil resources of the western Puente Hills area, southern California: U.S.Geological Survey Professional Paper 420-C, 63p.

Yerkes, R.F.,1985, Geological and seismologic setting-in Ziony,J.I.,ed.,Evaluating erthquake hazards in the Los Angeles region-an earth-science perspective: U.S.Geological Survey Professional Paper 1360, 505p.

Yerkes, R.F., Mc Culloch,T.H., Schoellhamer, J.E. and Vedder, J.G.,1965, Geology of the Los Angeles Basin-an introduction: U.S.Geological Survey Professional Paper 420-A, 57p.

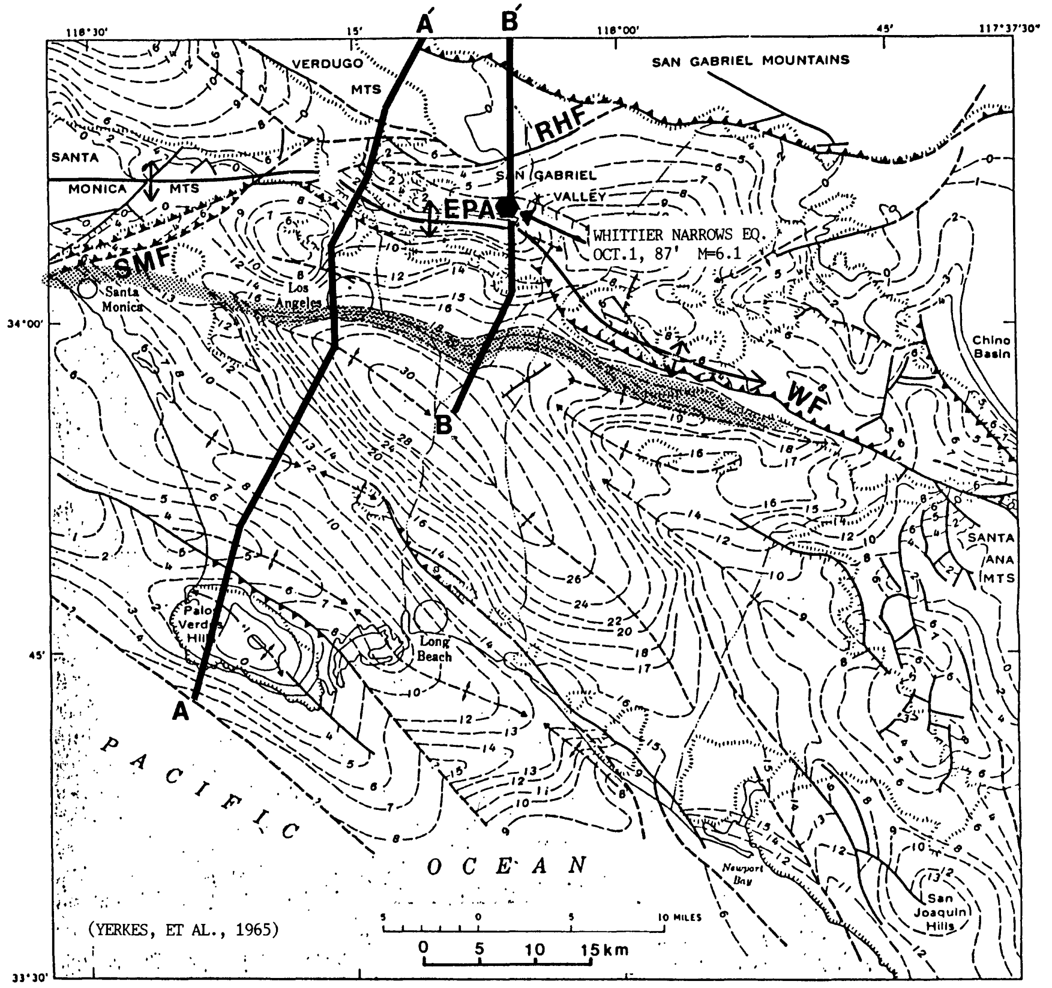

(YERKES, ET AL., 1965)

Figure 1. Location map of Los Angeles Basin showing cross section lines and epicenter for the Whittier Narrows earthquake(M=6.1) of Oct.1,1987. EPA=Elysian Park antiform, RHF=Raymond Hill fault, SMF=Santa Monica fault WF=Whittier fault.

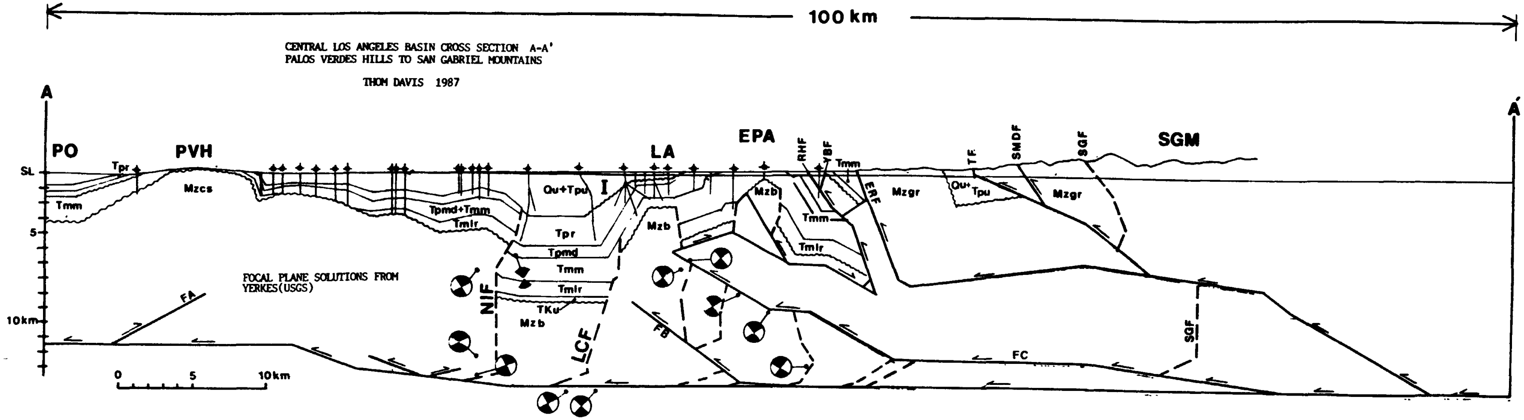

Figure 2. Retrodeformable cross section from Palos Verdes Hill(PVH) to the San Gabriel Mountains(SGM).Restoration is shown on Figure 3. PO=Pacific Ocean, LA=Downtown Los Angeles, EPA=Elysian Park antiform, FA=Fault A, NIF=Newport-Inglewood fault, LCF=Las Cienegas fault, FB=Fault B, RHF=Raymond Hill fault, YBF=York Blvd.fault, FC=Fault C, ERF=Eagle Rock fault, TF=Tujunga fault, SMDF=Sierra Madre fault, SGF=San Gabriel fault.

Rock units: Mzcs=Catalina Schist, Mzb=undifferentiated schist, metaigneous rocks, and slate-includes Santa Monica Slate and possibly Catalina Schist, Mzgr=granitic rocks and Precambrian gneissic and granitic rocks; TKu=undifferentiated upper Cretaceous and lower-middle Tertiary strata, Tmlr=Middle Miocene strata(Luisian and Relizian), Tmm=Upper Miocene strata(Mohnian), Tpmd=Uppermost Miocene and lowermost Pliocene strata(Delmontian); Tpr=lower Pliocene strata(Repetto), Tpu=upper Pliocene strata, Qu=undifferentiated Quaternary strata.

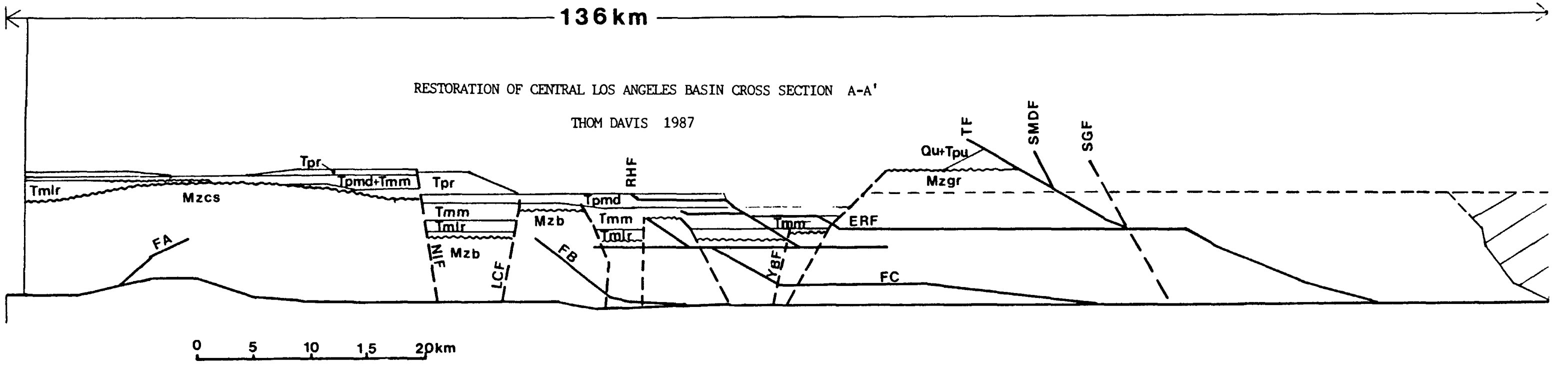

Figure 3. Restoration of cross section A-A'. Cross section has been restored so that top of Delmontian(4.0 Ma) strata is horizontal. Repetto(4.0-2.6 Ma) strata was then added on the section. Angular unconformities and onlapping relationships indicate that major compression started about 3.0 Ma or near the end of Repetto deposition. Diagonally lined area at right of section is restoration error which is less than 5% of area of the section. Abbreviations are explained in Figure 2.

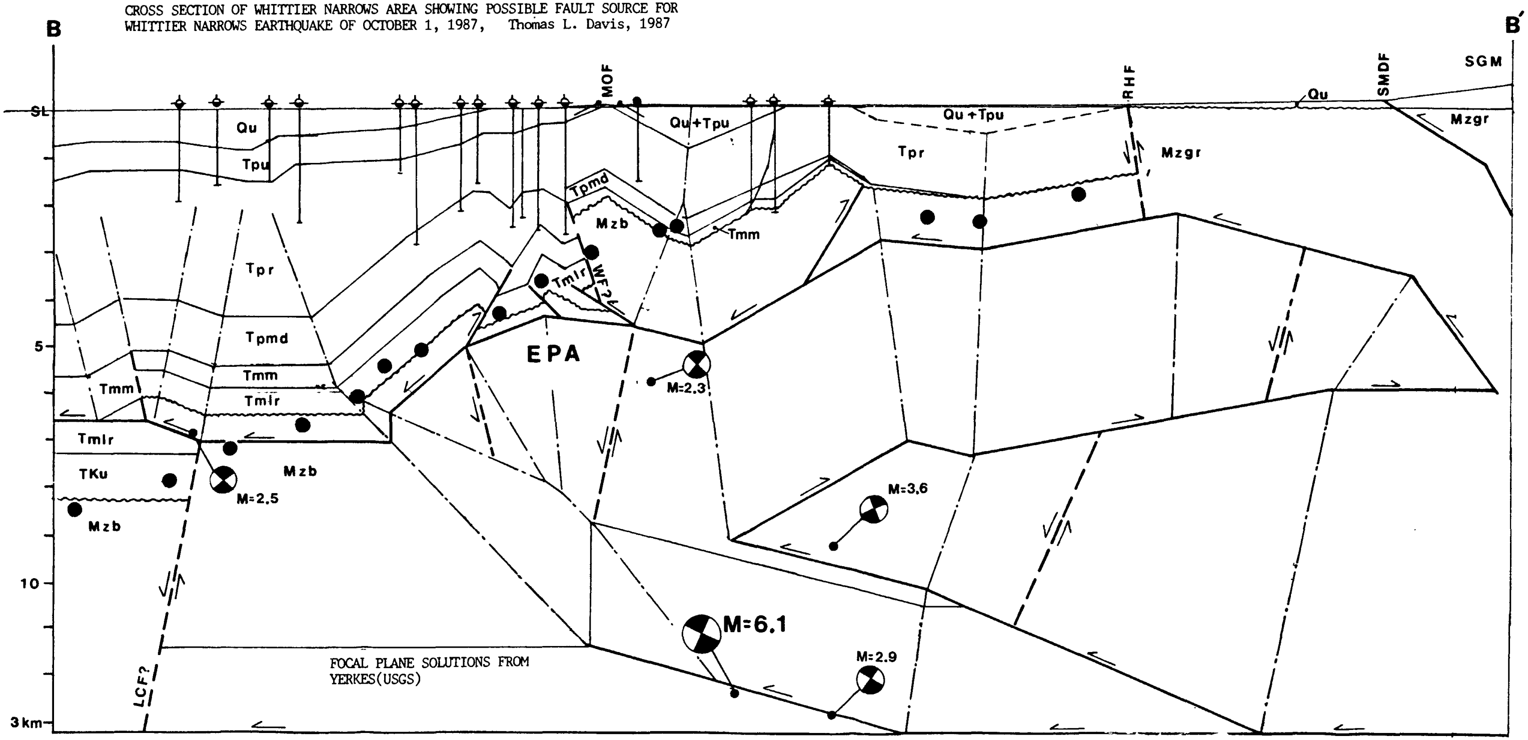

CROSS SECTION OF WHITTIER NARROWS AREA SHOWING POSSIBLE FAULT SOURCE FOR WHITTIER NARROWS EARTHQUAKE OF OCTOBER 1, 1987, Thomas L. Davis, 1987

FOCAL PLANE SOLUTIONS FROM YERKES(USGS)

Figure 4. Cross section across the Whittier Narrows showing hypocenter location and focal plane solution for the Oct.1,1987 Whittier Narrows Earthquake(M=6.1). The heavy black dots represent the top of the crystalline basement as determined by gravity and additional deep well data(B.Yerkes, personal communication). WF=westward projection of the Whittier fault, other abbreviations are explained in Figure 2.

Stress Transfer, Nonlinear Stress Accumulation and Seismic Phenomena at a Subduction-Type Plate Boundary

14-08-0001- G1367

R. Dmowska and J.R. Rice (P.I.)
Division of Applied Sciences and
Department of Earth and Planetary Sciences,
Harvard University
Cambridge, MA 02138
(617) 495-3452, 3445

1. Investigations. We have completed our work on a simple mechanical model of stress transfer in coupled subduction zones during the earthquake cycle; see previous summary reports. The model addresses the space and time distribution of the periodic perturbation stress (superposed on a time invariant mean stress) over the earthquake cycle in the area of great subduction earthquakes, in the zone of the outer-rise, adjacent to the thrust area, and in the down-going slab to depths of approximately 300 km (Dmowska et al., 1988). Also, we have continued research into the mechanics of mature seismic gaps in coupled subduction zones, seeking possible intermediate-term precursors (Dmowska and Lovison, 1988).

2. Results. It is reasonable to expect that in a mature seismic gap in a coupled subduction zone the locking of the interplate boundary in presence of sustained gravitational driving forces would result in the compression of (at least) the deeper portions of the oceanic lithosphere in the outer-rise zone adjacent to the locked area, and increased tension of the downgoing slab. Such expectations are confirmed by our recent simple mechanical modeling of subduction zone mechanics. Fig. 1 shows schematically our model situation, with subducting oceanic lithosphere of thickness H and velocity averaged over many earthquakes cycles equal V_{pl}. Fig. 2 (Dmowska et al., 1988) presents the extensional stress perturbation σ' in the subducting slab, downdip from the thrust contact, at $x=3H$, $4H$, $5H$ and $6H$, and at location $x=2H$ beneath the thrust contact. These stresses average to zero over the earthquake cycle and represent only that part of the stress field that pulsates in time. Fig. 2 shows their behavior during one cycle, in dimensionless time $o < t/T < 1$. In the first part of the cycle these stresses are compressional, and they turn tensional in the latter part of the cycle. It should be noted that the stresses experienced by the slab consist of these pulsating stresses and the mean background stresses associated with subduction.

Fig. 3 (Dmowska et al., 1988) presents the same pulsating stresses σ' associated with the earthquake cycle, but for the area updip from thrust contact zone, in the region of the outer-rise. The stresses are shown for distances $x=0$, $-2H$, $-3H$ and $-4H$. The outer-rise zone is under tension in the first part of the cycle and under compression in the latter part. Again, this is only the pulsating part of the stress field, and the total field, consisting of the sum of the background stresses (in this case the bending stresses) and the pulsating ones, is shown schematically in Fig. 4. Recent observational work of Christensen and Ruff (1988) on the presence and mechanisms of outer-rise earthquakes confirms such supposition in that there are many tensional outer-rise earthquakes following large subduction events, and some compressional ones preceding such earthquakes.

Even if the compressional outer-rise events are much rarer than their tensional counterparts, their presence is a sign of the locking of an adjacent section of the interplate boundary; that is, they are intermediate-term precursors to the approaching large subduction earthquake. In our observational work we assess the maturity of seismic gaps based on the presence and mechanisms of outer-rise earthquakes in the area adjacent to the gap, and intraplate earthquakes in the downgoing slab. Our results for 6 different areas are shown in Fig. 5-10, which cover two closed gaps: central Chile, area of March 3, 1985 earthquake (Fig. 5) and northern Chile, area of October 4, 1983 earthquake (Fig. 6), and four still-to-be closed gaps: Copiapo-Coquimbo region of northern Chile (Fig. 7), southern Mexico and coast of Guatemala (Fig. 8), Kurile Islands Trench Gap (Fig. 9) and northern New Hebrides (Fig. 10). In each area we present sequence of events and known mechanisms. We conclude, that the presence of both: compressional outer-rise events and tensional (normal) intraplate earthquakes in the downgoing slab is a useful intermediate-term precursor to the approaching large subduction earthquake. The full text (Dmowska and Lovison, 1988) is in press.

References

Christensen, D.H. and L.J. Ruff, Seismic coupling and outer-rise earthquakes, in revision for J. Geophys. Res., 1988.

Dmowska R. and L.C. Lovison, Intermediate-term seismic precursors for some coupled subduction zones, in press in Pure and Appl. Geophys. topical issue "Intermediate-Term Earthquake Prediction", eds. W.D. Stuart and K. Aki, v. **126**, N.2/4, 1988.

Dmowska, R., J.R. Rice, L.C. Lovison and D. Josell, Stress transfer and seismic phenomena in coupled subduction zones during the earthquake cycle, in revision for J. Geophys. Res., 1988.

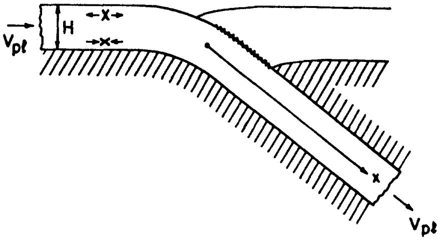

FIG.1.

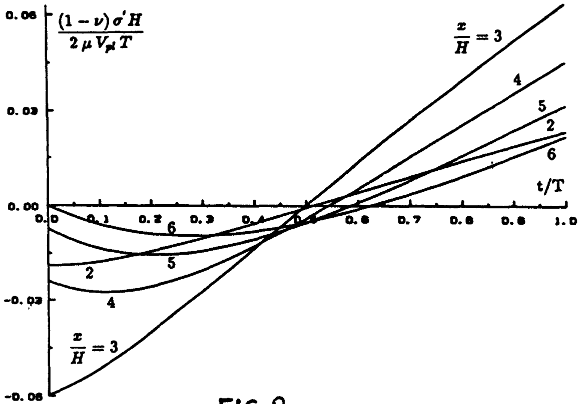

FIG.2.

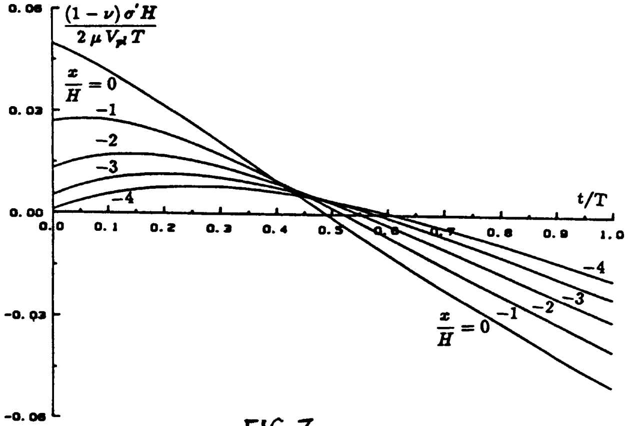

FIG. 3.

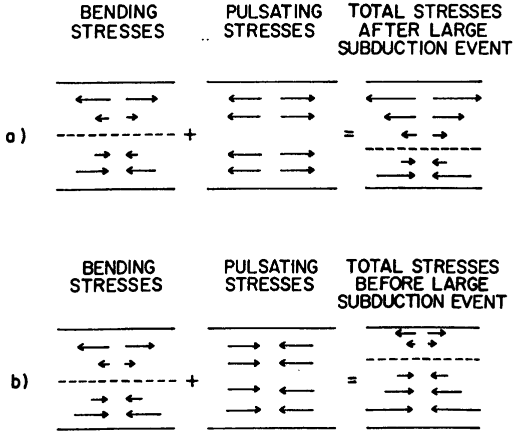

FIG. 4.

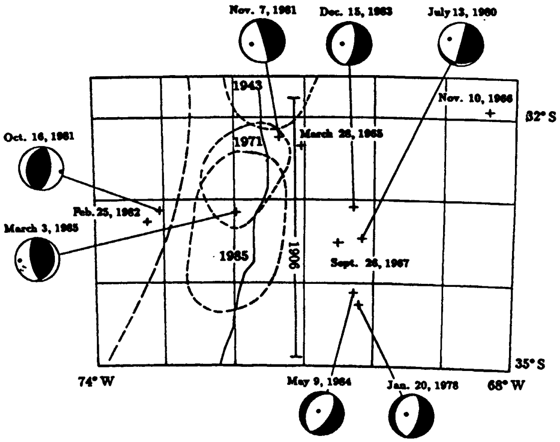

FIG. 5.

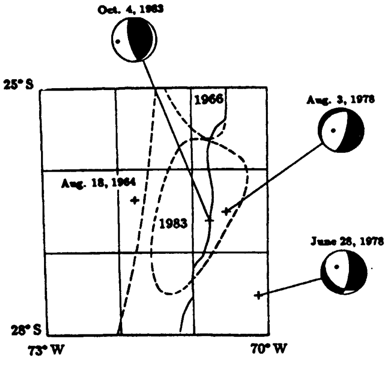

FIG. 6.

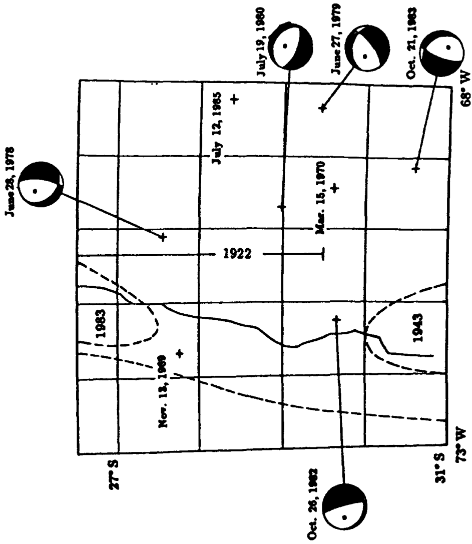

FIG. 7.

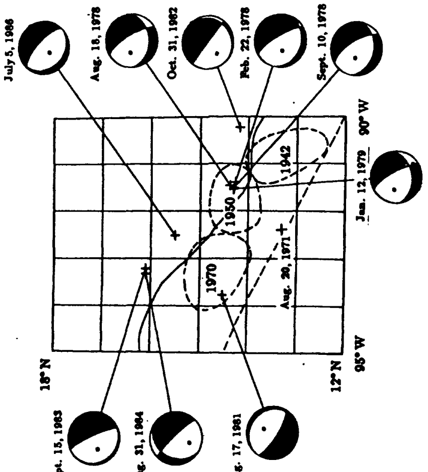

FIG. 8.

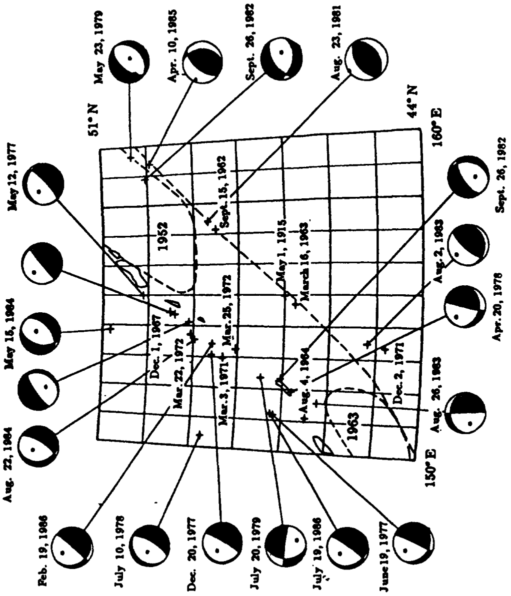

FIG. 9.

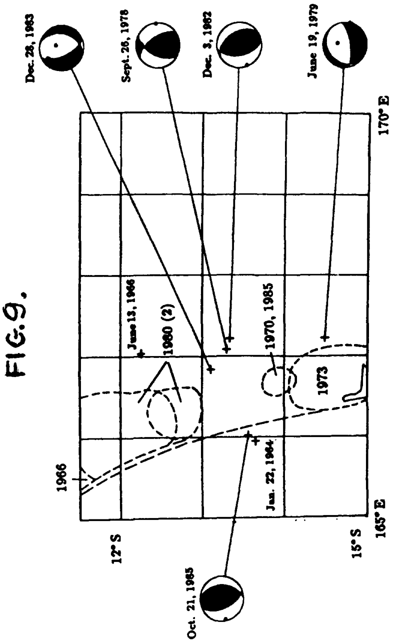

FIG. 10.

Investigations of Recent Crustal Deformation in South Coastal Oregon

14-08-0001-G1387

Harvey M. Kelsey and Galan McInelly
Department of Geology
Western Washington University
Bellingham, WA 98225

Terese Abelli, Raymond M. Burke and Gary A. Carver
Department of Geology
Humboldt State University
Arcata, CA 95521

Investigations

During the summer and fall of 1987, we investigated marine terraces at three areas in south coastal Oregon: 1) Brookings-Cape Ferrelo, 2) Port Orford-Cape Blanco-Floras Lake, and 3) Bandon-Cape Arago-Charleston. In each area, we mapped the sequence of marine terraces and investigated terrace cover stratigraphy. Soils were investigated to aid in regional correlation among these sites and to determine if a soils chronosequence developed further to the south in Humboldt County, California (Burke and others, 1986) is applicable to south coastal Oregon. The purpose of the terrace mapping and soils investigation is to ascertain the degree of late Pleistocene tectonic deformation recorded by these marine terraces. The following results constitute a progress report; studies under this contract are still underway. This report is not intended to be comprehensive, but rather to outline the most important findings to date. Primary researchers in each field area are Terese Abelli (Brookings); Harvey Kelsey, (Cape Blanco); and Galan McInelly and Harvey Kelsey (Cape Arago). Soils investigations in all the areas are under the supervision of Bud Burke and Gary Carver. Soils have so far been described near Brookings and near Cape Arago, and soils particle size analysis is presently underway.

Results

1. Brookings-Cape Ferrelo area

Marine terraces were investigated along 33 km of coast from the Chetco River to north of Cape Ferrelo. The terraces are cut on late Jurassic Dothan Formation sandstones. At least five, and possible several more, wavecut platforms are recognized. The two lower terraces are preserved to the south near Brookings, at elevations that range from 15-60 m. The upper terraces are preserved in the central and northern part of this coastal reach at 50-350 m elevation.

Terrace cover sediments consist mainly of poorly consolidated sands. These sediments range from a thickness of 1-2 m on the lower two platforms to 2-6+ m on the upper platforms.

One soil pit was excavated on each of the five terrace surfaces. Soils on the lower two surfaces show an approximately equal degree of development and these soils are significantly less developed than those on the upper three surfaces. Soils on the upper surfaces are also similar and not clearly distinguishable one from the other. Based on soils chronosequence work further south in California (Burke and others, 1986), soils on the lower two surfaces are probably on the order of 120 ka and those on the upper surfaces are probably 240 ka and older. One more soil pit is planned on each of the five surfaces.

The principal crustal movement recorded by these terraces is regional uplift. No obvious faulting or folding of these surfaces is evident, but it would be difficult to discern such deformation in any case because the terraces are exposed discontinuouly. The other two terrace sites further to the north provide better exposure for detection of regional deformation.

2. Port Orford-Cape Blanco-Floras Lake area

Janda (1969, 1970) mapped four marine terraces in this area, ranging from 60 m to 275 m elevation, and described the soils. Our mapping of terraces is essentially the same as that of Janda (1970), with the notable exception that we have identified a new, and youngest, marine terrace at Cape Blanco (the Cape Blanco terrace). This terrace has an 8 m backedge. Though the surface elevation of this terrace is lower than the next oldest (the Pioneer terrace), the wavecut platform elevation of the two terraces is essentially the same. Recognition of this new ycungest terrace at Cape Blanco may help resolve the controversy over correlation of the lower terraces at Cape Blanco with those at Cape Arago (see Adams, 1984).

On the beach 2.2 km south of Cape Blanco, an elevated (?) beach berm is well exposed in a gap in the othewise solid facade of seacliffs (Janda, 1970). The berm is underlain by sand and is composed of coarse cobbles of both resistant (recycled conglomerate clasts) and unresistant (local Miocene sandstone) lithologies. The deposit has a well developed imbrication that dips seaward. Janda (1970) reports a ^{14}C date on wood from this deposit of 3,010 +/- 250 years. The unresistant cobbles are full of pholadid borings with in-place pholadid shells; these shells have been submitted for an age determination as well. The deposit is approximately 19 m above sealevel and anywhere from 12.5-16 m above the upper limit of possible deposition by a storm generated with sealevel at its present height. The cobble berm may have been deposited by a tsunami, in which case no tectonic uplift is necessary. On the other hand, the deposit may indeed be a storm berm in which case (using the one available date and uncertainty as to the height of storm deposition), the deposit has been uplifted at a rate of 4.2 - 5.3 mm/a in the late Holocene. This deposit is potentially a key feature in understanding the late Holocene tectonic deformation in this area, and further investigation is underway.

The Beaver Creek fault zone is a major pre-Tertiary structure that offsets the fourth (previously, the third) highest terrace at Cape Blanco (Janda, 1970). Mapping indicates that late Pleistocene motion on the Beaver Creek fault zone has occurred on at least 6 separate faults within the 400 m wide fault zone. The fault zone has a normal movement sense and vertical separation of the wavecut platform is 37-43 m. The age of the platform is unknown, but if the platform was cut during the last interglacial (stage 5e, Chappell and Shackleton, 1986, and references therein), which is possible, then the late Pleistocene vertical slip rate on the Beaver Creek fault is .30-.35 mm/a.

The thickness of the sediment cover on each of the five terraces is large relative to cover thicknesses on terraces to the north and the south. Cover thicknesses on the first, second and fourth terraces (those that have been subject to the most study) are 6.4-9.0 m, 16.5 - > 28 m, and 35-40 m respectively. Nearshore, beach and aeolian facies are all represented, though not all facies are present at any one locality. In all cases, the cover sediments show a progradational sequence deposited during sealevel fall from a stadial or interstadial highstand. Both thickness and sedimentologic character of the different terrace deposits have been useful for correlation within and among terraces.

The marine terraces at the latitude of Cape Blanco tilt to the north and the south from a high point near the cape (Janda, 1970). The second highest terrace at Cape Blanco (the Pioneer) descends below sealevel to the south near Port Orford and descends below sealevel to the north at Floras Lake (Janda, 1970). There is also a landward tilt to the younger two surfaces, but landward tilt is not as pronounced as is the case for the Cape Arago terraces to the north.

3. Bandon-Cape Arago-Charleston area

Griggs (1945) mapped five terraces in the Cape Arago-Charleston area, the lower four of which are widespread and range from very well to well preserved. These terraces are all cut on relatively erosive Miocene or Eocene sandstones. We have remapped these terrace surfaces on the basis of elevation and cover bed stratigraphy. Griggs' mapping is essentially accurate. However, we have revised some of Griggs' mapping in the Charleston area where both faulting and tilt, plus a relatively low uplift rate, have obscured terrace relations.

Our detailed mapping focused on deformation of the youngest raised wavecut platform, the Whisky Run terrace (Griggs, 1945). The Whisky Run terrace is exposed almost continuously along a 30 km section of the coast from south of Fivemile Point northward to Cape Arago, then northeastward to Charleston and then up the eastern side of Coos Bay toward Empire, Oregon. The surface dips to the north and south from a high point near Cape Arago (Griggs, 1945; Janda, 1970). Detailed altimeter surveys of Whisky Run wavecut platform elevation indicates significant secondary flexure in the terrace, superimposed on top of the regional antiformal tilt. On the east shore of Coos Bay, the Whisky Run surface undulates above and below sealevel several times and at least one of these undulations is due to movement on a low angle thrust fault. The attitude of the fault, as exposed in overlying sands, is sympathetic to the bedding attitude in the underlying Miocene sandstones, suggesting that the fault is a bedding plane fexural slip fault. On the down-dropped side of this fault, there are several drowned Holocene trees in the intertidal zone, indicating Holocene movement on the fault. Samples of these trees have been submitted for dating. At another locality near Yoakam Point, Baldwin (1945) also documents offset of the Whisky Run surface by a bedding plane thrust. However, there are at least two instances where faults that offset the late Pleistocene marine terraces are not sympathetic with bedding. In the first instance, the Pioneer terrace is offset by a normal fault with at least 12 m of vertical separation in the vicinity of Charleston. In the second instance, the Whisky Run surface gradually descends below sealevel from Cape Arago southward to Whisky Run, then the wavecut platform is abruptly uplifted again above sealevel at Coquille Point in the vicinity of Bandon. This uplift is fault controlled. Both the fault near Charleston and the fault at Coquille Point are directly on strike (and have the same movement sense) as correlative faults mapped from seismic reflection profiling in the offshore by Clarke and others (1985).

The marine terraces in the Cape Arago area dip eastward toward the axis of the South Slough syncline (Baldwin, 1945; Griggs, 1945; Janda, 1970; Adams, 1984). However, it is unclear whether the downdip direction of this tilt is actually perpendicular to the South Slough syncline, as has been assumed (Baldwin, 1945; Adams, 1984). Preliminary detailed altimeter surveys of the Whisky Run surface suggest the downdip direction is more to the northeast, a tilt direction that is not easily reconciled with the south-trending South Slough syncline. It is also unclear when tilt occurred (relative to the ages of the lower four wavecut platforms), despite data that purportedly shows progressive tilt with time (Adams, 1984). Systematic collection of wavecut platform elevations on all the terraces, plus supporting elevation data from well logs, presently being collected, should elucidate these problems.

Six soil pits have been examined on terraces in the Cape Arago area, two each on the lower two surfaces (Whisky Run and Pioneer surfaces) and one each on the next upper two surfaces (Seven Devils and Metcalf surfaces). Duplicate pits on the lower two surface show substantial variability depending on local groundwater and vegetation characteristics at the sites, but the two surfaces nonetheless have soils that are not well developed and not easily distinguished based on the degree of profile development. Soils on the uper two surfaces are substantially more developed than those on the lower two, but again, the upper terrace soils are not distinctive one from the other in terms of profile development.

4. Correlation of wavecut platforms among the three areas

Correlation techniques that are potentially useful for this region include: 1) physically tracing a wavecut platform from one area to the adjacent one, 2) relative age correlation based on degree of soil development, 3) relative age correlation based on aminostratigraphy (Kennedy and others, 1982), and 4) correlation by absolute age determination at more than one site.

We have so far been able to employ the first two techniques based on our preliminary data. We agree with Janda (1970) that it is possible to physically trace the elevation of the wavecut platform of the Pioneer terrace from its type locality near Cape Arago across the Coquille River east of Bandon to the broad, well defined terrace to the east of Cape Blanco (which Janda also called the Pioneer). The Pioneer wavecut platform is discontinuously exposed in stream cuts and road cuts and can be identified in well logs. The platform reaches a low point in the vicinity of Fourmile Creek, approximately halfway between Bandon and Floras Lake.

Soils have yet to be studied in the Cape Blanco vicinity. However, the noteable change in the degree of development between the second and third terraces both at Cape Ferrelo and at Cape Arago suggests the second and third terraces in these two localities may be the same age. Further work is needed to confirm this tentative correlation.

Shells (Saxidomus giganteus) have been collected at the base of the classic molluscan fossil locality (Addicott, 1964) on the Cape Blanco terrace and also at the base of the Whisky Run terrace at Coquille Point near Bandon. Uncertainty over correlation of these two wavecut platforms may be resolved by collaborative studies, now in progress by D. Muhs of the U.S. Geological Survey, on the extent of racemization of amino acids in these shells.

More work on potential correlations by all of these techiques remains to be done, and will be a focus of future work in the area.

References

Adams, J., 1984, Active deformation of the Pacific northwest continental margin: Tectonics, v. 3, no. 4, p. 449-472.

Addicott, W. O., 1964, A late Pleistocene invertebrate fauna from southwestern Oregon: Journal of Paleontology, v. 38, no. 4, p. 650-661.

Baldwin, E. M., 1945, Some revions of the late Cenozoic stratigraphy of the wouthern Oregon coast: Journal of Geology, v. 52, p. 35-46.

Burke, R. M., Carver, G. A., and Lundstrom, S., 1986, Soil development as a relative dating and correlation tool on marine terraces of northern California: Geological Society of America abstracts with programs, v. 18, no. 2.

Chappell, J., and Shackleton, N. J., 1986, Oxygen isotopes and sealevel: Nature, v. 234, p. 137-140.

Clarke, S. H., Field, M. E., and Hirozawa, C. A., 1985, Reconnaissance geology and geologic hazards of the offshore Coos Bay basin, Oregon: U.S. Geological Survey Bulletin 1645, 41 pp.

Griggs, A. B., 1945, Chromite-bearing sands of the southern part of the coast of Oregon: U.S. Geological Survey Bulletin 945-E, p. 113-150 and 11 plates.

Janda, R. J., 1969, Age and correlation of marine terraces near Cape Blanco, Oregon: Geological Society of America abstracts with program, v. 3, p. 29-30.

Janda, R. J., 1970, Field guide to Pleistocene sediments and landforms and soil development in the Cape Arago-Cape Blanco area of Coos and Curry Counties, southern coastal Oregon, Friends of the Pleistocene, October 9-11, 1970, unpublished.

Kennedy, G. L., Lajoie, K. R., and Wehmiller, J. F., 1982, Aminostratigraphy and faunal correlations of late Quaternary marine terraces, Pacific Coast, USA: Nature, v. 299, p. 545-547.

Coastal Tectonics, Western United States

9910-01623

Kenneth R. Lajoie

Branch of Engineering Seismology and Geology
U.S. Geological Survey
345 Middlefield Road, MS 977
Menlo Park, California 94025
(415) 329-5641

Investigations:

1. Age and deformation of Pleistocene marine strandlines and sediments in the Los Angeles Basin.

2. Geologic/Tectonic evolution of the Mendocino triple junction.

Results:

1. Structurally, the eastern Los Angeles basin is a northwest-trending synclinal trough bounded on the southwest by a complex anticline centered along the Newport-Inglewood fault zone (NIFZ). Pleistocene and Holocene sediments (both marine and continental) up to 1000 m thick underlie the southwest-sloping Downy plain along the synclinal axis. Sedimentation rates are very high and, therefore, prevent the formation of a topographic low along the subsiding axis.

   Along the southeast coastline of the Los Angeles basin (Long Beach to Newport Beach) five low mesas separated by wide, partially filled alluvial channels lie along the souotheast segment of the NIFZ. Topographically, each mesa consists of two virtually horizontal planar surfaces separated by a moderately steep, sea-ward facing linear scarp (8-15 m high) near and roughly parllel to the present shoreline. Locally, broad mounds (2-15 m high) occur on and at the crest of these scarps. Several previous workers interpreted these linear scarps as fault scarps and some of the mounds as fault-bounded structural blocks. These interpretations imply very recent and rapid fault movement within the NIFZ. However, our preliminary geomorphic and geologic data indicate that the linear scarps on the four mesas between Seal Beach and Newport Beach are remnants of uplifted relict sea cliffs cut during a single sea-level highstand 85-125 ka ago. Also, the mounds on and at the crest of the scarps are stabilized dunes derived from the ancient beach on the abandoned wave-cut platform.

   The southeast margin of the Huntington Beach mesa is a remnant of an uplifted alluvial plain (with an abandoned incised stream channel) is graded to the emergent marine strandline. This plane grades uninterrupted into the emergent wave-cut platform below the ancient sea cliff. The lack of a linear scarp across this surface is evidence that the linear scarp to the northwest is of erosional, not tectonic, origin.

The higher surface capping each mesa is a remnant of a once continuous depositional marine platfrom probably 200-300 ka old. These platform remnants slope gently to the northeast toward basin's synclinal axis. Also, the upper and lower marine platforms rise gradually and diverge to the southeast before they merge with marine terraces cut into the northwest flank of the San Joaquin Hills. To the northwest the lower platform might slope below present sea level. The upper platform forms the broad northeast-sloping plain eroded into the western flank of Signal Hill.

In summary, our preliminary data indicate there is no topographic expression of any fault strand within the NIFZ southeast of Long Beach. However, the anticline along the NIFZ is clearly expressed by warped marine and alluvial surfaces as young as 85-125 ka. The numerous, broadly dispersed minor faults that offset Pleistocene sediments in this area are probably related to the anticlinal warping, or perhaps to more localized fault movement at depth.

2. P. McCrory completed her study of the Neogene tectonic history of the Humboldt basin and Mendocino triple junction. This basin provides an unique opportunity for studying the transition from convergent to transform plate motion and the northward migration of the triple junction.

Reports

None.

Coastal Tectonics in the Pacific Northwest

9910-04190

Kenneth R. Lajoie

Branch of Engineering Seismology and Geology
U.S. Geological Survey
345 Middlefield Road, MS 977
Menlo Park, California 94025
(415) 329-5641

Investigations:

1. A major need in Ouaternary geology is a widely applicable absolute dating technique with a range beyond that of ^{14}C (0-40 ka). In our studies of coastal tectonics we have developed relative dating techniques based on paleontology, amino-acid racemization in fossil shells, and sea-level history that provide numerical age estimates of emergent marine strandlines beyond 40 ka. However, because of inherent limitations (primarily resolution) in these techniques, we continually experiment with new dating techniques. Accordingly, we have recently initiated a feasibility study of dating fossil shells using ESR (Electron Spin Resonance). Hopefully, this technique will help resolve some uncertainties in age estimates of emergent Pleistocene marine strandlines along the coastline of Oregon and Washington.

2. The first problem of paleoseismicity in coastal areas is identifying and dating the Holocene strandline record of past earthquakes. Accordingly, we have accumulated data from numerous Pacific basin areas to test against theoretical models of episodic crustal movement in coastal areas.

3. Regional and subregional patterns of Pleistocene crustal deformation provide important information for understanding and interpreting current crustal movements. Accordingly, a preliminary summary of Quaternary crustal deformation in the coastal regions of California, Oregon, and Washington is being undertaken.

Results

1. Background gamma-radiation (dose rates) must be known to apply the ESR dating technique. Preliminary readings at several fossil localities with a portable micro-R meter yield dose rated of 5-25 micro-R/h. We are contracting with Battelle Laboratories to instrument four sites to obtain more complete information (sources, variability, *etc.*) and to calibrate the portable meter and passive dosimeters to be installed at numerous other sites.

   Samples of fossil shells must be artificially irradiated at various levels to determine the total dose of gamma radiation. We have developed sample holders and procedures to obtain the required doses from a ^{60}Co source. We are contracting with Battelle Laboratories for the irradiations.

Because there are no established procedures for this relatively new dating technique, we have done numerous ESR analyses of fossil shells to determine optimum grain and sample size. Fortuitously, the very small optimum sample size is very economical in terms of cost for artificial irradiation.

2. Theoretical (ideal) models of coseismic deformation in coastal areas indicate that even under the best geologic conditions (each coseismic event clearly recorded and well dated) no meaningful pattern of seismicity can be established if there has been significant post-earthquake recovery. This result suggests that we should carefully search for any evidence of post-earthquake recovery in the geologic record.

3. A preliminary summary of crustal deformation along the west coast of the United States is progressing. Initial conclusions are:

   A. In the region south of Mendocino triple junction lateral tectonic movements predominate. There, typical coastal uplift rates are 0.1-2.0 m/ka (mm/yr). These subregional uplift rates primarily reflect crustal thickening due to crustal shortening normal to major right-lateral faults. Locally, uplift rates reach 4-10 m/ka on anticlinal structures in subregions of rapid lateral crustal compression (Transverse Ranges and Cape Mendocino). It is only in these areas that coseismic uplift is recorded as emergent marine strandlines. Locally, subsidence occurs in fault-bounded structural troughs parallel to subregional tectonic structures.

   B. In the region north of the Mendocino triple junction oblique subduction predominates. There, Pleistocene uplift rates of 0.0-0.5 m/ka are generally lower than in the region to the south. However, in this region large coseismic vertical crustal movements may be followed by post-earthquake relaxation, resulting in minor net uplift and lower long-term uplift rates.

Reports

None.

NEOGENE MAGNETIC STRATIGRAPHY AND TECTONIC ROTATIONS, TRANSVERSE RANGES, CALIFORNIA: TIMING AND DEFORMATION RATES OF POTENTIALLY ACTIVE FAULTS

14-08-0001-G1353

Shaul Levi

Geophysics, College of Oceanography
Oregon State University
Corvallis, Oregon 97331
(503) 754-2915

PALEOMAGNETIC RESULTS FROM THE VAN NORMAN RESERVOIR, SAN FERNANDO, CALIFORNIA

Objectives: The long term objectives of our research have been to use magnetic stratigraphy and paleomagnetism (PM) to establish ages and sedimentation rates of Neogene formations in the Transverse Ranges, California, to determine the timing, deformation rates and tectonic rotations associated with potentially active faults in areas undergoing rapid urbanization.

The specific objectives of this study have been to determine the time of uplift of the Santa Susana Mountains and the initial movement along the Santa Susana fault, and associated tectonic rotations in the Van Norman reservoir area.

Results: Forty-five sites from the Saugus Formation, primarily from the lower Sunshine Ranch member (Saul, 1975), were sampled at the Van Norman reservoir (Figure 1), representing approximately a 1.05 km stratigraphic section.

Sites were chosen at the finer grain sedimentary interbeds, typically between 0.5 and 3 m in thickness. Three oriented hand samples were obtained at each site, and two specimens were cut from each sample. Pilot specimens were stepwise demagnetized thermally and with alternating fields (AF). Both demagnetization methods gave similar stable PM directions. The remaining specimens were stepwise AF demagnetized in at least six steps to 80 or 100 mT. For each site stable PM directions were determined by vector averaging of the remanence over 2 - 5 consecutive AF levels, chosen independently for each site (Table 1). Within each site the same AF steps were used to obtain the stable direction of each specimen.

The PM results are summarized in Table 1. Forty-three of the sites yielded the magnetic polarity, and for thirty-three sites meaningful PM directions were calculated. The sampled section is predominantly reversed, but it includes a 70 - 100 m zone of normal polarity, represented by six sites (Figures 2 and 3). By analogy with the reference section near Castaic (Levi et al., 1986) we infer that the Saugus section at the Van Norman reservoir was deposited in the Matuyama chron. Based on the stratigraphic position of the normal subchron and its duration, we speculate that it might represent the Olduvai event from 1.67 - 1.87 Ma (Mankinen and Dalrymple, 1979). A lower limit on the average sedimentation rate can be calculated by assuming that the sampled section represents the entire Matuyama chron, which lasted about 1.75 Ma. This leads to an average sedimentation rate of about 0.6 km/Ma. A similar value was obtained from the thickness of the normal subchron and the assumption that it is the Olduvai event. Extrapolating this crude estimate to the top of Saugus exposed at the Van Norman reservoir area suggests that the youngest Saugus in this area was deposited several hundred thousand years ago; this would indicate the time of uplift of the Santa Susana Mountains, which is consistent with the results of Treiman and Saul (1986).

The mean PM direction for thirty-three sites (Figure 3), where the directions were transformed to normal polarity, is $I = 48°$, $D = 1.8°$, $\alpha_{95} = 4°$. The mean inclination is very similar to the value in the Merrick syncline, (Levi, 1986), but it is 6° shallower than the expected value for a geocentric axial dipole at this location ($I = 54°$). The mean declination indicates that this section has not undergone significant tectonic rotation since Saugus deposition, in sharp contrast with neighboring blocks near Castaic and in Merrick syncline (Levi et al., 1986; Levi, 1986).

References:

Barrows, A.G., J.E. Kahle, R.B. Saul and F.H. Weber, Jr., 1975, Geologic Map of the San Fernando earthquake area 1:18,000, Calif. Div. Mines Geology Bull, 196.

Levi, S., 1986, Paleomagnetism of the Neogene Saugus Formation, Transverse Ranges, California: Timing and deformation rates of potentially active faults, U.S. Department of the Interior, Geological Survey, National Earthquake Hazards Reduction Program, Summaries of Technical Reports, v. XXII, Open File Report 86-383, p. 183-191.

Levi, S., D.L. Schultz, R.S. Yeats, L.T. Stitt, and A.M. Sarna-Wojcicki, 1986, Magnetostratigraphy and paleomagnetism of the Saugus Formation, near Castaic, Los Angeles County, California, in Field Trip Guidebook and Volume on Neotectonics and Faulting in Southern California and Baja California, Cordilleran Section, P.E. Ehlig, editor, p. 103-108, GSA, 82nd Annual, Los Angeles, California.

Mankinen, E.A. and G.B. Dalrymple, 1979, Revised Geomagnetic Polarity Time Scale for the interval 0-5 m.y.B.P., J. Geophys. Res., v. 84, p. 615-626.

Saul, R.B., 1975, Geology of the southeast slope of the Santa Susana Mountains and geologic effects of the San Fernando earthquake, Calif. Div. Mines Geology Bull., v. 196, p. 187-194.

Treiman, J. and R. Saul, 1986, The mid-Pleistocene inception of the Santa Susana Mountains, in P.E. Ehlig, editor, Fieldtrip Guidebook and Volume on Neotectonics and Faulting in Southern California and Baja California, Cordilleran Section, GSA, 82nd Annual, Los Angeles, California, p. 7-12.

TABLE 1

VAN NORMAN LAKE, SUMMARY OF PALEOMAGNETIC RESULTS

Site No.	N/n	D_R(°)	I_R(°)	k	α_{95}(°)	Demag Levels(mT)	Bedding Strike/Dip	VGP—North Pole Long(°)	Lat(°)
VNL10	4/6	195.6	-35.4	63	12	80-100(2)	275°/59°N	14.3	69.8
VNL09	5/5	Reversed					168°/54°N		
VNL08	6/6	Reversed							
VNL07	4/6	169.7	-46.1	58	12	40-50(2)	280°/54°N	116.5	78.8
VNL06	6/6	196.9	-52.6	73	8	40-50(2)	276°/59°N	-28.6	75.9
VNL05	6/6	201.1	-50.3	245	4	40-50(2)	279°/61°N	-24.0	72.0
VNL04	6/6	Reversed					269°/64°N		
VNL03	6/6	Reversed					265°/64°N		
VNL02	6/6	Reversed					277°/70°N		
VNL99	6/6	183.2	-41.9	673	2.6	30-80(5)		45.3	79.5
VNL98	6/6	188.4	-44.4	69	8.1	40-80(4)	270°/57°N	17.8	79.0
VNL96	6/6	Reversed					259°/53.5°N		
VNL95	5/6	203.6	-52.8	41	12.1	40-80(4)	271°/54.5°N	-32.5	70.4
VNL92	6/6	160.9	-66.6	54	9.2	40-80(4)		-156.3	69.5
VNL91	4/6	187.9	-51.4	21	14.9	30-60(4)	264°/65.5°N	-12.0	83.0
VNL90	6/6	173.4	-58.6	57	8.9	40-80(4)		163.0	82.7
VNL87	6/6	Reversed							
VNL86		Indeterminate							
VNL84	6/6	11.8	46.0	29	12.6	10-30(4)		2.7	77.7
VNL82	4/6	355.8	53.8	263	5.7	10-30(4)	259°/58°N	-206.7	86.5
VNL80	6/6	3.0	40.6	196	4.8	40-80(4)		47.4	78.6
VNL78	8/8	36.5	54.2	149	4.5	10-30(4)	277°/52°N	-39.9	60.1
VNL76	6/6	6.8	47.3	232	4.4	40-80(4)	265°/50°N	14.9	81.8
VNL01	6/6	7.6	50.4	81	7	40-50(2)	265°/60.5°N	-4.3	82.9
VNL74	6/6	187.3	-41.6	48	9.8	40-80(4)	247.5°/58°NW	28.0	77.8
VNL70	8/8	Reversed					258°/45°N		
VNL62	8/8	174.3	-25.3	33	9.8	10-30(4)	261°/45°N	76.7	68.4
VNL60		Reversed?					264°/45.5°N		
VNL54		Indeterminate				272.5°/37.5°N			
VNL50	5/6	Reversed					291°/36°NE		
VNL44	6/6	193.5	-34.8	64	8.4	40-80(4)	266°/30°N	19.7	70.7

Van Norman Lake, Summary of Paleomagnetic Results (cont.)

Site No.	N/n	D_R(°)	I_R(°)	k	α_{95}(°)	Demag Levels(mT)	Bedding Strike/Dip	VGP—North Pole	
								Long(°)	Lat(°)
VNL42	8/8	180.9	-45.7	76	6.4	40-80(4)		55.1	82.8
VNL40	7/8	169.7	-49.0	162	4.7	40-80(4)	259°/18°N	127.6	80.2
VNL37	5/6	181.2	-43.0	42	12.0	40-80(4)	280°/25°N	54.8	80.6
VNL36	5/6	195.1	-48.0	112	7.2	40-80(4)		-10.4	76.1
VNL35	3/6	188.0	-46.5	74	14.4	30-80(5)	253°/21°NW	12.9	80.5
VNL34	6/6	193.9	-64.8	61	8.6	30-80(5)	218°/13.5°NW	-82.5	73.7
VNL33	10/10	208.8	-63.8	144	4.0	40-80(4)		-64.1	65.4
VNL32	8/8	144.8	-56.2	99	5.6	40-80(4)		-193.3	61.4
VNL31	6/6	147.4	-51.1	45	10.1	40-80(4)		-204.5	62.7
VNL30	6/6	166.4	-45.8	65	8.4	40-80(4)	205.5°/21.5°NW	123.9	76.3
VNL23	8/8	166.5	-45.1	50	7.9	40-80(4)	241.5°/15.5°NW	121.8	76.1
VNL22	6/6	174.8	-29.3	64	8.4	40-80(4)	237.5°/29.5°NW	76.9	70.8
VNL21	6/6	169.9	-39.0	82	7.4	40-80(4)		100.0	74.9
VNL20	6/6	161.9	-33.5	173	5.1	40-80(4)	233.5°/27.5°NW	111.5	67.2
MEAN (Normal Directions)	33	1.8	48.1	34	4.4			44.5	84.6
MEAN (North VGPs)	33			26	5.0			39.8	85.4

N/n, number of specimens used in calculations/number of specimens measured.

D_R, I_R, structurally corrected declination (D) and inclination (I); rotated to horizontal using measured bedding attitude (strike/dip).

k, best estimate of precision parameter of Fisher distribution.

α_{95}, radius in degrees of the 95 percent cone of confidence about the mean direction.

Demag Levels (mT), range of consecutive AF demagnetization steps in millitesla used for obtaining the stable direction of each specimen; number of steps are given in ( ).

VGP Long., positive (negative) east (west) of Greenwich.

Site Location 34.30°N Lat., 241.51°E Long.

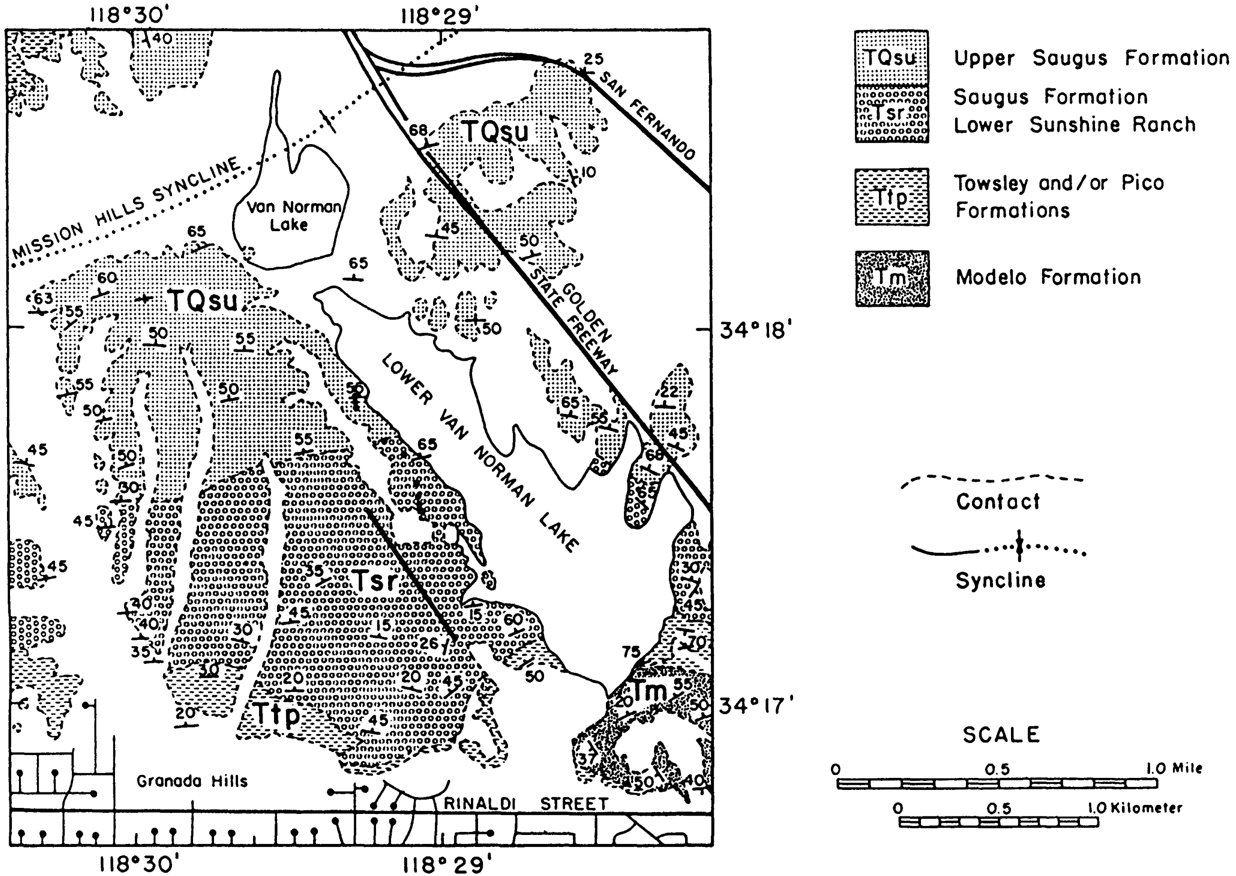

Figure 1. Geologic map of the Van Norman Lake reservoir area. Redrawn and simplified from the "Geologic Map of the San Fernando Earthquake Area," 1:18,000, Barrows et al. (1974). Closed circles represent individual sampling sites, and the heavy black bar trending NW-SE represents closely spaced sites, 20-90.

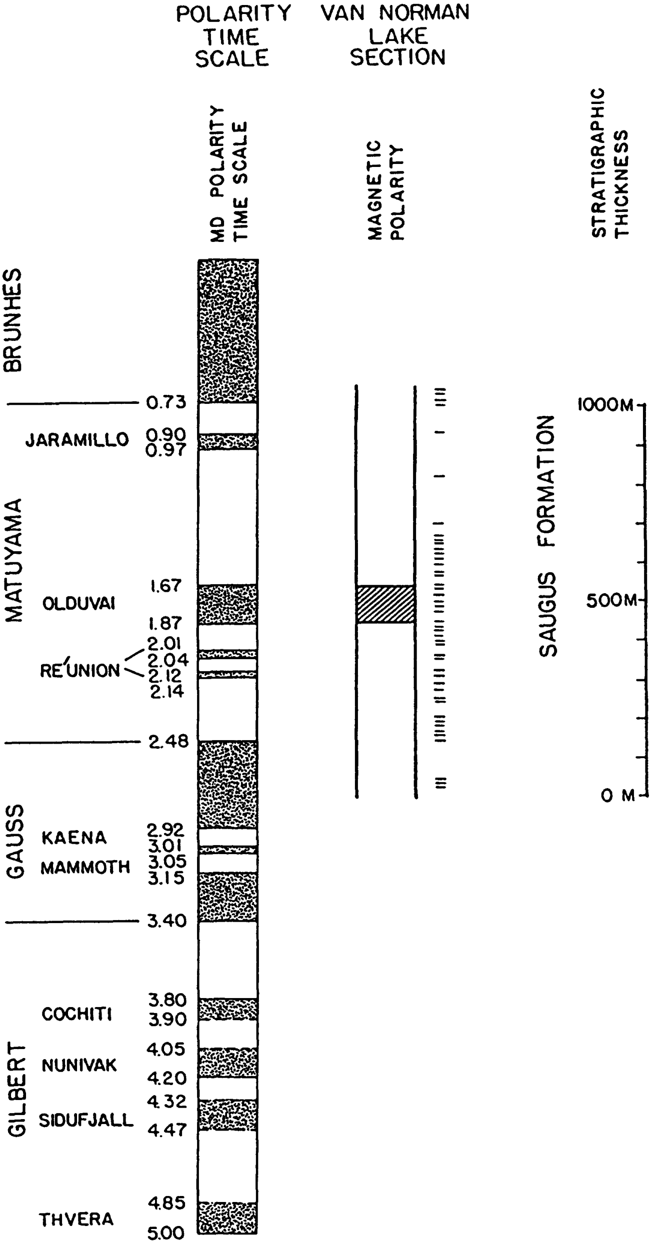

Figure 2. Magnetic stratigraphy along the Lower Van Norman Lake and the magnetic polarity time scale of Mankinen and Dalrymple (1979). Hatchured (white/unmarked) zones represent normal (reversed) polarity. Dashes along the right side of the stratigraphic column indicate paleomagnetic sampling sites.

VAN NORMAN LAKE

Site Mean Directions - Structurally Corrected

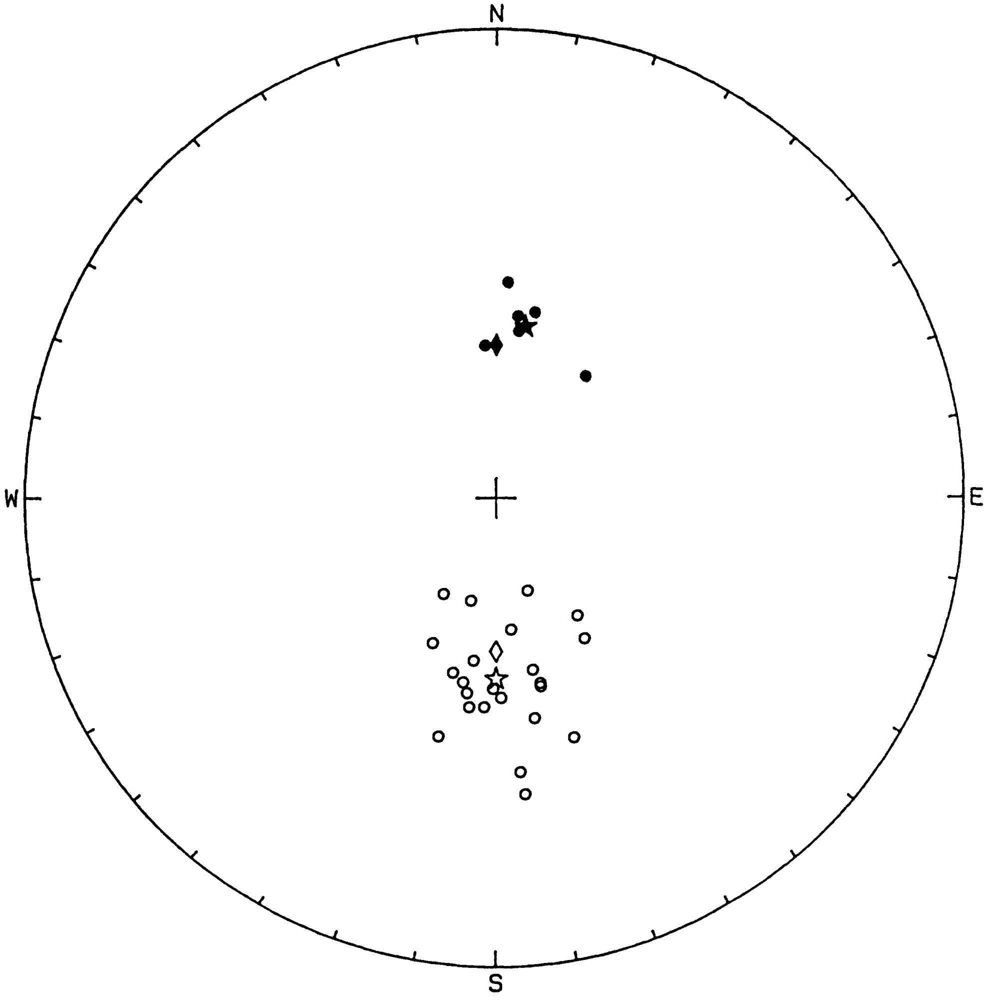

Figure 3. Stereogram of structurally corrected site mean PM directions (circles). Solid (open) symbols represent lower (upper) hemisphere directions. Diamonds represent the expected geocentric axial dipole directions. Stars indicate the mean PM directions of normal and reversed sites separately.

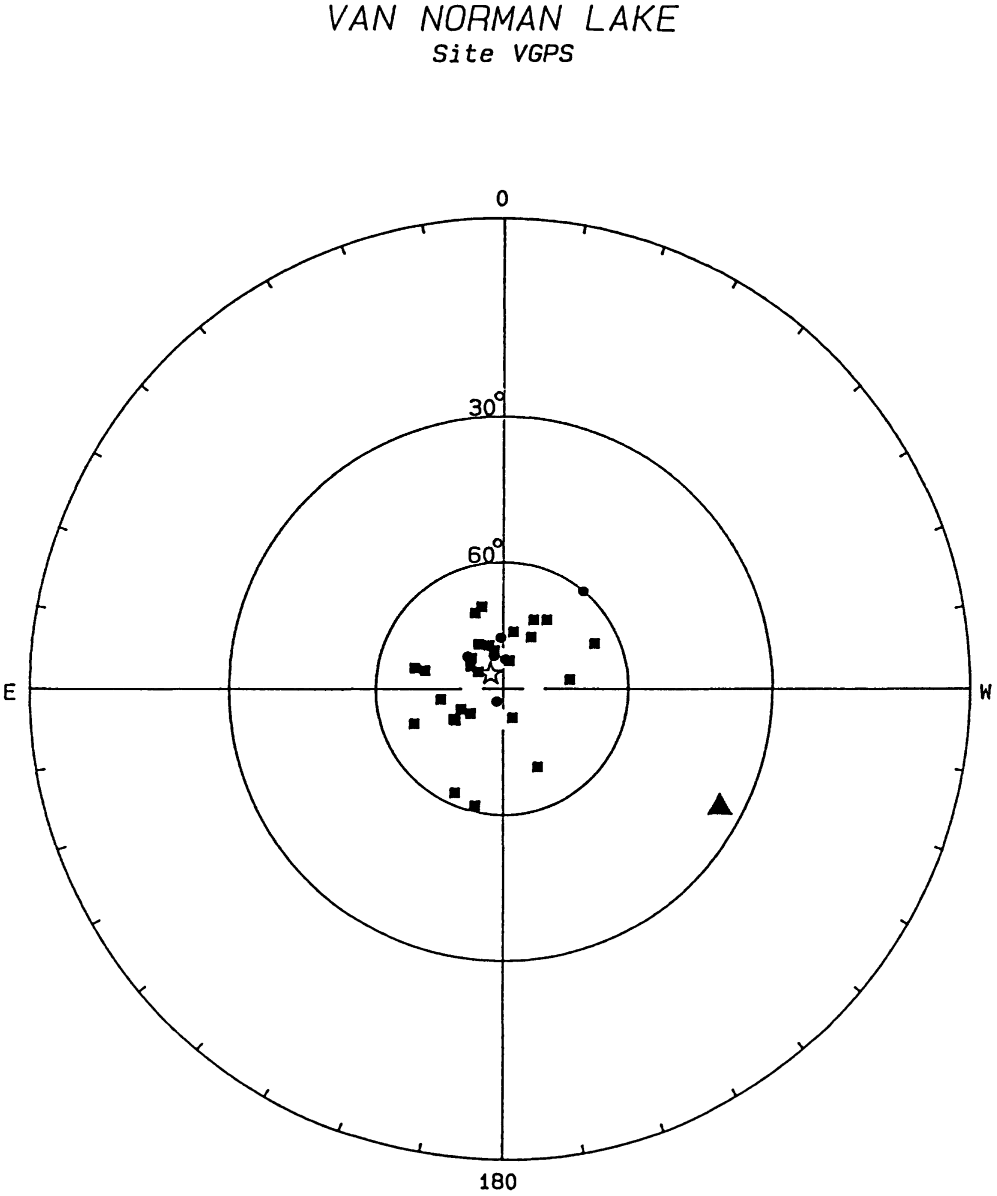

Figure 4. Northern hemisphere VGPs of structurally corrected Van Norman Lake sites. Triangle represents the sampling area at Van Norman Lake (34.30°N 241.51°E); the star denotes the mean VGP.

Holocene Displacements of the Alvord Fault and the Steens Fault Zone, Southeastern Oregon

Grant No. 14-08-0001-G1333

William D. Page, Mark A. Hemphill-Haley
Woodward-Clyde Consultants
100 Pringle Avenue, Suite 300
Walnut Creek, CA 94596-3564

Gary A. Carver, Raymond (Bud) Burke
Department of Geology
Humboldt State University
Arcata,CA 95521

Objectives

The proposed objectives for this project were to 1) better characterize the Steens Fault Zone (SFZ) and the Alvord fault along the eastern side of Steens Mountain in southeastern Oregon; 2) obtain data for scarp degradation analysis; 3) contrast and compare the results to tectonically similar faults in more densely populated areas of Nevada and Utah; and 4) add information to the fault length and displacement data base for normal faults in the Basin and Range province.

A line of low-sun-angle aerial photographs was flown along the eastern range-front of Steens Mountain and used to map the SFZ. Two trenches were excavated into the Alvord fault, one near the range-front in coarse, clastic deposits and the other in playa-dune deposits. In addition, profiles were measured normal to the scarp formed by the Alvord fault. Finally, shorelines within the Alvord basin were surveyed to analyze local deformation.

This project was conducted as a cooperative effort between Woodward-Clyde Consultants and professors and graduate students of Humboldt State University.

Preliminary Results

Low-sun-angle black and white aerial photographs were taken along the western margin of the Alvord Valley in June at a scale of 1:24,000. These photographs were then used for selection of trench sites and for detailed mapping of the SFZ.

The Alvord fault, a component of the SFZ, is a segment of a range-front fault that extends south of the study area for a distance of about 35 km to near Denio Junction, Nevada. The Alvord fault segment, approximately 22 km long and located at the base of the Central Steens, appears to be the most recent site of surface rupture within the SFZ. Other scarps to the south that extend southward to Nevada, although youthful, appear morphologically older than those of the Alvord fault.

Two trenches were excavated to expose the Alvord fault. One trench, near Alvord Hot Springs, exposed a near vertical fault with >2 m of normal slip. It appears that a portion of the collapsed, scarp free-face was preserved in the profile. Several tephra and charcoal samples were collected for possible age information.

A second trench was excavated in a dune field-playa complex away from the Steens Mountain range-front. The fault scarp which has been preserved in these fine-grained, poorly consolidated sediments can be as great as 2 m in height, however, dip-slip displacement along the near-vertical fault was no more than 0.5 m. Therefore, the scarp appears to be the surface expression of folding in the sediments, possibly acompanying predominantly strike-slip movement along that portion of the Alvord fault. Tephra samples were collected for analysis in this trench also.

Prominent shorelines which may record coseismic tilting were surveyed in the vicinity of the Alvord fault. Those data are being analyzed at this time.

A report detailing the findings of this project is now in preparation.

EARTHQUAKE RESEARCH IN THE WESTERN GREAT BASIN

Contract 14-08-0001-21986, October 1987

W.A. Peppin, M.K. Savage, and U.R. Vetter
Seismological Laboratory
University of Nevada
Reno, NV 89557
(702) 784-4975

Investigations

This program supports continued studies with research focused on: (1) seismicity in the White Mountains Gap; (2) magmatic processes in Long Valley Caldera; (3) relocations of Mammoth Lakes earthquakes; (4) focal mechanisms and stress distribution: (5) analysis of digital waveforms. The most interesting new results are described below.

Seismicity in the Mammoth - Bishop area between 01 January and 30 September 1987, comprising 2,609 earthquakes, (**Figure 1**) shows continued high activity in the Chalfant area, but nearly normal activity in the Round Valley-Wheeler Crest region. Activity also continues south of Long Valley caldera, where earthquakes clearly line up in N 10° E direction, a direction which is seen in the fault planes of many of the Mammoth area earthquakes studied earlier (e.g. Cramer and Toppozada, 1980, Vetter 1987).

A statistical study of earthquake focal mechanisms of small to moderate earthquakes in eastern California and western Nevada shows that the principal axes of extension (= T-axes), as inferred from these mechanisms, rotate clockwise from an azimuthal direction of 65° in the Mammoth Lakes area to 125° in the western Great Basin of Nevada to the east(**Figure 2**). The Walker Lane (WL), a Tertiary structure subparallel to the San Andreas fault and running in the study area from about 40 degrees N to 38 degrees N, lies east of this transition zone in western Nevada, apparently unrelated to the change: no change in the orientation of inferred T axes can be associated with the Walker Lane, in spite of clear evidence from Tertiary geology that this structure has recently separated provinces of markedly different tectonic styles: NNE-trending faults east and NNW-trending faults west of Walker Lane (Speed, 1979).

Earthquakes in west-central Nevada, NE of the Walker Lane, are 80% oblique and normal slip with inferred focal planes most commonly parallel to the direction of the basins and ranges; this is in accordance with the observations of normal faulting along almost all of the rangefronts. However, along the eastern front of the Sierra Nevada, the most spectacular of the normal-fault features in the Great Basin, most of the mechanisms show strike-slip faulting along trends not recognizable from the surface geology. Therefore, it remains an open question as to whether the focal mechanisms of small-to-moderate earthquakes in fact reflect the current tectonics in this region. In the eastern Sierra, the mechanisms of small earthquakes may be strongly influenced by local fracture patterns, produced in response to stresses long gone.

REFERENCES

Cramer, C. H., and Toppozada, T. R., A seismological study of the May 1980 and earlier earthquake activity near Mammoth Lakes, California, *Calif. Div. Mines Geol. Spec. Rep.*, *150*, 91-130, 1980.

Speed, R., 1979. Extensional faulting in the Great Basin: kinematics and possible changes with depth, *U.S.G.S. Open File Rept.* **79-1239**, 121-138.

Vetter, U.R. (1987). Characterization of regional stress patterns in the western Great Basin using grouped earthquake focal mechanisms, *Tectonophysics*, accepted for publ. Oct. 1987.

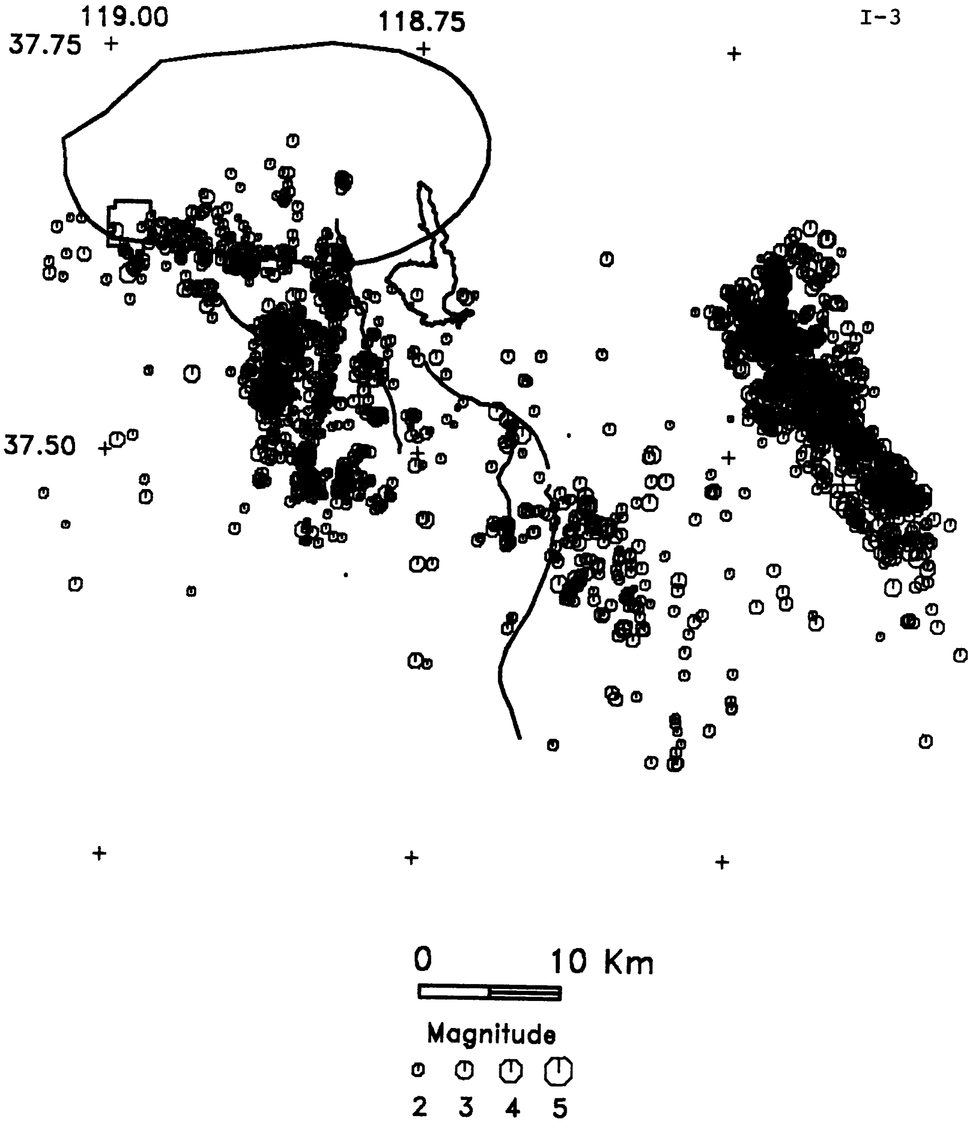

Figure 1. Seismicity near Mammoth Lakes for the time period 1 January to 30 September 1987. Activity south of the caldera continues to define NNE-trending lineups of earthquakes. Most of the earthquakes are aftershocks of the 1986 Chalfant Valley sequence, the irregular area to the right in the figure.

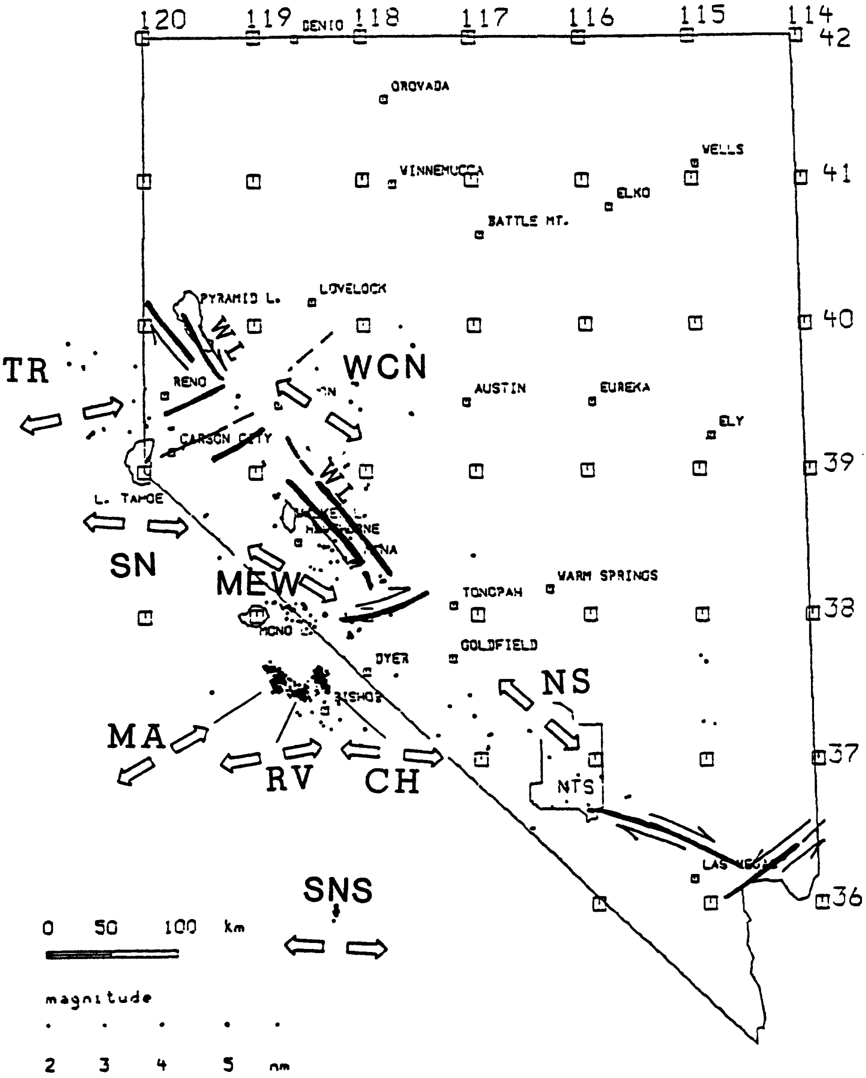

Figure 2. Averaged T-axes of stress (arrows) inferred from grouping of values obtained from focal mechanisms in various regions of western Nevada and eastern California. TR: Truckee region; WL: Walker Lane; WCN: west-central Nevada; SN: Sierra Nevada; MEW: Mono-Excelsior-Walker Lake; MA: Mammoth Lakes; RV: Round Valley 1984; CH: Chalfant Valley 1986; NS: Nevada south; SNS: Sierra Nevada south. There seems to be a relationship between these directions of extension and the NW-trending Walker Lane Tertiary structure.

EARTHQUAKE HAZARDS REDUCTION PROGRAM

SEMI-ANNUAL TECHNICAL SUMMARY: 1 April-30 September 1987

Project: Radiocarbon Geochmeistry and Geophysics
9570-01568
Project chief: Stephen W. Robinson
Branch of Iosotope Geology
U.S.G.S. , Mail Stop 937
FTS 459-4684

During the time period the radiocarbon laboratory was occupied with work on four investigations of earthquake related tectonics, one of which is not directly funded by the Earthquake program.

1. Project: Coastal Tectonics
   Chief: Kenneth Lajoie

2. Project: Quaternary Geology of the Washatch Front
   Chief: Michael Machette

3. Project: Puget Lowland Seismic Hazards
   Chief: Brian Atwater

4. Project: Alaska Coastal Environments
   Chief: Susan Bartsch-Winkler

Structure and Mechanics of Fault Jogs in Relation to Earthquake Rupturing

14-08-0001-G1331

Richard H. Sibson
Department of Geological Sciences
University of California
Santa Barbara
California 93106
(805) 961 4530

Investigations

Investigations of the geological structures which control the nucleation, perturbation and stopping of earthquake ruptures in major fault zones.

Results

1. More data on the effects of rupture interaction with jogs and isolated bends on strike-slip faults have been collected. An interesting directivity effect appears to be associated with slip transfer around isolated fault bends. Slip transfer across such structures involves dilation or compression across the adjoining fault segment depending on the direction of rupture propagation into the bend. Preliminary findings are that ruptures are more likely to terminate at isolated bends when slip transfer involves dilation, than when it leads to enhanced compression.

2. A presentation at the USGS Workshop "Directions in Paleoseismology" (Albuquerque, April 22-25, 1987) reviewing observed interactions of strike-slip ruptures with fault irregularities has been extensively revised, and has been submitted for inclusion in the Open-File Report on that meeting.

3. A collaborative study of mesothermal gold-quartz vein systems developed syntectonically in shear zones of mixed "brittle-ductile" character, cutting the granite-greenstone belts of the Canadian shield (and elsewhere), has been initiated with Drs. K. Howard Poulsen and Francois Robert of the Geological Survey of Canada. These shear zones are of relevance to modern earthquake source processes in similar structural settings (high-angle reverse or reverse-oblique faulting) because: (i) they appear to have developed at depths corresponding to the base of the seismogenic regime where larger earthquake ruptures nucleate, and (ii) the vein systems unequivocally demonstrate cyclic development of supra-lithostatic fluid pressures. A preliminary geomechanical model accounting for the observed structural relationships has been developed and is currently in internal review with the Geological Survey of Canada.

4. A preliminary visit to the Archean granite-greenstone terrain of the Slave Province at Yellowknife, N.W.T., Canada (8/30/87 to 9/7/87) to attend the Geological Association of Canada field meeting has allowed reconnaissance studies of:

(i) The mixed "brittle-ductile" high-angle reverse shear zones of Archean age within the greenstone belt which host mesothermal gold-quartz vein systems, exposed by mining over a depth interval approaching 2 km.

(ii) The younger Proterozoic left-lateral strike-slip faults which disrupt the Archean granite-greenstone terrain (and the older shear zones). Total left-slip across this fault system amounts to about 17 km, with as much as 5 km left-slip and some minor vertical displacement across the West Bay Fault, the dominant strand within the system.

These two shear systems both form attractive targets for continued work. Contact has been established with the mine geologists of both the Giant and Con mines, which it is hoped will allow future access to the vein systems within the Archean mixed "brittle-ductile" shear zones (see item 3, above). The younger brittle strike-slip system which is well-mapped in the vicinity of Yellowknife, and is surprisingly well exposed, forms an exhumed analog of comparable scale and complexity to the interweaving system of strike-slip faults now active in the southern reaches of the San Jacinto fault zone. Extensive local development of hydrothermally cemented (quartz-haematite) breccias along these otherwise brittle and well-localized faults appears related to major fault bends and intersections, and likely represents zones of slip-induced dilation.

Reports

Brown, N.N. and Sibson, R.H., 1987: Deformation at an antidilational fault jog: a study of the Ocotillo Badlands, Southern California (abstr.). Trans. Am. Geophys. Union - in press.

Sibson, R.H., 1987a: Earthquake rupturing as a hydrothermal mineralizing agent. Geology 15, 701-704.

----1987b: Effects of fault heterogeneity on rupture propagation. U.S. Geol. Surv. Open-File Report - in press.

----1987c: Fluid pressure cycling near the base of the seismogenic regime: evidence from mesothermal gold-quartz lodes (abstr.). Trans. Am. Geophys. Union - in press.

EARTHQUAKE GEOLOGY OF THE SAN ANDREAS AND OTHER FAULTS IN CALIFORNIA

Grant number 14-08-0001-G1370

Kerry Sieh
Division of Geological and Planetary Sciences
California Institute of Technology
Pasadena, CA 91125
(818)356-6115

Our work during the past six months involves four separate projects being undertaken as the Ph.D. dissertation work of Stephen Salyards, Patrick Williams, Carol Prentice and Marcus Bursik.

Paleomagnetic studies of warping at Pallett Creek

The objective of this study has been to determine the amount of non-brittle dextral shear at the Pallett Creek site during the past three large earthquakes, in AD 1857, 1812 and 1480 ± 15. This is slip beyond that which has been documented by Sieh (1984) as offset of piercing points across discrete fault planes. Our work is predicated upon the belief that any strike-slip rotational deformation should be visible as a rotation of the magnetic declination of the sediments. This information is important for three reasons: First, the slip rate determined across the faults at Pallett Creek is only 9 mm/yr for the past 1200 years. This is incompatible with all tectonic models of the fault. Recognition of non-brittle warping may solve this problem. Second, determination of the total dextral offset associated with the past few large earthquakes at Pallett Creek is important to understanding the behavior of the fault. How large are the offsets. Are they similar from event to event, or do they vary appreciably? Third, can paleomagnetics be used to determine the non-brittle offset across fault zones?

The results from the Pallett Creek site have met all three of these objectives. Several hundred samples were collected from the two layers that bracket the third earthquake back. In each layer groups of three samples were collected at regular intervals; one meter intervals out to 20 meters from the fault and at two meter intervals out to 48 meters. Dextral rotations of the paleomagnetic directions, relative to directions of the samples collected 48 meters from the fault, are present. Using the direction of the samples at 48 meters as a reference, this deformation in combination with the brittle slip gives an average slip rate over the past three full earthquake cycles of 35.8 ± 1.2 mm/yr. Total dextral offset during event V, in AD 1480 ± 15, was about 6 meters. Total offset during events X and Z (1812? and 1857) was about 12 meters. Sieh (1984) showed that the total brittle slip for these two events was 4 meters, with each event accounting for 2 meters. If the paleomagnetically-determined warping of 8 meters is also divided equally, each of the latest two events was associated with about 6 meters of dextral slip.

These values for the slip rate and offset per event are minimum values, because the paleomagnetic sampling traverse extended 48 meters northeast of the fault, but only 3 meters southwest of the fault. We believe, however, for reasons that we don't present here, that the values are likely to approximate the total offsets and slip rate across the entire zone of deformation.

Paleoseismic investigations of the San Andreas fault near the Salton Sea

Field studies by Patrick Williams in an area about 10 kilometers from the southern terminus of the San Andreas fault are recovering its slip history for the past 80-, 300- and 800- year intervals. Discrete fault offsets have been recovered from the strata of four lacustrine episodes. Lacustrine strata of ancient Lake Cahuilla have been offset across the San Andreas fault at Salt Creek and 40 km further northwest near Indio. A reduction in rate of slip and size of slip events appears to have occurred over the past millennium at both sites.

At Salt Creek three packets of lacustrine sediment yield radiocarbon dates of about AD 850, 925 and 1210; two of these overlay and are cut by the fault. About 6 m of slip occurred during rapid deposition in the oldest lake. No event approaching that size has occurred subsequently. There is, however, 3.5 m of offset of upper oldest lake and second lake strata. This could be wholly aseismic slip (creep at the site has averaged 1.75 mm/yr over the past 80 years); alternatively, a relatively small slip event could account for part of this figure.

The southern 100 kilometers of the San Andreas fault has been aseismic during the entire period of instrumental record. However, we find that the fault has exhibited slip at 10 to 20 % of its long-term rate for the past 40-, 80- and, perhaps, 300- year periods. Offset strata at Indio dates the latest large (> 2m) offset along this trace at AD 1680 ± 40. Additional data indicate that the long-term slip rate is at least 25 mm/yr. Displacements subsequent to about 1680 are recorded by numerous features along this segment of the fault: lacustrine strata deposited shortly after the 1680 earthqauke are offset about 1 m at Indio and at Ferrum, near the Salton Sea; Salton Sea sediment deposited over the fault at Salt Creek during a high-stand in 1907 has been offset about 14 cm; and a canal built in 1949 at Indio has been offset 6.8 cm. These data yield average slip rates of between 1.5 and 4 mm/yr, far lower than the long-term rate. These data demonstrate that these low slip rates have been relatively uniform over the past 80 and perhaps 300 years. This suggests that aseismic slip along the southern San Andreas fault is not a short-term precursor to much larger seismogenic rupture.

Paleoseismic studies of the northern San Andreas fault

Last spring Carol Prentice spent several weeks in the lab separating zircon crystals from an ash collected from the Ohlson Ranch formation. The zircons were sent to Dr. Naeser of the USGS in Denver for fission track analysis. The age of this ash will constrain the age of a unit offset approximately 50 kilometers across the San Andreas fault in northern California.

Over the summer, Prentice made a series of excavations across th fault near Point Arena. These excavations yielded both paleoseismic and slip-rate data. Carbon samples will be sent to labs for age determination to provide constraints on the ages of paleoseismic events and a buried channel offset approximately 67 meters across the fault.

Mapping of the marine terraces between Fort Ross and Point arena is continuing and will provide information on deformation and slip rate since late Pleistocene time.

Volcanotectonic studies in the Mono Basin

Graduate student Marcus Bursik is studying the eastern Sierra Nevada range front. We are investigating the relationship between tectonic and volcanic processees in an active extensional environment. Our ultimate objective is to determine the possibility of forecasting both earthquakes and volcanic eruptions by understanding their behavior as recorded in the geological record. Bursik's research focuses on 1) comparison of the geometric relationships between active tectonic and volcanic features, and 2) determination of rates of faulting and injection of dikes underneath the Mono and Inyo Craters within the late Quaternary period. He is testing the hypothesis that volcanic dike formation and eruption, as well as normal faulting, occurs as an extensional strain relief mechanism.

In the past six months Bursik finished a study of flow foliations and faults on domes within the Mono Craters chain. These data are being compared with our previously constructed maps of late Quaternary faults to understand the orientations af regional strains and stresses, and how they are manifested differently in the volcanoes and the faults. We have also finished measuring seismic velocities in clasts on moraines that cross the Sierran rangefront. These data are enabling us to date the late Pleistocene moraines offset by range-front faults. From these determinations we will determine fault slip rates and extension rates.

Modeling of Induced Seismicity and Implications for Earthquake Prediction

14-08-0001-G-1358

D.W. Simpson
Lamont-Doherty Geological Observatory of Columbia University
Palisades, New York 10964
(914) 359-2900

Two Types of Induced Seismicity

The temporal distribution of induced seismicity following the filling of large reservoirs shows two types of response. At some reservoirs, seismicity begins almost immediately following the first filling of the reservoir. At others, pronounced increases in seismicity are not observed until a number of seasonal filling cycles have passed. These differences in response may correspond to two fundamental mechanisms by which a reservoir can modify the strength of the crust - one related to rapid increases in elastic stress due to the load of the reservoir and the other to the more gradual diffusion of water from the reservoir to hypocentral depths. Decreased strength can arise from changes in either elastic stress (decreased normal stress or increased shear stress) or from decreased effective normal stress due to increased pore pressure. Pore pressure at hypocentral depths can rise rapidly, from a coupled elastic response due to compaction of pore space, or more slowly, with the diffusion of water from the surface.

Modeling of Transient Response in Reservoir Induced Seismicity

One of the characteristics of reservoir triggered seismicity observed at a number of sites is that it depends on the rate of filling of the reservoir - increased seismicity tends to follow times of rapid filling but is less likely to occur following slower filling to the same absolute water level. This implies a transient response to loading that can have a decay time short compared to the loading rate. Transients in pore pressure can be produced at depth beneath a reservoir by elastic compression of pore space in localized zones of small spatial dimension. Equilibration of pore pressure in these zones can occur on time scales that are short compared to that necessary for fluid diffusion from the surface. If the rate of loading at the surface is slow compared to this equilibration time, the pore pressure dissipates and there is little effect on strength. If the loading rate is more rapid, the effect is additive and significant decreases in strength can occur.

Localized zones of pore pressure increase can be produced by heterogeneities in the elastic and fluid properties of the crust. We have modeled the elastic influence of localized zones of high strength in an otherwise weak fault and the temporal changes of coupled pore pressure following the imposition of a surface load. The resulting variations in pore pressure and effective stress are in much closer agreement with the temporal and spatial characteristics of observed cases of induced seismicity than for models with homogeneous elastic properties.

One type of elastic heterogeneity may be asperities on faults, which can lead to localized stress concentrations and, through elastic compression, corresponding increases in pore pressure. Diffusion of pore pressure into surrounding areas can extend both the temporal and spatial influence of the stress concentration. These processes may relate to failure during natural episodes of stress accumulation and the role of fluids in triggering earthquakes may be important in understanding both the earthquake source and processes precursory to large earthquakes.

Induced Seismicity at Aswan Reservoir

A continuing sequence of earthquakes at Aswan Reservoir began with a magnitude 5.3 event on November 11, 1981 when the reservoir level was close to its maximum since filling started in 1964. During the recent African drought, the water level in the reservoir has dropped by more than 20 m and the level of seismicity has also decreased. However, a sequence of more than 180 earthquakes in June 1987, with maximum magnitude of 3.8, following an abrupt change in rate of water withdrawal, shows that the area is still active and under the influence of the reservoir.

The seismicity at Aswan is concentrated in clusters along the Kalabsha fault zone, a major east-west structure that intersects the reservoir about 45 km south of the High Dam. The mainshock and highest density of early aftershocks occur at depths of 15 - 25 km, deeper than other cases of induced seismicity and deep for intraplate earthquakes in general, with no activity above the mainshock at depths less than 15 km. Lower level activity on adjacent segments of the same and conjugate faults is confined to depths of 0 - 10 km, with no deeper activity. The earthquakes show clear lineations in epicentral strike, which are in close agreement with fault plane solutions showing almost pure strike-slip faulting, but which are rotated with respect to the average strike of the geological expression of the faults on which they are located.

Early in the sequence, depths in both the shallow (0-10 km) and deep (15-25 km) groups of activity extend fairly uniformly over these ranges. As the level of activity decreases with time, however, the depth range over which the activity occurs becomes smaller, so that by mid-1985 there are two localized concentrations near 5 and 18 km. These depths may indicate concentrations of stress induced by the reservoir or variations in strength along the fault.

The temporal distribution of seismicity detected since a telemetered network was installed in July 1982 shows that the seismicity increased following each of the yearly maxima in water level 1982 - 1985. When the seismicity is separated into the deep activity near the mainshock and the shallower activity elsewhere, the deeper activity gradually decreases and after 1982 the seasonal maxima are almost entirely confined to the shallow activity closer to the central part of the reservoir.

Because of the flat topography of the reservoir area, the final 15 - 20 m change in water level at the end of the filling at Aswan (1972 - 76) or the recent drop in reservoir level of the same magnitude, is much more significant than a simple 15 -20 m change in water head. In the early stages of filling, the old Nile channel confined the reservoir to within a few km of the center of the old river course.

In 1976, a bay along the Kalabsha fault flooded and rapidly extended the reservoir surface to the west. From deep piezometer wells it is known that the groundwater level in the epicentral area prior to flooding was near an elevation of 105 m, 70m below the eventual level of the reservoir. We propose that as the reservoir entered the Marawa area, water from the lake flowed into the sandstone, raising the groundwater level until it became continuous with the lake itself. Both in terms of the increased water head (70m) and the volume of water added to the porous sandsone (~ 10 km^3) the flooding of the Kalabsha bay alone is therefore comparable to the filling of many large reservoirs. This effect in the epicentral area is in contrast to that near the Nile channel, where the groundwater prior to filling was already near the surface and the seepage from the reservoir affected only a narrow prism near the river edge. Analysis of data on the water budget of the reservoir, from measurements of inflow and outflow on the Nile, show losses due to seepage that are in agreement with our estimates of the volume of water lost to the sandstone in the epicentral area.

In the early stages of development of Aswan reservoir, it was realized that seepage into the very porous Nubian sandstone could account for significant losses of water from the reservoir storage. To monitor changes in the regional water table and the flow from the reservoir, a series of profiles of monitoring wells were established in 1964 at the start of the filling of the reservoir. Three profiles cross the reservoir upstream from the dam. Each profile consists of 4-8 shallow wells (< 80 m) on each side of the river at distances of up to 10 km from the old Nile channel. At the ends of the profiles are deep wells (< 400m) which penetrate to basement. In addition, there are 4 deep wells in the northern reservoir area. Because of the importance of the groundwater in determining the gross influence of the reservoir, we realized that the piezometer wells could provide a wealth of unique data on the changes in the ground water system, its influence on the reservoir volume and the properties of the rock system. Two additional wells were drilled in 1985 as part of the earthquake study, and these, along with three of the original wells, have been instrumented to measure water level (1mm resolution), temperature and atmospheric pressure. The field units sample and store data every 12 minutes and telemeter to the central recording station once an hour, where all data are recorded on floppy disk.

The long term response of the wells near the reservoir clearly shows a substantial rise in water level due to bank storage as water enters the porous Nubian sandstone. In the intermediate term, seasonal variations in the reservoir level are seen in some of the deeper wells. The short term response is dominated by the influence of atmospheric and tidal loading. The responses to diurnal and semi-diurnal earth tides and atmospheric pressure changes are clearly seen. The spectral response of the wells to these narrow band harmonic signals, plus the broader band components in the atmospheric pressure, allow the extraction of hydraulic properties of the aquifer system.

Publications

Simpson, D.W., Triggered earthquakes, *American Review of Earth and Planetary Sciences, 14*, 21-42, 1986.

Kebasy, R.M., M. Maamoun, E. Ibrahim, A. Megahed, D.W. Simpson, and W.S. Leith, Earthquake studies at Aswan Reservoir, *Journal of Geodynamics, 7,* 195-203, 1987.

Simpson, D.W., R.M. Kebeasy, C. Nicholson, M. Maamoun, R.N.H. Albert, E.M. Ibrahim, A. Megahed, A. Gharib, and A. Hussain, Aswan telemetered seismograph network, *Journal of Geodynamics, 7,* 173-193, 1987.

Simpson, D.W. and T.N. Narasimhan, Reservoir induced earthquakes and the hydraulic properties of the shallow crust, *EOS, Trans. AGU, 67,* 242, 1986.

Simpson, D.W., W.S. Leith, and C.H. Scholz, Two types of reservoir induced seismicity, submitted to *Bulletin of the Seismological Society of America*, 1987.

Simpson, D.W., Triggered earthquakes and their implications for earthquake source processes, *International Union of Geodesy and Geophysics (IUGG), XIX General Assembly, Vancouver, Canada* , pg 341, August 9-22, 1987.

Kebeasy, R.M., D.W. Simpson, A. Gharib, Induced Seismicity around Aswan Lake, Egypt, *International Union of Geodesy and Geophysics (IUGG), XIX General Assembly, Vancouver, Canada,* pg 272, August 9-22, 1987.

Beavan, J., K. Evans, D.W. Simpson, Broad-Band Response of Water Wells to Applied Stress and Estimates of In-Situ Elastic Properties, *AGU Meeting -Spring 1987, Additional Abstracts,* pg 63.

DETAILED GEOMORPHIC STUDIES TO DEFINE LATE QUATERNARY FAULT BEHAVIOR AND SEISMIC HAZARD, CENTRAL NEVADA

Contract #14-08-0001-G136

Steven Slaff, Philip Pearthree, William Bull, Karen Demsey,
Julia Fonseca, Suzanne Hecker, and Oliver Chadwick
Department of Geosciences
University of Arizona
Tucson, Arizona 85721
(602)621-6024

Investigations

The Central Nevada Seismic Belt (CNSB) is a 360 km-long zone of active faulting and historical surface rupture in the Basin and Range physiographic province. During this century, four events of $M_s \geq 7.0$ have occurred in the zone (Slemmons, 1967). Wallace (1978) proposed that a belt-filling sequence of earthquakes may be in progress and identified the Stillwater Seismic Gap as a likely location for future faulting. The present study applies geomorphic techniques to determine the spatial and temporal distribution of late Quaternary surface ruptures in central Nevada and the severity of associated seismic hazards. Evidence supporting the belt-filling hypothesis is also being examined. The effort is concentrated in the CNSB and in adjacent similar structural belts of central Nevada. Several subareas have been or are being investigated in detail and a general picture of the entire region is emerging.

The approach includes the following methods of investigation: (1) Tectonic landform analysis to determine relative tectonic activity classes of mountain fronts and their segments (a reconnaissance-level tool, see Bull and McFadden, 1977; Bull, 1984); (2) Quantification of soil-profile development by using the Profile Development Index (Harden, 1982) to determine the relative ages of pertinent geomorphic surfaces; (3) Mapping and correlation of faulted and unfaulted late Quaternary geomorphic surfaces; and (4) Analysis of surveyed topographic profiles of alluvial fault scarps using solutions to the diffusion equation (Hanks, 1984) to obtain numerical estimates of scarp ages.

Results

Active uplift of the Wassuk Range is attested to by two large-magnitude ($M_s \geq 7.0$) Holocene faulting events along the east front of the range (Demsey, 1987), but there has been no historical ground rupture. Latest Pleistocene (∿12 ka) highstand shoreline features of Lake Lahontan (Benson and Thompson, 1987) are preserved on the west side (eastern front of the uplifting Wassuk Range) and east side (western front of the stable Gillis Range) of the Walker Basin. The shoreline features provide a basis for quantifying rates of faulting, scarp degradation, soil formation, and mountain-block uplift. Age and rate estimates determined from soil-profile development and diffusion-equation modeling may thus be checked and calibrated.

The eastern front of the Wassuk Range was divided into four segments based on the occurrence, preservation, and morphology of fault scarps. The longest segment is ∿35 km long, but the most recent rupture extended through more than one segment and offset a 50 km-long zone of the northern part of the range. Average surface displacement was 2.5 m. A shorter southern segment 30 km long ruptured independently earlier in the Holocene, with average surface dislacement of ∿2 m.

Soils examined range in estimated age from less than 500 years to 13-15 ky. The rate of soil genesis was quantified by using the Profile Development Index (Harden, 1982). Soil properties that vary the most systematically with time in the Walker Basin are related to clay accumulation and include texture, dry consistence, structure, and frequency and thickness of clay films. Soil profiles developed in Lake Lahontan highstand shoreline deposits and numerical dates obtained from tephra, charcoal, and wood deposits associated with the soils were used to calibrate the chronosequence reprsented by the Profile Development Index values.

Diffusion-equation modeling of alluvial fault-scarp degradation was applied successfully to the Wassuk Range frontal scarps. A variety of diffusivity coefficients was tested (Hanks and others, 1984; Pierce and Colman, 1986; Andrews and Bucknam, in press) and one derived in the course of this project specifically for the Walker Basin proved to be the most useful.

Deformation of originally-horizontal shoreline features formed during Lake Lahontan's most recent highstand is another indication of vertical tectonic movement of the Wassuk Range. A detailed topographic survey was made of the present altitudes of shoreline remnants on upthrown, downthrown, and unfaulted portions of the Walker Basin to determine the amount of Holocene uplift along the Wassuk Range front. The Gillis Range, on the east side of the basin, served as a stable reference from which to estimate regional deformation as well as localized uplift of the Wassuk Range. Data from near Rose Creek Canyon in the central portion of the range indicate that there has been 6-7 m of Holcoene fault displacement, which is consistent with estimates based on fault-scarp offsets. Fault-generated uplift of this portion of the Wassuk Range fault zone averages ∿1.5 m.

The average Holocene slip rate on the Wassuk Range fault zone is 0.4-0.5 m/ky. The most recent faulting of the southern segment occurred 4-7 ka along a 30 km-long zone. Differences in timing of surface ruptures along the three segments to the north cannot be demonstrated conclusively. If separate breaks did occur each was within the period from 2-3 ka and the central segment ruptured most recently.

Analysis of data collected along the eastern front of the Toiyabe Range in central Nevada suggests that Holocene faulting has occurred along the southern and central segments of the range.

Additional work is in progress to match Holocene and late Quaternary uplift rates with relative mountain-front tectonic activity classes, which describe Quaternary uplift patterns.

References

Andrews, D.J., and Bucknam, R.C. (in press). Fitting degradation of shoreline scarps by a model with nonlinear diffusion, Jour. Geophys. Res.

Benson, L.V., and Thompson, R.S. (1987). Lake-level variations in the Lahtonton basin for the past 50,000 years, Quat. Res., **28**, 69-85.

Bull, W.B. (1984). Tectonic geomorphology, Jour. Geol. Educ., **32**, 310-324.

Bull, W.B., and McFadden, L.D. (1977). Tectonic geomorphology north and south of the Garlock fault, California, in Geomorphology in arid regions, Doehring, D.O., ed., Proc. 8th Ann. Geomorph. Symp., State Univ. N.Y., Binghamton, 115-138.

Demsey, K. (1987). Holocene faulting and tectonic geomorphology along the Wassuk Range, west-central Nevada, M.S. prepub. manuscr., Univ. of Arizona, 1-64.

Hanks, T.C., Bucknam, R.C., Lajoie, K.R., and Wallace, R.E. (1984). Modification of wave-cut and faulting-controlled landforms, Jour. Geophys. Res., **89**, 5771-5790.

Harden, J.W. (1982). A quantitative index of soil development from field description: Examples from a chronosequence in central California, Geoderma, **28**, 1-28.

Pierce, K.L., and Colman, S.M. (1986). Effect of height and orientation (microclimate) on geomorphic degradation rates and processes, late-glacial terrace scarps in central Idaho, Geol. Soc. Amer. Bull., **97**, 869-885.

Slemmons, D.B. (1967). Pliocene and Quatenary crustal movements of the Basin and Range province, USA, Jour. Geoscience, Osaka University, **10**, 91-103.

Wallace, R.E. (1978). Patterns of faulting and seismic gaps in the Great Basin province, in Proceedings of Conference VI, Methodology for identifying seismic gaps and soon-to-break gaps, U.S. Geol. Surv., Open-File Rept. 78-943, 857-868.

Central California Deep Crustal Study

9540-02191

Carl M. Wentworth
Branch of Western Regional Geology
U.S. Geological Survey
345 Middlefield Road, MS 975
Menlo Park, California 94025
(415) 329-4950

Structure Across the Coast Ranges Boundary; Parkfield

Investigations

1. Final delivery has finally been made by the contractor of processed reflecion profiles extending from the Diablo Range across the northern San Joaquin Valley and into the Sierran foothills (lines CC-1 and CC-2).

2. A manuscript has been completed on the implications of the 1983 Coalinga earthquake on late Cenozoic deformation along the whole 600-km length of the east front of the California Coast Ranges.

3. A computer file of wells that reach crystalline basement in the California Great Valley has been prepared. Perhaps 50 wells in the San Joaquin Valley have yet to be incorporated in the file.

4. Young scarps found through photo interpretation off the San Andreas in the Parkfield area were field checked.

Results

1. The 600-km-long eastern front of the California Coast Ranges (Coast Ranges boundary) is marked by a remarkable association between parallel-striking uplift, folding, and basement structure and perpendicularly oriented directions of maximum horizontal stress. The 1983 Coalinga earthquake at the Coast Ranges boundary resulted from northeast-directed thrusting that, over the past 2 m.y., has produced Coalinga anticline above the blind eastern tip of the Coalinga thrusts. Late Cenozoic deformation associated with the whole length of the Coast Ranges boundary, probably including uplift of the eastern Coast Ranges, results from such compression and is closely adjusted to the shape of the southwest-facing basement buttress beneath the western Great Valley. We suggest that the easternmost Coast Ranges are underlain by thrusts, some of which extend out from beneath the range front to produce associated folding. This process has probably been underway since the slight clockward shift in the relative motion of the North American plate 4-5 m.y. ago.

2. Computer calculation of structure contours on the surface of crystalline basement beneath the Great Valley of California reinforces the results of earlier hand contouring. The surface really is extraordinarily smooth, with a local relief along strike typically much less than 200 m.

3. Two previously unrecognized sites of probable Quaternary faulting have been found in the vicinity of the Parkfield segment of the San Andreas fault. Due east of Cholame at the north side of Antelope Valley, a 35-foot high scarp in alluvium occurs along the trace of one of the east trending thrust faults mapped by Marsh (1960). West of the San Andreas and south of Cholame, alluvium is warped and apparently faulted in and near Gillis Canyon along the trend of the Red Hills fault mapped by Dibblee (1974).

Reports

Wentworth, C.M., 1987, Implications for crustal structure in the western Coast Ranges, California, from studies along their eastern margin (abs.): American Geophysical Union, EOS, Fall 1987 meeting.

Wentworth, C.M., Simpson, R.W., and Jachens, R.C., 1987, Late Cenozoic deformation around the Parkfield segment of the San Andreas fault (abs.): American Geophysical Union, EOS, Fall 1987 meeting.

Wentworth, C.M., Zoback, M.D., Griscom, Andrew, Jachens, R.C., and Mooney, W.D., 1987, A transect across the Mesozoic accretionary margin of central California: Royal Astronomical Society Geophysical Journal, v. 89, p. 105-110.

Convergence Rates Across Western Transverse Ranges

14-08-0001-G1372

Robert S. Yeats and Gary J. Huftile
Department of Geology
Oregon State University
Corvallis, Oregon 97331-5506

Investigations

We are concentrating on convergence rates in four cross sections: (1) San Miguelito and Rincon anticlines south to Oak Ridge fault, building on Grigsby (1986), (2) Ventura Avenue anticline at Ventura River south to Oak Ridge fault, (3) Silverthread oil field in Upper Ojai Valley south to Oak Ridge fault at Saticoy, and (4) Timber Canyon oil field south to the Santa Rosa Valley south of the Simi fault in Camarillo. In addition, Gary Huftile completed mapping in Piru Creek to correlate the fold belt east of Piru Creek to the strata in the hanging-wall block of the San Cayetano fault.

Results

A paper, "The Ventura Fold Belt and the Oak Ridge Fault, Western Transverse Ranges, California" by R. S. Yeats, G. J. Huftile, and F. Bryan Grigsby is being reviewed internally prior to submitting it to either Geology or Tectonics. This paper deals with the problem of why the slip on the Oak Ridge fault in the last 200,000 years decreases from nearly 2.5 km at South Mountain and Santa Paula to zero west of Oak Ridge at Saticoy. Previously we thought that the loss of separation was due to the change westward from dip slip to strike slip as the fault turns from a west to a southwest strike. However, this does not explain the zero separation in the last 200,000 years on the offshore Oak Ridge fault which has the same strike as it does at Santa Paula. Also, electric logs of Quaternary aquifers can be correlated directly across the Oak Ridge fault west of Saticoy.

Huftile (1987) found that the Sisar, Lion, and Big Canyon thrust faults extend downward into a decollement in the lower Miocene Rincon shale, and cross-section balancing shows that strata above the decollement are 6.2 km longer than competent strata (Vaqueros, Sespe, and marine Eocene) below it. For a cross section to be truly balanced, some way has to be found to account for the 6.2 km shortening in the competent section below the decollement.

The paper resolves this by making the Sisar fault system a frontal thrust system of the Oak Ridge fault. There is a transfer of displacement in the last 200,000 years from the Oak Ridge fault itself at South Mountain and farther east on Oak

Ridge through the decollement to the Sisar system in the Upper Ojai Valley. The transfer of displacement takes place along a NE-SW trending zone between Saticoy west of Oak Ridge and Timber Canyon oil field, where the Sisar fault turns sharply into the San Cayetano fault and disappears. West of this zone, rootless folds appear within the Ventura trough: Ventura Avenue, San Miguelito, and Rincon anticlines, each with a south-dipping thrust fault arching over the crest, so that each anticline is a fault-propagation fold, as first postulated by Grigsby (1986). The NE-SW orientation of the displacement transfer zone is consistent with aftershocks of microearthquakes on the Red Mountain and San Cayetano fault, deep aftershocks on the 1973 Point Mugu earthquake, and a slip vector on the Oak Ridge fault at Saticoy oil field, all of which trend NE.

The most important societal implication of this new hypothesis is that the Oak Ridge fault must be considered as active and seismogenic west of Oak Ridge despite the lack of post-200,000-year displacement. In addition, if the post-200,000-year displacement reaches the surface on the Sisar fault system, the southern margin of the Upper Ojai Valley must be considered to be subject to ground-rupture hazard.

Our present strategy is to work out the convergence and convergence-rate budget from east to west across the Ventura basin and from 2 Ma to the present.

Reports

Grigsby, F. B., 1986, Quaternary tectonics of the Rincon and San Miguelito oil fields area, western Ventura basin, California: M.S. thesis, Oregon State University, Corvallis, 110 p.

Huftile, G. J., 1987, Thin-skinned tectonics of the Upper Ojai Valley: EOS, Trans. Am. Geophys. Un., in press.

Huftile, G. J., 1987, Thin-skinned tectonics of the Upper Ojai Valley and Sulphur Mountain and vicinity, Ventura basin, California: M.S. thesis, Oregon State University, Corvallis, in prep.

Yeats, R. S., Lee, W. H. K., and Yerkes, R. F., Geology and seismicity of the eastern Red Mountain fault, Ventura County, California: U. S. Geological Survey Professional Paper 1339, in press.

VERY PRECISE DATING OF EARTHQUAKES AT PALLETT CREEK AND THEIR INTERPRETATION

Grant number 14-08-0001-G1086

Kerry E. Sieh
Division of Geological and Planetary Sciences
California Institute of Technology
Pasadena, CA 91125
(818)356-6115

Improved methods of radiocarbon analysis have enabled us[1] to date more precisely the ruptures of the San Andreas fault that are recorded in the sediments at Pallett Creek. Previous dates of these events had 95-%-confidence errors of 50 to 100 years. New error limits are 13 to 22 years for all but two of the dated events. This greater precision is due to larger sample size, longer counting time, lower background noise levels and more precise conversion of radiocarbon ages to calendric dates. The new, narrower date ranges, with one exception, fall within the broader ranges estimated previously (Sieh, 1984).

The average interval between the latest 10 episodes of faulting is 131 ± 1 years, a value equal to the present period of dormancy. However, variability about this mean is much greater than was suspected previously. Five of the nine intervals are less than 100 years long; three of the remaining four are about two to three centuries long. Our preliminary statistical analyses of these data indicate that the likelihood of a large earthquake associated with rupture of the fault at Pallett Creek within the next 30 years is less than values estimated previously by us and other workers.

The past 10 earthquakes appear to occur in four clusters, each cluster comprising two or three events. Earthquakes within the clusters are separated by periods of several decades, but the clusters are separated by dormant periods of two to three centuries. The time since the occurrence of the latest large earthquake — 131 years — suggests that the section of the fault represented by the Pallett Creek record is currently in the middle of one of its longer periods of repose between clusters. If this is true, the likelihood of a large earthquake along this section of the San Andreas fault in the next 30 years is quite small.

The greater precision of dates now available for large earthquakes recorded at the Pallett Creek site enables less speculative correlation of events between paleoseismic sites along the southern half of the San Andreas fault. A history of great earthquakes with overlapping rupture zones along the Mojave section of the fault remains one of the more attractive speculations.

---

[1] This work is being conducted in collaboration with Minze Stuiver (Quaternary Isotope Laboratory, University of Washington) and David Brillinger (Department of Statistics, University of California at Berkeley).

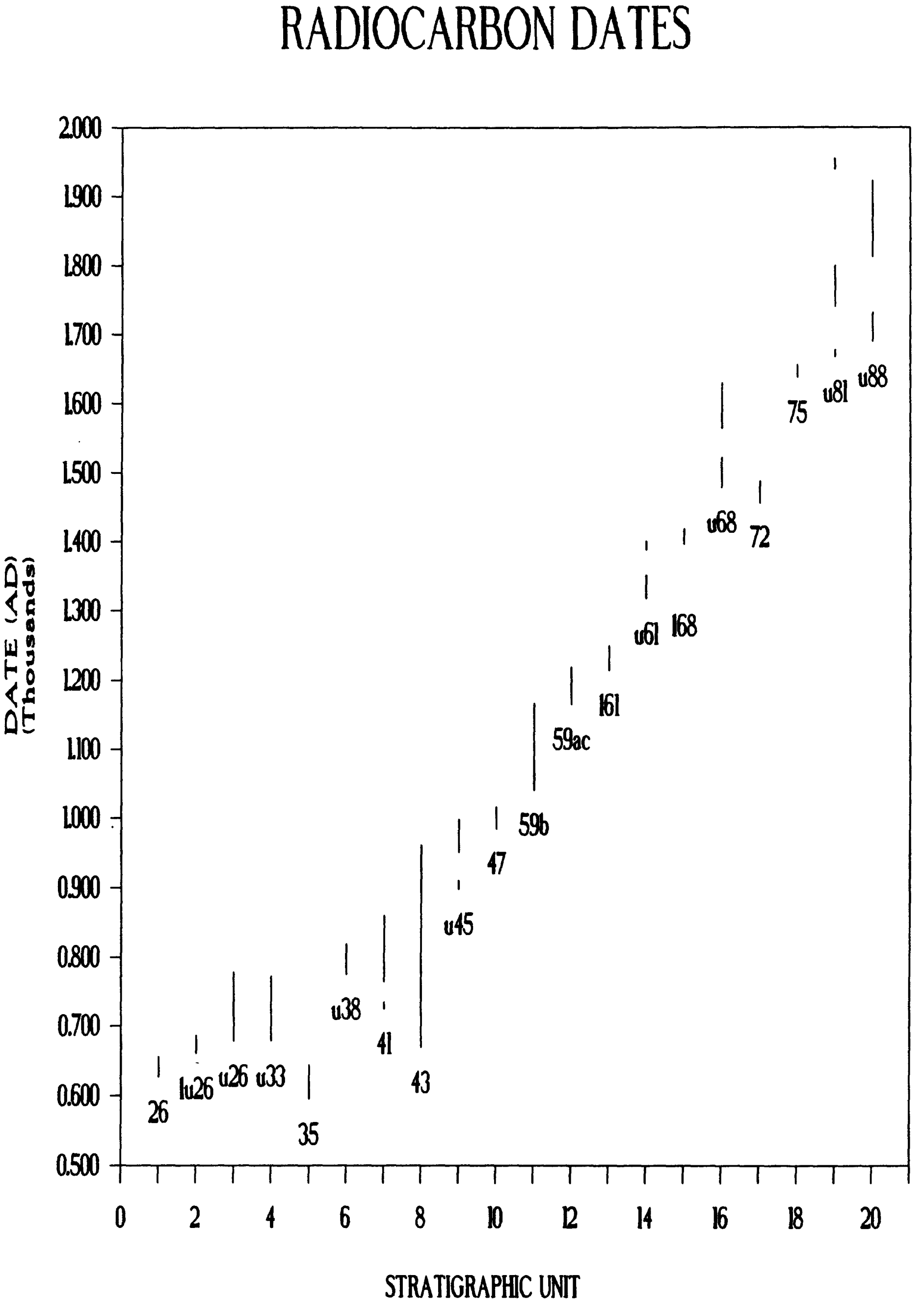

Figure 1. This plot of calendric date versus stratigraphic position shows the internal consistency of the radiocarbon analyses performed for this study.

EARTHQUAKE DATES

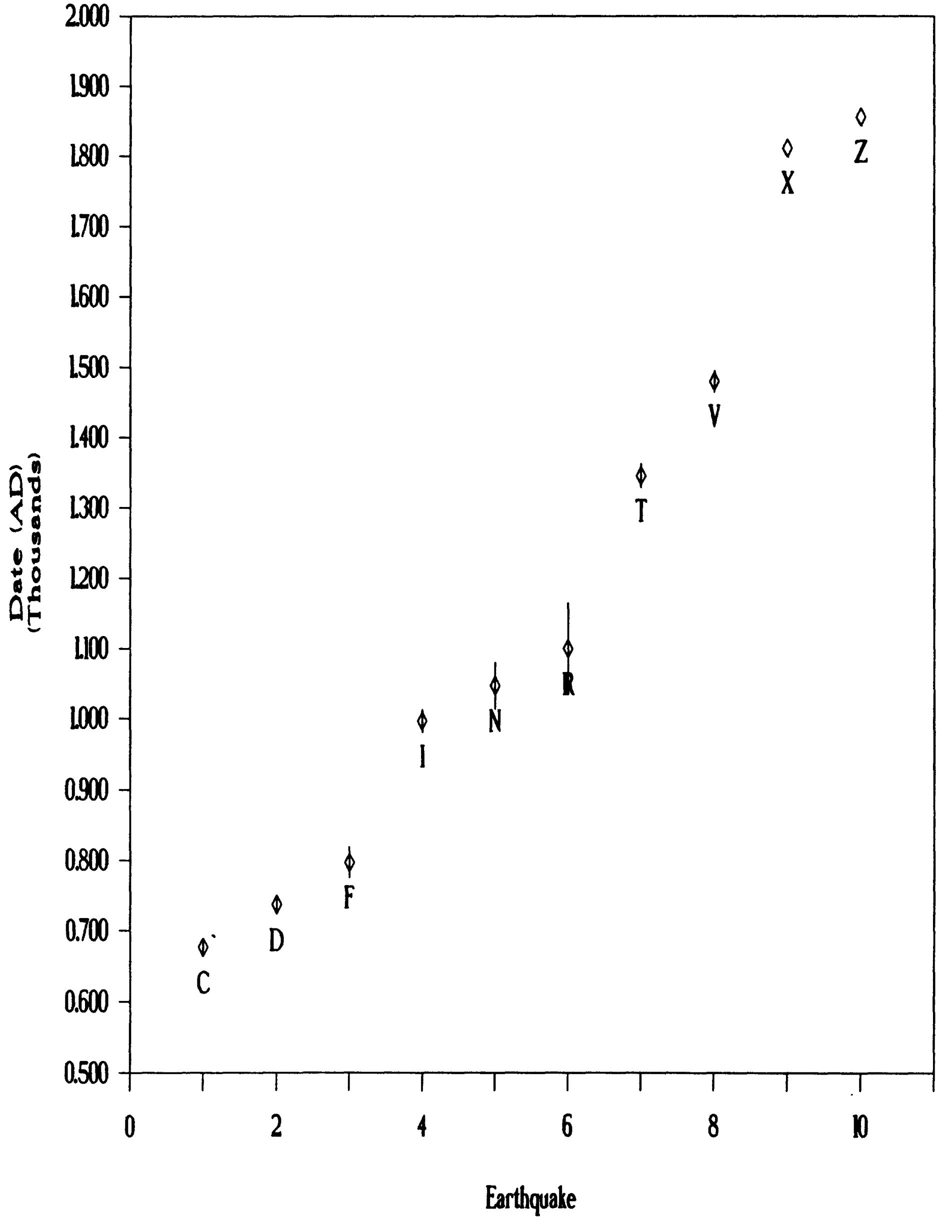

Figure 2. New date estimates for earthquakes recorded in the sediments at Pallett Creek.

Oak Ridge Fault, Ventura Basin, California: Slip Rates and Late Quaternary History

14-08-0001-G1194

Robert S. Yeats
Department of Geology
Oregon State University
Corvallis, Oregon 97331-5506

David A. Gardner
Staal, Gardner & Dunne, Inc.
121 N. Fir Street, Suite F
Ventura, California 93001
805-653-5556

Investigations

This project has been completed, and the final report is being written in four parts. First, a paper written by R. S. Yeats entitled "Late Quaternary Slip Rates on the Oak Ridge Fault, Transverse Ranges: Implications for Seismic Risk" is being reviewed prior to submitting it to Journal of Geophysical Research. Second, a report is being submitted to USGS for open file consisting of several maps of the Oak Ridge fault at a scale 1:48,000; these maps include (1) surface geology, (2) fault contours, (3) structure contours on a 1 Ma marker, and (4) location of wells used in study. Third, a paper describing late Quaternary features of the fault is being written by John Powell of Staal, Gardner & Dunne with several coauthors. Fourth, a paper entitled "The Ventura Fold Belt and the Oak Ridge Fault, Western Transverse Ranges, California will be submitted either to Geology or Tectonics. This paper is also a product of Contract 14-08-0001-G1372 and is discussed in the Technical Report Summary covering that contract.

Despite the official end of USGS funding of the Oak Ridge project, the work goes on. S. Levi of OSU, under another contract, is constructing a paleomagnetic section on the south side of South Mountain to better constrain the slip rate on the Oak Ridge fault (see discussion below under Results). In addition, a large new cut has been made on the Victoria pressure ridge across from the K-Mart on Victoria Avenue in Montalvo, and John Powell, Ed Hall, and Tom Rockwell are describing this cut and trying to get a radiocarbon sample from the tilted sediments that overlie the Saugus with angular unconformity.

Results

The paper to be submitted to Journal of Geophysical Research proposes a slip rate of 12.3 mm/yr on the Oak Ridge fault for the last 200,000 years. This rate is based on an age of 200,000 years for the end of Saugus deposition, as determined near

Ventura by Ken Lajoie using amino-acid age estimates, with the top of the Saugus correlated to Santa Paula and Balcom Canyon by us. We project the top of the Saugus from the outcrop south of South Mountain to the crest of the Oak Ridge anticline, and we recognize the top of the Saugus in the Santa Clara syncline on the basis of an angular unconformity between flat-lying Santa Clara River gravels and steeply-dipping Saugus close to the Oak Ridge fault (Figure 1). The vertical separation between the top of the Saugus at the crest of the anticline and the trough of the syncline (line AB of inset, Figure 1) can be converted to dip separation because the dip of the fault is known to -3km. Fault slip at seismogenic depth is calculated by adding the near-surface fault slip (line DE of inset, Figure 1) and the displacement due to drag folding.

Assuming that all slip is released seismically in events averaging 3 meters of slip, the most realistic average recurrence interval is 245 years. By using more conservative but less likely parameters: 400,000 years as the age of the top Saugus and an alternate projection of the top Saugus over the crest of the Oak Ridge anticline (also shown in Figure 1), a slip rate as low as 5 mm/yr is possible, with an average recurrence interval of 500 to 600 yr. The Red Mountain and San Cayetano faults probably have slip rates as high as those for the Oak Ridge fault, although this cannot be demonstrated because Pliocene and Pleistocene sediments are not preserved in the hanging-wall blocks of these faults.

Vertical separation of 1.5 m in alluvial-fan materials radiocarbon dated as 2000 years old occurred on a secondary fault in a trench in the hanging wall block of the Oak Ridge fault at Bardsdale; this separation occurred in a single event and apparently accompanied an earthquake. However, the total relief on the scarp at Bardsdale is 9 m, consisting of a broad warp of the alluvial fan, including the dated Holocene sediments. If the broad warp is the surface expression of a fault at depth, and displacements on this fault were 3 m per event (with the 1.5 m displacement on the fault in the trench representing only part of the displacement on the fault at depth), an average recurrence interval of 650 years on the secondary fault underlying this scarp (not the main Oak Ridge fault) is obtained. In Ventura, near the County Government Center, Holocene sediments of the Harmon alluvial fan are cut by vertical cracks filled with clay, silt, and/or fine sand that are best explained as liquefaction features accompanying an earthquake.

There has been no damaging earthquake on the Oak Ridge, Red Mountain, or San Cayetano faults in the 200 years of record keeping. However, the recurrence intervals documented for the Oak Ridge fault and surmised for the other two faults, together with the evidence for paleoseismicity, indicate that the lower Santa Clara Valley will be the site of a large, damaging earthquake in the near future.

Because this paper concludes with a long-range earthquake prediction for a heavily-populated area, it has been submitted to USGS for review prior to making the prediction public.

Reports

Powell, J. R., Gardner, D. A., Yeats, R. S., and Rockwell, T. K., 1987, Evidence of late Quaternary activity, Oak Ridge fault, Ventura, California: Association of Engineering Geologists Newsletter 30/1, p. 17.

Yeats, R. S., 1987, Vertical separation rates on the Oak Ridge fault, Ventura basin, California: Geological Society of America Abstracts with Programs, v. 19, p. 902.

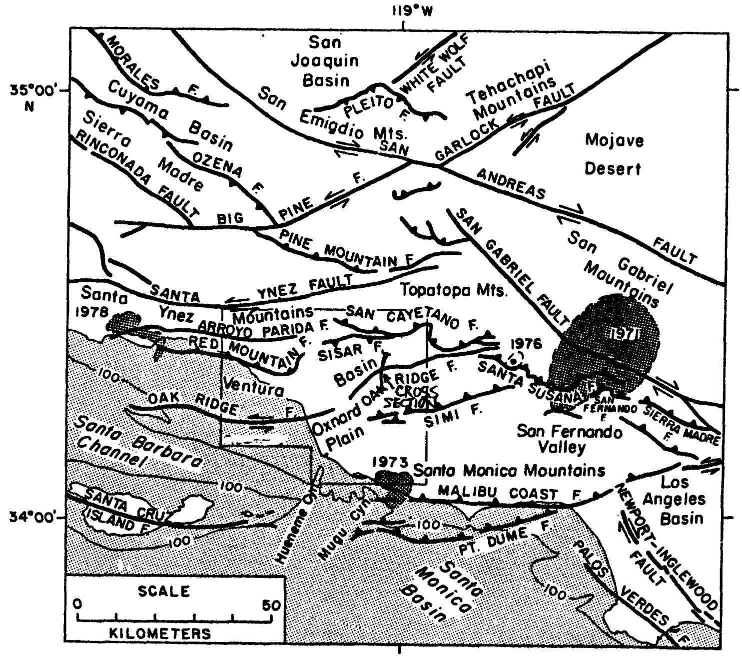

Figure 1. Cross section used in slip-rate determination.

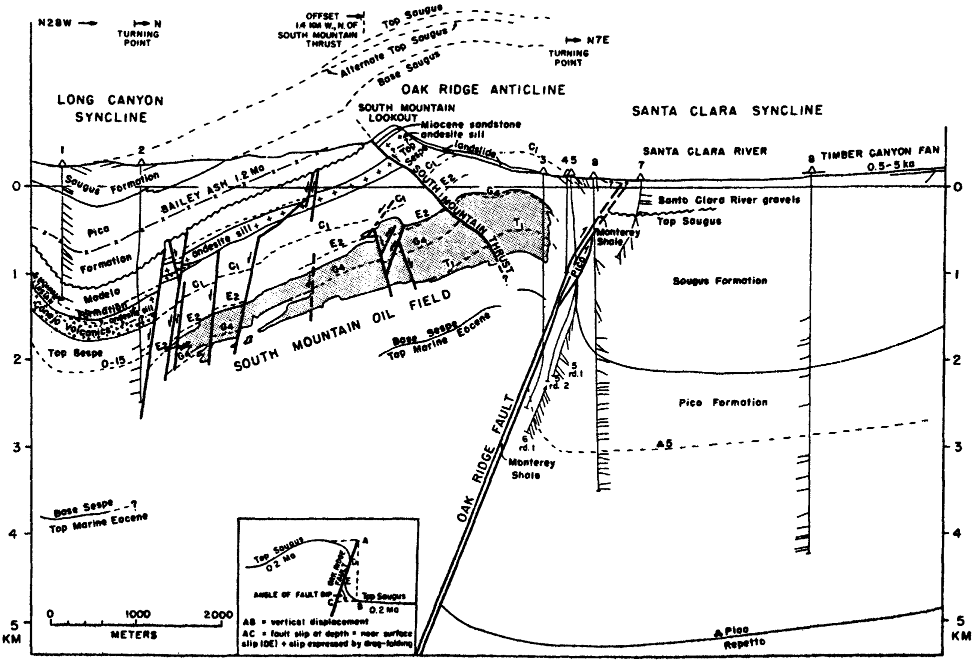

Analysis of Southern California Seismic Network Data for Earthquake Prediction

14-08-0001-G1381

Keiiti Aki
Dept of Geological Sciences
University of Southern California
Los Angeles, CA 90089-0740
(213) 743-3510

Objective: The temporal and spatial change of coda Q^{-1} associated with earthquake occurrences have been reported world-wide. Some researchers found the coda Q^{-1} increased before the mainshock, but some others found the opposite results. A rather complex spatial and temporal change in coda Q^{-1} were observed in the case of Round Valley, California earthquake. Why do the temporal and spatial changes of coda Q^{-1} show such diverse patterns? Are there any physical significance in them? The purpose of this study is to use seven-year data on earthquakes in the North Palm Springs area to further investigate the coda Q^{-1} change in time and space associated with the North Palm Springs earthquake (M=5.6) which happened on 8 July 1986 at the epicenter at φ=116°39W and λ=33°59N.

Result: We determined coda Q^{-1} using the single back-scattering model (Aki & Chouet, 1975). To look for the change of coda Q^{-1} in the source region, we chose earthquakes within a small area covered by longitude from 116°25 to 116°50' and latitude from 33°51' to 34°10' and limit our stations to be within 25 km from the mainshock epicenter. The coda wave were sampled after twice the shear wave travel time and before the time at which the power spectrum of signal already corrected for the noise is equal or less than a half of the power spectrum of the noise. We calculated coda Q^{-1} for different lapse time window, and obtained some interesting results.

1. The precursory phenomena

Fig. 1 shows the results of mean of coda Q^{-1} vs. time for frequencies 1.5, 3.0, 6.0, and 12.0. The lapse time period for f=1.5 is from 15^s to 30^s and those for f=3.0, 6.0, and 12.0 are from 10^s to 20^s. Each point on the curve represents the mean of 30 measurements of coda Q^{-1} with 15 points overlapping at neighboring points. The error bar indicate the standard error of the mean. From Fig. 1, we see that the mean of coda Q^{-1} gradually increases for several years period of time before the mainshock and then gradually decreases. The pattern of the change is different for different frequency. The lower the frequency, the anomalous increase in Q^{-1} appears earlier. This may be explained if we consider larger cracks are responsible for the attenuation and scattering of lower frequencies, because larger cracks are more sensitive to minute stress changes than smaller cracks.

2. The difference in Q^{-1} change between different lapse time windows

The solid line in Fig. 2 represents the coda Q^{-1} obtained from lapse time window from 15^s to 40^s. Although the mean of coda Q^{-1} shows a little increase after mainshock especially for high frequencies, there is no significant change during the whole time period. This may be explained if the long and late time window sampled coda scattered over a large area. Fig. 1 is reproduced here in dashed lines for comparison. From this figure, we see a remarkable difference between coda Q^{-1} behaviors obtained from lapse time 10 to 20 sec. and 15 to 40 sec. After the mainshock, the difference decreased for (all) frequencies, but especially drastically for high frequencies. This probably means that there was a small high Q^{-1} region in the mainshock area before its occurrence. The high Q^{-1} may be caused by an increased crack density before the earthquake. The decrease in difference between the two time windows for high frequency after the earthquake may mean that smaller cracks affecting Q^{-1} at higher frequencies might have been closed by the M5.6 earthquake, but larger ones were not affected. In any case, the result from the North Palm Springs earthquake encourages a further study on coda waves for the earthquake prediction research.

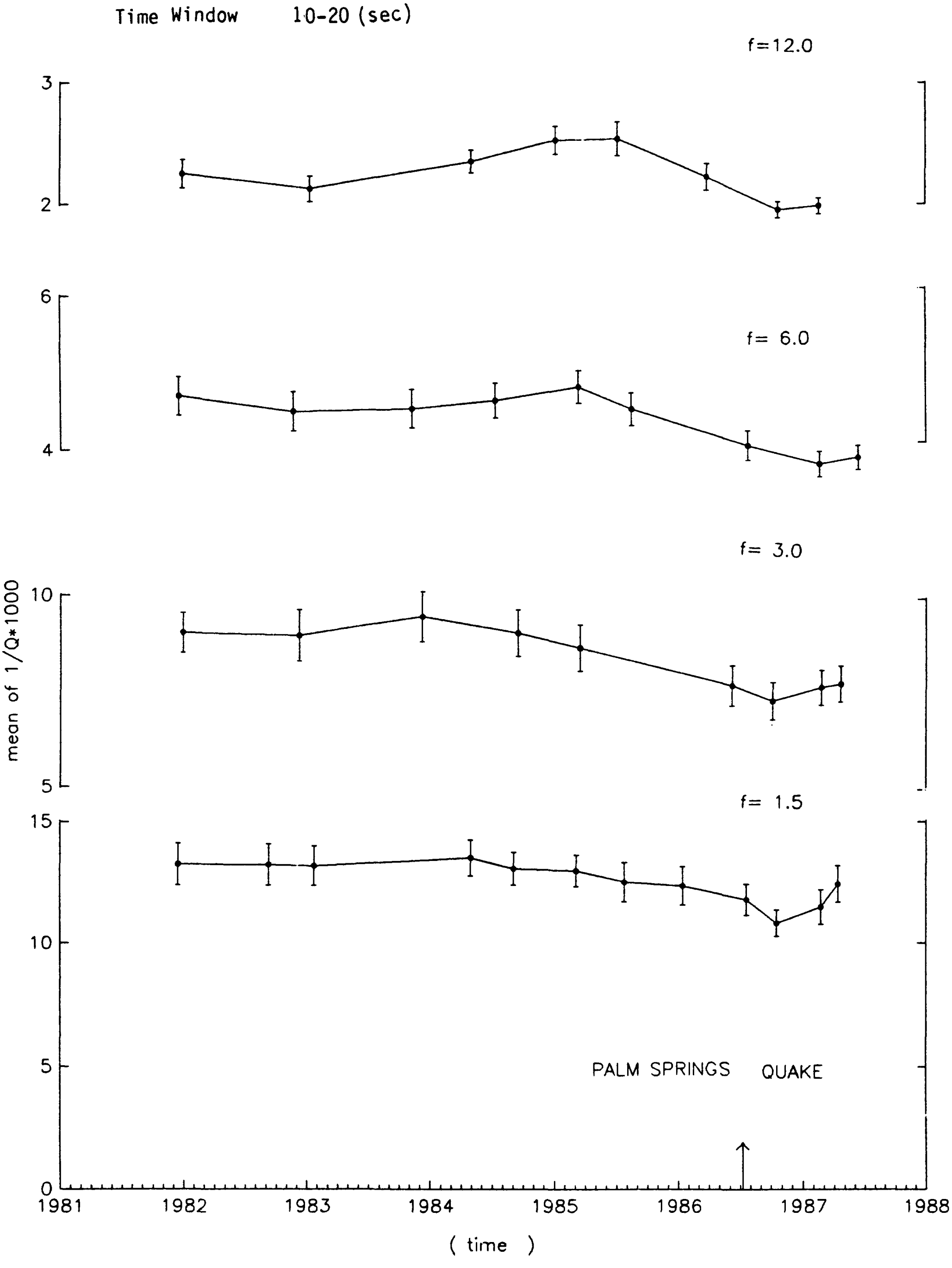
Time Window 10-20 (sec)
f=12.0
3
2
6
f= 6.0
4
f= 3.0
10
mean of 1/Q*1000
5
f= 1.5
15
10
5
0
PALM SPRINGS QUAKE
1981
1982
1983
1984
1985
1986
1987
1988
(time)

Figure 1

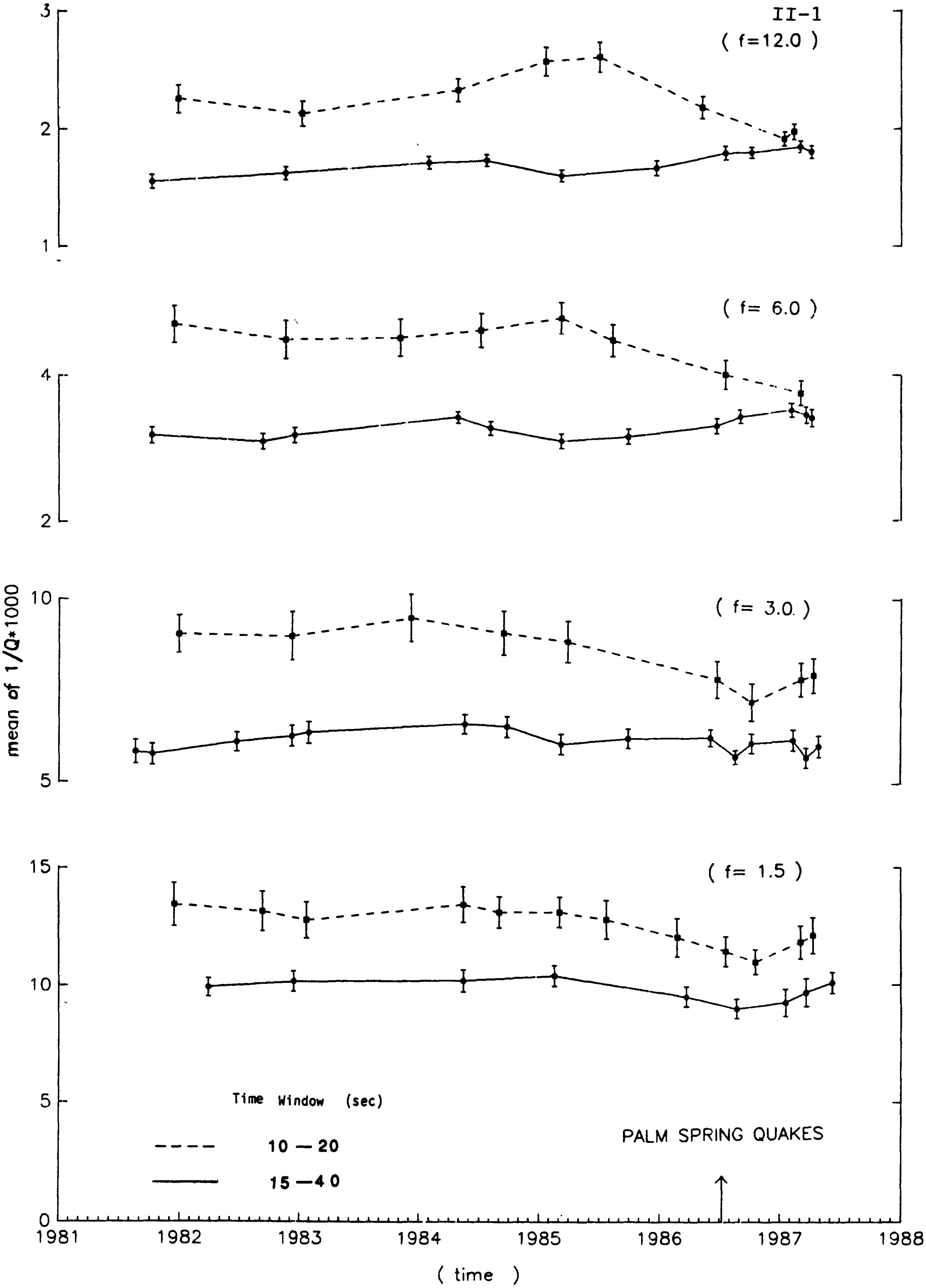
II-1
(f=12.0)
(f= 6.0)
(f= 3.0)
(f= 1.5)
mean of 1/Q*1000
3
2
1
4
2
10
5
15
10
5
0
1981
1982
1983
1984
1985
1986
1987
1988
(time)
Time Window (sec)
10 — 20
15 —4 0
PALM SPRING QUAKES

Figure 2

On-Line Seismic Processing

9930-02940

Rex Allen
Branch of Seismology
U.S. Geological Survey
345 Middlefield Road, MS 77
Menlo Park, California 94025
(415) 329-4731

Investigations and Results

A Motorola 68020 system with a 12 Mhz clock rate has been installed as the realtime backup for the subset of 48 seismic stations covering the Parkfield area. The new system currently emulates the Mk I RTP in producing only phase card descriptors of events, but incorporates the software required for saving the digital records when required. Running the new system as a backup on a set of stations also covered by the Mk I system has allowed us to evaluate its performance against a known standard. It appears to have a significantly lower detection threshold for small events, and the use of later 16Mhz or 20 Mhz processors would allow the covering of proportionally more stations. The relatively small increment, however is not up to handling the whole of CALNET, so this machine will probably remain as is, and we will concentrate on a more general solution for expansion.

The next development phase on the 68020 Mk II systems will require the use of multiprocessors on the VMEbus to allow handling about 500 stations and saving the digital records from selected stations during seismic events. I am proceeding with this work on the new development system, and hope to have a multiprocessor in operation within a few months.

Jim Ellis has continued work on the multiproject effort to develop new digital field instruments.

The Mk I RTP's at Menlo Park and at the University of Washington and the University of Utah have continued to operate satisfactorily.

Soil Amplification at Anza

9910-04187

Lawrence M. Baker, Joe Fletcher, Hsi-Ping Liu, Tom Moses
Branch of Engineering Seismology and Geology
U. S. Geological Survey
345 Middlefield Road MS977
Menlo Park, CA 94025
(415) 329-5608 FTS 459-5608

Investigations

In FY87, the U. S. and French Nuclear Regulatory Commisions funded the USGS and U. C. Santa Barbara to begin a cooperative program to study soil amplification at Anza, California, in particular, the effects of a thin, near-surface soil layer overlying a basement of hard rock on upgoing seismic waves. Such layers are frequently characterized by unusually low S-wave velocities, which are indicative of the low rigidities necessary for large S-wave amplifications. These amplifications can have a dominant effect on strong ground shaking, and therefore understanding these effects is critical for estimating the risk to nuclear reactors from earthquake-generated ground shaking.

In support of this program, the USGS was assigned responsibility for the following tasks:

- Drill holes for seismometer emplacement (Moses).
- Log deepest hole for shear-wave velocity (Liu).
- Analyze and specify the hardware for the data acquisition system to be procured by UCSB (Baker).
- Program the real-time data acquisition software on a MicroVAX II computer system to be provided by UCSB (Baker).

Results

One test hole has been drilled by UCSB. Drilling and logging of the instrument holes awaits approval of the site by the French NRC, followed by lease negotiations with the land owner.

Hardware for the data acquisition system has been specified and an analog-to-digital converter has been ordered by UCSB. Preliminary work on the computer software has been done using similar USGS-owned equipment. Completion of the remaining work awaits delivery of the data acquisition hardware and the subsequent transfer of this equipment and the MicroVAX II from UCSB to the USGS.

Assuming the site is approved by the French NRC, and the landowner grants us permission to occupy the site, the installation should begin by Spring 1988, and should be fully operational by Summer 1988.

Reports

None.

Crustal Deformation Observatory Part F

14-08-0001-G1355

John Beavan, Roger Bilham

Lamont-Doherty Geological Observatory of Columbia University
Palisades, New York 10964
(914) 359-2900

Investigations

We operate a 535 m long-baseline half-filled water tube tiltmeter (Fig. 1) at Pinon Flat Observatory. This is used in conjunction with a similar instrument operated by the University of California, San Diego, to investigate:

(1) sources and magnitudes of noise affecting the tilt signal;
(2) water level sensor design and reliability;
(3) methods of referencing tiltmeter to depth.

Results (as of October 30, 1987)

1. LDGO/UCSD tiltmeter interconnection

Data collected to date from the two tiltmeters suggest that it will be possible to monitor secular tilt changes at much better than the 10^{-7}/year level with this type of instrument. However, observed differences in long-term tilt rate between the LDGO and UCSD tiltmeters at the 10^{-7}/year to 10^{-8}/year level led us to suggest interconnecting the two tiltmeters in order to investigate the source of the discrepancy. The 535 m tiltmeters run parallel about 10 m apart, and both are referenced to approximately 30 m depth, so we would expect nearly identical behavior even in the long term. Possible sources of the discrepancy are the different sensors, different methods of referencing to depth, and the methods used for filling the inevitable gaps in the data. See Open File Report 87-374 and earlier reports for more details.

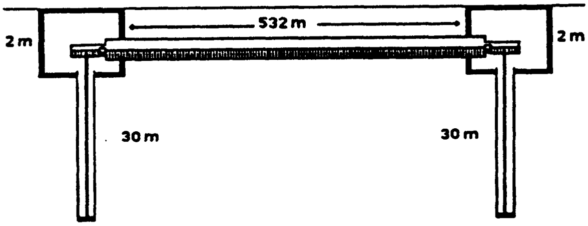

Figure 1. Schematic of PFO long baseline tiltmeters. The tiltmeters are referenced to fiducial points at 30 m depth.

Since the water levels in the two tiltmeters are some 20 cm different, the interconnection was achieved by bringing a pipe from each end of the LDGO tiltmeter into the adjacent UCSD vault. The water level in this pipe is then measured with respect to the granite table on which the UCSD tiltmeter sensor is mounted. The interconnection was completed last year, with much help from the UCSD group, and newly designed micrometer sensors have recently (October 1987) been installed in both the LDGO and UCSD vaults for reading the water levels. We did not have sufficient funds to install continuously recording sensors, and we also believe that periodic readings of the micrometer sensors will be sufficient to resolve our questions about long-term stability. The micrometers have been completely redesigned from those used previously in the LDGO vaults, so that they are easier to read and easier to clean. In tests prior to installation, several different observers obtained repeatibility within about ± 2 microns, which corresponds to better than 10^{-8} μrad in the PFO tiltmeter. The micrometer installation is too new to be able to present data in this report.

2. Tiltmeter Installations Outside Pinon Flat

It is our belief that the long baseline tiltmeter has been well enough proved at Pinon Flat that it is ready for installation elsewhere. This is not to say that the experiments at Pinon Flat are completed - on the contrary, the investigation of the ultimate accuracy of these instruments is of great importance for certain tectonic requirements in the future. However, there are some sites where stabilities of 10^{-7}/year are definitely adequate for the expected signal levels, and it is also important to install instruments in sites other than competent granite in order to investigate data quality and stability in such environments.

To these ends, and using funds largely outside this grant, we have been pursuing tiltmeter installations at Mammoth Lakes, California, and in the People's Republic of China. Some funds from this grant *have* been used in a major redesign of the interferometer mechanics and electronics. These improvements make the interferometer far easier to align, give a four times increase in resolution, and are intended to allow the interferometer to run continuously for many months without loss of datum. The new electronics will be installed on the PFO instrument in November 1987.

2.1 Mammoth Lakes

The USGS has used funds outside this grant to fund a Mammoth Lakes tiltmeter installation by Roger Bilham (now at University of Colorado) and ourselves. The tiltmeter will be used to monitor magma chamber inflation episodes, and it is hoped to be able to reduce the amount of conventional surveying that is necessary in the area. The data are transmitted by GOES satellite in near-real-time and are archived on the Menlo Park computers. The bulk of the construction of the two-component, 450 m per arm, tiltmeter was undertaken by subcontractors supervised by Roger Bilham. Funds to install deep references have unfortunately been so far unavailable. The new LDGO interferometer end sensors and electronics were recently installed (October 1987) and the first week of data is shown in Figure 2. One of the four end sensors is not recording correctly at present, but this will be fixed by early November 1987. The data appear very quiet, and the tilt measured on the east-west component is extremely stable despite a fairly large drift at each end. (This is presumably due to temperature effects or to a small leak.)

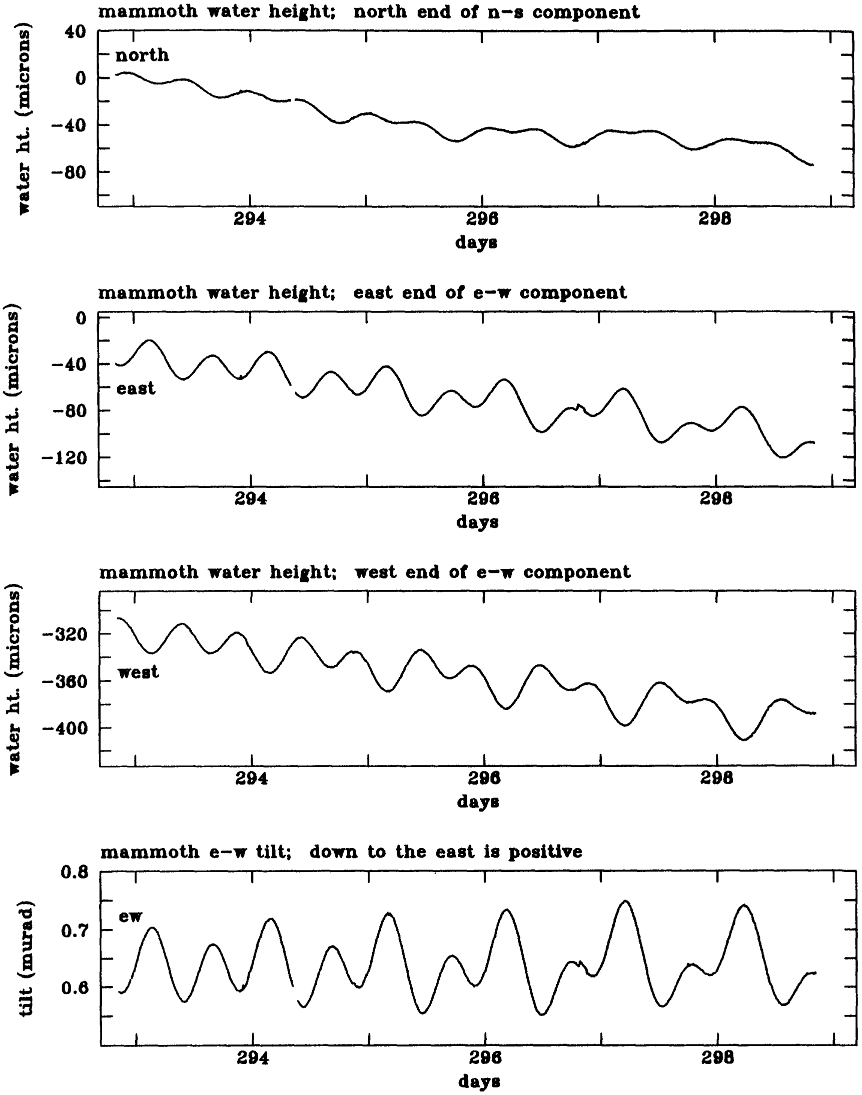

Figure 2. The first week of data from three of the four sensors in the Mammoth Lakes two-component tiltmeter. The fourth frame shows the derived east-west tilt.

2.2 Near Beijing, PRC

As part of a United Nations Development Project, we are supplying four tilt end sensors and electronics to the Centre for Analysis and Prediction, State Seismological Bureau, Beijing. These will be installed in an experimental underground facility north of Beijing, where they will be used with many other instruments to monitor seismic hazard in the region. The instruments will be shipped to China in November 1987, and should be installed by early 1988. The current installation plans are to use the sensors in 40 m instruments. This is unfortunate due to the inherent resolution limit of the sensors of about 0.25 micron water level change per count. However, the instruments will be excellent monitors of long-term tilt, even if their usefulness for studying effects such as tidal admittance variations will be degraded. We are continuing to encourage the Chinese to install the sensors on longer instruments.

2.3 Wuhan, PRC

We negotiated an exchange agreement with the Institute of Seismology, Wuhan, whereby we would mutually exchange our top-of-the-line tiltmeter end units for evaluation and testing purposes. The Chinese supplied us with two float-type end units last year. Tests on the magnetic sensor used as a transducer proved it grossly inferior to LVDT sensors, both in its linearity and in its sensitivity to lateral motions. Roger Bilham now has the Chinese end units and intends at some point to install them, using LVDT transducers, alongside one of our instruments at Mammoth Lakes or Pinon Flat. We will supply the Wuhan group with a complete end unit, including electronics and fabrication instructions, by the end of 1987. We hope that they will evaluate it favorably against their instruments and will be inclined to duplicate the instrument themselves. We will encourage them to install it in long-baseline, near-surface sites.

Crustal Deformation Measurements in the Shumagin Seismic Gap

14-08-0001-G1379

John Beavan

Lamont-Doherty Geological Observatory of Columbia University
Palisades, New York 10964
(914) 359-2900

Investigations

1. Nine short (~1 km) level lines are measured approximately annually within the Shumagin seismic gap, Alaska (Fig. 1). Surface tilt data are interpreted in terms of tectonic deformation at the Pacific-North American plate boundary.

2. Five absolute-pressure sea-level gauges are operated in the Shumagin Islands in an attempt to measure vertical deformation associated with the Aleutian subduction zone. A two-component short-baseline tiltmeter is operated at one site.

3. Data from the sea-level and tilt sensors are transmitted to Lamont by satellite in near real time, and are examined for possible tectonic signals. Studies of noise level as a function of frequency are used to determine the relative usefulness of different types of measurement, and to evaluate the minimum size of tectonic signal that will be visible above the noise. Our data are compared with other crustal deformation data from the Shumagin gap.

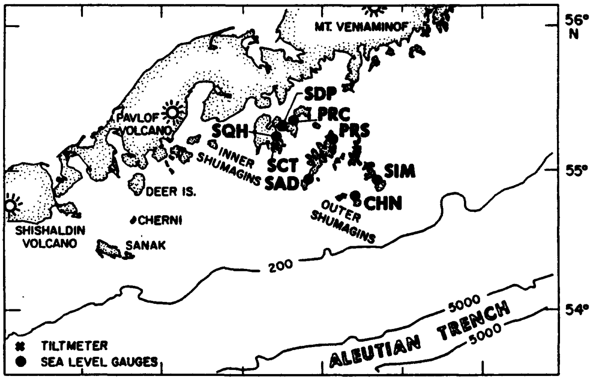

Figure 1. Location of the Shumagin Islands with respect to the trench and the volcanic arc. Depth contours are in metres. The seismic gap stretches from approximately Sanak Island in the west to 50 km east of the Shumagin Islands. Also shown are the sites of sea-level gauges operated by Lamont-Doherty and by the National Ocean Survey (SDP). Site SAD is no longer operated because of repeated storm damage. All LDGO sites now use Paroscientific quartz pressure sensors, and housings that are substantially improved over those described by Beavan et al. [1986]. As of this writing, all gauges but SQH are operating perfectly.

Results (as of October 30, 1987)

Sea level gauge and level line locations are given in Figures 1 and 2. This report will deal principally with the leveling data. See USGS Open File Report 87-374 for a recent discussion of the sea level data. The level line data are shown in Figure 3, and the 1980-87 tilt rates derived from these data are given in Table 1. The pre-1984 level data, including the apparent 1978-80 tilt reversal, are discussed by Beavan *et al.* [1984].

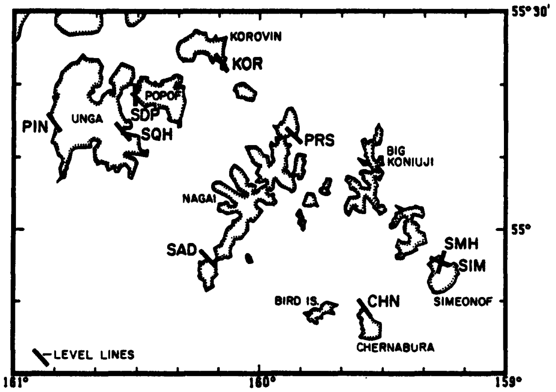

Figure 2. Locations and directions of first-order level lines, whose lengths vary from 600 - 1200 m. The resultant of data from SDP and SQH is used to estimate the tilt direction in the Inner Shumagins. The resultant of SIM and SMH is used for the Outer Shumagins.

Table 1. Shumagin 1980-87 tilt rates

Site	Interval	Rate (µrad/yr)*	Azimuth*	Confidence
Inner Shumagins				
SDP/SQH	1980-87	-0.31±0.13	-53°±32°	95%
PIN	1980-86	-0.16±0.12	NW†	-
KOR	1980-87	0.09±0.09	NW†	-
Central Shumagins				
PRS	1981-87	-0.02±0.12	NW†	-
SAD	1980-87	-0.26±0.14	NW†	-
Outer Shumagins				
SIM/SMH	1980-87	0.16±0.12	12°±42°	-
CHN	1980-86	0.43±0.15	NW†	95%

* Positive rates indicate tilt is down towards the given azimuth
† Level line in only one azimuth, so tilt only determined in that azimuth
Errors quoted are 1 standard deviation

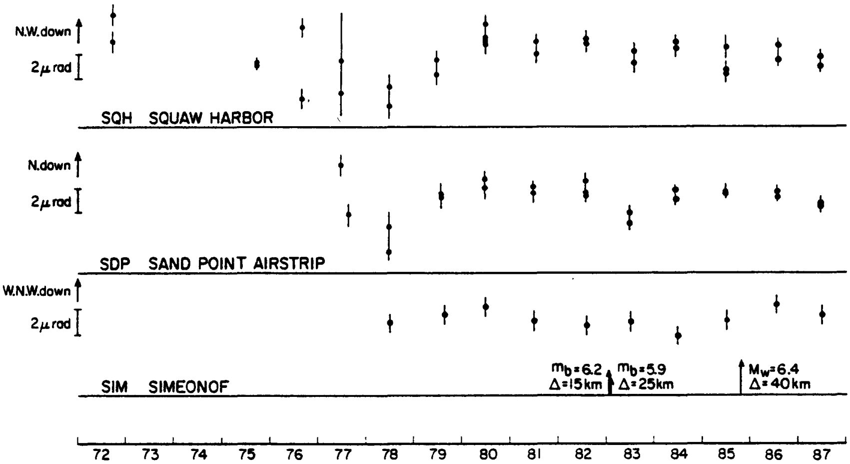

Figure 3a. See also Figure 3b. All data (1972-1987) from level lines in the Shumagin Islands. All lines except SMH are oriented approximately in the direction of relative plate motion. The two data points each year represent the forward and backward runs of leveling. The error bars are ±1σ, based on variations in multiple readings of each stadia rod from each tripod position. The height differences between the ends of the lines have been converted to slope by dividing by the line length; changes in slope from year to year are due to ground tilt (or noise in the data). Several benchmarks are set at each end of each line to guard against benchmark instability. Lines SIM and SAD have only one data point plotted for each year; this is because they have benchmarks between almost every tripod position and the overall tilt is estimated by averaging tilts between adjacent benchmarks. Most of the NW-SE oriented lines show tilt rates since 1980 that are not significantly different from zero, though there is a general tendency for tilting down towards the trench since 1980 in the Inner and Central Islands (see Table 1). Clusters of microseismicity at shallow depths below KOR in 1978 through 1980 may contribute to its noisy behavior. The 1980 measurement on CHN was made immediately after setting the benchmarks, so there may be some settling error due to hardening of the concrete. CHN shows a significant tilt rate, with tilting down towards the north. However, this is controlled largely by the initial measurement. The 1986 measurement may also be affected by the Oct - Nov 1985 earthquakes, whose aftershock zone extended beneath CHN.

The only leveling data that show tilt rates different from zero at the 95% confidence level are SQH and CHN. However, there is a general tendency for slight tilt down towards the trench in the inner and central islands. This is the direction that would be expected for most simple models of a locked plate boundary [e.g. Savage, 1983]. However, the rates are a factor of two or more lower than expected for a subduction rate of about 6 cm/yr. Savage and Lisowski [1986] also find much lower than expected (for simple models of a locked boundary) strain rates in this area, a result that is supported by their 1987 measurements [Savage, pers. comm., 1987]. Several explanations are available for these results.

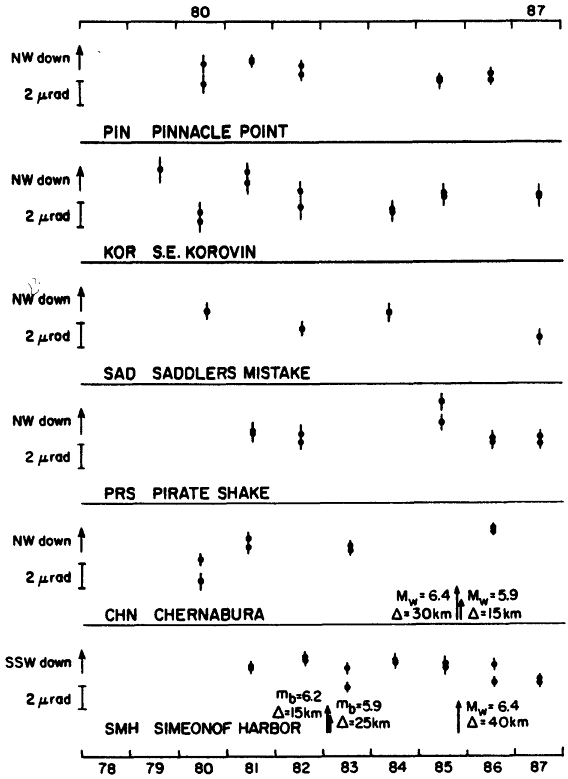

Figure 3b.
See Figure 3a.

(1) The entire gap may fail aseismically, as suggested by Savage and Lisowski [1986]. The historical evidence for great earthquakes in 1788 and 1848 [Davies et al., 1981], and more especially the recently uncovered instrumental evidence for a gap-filling event in 1917 [Jacob and Taber, 1987; Boyd et al., 1987] make this expanation highly unlikely in our view.

(2) The eastern one third of the gap, where the Shumagin Islands themselves are located, and where both the strain and tilt measurements are made, may fail aseismically, while the remainder of the gap fails in great earthquakes. This explanation is suggested by pronounced changes in microseismicity patterns between the two parts of the gap [Hudnut and Taber, 1987; Boyd et al., 1987]. This would explain both the seismological evidence for great earthquakes and the geodetic evidence for low strain and tilt rates. However, it begs the question of why such a narrow regime of aseismic slip should be present along an otherwise seismogenic plate boundary.

(3) The gap may be nearing time of failure in a great earthquake, and the rates of deformation may be slowing down through a mechanism such as that suggested by Thatcher and Rundle [1984]. Simple extrapolation of historical repeat times suggest that the gap is indeed approaching failure. The lack of strain accumulation noted by Savage and Lisowski [1986] between a 1913 triangulation survey and their current measurements could also be used as evidence that the strain state in the gap is

approaching failure, since the 1913 survey was just before the 1917 earthquake. (Of course, this can also be used as evidence for aseismic subduction, but only if the effects of the 1917 earthquake are discounted.) Finally, results of an early 1950's survey, reported by Savage and Lisowski [1986], weakly suggest strain accumulation between then and now that is consistent with the simple locked plate boundary models.

(4) The strain and tilt measurement networks may be located so as to be insensitive to the strain accumulation that is occurring. It is possible that the upper 20 km or so of the plate interface slips aseismically due to the presence of high fluid pressures or weaker rock at the interface [Byrne et al., 1986, 1987]. If this is the case, the simple strain accumulation model that consists of a virtual dislocation [Savage, 1983] between about 20 km and 50 km depth in an elastic half space, shows rather low average strain rates, comparable to those observed, across the area occupied by the trilateration array. However, such a model does not fit the observed tilts very well, and Savage [pers. comm., 1987] disputes whether our elastic half-space model is justifiable when there is weaker rock abutting the shallower part of the plate interface; we are currently investigating this further.

None of these proferred explanations avoid special pleading of one form or another. We currently feel that explanations (2) or (3) require the least.

References

Beavan, J., R. Bilham, and K. Hurst, Coherent tilt signals observed in the Shumagin seismic gap: Detection of time-dependent subduction at depth?, *J. Geophys. Res., 89,* 4478-4492, 1984.

Beavan, J., K. Hurst, R. Bilham, and L. Shengold, A densely spaced array of sea level monitors for the detection of vertical crustal deformation in the Shumagin seismic gap, Alaska, *J. Geophys. Res., 91,* 9067-9080, 1986.

Boyd, T.M., J.J. Taber, A. Lerner-Lam and J. Beavan, Seismic moment release and arc segmentation within the Shumagin Islands seismic gap, Alaska, *in preparation,* 1987.

Byrne, D.E., D.M. Davis and L.R. Sykes, Forearc mechanics and the seismogenic zone, *EOS, 67,* 1196, 1986 (abstract).

Byrne, D.E., D.M. Davis and L.R. Sykes, Forearc mechanics and the seismogenic zone, *Tectonophysics,* submitted, 1987.

Davies, J.N., L.R. Sykes, L. House and K. Jacob, Shumagin seismic gap, Alaska peninsula; History of great earthquakes, tectonic setting, and evidence for high seismic potential, *J. geophys. Res., 86,* 3821-3856, 1981.

Hudnut, K.W. and J.J. Taber, Transition from double to single Wadati-Benioff zone in the Shumagin Islands, Alaska, *Geophys. Res. Lett., 14,* 143-146, 1987.

Jacob, K. and J.J. Taber, Analysis of seismic data from the Shumagin Seismic gap, Alaska, *USGS Open File Report, 87-374,* 300-302, 1987.

Savage, J.C., A dislocation model of strain accumulation and release at a subduction zone, *J. geophys. Res., 88,* 4984-4996, 1983.

Savage, J.C. and M. Lisowski, Strain accumulation in the Shumagin seismic gap, Alaska, *J. geophys. Res., 91:B7,* 7447-7454, 1986.

Thatcher, W. and J.B. Rundle, A viscoelastic coupling model for the cyclic deformation due to periodically repeated earthquakes at subduction zones, *J. geophys. Res., 89,* 7631-7640, 1984.

Tectonic Tilt Measurement: Salton Sea

14-08-0001-G1392

John Beavan

Lamont-Doherty Geological Observatory of Columbia University
Palisades, New York 10964
(914) 359-2900

Investigations

1. Historical water level measurements at three sites on the Salton Sea are being investigated to determine tectonic tilting, taking account of as many noise and error sources as possible.
2. The tectonic tilt derived from Salton Sea records is being carefully compared with leveling data from the area.
3. LDGO-designed pressure sensor gauges are being installed at several sites around the Sea to measure water level continuously, to investigate noise sources, to determine the level of detectability of tectonic tilt signals in the data, and to measure tectonic signals.

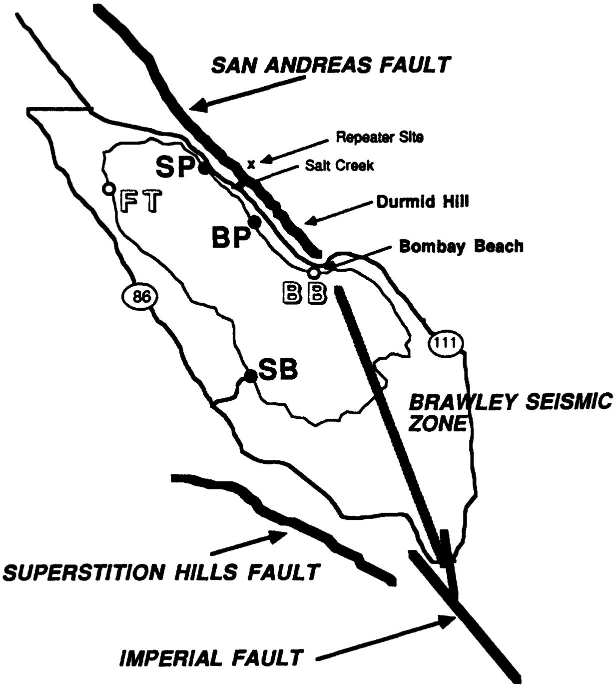

Figure 1. Map of the study region, showing the tectonic setting and the sea-level gauge network. Historical sea-level data have been collected at FT and SB since 1950, and at SP since 1970. Continuously recording pressure gauges have operated at SP since May 1985, at SB since January 1986, at BP since December 1986, and at BB and FT since May 1987.

Results (as of October 31, 1987)

1. Historical data

We have nearly completed re-analysis and updating of the historical (1950 - 1986) sea level records, as described in USGS Open File Report 87-374. The final part of this work is the checking of the stability of the gauges by repeating old leveling surveys that were used to set the gauge datums. We almost completed the leveling to the FT gauge in May and June 1987, but some inconsistencies between that leveling and previous levelings caused us to repeat some of the leveling again in October 1987. The field party is still in California as of this writing, so we do not yet have the results. A paper on the data is virtually complete, and will be submitted within the next few weeks.

2. Instrumental installations

Continuously recording gauges using Paros differential pressure sensors have been installed at SP, SB, BP, BB and FT (see Fig. 1). Data are sampled every 12 minutes, and are digitally transmitted to a central recording site every hour. All data are transmitted twice to guard against short power outages or transmission errors. The recording system is an IBM-PC powered via an uninterruptible power supply, with a watchdog timer to ensure clean power-up. A new operating system has just been installed that allows us to access the data by phone, instead of the previous system in which floppy disks were mailed to us weekly. The recording system has worked very reliably, but during the past 6 months several instrument-months of data have been lost due to various problems with solar panels and gauges. These problems are being corrected by a party currently in the field.

Arrays of local benchmarks have been installed and measured near all five gauges, so that the measurement datum is not lost even when a gauge fails for a period of time. The local arrays are used to check gauge elevations at every visit. SB and SP have also been tied to more remote benchmarks on the main leveling routes; these ties will be repeated every few years to check the stability of the local array. During field trips in May and October, 1987, the gauges at BP, BB and FT were also tied to the main leveling routes.

Sources of Errors in GPS Measurements of Crustal Deformation

14-08-0001-G1335

Yehuda Bock and Robert W. King
Dept. of Earth, Atmospheric, and Planetary Sciences
Massachusetts Institute of Technology
77 Massachusetts Avenue
Cambridge, MA 02139
(617) 253-7360

Objectives: Understanding the structure and geometry of seismogenic zones is a key element in the prediction of earthquakes. Geodetic measurements contribute to this understanding through the mapping of present-day crustal deformations. Three-dimensional relative-positioning using the Global Positioning System (GPS) appears to be the most accurate and cost-efficient method for measuring crustal deformations over distances of tens to hundreds of kilometers. The objective of our research is to investigate sources of error and optimum analysis techniques for high-precision GPS measurements. Progress in these areas will lead directly to more accurate measurement of deformation in areas of high seismogenic potential.

Investigations undertaken: A major component in using a particular measurement technique to monitor deformations is understanding and reducing any inherent systematic errors. Otherwise, these effects may obscure the deformation signal or propagate into erroneous relative-position measurements and incorrect interpretations of deformation. In order to understand and model systematic errors and to improve analysis techniques, it is advantageous to collect data under different observing conditions (time of day, season, weather, etc.) and over a wide range of spatial scales. In this context, we are examining several sets of GPS data, collected in central and southern California, which fulfill these conditons.

1) In collaboration with investigators at the USGS in Menlo Park (Prescott, et al., this volume), we are examining GPS data collected at a quadrilateral of stations spanning the San Andreas fault near Parkfield, California (Figure 5 in Prescott, et al.). Variations of 10-15 mm/yr are expected in the lengths of four baselines crossing the fault (W. Prescott, private communication). The distances between the sites range from 2 - 11 km. The four sites have been occupied, in two day bursts, fifteen times over the past 18 months. Using the MIT GPS software package, we have analyzed three bursts spanning 106 days between January and May 1986. The results of the comparison between the MIT baseline-vector results and those obtained by Dr. Prescott using the Phaser and Bernese software packages are described in this report.

2) We are examining a large GPS data set collected over an approximately 400 km^2 region in central and southern California to monitor crustal deformations west of the San Andreas fault (Agnew et. al., 1987). The data has been collected at a network of sites that includes five regional "fiducials" and about 20 other sites of interest, all in California, and at several other sites distributed over North America. A subset of the sites has been occupied in Dec. 1986 - Jan. 1987, May - June, 1987 and September, 1987. This network has been designed to study systematic errors in GPS measurements by repeat observations covering a broad range of lengths and under widely varying conditions. In this report, we discuss preliminary results using regional orbit improvement techniques.

Analysis and Results:

1) Three measurements (spanning six days) of the Parkfield quadrilateral were analyzed using the MIT GPS software package. On each of the days, the carrier-beat-phase data from the three receivers were analyzed simultaneously in the session mode to yield a self-consistent set of three baseline vectors. The observables were L1 and L2 carrier-beat-phase (the ionosphere-free linear combination was not used because of the short baseline lengths, e.g., Schaffrin and Bock, 1987). The orbits used in the analysis were obtained by using MIT program NAVSTR to numerically integrate, over the four-hour observation span, an orbit for each of the six observed satellites, using as initial conditions the "precise ephemerides" supplied by the Naval Surface Weapons Center in Dahlgren, Virginia. From previous experience, these orbits should be accurate at the 0.5 - 1 parts per million level, or 5-10 mm on a 10 km baseline.

With this limited data set , the (rms) repeatability of the baseline vectors over the three bursts, is at the 0.5 - 1.0 ppm level in the north and east components, 1-3 ppm in the vertical component and 0.5 ppm in the distance component. The repeatability in the horizontal components is consistent with the postulated orbital uncertainties. The repeatability in the vertical component is due to a combination of orbital errors, tropospheric refraction, and quite possibly a blunder in recording the antenna heights. All components are affected by multipath errors, as well. The precision in the baseline length should allow for the detection of 1 microsrain/year which is more than half the expected deformation. Thus, it should be possible to detect fault motion confidently after the analysis of two years of similar quality data.

The results of the intercomparison of baseline lengths estimated by the MIT, Phaser, and Bernese software are given in Figure 6 (in Prescott, et al., this voume). The shorter baselines agree at the several mm level but there are disturbing disagreements of greater than a cm in the lengths of the longer baselines. We are investigating the reasons for these differences.

We plan to continue the analysis and intercomparison for all the Parkfield quadrilateral data collected. Continental orbit tracking data from the National Geodetic Survey will be used, when available, in order to reduce errors due to orbital uncertainties.

2) We have analyzed the "first" experiment of the December, 1986 GPS data. This includes repeated observations from five fiducials (Vandenberg, Ft. Ord, Owens Valley, Mojave, and Palos Verdes, and four other sites (Black Hill, Pozo, Santa Paula, and Lospe). The first objective of the experiment was to tie the VLBI sites at Vandenberg, Santa Paula and Palos Verdes to the NGS triangulation site on north Vandenberg, to Pozo, and to the USGS triangulation site on Black Hill. The second objective was to provide, along with the "second" experiment not described here, first-epoch data for studying tectonic deformation across the Santa Maria Basin. We wanted to test the hypothesis that motion along the Hosgri fault system is transferred to faults in the Santa Barbara Channel by deformation within the Santa Maria Basin east of Vandenberg, to estimate any compressive deformation perpendicular to the San Andreas fault, and to test the stability of the southern end of the Salinian block.

Previous high-accuracy GPS studies in California have relied on simultaneous continental-scale GPS measurements in order to provide improved satellite ephemerides (e.g., Bock et al., 1986). Recent studies have indicated that it is possible to use a fiducial network, enclosing the region of interest, to reduce the errors due to orbital uncertainties to the same level as obtained from continental tracking (King et al., 1987). Since the first experiment did not include a significant amount of continental tracking support, we had no choice but to use the regional orbit-improvement approach. For each of the five days, we performed a session-mode least-squares adjustment of all the carrier-beat-phase data collected that day. To define a regional reference frame, we fixed the coordinates sites of three of the previously well-determined fiducial sites (Vandenberg, Owens Valley and Ft. Ord). We adjusted, using the ionosphere-free phase observable, the remaining station coordinates, six orbital parameters for each of the six observed satellites, tropospheric zenith-delay parameters for each site, and phase bias parameters. Except for tropospheric constraints which we applied to the zenith-delays (Murray et al., 1987), all parameters were completely free to adjust.

The scaled formal uncertainties for the adjusted baseline components of each day ranged from 3-6 mm in the north component, 10-25 mm in the east component, and 15-35 mm in the vertical component. The baseline ranged in length from 35 - 460 km. The higher uncertainties in the east component are due to the primarily north-south satellite ground tracks in California and to the fact that in these preliminary analyses we used the ionosphere-free observable and did not fix any phase biases to integer values. The higher uncertainties in the vertical component are due to geometric considerations and to the estimation of zenith delay parameters.

The rms scatter for each baseline vector was computed from the mean of five days, for the north, east and vertical components. These are displayed in the figure as a function of baseline length in units of mm and in length-proportional units of parts per billion. It is apparent, for each component, that any systematic errors are mapping into baseline repeatability at a constant level. There seems to be little functional dependence on baseline length. The absolute repeatability in the vertical component is somewhat better for the shorter baselines over which the tropospheric refraction errors are still correlated and are thereby reduced in the between-stations phase-difference. The decrease in proportional repeatability with increased baseline length, for all components, indicates that orbital uncertainties are not a significant source of error for these baselines, since orbital errors map into increasing baseline error proportionately with increasing baseline length. It can be inferred from the plots that the errors due to orbital uncertainties are below the 20-30 parts per billion level.

An examination of the double-difference post-fit residuals for the various baselines indicates that the rms scatter is similar (approximately 1- 2 cm) for all length baselines. Comparisons on repeated baselines indicate highly correlated systematic behavior from day to day that can only be due to multipath errors. This behavior is particularly evident on the shorter baselines and at particular sites. We cannot attribute the level of baseline repeatability to multipath errors since these errors are so highly correlated from day to day (to the extent that the observation schedules repeat from day to day). Multipath errors will, of course, degrade accuracy.

In summary, it is evident, albeit from this small sample, that the concept of regional orbit improvement is a powerful tool for crustal deformation monitoring on scales of tens to hundreds of kilometers. We now have at our disposal a GPS data set collected over the same network, spanning 10 months. We plan to use this data set to continue our study of regional orbit and network improvement and systematic error sources.

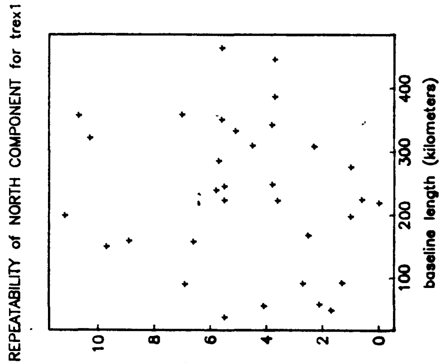
REPEATABILITY of NORTH COMPONENT for trex1
millimeters
0
2
4
6
8
10
baseline length (kilometers)
100
200
300
400

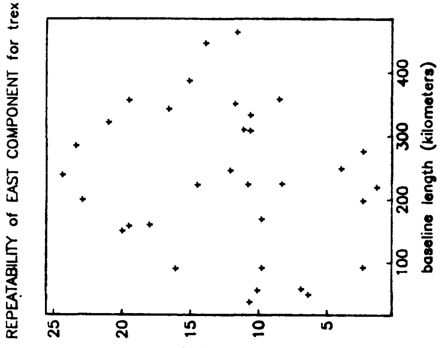
REPEATABILITY of EAST COMPONENT for trex1
millimeters
5
10
15
20
25
baseline length (kilometers)
100
200
300
400

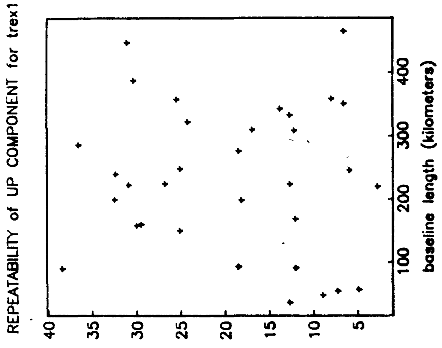
REPEATABILITY of UP COMPONENT for trex1
millimeters
5
10
15
20
25
30
35
40
baseline length (kilometers)
100
200
300
400

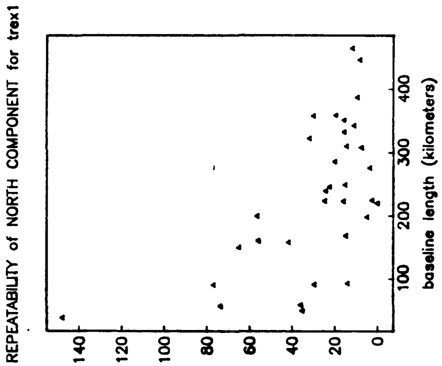
REPEATABILITY of NORTH COMPONENT for trex1
parts per billion of baseline length
0
20
40
60
80
100
120
140
baseline length (kilometers)
100
200
300
400

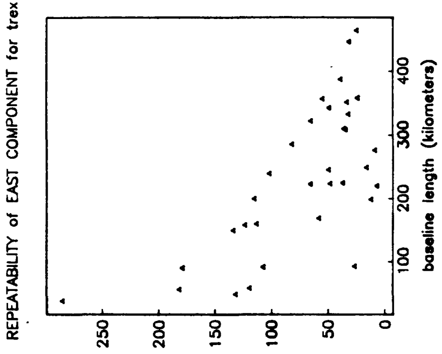
REPEATABILITY of EAST COMPONENT for trex1
parts per billion of baseline length
0
50
100
150
200
250
baseline length (kilometers)
100
200
300
400

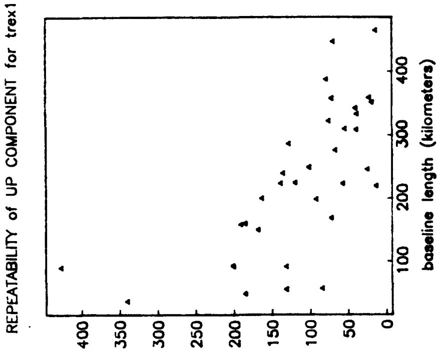
REPEATABILITY of UP COMPONENT for trex1
parts per billion of baseline length
0
50
100
150
200
250
300
350
400
baseline length (kilometers)
100
200
300
400

References:

Agnew, D. C., Y. Bock, T. H. Jordan, R. W. King, T. H. Dixon, B. H. Hager, D. D. Jackson, W. H. Prescott, J. L. Stowell, B. E. Schutz, and W. E. Strange, GPS measurements in central and southern California (abstract), *Eos Trans*. AGU, **68**, p. 282, 1987.

Bock, Y., R. I. Abbot, C. C. Counselman, and R. W. King, A demonstration of 1-2 parts in 10^7 accuracy using GPS, *Bulletin Geodesique*, **60**, pp. 241-254, 1986.

King, R. W., Y. Bock, M. H. Murray, and D. N. Dong, Optimal networks for GPS orbit determination, Union Symposium on the Impact of GPS on Geophysics, IUGG General Assembly, British Columbia, August, 1987.

Murray, M. H., Y. Bock, K. L. Feigl, and J. L. Davis, Assessing the effects of atmospheric error on estimates of relative position obtained from GPS data, Union Symposium on the Impact of GPS on Geophysics, IUGG General Assembly, British Columbia, August, 1987.

Prescott W. H., J. C. Savage, M. Lisowski, Crustal Strain project report, this volume.

Shaffrin, B. and Y. Bock, A unified scheme for processing GPS phase observations, *Bulletin Geodesique*, in press, 1987.

FAULT ZONE TECTONICS

9960-01188

Sandra Schulz Burford
Branch of Tectonophysics
U.S. Geological Survey
345 Middlefield Road, MS/977
Menlo Park, California 94025
(415) 329-4814

Investigations

1. Directed maintenance of creepmeter network in California.

2. Updated archived creep data on PDP 11/44 computer and moved entire data set to new ISUNIX LOW FREQUENCY computer.

3. Installed three new creepmeters in the Parkfield area.

4. Continued to establish and survey alinement arrays on California faults.

5. Monitored creepmeter and alinement array data for possible earthquake precursors. Submitted two abstracts for the Fall 1987 Meeting of the American Geophysical Union.

Results

1. Currently 32 extension creepmeters and one contraction creepmeter operate; 25 of the 32 have on-site strip chart recorders, and 23 of the 25 are telemetered to Menlo Park (Figure 1).

2. Fault creep data from USGS creepmeter sites along the San Andreas, Hayward, and Calaveras faults have been updated through September 1987, and stored in digital form (1 sample/day). Telemetry data are stored in digital form (1 sample/ten minutes), updated every 10 minutes, and merged with daily-sample data files to produce timely data.

3. During the period April-June, three new creepmeter pairs were installed at Parkfield. These three, together with two pairs installed last summer, fulfill our proposal funded in 1986 by the State-Federal Joint Prediction experiment to install five new creepmeters by June 30, 1987.

A creepmeter pair consists of a 25-mm-range invar wire instrument and a 30-cm-range strong-motion stainless steel cable instrument. The invar wire and the steel cable share the same 30-meter conduit, but have separate anchor points. The invar wire instrumentation is mounted on piers isolated from the surrounding vaults, while the stainless steel cable instrumentation is attached directly to the vaults. The three newest sites, shown on Figure 2, are:

XVA1 (Varian Ranch) - across the center of the VAR4 alinement array, 3.1 km southeast of XMD1 (Middle) Ridge) creepmeter and 2.9 km northwest of XPK1 (Parkfield) creepmeter. There are now four creepmeters spaced approximately 2-3 km apart along Middle Mountain (XMM1, XMD1, XVA1, XPK1).

XRSW (Roberson southwest) - on the southwest trace on projection of a line from en echelon cracks across Parkfield-Slack Canyon Road 150 m to the northwest, to an offset measured between monuments 2 and 3 of the Kester alinement array (PKW4) 50 m to the southeast.

XHSW (Hearst southwest) - near HSW4 alinement array on the southwest trace, 0.6 km south-southeast of Parkfield cemetery (south of Turkey Flat Road) and 2.25 km west-northwest of WKR1 (Work Ranch) creepmeter.

Coordinates of all five new creepmeters are as follows: (listed north to south).

STATION NAME	LATITUDE	LONGITUDE	INSTALL. DATE	TYPE
XMD1 (Middle Ridge)	35 56.6'	120 29.1'	July 1986	extension
XVA1 (Varian)	35 55.3'	120 27.7'	April 1987	extension
XRSW (Roberson SW)	35 54.4'	120 27.6'	May 1987	extension
XHSW (Hearst SW)	35 51.7'	120 24.9'	June 1987	extension
X461 (Hwy 46 SO)	35 43.3'	120 16.7'	August 1986	contraction

4. A final set of surveys of five Parkfield alinement arrays were performed by the private contractor during the reporting period, completing a 1-year contract. The other Parkfield arrays were surveyed by Project personnel James Wilmesher, F. Brett Baker, and Sandra Burford, with assistance from volunteer Kay Schulz. A survey monument (MIDO)

was installed near two-color laser reflector site MIDE, and the angle between MIDE and the Car Hill laser observatory measured to establish a baseline value. Future measurements of the angle will help determine if an active fault trace exists between the MID-E site and Car Hill.

5. Project personnel continued to monitor creepmeter and alinement array data for possible precursors. Special attention continued to be focused on Parkfield instruments and lines, and low-level alarm criteria thresholds for the Parkfield Prediction Experiment were reached several times during the reporting period. Project personnel supplied creep data to the Water Well Monitoring project for correlation between creep events and changes in water level, and to the two-color laser project for correlation between near-fault creep and long-line length changes.

Products

Baker, F. Brett, Wilmesher, James, and Burford, Robert O., 1987, Fault creep at Parkfield, California as determined by alinement array measurements (abstract submitted to American Geophysical Union for Fall 1987 Meeting).

Poley, C.M., Lindh, A.G., Bakun, W.H. and Schulz, S.S., 1987, Temporal changes in microseismicity and creep near Parkfield, California, Nature, v. 327, n. 6118, pp. 134-137.

Schulz, S.S., Mavko, Gerald, M., and Brown, Beth D. (in press), Response of creepmeters on the San Andreas fault near Parkfield to the earthquake, <u>in</u> Rymer, Michael J. and Ellsworth, William L., editors, The Coalinga, California, earthquake of May 2, 1983, U.S. Geological Survey Professional Paper, chapter 22.

Schulz-Burford, Sandra S., 1987, An update of creep observations at Parkfield, California (abstract submitted to American Geophysical Union for Fall 1987 Meeting).

Simpson, R.W., Schulz, S.S., Dietz, L.D., and Burford, R.O., 1987, (in press), The response of creeping parts of the San Andreas fault to earthquakes on nearby faults--two examples, Redbook for U.S. Geological Survey Conference on Intermediate Term Precursors.

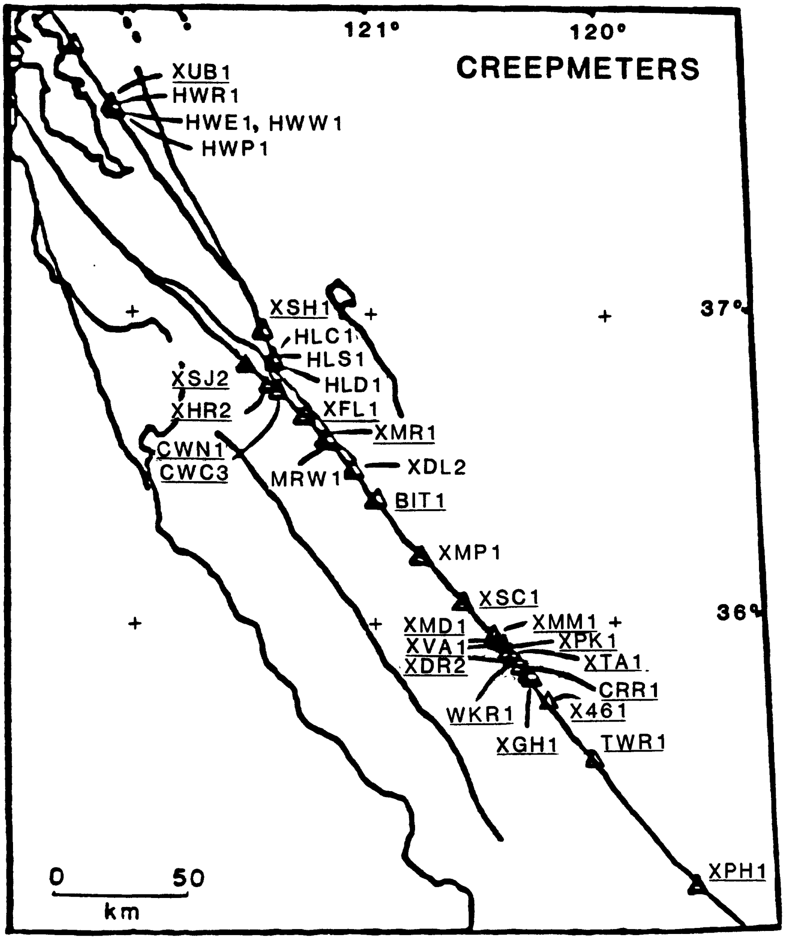

FIGURE 1. USGS creepmeter stations in Northern and Central California. Instruments with underlined names transmit on telemetry. NOT SHOWN: XRSW, XHSW on Southwest fracture near Parkfield. See Figure 2.

Creep and Alinement : Parkfield, CA

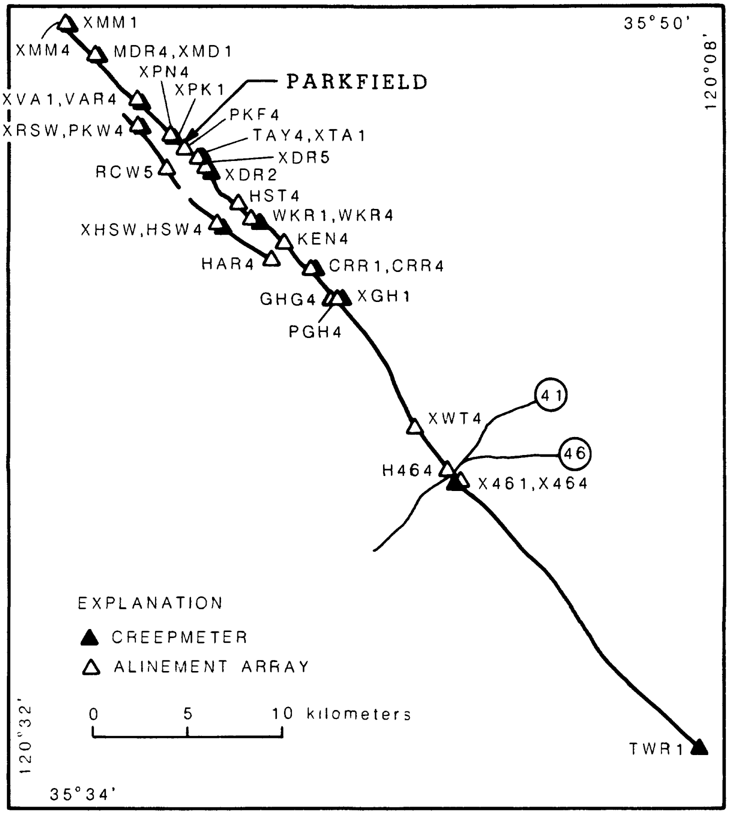

CREEPMETER AND ALINEMENT ARRAY SITES IN PARKFIELD
JULY, 1987

Creepmeter station names end with "1" or "2";
(stations on the southwest trace end with "W")

Alinement array site names end with "4" or "5"

FIGURE 2.

Remote Monitoring of Source Parameters for Seismic Precursors

9920-02383

George L. Choy
Branch of Global Seismology and Geomagnetism
U.S. Geological Survey
Denver Federal Center
Box 25046, Mail Stop 967
Denver, Colorado 80225
(303) 236-1506

Investigations

1. Enhancement of NEIC reporting services. We are integrating techniques of analyzing broadband data into the data flow of the NEIC. Broadband data can then be used routinely to increase the accuracy of some reported parameters such as depth and to compute additional parameters such as radiated energy.

2. Teleseismic estimates of radiated energy and strong ground motion. On a world-wide basis, the relative paucity of near-field recording instruments hinders the prediction of strong ground motion radiated by earthquakes. We are developing a method of computing radiated energy and acceleration spectrum from direct measurements of teleseismically recorded broadband body waves. From our method, the maximum expectable spectral level of acceleration and lower bounds of stress drops can be made for any event large enough to be teleseismically recorded.

3. Rupture process of large- and moderate-sized earthquakes. We are using digitally recorded broadband waveforms to characterize the rupture process of selected intraplate and subduction-zone earthquakes. The rupture processes thus delineated are used to complement seismicity patterns to formulate a tectonic interpretation of the epicentral regions.

Results

1. The advantages of using broadband data to determine the differential arrival times of direct P and depth phases was demonstrated in Choy and Engdahl (1987). Differential times are much more accurate in determining depth of an earthquake than arrival times of P waves alone. An automated processing package utilizing the method of Choy and Boatwright (1981) and Harvey and Choy (1982) has been implemented and is now routinely obtaining broadband records of displacement and velocity from digital data of the GDSN. The NEIC now uses broadband waveforms to routinely: (1) resolve depths of all earthquakes with $m_b > 5.8$; (2) resolve polarities of depth phases to help constrain first-motion solutions; and (3) present as representative digital waveforms in the monthly PDE's. We have developed and implemented a semi-automated package that uses the algorithm of Boatwright and Choy (1986) to routinely compute radiated energy for all earthquakes with $m_b > 5.8$.

2a. Subduction-zone events. We have applied our algorithm for the computation of radiated energy to a number of large subduction-zone earthquakes. Generally, indirect estimates of energy (e.g., those using simplistic relations with moment) may overestimate energy if the rupture process involves a sizeable component of aseismic slip. In the frequency range 0.1-1.0 Hz, a teleseismically derived acceleration spectrum compares well with the spectra from near-field accelerograms. This implies we can make routine estimates of strong ground motion from large earthquakes with teleseismic data.

2b. Intraplate events. We have applied our algorithm for the computation of acceleration spectra to a series of shallow intraplate earthquakes. Most of these events are characterized by a flat spectral level at high frequencies but an intermediate slope before an ω^2 falloff at low frequencies. The high-frequency spectral levels of these intraplate earthquakes are the same as the levels of subduction-zone earthquakes with the same seismic moments, although the spectral shapes are different.

3a. A study of the Yemen earthquake of 13 December 1982, has been completed. This event was found to consist of two events that occurred 3 s apart on a steeply dipping fault that trended NNW. Correlation with aftershock distribution confirms the hypothesis of Langer et al. (1987) that conjugate faulting occurred.

3b. We have completed a study of the Chilean earthquake of March 1985, and its aftershocks. The main shock was a complex event consisting of three events. The first two events released minor amounts of energy; the major release of energy occurred with the third event that nucleated downdip of the first two events. The size of the early aftershock zone far exceeds the dimension of the major shock; the strong frequency dependence of scalar moment implies that substantial slow slip occurred that was not associated with major energy release.

Reports

Boatwright, J., and Choy, G. L., 1987, Acceleration source spectra for large earthquakes in Northeastern North America [abs.]: EOS (American Geophysical Union, Transactions) (in press).

Choy, G. L., and Dewey, J. W., 1987, Rupture process of an extended earthquake sequence: Teleseismic analysis of the Chilean earthquake sequence of 3 March 1985: Journal of Geophysical Research (submitted).

Choy, G. L., and Dewey, J. W., 1987, Rupture process of an extended earthquake sequence associated with a great thrust-fault earthquake [abs.]: EOS (American Geophysical Union, Transactions) (in press).

Choy, G. L., and Engdahl, E. R., 1987, Analysis of broadband seismograms from selected IASPEI events: Physics of the Earth and Planetary Interiors, v. 47, p. 80-92.

Choy, G. L., and Kind, R., 1987, Rupture complexity of a moderate-sized (m_b 6.0) earthquake: Bulletin of the Seismological Society of America, v. 77, p. 28-46.

Seismic Analysis of Large Earthquakes and Special Sequences in Northern California

9930-03972

Robert S. Cockerham
Jerry P. Eaton
A.M. Pitt
Branch of Seismology
U.S. Geological Survey
345 Middlefield Road, Mail Stop 977
Menlo Park, California 94025
(415) 329-4790

Investigations:

1. Tectonic analysis of northern and central California on the basis of the distribution of microearthquakes and focal mechanisms of the larger earthquakes (Eaton).

2. Continued monitoring and analysis of the seismicity of the White Mountian Seismic group (Mono Lake to Bishop) area of eastern California and western Nevada. (Cockerham)

3. Completion of a USGS Yellowstone seismic catalog covering the years 1964 through 1984. (Pitt)

4. Collection and analysis of data from large earthquakes recorded by the Central and Northern California telemetered seismic network in support of:
   - (a) Developement of better velocity models and associated station travel time corrections, (Eaton, Cockerham and Katie Poley)
   - (b) Evaluation of magnitude calculation based on maximum amplitude and associated period. (Eaton)
   - (c) Calculation of regional variations in focal mechanisms of large (M > 4) California earthquakes. (Cockerham and Eaton)

Results:

1. Earthquakes in the Mendocino seismic zone from 1980 through 1986 (figure 1) have been examined in the light of the plate tectonic elements with which they are associated. These elements include the Mendocino fracture zone between the Pacific and Gorda/Juan de Fuca plates, the subduction zone between the Gorda/Juan de Fuca and North American plates, and the San Andreas fault between the North American and Pacific plates. These three elements come together at the Mendocino triple junction at the inferred junction of the MFZ and the San Andreas fault near Cape Mendocino. The exact location and nature of the triple junction and contiguous parts of the boundaries between the plates, as well as the nature of the processes that occur along them, are not yet well understood. The recognized boundaries between the plates as well as the relative velocities between the plates deduced from geologic and geodetic analysis (Atwater, 1970) are indicated in figure 1.

Relative to North America, the Pacific plate is moving northwestward along the San Andreas fault about 6 cm/yr and the Gorda plate is subducting northeastward (obliquely), along the coast north of Cape Mendocino, about 2 1/2 cm/yr. The Gorda plate is retreating ahead of the northwestward-advancing Pacific plate. Relative to the Pacific plate and their common boundary, the Mendocino fracture zone, the Gorda plate is moving eastward along the MFZ about 5 cm/yr and southward toward the Pacific plate about 2 1/2 cm/yr. Exactly how the convergence between the Gorda and Pacific plates is accommodated is not entirely clear, but it is generally believed that the Gorda plate is being internally deformed and is not subducting along the MFZ. The Mendocino triple junction is closely associated with the northeastern corner of the Pacific plate (junction of the San Andreas fault and the MFZ) and is presumed to move northwestward relative to North America with the Pacific plate.

Earthquakes for the internal 1980-1986 in the Mendocino seismic zone can be separated into three groups (figure 1): 1) earthquakes concentrated along the eastern end of the Mendocino fracture zone, 2) aftershocks of the M 7.2 Nov. 8, 1980 Eureka earthquake (left lateral strike slip), and 3) a broadly dispersed swarm of earthquakes centered on the coast between Cape Mendocino and Punta Gorda and lying principally north of the MFZ and its landward extension. These groups of earthquakes can also be resolved on a series of five contiguous cross sections perpendicular to the N 75°W trend of the concentrated zone of earthquakes on the MFZ (figure 2). The events along the east end of the MFZ are concentrated in a steep (70°-75°) northward dipping zone at depths of 10 km to 35 km (sections A and B, figure 2). Aftershocks of the 1980 earthquake run diagonally across section A and are well represented between about 120 km and 180 km. The scattered events centered on Cape Mendocino are represented on all five sections, but sections B and C appear to be most diagnostic of their nature. On these sections the earthquakes appear to lie in a sheet about 10 km thick with its center about 25 km deep. The sheet extends from about 140 km on the profile to about 90 km on the profile where its southern edge appears to be bent downward. Farther east (section E) this zone contains only a few events and its southern edge descends to about 50 km. West of the coastline the zone of scattered earthquakes blends into the 1980 aftershocks on the north and the earthquakes along the fracture zone on the south, and it appears to be somewhat shallower in its central and northern parts. On the south, however, this zone appears to thicken. Its base descends to about 35 km and its top rises to as shallow as 10 km (section B). On section B, where earthquakes along the MFZ are most numerous, the scattered earthquakes north of the MFZ combine with those along the MFZ to define a wedge-shaped zone of earthquakes with its "base" on the MFZ and its apex about 30 km north of the MFZ and 20 km deep.

The distribution of earthquakes on the map and cross sections (figs 1 and 2), along with the plate tectonic setting of the Mendocino seismic zone, suggest the following processes are at work in the region. The relatively young and weak Gorda plate is being driven obliquely against the northeastern corner of the older stronger Pacific plate. The persistent swarm of earthquakes along the eastern end of the MFZ is caused primarily by the component of that motion parallel to the MFZ. Strong N-S compression of the Gorda plate resulting from the component of Gorda motion perpendicular to the MFZ effectively crushes the Gorda plate against the Pacific plate with two consequences: 1) left lateral strike slip faulting on northeast trending planes (as in 1980) combined with right lateral strike slip motion on the MFZ, and perhaps on northwest trending planes, permits the southeastern corner of the Gorda plate to expand eastward in response to its north-south shortening, and 2) the southern edge of the Gorda plate is thickened by compression against the Pacific plate "anvil" as the brittle Gorda seismogenic layer is deformed by bending and reverse faulting in the seismic wedge along and north of the MFZ.

The wedge of Gorda debris impacted against the north edge of the Pacific plate extends from the sea floor, where it has access to sediments derived from North America, to a depth of at least 35 km; and it is subjected to intense right lateral shearing between the Gorda and Pacific plates. This crustal "mill" that operates along the east end of the MFZ may be the source of the melange and broken formation found in the Franciscan complex of the Coast Ranges. The important role of the northeast corner of the Pacific plate in this process as the "anvil" against which the Gorda plate is crushed and ground up is highlighted by the abrupt termination of concentrated seismicity on the MFZ east of its junction with the San Andreas fault at the triple junction (northeast corner of the Pacific plate). East of the shoreline where the northeast-moving Gorda plate descends gradually beneath the North American plate, part of the disrupted Gorda crust and superjacent sediments are scraped off and accreted to the western edge of the continent and part moves eastward on the descending Gorda mantle beneath North America. As it moves eastward beyond the triple junction the broken Gorda plate finds itself increasingly in the NW-SE shearing regime between the North American and Pacific plates and responds with the appropriate earthquakes.

2. The overall spatial distribution of seismicity in the immediate Long Valley cadera remained unchanged compared with the previous six month period (Fig. 3b). Analysis of the 5 yr. period August 1982 through August 1987 is continuing and will be completed by the end of calendar 1987 with a paper submitted for journal review.

<u>Reports:</u>

Pitt, A. M., 1987, Catalog of earthquakes in the Yellowstone Park-Hebgen Lake region for the years 1973 to 1981. U.S. Geological Survey Open-File Report 87-611, 65 p.

Pitt, A. M., (in press), Maps showing earthquake epicenters (1964-1981) in Yellowstone National Park and vicinity, Wyoming, Idaho, and Montana. U.S. Geological Survey, Miscelaneous Field Studies Map, MF-2022, scale 1:250:000.

Savage, J. C., and Cockerham, R. S., Quasiperiodic occurance of earthquakes in the 1978-1986 Bishop-Mammoth Lakes sequence, eastern California, Bull. Seismo. Soc. Amer., <u>v. 77 (4)</u>, 1347-1358, 1987.

Figure 1. Plate tectonic setting and distribution of microearthquakes in the Mendocino seismic zone for 1980-1986. The vectors indicate relative plate velocities (from Atwater, 1970).
MFZ = Mendocino fracture zone
SAF = San Andreas fault

Figure 2. Cross sections of the Mendocino seismic zone corresponding to the boxes A-A', E-E' on figure 1. Events are projected onto a vertical plane parallel the long axis of the box, which is parallel the coast north of Cape Mendocino and perpendicular to the concentrated zone of earthquakes on the east end of the Mendocino fracture zone. The vertical line at 75 km indicates the location of the southern edge of that zone of earthquakes and its landward projection.

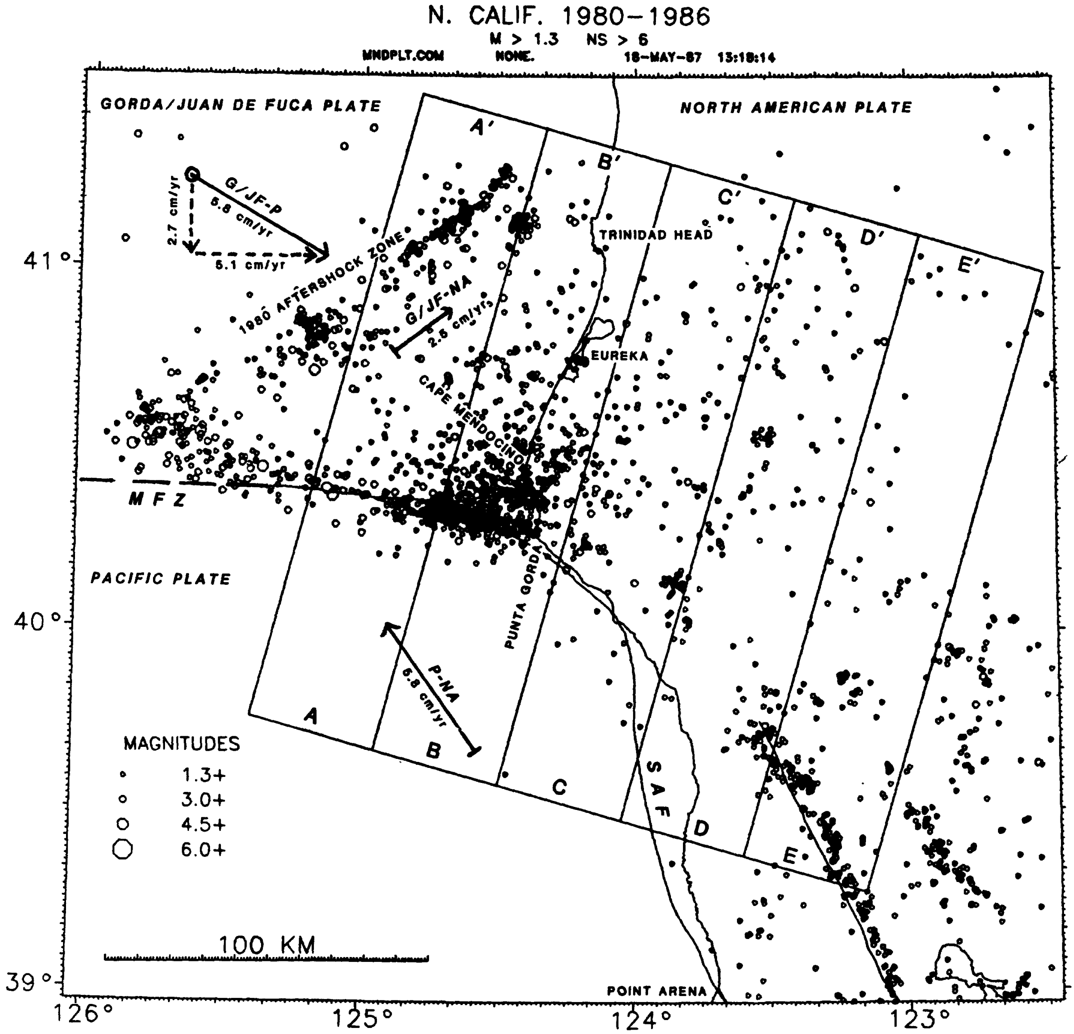
N. CALIF. 1980–1986
M > 1.3 NS > 6
MNDPLT.COM NONE. 18-MAY-87 13:18:14
GORDA/JUAN DE FUCA PLATE
NORTH AMERICAN PLATE
PACIFIC PLATE
G/JF-P
5.8 cm/yr
2.7 cm/yr
5.1 cm/yr
1980 AFTERSHOCK ZONE
G/JF-NA
2.5 cm/yr
P-NA
5.8 cm/yr
TRINIDAD HEAD
EUREKA
CAPE MENDOCINO
PUNTA GORDA
POINT ARENA
MFZ
SAF
A
A′
B
B′
C
C′
D
D′
E
E′
MAGNITUDES
1.3+
3.0+
4.5+
6.0+
100 KM
41°
40°
39°
126°
125°
124°
123°

Fig. 2
II.1

MENDOCINO SEISMIC SECTIONS
TRANSVERSE

M > 1.5 NS > 6

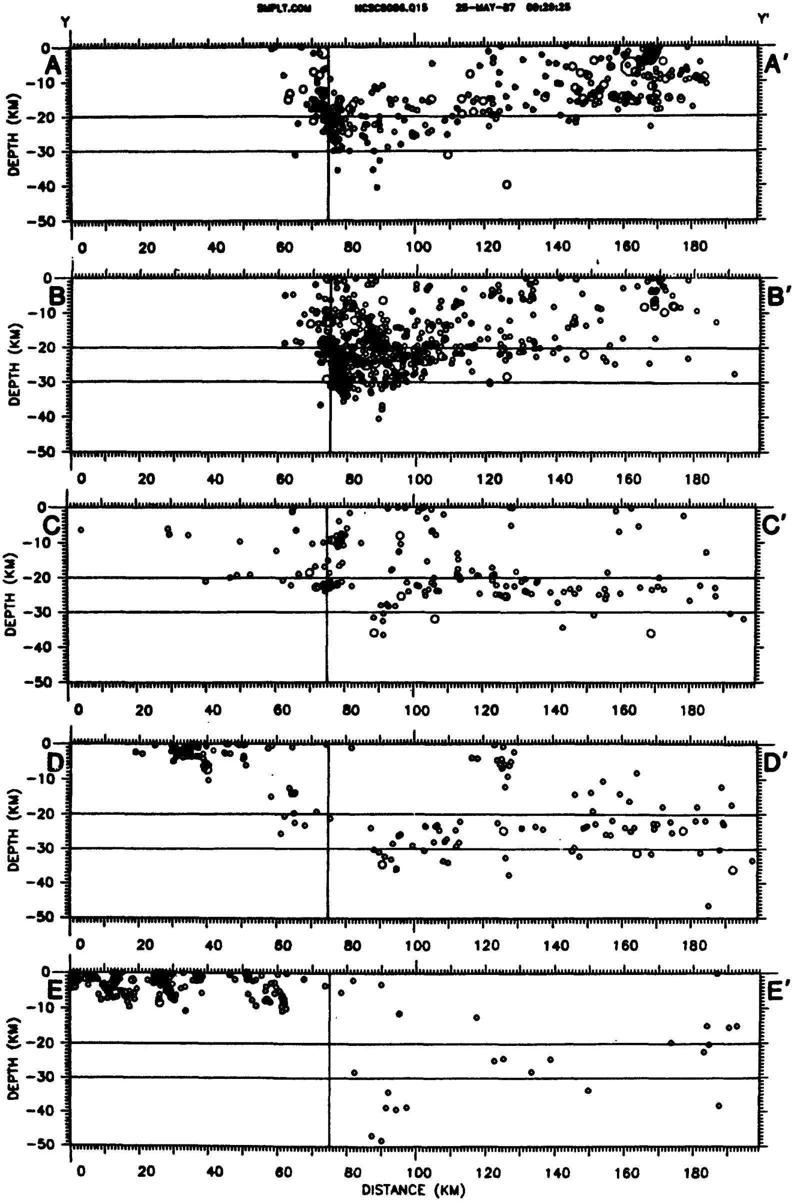

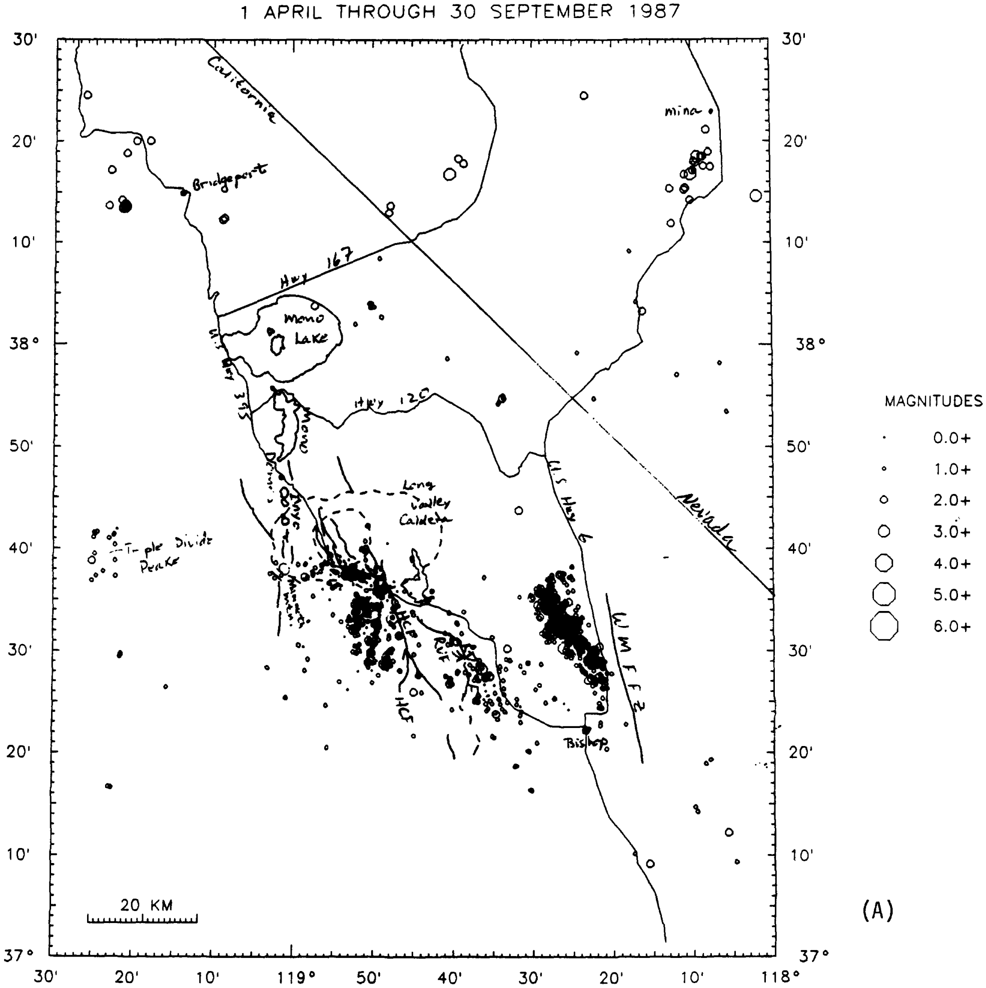

Figure 3. Epicentral map of seismicity in the Mono Lake to Bishop area of eastern California during the periods (A) April through September 1987 and (B) October 1986 through March 1987. WMFFZ - White Mountain Frontal Fault Zone; HCF - Hilton Creek Fault; RVF - Round Valley Fault. The heavy concentration of epicenters just west of the WMFFZ represents continuing high level of aftershock activity in the Chalfant zone.

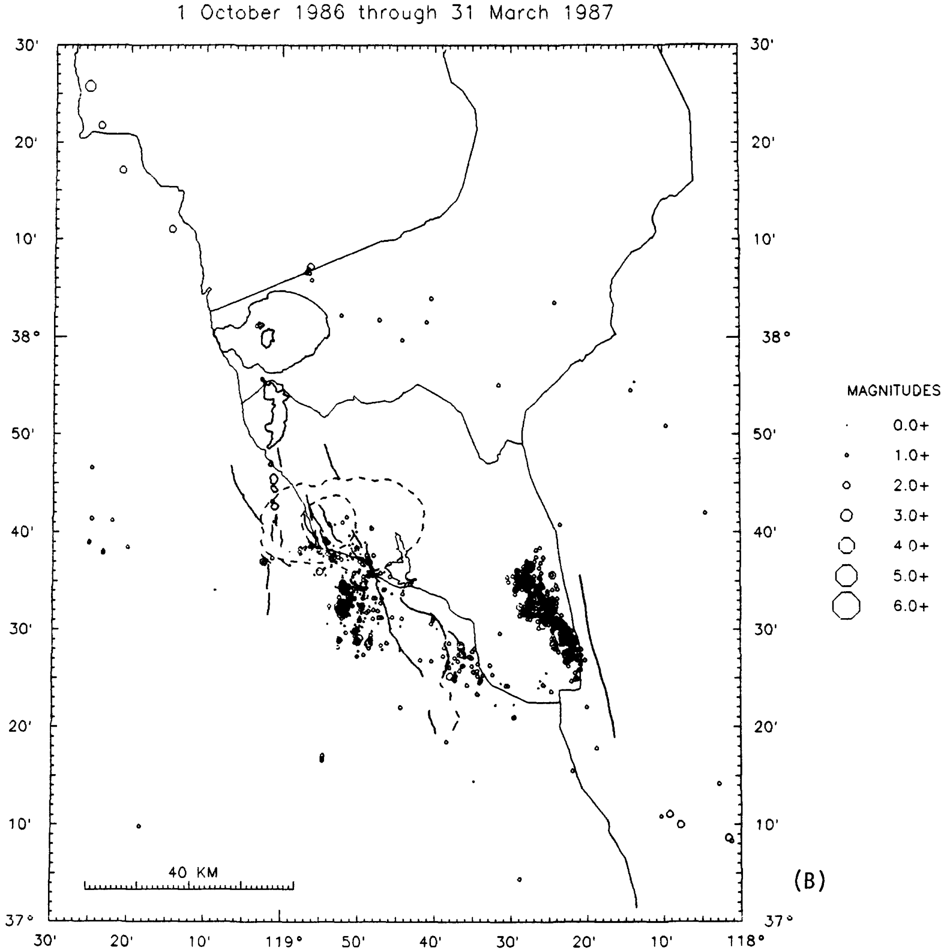
1 October 1986 through 31 March 1987
30'
20'
10'
38°
50'
40'
30'
20'
10'
37°
30'
20'
10'
119°
50'
40'
30'
20'
10'
118°
40 KM
MAGNITUDES
0.0+
1.0+
2.0+
3.0+
4.0+
5.0+
6.0+

(B)

TEMPORAL CHANGES IN SHEAR-WAVE SPLITTING: ADVANCES TOWARDS EARTHQUAKE PREDICTION

14-08-001-G1380

Stuart Crampin
British Geological Survey, Murchison House,
West Mains Road, Edinburgh EH9 3LA, Scotland UK
(031-667-1000)

Background

Technological advances of the last few years allow three-component digital recording at high enough sampling rates for shear-wave splitting to be easily observed for the first time, and splitting is now seen along almost all suitable shear-wave raypaths in the crust. There is rapidly increasing evidence from this splitting that most rocks in the Earth's crust are effectively anisotropic due to an internal structure of stress-aligned fluid-filled microcracks, and shear-wave motion can be interpreted in great detail in terms of the crack- and stress-geometry within the rockmass (reviewed by Crampin 1987a). These distributions of microcracks are known as *extensive-dilatancy anisotropy* or *EDA*. The data demonstrate that most *in situ* rocks contain an internal structure of stress-aligned fluid-filled microcracks (EDA-cracks) whose geometry can be estimated from three-component shear-wave motion recorded at a distance from the cracked rock.

Objectives

Changes in stress before an earthquake are expected to modify the geometry of EDA-cracks and lead to corresponding changes in the behaviour of shear-wave splitting. It is suggested that monitoring shear-wave splitting could form the basis for the routine prediction of earthquakes (Crampin 1987b). The importance for predicting earthquakes is that the most immediate and direct action of a change of stress before an earthquake is to change the strain on the rockmass and modify the geometry of the fluid-filled microcracks within the rockmass. These modifications will change the behaviour of shear waves propagating through the rockmass, and the effects should be visible on shear waves recorded remotely.

The objective is to seek temporal changes in shear-wave splitting before earthquakes, relate any such changes to the earthquake source process, and improve the understanding of the phenomenon of EDA.

Results

Shear-wave splitting is observed above small earthquakes in the Anza seismic gap on the San Jacinto Fault, Southern California, displaying the effective anisotropy of distributions of vertical fluid-filled EDA-cracks. Only one station (KNW) has arrivals from a wide range of azimuths and angles of incidence within the shear-wave window. The delays between the split shear-waves in part of this shear-wave window at KNW increase significantly over the three years of available records

(Peacock et al. 1987). These changes can be modelled by an increasing aspect ratio ("bowing") of the stress-oriented microcracks, which is one of the expected elastic effects of an increase of stress on a rockmass containing a distribution of fluid-filled microcracks (Peacock et al. 1987; Crampin 1987b).

This is the first time that temporal variations of shear-wave splitting have been observed, and suggests that shear-wave splitting can be used to monitor the detailed changes in the build-up of stress before earthquakes. Since the volume of rock affected by the build-up of stress before an earthquake is likely to be extensive, the microcrack geometry could be modified several tens of kilmometres away from the eventual epicentre of a large earthquake and monitoring shear-wave splitting could be a sensitive technique for diagnosing stress changes.

The epicentre of the $M = 5.9$ Palm Springs earthquake of July 8th 1986 was 33 km away from KNW and seems to provide an opportunity to examine the effects of a release of stress by an earthquake. **Preliminary observations suggest that the aspect ratio of the microcracks decreased immediately following the earthquake.** If these observations are confirmed, it would be a fundamental advance towards earthquake prediction, as monitoring shear-wave splitting appears to be most direct way to monitor the changes of stress on the rockmass.

Acknowledgements
I thank Russ Evans and David C. Booth for their comments on this note. The major part of this research was supported by the Natural Environment Research Council and is published with the approval of the Director of the British Geological Survey (NERC).

REPORTS OF RESEARCH PARTIALLY SUPPORTED BY USGS CONTRACTS

Booth, D.C., S. Crampin, E.M. Chesnokov, and M.A. Krasnova, The effects of near-vertical parallel cracks on shear-wave polarizations, *Geophys. J.R.astr.Soc.*, *87*, 583-594 (1986).

Bush, I., and S. Crampin, Observations of EDA and PTL anisotropy on shear-wave VSPs, *Expanded Abstracts, 57th Ann.Int.SEG Meeting, New Orleans, 1987*, 646-649 (1987).

Chen, T.-C., D.C. Booth, and S. Crampin, Shear-wave polarizations near the North Anatolian Fault - III. Observations of temporal changes, *Geophys.J.R.astr.Soc.*, in press (1987).

Crampin, S., Geological and industrial implications of extensive-dilatancy anisotropy, Nature, *328*, 491-496 (1987a).

Crampin, S., The basis for earthquake prediction, *Geophys.J.R.astr.Soc.*, in press (1987b).

Crampin, S., The scattering of shear-waves in the crust, Pure Appl. *Geophys.*, in press (1987c).

(cont.)

Crampin, S., and I. Bush, Shear waves revealed: extensive-dilatancy confirmed, *Expanded Abstracts, 56th Ann.Int.SEG Meeting, Houston, 1986*, 481-484 (1986).

Crampin, S. and R. Evans, Neotectonics of the Marmara Sea region of Turkey, *J.geol.Soc., 143*, 343-348 (1986).

Crampin, S., McGonigle, R. and Ando, M., Extensive-dilatancy anisotropy beneath Mount Hood, Oregon, and the effect of aspect ratio on seismic velocities through aligned cracks, *J.geophys.Res., 91*, 12703-12710 (1986).

Evans, R., D. Beamish, S. Crampin, and S.B. Üçer, The Turkish Dilatancy Project (TDP3): multidisciplinary studies of a potential earthquake source region, *Geophys.J.R.astr.Soc.*, in press (1987).

Liu, E. and S. Crampin, Effects of crack anisotropy on cross-hole shooting, *Expanded Abstracts, 57th Ann.Int.SEG Meeting, New Orleans, 1987*, 662-664 (1987).

Peacock, S., S. Crampin, D.C. Booth, and J/B. Fletcher, Shear-wave splitting in the Anza seismic gap, Southern California: temporal variations as possible precursors, J.geophys.Res., in press (1987).

Analysis of Natural Seismicity at Anza

9910-03982

Joe Fletcher, Art Frankel, Leif Wennerberg, and Linda Haar
Branch of Engineering Seismology and Geology
U.S. Geological Survey
345 Middlefield Road, MS 977
Menlo Park, California 94025
(415) 329-5628 or (415) 329-5612

Investigations:

1. The purpose of this project is to maintain the 10-station digital array of seismometers at Anza, California, compute source parameters from the digital seismograms, and analyze those source parameters with respect to the generation and propagation of high frequency seismic waves.

2. Measurements of attenuation by coda methods and by spectral ratios of body waves give a Q that is frequency-dependent whereas laboratory measurements and other field data suggest that a frequency-independent Q is sufficient to explain the data. It appears that calculating the true geometrical spreading (rather than just correct for a 1/distance fall-off) for reasonable layered models can bring the data on which the frequency-dependent models were based into line with the frequency-independent models.

Results:

1. Source parameters for about 640 earthquakes have been processed since October 1982. Figure 1 shows the epicenters for those earthquakes. Most of the earthquakes continue to occur at the same clusters identified in the early data. A number of the earthquakes from the North Palm Springs earthquake were recorded by the array and source parameters for many of those events have now been processed. The largest events recorded by the array continue to be in the 10^{20} to 10^{21} dyne-cm range: few events above $M_L = 3.5$ have occurred at Anza since the array was installed.

2. Studies that report on frequency-dependent Q usually use a correction of 1/distance to normalize the records for the different distances of the stations used in the analysis. However, it appears that ray theory and finite difference synthetics suggest that for reasonable velocity models that employ gradients a true geometerical spreading correction would be more severe than 1/distance. This strong decay with distance is found for upgoing rays and downgoing rays with turning points at depths with small velocity gradients. To check this result, data from the North Palm Springs earthquake were analyzed for the distance-dependent attenuation. A section of the coda was deconvolved from the body wave to correct for the site response. Out to distances of about 80 km the amplitudes at 1 Hz decay at about the same rate as amplitudes at 15 Hz. Although at first glance this might suggest that Q would be frequency-dependent a true geometrical spreading correction can explain most of this result and still be consistent with a frequency-independent Q.

Reports:

Frankel, A., and Wennerberg, L., 1987, On the frequency dependence of shear-wave O in the crust from 1 to 15 Hz. Submitted to American Geophysical Union Fall Meeting 1987.

Figure Caption

Figure 1. Map of epicenters determined from the digital array at Anza. Triangles and three-letter codes show the station sites. Sizes of the circles is proportional to moment: the range is from about 10^{17} dyne-cm to 10^{21} dyne-cm.

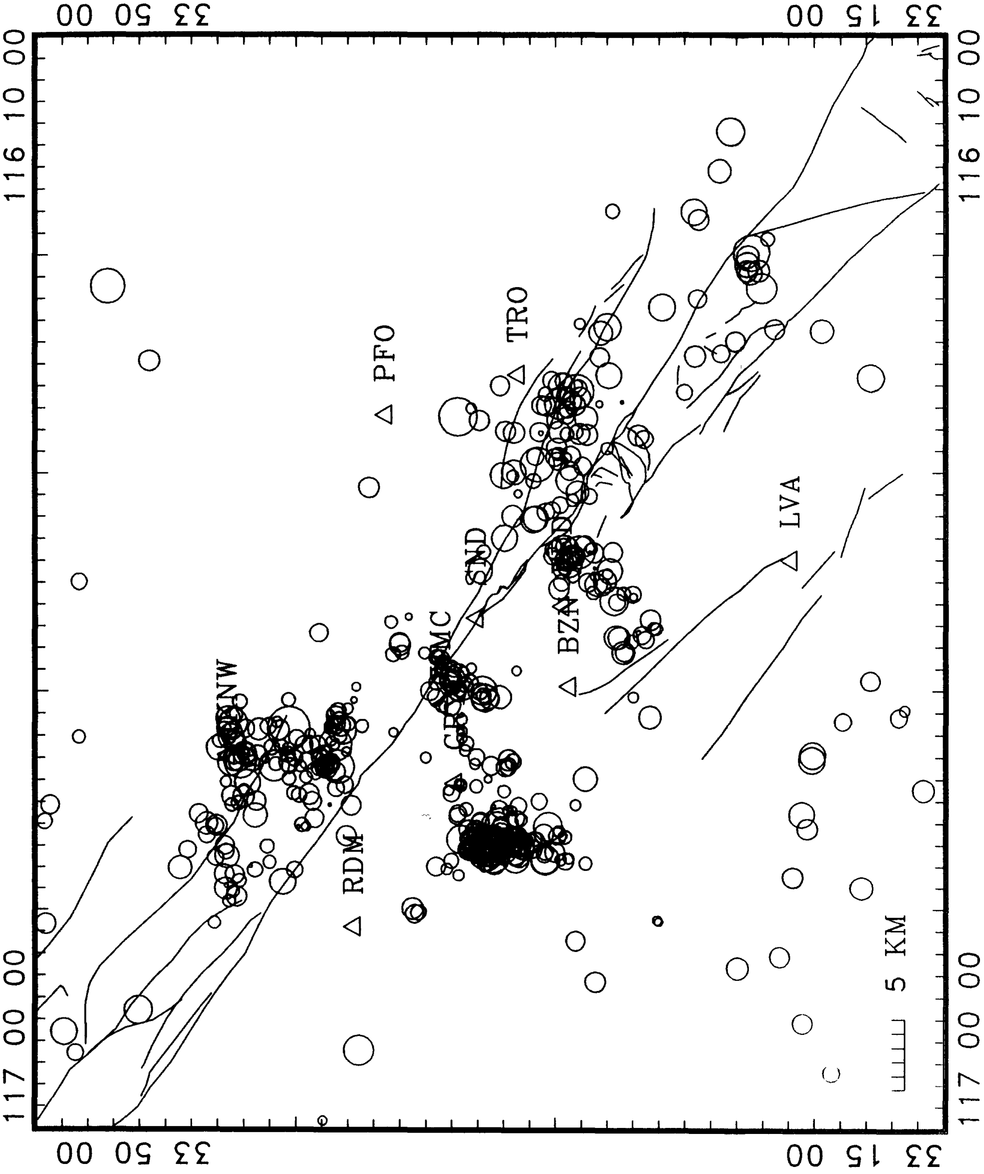
33 50 00
33 15 00
116 10 00
117 00 00
PFO
TRO
LVA
SND
BZN
KNW
RDM
5 KM

Attenuation/Amplification at Hard Rock Sites at Anza, California

9910-04188

Joe Fletcher and Linda Haar
Branch of Engineering Seismology and Geology
U.S. Geological Survey
345 Middlefield Road, MS 977
Menlo Park, California 94025
(415) 329-5628

Investigations

1) Several investigators have recently suggested that the dependence of stress drop on moment for earthquakes at Anza (moments $\leq 10^{20}$ dyne-cm) may be due to attenuation in the upper crustal layers beneath the receiver. Although such arguments are plausible, only by directly measuring the attenuation at Anza stations can we answer these questions. We have drilled boreholes at stations KNW and PFO and will use shear waves generated by earthquakes as well as air-driven shear wave hammers to determine the site response in the upper 300 m at these two sites.

Results

1) Seismograms recorded on the downhole sensors (see fig. 1) at station KNW are clearly higher in frequency content than the surface records at the same site. Additionally, the coda for the P wave is usually larger and dies off much more slowly than at the surface. In fact, some of the smaller events that have S-P times of about 2 sec. do not have a P-wave corner frequency inside of 100 Hz. We have computed spectral ratios of a suite of these events (fig. 2) and have found that while the ratios are highly variable, most show resonances in the surface records as compared to those downhole. There is a broad amplification between 7 and 40 HZ with narrow band resonance peaks superimposed on the broad amplification. Above about 40 Hz the ratios generally fall-off suggesting attenuation is important at the higher frequencies.

   Haskell modeling of the spectral ratios shows that the elastic response of the rock does explain most of the amplification and resonances. We have not tried to fit individual resonant peaks as these are highly variable in amplitude and frequency, but rather to qualitatively fit the frequency band and average size of the amplification and to note that some higher peaks occur within that band. It appears that a frequency-independent Q will not explain the ratios as Q can be adjusted to fit where the ratios start to fall-off but not the amount. The ratios fall-off faster than a frequency-independent Q model would predict. This is what might be expected if cracks with a small cross section were causing most of the attenuation.

   Although a second set of downhole seismometers was installed at Pinon Flat Observatory in August, they have not as yet produced any data as they suffer from a 60 Hz pickup problem, and their gains were initially set too low.

When the holes were first drilled they were logged for both P and S wave velocities by using a hammer source at the surface while a three-component geophone system was lowered into the borehole. The data has been analyzed for velocities for both Pinon Flat Observatory and Keenwild. Pinon Flat appears to have very high shear wave velocity of 3.2 to 3.3 km/sec at 1000 ft depth and 5.7 km/sec P-wave velocity at the same depth. The site at station KNW on the other hand has a somewhat slower shear wave velocity of 2.6 to 2.7 km/sec and a 5.4 km/sec P-wave velocity.

The difference in velocities are similar to other geophysical observations such as the distribution of seismicity and the shear strain accumulation. Pinon Flat Observatory is in a block of the southern California batholith between the San Andreas and San Jacinto faults that has a low shear accumulation and is low in seismicity: it appears to be more "monolithic" than surrounding rock. Station KNW, however, is very near the Hot Springs fault. It may be close enough to be within a a fractured zone associated with the fault. We are now analyzing the televiewer logs to confirm the crack densities and orientations in each hole.

Reports

Haar, L.C., Fletcher, J.B., Liu, H.-P., Warrick, R.E., and Westerlund, R.E., 1987, Near-surface effects at Anza: comparisons of surface and borehole data: *Seismological Research Letters*, v. 58, p. 26.

Haar, L.C., Fletcher, J.B., Liu, H.-P., Warrick, R.E., and Westerlund, R.E., 1987, Preliminary results from a borehole experiment at Anza, California, to investigate near-surface effects of seismic wave propagation: submitted to the Spring Meeting of the American Geophysical Union, Baltimore, MD.

Liu, H.-P., Warrick, R.E., Fletcher, J.B., and Westerlund, R.E., 1987, A three-component borehole seismometer for controlled-source earthquake seismology: submitted to the Spring Meeting of the American Geophysical Union, Baltimore, MD.

Liu, H.-P., Warrick, R.E., Fletcher, J.B.., and Westerlund, R.E. 1987, A three-component borehole seismometer for controlled-source and earthquake seismology: *Seismological Research Letters*, v. 58, p. 11.

Wennerberg, L., and Frankel, A., 1987, Site response and spectra of earthquakes determined from the Anza network: *Seismological Research Letters*, v. 58, p. 25.

Figure Captions

1) Seismograms from the two downhole systems at station KNW: D01 at 1000 ft and D02 at 500 ft depths. Seismograms from seismometers installed at the surface (SUR) are also shown. Generally the downhole systems are more impulsive than than the surface system.

2) Spectral ratios between seismograms recorded at the surface and the sensor at 1000 ft depth. The ratio shows a broad amplification between about 8 and 40 Hz with sharper resonant peaks superimposed on top of the amplification.

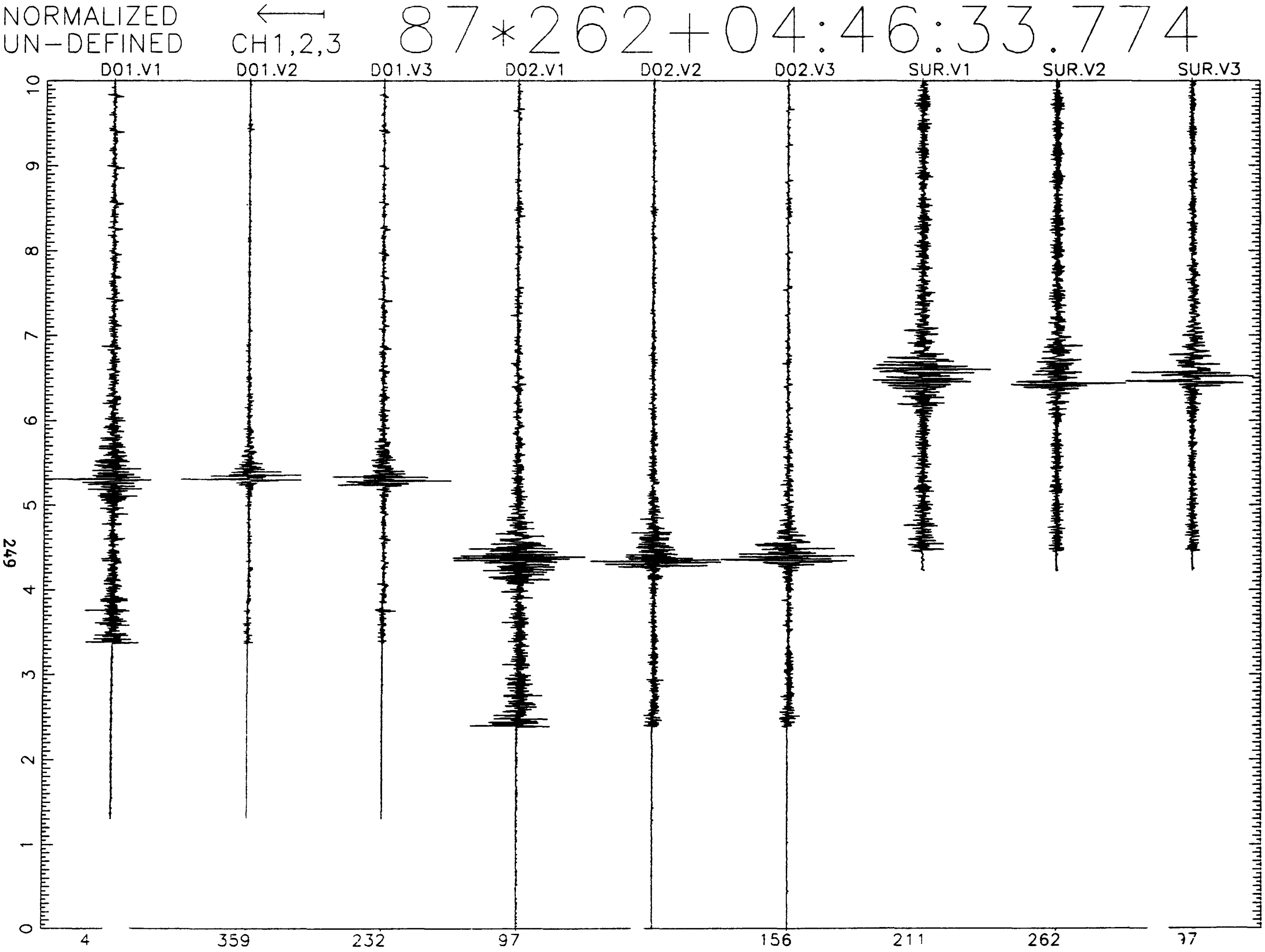
NORMALIZED
UN-DEFINED
CH1,2,3
87*262+04:46:33.774
D01.V1
D01.V2
D01.V3
D02.V1
D02.V2
D02.V3
SUR.V1
SUR.V2
SUR.V3
10
9
8
7
6
5
4
3
2
1
0
4
359
232
97
156
211
262
97

Figure 1.

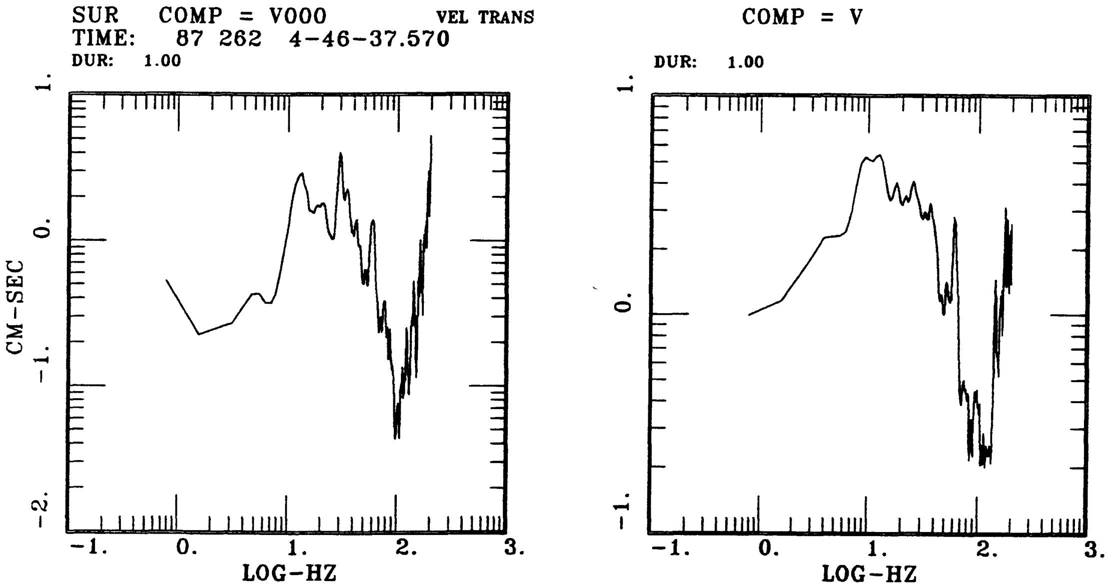

```
--------CORRECTIONS--------
WINDOW = 3
DIVIDED BY W
FILTER:  FHC = 100.00     M = 7
INSTR:   FN = 2.0000     DAMP = .70000
```

Figure 2.

Instrument Development and Quality Control

9930-01726

E. Gray Jensen
Branch of Seismology
U.S. Geological Survey
345 Middlefield Road - Mail Stop 977
Menlo Park, California 94025
(415) 329-4729

Investigations

This project supports other projects in the Office of Earthquakes, Volcanoes and Engineering by designing and developing new instrumentation and by evaluating and improving existing equipment in order to maintain high quality in the data acquired by the Office.

Results

During this period the Seismology computer area, electronics labs and offices were completely moved to temporary offices on different floors and then back to permit asbestos removal from the building. These moves were done one floor at a time in sequence. In addition to spending a lot of time moving the offices and labs themselves, a considerable effort went into accomodating the electronic changes required. Many terminal lines, communications lines, network cables and antenna leads were removed and some were later replaced. Data collection, processing and display equipment was moved or modified to accommodate the clean-up. Temporary terminals were set-up to allow work to continue.

In between these moves some normal tasks were completed. A 9600 baud modem link from Carr Hill in Parkfield to a VAX in our office via the microwave system was established. Assistance and equipment were provided to cooperative projects in Garm, USSR and Manizales, Colombia. A new 75 KVA backup power generator was installed at this office to provide power for critical data collection and processing equipment during outages. A 35 KVA uninterruptible power supply (UPS) will be installed soon to eliminate power loss during generator start-up. Personnel from this project again assisted in this year TACT refraction profiles in Alaska and in Arizona.

Purchases for new instruments for evaluation were made. Five EDA PRS-4 solid-state refraction recorders were bought and will arrive shortly. Two Nanometrics RD-3 remote seismic digitizers have also been purchased. These units will digitize and store data on site and will relay their data back to the office via packet radio. A PC-AT equivalent, which was recently acquired, which will act as the system controller and central data collector. Also acquired recently were two new computer-aided-design programs. The first is the Altera A-Plus system which permits straightforward programming of EPLD low-power programmable logic devices thus allowing us to make custom logic I.C.'s. The second is PADS PCB which is a very sophisticated printed-circuit layout program with auto-routing and direct disk-to-film output.

As usual a lot of time has been spent augmenting and maintaining the microwave telemetry network. Many CalNet, Parkfield and Yellowstone seismic stations were visited for maintenance, repair and upgrading. Also, numerous telemetry radios and seismometers were repaired, adjusted or calibrated.

Southern California Earthquake Hazard Assessment

7-9930-04072

Lucile M. Jones and Douglas D. Given
Branch of Seismology
U. S. Geological Survey
Seismological Laboratory 252-21
California Institute of Technology
Pasadena, California 91125

INVESTIGATIONS

1. Routine Processing of Southern California Network Data.

Routine processing of seismic data from stations of the cooperative southern California seismic network was continued for the period April through September 1987 in cooperation with scientists and staff from Caltech. Routine analysis includes interactive timing of phases, location of hypocenters, calculation of magnitudes and preparation of the final catalog using the CUSP analysis system. About 800 events are detected in most months with a regional magnitude completeness level of 2.0. Two backlogs, July to September 1986 created by the large number of earthquakes in the three mainshock sequences in July 1986 and October to December 1985 created during a switch in computer systems, have both been eliminated. A complete set of computer-timed locations and calibrated magnitudes now exist for 4 years from 1983 to the present. As processing time becomes available, data gaps before 1983 will be eliminated.

2. Characteristics of Earthquake Clusters in Southern California.

The properties of earthquake clusters in southern California are being analyzed. Earthquakes in the southern California catalog from 1932 to 1986 have been grouped into spatio-temporal clusters using Reasenberg's (1985) clustering algorithm. The b-values of clusters and regions have been compared to the magnitude distirbutions of the clusters and to the seismotectonic region.

3. Investigation of Southern California Earthquake Sequences.

The $M_L = 5.6$ North Palm Springs earthquake of July 8, 1986 and its aftershocks are being analyzed. Focal mechanisms are being determined for the M $\geq$3.0 aftershocks. These data are inverted for changes in the state of stress on the Banning fault caused by the earthquake. All of the aftershocks are being relocated using a master event technique. The results are compared to the geologic structures to better understand the deformation occurring along the southern San Andreas fault. The $M_L = 5.3$ Oceanside earthquake of July 8, 1986 and its aftershocks are also being analyzed. The aftershocks are being relocated and the focal mechanisms of the aftershocks determined.

4. Segmentation of the southern San Andreas fault.

The Mojave segment of the southern San Andreas fault, from Fort Tejon to Cajon Pass, and the Indio segment from Cajon Pass to the Salton Sea are near the end of their respective seismic cycles. If the segments rupture together, a more destructive great earthquake would result than if they fail separately. The slip deficit on these segments, together with the previously observed scaling of rupture length with seismic moment, are analyzed for information about segmentation of the San Andreas in future great earthquakes.

RESULTS

1. Routine Processing of Southern California Network Data.

The projects to upgrade the southern California seismic network are continuing. To increase the accessibility and research potential of the seismic data, a series of semi-annual Network Bulletins have been issued since 1985. These bulletins provide information about how to access data from the network, problems with the data, details of the processing computer systems, and earthquakes in southern California. As part of this project, documentation of past and present station configurations has been compiled. Hardware upgrades of the network have also been undertaken, including the installation of 50 new VCO's in the field for data transmission back to the central recording site. Three new six-component stations (3 high gain and 3 low gain (FBA) components) have also been installed.

2. Characteristics of Earthquake Clusters in Southern California.

The rate, sequence type and magnitude frequency distribution of earthquakes in southern California have been determined and compared to tectonic regime. Magnitude gap, the difference between the largest earthquake and the second and third largest events in a sequence, of southern California sequences forms a continuous distribution without a clear delineation between swarms and mainshock sequences. We define sequences with magnitude gap greater than 0.5 to be mainshock-aftershock sequences and find they are most common in San Jacinto and Santa Barbara. Sequences with small magnitude gaps (< 0.5) are classified as swarms and are most common in areas of high heat flow and extensional tectonics. Swarms are much more likely to have foreshocks than mainshock sequences are. Foreshocks are three times as likely to occur in extensional regimes where they precede 58% of the mainshocks than in reverse faulting regimes where only 17% of the mainshocks have foreshocks. B-values calculated for sequences in the Southern California catalog show great variability but no coherent pattern to the variation. The only obvious regional characteristic of the b-values of sequences is a cluster of very high b-value sequences in Owens Valley. No systematic relationship can be discerned between b-values and magnitude gap. Regional b-values calculated from the complete catalog show significant regional variation, with Imperial Valley having an unusually low value, and Whittier having an unusually high b-value. When regional b-values are calculated from the declustered catalog, the values are usually slightly less then the b-values from the complete catalog and less variable. Imperial Valley, San Jacinto and Santa Barbara have lower than average b-values, and Whittier, San Bernardino and Los Angeles have higher than average b-values. The variations in regional b-value are too large to be explained as random variations but are not obviously correlated with any tectonic feature. The large differences between regional and sequence b-values suggests that regional characteristics such as ambient stress or structural features cannot be determining the b-values.

3. Investigation of Southern California Earthquake Sequences.

The Oceanside mainshock occurred 55 km offshore at 32°58.2'N and 117°52.2'W, southwest of Oceanside in San Diego County. The mainshock was followed by an extensive aftershock sequence with 55 events of ($M_L \geq 3.0$) during July 1986. The preliminary epicenters of the mainshock and aftershocks are located at the northern end of the San Diego Trough-Bahia Soledad fault zone (SDT-BS). The spatial distribution of aftershock epicenters indicates a unilateral 5 - 10 km long rupture to the east away from the epicenter of the mainshock. The focal mechanism of the mainshock shows a northwest trending reverse fault.

4. Segmentation of the southern San Andreas fault.

A constant ratio of seismic moment to rupture length implies both a constant stress drop and a constant ratio between slip and length. Previously published data on rupture length and slip for strike-slip earthquakes in California have been collected and analyzed. These data show linear correlations between length and moment and between coseismic slip and length, within a factor of 1.5. This correlation predicts that a strike-slip earthquake with 4 m of average slip should rupture a length of 380 ± 130 km. Sieh has shown that the slip deficit at Indio is at least 7.5 m. Even if the average slip in the next event is only half that, the slip-length relation still requires the rupture zone to be twice the length of the 175 km long Indio segment. The slip deficit on the Mojave segment averages 3.2 - 4.5 m, also suggesting that a future earthquake could not be confined to the 175 km of the Mojave segment. Assuming coseismic slip of 4 m and fault width of 12 km, an earthquake on both segments (length = 350 km) would have a seismic moment of $\sim 5 \times 10^{27}$ dynes-cm ($M_w = 7.8$). If the slip deficit is only partially relieved in the next earthquake, then the event could be confined to an individual segment of 175 km length, with a slip of $\sim$ 2 m and a moment of $\sim 1 \times 10^{27}$ dynes-cm ($M_w = 7.3$).

5. Review of Earthquakes in Southern California.

The earthquake history and seismotectonic setting of southern California has been reviewed for the Geologic Society of America's Decade of North American Geology project. The broad plate boundary between the North America and Pacific Ocean plates in southern California produces a high level of seismic activity. Two great earthquakes of $M \simeq 8.0$ have occurred; one on the San Andreas fault in 1857 and the other in Owens Valley in 1872. Large earthquakes (M_L= 6.5–8) occur most frequently along the San Jacinto fault and in Imperial Valley. Most, but not all, $M_L \geq 6.0$ earthquakes in southern California occur on recognizable Quaternary faults. In some cases the small earthquakes form broad seismicity clusters coinciding with major Quaternary faults. Swarms of earthquakes are reported in Imperial Valley, Sierra Nevada and southern Basin and Range and Santa Barbara channel.

With the exception of parts of the San Jacinto fault, major faults that accommodate most of the plate boundary slip such as the San Andreas fault are seismically quiescent at the microseismic level during the interseismic period of the seismic cycle. Depths of earthquakes in southern California range from near the surface to depths of 10–15 km, with a few earthquakes in certain areas as deep as 20–25 km. Southern California is primarily a transform plate boundary with right-lateral strike-slip motion, although normal and reverse fault plane solutions occur throughout the region. The rate of reported seismicity is approximately 1000 earthquakes ($M_L \geq 1.0$) per month when excluding major aftershock sequences.

PUBLICATIONS

Given, D. D., L. K. Hutton, and L. M. Jones, 1987, The Southern California Network Bulletin, July - December, 1986, *U.S. Geol. Surv. Open-file Rep. 87-488.*

Jones, L.M., 1987, Focal mechanisms and the state of stress on the San Andreas fault in southern California, *J. Geophys. Res.*, in press.

Hutton, L. K., L. M. Jones, E. Hauksson, and D. D. Given, 1987, Seismotectonics of Southern California, submitted to **Tectonics of North America**, Decade of North American Geology, Geological Society of America.

Jones, L. M., and E. Hauksson, 1987, The size and locatio of the next great southern California earthquake: Implication of constant stress drops, *Trans. Amer. Geophys. U.*, in press.

Hauksson, E., and L. M. Jones, 1987, The July 1986 Oceanside earthquake sequence ($M_L = 5.3$) in the continental borderland, southern California, *Trans. Amer. Geophys. U.*, in press.

State of Stress Near Seismic Gaps

Grant No. 14-08-0001-G1356

Hiroo Kanamori
Seismological Laboratory, California Institute of Technology
Pasadena, California 91125 (818-356-6914)

Investigations

1. Large Intermediate Depth Earthquakes and the Subduction Process.
   Luciana Astiz, Thorne Lay, and Hiroo Kanamori

2. The mechanism of November 14, 1980, Hua-lien, Taiwan earthquake.
   Lorraine J. Hwang and Hiroo Kanamori

Results

1) Large Intermediate Depth Earthquakes and the Subduction Process.

Preliminary results of this study have been reported previously. We have just completed this study and the results are summarized in a paper which is in press in Physics of the Earth and Planetary Interiors. This study provides an updated overview of intermedate-depth earthquake phenomena, placing an emphasis on the larger, tectonically significant events. The historic record of both intermediate and deep focus events with $m_B \geq 7.0$ is first considered, with the spatio-temporal relationship with large interplate activity being emphasized. Then, a substantial catalog of intermediate depth (40 - 200 km) events with known focal mechanisms and $m_b \geq 6.0$ for the years 1960 to 1984 is compiled. The spatio-temporal characteristics of the 335 events in this catalog, which is probably complete for $m_b \geq 6.5$ after 1963, are discussed with regard to both static and dynamic stresses in the subducting slab. Four categories were defined: 1) Normal fault events (44%), and 2) reverse-fault events (33%), both with a strike nearly parallel to the trench axis; 3) Normal or reverse fault events with a strike significantly oblique to the trench axis (10%) and 4) tear faulting events (13%). The focal mechanisms of Type 1 events occur at the base of strongly or moderately coupled subduction zones: similar-type events occur near the trench axis in uncoupled zones. Type 2 events have near vertical tension axes and occur mainly in regions that have partially coupled or uncoupled subduction zones, and where the observed continuous seismicity extends deeper than 300 km. We advanced a simple model, in which the increased dip of the downgoing slab associated with weakly coupled subduction zones induces nearly vertical tensional stress at intermediate depth and consequently, the change in focal mechanism from Type 1 to Type 2 events. Events of Type 3 occur where the trench axis bends sharply, causing horizontal (parallel to the trench strike) extensional or compressional intraplate stress. Type 4 are hinge-faulting events associated with lateral segmentation of the subducting slab.

We have also considered the variation of focal mechanisms of moderate and large intermediate-depth earthquakes in relation to local variations of the strength of interplate coupling in a region. Temporal changes due to the occurrence of large underthrusting earthquakes were explored. Detailed regional observations of focal mechanisms of moderate and large intermediate-depth earthquakes in relation to spatial or temporal changes of the strength of interplate coupling support the idea that the subducting lithosphere acts as a stress guide.

In conclusion, this overview has confirmed the general complexity of the spatio-temporal occurrence of intermediate depth earthquakes, with slab pull forces and lateral slab deformation playing the principal role in causing the earthquake occurrence. We have presented numerous instances in which temporal variations in the level of activity or stress orientation in the intraplate environment are associated with large interplate thrust events. Given that such variations are observed for the very largest events, future investigations of all intraplate activity within the subducted slabs promise to reveal additional features of the seismic cycle.

2) The mechanism of November 14, 1986, Hua-lien, Taiwan earthquake.

The November 14, 1986 Hua-lien earthquake (filled star in Figure 1), (21h 20m 10.5s UTC, 23.901° N, 121.574° E, h=34 km, $M_s = 7.8$, NEIC) occurred near the plate juncture between the Eurasian and Philippine Sea plates. Here the boundary beteween the two plates changes from the south from a northeast trending oblique slip transform fault, the Longitudinal Valley fault (LVF), to an east-west trending thrust fault with the Philippine Sea plate subducting northward under the Eurasian plate to the north. The event was preceded by a foreshock ($m_b = 5.4$) approximately 5 seconds before the main event. Aftershocks of this event are concentrated in a small offshore region (shaded area in Figure 1) to the east of the main event. The seismicity map also shows the $m \geq 5.0$ earthquakes from 1973-1985 and the earthquake swarm of March 1986. Two other major earthquakes in this region in 1951 were accompanied by reverse oblique slip on the LVF.

The focal mechanism for the main event was determined from 45 long-period WWSSN and GDSN stations (Figure 2a). The first-motion data fix one of the nodal planes. Waveform inversion of Rayleigh and Love waves recorded by the GDSN stations over a period range of 100 to 300 sec yielded a solution which is consistent with the first motion data. The second plane is determined from the slip vector of the moment tensor solution. The first plane, dip 56°, rake 64° and strike 13°, is chosen as the fault plane. This is consistent with the orientation and dip of the LVF (Tsai et al., 1977) even thought the mechanism does not have a large component of left-lateral motion. The seismic moment of the best double couple is 1.47×10^{27} dynes-cm. Also shown are focal mechanism solutions for earthquakes in the Taiwan area during 1981-84 recorded by temporary seismic networks [after Tsai, 1986].

Amplitudes of body and surface waves from short-period vertical component WWSSN and GDSN instruments yield a magnitude of $\hat{m}_b = 6.4$ (19 stations $\sigma = .29$) and $M_s = 7.3$ (11 stations, $\sigma = .40$) from WWSSN instruments only. Note this estimate is substantially less than the reported NEIC value.

The average acceleration spectrum is computed from 7 teleseismic P-wave seismograms. We compare our results from the teleseismic study with the near-field accelerations from the SMART1 array in Lotung, approximately 79 km to the north of the event. Shown with a thick line in (Figure 2b) is the average acceleration spectra from the horizontal components SMART1 array. Shown in a thin line is the acceleration spectrum predicted for this site from the teleseismic acceleration spectrum. This predicted strong motion spectrum is approximately an order of magnitude less in amplitude than the actual strong motion. The situation of the array on an alluvial surface partly contributes to this difference.

References

Astiz, Luciana, Thorne Lay and Hiroo Kanamori, Large intermediate depth earthquakes and the subduction process, Physics of the Earth and Planetary Interiors, in press, 1988.

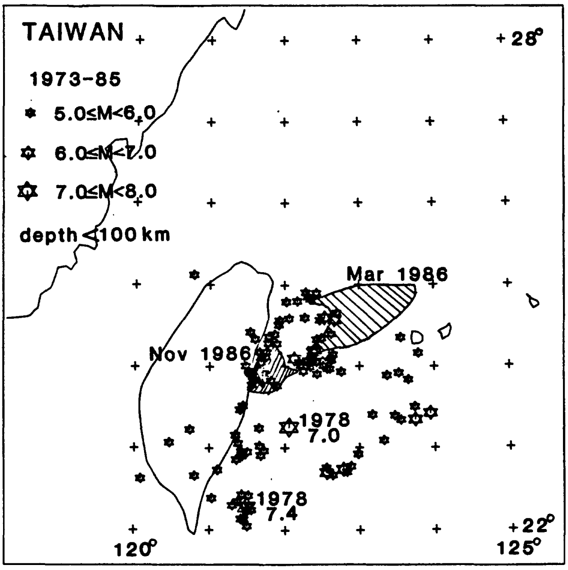

Figure 1 The epicenter of the Nov. 1986 earthquake and seismicity in the region.

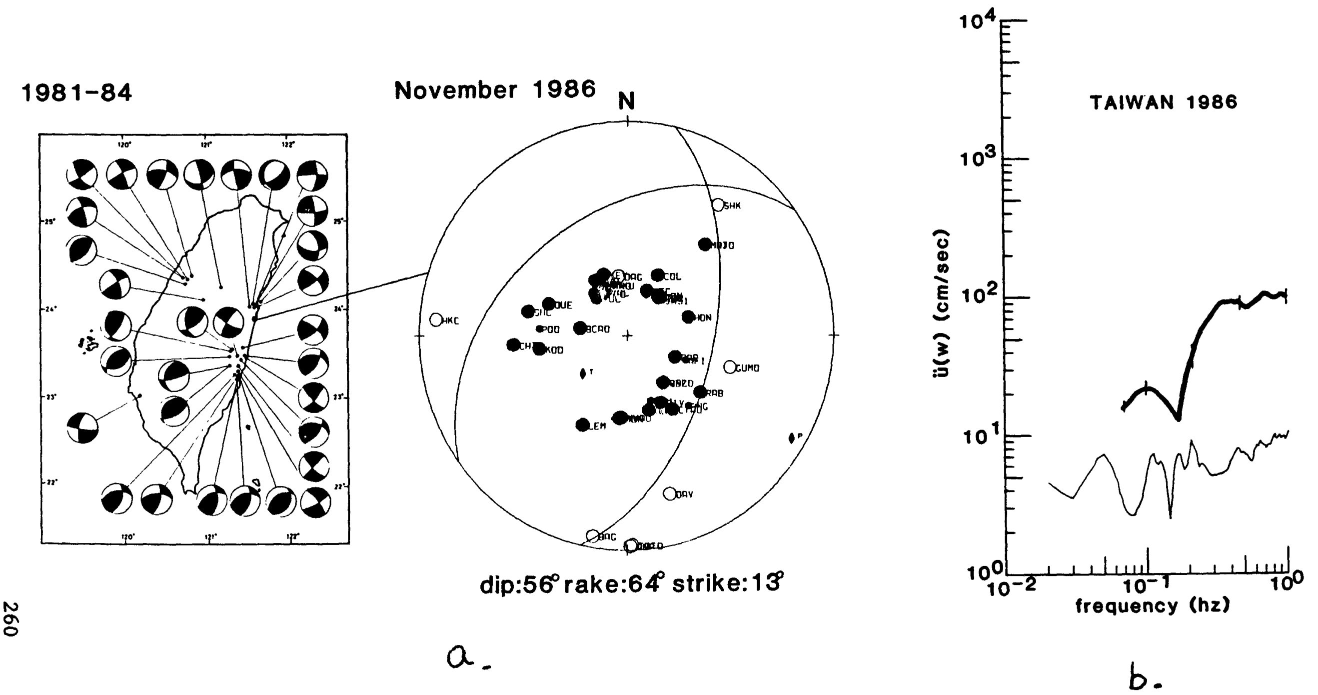

Figure 2 a) The mechanism of the Nov. 1986 earthquake. b) Comparison of the acceleration spectrum obtained from the SMART1 array data and that inferred from the far-field P-wave spectrum. The difference is due to the site response and the propagation effect.

FAULT MECHANICS AND CHEMISTRY

9960-01485

C.-Y. King
Branch of Tectonophysics
U.S. Geological Survey
345 Middlefield Road, MS/977
Menlo Park, California 94025
(415) 329-4838

Investigations

1. Water temperature and radon content were continuously monitored at three water wells in San Juan Bautista and Parkfield, California.
2. Water level was continuously recorded at six other wells.
3. Water temperature and electric conductivity were periodically measured, and water samples were taken from most of these wells and two springs in San Jose for chemical analysis.
4. Radon content of ground gas was continuously monitored at Cienega Winery, California, and at Nevada Test Site.
5. Migration pattern of historical earthquakes in California is examined.

Results

Migration of historical earthquakes in California.

Most large earthquakes of magnitude ≥ 6.0 in California during 1852-1984 as compiled by Toppozada *et* al. (1986) appear to show a south-to-north tendency of epicenter migration. This finding is consistent with earlier findings of Savage (1971) for a relatively few large earthquakes along the west coast of North America, and of Wood and Allen (1973) for smaller events along the San Andreas fault in central California. The average speed of migration is approximately 130 km/yr, which is within the range of speeds observed for other major seismic zones in the world. The epicenter migration in California may be the result of some small but broad-scaled episodic strain changes associated with creep waves induced by magma injections at the East Pacific Rise and propagating along a broad transform boundary between the Pacific and North American plates at subseismogenic depths as proposed by Savage (1971).

Reports

King, C.-Y. and Ma, Z. (1987). Migration of historical earthquakes in California (abs.): EOS (Transactions of the American Geophysical Union), in press.

King, C.-Y. (1988). Hydrological and geochemical approaches to earthquake prediction, in Proceedings of Indian Symposium on Earthquake Prediction.

CALIFORNIA AND HAWAII SEISMICITY STUDIES

Project 9930-03563

Fred W. Klein
Branch of Seismology
U.S. Geological Survey MS 977
345 Middlefield Rd.
Menlo Park CA 94025

Investigations

The overall objective is to look for long-term seismicity and tectonic patterns in the Northern California and Hawaii earthquake catalogs. The two catalogs are in very different states of self-consistency and usefulness for research, however. Accordingly, the Hawaiian work uses a completely reprocessed catalog and focuses on research. The Northern California effort presently involves cleaning up the raw phase data and developing methods for reprocessing this data into a self-consistent catalog. This reprocessing is necessary before many types of research become meaningful. The emphasis is on applying methods developed for Hawaiian processing and earthquake display to the California catalog.

The Hawaiian seismic investigation is a detailed study of the vertical magma conduit feeding Kilauea Volcano's shallow (3-7 km depth) magma reservoir. The seismically active conduit extends downward to about 55 km to the top of the magma source region.

The work on the Northern California earthquake catalog is being shared by several colleagues in the branch. This project has assumed responsibility in several areas: (1) Develop a data base of seismic stations including a new systematic set of station codes and apply it to the reprocessing of the earthquake catalog. (2) Develop a computer file system or data base for storing both raw and processed earthquake phase data. (3) Develop and modify the HYPOINVERSE earthquake location program to handle the various tasks needed for Northern California processing. These include archival storage of various data, implementation of a revised coda magnitude procedure, ability to obtain interactive locations in the CUSP processing environment, and use of regionalized crustal and station delay models. (4) Revise the QPLOT geophysical data plotting program as necessary for real-time and other display tasks needed for research, monitoring and reprocessing of seismicity data.

Results

The research on Kilauea's magma conduit suggests that the earthquakes require external sources of stress and are not simply generated by excess magma pressure, as with rift zone intrusions. Dramatic evidence for an external stress cause is the major drop in earthquake rate following the M=7.2 Kalapana earthquake in 1975. This event thus released stress in the entire volcanic system in addition to the rupture zone in Kilauea's south flank. Seismic gaps occur along the conduit centered at about 5, 13 and 20 km depths. The 3-to-7-km gap is the main magma reservoir, the 13 km gap appears to result from the layer of buried ocean sediments at the base of the volcanic pile, and the 20-km gap is present under the whole island. The latter may be a depth of low or "neutral" stress within the flexing lithosphere. Lateral extension is characteristic of the focal mechanisms within the volcanic pile (above the 13 km gap) and lateral compression occurs just below. Stresses are thus decoupled at the boundary of the volcanic pile with the underlying oceanic crust. Focal mechanisms below 20 km depth are similar to those in Kilauea's south flank and show southward motion of the upper block on a near-horizontal plane. Stresses do not reverse above and below 20 km depth, so this gap is more complex than simply a plane of neutral stress within the flexing lithosphere.

The reprocessing of the Northern California earthquake catalog is underway. Contributions from this project to date include: (1) A growing data base of seismic stations has been assembled, including assignment of unique 5-letter codes to each station ever used in our phase data. Several programs use the station data base, including one that converts all of the chaotic station codes in our phase data to the new system. (2) The HYPOINVERSE location program now uses multiple crustal and station delay models assigned to different geographic areas. The regional models developed by others have been assigned to 17 areas and are undergoing revision of models and delays. The algorithm uses a weighted average technique to combine up to three different models for epicenters near model boundaries. (3) The QPLOT plotting program has been continually revised, and now plots both maps and time-series in real-time to monitor both seismicity and the status of real-time processing.

Reports

Klein, F.W., User's guide to five VAX FORTRAN programs for manipulating HYPOINVERSE summary and archive files: SELECT, EXTRACT, SUMLIST, ARCPRINT and FORCON, U.S. Geological Survey Open File Report, 1987.

Southern California Co-Operative Seismic Network

8-9930-01174

Charles Koesterer
Branch of Seismology
525 S. Wilson Avenue
Pasadena, CA 91106

Investigations

1. Continuation of operation, maintenance, and recording of the southern California seismic network consisting of 209 U.S.G.S. short period siesmic stations and 66 other agency instruments. All of the stations are being recorded onto the CUSP analysis system and 205 stations recorded on FM tape units for back-up of digital recording.

2. Continuation of computer support for the Pasadena field office.

3. Continued provision of logistics and mangement for co-projects within the Pasadena field office.

Results

1. Operation and maintenance of field stations and office recording systems continued with little failure during this reporting period.

Tilt Measurements at Pinon Flat Observatory, California

14-08-0001-G1338

Judah Levine
Joint Institute for Laboratory Astrophysics
University of Colorado
Boulder, Colorado 80309
(303) 492 - 7785

Objective: We have installed two borehole tiltmeters at Pinon Flat observatory to investigate the coherence among tiltmeters installed at different depths. The instruments are also part of a larger group of instruments installed at the Observatory, with the long-term goal of obtaining a coherent picture of the local and regional deformation and of evaluating the utility and performance of the different kinds of instruments.

Approach: Data from our instruments are recorded both by the central Pinon Flat data acquisition system and by our own system located in the boreholes. Data from our acquisition system are transmitted every day to our analysis facility in Boulder, Colorado. Preliminary analysis techniques include estimation of the secular drift and the tidal amplitude and phase. We also examine the record for other events such as earthquakes or sudden changes in tilt or tilt rate. A more comprehensive analysis involves coherence estimates both among our data sets and between our data and the data obtained by other investigators at the site. Included in this work are estimates of the sensitivity of the instruments to various extraneous effects such as temperature, barometric pressure and rainfall.

Results: Our results to date are really just preliminary, since much of the more comprehensive analyses are still in progress. Many events, including the tilt resulting from a local drilling effort produce coherent signals on the deeper borehole instruments and the long-fluid tiltmeter, but there are discrepancies that are not easily understood. We think that these discrepancies originate from a complex interaction between secular effects, ocean loads and the classical body tide, but our analyses are far from complete, and we are unable to make a definitive statement at this time.

Plans: We are continuing to operate our two instruments and to analyze the data along the lines outlined above. We have requested funds to install a third instrument in a deeper borehole next year.

High Sensitivity Monitoring of Resistivity and Self-Potential Variations in The Palmdale and Hollister areas for Earthquake Prediction Studies

14-08-0001-G1378

Theodore R. Madden
Department of Earth, Atmospheric and Planetary Sciences
Massachusetts Institute of Technology

Due to the discontinuance of the Cal Tech data collection system, which we used on our telluric arrays in Hollister and Palmdale, we had to install our own remote data collection system. At each location the data is now digitized and stored on a hard disk. Each day's data is analyzed straightforwardly and the analysis results are sent out on a network mail system which we can access from Cambridge. These communications also serve as checks on the system clocks. At intervals of between 1 or 2 months the most recent data is copied onto a floppy disk by volunteers at the recording stations and mailed back to Cambridge for a more detailed analysis and archiving. The system could make use of better modems, as the communications do not always come through, but at present we do not have funds for such improvements. Otherwise the systems are performing quite satisfactorally.

We have just received our latest data from Palmdale which is of special interest because of the Whittier earthquake on October 1. The data is unusually noisy, but we haven't had the chance yet to try and determine if this noise is earth-produced or due to telephone line problems. The relative dipole amplitudes show large fluctuations, especially so for the Azusa-Sunland dipole. The data coherencies are at a level where we usually discard the data, but the correlations in the analysis results and the timing of the relative telluric amplitude changes with respect to the Whittier earthquake lead us to conclude we must take a careful look at this data. Figure 2 shows this data which has been smoothed by running averages weighted inversely by the data noise variances. The dipole locations are shown in figure 1. Channel G records a dipole made up of the closure of the two reference dipoles and is thus a check on the reference dipole amplifiers and the digitizer.

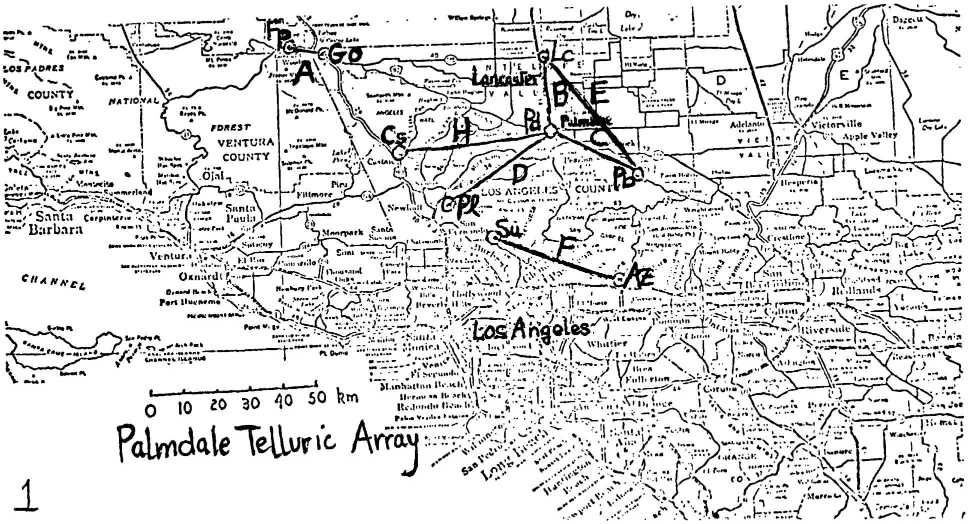

Palmdale Telluric Array

Fig 1

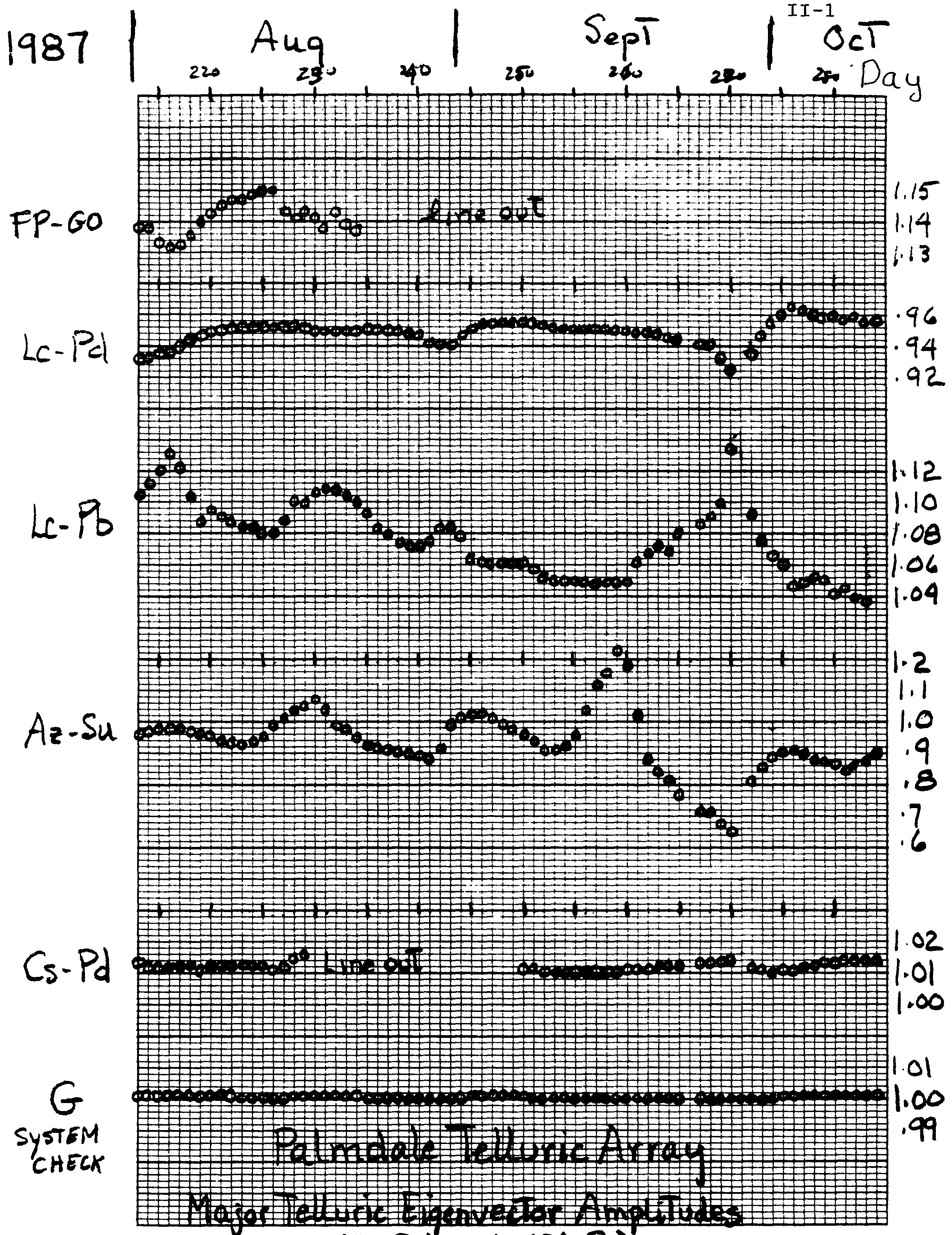

Palmdale Telluric Array

Major Telluric Eigenvector Amplitudes

using (Pb-Pd) and (Pl-Pd) references

Fig 2

MAGNETIC FIELD OBSERVATIONS

9960-03814

R. J. Mueller
Branch of Tectonophysics
U.S. Geological Survey
345 Middlefield Road, MS/977
Menlo Park, CA 94025
(415) 329-4857

INVESTIGATIONS

1) Investigation of total field magnetic intensity measurements and their relation to seismicity and strain observations along active faults in central and southern California.

2) Recording and processing of synchronous 10 minute magnetic field data and maintenance of the 12 station telemetered magnetometer network.

RESULTS

1. Routine processing and monitoring of differential magnetic field data in an effort to identify local anomalies. Data are monitored daily with particular attention to the seven stations operating in the Parkfield region of central California.

2. Assistance was given with installations of two tensor strainmeters in the Parkfield region.

3. Equipment was retrieved from two magnetometer stations which were shut down during this reporting period.

4. Processing and analysis of differential magnetic field data from networks near the northern end of the Red River fault in Yunnan Province, China and near Beijing, China was completed.

5. A lake level monitoring experiment, designed for measuring surface tilt, located at Crowley Lake was modified. The sample interval was changed from 10 minutes to 20 minutes and three of the four sensors now have differential pressure transducers rather than absolute.

6. Satellite telemetry was installed at a well near Lookout Mtn. in the Long Valley caldera. Water level and atmospheric pressure are being recorded.

7. A large portion of time and effort was spent this recording period with transferring software and data from the Unix44 computer system to the new Lowfreq IS machine. Presently, magnetic field data is being processed on both machines.

REPORTS

Mueller, R.J. and M.J.S. Johnston, Large-Scale Magnetic Field Perturbations Arising from the May 18, 1980, Eruption from Mount St. Helens (abs.) IUGG, Vancouver, Canada, August 1987.

Mueller, R.J., and M.J.S. Johnston, Seismomagnetic Observations During the July 8, 1986, Magnitude 5.9, North Palm Springs Earthquake in Southern California, Science, vol. 237, pp. 1201-1203, 1987.

"Variations in Electrical Properties Induced by Stress Along the San Andreas Fault at Parkfield, California"

USGS Grant No. 14-08-0001-G1357

Stephen K. Park and Tien-Chang Lee
Institute of Geophysics and Planetary Physics
University of California
Riverside, CA 92521
(714) 787-3438

Introduction

We have designed an experiment to monitor variations in resistivity at Parkfield. We will monitor telluric currents and look for relative changes of resistivity within our array. The mechanism producing earthquakes in Parkfield seems to be repeatable both in time and location, so we have positioned our array over the region most likely to deform. We use short (5 km) dipoles and try to look at smaller volumes of the crust than in previous experiments. In this sense, our experiment is focused on a specific segment of the San Andreas fault.

Field Survey

Our array will detect changes of the earth's response to telluric currents. These changes are proportional to, but not equal to, changes in the earth's resistivity. We must have an electrical model of Parkfield in order to determine what changes in resistivity caused the observed changes in the earth's response. We have now completed an electrical survey of the region which utilized DC resistivity, telluric, and magnetotelluric methods. Processing of the data is almost completed. Examination of preliminary results shows that the ocean exerts a major influence on electrical currents flowing in Parkfield. Most of the current flows in a southwesterly direction across the San Andreas fault. Our monitoring array will thus be sensitive to changes within the fault zone because the current flows through it. In particular, our dipole straddling Middle Mountain (Figure 1 - northwestern dipole) will be sensitive to changes in the hypocentral region.

Monitoring Array

Electrodes and electronics have been complete and installed in Parkfield since July. However, we still do not have the telephone lines needed to connect the electrodes to the electronics. The array is shown in Figure 1, and these locations are final. The telephone company is currently laying the cable between Halliburton Ranch and the switch office in Parkfield. The anticipated date for completion is in early November, and our array will come on line immediately after that. We cannot use RF telemetry because we must measure voltage differences between our electrodes. The telephone lines themselves are our dipoles for picking up telluric signals.

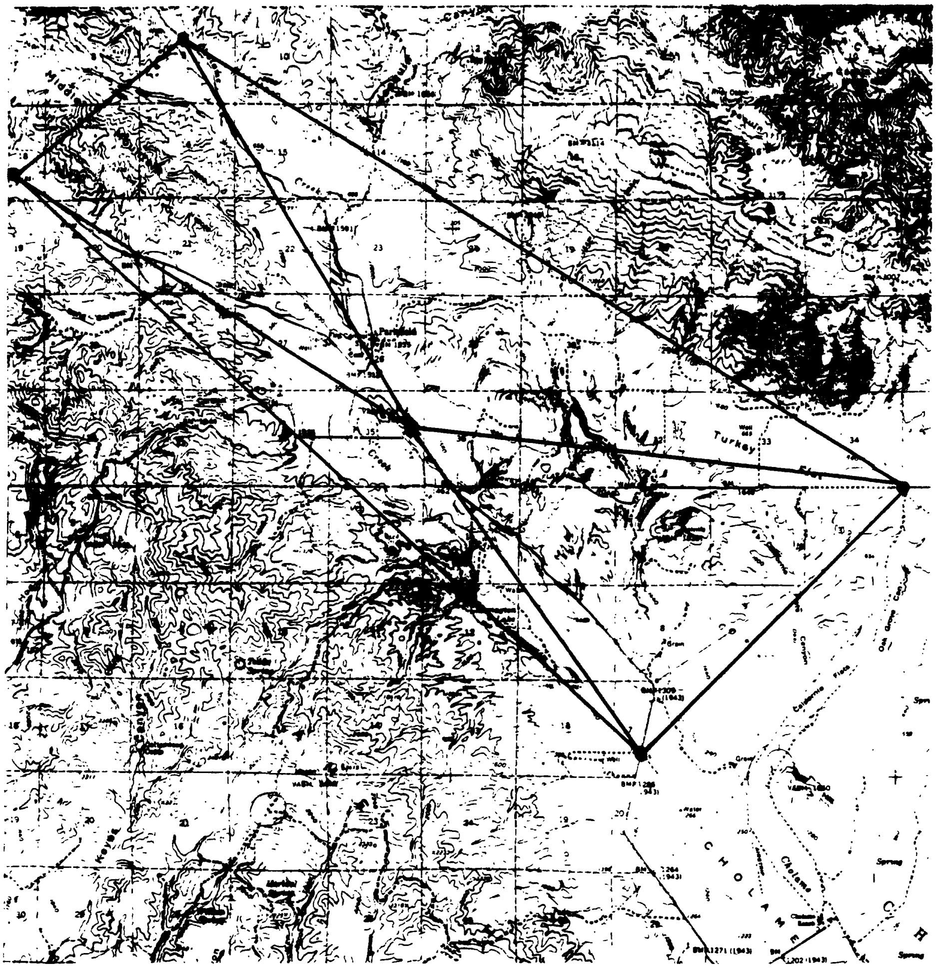

Figure 1 - Map showing locations of electrodes (solid dots) and telluric dipoles (heavy lines). Town of Parkfield is one mile northeast of center of array. (map from USGS 15' quadrangle)

CRUSTAL STRAIN

9960-01187

W.H. Prescott, J.C. Savage, M. Lisowski
Branch of Tectonophysics
U.S. Geological Survey
345 Middlefield Road, MS/977
Menlo Park, California 94025
(415) 329-4860

Repeated Global Positioning System Measurements near Parkfield, California

Since the beginning of 1986, we have observed the relative positions of four stations in the vicinity of Parkfield, California with TI-4100 Global Positioning System receivers. Four vectors have been observed more than 10 times and one has twice that many observations since it is observed twice each survey. The repeatability of these observations has been estimated from the misfit to a straight line. The one sigma uncertainty is 1.0 ppm in the east component, 0.7 ppm in the north component and 1.8 ppm in the vertical. Since these lines range in length from 5 to 11 km, the uncertainty in the worst component is only 2 cm and in the better components of the shorter lines the precision is a few mm. This precision is sufficient that even with less than two years of data it is possible to detect fault motion. The northernmost line crosses the San Andreas fault at Middle Mountain, near the epicenter of the 1966 earthquake. This line has been lengthening at a rate of +13.4 mm/yr. Two other fault crossing lines have rates of +9.8 mm/yr and -9.7 mm/yr. The two non-fault crossing lines have rates of 2 mm/yr and -3.3 mm/yr. One sigma uncertainties in all of the rates are about 5 mm/yr. All rates are consistent with right-lateral motion of 10-15 mm/yr on the San Andreas fault. In addition to the rates inferred from the changes in the lengths of the lines between the GPS stations, there is additional information in the individual components of the relative station positions. No significant changes have been detected in the vertical components. Because of the predominantly strike slip nature of the fault, a smaller signal is expected in this direction and the higher noise level makes the data less sensitive in this direction, so the absence of a detectable vertical change is not surprising.

Repeatability of Global Positioning System Observation

Since October 1985 the U.S. Geological Survey has made repeated Global Positioning System measurements of the 43 km long line Allison to LP1 located in central California. Between October 1985 and October 1986 the only source of orbit data came from the Department of Defense, either the **broadcast** orbits or orbits calculated at the Naval Surface Weapons Center in Dahlgren, Virginia. Based on this first year of observation, the standard deviation of line length as estimated from repeatability is 0.7 ppm. Since October 1986, the University of Texas has coordinated a satellite tracking effort involving stations at Westford, Massachusetts, Austin, Texas, and Mojave, California. During the time-span covered by this tracking effort there have been monthly observations of the Allison-LP1 line. This line is well suited to such a test for two reasons: it was observed over 20 times during the first year and has been observed more often than monthly since the improved tracking has been available; and secondly the length of this line is known independently to a precision of 0.2 ppm from early 100 Geodolite measurements. Preliminary analysis of the Allison-LP1 line using these three sources for satellite orbit information suggest that there is no discernible difference between the orbit sources. The three produce results that are highly correlated. At the present time all three orbits, broadcast, Dahlgren and Texas, are computed using pseudo-range tracking with TI-4100 receivers. The next step is to repeat the experiment using carrier-phase-determined orbits.

Absence of Significant Deformation in the Shumagin Seismic Gap, Southwest Alaska, 1980-1987

Precise surveys in 1980, 1981, 1983, 1985, and 1987 of a trilateration network that extends along the Shumagin Islands from the Alaska Peninsula to within 120 km from the trench show no significant deformation except for an arcward motion of about 5 ± 2 mm/yr at Simeonof Island, one of the outermost stations in the network. These measurements place an upper limit on the contraction perpendicular to the arc of about 0.04 µstrain/yr (95% confidence level), somewhat less than would be expected from simple dislocation models of subduction (0.1 µstrain/yr) or comparison with measured contraction at comparable subduction zones in Japan (0.3 µstrain/yr). Although other explanations may be available, the lack of strain accumulation in the Shumagin Islands is most readily explained if the main thrust zone, or at least the shallow main thrust zone, is slipping continuously (i.e., fault creep). The arcward motion of Simeonof Island would then be attributed to a local locked patch on the main thrust zone.

Principal Mode Analysis of 1983-1987 Geodetic Deformation Data from the Long Valley Caldera, Eastern California

Deformation can be interpreted as a consequence of one or more generalized coherent sources by means of principal component analysis (see factor analysis in Menke, Geophysical Data Analysis, 1984). By a generalized coherent source we mean any source that produces deformation that is time and space separable. Principal component analysis then gives the time and space factors that characterize each generalized coherent source. We consider as an example the geodetic measurements of deformation at Long Valley caldera in eastern California. A 40-line trilateration network surrounding the caldera was surveyed in midsummer 1983, 1984, 1985, 1986, and 1987. Principal component analysis indicates that the deformation can be represented by a single generalized coherent source. The time dependence for that source indicates uniform deformation in the 1984-1987 interval following a more rapid rate of deformation in 1983-1984. The spatial factor seems consistent with expansion of a magma chamber beneath the caldera accompanied by some right-lateral slip on the south moat fault. An independent principal component analysis of the 1983, 1984, 1985, and 1986 leveling surveys across the caldera is consistent with the analysis of trilateration data.

Resurvey of the Ogden (Utah), Hebgen Lake (Montana), and Yellowstone (Wyoming) Trilateration Networks

Three Geodolite networks in the northern Rocky Mountains were resurveyed in late summer 1987. Earlier surveys of the Ogden and Hebgen networks were described in Journ. Geophys. Res., 90, pp. 10310-10320, 1985, and the current surveys are on the trends previously established. That is, no significant strain accumulation has been detected in the Ogden network over the 1972-1987 interval, whereas a near-uniaxial extension rate of 0.25 ± 0.02 μstrain/yr N14°E ± 2° for the 1973-1987 interval has been observed in the Hebgen network. The strain rate at Hebgen Lake is consistent with continued extension across the fault system activated in the 1959 earthquakes. The Yellowstone network, which spans the Sour Creek resurgent dome in the Yellowstone caldera, has been surveyed in 1984, 1985, and 1987 in conjunction with leveling run across the caldera by the Cascades Volcano Observatory. The principal strain rates for the 1984-1987 interval are 0.10 ± 0.09 μstrain/yr N33°E ± 9° and -0.20 ± 0.09 N57°W ± 9° (extension reckoned positive). The significant deformation seems to be a contraction perpendicular to the long axis of the caldera.

Faulting Mechanism for the 1986 Chalfant Valley Earthquake (M_L=6.4)

Gross and Savage (Bull. Seismol. Soc. Am., v. 77, pp. 306-310, 1987) found the mechanism of the Chalfant Valley earthquake most consistent with the observed deformation of a precise trilateration network in the epicentral area involved 1.3 m right slip and 0.7 m normal slip on a 15-km-long buried fault dipping 50°S55°W. The inclusion of normal slip on the fault was not supported by most nodal-plane solutions for that earthquake. Postearthquake leveling by the National Geodetic Survey along Highway 6 north of Bishop shows only minor subsidence and uplift (±30 mm) in the epicentral area of the Chalfant Valley earthquakes. Those observations are not consistent with appreciable normal slip on the earthquake fault. A revised dislocation model that fits both the trilateration and leveling data involves 0.6 m right-lateral slip on the 15-km-long buried fault dipping 50°S55°W tht contains the hypocenter of the main shock and 0.8 m left-lateral slip on a near-vertical 7-km-long conjugate fault that passes through the epicenter of the M_L=5.7 foreshock.

Velocity Field Along the San Andreas Fault

The distribution of deformation across the San Andreas fault is inferred from the average rate of distance change between stations in trilateration networks that span the fault. Because the networks are not tied to an external coordinate system, rigid-body motions of the network are undetermined. We resolve this ambiguity by selecting the rigid body motion of the network as a whole that minimizes the rms velocity component perpendicular to a preselected direction (the so-called outer coordinate solution). Shown in Figure 1 is an N39°W outer coordinate velocity solution across the Salton Trough and Peninsular Ranges using data from the Salton, Anza, and Joshua networks. The station velocities are parallel to the local strikes of the San Andreas and San Jacinto faults with the zone of deformation becoming wider to the northwest. Shown in Figure 2 is a N65°W outer coordinate velocity solution across the Transverse Ranges using data from the Los Padres, Tehachipi, Palmdale, and San Gabriel networks. The station velocities parallel the local strike of the San Andreas. The velocity field for a N39°W outer coordinate solution is nearly identical. Shown in Figure 3 is a N33°W outer coordinate velocity solution for the San Francisco Bay Area. Relative station velocities parallel the local strikes of the San Andreas, Hayward, and Calaveras faults. Profiles show fault parallel relative velocity of 28 ± 3 mm/yr between end stations in the northern part of the network (Figure 4a) and 39 ± 3 mm/yr between end stations in the southern part of the network (Figure 4b). No significant contraction across the San Andreas or related faults is observed in any of the areas studied.

Deformation Near Cape Mendocino

Repeated geodetic surveys near the northern end of the San Andreas fault show relatively rapid deformation near the coast that decreases inland. Coseismic angle changes indicate the 1906 earthquake rupture is southwest of mountain peaks located 2 to 5 km from the coast line. The observed coseismic deformation is consistent with about 6 m of slip on a 0–10 km deep rupture surface. Repeated trilateration surveys from 1981 to 1984 of a network that extends from 40°00'N to 40°40'N and from 123°15'W indicate an average shear strain rate $\dot{\gamma} = 0.35 \pm 0.05$ zμrad/yr with the direction of maximum right-lateral shear ψ = N38°W ± 4°. This strain accumulation is similar to that observed in the same area in the intervals 1928–1942 and 1942–1981. Spatially varying strain was observed in the trilateration network: within 25 km of the coast $\dot{\gamma} = 0.47 \pm 0.08$ μstrain/yr and c = N45°W; 25 to 65 km from the coast $\dot{\gamma} = 0.32 \pm 0.07$ μstrain/yr and ψ = N32°W ± 5°; and in the part of the network north of the Mendocino triple junction $\dot{\gamma} = 0.21 \pm 0.08$ μstrain/yr and ψ = N23°W ± 13°.

Strain Accumulation in Northwestern Washington

Strain accumulation within a triangulation-GPS network that spans the Strait of Juan de Fuca has been redetermined using the method of simultaneous reduction for position and strain. Average strain rates and their uncertainties using this method are slightly lower than those estimated with Frank's method (reported in April 1987 summary). The new strain rates are summarized in Table 1. Significant strain accumulation with the direction of maximum contraction approximately parallel to the direction of convergence of the Juan de Fuca plate with the North American plate is observed within the network.

Table 1. Juan de Fuca Shear Strain Accumulation

Interval	$\dot{\gamma}_1$	$\dot{\gamma}_2$	$\dot{\gamma}$	β*	σ_o†
1892–1986	−0.13±0.05	−0.12±0.05	0.18±0.05	N69°E±8	0.99
1921–1986	−0.13±0.06	−0.04±0.04	0.14±0.06	N81°E±9	0.99
1942–1986					
All	−0.04±0.02	−0.04±0.02	0.08±0.02	N77°E±7	1.28
West	0.01±0.05	−0.07±0.04	0.07±0.04	N47°E±20	1.09
West Cent.	−0.09±0.07	−0.08±0.06	0.12±0.05	N67°E±17	1.12
East Cent.	−0.12±0.04	−0.04±0.03	0.13±0.04	N81°E± 7	1.33
East	−0.06±0.05	0.03±0.04	0.06±0.05	N76°W±21	0.98
1954–1986					
West	0.05±0.04	0.01±0.05	0.05±0.04	N 1°W±27	1.23

* β is the bearing of the axis of maximum contraction
σ_o is the rms of the normalized residuals

Reports

Savage, J.C., Effect of crustal layering upon dislocation modeling, *J. Geophys. Res.*, 92, 10595-10600, 1987.

Savage, J.C., and R.S. Cockerham, Quasi-periodic occurrence of earthquakes in the 1978-1986 Bishop-Mammoth Lakes sequence, eastern California, *Bull. Seismol. Soc. Am.*, 77, 1347-1358, 1987.

Savage, J.C., W.H. Prescott, and M. Lisowski, Deformation along the San Andreas fault 1982-1986 as indicated by frequent Geodolite measurements, *J. Geophys. Res.*, 92, 4785-4797, 1987.

Thatcher, W., and M. Lisowski, Long-term seismic potential of the San Andreas fault southeast of San Francisco, California, *J. Geophys. Res.*, 92, 4771-4784, 1987.

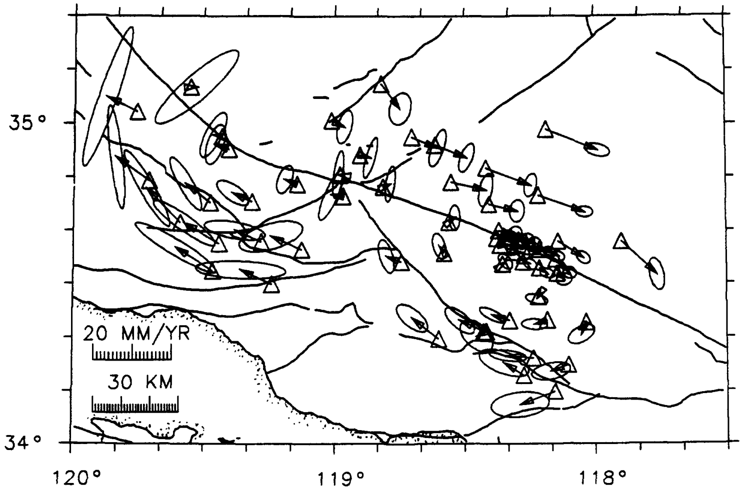

Figure 1. Velocity field inferred from surveys of trilateration networks in the central and western Transverse Ranges in the interval 1973–1986. The important faults are shown by the sinuous lines. The 95% confidence ellipse is shown at the end of each velocity vector.

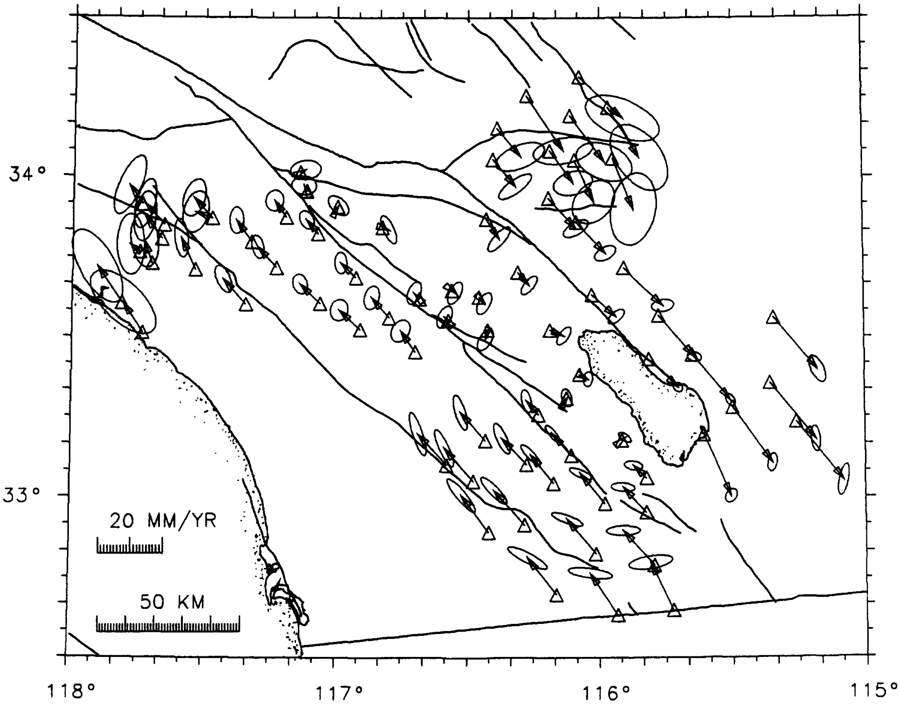

Figure 2. Velocity field inferred from surveys of trilateration networks that span the Salton Trough and Peninsular Ranges in the interval 1972–1987. The important faults are shown by the sinuous lines.

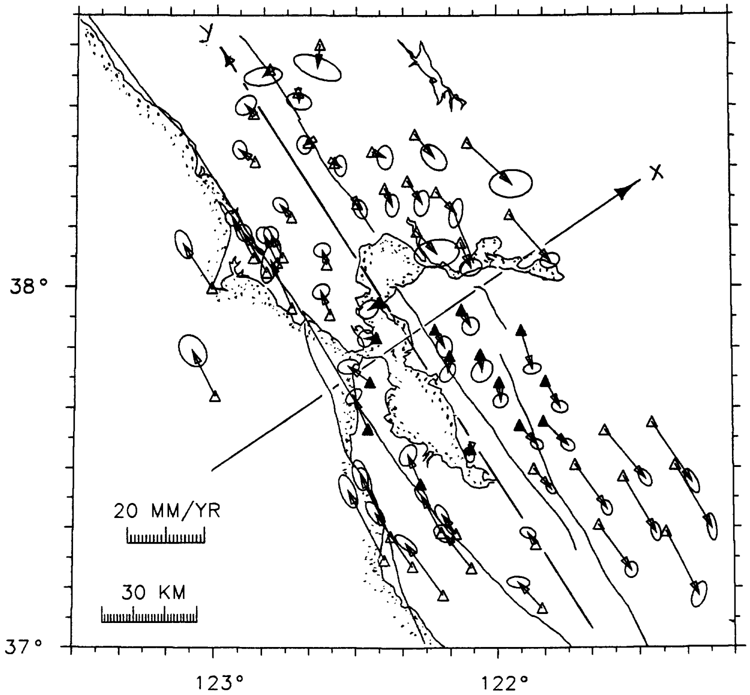

Figure 3. Velocity field inferred from trilateration surveys in the San Francisco Bay Area in the interval 1972–1984. A coordinate system with the y axis trending N33°W and origin near the center of the network are also shown. The network has been divided into northern, central, and southern parts, with the central stations shown by solid triangles. The important faults are shown by the sinuous lines. Velocity vectors are tipped with a 95% confidence ellipse.

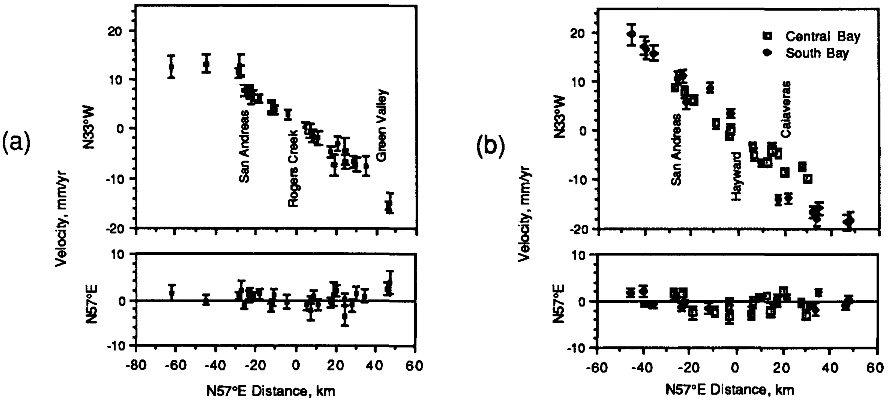

Figure 4. The x (lower) and y (upper) components of station velocity in the San Francisco Bay Area as a function of x. The coordinate system is shown in Figure 3. Velocities of stations in the northern part are shown in (a) and those of stations in the central and southern parts are shown in (b).

Seismic Studies of Fault Mechanics

9930-02103

Paul A. Reasenberg
Mark V. Matthews

Branch of Seismology
United States Geological Survey
345 Middlefield Road - MS 977
Menlo Park, California 94025
415-329-5002

Investigations

1. Analysis of fault-plane solutions of aftershocks of the M6.2 Morgan Hill, Ca., earthquake of April 24, 1984, and modeling of the regional stress field.
2. Investigation of the temporal and spatial variations in seismicity rate in the Kaoiki Seismic Zone, Hawaii, prior to the M 6.6 earthquake of November 16, 1983.

Results

1. This investigation is a collaboration among myself, David Oppenheimer and Robert Simpson. We have submitted a manuscript describing our findings to J.G.R. Fault-plane solutions for 946 aftershocks of the April 24, 1984 Morgan Hill, California M6.2 earthquake reveal a pattern of complex faulting within a 10-km-wide zone surrounding the Calaveras fault. The fault-plane solutions fall naturally into three groups: strike-slip mechanisms with vertical, north-northwest-striking dextral slip planes located along the Calaveras fault; strike-slip mechanisms with vertical, north-striking dextral slip planes located northeast of the Calaveras fault; and northwest-striking reverse mechanisms located southwest of the Calaveras fault.

   The average azimuth of P-axes for aftershocks located on the Calaveras fault is N10 ± 8°E. In contrast, the average orientations of P-axes for aftershocks northeast and southwest of the Calaveras fault are horizontal with azimuths N49 ± 13°E and N37 ± 11°E, respectively. By assuming that the earthquakes occur on pre-existing cracks, and that the stress field is uniform over the region, we infer from the observed slip directions that the direction of maximum horizontal compression is oriented approximately 80° from the local strike of the Calaveras fault.

   The combination of this inferred ambient stress field and changes in static stress field calculated for the 1984 mainshock offset successfully explains observed patterns in the spatial distribution of the aftershocks and orientation of their fault-plane solutions. Areas in which the Coulomb failure function increased by only a few tenths MPa correspond well to areas of intense aftershock activity. The calculated stress orientations agree with aftershock fault-plane solutions, except for the reverse mechanisms near Anderson Lake. Addition to the model of the static stress field change inferred for the 1979 Coyote Lake offset predicts these mechanisms as well.

A conceptual model to explain how fault-normal stress may arise near the Pacific-North American plate boundary consists of a vertical fault locked above the base of the seismogenic zone and slipping freely below in response to uniform right-lateral shear stress imposed on it. Slip on the lower fault surface effectively cancels the applied shear stress over most of the halfspace, but imposes large crack-tip shear stresses on the base of the seismogenic zone. When the applied shear is oblique to the fault, the resulting three-dimensional stress field includes fault-normal compression at seismogenic depth. This compressive stress may, in turn, contribute to the development of deformational features such as folds, reverse faults, and perhaps, the Coast Ranges.

2. This project is a collaboration with Max Wyss. An important factor in the analysis of seismicty rate fluctuations is the influence on the apparent rate imposed by man-made changes in the collection and processing of data for the catalog. Such artifacts are known to be significant in some cases. An analysis of apparent rate changes in the HVO catalog suspected of having artificial origin was made (by M.W.) We have developed a new software tool for the analysis of the spatial distribution of seismicity rate fluctuations analogous to the beta statistic for describing the temporal variations in seismicity rate (Matthews and Reasenberg, 1988). With this tool we are able to investigate, with resolution appropriate to the data, the three-dimensional spatial distribution of seismicity rate fluctuations identified in the time domain. Application of this technique to the Kaoiki Seismic Zone reveals significant differences in location, relative to the mainshock hypocenter, of identified episodes of extreme seismicity rate.

Reports

Oppenheimer, D. H., P. Reasenberg, and R. W. Simpson, Fault-plane solutions for the 1984 Morgan Hill, California earthquake sequence: Evidence for the state of stress on the Calaveras Fault, *submitted to* J. Geophys. Res., 64 pp.

Oppenheimer, D. H., and P. Reasenberg, 1987, Analysis of fault plane solutions for aftershocks of the M6.2 Morgan Hill, California earthquake, EOS, Tran. Am. Geophys. Union, 68, p. 362.

Zoback, M.D., M.L. Zoback, V.S. Mount, J.P. Eaton, J.H. Healy, D. Oppenheimer, P. Reasenberg, L. Jones, C.B. Raleigh, O. Scotti, and C. Wentworth, New evidence on the state of stress on the San Andreas Fault System, *submitted to* Science.

Matthews, M.V., and P.A. Reasenberg, Statistical methods for investigating quiescence and other temporal seismicity patterns, Pure and Applied Geophysics, *in press.*

Hydrogen Monitoring

9980-02773

Motoaki Sato and Susan Russell-Robinson
Branch of Igneous and Geothermal Processes
U.S. Geological Survey, MS/959, Reston, VA 22092
(703) 648-6766 (FTS 959-6766)

Investigations

Hydrogen (H_2) in soil along the San Andreas and Calaveras faults is continuously monitored at 5 sites in the Hollister area and 6 sites in the Parkfield area by using fuel-cell sensors and the data are telemetered to Menlo Park, CA. Goals are (1) to accumulate valid data, (2) to find patterns of correlation of the H_2 data with seismic data, (3) to understand the tectonic mechanism of H_2 emission along active faults, and (4) to constantly improve the monitoring method.

Results

Hollister Area:

The H_2 records are compiled into a composite plot shown in Fig. 1. In spite of the fact that there were no earthquakes of magnitudes greater than 4.0 in central California during the reporting period (Apr.- Oct. 1987), a 450-ppm peak occurred at Melendy Ranch (H2MR) on May 11. The level of H_2 remained high (confirmed in the field on May 16) for about a month. This was noteworthy because the event was the first unambiguous anomaly ever recorded at this site in its 6-year history. Although the H_2 anomaly was of moderate magnitude, it was not followed by an earthquake of a significant magnitude within 150 km and within a few months. The H_2 event, however, was preceded by a discrete 1-mm right-lateral creep two days earlier at this site. Morever, there was no rain in the preceding 10 days in the region, excluding the possibility of rain-induced creep and H_2 emission, which have occasionally been observed at Shore Road on the Calaveras fault. There may have been a deep crustal movement of some sort beneath this site, because this site did not respond to shallow (< 5 km) Stone Canyon earthquakes of 1986 in spite of its proximity to the epicenters.

Shore Road (H2SH) remained eventless throughout the period.

Wright Road (H2WR) had ended the broad elevated H_2 signal by the end of April. We are still uncertain as to whether the broad rise in the winter months was a natural H_2 increase related to a high regional stress during these months, which resulted in the M=5.0 Coalinga earthquake of March 14, or an artifact of cold temperature affecting the above-ground electronics vault. It must be remembered that this site responded to the Kettleman Hills earthquake of 1985 in spite of the long distance. We anticipate determining this by next spring.

San Juan Bautista (H2SJ) seems to have telemetry receiver problem. The signal became wild on April 13 and then became identical with the XSJ2 creepmeter record. Field checks in May and August of the sensor system and the transmitter confirmed no abnormalities. This suggests that the receiving end had been miswired, possibly during the asbestos removal operation in Building 8, USGS, Menlo Park, CA.

Cienega Winery (H2CW) recorded a 300-ppm peak on Aug. 10-12. This peak was not an artifact of telemetry nor rain. A barely recognizable peak (20 ppm) occurred at Melendy Ranch on Aug. 13-14. A 2-mm right-lateral creep was recorded at San Juan Bautista (XSJ2) on Aug. 16. We regret that the San Juan Bautista H_2 record, which might have shown a corresponding anomaly, was lost in the telemetry circuit somewhere. At any rate, there seems to be an inkling of a renewed tectonic activity in this segment of the San Andreas fault.

Parkfield Area:

The H_2 activities in this segment of the San Andreas fault were relatively low, particularly since late May, as shown in Fig. 2. There were some changes at Gold Hill (H2GH), Parkfield (H2PK), and Twisselman Ranch (H2TW) in April and early May. These changes appear to be the tail end of the activities that began in late September 1986 in this area (see USGS Open-File Report 87-374, p. 286).

There were no noteworthy changes recorded at Slack Canyon (H2SC), Middle Mountain (H2MM and H2M2), and Work Ranch (H2WK). Telemetry record for Twisselman Ranch has gone astray between May 1 and Aug. 7 somewhere in the telemetry circuit.

Forthcoming Project:

We are planning to install two geochemical well-water monitoring sites on the San Andreas fault as a part of the Parkfield Experiment. One of the well has already been drilled at Carr Hill (adjacent to the 2-color laser geodimeter station). This is a joint venture with Chi-Yu King, USGS, who will monitor radon. Initially, we will monitor CO_2, H_2, and conductivity. The sensors are state-of-the-art products characterized by low frequencies of field maintenance. At a later time, we hope to add methane, helium, hydrogen sulfide, and pH monitors to the new sites.

Publications:

An abstract has been submitted to the 1987 Fall AGU meeting on H_2 monitoring in the Parkfield area.

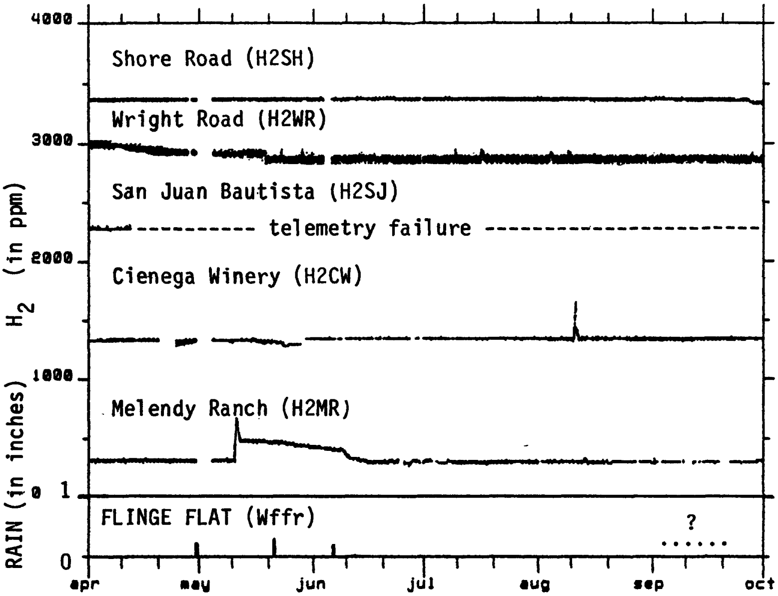

1987

FIGURE 1. Composite plot of hydrogen data for the northern segment of the instrumented portion of the San Andreas Fault and the instrumented portion of the Calaveras Fault. The hydrogen records are plotted on a relative scale in ppm. A 450-ppm peak was detected at Melendy Ranch on May 11. A 300-ppm peak was recorded at Cienega Winery between August 10-12. This peak was followed by a 20-ppm peak at Melendy Ranch on August 13-14. Rainfall data are given for the Flinge Flat site, which is in the Parkfield area. The dotted line indicates less than 0.2 inches of rain fell between September 2 and 21. There is no correspondence between the rainfall activity in this region and the H_2 increases.

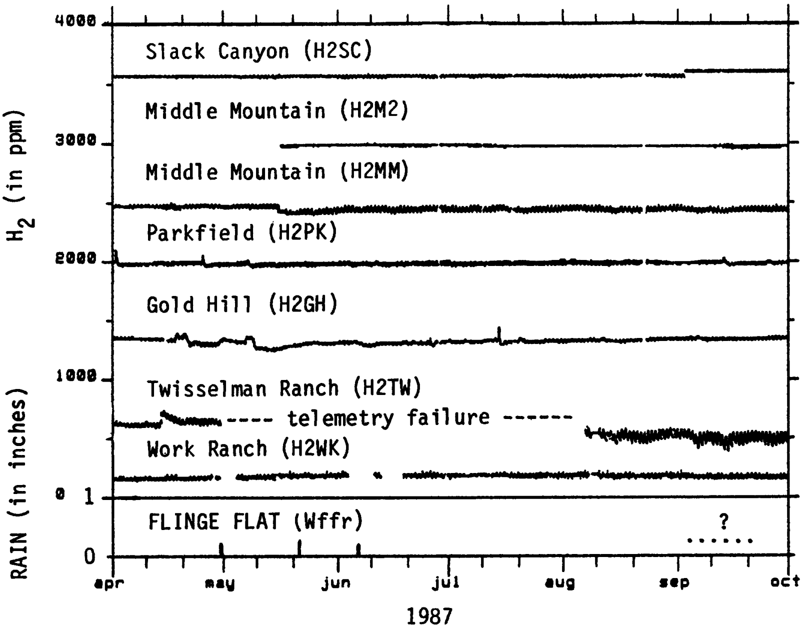

FIGURE 2. Composite plot of the hydrogen data for the instrumented portion of the San Andreas Fault defined as the Parkfield area. The hydrogen records have been plotted on a relative scale in ppm. There were minor changes at Gold Hill, Parkfield and Twisselman during April and early May. The second sensor at Middle Mountain was reinstalled in mid-May and the hydrogen record is very similar to that of the first sensor (H2MM) at that site. Rainfall data are given for the Flinge Flat site in inches. The dotted line indicates less than 0.2 inches of rain fell in this area between September 2 and 21. There is no correspondence between rainfall and H_2 increases in this region for this 6-month period.

FORESHOCKS AND THE NUCLEATION OF LARGE EARTHQUAKES

14-08-0001-G1339

Sean C. Solomon and Eric A. Bergman

Department of Earth, Atmospheric, and Planetary Sciences
Massachusetts Institute of Technology
Cambridge, MA 02139
(617) 253-3786

Investigation

The purpose of this project is to conduct a detailed study of foreshocks in order to investigate the nucleation process of large earthquakes. The study emphasizes multiple event relocation of all foreshocks in a sequence and, for the larger foreshocks, source studies with body waveform inversion techniques. A quantitative theoretical framework in which to interpret our investigations of the spatial-temporal patterns and source characteristics of foreshocks has been suggested by *Das and Scholz* (1981). In this model, which is based on the concept of subcritical crack growth, foreshocks arise from the interaction of a slowly-expanding nucleation zone with strength heterogeneities in the earthquake source zone. One of the goals of this project is to evaluate the utility of this model in characterizing actual foreshock-mainshock sequences.

Results

Our initial work on this project has focussed on the Kurile Islands earthquake sequence of January-March 1978, which culminated in two mainshocks (M_s 7.5 and 7.6) on March 23 and 24. We denote these two mainshocks as M1 and M2. This earthquake sequence is notable for the total number of foreshocks, the duration of the foreshock sequence, and the number of foreshocks large enough to permit teleseismic source studies. The neighboring sections of the southern Kurile subduction zone ruptured in 1963 (northeast) and 1969 (southwest). Detailed studies of the source processes of both earlier events have been conducted by *Schwartz and Ruff* (1985) and *Beck and Ruff* (1987). Our preliminary source studies of 5 of the largest foreshocks indicated that the 1978 earthquakes ruptured the shallow portion of the plate boundary, to a depth of about 35 km. The deeper portion of the plate interface apparently failed in the large ($M_w = 8.3$) Etorofu earthquake of 1958 (*Schwartz and Ruff*, 1987).

Further refinement of our body waveform inversion studies of five of the larger foreshocks strengthens our earlier conclusion that they are confined to a very narrow quasi-planar zone representing the interface between the Pacific and Eurasian plates (Figure 1). The earthquakes lie between 50 and 90 km from the trench axis at depths of 15-25 km beneath the seafloor. The dip of the interface in this region is close to 15°.

Preparatory to beginning multiple event relocation studies of the foreshock sequence, we have investigated the details of the spatial-temporal pattern of foreshock activity using the ISC epicentral data. For this purpose we assembled data for all earthquakes within 6 months of and closer than 200 km to M1. The 6 months of aftershocks define an approximately rectangular fault surface about 145 km long and extending about 70 km down-dip.

We examined the distribution of epicenters which occurred during the 40 hours between the two mainshocks in order to estimate the rupture area of M1, the epicenter of which is about 40 km northeast of that of M2. The rupture area is well-defined, occupying the northeastern two thirds of the full rupture area. The epicenter of M1 is at the bottom edge and near the southeastern end of its rupture zone. The distribution of aftershocks following M2 is more diffuse, because of the continued aftershock activity within the rupture zone of M1, but the rupture area of M2 may be characterized as approximately equal in area to that of M1, extending somewhat further both up- and down-dip, and overlapping that of M1 by 30-40 km (Figure 2). With these estimates of the rupture surfaces for the two mainshocks, we investigated the spatial-temporal patterns of the foreshock sequence with respect to these rupture zones.

From 6 months to 3 months prior to M1, the earthquakes are small ($m_b < 5.4$) and scattered throughout the region. Between the middle of January and early February, 1978 a cluster of earthquakes, including two for which we have performed source studies, occurred at the northeastern edge of the ultimate rupture area of M1. There was virtually no other seismic activity in the region during this time. From the depths determined in our body waveform inversions, this seismicity, which we consider to be the onset of foreshock activity, began near the lower edge of the ultimate rupture zone and propagated up-dip. In the last month before M1, except for the final 24 hours, there were only two small earthquakes in the region, one of which occurred in the cluster of foreshocks at the northeastern end of the rupture area of M1.

In the final 24 hours before M1 there was a great acceleration of foreshock activity, culminating in a M_s 7.3 foreshock 3 hours before M1. All this activity occurred on the southwestern end of the rupture zone of M1, in the region of overlap with the rupture zone of M2 (Figure 2). From our source studies of the larger events in this sequence, the progression of foreshock activity began in the shallow portion of the fault zone and propagated down-dip.

The observation of down-dip progression of foreshock activity is quite unusual and runs counter to current thinking about the nucleation process of subduction zone earthquakes. It is generally thought that ductile flow beneath the portion of the plate interface which behaves in a brittle fashion will gradually load the deepest levels of the fault zone, causing preslip to occur there (e.g., *Li and Rice*, 1983). Our working hypothesis relates the occurrence of foreshocks to this phase of preslip, as small patches of the fault fail seismically prior to the large-scale instability leading to the mainshock. The earliest foreshock activity, at the northeastern edge of the rupture zone, did follow the expected pattern. One possible scenario is that the nucleation phase of this earthquake sequence then propagated aseismically along strike toward the southwest before triggering the final acceleration of rupture in the last 24 hours before M1. In numerical simulations of earthquake nucleation, downward propagation of preslip was observed in a small number of cases by *Tse and Rice* (1986).

Further work on the 1978 Kurile earthquake sequence will focus on the unusual pattern of foreshock migration noted above and the role of the zone of overlap of the rupture zones of M1 and M2 in controlling the initiation of rupture in this part of the Kurile subduction zone. We speculate that the region of overlap (and of extensive foreshock activity) is a geometric or strength barrier within the subduction zone. We are continuing to investigate this structure with detailed earthquake relocation and source studies.

References Cited

Beck, S. L., and L. J. Ruff, Rupture process of the great 1963 Kurile Islands earthquake sequence: Asperity interaction and multiple event rupture, *J. Geophys. Res.*, in press, 1987.

Das, S., and C. Scholz, Theory of time-dependent rupture in the earth, *J. Geophys. Res., 86*, 6039-6051, 1981.

Li, V. C., and J. R. Rice, Preseismic rupture progression and great earthquake instabilities at plate boundaries, *J. Geophys. Res., 88*, 4231-4246, 1983.

Schwartz, S., and L. Ruff, The 1968 Tokachi-Oki and the 1969 Kurile Islands earthquakes: Variability in the rupture process, *J. Geophys. Res., 90*, 8613-8626, 1985.

Schwartz, S., and L. Ruff, Asperity distribution and earthquake occurrence in the southern Kurile Arc, *Phys. Earth Planet. Inter.*, in press, 1987.

Tse, S. T., and J. R. Rice, Crustal earthquake instability in relation to the depth variation of frictional slip properties, *J. Geophys. Res., 91*, 9452-9472, 1986.

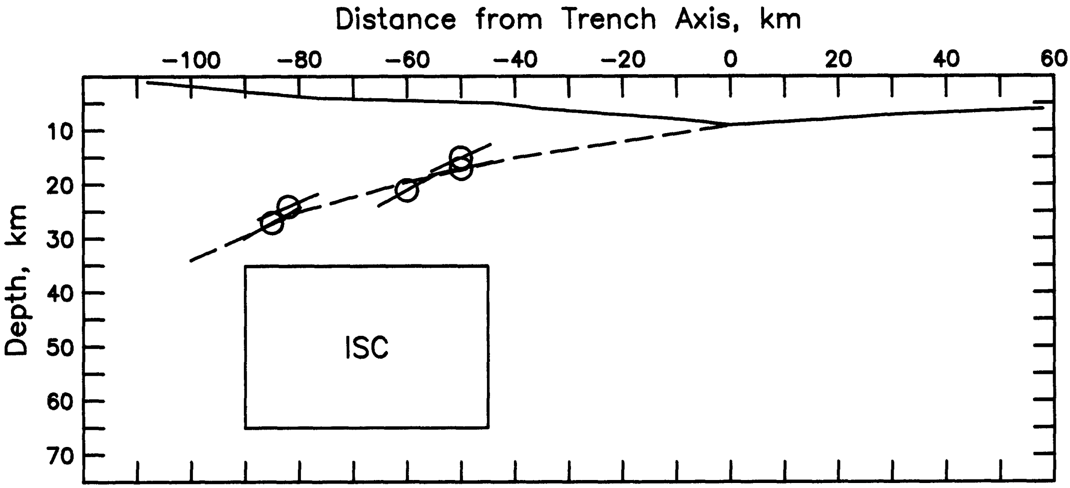

Figure 1. Cross section through the source region of the 1978 Kurile Islands earthquake sequence, showing the range of focal depths indicated by the ISC from reported pP-P times and the centroid depths obtained from body waveform inversion studies of 5 of the events. Dip angles are shown by lines through the circles representing the centroids. The inferred plate interface is shown by a dashed line. No vertical exaggeration.

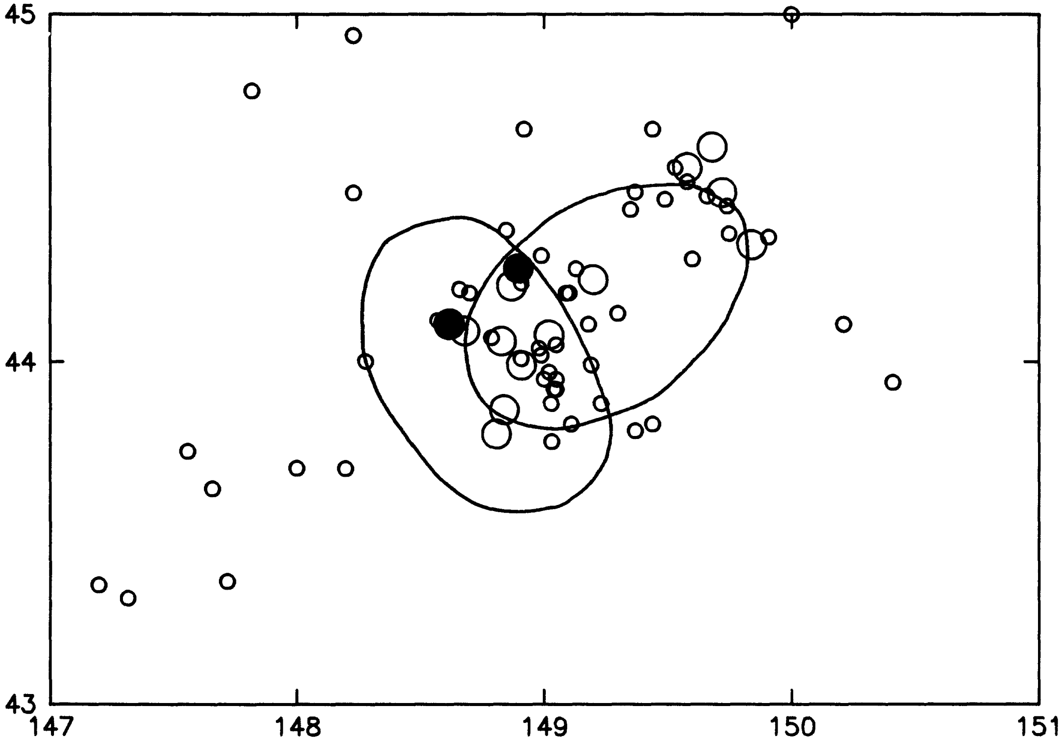

Figure 2. ISC epicenters of all earthquakes in the 6 month period before the first mainshock on March 23, 1978. The epicenters of the two mainshocks are shown by solid circles. Larger symbols indicate earthquakes with $m_b \geq 5.4$. The aftershock areas of the two mainshocks are indicated.

Analysis of Seismic Data from the Shumagin Seismic Gap, Alaska

14-08-0001-G-1388

John Taber and Klaus H. Jacob
Lamont-Doherty Geological Observatory of Columbia University
Palisades, New York 10964
(914) 359-2900

Investigations

Digitally recorded seismic data from the Shumagin seismic gap in eastern Aleutian arc, Alaska, are analyzed for detecting space-time variations in the seismicity, focal mechanisms, and dynamic faulting parameters that could be precursory to a major earthquake expected in this seismic gap. The seismic results obtained from the network data are being integrated with crustal deformation data that are independently collected, with volcanicity data of nearby Aleutian volcanoes, and with teleseismic information to identify basic tectonic processes which may be precursory to a great earthquake.

Results

We have continued our analysis of an M_s=7.9 earthquake in 1917 (Abe and Noguchi, 1983) that has been instrumentally located within the Shumagin gap. The location and magnitude of the 1917 event had been uncertain because it does not appear in the catalogues of Gutenberg and Richter (1954) or Gutenberg (1956). Arrival times for the mainshock on May 31, 1917 and 5 aftershocks were used by Boyd and Lerner-Lam (1987) to recalculate the epicenters. While the location of the mainshock is near the boundary between the Shumagin gap and the 1938 rupture zone, three of the five aftershocks are clearly within the Shumagin gap. To more carefully define the edges of the gap and the along arc extent of the 1917 earthquake, we have relocated the mainshocks and all well recorded aftershocks of events adjacent to and within the gap (Figure 1, and Boyd et al, 1987) using additional phases and clock corrections not used by Sykes (1971). It appears that at least 70% of the Shumagin gap has ruptured in large (M_s<8.0) earthquakes within the past 90 years. The 1917 earthquake ruptured up to a 200 km long arc segment in the eastern and central portions of the gap, while an event in 1948 (M_s=7.5) appears to have ruptured the deeper part of the central 75 km of the gap. A poorly documented earthquake that occurred in 1899 (M_s=7.2) may have ruptured the westernmost portion of the gap near Sanak Island. The interpretation of the 1899 earthquake, however, is based only on macroseismic observations.

The documentation of these earthquakes suggests that the gap can be divided into two or three smaller arc segments, each of which appears to be capable of rupturing separately. Observations of microseismicity by the local seismic network also suggest that downdip segmentation may exist. Microseismicity recorded by the Shumagin seismic network shows an abrupt change in the dip of the main thrust zone at about 30 km depth. The 1948 earthquake may have ruptured the lower portion of the main thrust zone while the 1917 event ruptured only the upper portion, allowing the along-arc extent of the rupture zones to overlap without any portion of the thrust zone rupturing more than once. These observations do not preclude the possibility of failure of the entire region in a single great earthquake (M_w=8.4) in the near future, and in fact historic observations of earthquakes that occurred in 1788 and 1847 suggest that portions of the Shumagin Gap and the adjacent 1938 rupture zone have failed simultaneously in the past. Such an extended rupture could occur again, based on the high probability of an event within the 1938 zone (Nishenko and Jacob, 1986). Assuming that the 1788, 1847, and 1917 earthquakes all ruptured the Shumagin Islands region, the two historically documented recurrence intervals for this portion of the arc are 59 and 70 years, and it has currently been 70 years since the 1917 earthquake. If the average recurrence interval for large earthquakes within the Shumagin Islands region is 65 years, the conditional probability of a large earthquake rupturing this portion of the arc in the next 20 years is about 65%. The average recurrence interval is, however, poorly constrained and allows for conditional probability estimates anywhere between 10 and 70%.

As a first step towards the calculation of conditional probabilities of future earthquakes based on recent microseismicity within the Shumagin gap, we have written a computer program to estimate the conditional probability of the occurrence of a large earthquake based on a statistical method developed by Feng et al. (1985). The technique uses six fundamental regional seismicity indices: number, average magnitude, and maximum magnitude of earthquakes with magnitude above the threshold magnitude within a time window, and their time derivatives. These statistical indices are first calculated from the earthquake catalogue. The conditional probability is then calculated from values of each statistical index in the previous time intervals.

We have applied this method to an Aleutian regional catalogue. The catalogue is a subcatalogue of the PDE catalogue that covers the area between 50-55N and 160-180W. The time period covers 1963-1985 and the cutoff magnitude was 5. Our goal is to predict magnitude 6 and above earthquakes using this catalogue. We divided the catalog into two parts, the learning and prediction periods. The learning period covers the time period between July, 1963 and February, 1979. The prediction period covers the time period between March, 1979 and December, 1985. Our most successful case thus far uses a window length of two months, a magnitude interval of 0.5, and 5 windows (10 months) of precursory time. For this case we have predicted 4 out of 6 earthquakes with magnitude 6 and above and we have 3 false alarms. This means we have correctly predicted 36 out of 41 time intervals.

The next step is to apply this method to the Shumagin network catalogue. Since this method can use any data that is continuous in time, it can easily be extented to include other possible precusory parameters such as regional stress patterns and sea level data. We can also use this method to identify and evaluate precusory patterns in space and time.

References

Abe, K., and S. Noguchi, Revision of magnitudes of large shallow earthquakes, 1897-1912, *Phys. Earth Planet Inter.* *33*, 1-11, 1983.

Boyd, T.M., and A. Lerner-Lam, The spatial distribution of turn of the century seismicity along the Aleutian Arc, *Bul. Seismol. Soc. Am.,* in press, 1987.

Boyd, T.M., J.J. Taber, A. Lerner-Lam, and J. Beavan, Seismic moment release and arc segmentation within the Shumagin seismic gap, Alaska, submitted to *Geophys. Res. Lett.*, 1987.

Feng, De-Yi, Jing-Ping Gu, Ming-Zhou Lin, Shao-Xie Xu, Xue-Jun Yu, Assessment of earthquake hazard by simultaneous use of the statistical method and the method of fuzzy mathematics, *Pageoph,* *122*, 982-997, 1985.

Gutenberg, B., Great earthquakes 1896-1903, *Transactions, American Geophysical Union 37*, 608-614, 1956.

Gutenberg, B., and C. Richter, *Seismicity of the Earth*, 2nd ed., Princeton Univ. Press, 310 pp, 1954.

Nishenko, S.P. and K. Jacob, Hazards evaluation for large and great earthquakes along the Queen Charlotte-Alaska-Aleutian seismic zone: 1985-2005, *USGS Open File Report 86-92*, 91-102,1986.

Sykes, L.R., Aftershock zones of great earthquakes, seismicity gaps, and earthquake prediction for Alaska and the Aleutians, *J. Geophys. Res., 76*, 8021-8041, 1971.

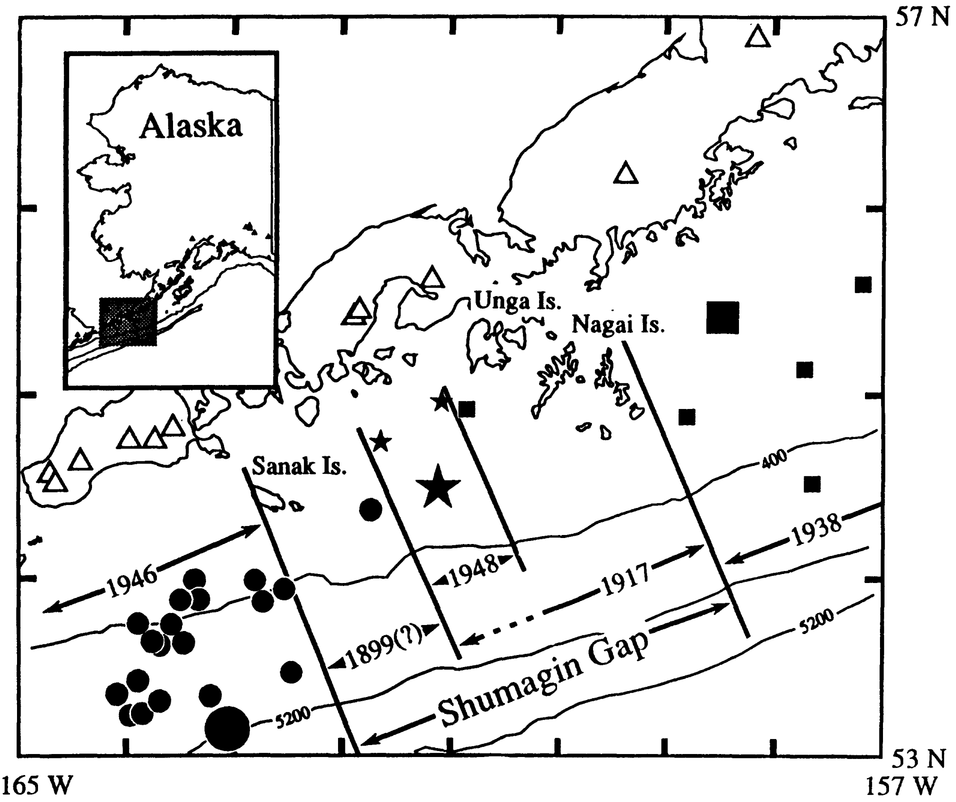

Figure 1. Relocations of the 1938 (squares), 1946 (circles), and 1948 (stars) mainshock and aftershock sequences. Larger symbols are the mainshocks, smaller symbols are the aftershocks that occurred within two months of each mainshock. Inferred along-arc rupture extents of each of these earthquakes plus those of the 1917 and 1899 earthquakes are also indicated. Inset shows the geographical position of the large-scale map. Open triangles show the positions of volcanoes and bathymetry is in meters.

Seismic Evidence for Tectonic Processes

9930-03353
Peter L. Ward
Branch of Seismology
U.S. Geological Survey
345 Middlefield Road, Mail Stop 977
Menlo Park, Ca. 94025
(415) 329-4736

Reese Cutler
Cutler Digital Design
2215 Sun Mor Ave.
Mountain View, Ca. 94040
(415) 964-1481

Investigations

Digital computer systems have proven to be the most desirable method to monitor and record data from local seismic networks but have typically cost between $50k and $100k. We developed a much lower cost computing system for installation in Katmai National Park, Alaska. Our design ideas were heavily influenced by the time available. Funding for this network was received in late April, 1987, and the system was installed in Alaska in early September, 1987.

Results

Design Principals

A major factor in the design of computer systems is the cost of the software both in terms of time and programmers' salary. Nearly all of the software that we needed to detect, process online, and interactively reprocess earthquake data exists and is running on a variety of minicomputers throughout the world. Much of this software has been written on systems with virtual memory capability and it would be difficult to trim these programs to fit computers with a severely limited address space. Thus our first fundamental decision was that the system must have virtual memory capability (address space of at least 16 megabytes) and should have a processing capability of at least 1 MIPS (Million Instructions Per Second).

The next decision was that the processor must have true multi-user and multi-tasking capability so that many programs could be run simultaneously without our software having to distribute system resources. In this way the large pool of existing software could be implemented rapidly and the configuration of software could be changed easily depending on need.

The third basic decision was to use the UNIX operating system (UNIX is a trademark of Bell Laboratories). All of the software needed was already running under UNIX. UNIX has become the industry standard portable, multi-user, multi-tasking operating system. Nearly all manufacturers of minicomputers now sell and support UNIX for their hardware. IBM and Apple have announced their intent to sell and support UNIX on the new generation of personnal microcomputers being introduced this year. Thus by chosing UNIX, not only can existing software be readily ported to our system, but our system can then be readily ported to hundreds of models of computers being developed by dozens of manufacturers. The choice of UNIX put some constraints on design of the analog-to-digital converter as discussed below.

These decisions ruled out use of IBM PC, XT, and AT compatible and Apple II and Macintosh I personnal computers. We reconsidered this result carefully because, after all, these computers are inexpensive, widely available, and easily maintainable worldwide. These machines do not have sufficient power for large seismic networks and programming to fit their addressing and processing limitations would negate any apparent cost savings. Furthermore these systems are soon to be replaced by new models that will meet the above criteria and that would make such special programming obsolete. While there are good arguments for ultimately using such mass-produced computers, we decided that the most expeditious way to proceed in 1987 was to do the development on the best machine available, but to use industry standards so that we could readily port our system to whichever hardware was best in the future.

The next decision involved how to interface the analog-to-digital converter (A/D) to the computer. The standard approach for large microcomputers and minicomputers is via a bus such as VME bus or Multibus. Processors using such high-performance buses, however, are typically expensive. The most powerful and least expensive processors typically use the Small Computer Systems Interface or SCSI bus to connect to peripherals. SCSI is rapidly becoming an industry standard as increasing numbers of disk drive and tape drive manufacturers are producing systems to connect directly to this bus. Several manufacturers provide chips that do all of the low level interface to this bus so that interfacing a new device is relatively easy. SCSI will be available for many of the new generation personnal computers announced this year. We decided that if we could make our A/D look like a read-only disk on the SCSI bus, then it could be readily interfaced to a wide variety of processors.

UNIX is not a realtime operating system. In other words it can not guarantee to service any specific process on a set schedule within fractions of a second. In fact most multi-user, multi-tasking operating systems are not as realtime oriented as single task processors. High performance A/D systems get around this problem by using buffering. Thus we concluded that if the A/D could buffer data for as much as a few seconds, it should be able to work properly even in a heavily laden UNIX environment. Within UNIX it is possible to lock a given process in core and to give it the highest priority, so that it will be serviced regularly.

Our design goal was to build a system capable of digitizing data from 128 seismic components at a rate of 100 samples-per-second each. We wanted to use as many off-the-shelf components as possible to reduce development time and to minimize cost.

Overall Design

We researched all computer systems available that would meet the above criteria and would cost under $20k including disk and tape subsystems. We concluded that the most mature and powerful (1.5 MIPS) processor available in mid 1987 for the lowest price was the SUN Microsystems Model 3/50 Workstation. This system with a floating-point processor, 4 megabytes of memory, 142 megabytes of disk storage, and 60 megabytes of cartridge tape storage was available for about $10k.

We were unable to find a buffering A/D interfaced to the SCSI bus and were thus forced to build our own. A/D chips, however, can be bought off the shelf, so that what we had to build was only an A/D controller. SCSI controllers are also available off the shelf, but we were unable to get one within a reasonable time period and thus had to build our own. The overall design of the A/D unit is shown in Figure 1.

The dynamic range of the seismic telemetry system is less than 60db, so that a 12 bit A/D is more than adequate. This leaves 4 bits of each 16 bit word unused. We decided to use these extra bits to record time information. The Kinemetrics/True Time GOES Satellite Synchronized Clock (Model 468-DC) provides absolute time accurate to a millisecond and has an option for parallel output of the time information in BCD format. Thus by using each set of 4 bits for one BCD digit, the complete time of year from day of year thru millisecond can be encoded in 12 samples. The clock also puts out 4 error bits. The clock data are latched into registers at the beginning of each sweep and then added 4 bits per data word to the A/D data stream. By placing the time information in the least significant bits, i.e. in the noise, the data can be processed without removing the time information.

The A/D is a Burr-Brown SDM854 Hybrid Data Acquisition System that contains not only an A/D, but a sample and hold amplifier, 16 channel multiplexer, clock, delay timer, and multiplexer address latch. Each channel of this internal multiplexer can then receive data from an external multiplexer (Burr-Brown MPC16S CMOS Analog Multiplexer) giving input from up to 256 channels. For ease of design and buffering, the number of channels in our system is selectable in units of 16, the number of multiplexers active. Similarly the sample rate is adjustable only to 50, 100, or 200 samples per second.

The output of the A/D and clock goes into a FIFO (Integrated Device Technology Model IDT7202) to provide some flexibility in the processor's response to the data stream. At high throughputs near 25.6K samples per second, the processor might otherwise miss some samples.

Our initial idea was to use a large FIFO as the whole data buffer and use Programmable Array Logic (PAL) to control the A/D and SCSI bus. The cost of 600K bytes of FIFO, however, is prohibitive. Furthermore the SCSI interface chip is designed to talk to a processor. Several people who had designed SCSI interfaces advised us that debugging a PAL-based SCSI system would be very difficult. Thus we decided to use a processor for buffering and control. The most inexpensive and well proven processor readily available to us was an Intel 8088 in the form of an IBM-XT clone. A fully configured XT was available for development with a cross assembler and a prom burner. Thus we could write and compile the program in a standard working environment, burn a prom, and insert it into the A/D. This established the physical configuration of the A/D as an XT clone case, power supply, and motherboard containing processor and memory. We then used standard XT full-length plugin prototype boards to hold the custom wire-wrap circuitry. All of these components were readily available over the counter. In addition a serial RS-232 port board was purchased to provide printer output during debugging of the SCSI interface.

The software that runs the processor as a standalone program is loaded in a 2K ROM. It uses an 8K byte segment of processor memory (RAM) for program variables and the remaining 632K bytes for buffer space.

A binary digital counter operates 8 LEDs that display the numbers of buffers waiting to be read over the SCSI bus. A buffer is 4096 bytes. This display shows immediately how well the interface to UNIX is working and whether the A/D is functioning properly.

SUN Microsystems Consulting Group sells a generic SCSI bus driver called CONSULT-SIP. This software provides the appropriate interfaces for the C Language subroutine calls open, close, read, write, and several options under ioctl (the IO control subroutine) that we used to identify the A/D, to reset the A/D, and to report errors. We designed the A/D interface to provide what this software expected. Porting this device to another machine will require a similar appropriate driver. A real benefit of the SCSI bus is that such a generic driver can be used. Writing a new SCSI bus driver would be a major undertaking.

Performance

The noise on the analog channels was about 5 mv peak-to-peak with reference to a plus and minus 5 volt maximum input causing jitter in the second data bit. Since the seismic signals input to the multiplexers had noise greater than this, no effort was made to reduce this noise.

The A/D was run for days into a program that read the header information, checking that the time between samples was always between 9 and 11 milliseconds, checking that the multiplexer numbers were sequential, and checking that the distinct numbers were always in their proper place. The only errors found were traced to poor reception by the Satellite Clock due to a misaligned antenna and automatic seeking between the two satellites. Over a period of hours the time between samples did not change 8 specific times and then suddenly changed 80 milliseconds as the internal clock in the receiver was resynchronized to the satellite. Reorientation of the antenna and setting the receiver to use only one satellite corrected this problem. No loss of data by the A/D was ever detected.

Throughput of data proved to be no problem for up to 256 channels at 100 samples per second or 25.6K samples per second. The Burr-Brown Hybrid Data Acquisition System is rated at 27K sps. The FIFO and processor had no problem maintaining this rate because DMA channels were used and the processor was dedicated to data collection and transmission. This rate would not be attainable using the MSDOS operating system. The bandwidth of the SCSI bus is up to 4 megabytes per second with DMA input and output. The SUN 3/50 was able to receive the data and write it to disk at 25.6K sps. For testing purposes we installed a do loop in the main program on the SUN doing integer multiplies and discovered that 4 such multiplies per sample could be done without losing data. There was some indication that data may have been lost by the disk at specific moments, perhaps during switching of disk tracks. This problem was not regular, however, and we did not have time to investigate it fully. In cases where the highest throughputs are required, it may be wise to use a higher cost SUN model including a VME bus so that data is input on the SCSI and output to disk on the VME bus. Throughput was influenced by system load. If the A/D reading program was run at standard priority (nice=0) and a large amount of other disk or tape I/O or computing was going on simultaneously, the number of buffers in the A/D would increase and decrease, sometimes causing buffer overflow. If the A/D program was run at highest priority (nice= -10) this was rarely a problem and never a problem for less than 200 channels (20K sps). When buffer overflow occurs, the A/D sends an error message and continues to collect data so that the buffer always contains the most recent data. The possibility of overflow can be further decreased by a program called plock that is available from SUN Consulting to lock a process in core. We did not buy or test the effect of this on throughput, because we never expected to use more than 128 channels.

A standard long-term short-term detection program provided by J. W. Herriot of the U.S.G.S. was used to select and save earthquake data. We could run 224 channels of data through this program without losing data and using all of the system bandwidth. We tested the program extensively with data from 32 stations near Parkfield, California. Running the complete detection algorithm on all 32 stations and saving suspected events on disk used less than 10 percent of the computer resources. While this task was running in background, we could use the rest of the computer resources for editing, compiling, and other computing. We also modified this program so that the data was not only scanned with suspected earthquakes saved to disk files, but also written continuously to magnetic tape. This allows us to collect continuous data from the network when desired.

The only task that would backup buffers in the A/D was extensive use of the cartridge streamer tape drive. This tape drive hogs the SCSI bus even while rewinding, a problem that should be corrected by a better controller. A major feature of the SCSI bus is that when a device is asked to do something that will take a long time, the device can disconnect from the bus and then reconnect once the data are available. We use this feature in reading the A/D. The SUN requests one buffer (4096 bytes). If the A/D does not have one ready, it disconnects and then reconnects when the buffer is ready. The tape controller should do this but does not. Thus it is possible to lose some data from the A/D when writing a very long cartridge tape. There may be ways to mitigate this problem, but in our case we concluded that the problem was likely to occur so rarely, that we would not spend more time on it.

Reports

Ward, P.L., and Cutler, R., An inexpensive, buffered analog-to-digital converter for use on the SCSI bus with the UNIX operating system, U.S. Geological Survey Open-File Report, 81p.,1987.

Ward, P.L., and Cutler, R., Economical seismic-network processing, Seismological Society of America Eastern Section Abstract, in press, 1987.

Ward, P.L., and Cutler, R., Economical seismic-network processing, Transactions American Geophysical Union, v. 68, in press, 1987.

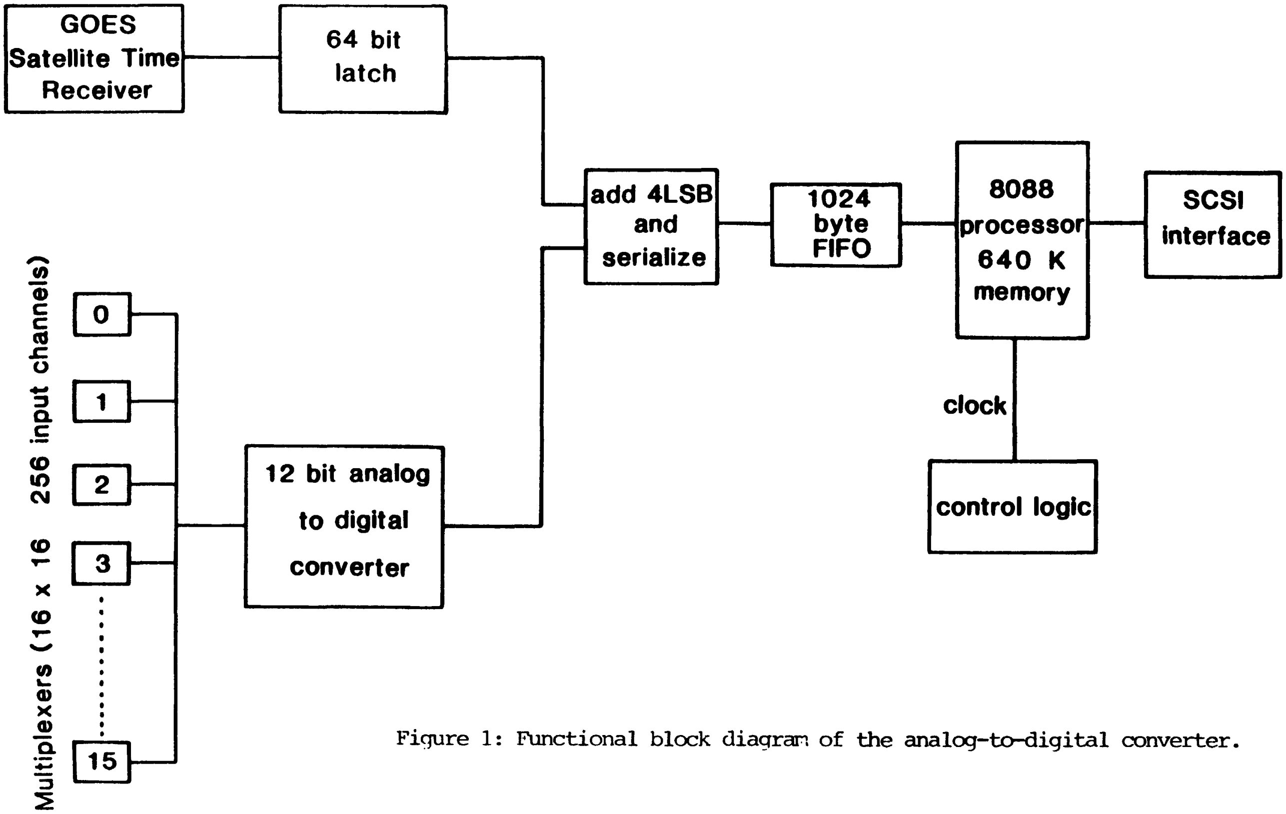

Figure 1: Functional block diagram of the analog-to-digital converter.

LATIN AMERICAN VOLCANOES AND EARTHQUAKES

Project #9930-01163

Randall A. White and David H. Harlow
Branch of Seismology
U.S. Geological Survey
345 Middlefield Road, MS/977
Menlo Park, California 94025
(415) 329-4746

Investigations: **SEISMOLOGICAL ASPECTS OF THE SAN SALVADOR EARTHQUAKE OF OCTOBER 10, 1986 AND COMPARISON WITH OTHER LOCAL MICROSEISMICITY**

The magnitude (Mw) 5.6 San Salvador earthquake of October 10, 1986 resulted in about 1500 deaths, 10,000 injuries, and 150,000 people left homeless. The earthquake originated along the Central American volcanic chain within the upper crust of the Caribbean Plate. Results from a local seismograph network show a tectonic style main shock-aftershock sequence. The hypocenter was located 7.3 km below the south edge of San Salvador. The main shock ruptured along a nearly vertical plane toward the north-northeast. A main shock fault-plane solution shows a nearly vertical fault plane striking N32°E, with left-lateral sense of motion. This earthquake is now the second Central American volcanic chain earthquake documented with left-lateral slip on a fault perpendicular to the volcanic chain (being similar in this and many other respects with the 1972 Managua earthquake). Strong ground motion lasted for only 3 to 5 sec, but the shallow focus and amplification of seismic waves by surface deposits of volcanic tuff combined to produce horizontal ground accellerations up to 0.72g at a period of 0.8 seconds.

During the 2 1/2 years preceeding the 1986 San Salvador earthquake, minor microseismicity was noted near the epicenter, but this has been common along the volcanic chain since at least 1953. San Salvador was previously damaged by a volcanic chain earthquake on May 3, 1965. The locations of six foreshocks of the 1965 earthquake show a distinctly WNW-trending distribution. Together with the distribution of damage and a fault-plane solution, this, we believe, documents the first instance of right-lateral slip along a fault sub-parallel with Central American volcanic chain. This earthquake was also unusual in that it was preceded by a foreshock sequence more energetic than the aftershock sequence! Earlier this century, on June 08, 1917, an M_S 6.4 earthquake occurred 30 to 40 km west of San Salvador Volcano. Only 30 minutes later, an M_S 6.3 earthquake occurred, centered at the volcano, and about 35 minutes later the volcano erupted. In 19 an M_S 6 earthquake occurred, centered at about the epicenter of the 1986 earthquake. We conclude that the volcanic chain is seismically very active with variable styles of seismicity.

Reports

White, Randall A., and Ines Lucia Cifuentes, Seismic history of the Middle America Trench spanning the Guatemala Triple Junction and an earthquake forecast: BSSA (received July 1987).

Harlow, D.H., White, R.A., Rymer, M.J., Alvarez, Salvador, and Carlos Martinez, The San Salvador earthquake of 10 October 1986 and its historical context: Science (submitted October 1987).

Figure Captions

Figure 1 - The M_S 5.4 main shock (large octagon) was located near the south edge of the city of San Salvador using P-wave arrival times at five seismic stations within 30 km and S-P intervals from five strong-motion accelerographs within 15 km. The MM VII and VIII intensity contours are also shown. The fault plane solution is shown at lower left. Aftershocks were located using P-wave arrivals from at least the four seismic stations within 30 km and S-wave arrivals were also used for all events with M <4. The first locateable aftershock, 14 minutes after the mainshock, was also the largest aftershock (M 4.8). It is the northernmost M >4 event on the figure. The cross-section of the aftershocks along A-A'shows that the after-shocks define a nearly vertical plane extending from the surface to 15-km depth. The strike of this plane is compatible with the NNE-striking plane of the fault plane solution.

Figure 2 - Locations of microearthquake swarms, with more than 10 events/month, since 1953 are shown as hatched areas. The swarms prior to 1984 were recorded by low-gain seismographs. The month and year of the swarms are shown next to them with the number of recorded events in parentheses. Data are from the bulletins of the Centro de Investigaciones Geotecnicas (This is not a complete accounting - bulletins were only available to us for about 40% of the months between 1953 and 1987). Data for the hatched area at San Salvador, dated 1965, is presented in Figure 5. Note that all recorded microseismicity has occurred within 10 km of the Quaternary volcanic axis.

Figure 3 - Unlabelled octagons are foreshocks that occurred during the tremendous swarm of foreshocks before the May 3, 1965 San Salvador earthquake. The southernmost octagon is our relocation of the aftershock of May 25, 1965 located by Lomnitz and Schulz (BSSA:1966) at the the point indicated by the *. The Modified Mercalli (MM) intensity VII and VIII contours are also shown. The foreshock zone and MM VIII contour are essentially coincident. The main-shock fault-plane solution from Molnar and Sykes (JGR:1969) is shown below. The significant elongation of the foreshock zone and MM VIII contour along the WNW-ESE direction is compatible with the WNW-ESE-oriented plane of the fault-plane solution.

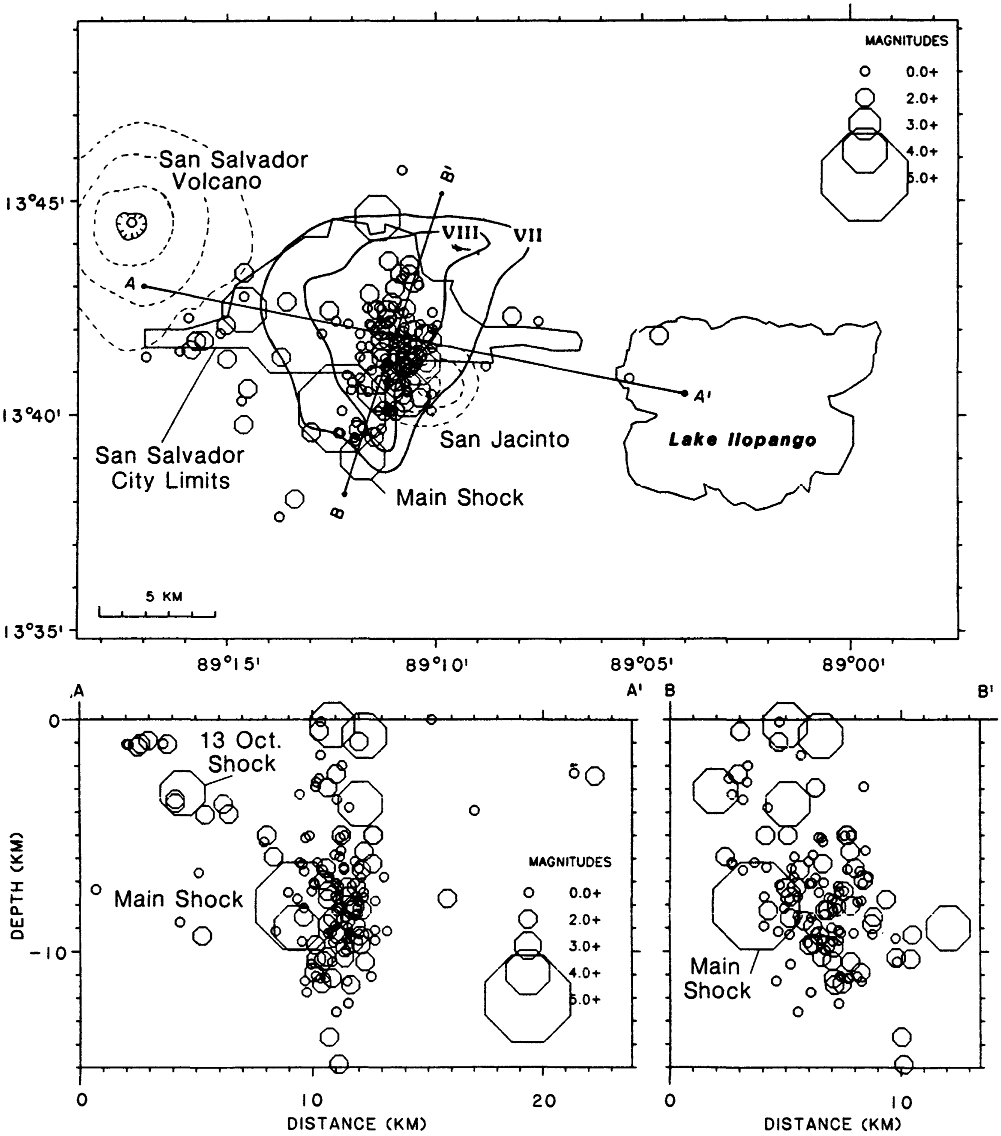
MAGNITUDES
0.0+
2.0+
3.0+
4.0+
5.0+
San Salvador Volcano
13°45'
13°40'
13°35'
A
A'
B
B'
VIII
VII
San Salvador City Limits
San Jacinto
Main Shock
Lake Ilopango
5 KM
89°15'
89°10'
89°05'
89°00'
13 Oct. Shock
Main Shock
DEPTH (KM)
0
-10
DISTANCE (KM)
0
10
20

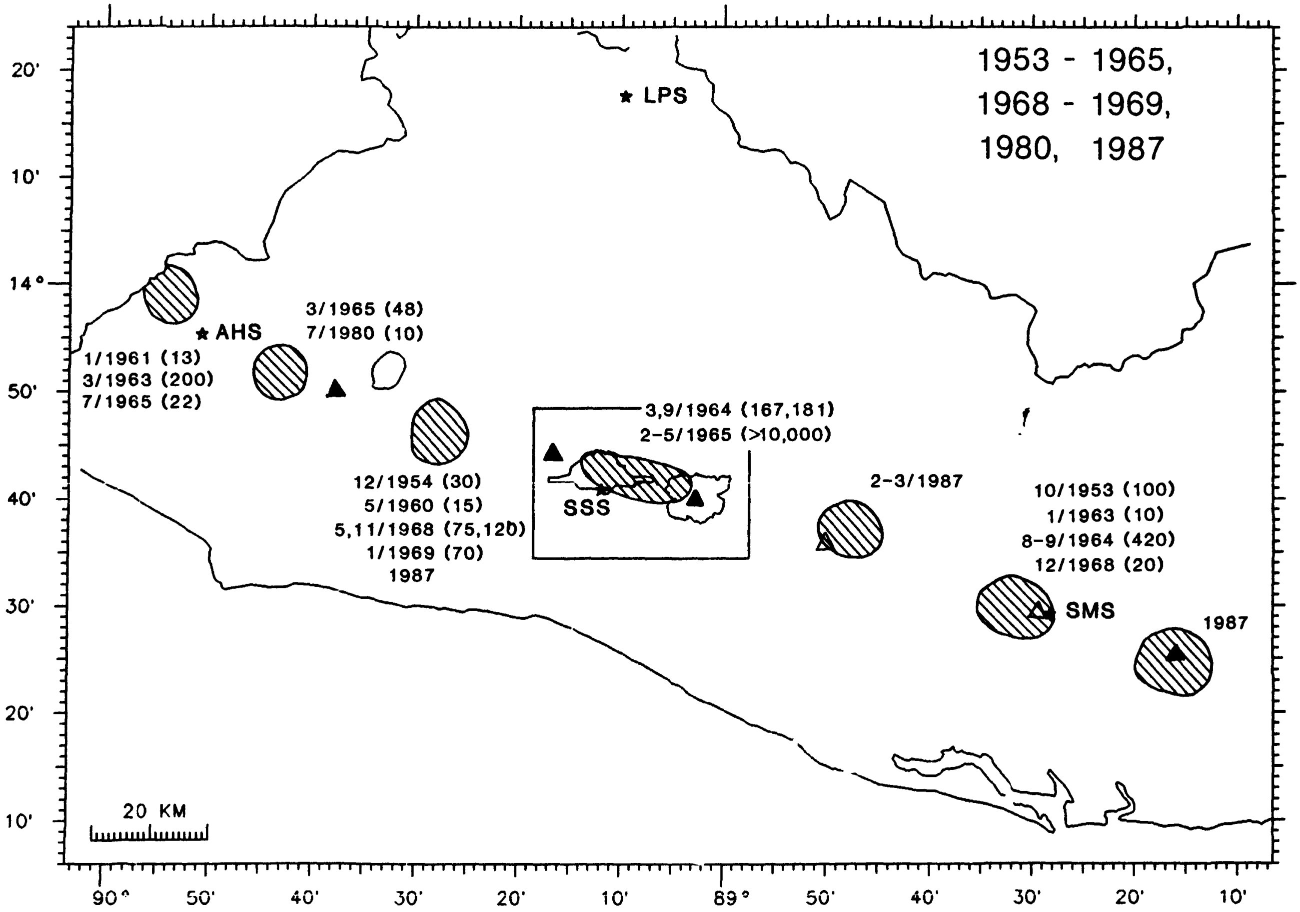
1953 - 1965,
1968 - 1969,
1980, 1987
LPS
AHS
SSS
SMS
1/1961 (13)
3/1963 (200)
7/1965 (22)
3/1965 (48)
7/1980 (10)
12/1954 (30)
5/1960 (15)
5,11/1968 (75,120)
1/1969 (70)
1987
3,9/1964 (167,181)
2-5/1965 (>10,000)
2-3/1987
10/1953 (100)
1/1963 (10)
8-9/1964 (420)
12/1968 (20)
1987
20 KM
20'
10'
14°
50'
40'
30'
20'
10'
90°
50'
40'
30'
20'
10'
89°
50'
40'
30'
20'
10'

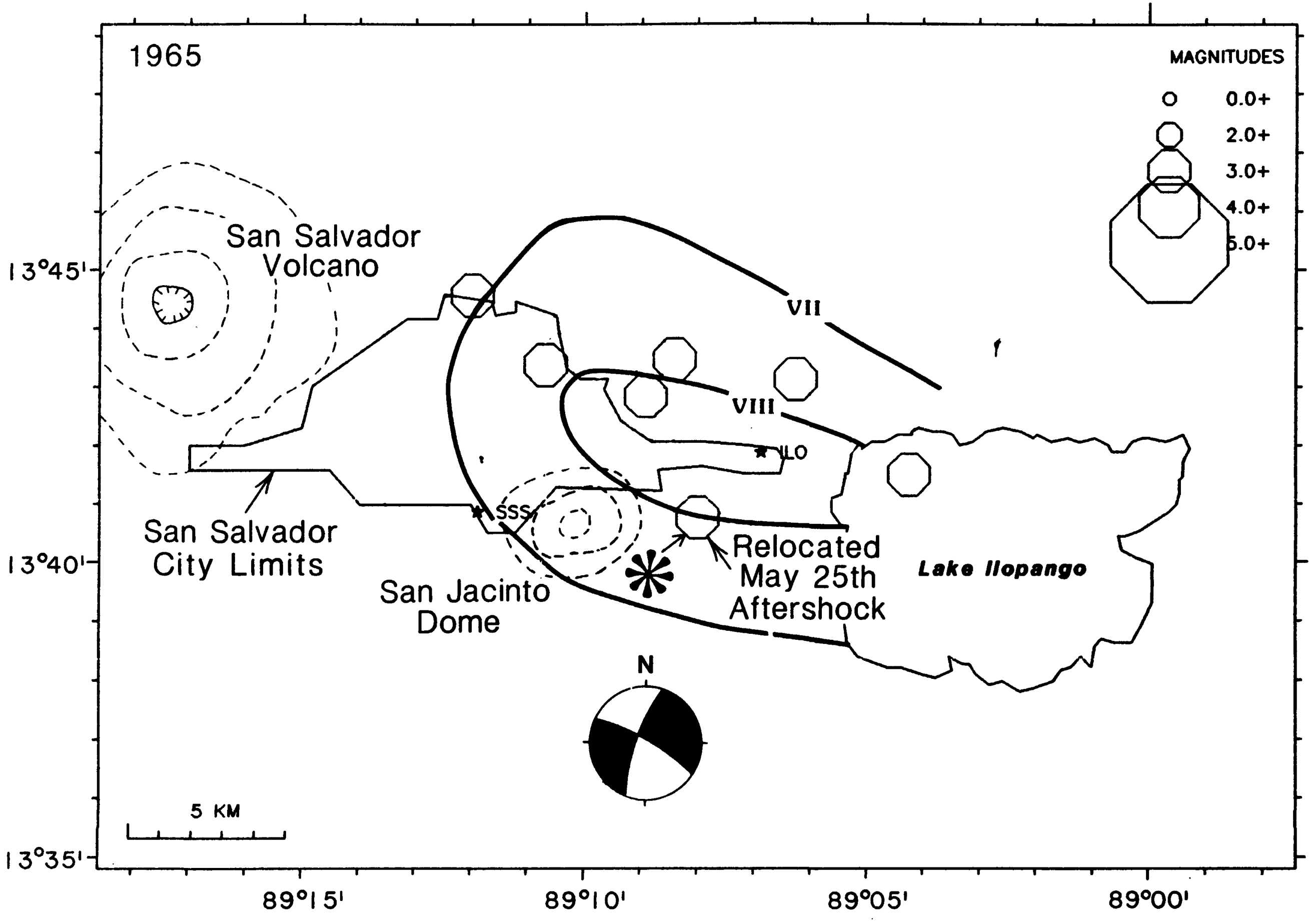
1965
MAGNITUDES
0.0+
2.0+
3.0+
4.0+
5.0+
San Salvador Volcano
VII
VIII
ILO
SSS
San Salvador City Limits
San Jacinto Dome
Relocated May 25th Aftershock
Lake Ilopango
N
5 KM
13°45'
13°40'
13°35'
89°15'
89°10'
89°05'
89°00'

Piñon Flat Observatory: Cooperative Studies with Outside Investigators

14-08-0001-G1197

Frank Wyatt and Duncan Carr Agnew
Institute of Geophysics & Planetary Physics
Scripps Institution of Oceanography
University of California, San Diego
La Jolla, CA 92093
(619) 452-2019

This grant provides assistance for independent investigators working at Piñon Flat Observatory (PFO) under the auspices of the U.S. Geological Survey. This assistance includes research coordination, instrument operation and testing, data logging, preliminary data reduction, and collaborative data analysis. Part of this is a cooperative program (the Crustal Deformation Observatory Project) to evaluate instruments for measuring long-period ground deformation. Such evaluation involves understanding and reducing noise in the instruments and also developing improved methods to describe measurement error. Most of the studies currently underway are conducted independently, with investigators establishing their own associations to compare results; in the Crustal Deformation Project there is a more formal agreement to share observations.

In the past few years several precise geodetic surveys have been made in the area around PFO (Figure 1); some of these are made by organizations operating independently, while for others we provide coordination and some support. The longest-running geodetic measurement around PFO is the Geodolite network surveyed by the USGS Crustal Strain group of Drs. W. H. Prescott and J. C. Savage. This network (observed since 1973) has given the best values of the secular strain near PFO, serving as the low-frequency constraint on our continuous measurements. A more recent addition is a 2-color EDM network established by Dr. J. Langbein in the spring of 1986, and surveyed again in the spring and summer of 1987. Preliminary results from these observations are that the 2-color net shows strain rates much larger than those seen on the Geodolite net. A comparison between the 2-color and laser strainmeter results is planned (aided by an NSF-funded upgrade to the NS strainmeter); this comparison of geodetic measurements and observatory-based results should help establish the quality of both.

With support from the National Geodetic Survey (NGS) and the NASA Crustal Dynamics Project (CDP), there have been several visits of the mobile VLBI antenna MV-3 to the National Crustal Motion Network (NCMN) monument at PFO. These VLBI measurements are beginning to establish differential motions across the plate boundary in Southern California. A data reduction by NGS (presentation by M. Abell and M. Morrison at the October CDP meeting) shows that relative to a fixed baseline between the VLBI stations at Owens Valley and Mojave, PFO is moving at 17 ± 2 mm/yr at an azimuth of 300°, about 15 mm/yr less than the motion seen at Monument Peak, on the other side of the San Jacinto fault. This suggests that current slip rates on the San Andreas and San Jacinto faults are about equal.

Several occupations of the same NCMN monument have been made for GPS surveying. In June of 1986 this monument was occupied both for regional surveys and to put a "footprint" of stations nearby (Figure 1). (These other stations included part of the

USGS 2-color net, the new level line, and the absolute gravity station). In January the NCMN monument was occupied for regional surveys (to be repeated annually) by observers from UCLA, working in coordination with the NGS and using a UNAVCO receiver. Another occupation is planned in March; at this time the mark will also be used as a GPS reference station for a survey by the Riverside County Flood Control District.

In June 1986 a group of closely-spaced class A rod marks was established near one end of the long fluid tiltmeters. Measurements at PFO by Dr. A. Sylvester (UCSB) had suggested that such marks did not in fact possess the high stability that they should. The purpose of this "bench mark farm" is to test this through repeated leveling (to be done largely by UCSB), that will compare these marks with each other and with the deep optical anchor on the adjacent UCSD tiltmeter.

A level line was constructed through the observatory; we devoted considerable time to ensuring that this would include ties to the NCMN mark, several of the rod marks, the absolute gravity station, and several of the UCSB marks. This line is part of a loop in a larger line (Figure 1) set up by Dr. R. Stein with an NGS contract crew. It was surveyed in July 1986 and again in August 1987. Repeated surveys of this line will give a check on the long-term tilt in the area—a useful comparison with the long-base tiltmeter results. Both ends of this line have also been surveyed with GPS—another source for useful comparisons.

Most of the sensors operated by outside investigators have continued to work well with only occasional attention, notably the various borehole tiltmeters, which include an Askania tiltmeter run in cooperation with Walter Zürn of Karlsruhe University; two tiltmeters (BOA, at 24 m, and BOB at 36 m) designed by Judah Levine and Charles Meertens of the University of Colorado; and three St. Louis University tiltmeters (STLA, STLB, and STLD, all at 4.5 m) developed by Sean-Thomas Morrissey. These last three replace the Kinemetrics TM-1B instruments formerly run at the same sites, and have shown similar behavior despite considerable difference in instrumentation. This provides near-conclusive evidence that the instabilities seen are in the soil around the instrument; at the same time it shows that the sensor stability exceeds that of the ground, so that deeper installation of these instruments would give improved results.

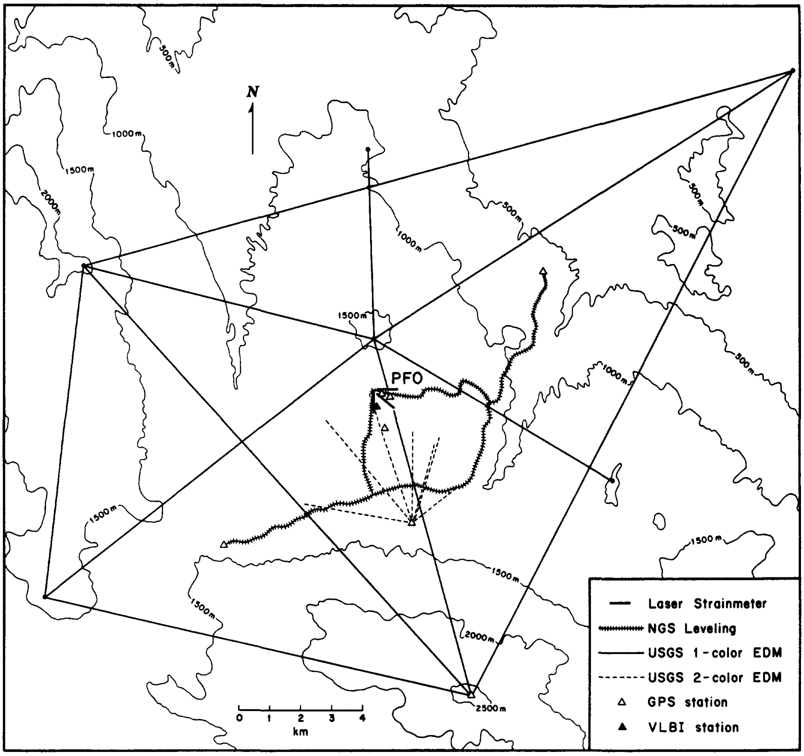
500m
N
1000m
1500m
2000m
500m
1000m
500m
500m
1500m
PFO
1000m
500m
1500m
1500m
1500m
1500m
2000m
2500m
0 1 2 3 4
km
Laser Strainmeter
NGS Leveling
USGS 1-color EDM
USGS 2-color EDM
△ GPS station
▲ VLBI station

Figure 1.

Piñon Flat Observatory: A Facility for Studies of Crustal Deformation

14-08-0001-G1178

Frank Wyatt, Duncan Carr Agnew,
Mark A. Zumberge, Jonathan Berger
Institute of Geophysics & Planetary Physics
Scripps Institution of Oceanography
University of California, San Diego
La Jolla, CA 92093
(619) 452-2019

This grant supports the operation of Piñon Flat Observatory (PFO) by providing one-half the funds needed for running the shared facility. Matching funds are provided by the National Science Foundation. The work done at PFO includes establishing the accuracy of instruments designed for measuring various geophysical quantities by comparing results from them with data from "reference standard" instruments. This comparison also allows reliable monitoring of strain and tilt changes in the area near the observatory, between the active San Jacinto fault and dormant southern San Andreas fault systems. All of this effort is intended to foster development of precision geophysical instrumentation.

In this report we present data from the three laser strainmeters (the operation of which is supported by this grant) for the Whittier Narrows earthquake of 1 October 1987. Our usual interest in strain data is at very long periods, so that the onsite recorders sample every 5 minutes; we also operate a higher-speed datalogger in our lab at La Jolla, recording off a telemetry link provided by Sandia Laboratories. We record continuously at 1 sample/second, with event-triggered recording at 10 times this rate. Since the strains associated with seismic waves can be very large, we had upgraded the fringe-counting system to have a higher dynamic range (16 bits) and adequate antialiasing filters.

All of this equipment worked as it should, providing us with an onscale recording of the complete event, through peak strains of over ± 100 nϵ. We have not yet attempted any detailed modelling of these data, but as a start have analyzed them for possible coseismic offsets. These are lost in the raw data because of the persistence of the coda. To bring them out we constructed a composite of the triggered and continuous data, 6 hours in length; the tides were removed from this by fitting a one diurnal and one semidiurnal constituent (skipping over the earthquake and coda). This detided series was then lowpassed to remove energy at periods less than 30 seconds.

The result (plotted in Figure 1) shows definite coseismic offsets on all three instruments. These are of the right size for an earthquake of magnitude 6.1 at a distance of 160 km, but it should be noted that they do not agree in detail with the halfspace predictions gotten from the local-network source mechanism. Whether or not this is caused by errors in the source mechanism remains to be seen, but we should note that the predicted (and observed) offsets are only about one fringe of the laser interferometer (each fringe is 0.43 nϵ), and at this level many noise effects are present that could produce spurious offsets. Within this range, the observed and theoretical strain offsets are in agreement; while the observations probably cannot provide much of a constraint on the earthquake source, they do show that anomalously large strain steps were not present.

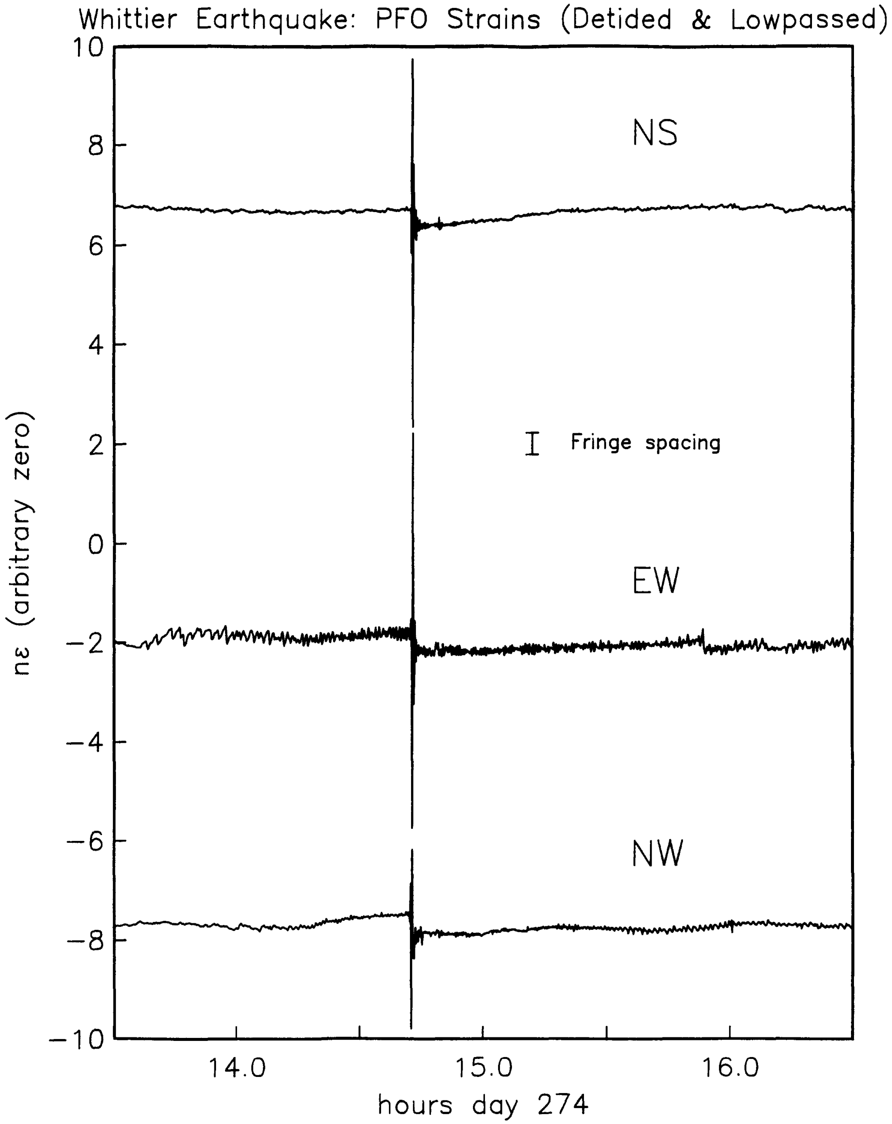
Whittier Earthquake: PFO Strains (Detided & Lowpassed)
nε (arbitrary zero)
10
8
6
4
2
0
−2
−4
−6
−8
−10
NS
EW
NW
Fringe spacing
14.0
15.0
16.0
hours day 274

Figure 1.

Towards a Widely-Deployable Long-base Tiltmeter: Sensors and Anchors

14-08-0001-G1336

Frank Wyatt, Mark Zumberge, Duncan Carr Agnew
Institute of Geophysics & Planetary Physics
University of California, San Diego
La Jolla, California 92093-0225
(619) 534-2411

The aim of this project is to design and construct new tiltmeter systems and to test them against existing long-base tiltmeters at Piñon Flat Observatory. For long-base tiltmeters to be generally useful in measuring crustal deformation, they must be engineered for easy use, and widely-applicable installation procedures must be devised. Our new design incorporates two important improvements over the earlier UCSD long-base tiltmeter. One is an improved absolute water-height gauge; the other is the use of optical fibers in vertical anchoring, to ease the greatest difficulty in the construction of observatory-based instruments: securely attaching the sensor to the underlying crust.

Our approach for testing the new equipment has been to install the combination of water-height gauge and optical anchor in a new vault (116 m from the original tiltmeter) so we could experiment with different arrangements. Extending the equipotential fluid-surface from the original tiltmeter over to the new vault allows us to compare our old system with the new one. In the absence of large tilts, we will not accumulate much signal between the new vault and the nearer of the original tiltmeter vaults, and we can correct for any tilt that does occur using the measurements from the present system.

The basic layout of the two sensors is shown in Figure 1. We are using a microprocessor controller and motorized micrometers to hold an optics stage a fixed distance above the fluid surface. (This uses a white light interferometer, which is an absolute displacement gauge and so is immune to power outages.) A displacement transducer then measures the motions of the optics stage relative to an invar spacer held securely at a depth of 3.9 m. From this depth we measure the displacement to bedrock with the fiber optics anchor. Two fibers are held taut at the surface and connected as arms of a Michelson interferometer. As the fibers strain (in the interval between the two ends of the fibers) the optical path lengths change, and this causes the interference pattern to change. The reason for the invar spacer is that optical fiber, while inherently stable, is very sensitive to temperature variations and can not be relied upon near the ground surface.

Figure 2 shows three weeks of recent records from the new sensors. For the water height, we actually measure its movement relative to two places: the invar spacer and the table. Because of the competence of the underlying rock, we expect most of the vault motion to appear as the difference of these records: in the near-surface material spanned by the invar spacer. The lower panel shows this signal to be quite small (3.25 μm on a 650-m-long tiltmeter is a tilt of only 5 nrad). Also shown in Figure 2 are the two fiber records (measured individually at this point, rather than in their eventual Michelson configuration) and their difference. Proper evaluation of this record involves determining the tilt seen on the original tiltmeter and projecting it to this vault, nevertheless the data look quite good. The fiber-difference seems well behaved, most especially in its immunity to temperature effects, and seems to show promise for general use.

Tiltmeter - Fiber Optics Anchor

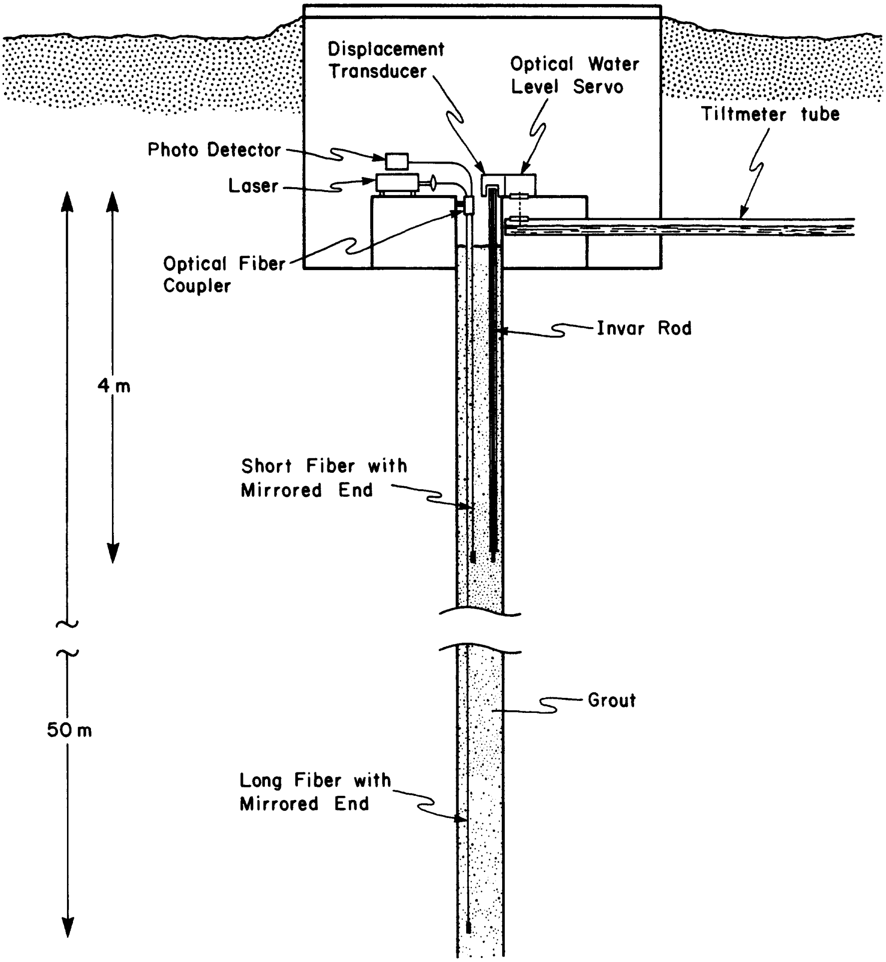

Figure 1.

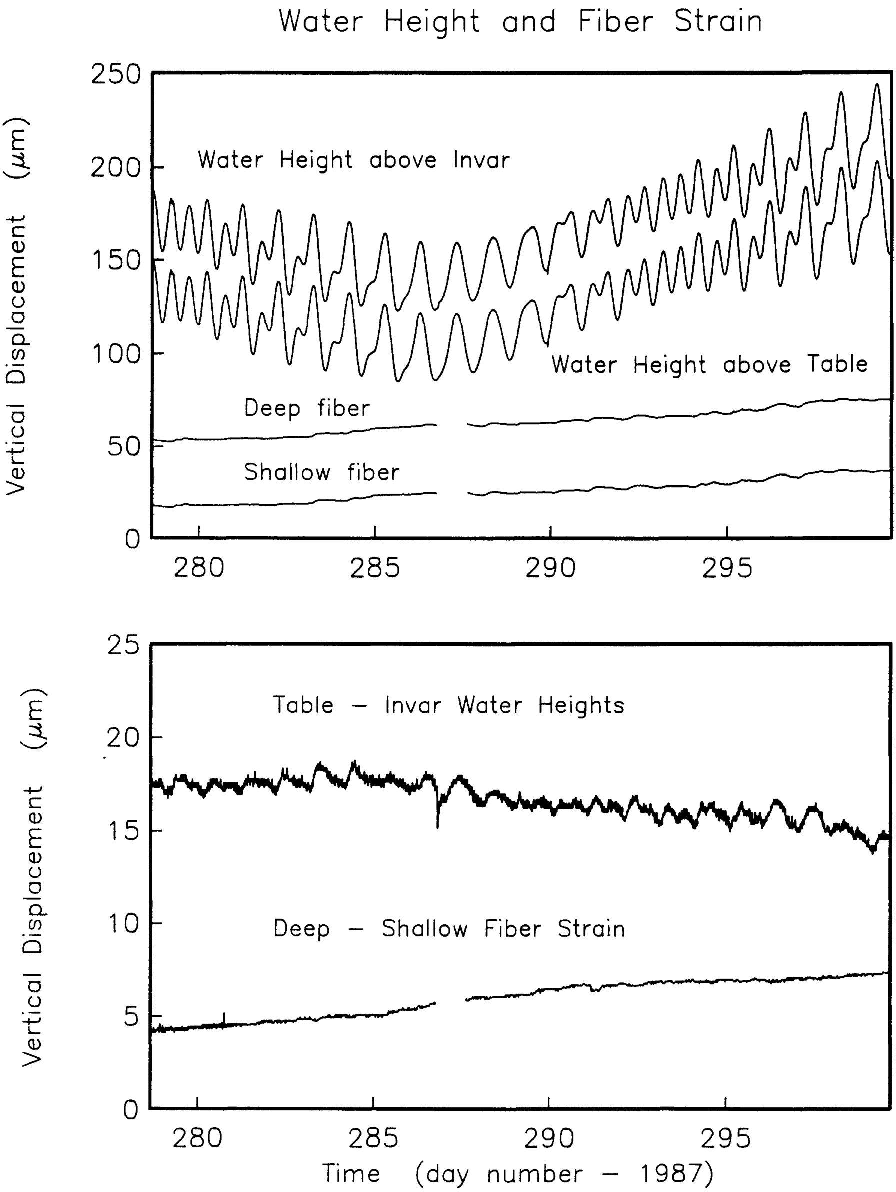
Water Height and Fiber Strain
Vertical Displacement (μm)
250
200
150
100
50
0
Water Height above Invar
Water Height above Table
Deep fiber
Shallow fiber
280
285
290
295
Vertical Displacement (μm)
25
20
15
10
5
0
Table – Invar Water Heights
Deep – Shallow Fiber Strain
280
285
290
295
Time (day number – 1987)

Figure 2.

Crustal Deformation Observatory: Part J
Askania Borehole Tiltmeter

14-08-0001-G1361

Frank Wyatt and Duncan Carr Agnew
Institute of Geophysics & Planetary Physics
University of California, San Diego
La, Jolla, California 92093-0225
(619) 534-2411

Walter Zürn
Geowissenschaftliches Gemeinschaftsobservatorium Schiltach
Universitäten Karlsruhe
D-762 Wolfach, Heubach 206, FRG

This grant supports the installation of an Askania biaxial borehole tiltmeter to a depth of 120 m at Piñon Flat Observatory and the analysis of observations from depth as well as those from its current 25-m-deep installation. This project is part of the overall Crustal Deformation Observatory program to understand vertical deformations and is a cooperative enterprise with Dr. Walter Zürn of Karlsruhe University (West Germany). The aims of this effort are to:

1) Establish techniques (and costs) for emplacing and orienting removable tiltmeters in boreholes of various depths, with special emphasis on developing methods that may be applied at depths of 100 m or more;
2) Compare these borehole tilt measurements with those from adjacent tiltmeters, including both long-base surface instruments and other borehole installations. Such comparisons will enable us to establish sources of instability and noise, and test the accuracy of different techniques; and
3) Monitor the signals produced by this high-quality borehole instrument to accurately record tilt in this tectonically active area.

Our primary task during this period has been to design the borehole casing and instrument housing for deep installation. The instrument requires a fully cased and dry well bore, vertical to within 3°. The housing will include a forced-alignment device, though, because of budgetary constraints, its orientation will not be known initially. Sometime in the next year we plan to remove the instrument temporarily and log the alignment guide using a gyro compass. This task will serve the additional purpose of investigating the sensor's response to removal and reinstallation: How quickly do the signals return to their previous trends?

Current records from the 25-m-deep installation show tilt rates of order 5×10^{-7} rad/yr, about 5 times greater than those from the adjacent long-base tiltmeters. We are continuing to investigate this sensor/installation's response to tides and high-frequency ground noise, both of which show unexpected behavior.

Creep and Strain Studies in Southern California

Grant No. 14-08-0001-G1177

Clarence R. Allen and Kerry E. Sieh
Seismological Laboratory, California Institute of Technology
Pasadena, California 91125 (818-356-6904)

Investigations

This semi-annual Technical Report Summary covers the six-month period from 1 April to 30 September 1987. The grant's purpose is to monitor creepmeters, displacement meters, and alignment arrays across various active faults in the southern California region. Primary emphasis focuses on faults in the Imperial and Coachella Valleys.

Results

Recent resurveys of alignment arrays across the eastern Garlock fault at CHRISTMAS CANYON and across the Mojave segment of the San Andreas fault at UNA LAKE, PALLETT CREEK, and CAJON show no evidence of creep, which is consistent with earlier behavior. On the San Jacinto fault zone, the alignment array at BAILEYS WELL continues to show 5 mm/yr of creep, as it has since installation in 1971. Farther southeast, the creepmeter at SUPERSTITION HILLS shows no slip since 1979, when ±11 mm of slip occurred in association with the Imperial Valley earthquake.

On the Imperial fault, recent resurveys of the alignment array at ALL AMERICAN CANAL show no clear evidence of creep, although most stations farther northwest along the fault do show evidence of continuing creep: At TUTTLE RANCH, creep ceased about 2-1/2 years following the 1979 Imperial Valley earthquake, but creep has now resumed at the pre-1979 rate of about 1 mm/yr. At HEBER ROAD, the creepmeter was continuing to register after-slip from the 1979 earthquake until January 1975, and recent readings indicate that the creep here has declined back to its pre-1979 rate of about 8 mm/yr. Data from the nearby ANDERHOLT ROAD nail-file array show a similar pattern. Likewise at ROSS ROAD, creep since July 1984 declined to its pre-1979 rate, at least up to the time the instrument was destroyed in 1985. A new invar-wire, satellite-telemetered creepmeter was installed here in April 1987, and no creep has been observed through September. Still farther northwest along the Imperial fault, alignment arrays at HIGHWAY 80 and WORTHINGTON ROAD show that creep is still occurring at rates well above that prior to 1979. Thus post-seismic slip related to the 1979 earthquake is still occurring on the northern Imperial fault.

Alignment arrays and creepmeters across the southernmost San Andreas fault in the Coachella Valley area have shown no anomalous behavior during the reporting period, although there tentatively appears to be a small triggered slip episode at the satellite-telemetered instrument at SALT CREEK at the time of the 1 October 1987 Whittier Narrows earthquake ($M_L = 6.1$), one day following the end of the reporting period.

Publications

Williams, P. L., McGill, S. F., Sieh, K. E., Allen, C. R., and Louie, J. N., submitted for publication, Triggered slip along the San Andreas fault after the July 8, 1986 North Palm Springs earthquake: Seismol. Soc. America Bull.

Digital Signal Processing of Seismic Data

9930-02101

William H. Bakun
Branch of Seismlogy
U.S. Geological Survey
345 Middlefield Road - Mail Stop 977
Menlo Park, California 94025
(415) 329-4793
(FTS) 459-4793

Investigations

Coordination of activities in the Parkfield prediction experiment. Analysis of USGS coda-duration measurements for magnitude determination.

Results

A real-time earthquake prediction experiment is underway at Parkfield.

Reports

Poley, C. M., A. G. Lindh, W. H. Bakun, and S. S. Shulz, 1987, Temporal changes in microseismicity and creep near Parkfield, California, Nature, vol. 327, p. 134-137.

Bakun, W. H., 1987 Future earthquakes, Contributions in Seismology, U.S. National Report to International Union of Geodesy and Geophysics 1983-1986; Reviews of Geophysics, vol. 25, pp. 1135-1138.

Bakun, W. H., 1987, Parkfield, California earthquake prediction experiment - An overview (abs.), EOS, American Geophysical Union Transactions, in press.

ATTACHMENTS: Following are the synopses from each of the Parkfield Data Review meetings held for months during the reporting period or meetings held during the reporting period.

PARKFIELD DATA REVIEW FOR MARCH 1987 Held 4/13/87

Although seismic activity was low at Parkfield in March, there were **two D-level seismic alerts** resulting from a M=1.8 shock at 11 km depth in MM3 on 3/14 at 1417 UTC and a M=1.5 shock at 11.7 km depth in MM3 on 3/27 at 1303 UTC. (The magnitude of the 3/27 shock was initially just below the M 1.5 threshold; subsequent processing resulted in a revised magnitude of 1.51.)

March was a very active month for creep happenings. The XPK1 and XMM1 instruments responded to rainfall of 3/5-3/6 with 1.0 mm and 0.7 mm of right-lateral movement respectively. The long-running **D-level creep alert at XMD1 (2/23-3/25)** due to 8.25 mm of continuing left-lateral movement, possibly due to rainfall and/or activity on the southwest fault trace, ended on 3/25 with a 1.0 mm right-lateral creep event, resulting in a **D-level creep alert** from 3/25-3/28. (A 0.3 mm right-lateral creep event occurred at XMM1 12 hours after the XMD1 creep event.) In addition, XTA1 had a **D-level creep alert** (3/15-3/18) due to 0.9 mm of left-lateral movement from 3/5-3/16, possibly related to rainfall and/or activity on the southwest fault trace. Finally, WKR1's 1.1 mm of right-lateral movement on 3/5-3/19, resulted in a **D-level creep alert on 3/15-3/19**; this alert was arbitrarily terminated on 3/19 by maintenance at the site. Reports of cracking along the southwest fault trace and felt reports of shocks by residents of Parkfield suggest that there is cause for increased awareness of the Parkfield monitoring networks.

The D-level seismic and creep alerts described above resulted, according to the combination rules, in **C-level alerts on 3/14-3/17 and on 3/27-3/30**. These C-level alerts were not recognized as such until after the fact: (1) The creep alerts from 3/14-3/17 were initially interpreted as effects of rainfall; (2) The seismic alert on 3/27 resulted from a late minor adjustment of a magnitude estimate.

There were no alerts on any of the continuous strain monitoring networks. The eight dilatational strainmeters are now recorded via the satellite telemetry and onsite by GEOS recorders. The tensor strainmeters at Eades and Froelich are now clearly showing north-south compression and east-west extension. There are now 7 water wells on satellite telemetry with 3 of the wells monitored at more than one perforation depth.

There were no alerts on the two-color geodolite network. (A level D alert would have been in effect on 3/19-3/24 using the proposed revised geodolite alert level criteria.) Loss of power on the blue laser coupled with poor visibility prevented some measurements early in the month; the blue laser failed completely on 3/14, was overhauled and returned to service on 3/16. (Some measurements early in March may have been biased owing to the weak return of the blue wavelength signal.) The effects of a strong areal dilatational trend are clear for early February through late March; this trend is similar to the beginning of the 3-month pattern preceding the 8/5/1985 Kettleman Hills shock.

Radon levels at the Miller Ranch located west of the San Andreas near Parkfield apparently changed by about a factor of 3 from mid-February to mid-March. Severe gaps in the data make interpretation difficult.

W.H. Bakun

II.2

PARKFIELD APRIL 1987 DATA REVIEW MEETING -Held 5/11/87

Seismic activity at Parkfield was at normal levels with one D-level alert (4/28/87 1916 UTC - 5/1/87 1916 UTC) from a M2.45 shock at 11 km depth in MM5. Most of the activity occurred in or north of the Middle Mtn. zone.

There was significant activity on the Parkfield creepmeters. Before 4/12 the creep rate at Slack Canyon was normal at about 23.8 mm/yr, but from 4/12-4/30 the sustained rate was 35.5 mm/yr. There were two D-level creep alerts caused by sustained (10 days) accelerated creep: XDR2 from 4/20-4/23 and XTA1 from 4/25-4/28. During April a creepmeter was installed on the Varian Ranch at the VAR4 alinement array site (nearly midway between XPK1 and XMD1).

No noteworthy unusual events of geophysical origin were recorded on the borehole strainmeter, tiltmeter, or magnetometer networks.

A changeover to higher resolution barometers during April is responsible for small offsets in the water levels reported; the offsets occur in the filtered water level data at the end of the barometer data gap. Permeability tests were performed at several wells in April; after the tests in the Middle Mtn. well, earth tide fluctuations were significantly reduced, perhaps because the 1/4" tube was clogged. A D-level water level alert was issued on 4/14 because of a rise in the deep well at Vineyard Canyon that began with an abrupt step of 4/9. A second abrupt step occurred on 4/16. On 4/17 the water level in the deep well at Middle Mtn. rose in association with a creep event recorded at XMM1, located about 1/2 km NW of the Middle Mtn. well. The total water level rise was 2.2 cm and the total slip at XMM1 was 0.7 mm.

Steady deformation at unusually high rates has been measured by the two-color network since about 4/17. Line-length change trends on lines to GOLD, MEL-S, MIDE, FLAT, BARE, CAN and BUCK range between 7.2 down to 2.4 times higher than previous long-term rates. The rates appear to be due to increased right-lateral slip on the main fault trace. The onset was more abrupt on lines near and SE of Car Hill than on lines to the northwest.

- W.H. Bakun

May 1987 Parkfield Data Review Meeting Held: June 8, 1987

Seismic activity was at a normal rate during May with no seismic alerts. There were 18 shocks, six of these at Middle Mtn. Two events occurred in MM3. There was unusual shallow activity (7 shocks) late in May (5/22-31) clustered near the northwest border of MM3.

There was in excess of 1.0 mm of right-lateral slip recorded 5/4-17 on the XTA1 creepmeter, resulting in a D(1)-level creep alert from 5/14-20. There was a 1.3 mm creep event on XGH1 on 5/28. Beginning 5/3, there was an apparent migration of right-lateral creep from XPK1 (1.4 mm on 5/3-10), to XMD1 (1.4 mm) and XMM1 (0.6 mm) on 5/7. The creep was seen as a 15.3 cm drop in the water level in the deep Middle Mtn. water well on 5/7. The first creepmeter on the southwest fracture zone was installed at the Kester Ranch (XRSW), near the location of the cracks on the Parkfield-Vineyard Canyon Rd. The Varian Ranch creepmeter (XVA1) installed last month is now on telemetry.

There were two D-level water well alerts. A level D alert (5/7-10) was caused by the 5/7 water level drop in the Middle Mtn. well, corresponding to 0.29 PPM volume strain. The slip at XMM1 (0.42 cm) is not large enough to account for the water level change which requires at least 5 mm of slip if the slip extended to 1 km depth. On 5/16, the water level in the deep well at Middle Mtn. rose 3.4 cm in association with a 0.6 mm creep event at XMM1, corresponding to a D-level alert (5/16-19)

There were no strain alerts in May. Although the Eades dilatometer detected a strain event associated with the early May creep event at XPK1, the Gold Hill strainmeters did not see any effects of the 5/28 XGH1 creep event, even though earlier comparable creep signals had been detected. The DCPS on the tensor strainmeters are broken, and the Eades tensor strainmeter "software" is broken.

Significantly higher rates of line length changes on the CAN, MIDE, BARE, BUCK, POMO, LANG, TODD, CREEK, FLAT, MEL S, and TABLE lines from 4/15-18, resulted in a D-level two color alert from 5/1-18. Because of the combination rules, there was a continuous C-level alert from 5/4-18. Because the two color alert was only recognized in retrospect, the C-level alert status was not recognized at the time.

There were no reported unusual signals in May on the tilt, magnetometer, or geochemistry networks operated at Parkfield.

- W.H. Bakun

JUNE 1987 PARKFIELD DATA REVIEW MEETING Held 7/13/87

Seismic activity was normal at Parkfield during June. Small earthquakes occurred in and north of the Middle Mtn. zone, but no shocks occurred in MM3. There was no seismic alerts.

June was a quiet month for the Parkfield creepmeter network as well. There were no alerts and only a few events. With the completion of the Varian Ranch (XVA1), Roberson southwest (XRSW) and the Hearst southwest (XHSW) creepmeters, the installation of the new creepmeters funded by AB938 has been completed.

The high rates of deformation recorded since mid-April 1987 by the two-color geodimeter network continued through June. Recent trends resemble the trends preceding the August 1985 North Kettleman Hills earthquake, except that the recent trends are significantly higher. While the rapid deformation near the northwest edge of the net slowed in early June, the high rates on the central part of the network continue, so that the D-level geodimeter alert in force since April continued through the month of June. (The number of two-color lines and the individual lines contributing to the alert status have changed over the past few months.)

There were no alerts on the dilatometer array although subtle coherent changes from 1-20 May are consistent with the geodimeter observations of the past few months. There were no alerts and no unusual changes in the water levels in the seven Parkfield wells now being monitored. Obstructions in the Middle Mtn. water well continue to negatively affect the utility of that well for observing fluctuations that might be tectonic in origin.

- W. H. Bakun

JULY 1987 PARKFIELD DATA REVIEW MEETING

held 8/10/87

(revised summary 8/17/87)

There were no **seismic** alerts at Parkfield during JULY. The largest event was the M=2.4 shock that occurred at 4 km depth near Gold Hill at 2122 UTC on JULY 9. The remainder of the planned GEOS-recorded FBA units were installed and are now fully operational. The CALNET stations Parkfield (PPF) and Turkey Flat (PTF) were removed at the request of the landowner.

There were no **creep** alerts during JULY. Two events were of interest: (1) a two-day 1.5 mm right-lateral surge on 7/12-14/87; and (2) a 1.3 mm right-lateral creep event at XGH1 on 7/30-31/87. The Durham Ranch creepmeter (XDR2) was removed at the request of the landowner.

There were no alerts or unusual signals on the **strainmeters**. The Donalee tensor strainmeter is again operational, thanks to replacement electronics boards sent by Mick Gladwin. The EADES dilatometer was removed at the reqeust of the landowner.

The **water level** rise of 4.5 cm at Flinge Flat on 7/3/87 at 0600 UTC should have been declared a **D-level alert**. The water level appeared to return to its previous level within the ten days after the rise.

The **D-level geodimeter** alert continued throughout the month of JULY, except for a 5-day span (7/13-17/87) when the number of lines with unusual rates of extension fell below 3 (the minimum required for an alert). From 4/12/87 to 7/29/87 the pattern of deformation has deviated from the background (1984-1987) pattern in that shallow slip monitored by the two-color network (and confirmed by the creepmeter observations) has been peaked at Middle Mtn. and near Car Hill, with a well-developed minimum in between. **Two-color** reflector sites at NORM and FLAT were removed at the request of the landowner; the line to FLAT has been replaced by a similar line to TURK and the replacement for NORM (to be NORE) is scheduled.

The **D-level water well** alert (7/3-6/87) and the continuous **D-level geodimeter** alert combine to give a **C-level alert** for 7/3-6/87. Because these alerts were not recognized immediately, the notifications (to Chief OEVE, and to OES) appropriate to a **C-level alert** were not carried out.

- W.H. Bakun

AUGUST 1987 PARKFIELD DATA REVIEW MEETING Held 9/14/87

Seismic activity during August was normal in number of shocks, but unusual in that there were 5 D-level seismic alerts:

8/7/87	0425 GCT	M=2.3	9.9 km depth	MM3
8/7/87	1055 GCT	M=1.3	10.2 km depth	MM3
8/15/87	1604 GCT	M=2.6		Simmler
8/15/87	1752 GCT	M=2.5		Simmler
8/28/87	2039 GCT	M=2.1	10.4 km depth	MM3.

The 5 Simmler shocks on 8/15/87 are interesting in that earlier unusual Simmler activity has been correlated with significant seismicity elsewhere in the region; the 8/15/87 shocks are not correlated with any obvious external trigger events.

Three was a C-level creemeter alert on 8/3/87 with nearly simultaneous events at the adjacent XMD1 (1.5 mm right-lateral slip beginning 0940-0950 GCT) and the XMM1 (0.9 mm right-lateral slip beginning 1020-1030 GCT) sites. Overall, the creepmeter network shows typical movements for this time of year.

There was a D-level water well alert on 8/3/87 starting 0946 GCT and 1001 GCT when the water level dropped in both the deep and shallow intervals of the Middle Mtn. well. The onset of the water level drop is between the onset of creep at XMD1 and XMM1 and precedes by 4 days the D-level shocks on 8/7 in MM3 that were described above. Recent delivery of long-awaited recorders and DCPs should allow for significant expansion of the water wells monitored at Parkfield.

There were no dilatometer, magnetometer, or tiltmeter alerts. The only unusual and unexplained strainmeter signal occurred at the Jack Canyon dilatometer beginning 8/28/87: Magnetic field data recorded at Turkey Flat (TFLM) indicate a change starting the end of May 1987 of about 0.9 nT; If the current rate of change continues, the 1 nT D-level threshold would be exceeded during September.

Deformation recorded by the 2-color geodimeter netwowrk during August was complex, including shallow slip at high rates along the main fault trace, areal extension, and reversal of trends for stations BUCK and HUNT. Level-D two-color geodimeter alerts were in effect 8/5-21/87. Revision of the processes for identifying level-D two-color alerts are in preparation, largely because the current procedures result in an unacceptably high background of two-color alerts.

- W.H. Bakun

SEPTEMBER 1987 PARKFIELD DATA REVIEW MEETING Held 10/13/87

The highlight of the month was the unique pattern of creep and seismicity that were observed during September 13-23, 1987. The events are described in detail in the attached memo (dated 9/23/87) to John Filson. These events were treated with considerable concern, consistent with that of a C-level alert.

There were a total of 11 shocks, the largest being M=1.9, in the swarm location in MM3 that is described in the attached memo. Because these shocks were at 6 km depth, they did not constitute any formal alerts, even though they were a cause of concern at the time. There was a level D seismic alert on 9/22/87 at 0031 GCT due to a M1.7 shock at 7.5 km depth in MM3.

Although there were no creep alerts in September, the unusual creep surges described in the attached memo were a major part of the 9/13-23/87 concern. There was a 0.7 mm right-lateral creep event at XMM1 on 9/22/87.

Water level rises occurred in 9/22/87 in both the deep and the shallow intervals of the Middle Mtn. well, essentially simultaneous with the XMM1 creep event. On 9/24/87 the rise in the deep interval reached 2.5 cm, the level D threshold for that sensor. The seismic D alert and the water level D alert combined for a C-level alert for 9/24-25/87.

There were no unusual signals or alerts on the dilatometer, magnetometer, or two-color geodimeter networks during September. Although the rates of the geodimeter line length changes were faster than the long-term rates, they were slower than the unusual rate changes of the last few months.

- W.H. Bakun

United States Department of the Interior

GEOLOGICAL SURVEY
OFFICE OF EARTHQUAKES, VOLCANOES, AND ENGINEERING
Branch of Seismology
345 Middlefield Road, Mail Stop 977
Menlo Park, California 94025

September 22, 1987

TO: John Filson
FROM: Bill Bakun Bill
RE: The Unique Parkfield Creep and Seismicity Patterns of September 13-22, 1987

Creep. Beginning September 13, 1987, the Parkfield (XPK1), Taylor Ranch (XTA1), and Carr Ranch (CRR1) creepmeters recorded an essentially simultaneous onset of a creep surge that by September 21, 1987 has totalled 0.9 mm, 1.1 mm, and 0.4 mm of right-lateral slip respectively. The signals at these three sires are highly correlated, suggesting coherent shallow slip over a 10-15 km length of fault within the 1966 Parkfield rupture zone. Although the near simultaneous nature of the creep signals was not explicitly described in "Parkfield, California earthquake prediction scenarios and response plans" (USGS OFR 87-192), the coherence of several signals is unprecedented not only for Parkfield observations, but for creepmeter observations in general.

The Middle Ridge creepmeter (XMD1), which normally records 1 mm of right-lateral slip/10 days, recorded 1.0 mm for 9/11 - 9/21, so that it is consistent with the XPK1 and XTA1 observations for 9/13 - 9/21. In this context, the unusual creep recordings can be viewed as an extraordinary high creep rate over the 10-15 km south of XMD1 equaling the normal high creep rate seen at the XMD1 site. Note that the Work Ranch (WKR1) and Varian Ranch (XVA1) creepmeters have not yet participated in the ongoing creep surge; even though XVA1 lies between XMD1 and XPK1 and WKR1 lies between XTA1 and CRR1. The rate has decreased in the past few days, although the creep surge has not yet ended.

On September 22 at 8:30 A.M. PDT, a large creep event (1/2 mm of right-lateral slip in the first 40 minutes) occurred at XMM1. The event just missed triggering a D level alert (1/2 mm in first 30 minutes).

Seismicity. On September 18, a swarm of five M1-2 shocks occurred in a 7 minute span at 5 km depth on the San Andreas fault just north of XPK1. (see the attached epicenter lists for September). The swarm nature of seismicity is unprecedented in the detailed recordings of Middle Mtn. seismicity since 1971. Three more shocks (M 2.0, M 1.5, M 1.5) occurred at the same hypocenter on 9/19, and an M 1.3 shock occurred there on 9/21.

On September 21 5:30 P.M. PDT a magnitude 1.6 shock occurred at 7km depth in MM3. This constitutes a D-level seismic alert. This shock is just north and a little northwest of the swarm hypocenter.

Other Networks. Examinations of the water well, dilatometer, tensor strain, and 2-color geodimeter network observations have revealed no evidence for significant slip at depth over the 9/13 - 9/21 time span. That is, there is no evidence, other than the microearthquake swarm described above (spatial extent approximately 100-200 m), that the 1 mm slip recorded by the creepmeters extends deeper than about 1 km.

We are continuing to monitor the situation closely for any indication that the fault at depth is participating significantly in the current Parkfield happening. We emphasize that the unique nature of both the creep and siesmicity are cause for serious concern. The Parkfield Working Group is proceeding according to the response for a C-level Parkfield alert, even though formally we are at a D level condition. Note that the finite set of conditions described in USGS OFR 87-192 anticipated neither the current creep nor the current seismicity patterns so that the formal plan cannot adequately reflect the Parkfield Working Group's current assessment of the seismic hazard in the Parkfield area.

Parkfield

87	9	2	747	55.99	36	1.49	120	34.69	2.72	1.40	6	152	4.8	0.11	0.8	2.7
87	9	7	749	8.61	36	1.45	120	34.76	5.08	1.80	10	150	4.8	0.10	0.6	1.9
87	9	6	437	15.41	35	58.59	120	32.17	3.90	1.50	7	148	4.2	0.02	0.5	2.3
87	9	8	1631	44.08	35	53.48	120	26.53	10.74	1.30	9	193	4.3	0.05	1.0	1.2
87	9	8	2245	1.70	36	4.23	120	30.00	6.94	1.80	14	62	2.3	0.10	0.3	0.8
87	910		440	19.45	35	58.95	120	33.08	7.35	1.20	5	168	4.6	0.01	1.0	1.3
87	910	11	6	30.78	36	0.78	120	34.49	5.70	1.20	4	211	3.9	0.00	2.3	2.1
87	913	16	1	52.00	36	0.33	120	34.34	5.70	1.90	21	100	3.5	0.07	0.2	0.3
87	914		726	45.97	36	3.58	120	37.86	6.15	1.40	4	206	8.7	0.01	3.5	1.9
87	918		1050	28.28	35	55.30	120	28.10	5.21	1.90	10	76	3.7	0.11	0.5	1.5
87	918		1050	40.45	35	55.14	120	28.36	5.04	1.20	7	157	3.4	0.11	0.8	1.6
87	918		1055	5.17	35	55.61	120	26.17	5.25	1.80	18	124	3.5	0.08	0.3	0.4
87	918		1056	17.60	35	55.27	120	29.03	5.63	1.50	6	194	2.4	0.03	0.9	1.0
87	918		1057	34.76	35	55.57	120	28.19	5.25	1.70	9	161	3.5	0.05	0.5	0.8
87	919	0	2	31.48	35	55.32	120	24.45	5.07	2.00	22	131	3.2	0.07	0.4	0.4
87	919		235	25.70	35	55.26	120	28.98	5.64	1.50	7	190	2.5	0.02	0.9	1.0
87	919		347	57.44	35	55.42	120	29.01	5.32	1.50	6	196	2.3	0.03	0.9	0.9
87	921		1046	25.67	35	55.46	120	29.03	5.25	1.30	6	195	2.3	0.03	0.9	0.9
87	922		031	3.16	35	57.85	120	31.10	7.34	1.70	16	75	2.0	0.08	0.4	0.5

Middle mountain relocations

87	9	6	437	15.38	35	58.80	120	31.97	3.39	1.50	7	158	4.2	0.02	0.5	1.5
87	910		440	19.42	35	59.14	120	32.95	7.45	1.10	5	172	4.8	0.00	1.4	4.4
87	918		1050	28.29	35	55.39	120	28.28	5.14	1.90	10	76	3.4	0.06	0.4	1.1
87	918		1050	40.43	35	55.43	120	28.42	5.20	1.20	7	147	3.2	0.06	0.5	1.0
87	918		1055	5.20	35	55.48	120	28.13	5.37	1.80	20	76	3.2	0.06	0.3	0.4
87	918		1056	17.50	35	55.47	120	28.41	5.73	1.50	6	218	3.2	0.03	1.2	1.0
87	918		1057	34.78	35	55.42	120	28.19	5.53	1.70	9	154	3.0	0.03	0.5	0.7
87	919	0	2	31.44	35	55.44	120	28.41	5.26	2.00	24	104	3.2	0.06	0.3	0.3
87	919		235	25.60	35	55.44	120	28.44	5.77	1.50	7	217	3.2	0.03	1.1	1.0
87	919		347	57.34	35	55.62	120	28.37	5.30	1.50	6	220	3.2	0.04	1.1	0.9
87	921		1046	25.56	35	55.67	120	28.39	5.30	1.30	6	221	3.2	0.03	1.1	0.9
87	922		031	3.19	35	57.94	120	31.11	6.85	1.70	16	76	2.2	0.03	0.3	0.5
87	922		1654	44.9	36	1.98	120	35.49	6.10	1.00	6	201	5.4	0.01	0.1	0.1

Earthquake Prediction Research in the Anza-Coyote Canyon Gap

14-08-0001-G1373

Jonathan Berger and James Brune
Institute of Geophysics and Planetary Physics
Scripps Institution of Oceanography
University of California, San Diego
La Jolla, CA 02193
(619) 534-2889

Introduction. We have found a model for the laterally averaged crustal P-wave velocity structure in the region of the Anza Seismic Array on the San Jacinto fault using the simultaneous earthquake location-velocity inversion method outlined by Spencer and Gubbins (1980) and Pavlis and Booker (1980). Patterns of seismicity are much clearer using events relocated with the new structure though some residual signal indicates the need for a 3-D model.

Data. The dataset consists of 314 events recorded by both the Anza Seismic Array and the Caltech SCARLET Array. A total of 5054 P-wave arrival times from the 10 Anza stations and 13 Caltech stations are used in the inversion. Only high quality picks with assigned weights of 0 or 1 are included. All of the stations are located entirely within the Peninsular Range Batholith, a body of intrusive and metamorphic rocks present on both sides of the San Jacinto Fault Zone (Fig. 1). The lack of large sedimentary features within the study area should help to minimize lateral variations of the velocity structure. There is tremendous topographic relief in the area. The lowest station, LAQ, is at 49 meters elevation and the highest, TRO, is at 2657 meters. For this reason the ray tracing algorithm traces rays directly to the elevation of the station rather than applying an *a priori* station delay model to the data.

Modeling. The velocity model is parameterized as a sequence of velocities specified at fixed depth nodes. The velocity gradient is constant between model nodes. This type of model is chosen as opposed to a homogeneous layered model because the crystalline geology of the region would not be expected to require sharp discontinuities. Measurements of shear and compressional velocities in boreholes at two of the stations, KNW and PFO, (Joe Fletcher, unpublished data, 1987) are used to constrain the surface velocity (5.2 ±.1 km/sec). The starting model is taken from laboratory measurements of granite as a function of pressure (Press, 1966). The solution vector is cast as the differences between consecutive model node slownesses. Thus, by using fewer than the total number of singular values from the eigenvalue decomposition of the matrix, we are effectively finding models with the minimum velocity gradient. In the inversion we incorporate the idea of projecting the data onto the nullspace of the earthquake hypocenter parameters before inverting for the velocity parameters (Pavlis and Booker, 1980). In this way, we can treat an arbitrary number of events without computational difficulty.

Results. After two iterations the velocity model converged to the following (Fig. 2):

Velocity (km/sec)	Depth (km)
5.22	0.00
5.42	2.00
5.66	4.00
5.94	6.00
6.07	8.00
6.13	10.00
6.16	12.00
6.18	15.00
6.18	20.00
6.18	25.00

The 314 events are relocated with this model. Comparing the locations made with only arrival times from the Anza array (Fig. 4) with the locations using both arrays (Fig. 5), we see that clusters of events have become more linear features. Notice in particular the cluster of events just southwest of station CRY and the cluster just south of station KNW. The CRY cluster clearly shows up in cross section (Fig. 6) as a small steeply dipping fault at about 5 km depth. The events in the KNW cluster are considerably deeper than the other events. This may be due to tradeoffs between velocity and depth in the inversion and should become better resolved in future inversions in which S-wave arrival times will be included.

Station corrections are not included in the inversion, but will be incorporated in the future, probably using the same method of projection in order to separate the station corrections from the velocity parameter inversion. Mean travel-time residuals are calculated at each station using the relocated events. These should roughly correspond to the station corrections had they been included in the inversion. Some of the stations, such as WMC, have significantly higher or lower means (Fig. 3). But some stations, such as CAH, have a bimodal distribution. This may be due to lateral differences in velocity structure for paths from events in the CRY cluster and paths from the rest of the events.

Acknowledgements. This report summarizes research carried out by Jennifer Scott and Frank Vernon. We would like to thank Susanna Gross and Lucy Jones at U.S.G.S. Pasadena and Joe Fletcher and Linda Haar at U.S.G.S. Menlo Park for their help in acquisition of the dataset. The helpful advice of Guy Masters at I.G.P.P. is also greatly appreciated.

REFERENCES

Pavlis, G. L. and Booker, J. R. The mixed discrete-continuous inverse problem: Application to the simultaneous determination of earthquake hypocenters and velocity structure. *J. Geophys. Res.* **85**: 4801-4810, 1980.

Press, F. Seismic Velocities, in *Handbook of Physical Constants*, G.S.A. Memoir 97, 195-218, 1966.

Sanders, C. O. Seismotectonics of the San Jacinto Fault Zone and the Anza Seismic Gap, Ph.D. Thesis, California Institute of Technology, Pasadena, 179 p., 1986.

Spencer, C. and Gubbins, D., Travel-time inversion for simultaneous earthquake location and velocity structure determination in laterally varying media. *Geophys. J. R. Astr. Soc.* **63**: 95-116, 1980.

FIGURES

Figure 1. Map of Anza Array and Caltech SCARLET Array stations that were used. All stations are located within the Peninsular Range Batholith, the shaded region.

Figure 2. Velocity model derived after two iterations and used for relocations of events. The velocity at surface was fixed at 5.2 ±.1 km/sec. Depth is measured from the top of the model at 2657 meters elevation.

Figure 3. Example of residuals at two stations after relocation of events. Note the bimodal distribution at CAH due to two distinct source areas.

Figure 4. Events located with only Anza Array stations using a model consisting of 3 homogeneous layers. Events tend to fall in clusters.

Figure 5. Events located with Caltech and Anza Array stations using the model derived in this inversion. Notice the linear trends of events. Locations of cross-sections are shown.

Figure 6. Vertical sections along the lines shown in Figure 5. The maximum projection distance is 6 km. Fault planes can be seen clearly in section C-C′. The depth distribution of events is similar to that found by Sanders (1986) but linear trends associated with faults are clearer.

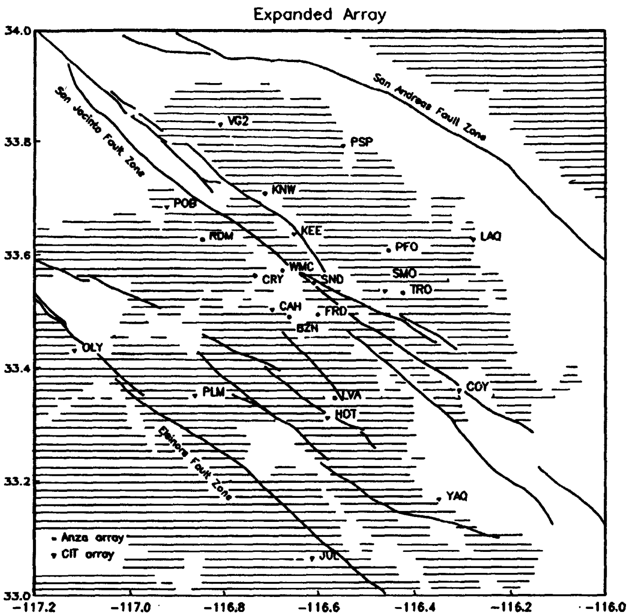

Figure 1

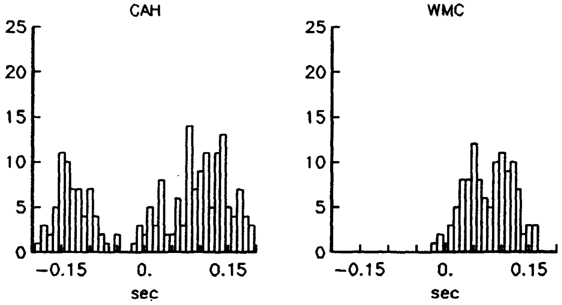

Figure 3

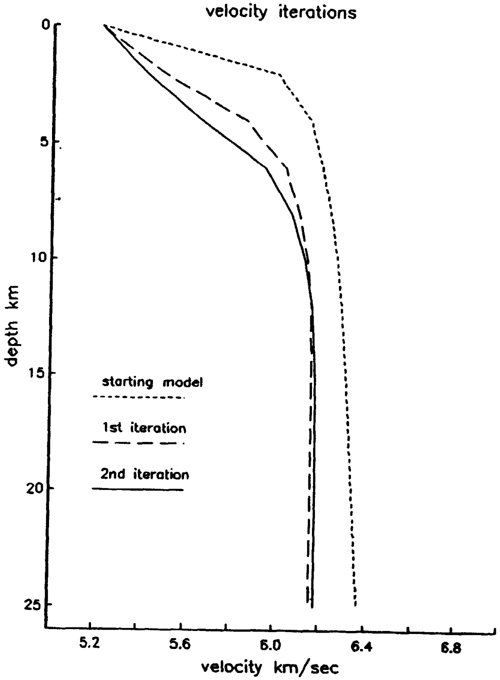

Figure 2

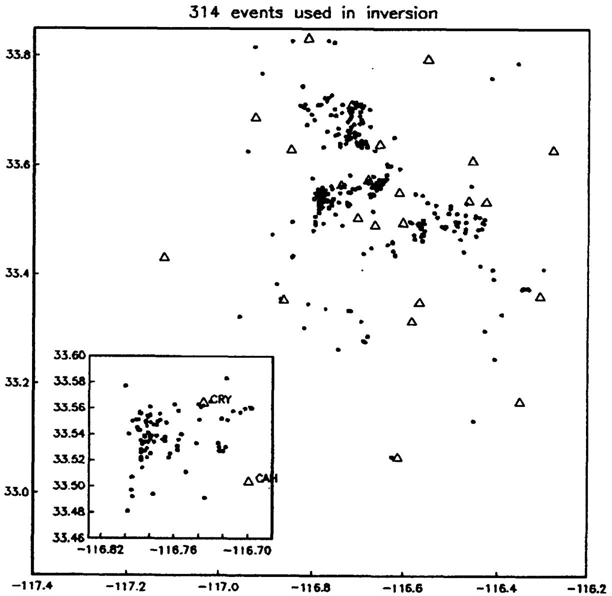

Figure 4

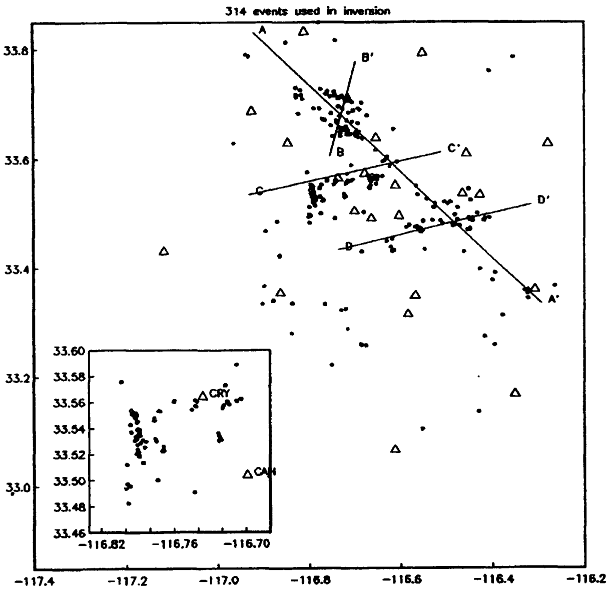

Figure 5

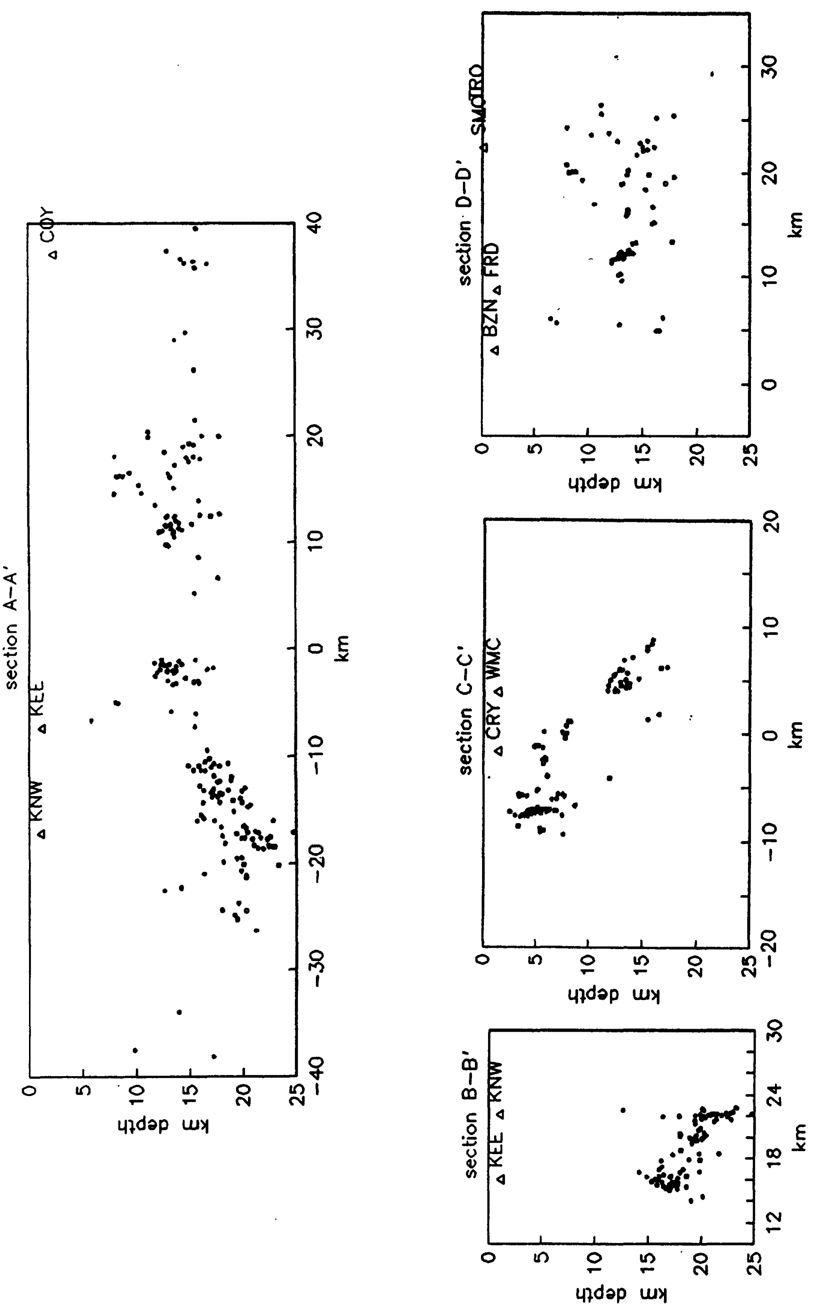
section A-A'
KNW
KEE
COY
km depth
0
5
10
15
20
25
-40
-30
-20
-10
0
10
20
30
40
km
section B-B'
KEE
KNW
12
18
24
30
section C-C'
CRY
WMC
-20
-10
0
10
20
section D-D'
BZN
FRD
SMC
TRO

Figure 6

Acceleration, Velocity, and Volumetric Strain from Parkfield GEOS Network

9910-02089

Roger D. Borcherdt, Malcolm J. Johnston, Allan Lindh
Branch of Engineering Seismology and Geology
345 Middlefield Road, MS 977
Menlo Park, California 94025
(415) 329-5619

Investigations

As part of Parkfield Prediction Experiment install GEOS network to acquire on-scale, broad-band, high-resolution measurements for earthquakes occurring on and near the segment of the San Andreas fault that ruptured during the 1966 Parkfield earthquake. On-scale measurements of ground acceleration for events in the preparation zone are intended for all events larger than magnitude 2. On-scale measurements of pre-, co-, and post-seismic volumetric strain are intended for all events with sensitivities exceeding 10^{-11} strain near 1 Hz.

Results:

1) Installation of a 14 station network surrounding the 1966 rupture zone was completed July, 1987 by T. Noce working in conjunction with project principals, G. Glassmoyer, D. Myren and T. Burdette. Location map for stations is given in figure 1. Five of the stations are configured to record three components of ground acceleration (Kinemetrics FBA-13) together with three channels of volumetric strain (Sacks-Evertson dilatometer; 2 channels in AC coupled mode at 2 gain levels, and 1 channel in DC coupled mode). One of the stations is configured to record three components of ground velocity together with three channels of volumetric strain. Eight of the stations are configured to record three components of acceleration and three components of ground velocity. The signals from the sensors at each of the sites are being recorded with the GEOS programmed to operate in a six-channel, event trigger mode at 200 sps per channel. Data is being played back using the PDP 11-70 RSX system at Menlo Park. Stations at Gold Hill, Vineyard Canyon, and Joaquin Canyon have been in operation since 1984-85. The other eleven stations were put into operation during the time interval November 1986, July 1987.

2) Several small events with magnitude less than 2.8 have been recorded at individual stations, but as of end of report period no larger events had occurred in vicinity of network.

Reports

See related project reports: Borcherdt, 9910-02689; Maxwell and Borcherdt, 9910-03009.

10/87

PARKFIELD GEOS STATIONS

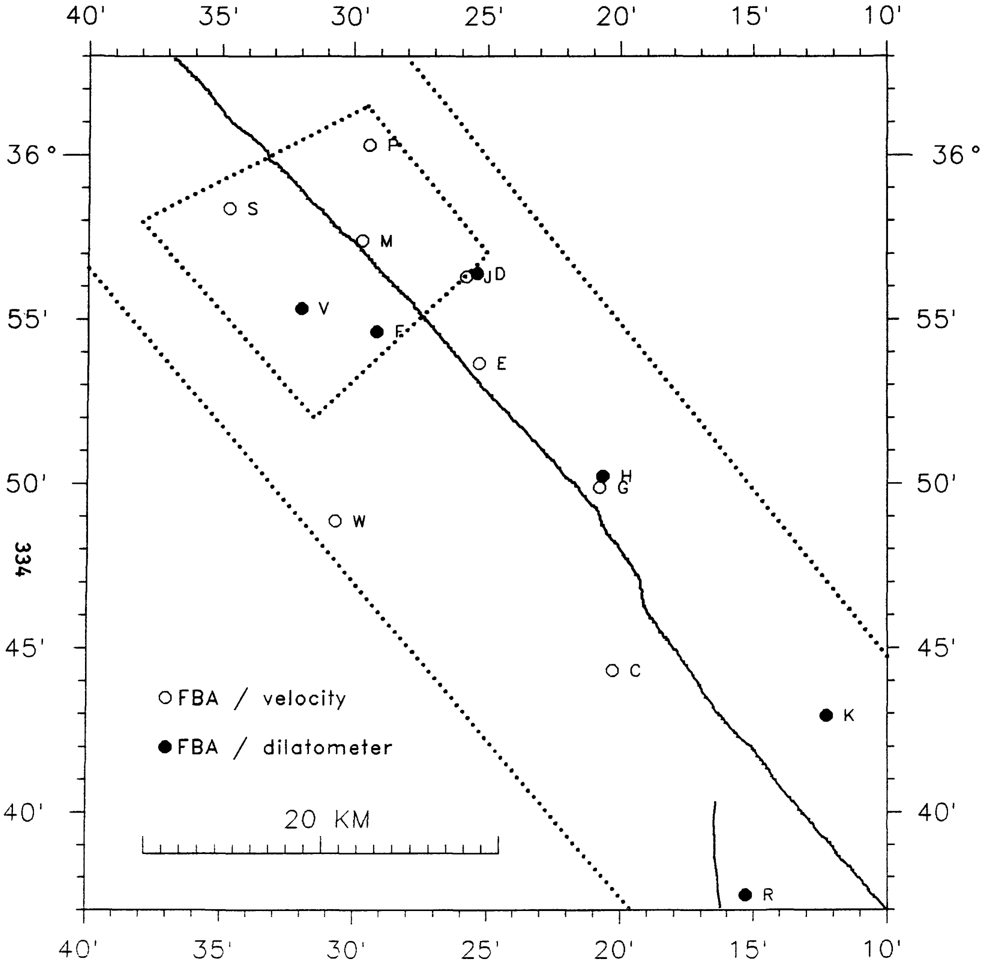

P = Reason Peak
S = Stockdale Mountain
M = Middle Mountain
D = Donnalee
J = Joaquin Canyon
V = Vineyard Canyon
F = Froelich
E = Eades / Taylor
H = Gold Hill 2
G = Gold Hill
W = Work Ranch
C = Cholame Hills / White Canyon
K = Jack Canyon
R = Red Hills

FIGURE 1

PARKFIELD TWO-COLOR LASER STRAIN MEASUREMENTS

9960-02943

Robert Burford
Branch of Tectonophysics
U.S. Geological Survey
345 Middlefield Road, MS/977
Menlo Park, California 94025
(415) 329-5922

and

Larry Slater
CIRES
University of Colorado
Boulder, Colorado 80309
(303) 492-8028

Investigations

Operation of the CIRES two-color laser geodimeter at the Car Hill Observatory near Parkfield, California was continued during the period April 1 through September 30, 1987. Lines to permanent reflector sites that were monitored for length changes during this period are shown in Figure 1. Additional measurements were made occasionally to monumented points without permanent reflectors as well as to reference marks adjacent to the permanent reflectors.

Results

Plots of detrended length-change histories for the 19 lines to permanent reflector points are shown in Figure 2. The average rate of length change determined by linear least-squares approximation for each line is given in Table 1. Average station velocities relative to Car Hill for motion constrained to be parallel to the strike of the San Andreas fault zone are also given in Table 1 (negative values denote apparent left-lateral motion).

Reports

Burford, R.O., Langbein, J.O., Slater, L.E., and Hamann, D.M., 1987, Deformation within the two-color laser geodimeter network across the San Andreas fault at Parkfield, California (abs.): EOS, Program for Fall AGU, San Francisco.

Table 1

Summary of Monitoring Results
Two-Color Laser Geodimeter Network at Parkfield
April 1 through September 30, 1987

Permanent 2-Color Reflector Sites		Measurements Started	Location Relative to Car Hill	Average Extension Rate, mm/yr	Fault Parallel R.L. Station Velocities
1.	Can	10/09/84	5.7 km N03°W	-06.84 ± 0.46	08.85 ± 0.60
2a.	Nore	08/13/87	1.1 km N44°E	-06.48 ± 1.36	(136.00 ± 28.55)
2b.	Norm	11/14/85	1.1 km N45°E	+03.90 ± 0.51	(-74.51* ± 9.69)
3.	Table	10/09/84	6.2 km N69°E	+09.04 ± 0.54	(25.45 ± 1.52)
4.	Hunt	07/28/85	2.7 km S72°E	+13.38 ± 0.29	15.53 ± 0.33
5.	Mel-S	10/14/84	5.4 km S68°E	+13.01 ± 0.47	14.51 ± 0.52
6a.	Flat	09/25/85	1.8 km S60°E	+23.30 ± 0.48	24.50 ± 0.51
					17.98 ± 0.68(avg)
6b.	Turk	07/10/87	2.3 km S47°E	+09.38 ± 0.83	9.78 ± 0.87
7.	Gold	04/18/86	9.2 km S49°E	+18.35 ± 1.16	18.48 ± 1.17
8.	Creek	06/27/84	5.7 km S36°E	+11.42 ± 0.56	-11.49* ± 0.57
9.	Mason-W	06/26/84	6.3 km S11°W	+03.02 ± 0.53	-4.98* ± 0.88
10.	Todd	08/07/85	3.7 km S15°W	+18.36 ± 0.37	-33.26* ± 0.68
11.	Hog-S	07/25/84	5.0 km S62°W	+01.28 ± 0.43	(5.29 ± 1.78)
12.	Lang	07/25/84	4.1 km N72°W	+00.14 ± 0.41	0.16 ± 0.47
13a.	Pomo	04/29/86	5.6 km N51°W	+11.55 ± 0.49	11.71 ± 0.50
13b.	Pitt**	10/09/84	5.7 km N47°W	not determined	-------------
14.	Mid	08/23/84	5.0 km N43°W	-00.21 ± 0.45	00.21 ± 0.45
15a.	Mid-E	08/21/84	4.5 km N35°W	-34.85 ± 0.38	35.13 ± 0.39
15b.	Buck	07/31/86	3.1 km N32°W	-13.91 ± 0.32	14.10 ± 0.33
16.	Bare	10/09/84	4.8 km N12°W	-15.73 ± 0.42	18.13 ± 0.48

NOTE: (*) Indicates apparent left-lateral station movement (column 5)
( ) Fault-parallel projection values in column 5 are unreliable owing to orientation of line nearly normal to fault strike.
(**) Routine measurements discontinued after June, 1986.

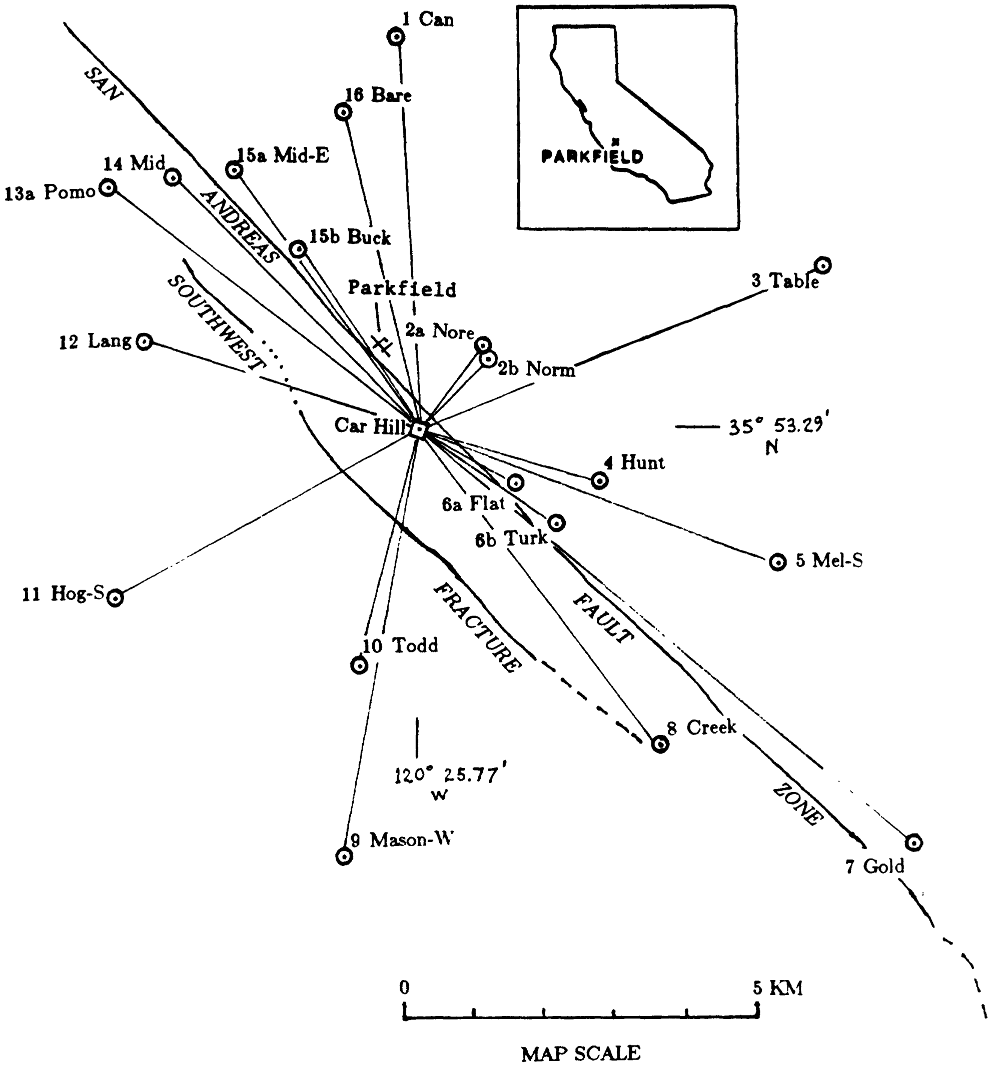

Figure 1. Two-color laser geodimeter network at Parkfield, California.

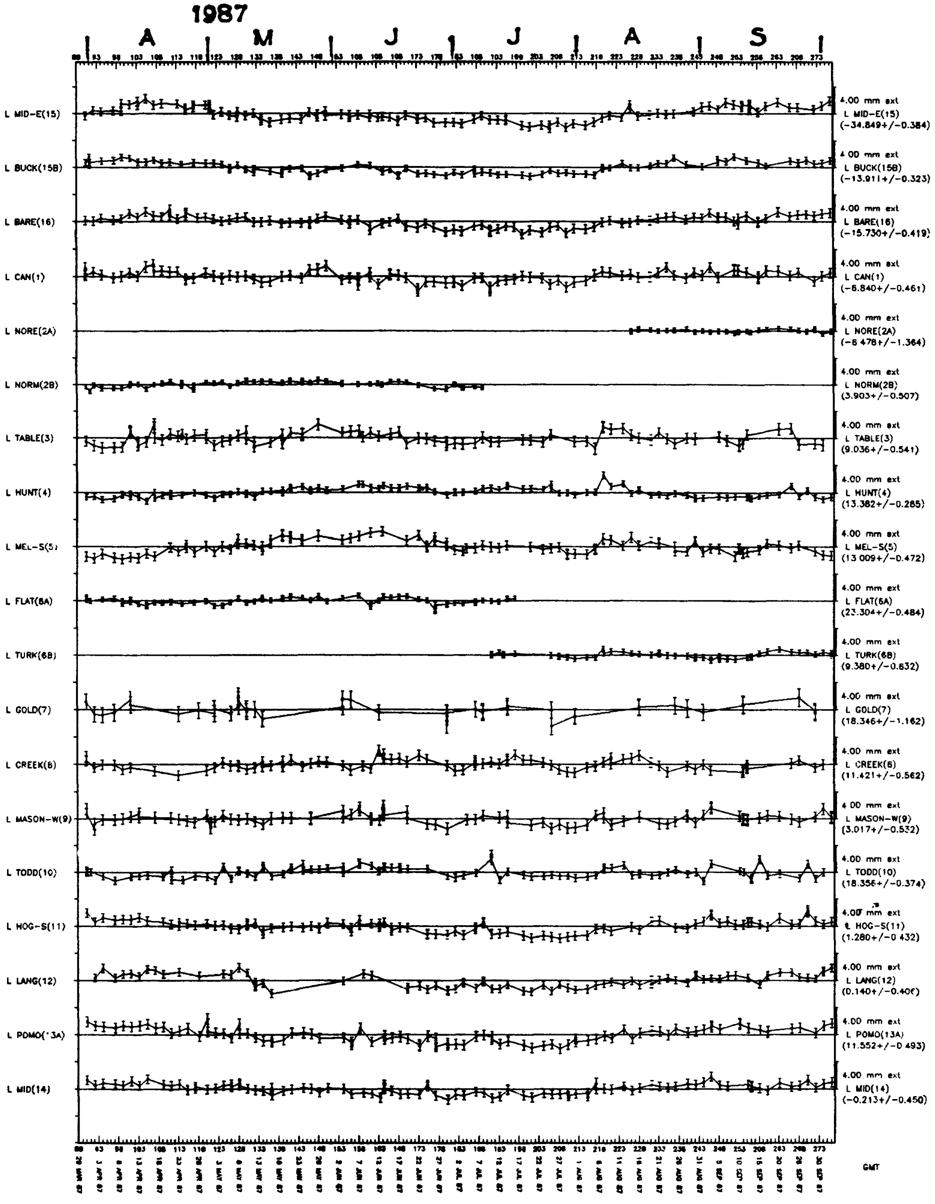

DETRENDED TWO-COLOR DATA, APRIL-SEPTEMBER, 1987

Figure 2. Detrended line-length histories, Parkfield two-color geodimeter network, April through September, 1987.

Theodolite Measurements of Creep Rates on San Francisco Bay Region Faults

14-08-0001-G1186

Jon S. Galehouse
San Francisco State University
San Francisco, CA 94132
(415) 338-1204

We began measuring creep rates on San Francisco Bay region faults in September 1979. Amount of slip is determined by noting changes in angles between sets of measurements taken across a fault at different times. This triangulation method uses a theodolite to measure the angle formed by three fixed points to the nearest tenth of a second. Each day that a measurement set is done, the angle is measured 12 times and the average determined. The amount of slip between measurements can be calculated trigonometrically using the change in average angle.

We presently have theodolite measurement sites at 20 localities on ten active faults in the San Francisco Bay region (see Figure 1). Most of the distances between our fixed points on opposite sides of the various faults range from 75-215 meters. The precision of our measurement method is such that we can detect with confidence any movement more than a millimeter or two between successive measurement days. We remeasure most of our sites about once every two months.

The following is a brief summary of our results thus far.

San Andreas fault - Since March 1980 when we began our measurements across the San Andreas fault in South San Francisco (Site 10), no net slip has occurred. Our Site 14 at the Point Reyes National Seashore Headquarters has also shown no net slip since we began measurements in February 1985. Our Site 18 (not shown on Figure 1) in the Point Arena area has averaged about one millimeter per year of right-lateral slip in the 6 years from January 1981 to January 1987. These results indicate that the northern segment of the San Andreas fault is virtually locked, with very little, if any, creep occurring.

Hayward fault - Since we began our measurements on the Hayward fault in September 1979 in Fremont (Site 1) and Union City (Site 2), the average rate of right-lateral slip is 4.3 millimeters per year in Fremont and 4.1 millimeters per year in Union City (see Figure 2). It is interesting to note that U.S. Geological Survey creepmeter data from an area between these two sites show an average of about 4.2 millimeters per year from 1978 to 1982 (Schulz, et al., 1982, p. 6979).

Since we began measuring two sites within the City of Hayward in June 1980, the average annual rate of right-lateral movement is 4.6 millimeters at D Street (Site 12) and 4.8 millimeters at Rose Street (Site 13).

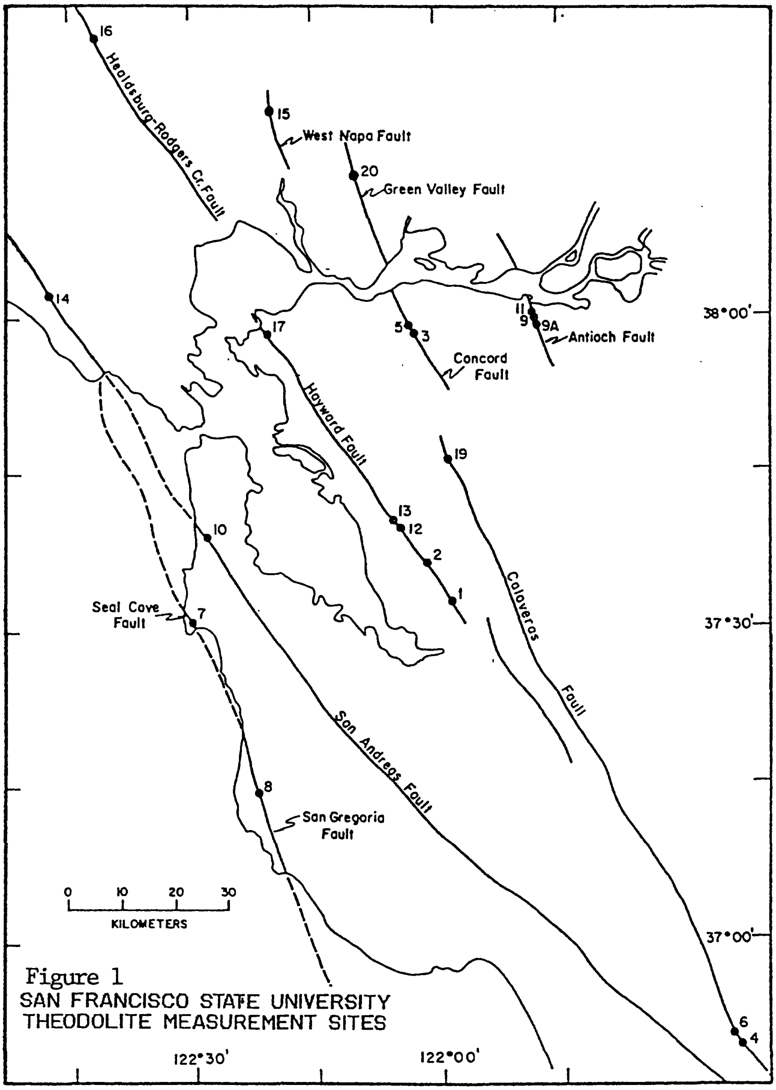

Figure 1
SAN FRANCISCO STATE UNIVERSITY
THEODOLITE MEASUREMENT SITES

FIGURE 2 HAYWARD FAULT

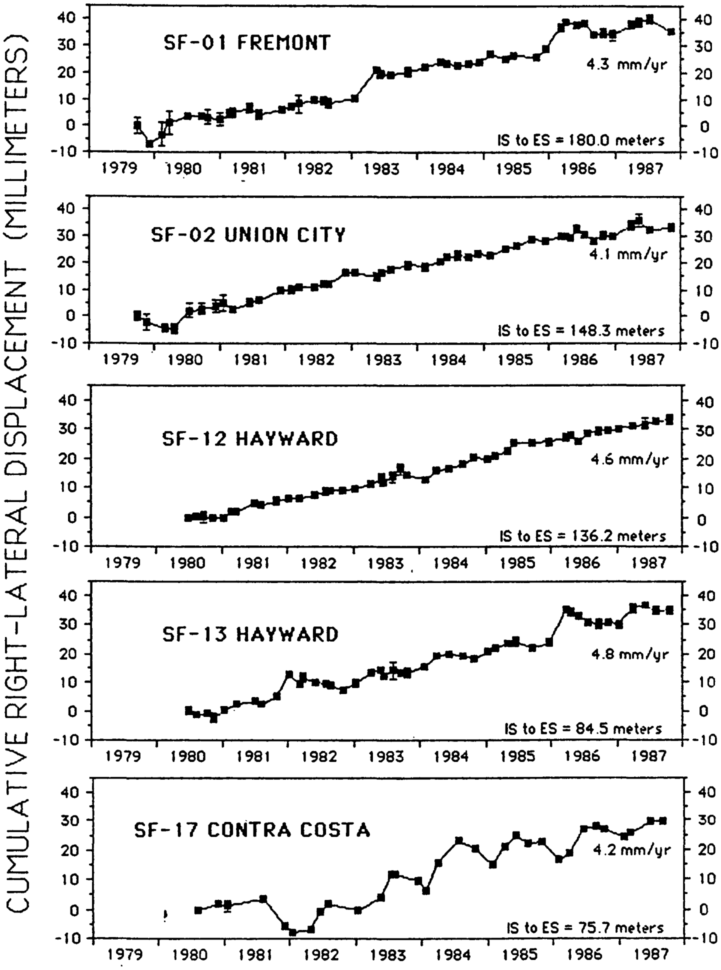

Since we began measurements in San Pablo (Site 17) near the northwestern end of the Hayward fault in August 1980, the average rate of movement has been about 4.2 millimeters per year in a right-lateral sense. However, superposed on this overall slip rate are changes between some measurement days of up to nearly a centimeter in either a right-lateral or a left-lateral sense. Right-lateral slip tends to be measured during the first half of a calendar year and left-lateral during the second half. U.S. Geological Survey creepmeter results also show occasional aberrations in apparent direction of movement on the Hayward fault (e.g. Schulz and Burford, 1979).

In summary, the average rate of right-lateral movement on the Hayward fault is about 4 to 5 millimeters per year over the past 7 to 8 years.

Calaveras fault - We have three measurement sites across the Calaveras fault and the nature and amount of movement are different at all three (see Figure 3). We began monitoring our Site 4 within the City of Hollister in September 1979. Slip along this segment of the Calaveras fault is quite episodic, with times of relatively rapid right-lateral movement alternating with times of little net movement. For the past 7.9 years, the fault has been moving at a rate of 6.1 millimeters per year in a right-lateral sense.

At our Site 6 across the Calaveras fault just 2.3 kilometers northwest of our site within the City of Hollister, the slip is much more steady than episodic. In the 7.8 years since October 1979, the Calaveras fault at this site has been moving at a rate of 12.9 millimeters per year in a right-lateral sense, the fastest rate of movement of any of our sites in the San Francisco Bay region.

U.S. Geological Survey creepmeter results in the Hollister area are quite similar to our theodolite results (Schulz, et al., 1982). Creepmeters also show a faster rate of movement at sites on the Calaveras fault just north of Hollister (13.5 millimeters per year between 1971 and 1982) than within the city of Hollister itself (7.3 millimeters per year between 1970 and 1982). This striking comparison between our theodolite triangulation data and U.S. Geological Survey creepmenter data helps increase confidence in the validity of both methods for accurately determining creep rates.

In contrast to the relatively high creep rates in the Hollister area, our Site 19 in San Ramon near the northwesterly terminus of the Calaveras fault has shown less than a millimeter per year of right-lateral movement for the past 6.6 years.

Based on our theodolite data and field observations of the Calaveras fault, we contributed two papers (Galehouse, 1987; Galehouse and Brown, 1987) to the U.S. Geological Survey Bulletin 1639 on the Morgan Hill earthquake.

Concord fault - We began our measurements at Site 3 and Site 5 on the Concord fault in the City of Concord in September 1979. Both sites showed about a centimeter of right-lateral slip during October and November 1979, perhaps the greatest amount of movement in a short period of time on this fault in the past three decades.

FIGURE 3 CALAVERAS FAULT

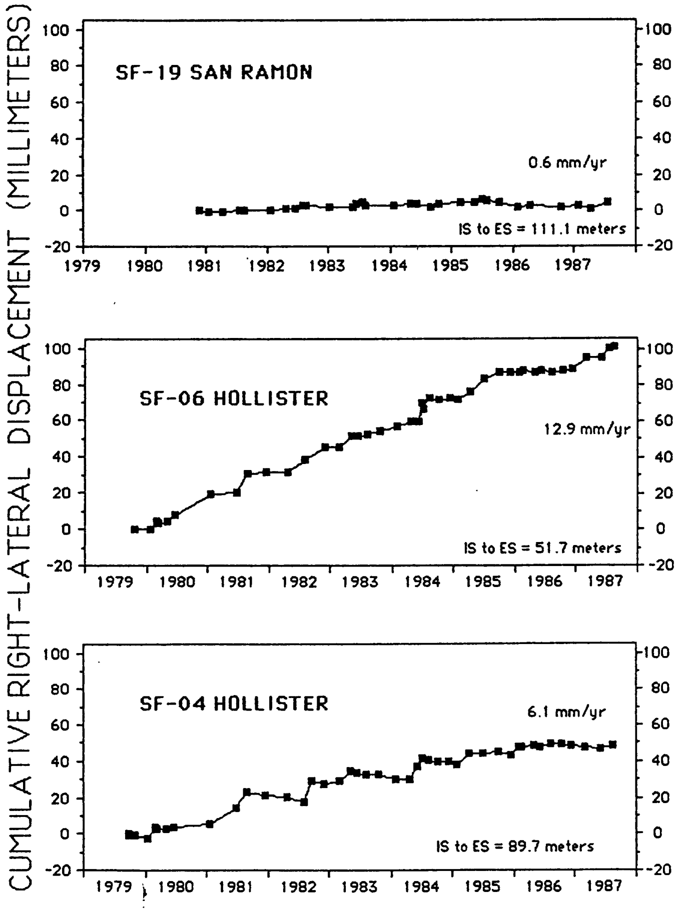

After the relatively rapid slip on the Concord fault in late 1979, both sites showed relatively slow slip for the next four and one-half years at a rate of about one millimeter per year right-lateral. However, in late Spring-early Summer 1984, both sites again moved relatively rapidly, slipping about seven millimeters in a right-lateral sense in a few months. The rate has again slowed since late August 1984.

The overall rate of movement on the Concord fault (combining the two periods of relatively rapid movement with those of slower movement) is 3.4 millimeters per year (Site 3) and 2.7 millimeters per year (Site 5) of right-lateral slip in the past 7.9 years.

Other faults - The Seal Cove fault (Site 7) and the San Gregorio fault (Site 8) have shown very little net slip for the past 7.8 and 5.3 years respectively. However, both sites often show large variations in the amounts and directions of movement from one measurement day to another.

Seasonal and/or gravity-controlled mass movement effects are also present at our sites on the Antioch fault (9A and 11), Rogers Creek fault (16), and West Napa fault (15). Although there have been large variations from one measurement day to another, all these sites show very little net movement for the past 5 to 7 years. Because our line of sight at Site 16 on the Rodgers Creek fault became obscured, we had to abandon the site in early 1986. We have established a new site on the Rodgers Creek fault and will give our results in subsequent reports.

Since we established Site 20 on the Green Valley fault in June 1984, measurements show right-lateral slip at a rate of about 5 millimeters per year. Large variations also tend to occur between measurement days here. Continued monitoring over a longer period of time will confirm whether or not this apparently high rate of slip is real.

References Cited

Galehouse, J.S., 1987, Theodolite measurements: Chapter 15 of "The Morgan Hill, California, Earthquake of April 24, 1984"; U.S. Geol. Survey Bull. 1639, pp. 121-123.

Galehouse, J.S. and Brown, B.D., 1987, Surface displacement near Hollister: Chapter 7 of "The Morgan Hill, California, Earthquake of April 24, 1984"; U.S. Geol. Survey Bull. 1639, pp. 69-72.

Schulz, S.S. and Burford, R.O., 1979, Catalog of creepmeter measurements in central California for 1976 and 1977: U.S. Geol. Survey Open-File Report 79-1609, 375 pp.

Schulz, S.S., Mavko, G.M., Burford, R.O., and Stuart, W.D., 1982, Long-term fault creep observations in central California: J. Geophys. Res., v. 87, no B8, pp. 6977-6982.

DEEP BOREHOLE PLANE STRAIN MONITORING
14-08-0001-G1190 / 14-08-0001-G1376

Michael T Gladwin,

Department of Physics
University of Queensland
St.Lucia, 4067
AUSTRALIA.

ACTIVITIES

1. Processing of the data from the two borehole tensor strainmeters installed in California in 1983 has been continued. Both instruments have continued to provide data of excellent quality.

2. Three new instruments were installed in the Parkfield region during 1986 summer field season. In the new instruments, electronic noise has been reduced by more than 30 dB compared with the instruments presently in operation in San Juan Bautista and Pinon Flat.

3. Two of these new instruments are capable of broad band strain monitoring over the band D.C. to 10 Hz. A manually operated test of the high frequency capability was performed at one of the sites soon after installation. Data from a nuclear test shot at NTS was obtained.

RESULTS

1. Data for 1985-87 from the instrument at San Juan Bautista is shown in Figure 1. Pinon Flat data from 1984 is shown in Figure 2. A change in shear strain rate, with no concurrent dilatation rate change, is evident from the time of the July 8, 1986 Palm Springs earthquake. This shear strain rate was 0.6 microstrain per year prior to the event, and has now decreased to 0.1 microstrain per year.

2. Sites instrumented in the Parkfield region are shown in figure 3. The identifications are "DLT", "FLT" , and "EDT" clustered at the southern end of Middle Mountain. There are DTM Sack's-Evertson dilatometers in close proximity at each site.

3. Data reduced to areal and shear strains during 1987 operation are shown in figures 4, 5, 6. The modified deployment procedure and schedule imposed did not allow proper closing of the holes following instrument implant except in the case of the FLT site. Performance of the instruments DLT and EDT is abnormal as a consequence (neither show the appropriate initial compression due to grout cure), and the long term value of these sites remains in question. Evaluation of these sites will continue during the remainder of the year. The DLT site had the added disadvantage that prior to installation, it was making water to the surface from about 8 feet below the instrument site. This aquefer was (hopefully) sealed with grout prior to installation but its effects in local strain will probably always be evident at this site.

4. Processing of the data obtained from the NTS event is continuing. This data which was recorded using a GEOS recorder provided by R. Borcherdt of the USGS.

Two samples of the data are shown in figure 7 and 8. In figure seven, raw data from the three strain components are presented with three normal seismic signals observed at the surface above the strain meter. The strain seismograms, as has been demonstrated previously with dilatometers, last for much longer than conventional seismograms, being essentially flat to D.C. In the present instance, significant energy continued for about nine minutes. Figure 9 shows the early arrivals on seismometers and the tensor strain meter.

PUBLICATIONS

Gladwin, M. T., High Precision multi component borehole deformation monitoring. *Rev.SciInstrum., 55*, 2011-2016, 1984.

Gladwin, M.T., Gwyther, R., Hart, R., Francis, M., and Johnston, M.J.S., Borehole Tensor Strain Monitoring in California. *J. Geophys. Res.* V 92, No B8, July 10,1987.

Gladwin, M. T. and Hart, R. Design Parameters for Borehole Strain Instrumentation. *Pageoph.,123,* 59-88, 1985.

Gladwin, M. T., Gwyther, R.L. and Hart, R. Tidal Calibration of Borehole Vector Strain Instruments.*EOS, (Trans. Am. G. Un.) 66,* 1057, 1985.

Gladwin, M. T. and Johnston, M.J.S. Strain Episodes on the San Andreas Fault following the April 24 Morgan Hill, California Earthquake. *EOS,(Trans. Am.G.Un.), 65,* 852, 1984.

Gladwin, M.T., and Johnston, M.J.S. Coseismic moment and total moment of the April 24, 1984, Morgan Hill and the January 26, 1986, Quiensabe earthquakes. *EOS,(TransAm.G.Un.), 67, R 308, 1986.*

Gladwin, M. T. and Wolfe, J. Linearity of Capacitance Displacement Transducers. *J.ScInstr. 46,* 1099-1100, 1975.

Johnston, M.J.S., Gladwin, M.T., and Linde, A.T. Preseismic Failure and Moderate Earthquakes. *I.A.S.P.E.I.* , Tokyo, August 19-30, S7-65, 35 , 1985.

Johnston, M. J. S., Linde, A.T., Gladwin, M.T., and Borcherdt, R.D. Fault Failure with Moderate Earthquakes. Tectonophys., In Press.

Johnston, M.J.S., Borcherdt, R.D., Glassmoyer, G., Gladwin, M.T., and Linde, A.T. Static and Dynamic Strain during and following January 26, 1986, Quiensabe, California, Earthquake. *EOS,(Trans., Am. G. Un.), 67,* 16, 308, 1986.

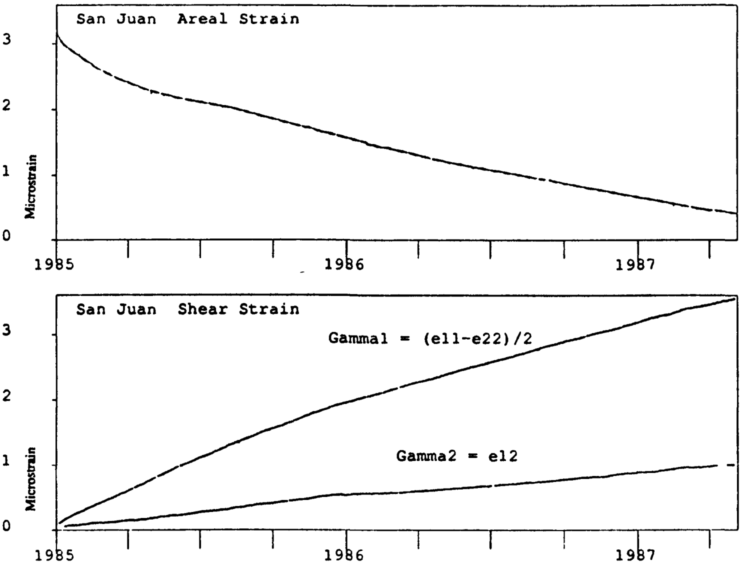

1. Areal and shear strains for the site SJB in southern California since 1984.

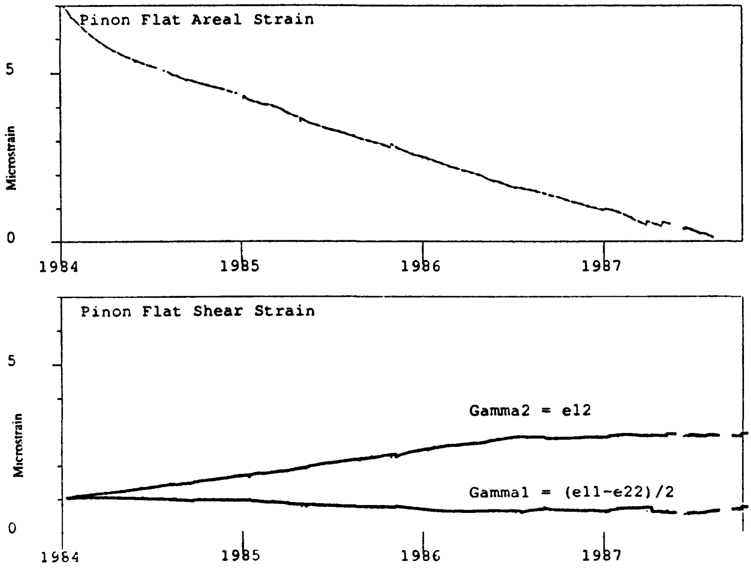

2. Areal and shear strains for Pinon Flat site since 1983. The only significant change of shear strain gradient over the four years of data occurs at the the July 8 1986 Palm Springs event.

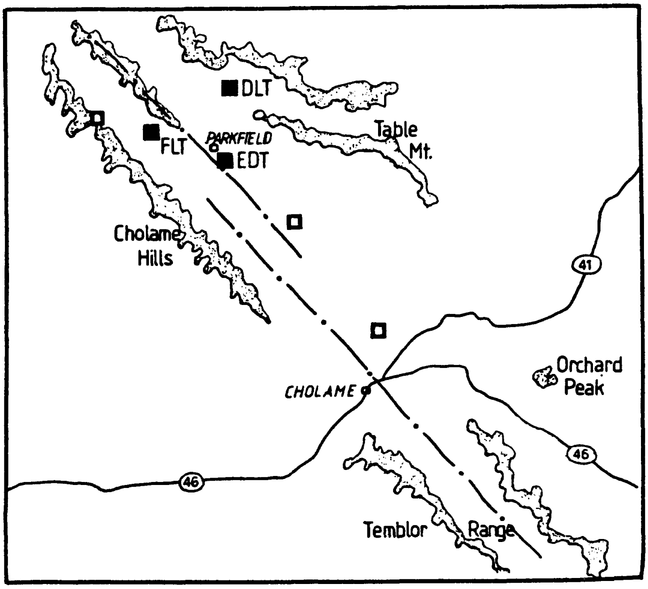

3. Location of newly installed sites in the Parkfield region.

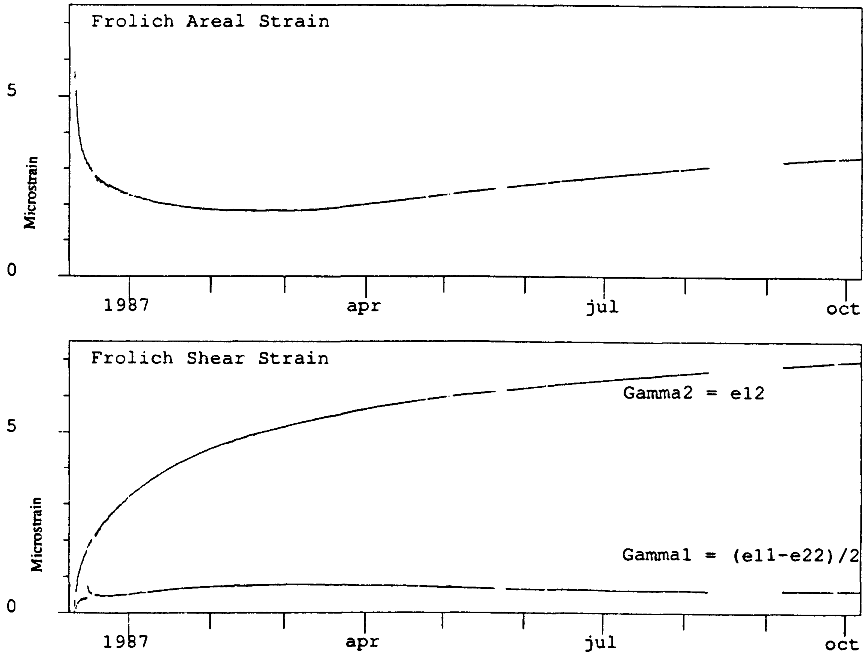

4. Areal and shear strains for the site FLT. Behaviour is fairly normal for a newly drilled situation.

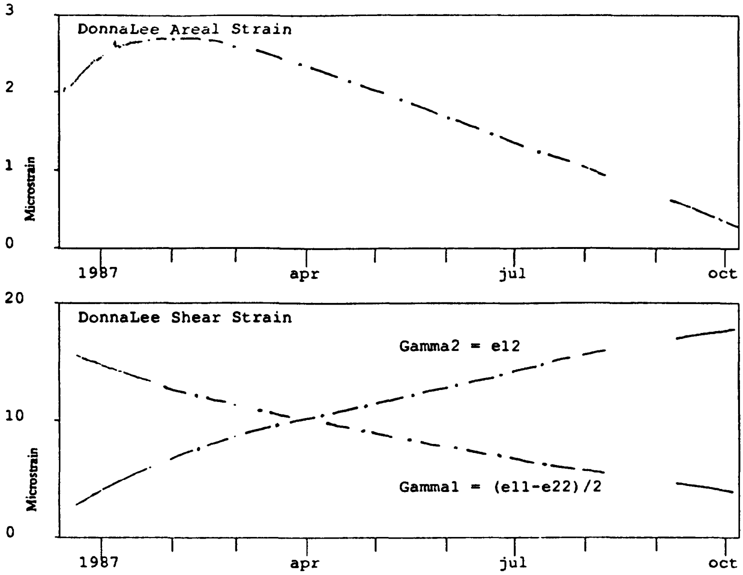

5. Areal and shear strains for the site DLT since installation. Note the absence of the expected initial compression. The installation procedure imposed did not allow adequate pre-load conditions for the grout cure at either this site or at EDT site.

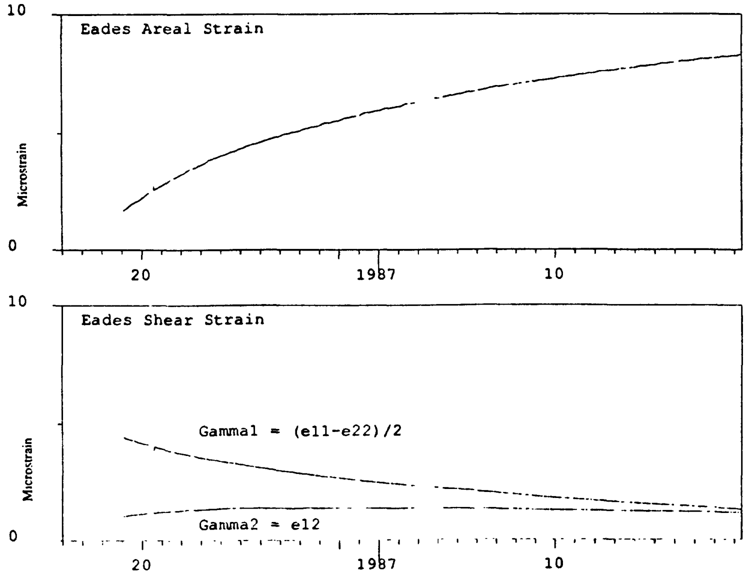

6. Areal and shear strains at the site EDT. Note that the abnormal initial expansion of the instrument is exacerbated by a plug of 140 feet of drilling mud entrained immediately above the instrument.

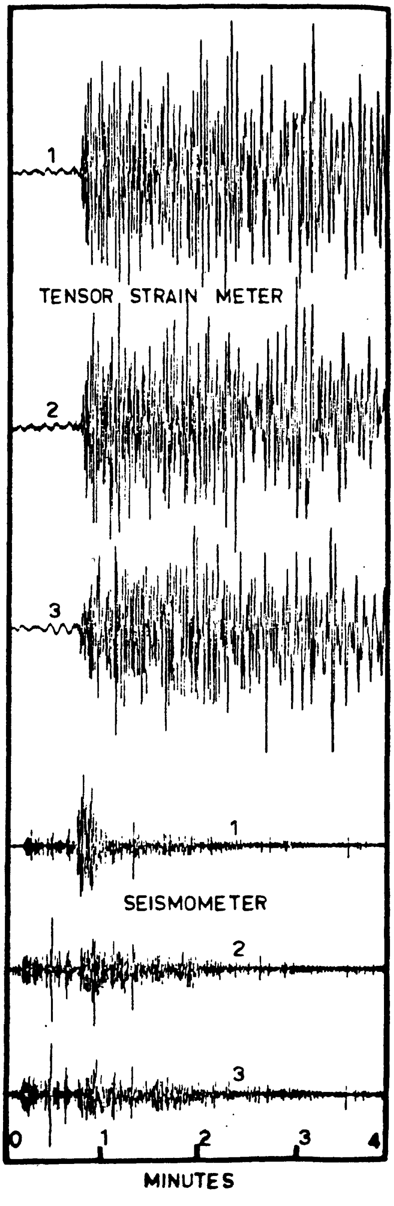

7. Composite raw three component seismograms and three component strain data at the site DLT from the NTS event early in December.

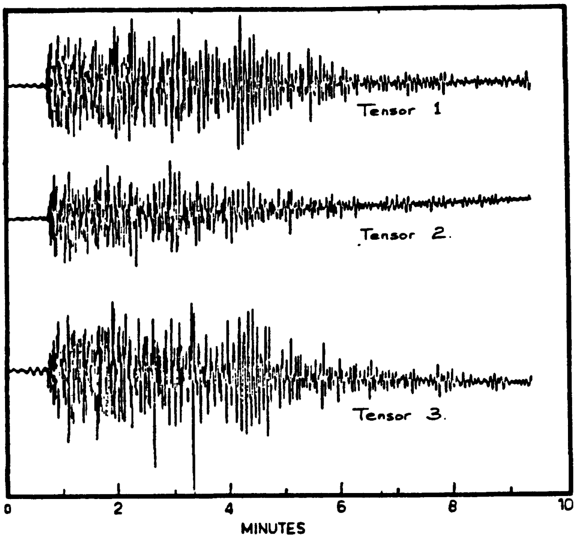

8. Three components of the complete straingram. Note the duration of the event which lasted more than nine minutes.

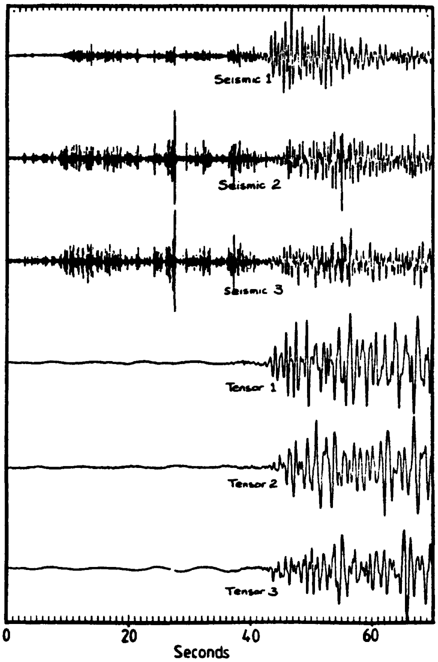

9. Detail of the first arrivals on seismometers and on the tensor strain components. Data have not been rotated to compatible directions.

Spatial and Temporal Patterns of Seismicity in the Garm Region, USSR: Applications to Earthquake Prediction and Collisional Tectonics

14-08-0001-G1382

Michael W. Hamburger
Department of Geology, Indiana University
Bloomington, Indiana 47405
(812) 335-2934

Investigations

This report summarizes the second half-year of a new NEHRP research program, which focuses on the highly active seismic zone between the Pamir and Tien Shan mountain belts in Soviet Central Asia. The Garm region, shown in Figure 1, is located directly atop the collisional boundary between the Indian and Eurasian plates. Active deformation of this mountainous area is marked by a complex tangle of thrust and strike-slip faults, and by the densest concentration of earthquakes in the USSR. As the home of the Complex Seismological Expedition (CSE), whose primary mission is the prediction of earthquakes in the USSR, Garm has been the site of some of the most intense observation of earthquake-related phenomena in the world (Nersesov et al., 1979). Since 1975, the USGS, in cooperation with the CSE, has operated a telemetered seismic network nested within a stable CSE network that has operated in the area since the early 1950's. The fundamental aims of this research are twofold: (1) to elucidate the structures and processes involved in active deformation of the broad collisional boundary of the Indian and Eurasian plates and their influence on the earthquake generation process, and (2) to examine the temporal variations in seismicity near Garm, in the form of changing spatial, depth, and stress distribution of microearthquakes that precede larger events. The data base includes the combined resources of the global, regional, and local seismic networks.

Results

The first phase of the project, prior to field work at Garm during the summer of 1987, focused on the compilation and evaluation of the earthquake catalogs that provide a basis for all subsequent investigations. We now have compiled data from the following earthquake sources: (1) *historical earthquake catalogs*, including all events of $M_s \geq 6$ from a variety of historical sources; (2) *global seismicity catalogs*, from the ISC and PDE bulletins and their precursors; (3) the *Soviet regional catalog* ("Earthquakes in the USSR," Acad. Sci. USSR) has been compiled in computer-readable form by David Simpson (Lamont-Doherty Geol. Obs.) and is shown in Figure 2; (4) the *CSE network* based at Garm has recorded over 70,000 events since the early 1950's. Arrival times and event locations from this network will be made available as part of the Soviet-American exchange; (5) the *USGS/CSE network data* provide the most detailed spatial information on earthquake distribution. This network includes 13 radio-telemetered stations operated jointly by the USGS and the CSE since 1975 (Wesson *et al.*, 1976; Pelton and Fischer, 1981).

The large shallow earthquakes within Soviet Central Asia are concentrated near the edges of the Pamir and Tien Shan mountain belts; near Garm, these two zones coalesce into a single dense nest of activity. Earthquake depths in the Garm region are largely restricted to the upper crust; however, this area is also the site of the world's densest concentration of intracontinental intermediate-focus seismicity. The Pamir-Hindu Kush zone, shown by filled circles in Figures 1 and 2, provides an extremely reliable supply of subcrustal earthquake sources that may be used for studies of spatial and temporal variations of seismic properties of the crust.

Results of Field Investigations. This phase of the project included a one-month field trip to the Soviet Union during June, 1987. The trip included approximately one week each in Moscow and Dushanbe, and two weeks in Garm, and included meetings with scientists at the Institutes of Geology and Physics of the Earth (Moscow), the Tadjik Institute of Seismo-resistant construction and Seismology (Dushanbe), and the Complex Seismological Expedition (Garm). The primary goals of the trip were to review the extensive Soviet work in the Garm region since the early 1950's, as well as to establish a basis for future collaborative work with Soviet seismologists and geologists working in Garm. I was able to return with extensive published literature on previous seismological and geological work at Garm, as well as a catalog of arrival times from the USGS telemetered network for 1975-1977 and 1980-1982. Arrangements were also made for provision of the earthquake locations and arrival time data from the Soviet (CSE) network at Garm.

Analysis of Regional Network Data. Much of our efforts during this period have been directed toward elucidation of spatial and temporal structure within this very complex seismic zone. The Soviet regional catalog (Figure 2), which includes events to magnitude 3, provides an extremely stable, long-term basis for examining seismicity of the Garm region. Earthquakes in this area are tightly clustered along discrete seismogenic features within the India/Eurasia plate boundary. Large and moderate-sized earthquakes ($M \geq 4.5$) are concentrated along the Gissar-Kokshal seismic zone that bounds the Tien-Shan range on the south. A densely populated band of smaller events extends southward from the Gissar-Kokshal zone into the Tadjik Depression fold-thrust belt (southwest of Garm). Earthquake distribution for intermediate-depth events is very tightly concentrated in the Pamir-Hindu Kush nests.

The vast size of the Soviet regional catalog, which includes over 30,000 earthquake locations in the Central Asian region since the early 1950's, has required us to consider alternative methods of analyzing the data. Our approach centers on application of a new method to identify and quantitatively characterize non-randomness in the spatial and temporal distribution of earthquakes. The approach compares the observed distributions of distances and time intervals among all possible pairs of events with expected distributions derived from *a priori* models (in this case, events uniformly scattered in space and time). By subtracting the expected from the observed distributions, we obtain residual distributions that provide a basis to estimate the degree of non-randomness within an earthquake sequence. This approach can be used to discriminate clustering or to characterize the overall nature of non-uniformity in earthquake occurrence. The preliminary results reported here support our findings in other seismically active zones, that the earthquake process appears to be non-uniform in space, independent of the size of the study area (Eneva and Pavlis, 1987; Eneva *et al.*, 1987). In many cases this can be attributed to spatial alternation of areas with different levels of seismic activity, as observed at both small and large scale. Such features are related to fault segmentation and are consistently observed in both background seismicity and within aftershock sequences (Eneva and Pavlis, 1987; Eneva *et al.*, 1987).

We have examined various subsets of the data within different spatial, time, and magnitude ranges. Deviations from the expected spatial and temporal distributions are observed on all scales: within small zones within the Tadjik Depression, as well as within the regional-scale Gissar-Kokshal zone. For virtually all subsets considered, we observe marked spatial clustering at small epicentral distances.

Such spatial clustering persists even when aftershock sequences and swarms are excluded from consideration (Eneva and Hamburger, 1987)

Figure 3 presents an example of the statistical analysis used to discriminate spatial patterns within an apparently homogeneous seismic zone. Figure 3A shows the epicentral map for a 30x150 km^2 area in the Tadjik Depression. The respective residual distribution of distances between events is shown on the right. The dotted lines indicate the tolerance limits (that include with 95% confidence 90% of the residual frequencies from single random generations). Although the map has the appearance of a random scattering of events, the excess of pairs above the tolerance interval for small distances (< 20 km) can be attributed to spatial clustering (i.e., non-randomness) that involves about 24% of the events in the area. For comparison, Figure 3B presents a randomly generated epicentral map for earthquakes in the same area. In this case, the residual distribution (shown on the right) falls well within the tolerance limits. Thus, while the maps shown on the left of the figure appear to be similar, the distributions shown on the right provide a powerful discriminant of significant non-randomness in earthquake occurrence.

We applied the same techniques to the larger scale of the Gissar-Kokshal seismic zone (100x500 km^2). Unlike the Tadjik Depression, this zone is characterized by a concentration of events with magnitude greater than 5.0, and several events with magnitudes greater than 7.0. Almost 40% of the larger events ($M \geq 4.5$) in the Gissar-Kokshal zone show a similar clustering for distances ≤ 40 km. Anomalous grouping of events is also observed at larger epicentral distances (≥ 100 km). This pattern is due to spatial alternation of areas with different levels of seismic activity and may reflect long-term rheological or geometric segmentation of the Gissar-Kokshal fault zone. The temporal pattern of earthquake occurence within these seismic zones also deviates from a random distribution. Clustering at short time intervals (≤ 5 years) along the Gissar-Kokshal zone reflects periods of increased activity following several major events (Eneva and Hamburger, 1987).

References

Eneva, M., and G.L. Pavlis, 1987, Application of pair analysis statistics to aftershocks of the 1984 Morgan Hill, California, earthquake, Submitted to *J. Geophys. Res.*

Eneva, M.G., G.L. Pavlis, and M.W. Hamburger, 1987, Discrimination of non-random features in the space-time distribution of earthquakes [abstract], *Seis. Res. Lett.*, in press.

Eneva, M.G., and M.W. Hamburger, 1987, Space-time seismicity patterns within the Gissar-Kokshal and Tadjik Depression seismic zones, Soviet Central Asia [abstract], *EOS, Trans. AGU*, in press.

Nersesov. I.L., Yu, P. Skovorodkin, and T.V. Guseva, 1979, Results of complex studies in the Garm geodynamic polygon, *Izvestiya, Physics of the Solid Earth, 15:4*, 47-55.

Pelton, J., and F.G. Fischer, 1981, An earthquake catalog and velocity model for the USGS Peter the First Range seismic array, Tadzhikistan, USSR. *U.S. Geol. Surv. Open-File Rept. 81-1150*, pp. 221-246.

Wesson, R.L., 1986, Seismicity of the Pamir-Alai region, Soviet Central Asia. Submitted to *J. Geophys. Res.*

Wesson, R.L., V.G. Leonova, A.B. Maksimov, I.L. Nersesov, and F.G. Fischer, 1976, Results of cooperative field seismological investigations in 1975 in the Peter I Range region [in Russian], in *Collection of Soviet-American Works on Earthquake Prediction*, v. 1, book 1, pp. 43-69.

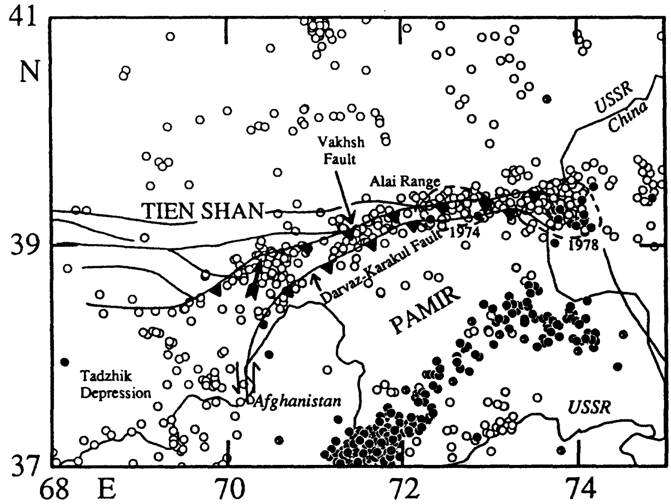

Figure 1. Teleseismically located earthquakes and active faults of the Garm region. Earthquakes recorded from 1964-1984 and located by ≥ 20 stations, are from the ISC catalog. Open circles represent earthquakes at ≤ 70 km depth; filled circles: $h > 70$ km. Fault maps are adapted from Keith et al. (1982) and Wesson (1986). Dashed ellipses indicate aftershock zones of 1974 Markansu and 1978 Daraut-Kurgan earthquakes. Heavy arrow shows the location of Garm.

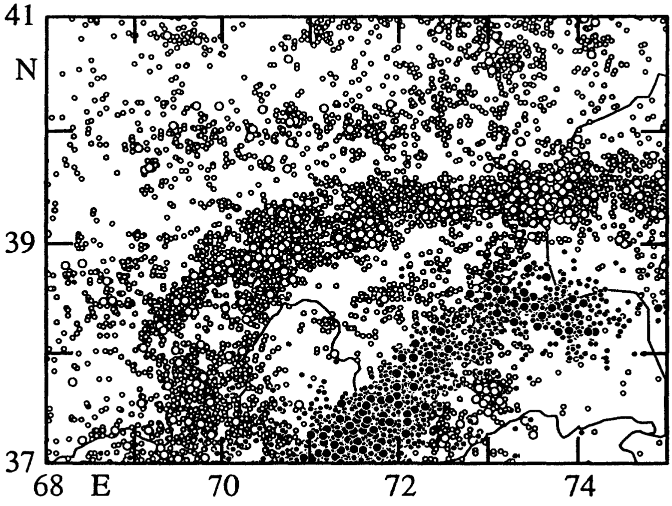

Figure 2. Earthquakes located by the Soviet Regional Network, 1964-1980, classified by magnitude and depth: open circles: $h \leq 70$ km; filled circles: $h > 70$ km. Small symbols: $M \leq 4.0$; large symbols: $M > 4.0$. We have arbitrarily "randomized" the coordinates of poorly located events on the margins of the seismic network whose position was given in 0.1° increments in order to remove an apparent gridding of epicenters.

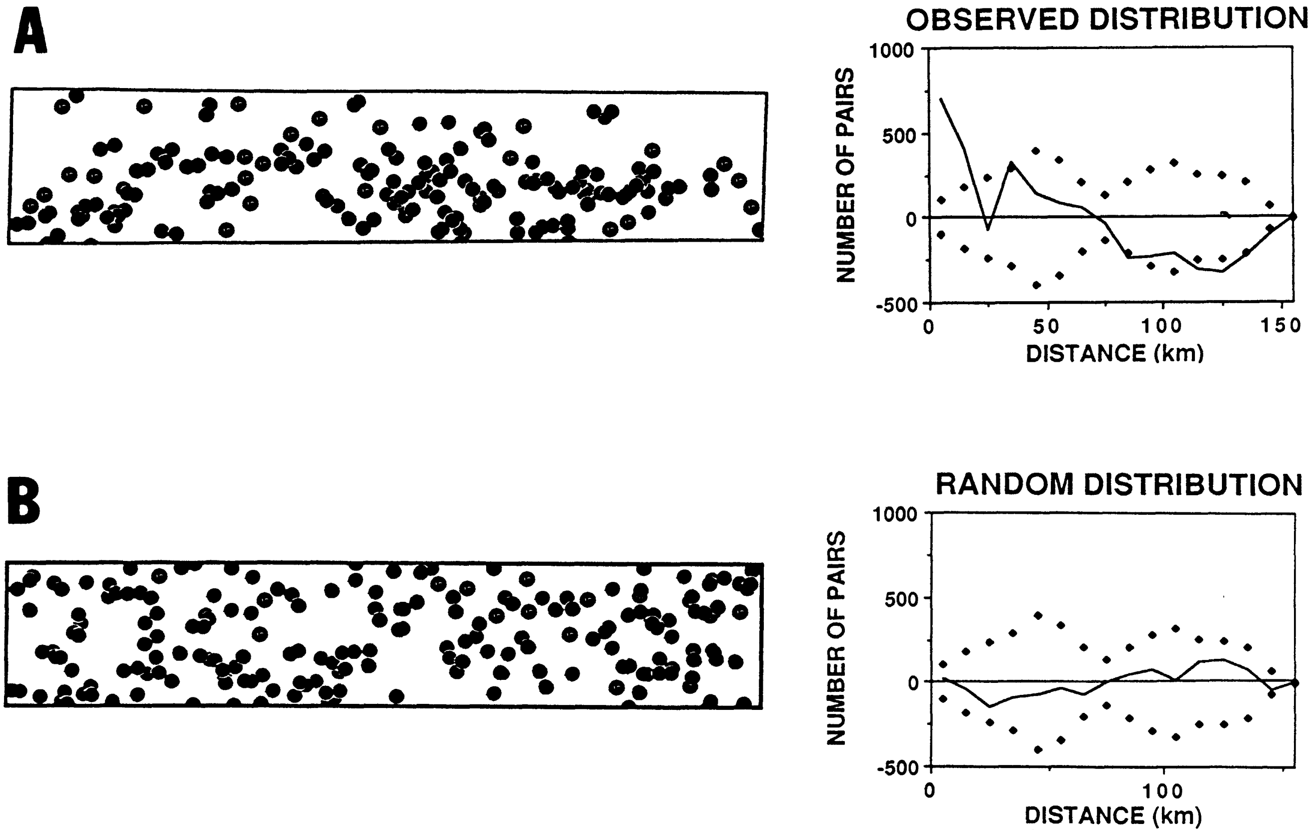

Figure 3. Comparison of observed and random spatial patterns of earthquake distribution in a 30x150 km^2 area in the Tadjik Depression. Figures on the left show epicentral maps for the study area; figures on the right show residual distributions of epicentral distances between events (i.e., observed minus expected distributions). The dotted lines indicate the tolerance limits for the expected distributions. (A) Observed distribution of earthquakes with magnitudes larger than 3.3 for the period 1964-1980. (B) Randomly generated distribution of earthquakes within the same area.

TILT, STRAIN, AND MAGNETIC FIELD MEASUREMENTS

9960-2114
M. J. S. Johnston
Branch of Tectonophysics
U. S. Geological Survey
Menlo Park, California 94025
415/323-8111, ext. 2132

Investigations

[1] To investigate the mechanics of failure of crustal materials using data from both deep borehole tensor and dilational strainmeters and near surface strainmeters, tiltmeters, and arrays of absolute magnetometers.

[2] To develop physical models of incipient failure of the earth's crust by analysis of real-time records from these instruments and other available data.

Results

[1] Deep and Near-surface Fault Creep Near Parkfield, California.

Surface observations of aseismic fault displacement (fault creep) exhibit episodic behavior (creep events) whose sources are typically limited in extent and complex in character. Strain, tilt and displacement data obtained near and across the fault segments where these events are occurring indicate that they are triggered by deeper slip of longer duration. On August 18, 1986, fault displacement of 1.5 mm was observed on a creep meter XGH1 at Gold Hill near Parkfield, California. At this location, two borehole dilational strainmeters are installed at distances of 1.0 km and 1.35 km from the fault. Strain changes preceding and during the creep event have similar form but maximum amplitudes of 22 and 5 nanostrain, respectively. These data are consistent with a slip moment for the creep event of $2*10^{19}$ dyne-cm. If centered on the creepmeter, the patch that slipped could be several hundred meters square. During the previous two weeks, and at other times, strain transients of several hundred nanostrain occurred. The apparent rupture velocities obtained by replicating the strain data with simple quasistatic models of the deep creep are about 1 km/day or less. These apparent deeper slip episodes could explain the general correspondence over periods of months between higher than normal average creep and higher rates of occurrence of moderate seismicity reported previously and should be easily detected with a small 2-dimensional arrays of low-noise borehole strainmeters planned for this area. Routine detection of these episodes may allow prediction of related moderate magnitude earthquakes in this creeping/locked transition zone

[2] Strain and Geomagnetic Variation in the Northern End of the Red River Fault System near Eryuan in Western Yunnan, China

Arrays of absolute differential magnetometers and intermediate baseline geodetic nets have been installed and surveyed since 1980 at the northern end of the Red River fault in western Yunnan, China. On the basis of data obtained and analysed usimg linear regression and inversion techniques, local magnetic field changes, shear strain rates, dilational strain rates, principal strains and net displacement vectors have been determined for these areas. Near Eryuan, local fields and strain rates of as much as 2 nT/a and 0.8 μstrain/a, respectively, are occurring. Similar strain rates are occurring near Liantie. However, no significant magnetic field change have occurred.

[3] Static and Dynamic Strain during the July 8, 1986, M 5.9 North Palm Springs, Ca, Earthquake

Crustal strain during the July 8, 1986, North Palm Springs earthquake (M 5.9) was recorded on several Sacks-Evertson dilatometers (PUBS at 125 km, AMSS at 127.2 km, BBSS at 121 km and others at greater distances), a 3-component (tensor) strainmeter (MPFS - 24.3 km distant), all installed at depths of about 200 m, and 3-component surface seismic velocity transducers at the PUBS and more distant dilatometer sites. Dynamic strain and velocity for the foreshock, mainshock, and aftershocks were recorded at a 300 Hz sampling rate and high gain on digital recorders (GEOS). The moment of the earthquake was estimated from displacement spectra generated using the dynamic strain and velocity seismograms and also from the static strain offsets recorded on the strainmeters. The seismic moments determined from the surface velocity tranducers at the dilatometer locations are between $0.6\text{-}1.4*10^{25}$ dyne-cm. The static moments are larger (between $2\text{-}3*10^{25}$ dyne-cm). Post-seismic strain, consistent with continued failure on the rupture plane, continued for about 30 minutes. This was followed by apparent rebound for several days after the earthquake. The post-seismic moment was less than 10% of that of the earthquake. Precursive strains during the period days to 10 minutes before the event are not apparent in the data from the closest instrument, MPFS. The coseismic shear strain decrease and normal strain increase at this 3-component strainmeter site was 0.06 and 0.02 μ strain, respectively. The North Palm Springs earthquake decreased the effective strength (σ_p-$0.6\sigma_n$) for right-lateral failure in nearby sections of the San Jacinto fault and, therefore, increases the probability of earthquakes in sections of this fault.

[4] Borehole Strain Array near Parkfield, California.

A network of 8 borehole dilatometers and 3 borehole tensor strainmeters has been installed along a 36-km segment of the San Andreas fault zone near Parkfield California. All instrument are installed at depths between 117-m and 324-m and all are between 1-km and 5-km of the surface trace of the fault. High frequency dilatometer data in the frequency range 0.005 Hz to 100 Hz are recorded on 16-bit GEOS digital recorders with least count noise of less than 10^{-11}. Lowfrequency data from zero frequency to 0.002 Hz are transmitted using a 16-bit digital telemetry system through the GOES satellite to Menlo Park, California. Least-count noise on the satellite telemetry system is about $2*10^{-11}$ on the high gain channels and about $1.2*10^{-9}$ on the low gain channels. Earth strain tides, strain transients of which some are related to subsequent surface observations of fault creep, and numerous strain seismograms from local and teleseismic earthquakes with magnitudes between -1 and 6 have been recorded on these instruments. Strain seismograms are used to calculate the dynamic earthquake moments. Static moments and total earthquake moments are determined from the co-seismic strains and total strain changes observed with larger events. Should preseismic strains occur before the expected Parkfield earthquake, they can be resolved at about the 10^{-11} level if they occur quickly, and about the 10^{-9} level if they occur from days to weeks before the event.

[5] Characteristics of Seismic Waves from Volumetric Strainmeters

Theoretical descriptions of volumetric and displacement fields for radiated seismic energy predict that simultaneous observations of each on colocated sensors allow determination of 1) the superimposed P and S radiation fields, and in particular, superimposed P and S waves reflected at the free surface, 2)angle of incidence and apparent phase velocity based on amplitude on amplitude ratios and, 3) intrinsic material absorption and characteristics of low-loss inhomogeneous wave fields. Several hundred local, regional and large teleseismic events including the recent Wittier, Chalfant, and North Palm Springs eevents, have been observed on colocated volumeteric strain meters and seismometers using broad-band high-resolution recorders (GEOS) at fourteen sites near the San Andreas fault, CA, and in Long Valley. These observations have been used to determine site and propagation characteristics, earthquake moments, conversion efficiencies, long period characteristics, and information during the immediate pre-rupture interval.

[6] Static and Dynamic Strain During the M_L 5.9, Banning, California, Earthquake on July 8, 1986.

Changes in crustal strain generated by the July 8, 1986, North Palm Springs earthquake (M 5.9) were recorded on several Sacks-Evertson borehole dilatometers (PUBS at 125 km, AMSS at 127 km, BBSS at 121 km and others at greater epicentral distances), and a 3-component (tensor) borehole strainmeter (MPFS - 24.3 km distant). Dynamic strain and 3-component ground velocity were simultaneously recorded at PUBS and more distant dilatometer sites for the foreshock, main shock, and aftershocks with on-site 16-bit digital recorders (GEOS). The moment of the earthquake was estimated from displacement spectra generated using the strain and velocity seismograms and also from the static strain offsets recorded on the strainmeters. The seismic moments determined from straingrams and seismograms are $0.6\text{-}1.7*10^{25}$ dyne-cm. The static moments are larger ($2\text{-}3*10^{25}$ dyne-cm). MPFS recorded post-seismic strains, consistent with continued failure on the rupture plane, for about 30 minutes. This was followed by apparent rebound for several days after the earthquake. The post-seismic moment was less than 10% of that of the earthquake. Precursive strains are not apparent in the data from any of the instruments before the event. The coseismic shear strain decrease and normal strain increase at the 3-component strainmeter site was 0.06 and 0.02 μ strain, respectively. These data suggest the effective strength $(\sigma_p - 0.6\sigma_n)$ for right-lateral failure on nearby sections of the San Jacinto and the San Andreas faults was decreased by the North Palm Springs event with the implication that the probability of earthquakes on these sections was increased by this event.

[7] Crowley Lake Level Monitoring

Four water level monitoring sites have been installed on Lake Crowley in the Long Valley/ Mammoth Lakes region. These stills provide differential water level measurements (tilt) equivalent to 6 independent tiltmeters with baselines of up to 8 kilometers at varying angles to the center of the resurgent dome. Each site has been surveyed into the existing level line routes around the lake. The time constants of the stills are approximately 40 minutes to minimize effects from the primary seiche periods at 18 minutes and 13 minutes, respectively. The water level data, together with water temperature, wind speed, and other parameters, are being transmitted by the low frequency satellite data collection system to Menlo Park at a 2-min sample period. The maximum change in differential elevation that could have occurred during the past year is less than 1 cm (ie < 1 μradian).

[8] Episodic Strain Signals, Aseismic Slip, and Seismicity

Slow strain signals have been recorded near Parkfield, California near Tohoku, Japan, and in southern Iceland before moderate to large earthquakes and aseismic fault slip. The strain signals are consistent with aseismic slip on a section of fault near the observation stations. In one region (Tohoku), these slow episodic signals were followed by a major earthquake; in the other areas an earthquake is expected to occur soon.

Reports

Gladwin, M. T., Gwyther, R. L., Hart, R., Francis, M., and Johnston, M. J. S., 1987, Borehole Vector Strain Measurements in California, J. Geophys. Res., **92**, 7981-7988.

Johnston, M. J. S., Tectonomagnetism and Tectonoelectricity, 1987, Reviews of Geophysics,**25**, 983-988.

Johnston, M. J. S. Review of Tectonomagnetic, Seismomagnetic, and Volcanomagnetic Observations in Western U.S.A., 1974-1986, 1987, Abs. IUGG, Vancouver, Canada, August 9-22, 1987, v1, p388.

Linde, A. T., I. S. Sacks, A. Takagi, R. Stefansson and M. J. S. Johnston, Episodic Strain Signals, Aseismic Slip, and Seismicity, 1987, Abs. IUGG, Vancouver, Canada, August 9-22, 1987, v1, p268.

Johnston M. J. S. and R. J. Mueller, Seismomagnetic Observations During the 8 July, 1986, Magnitude 5.9 North Palm Springs, California, Earthquake, 1987, Science v237, 1202-1203.

Mueller R. J., and M. J. S. Johnston, Large-Scale Magnetic Field Perturbations Arising from the May 18, 1980, Eruption from Mount St. Helens, 1987, Abs. IUGG, Vancouver, Canada, August 9-22, 1987, v1, p385.

Chen Zhong-yi, M. J. S. Johnston and R. J. Mueller, Strain and Geomagnetic Variation in the Northern End of the Red River Fault System near Eryuan in Western Yunnan, China, 1987, Abs. IUGG, Vancouver, Canada, August 9-22, 1987, v1, p385.

Borcherdt R. D., and M. J. S. Johnston, A Broad-Band Wide-Dynamic Range Strong-Motion Network near Parkfield, California, USA, for Measurement of Acceleration and Volumetric Strain 1987, 9 th World Conference on Earthquake Engineering (in press)

Myren, G. D., M. J. S. Johnston, A. T. Linde, M. T. Gladwin, and R. D. Borcherdt, 1987. Borehole Strain Array near Parkfield, California. Trans. AGU. (in press).

Johnston, M. J. S., R. D. Borcherdt, M. T. Gladwin, G. Glassmoyer, and A. T. Linde, 1987. Static and Dynamic Strain During the M_L 5.9 Banning, California, Earthquake on July 8, 1986. Trans. AGU, (in press)

Borcherdt, R. D., and M. J. S. Johnston, 1987. A Broad Band Wide- dynamic Range Strong-Motion Network near Parkfield, California, USA, 1987, Trans AGU, (in press)

Johnston, M. J. S., A. T. Linde, and M. T. Gladwin, 1987. Static Moment of the October 1, 1987, Wittier Narrows Earthquake from Borehole Strain Data, 1987. Trans. AGU, (in press).

Earthquake and Seismicity Research Using SCARLET and CEDAR

Grant No. 14-08-0001-G1354

Hiroo Kanamori, Clarence R. Allen, Robert W. Clayton
Seismological Laboratory, California Institute of Technology
Pasadena, California 91125 (818-356-6914)

Investigations

1. Recent Seismicity Along the San Jacinto Fault
   Hiroo Kanamori and Harold Magistrale

2. Comparison of Iterative Back-Projection Inversion and Generalized Inversion Without Blocks: Case Studies in Attenuation Tomography for the Imperial Valley and Coso-Indian Wells Valley
   Phyllis Ho-Liu, Jean-Paul Montagner, and Hiroo Kanamori

Results

1. Recent Seismicity Along the San Jacinto Fault

The seismicity cross section along the San Jacinto fault, southern California, shows almost complete absence of seismic activity along an 80 km long section at depths above 13 km (Figures 1 and 2). The last large earthquake which occurred in this section was in 1918, and the seismic quiescence suggests steady strain accumulation there. Assuming that the slip rate is 1 cm/year, we estimate that strain energy corresponding to an earthquake with a seismic moment of at least 2.2 x 10^{26} dyne-cm (M_w=6.8) is accumulated there. The empirical relation between the fault length and the seismic moment of shallow strike-slip earthquakes in active plate boundaries suggests that the accumulated energy in this section is comparable (within a factor of 2) to the ultimate strain energy that can be stored in an 80 km fault section. Although this type of empirical data does not allow prediction of the exact time of an earthquake, it provides a physical framework for further prediction experiments.

2. Comparison of Iterative Back-Projection Inversion and Generalized Inversion Without Blocks.

We have earlier reported the results of attenuation tomography for the Imperial Valley and Coso-Indian Wells Valley. We examined the results using a different inversion method.

Iterative back-projection tomography and generalized tomography without blocks are two different inversion techniques developed recently, and are commonly applied to inversions of travel-time data. In this study, we compared the two methods and derived one from the other under certain assumptions, then we applied them to an attenuation problem, inverting for the quality factor of the medium.

We applied the methods to the data sets obtained for two areas in southern California: Coso-Indian Wells region and Imperial Valley. The results obtained by the two methods are very similar (Figure 3). The back-projection tomography is a direct and fast method for this type of problem; however, it does not provide formal error estimates and resolution. The no-block inversion requires more computational time, but formal errors and resolution can be directly computed for the final model. Thus, application of the two methods to the same data set enhances the objectivity of the final result.

References

Kanamori, Hiroo and Harold Magistrale, State of stress in seismic gaps along the San Jacinto fault, in press, Berkeley Centennial Volume, 1988.

Sanders, Chris, David Rinn, Phyllis Ho-Liu, and Hiroo Kanamori, Anomalous shear-wave attenuation in the shallow crust beneath the Coso Region, California, J. Geophys. Res., in press, 1987.

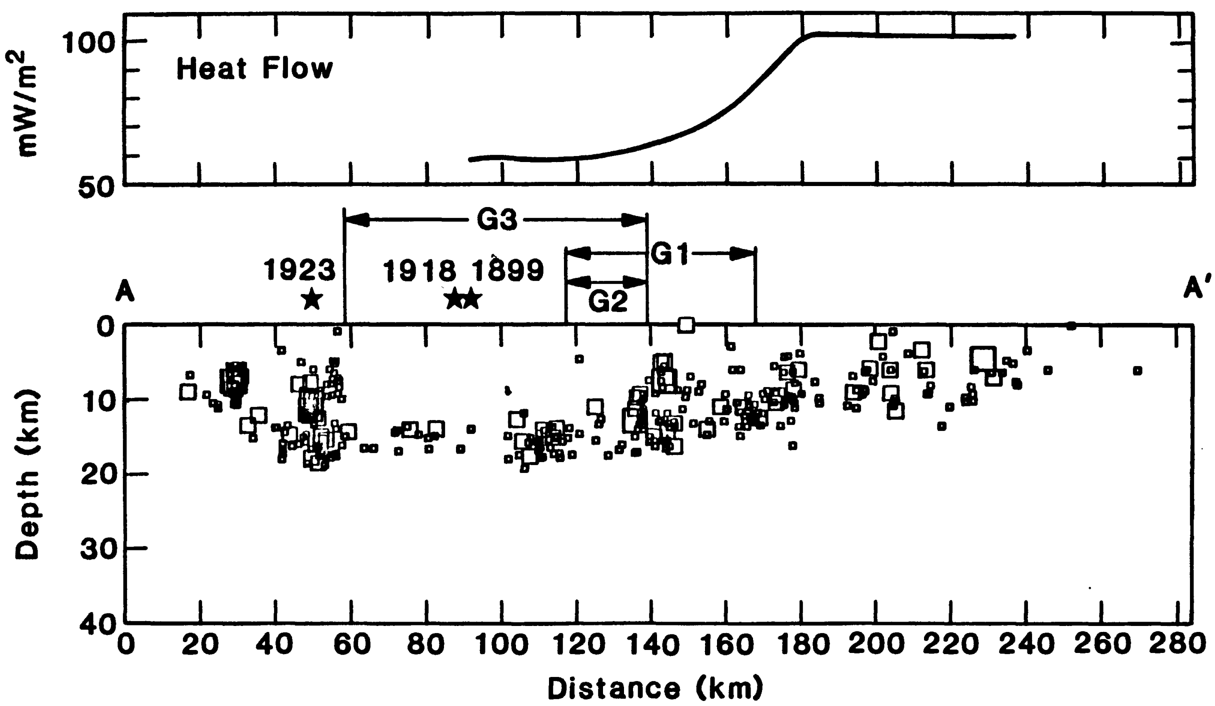

Figure 1. Seismicity along the San Jacinto fault, southern California, for the period Jan. 1, 1987 to June 30, 1987. The data are taken from the catalog of the southern California Seismic Network. All the events in the polygon are shown. The narrow box A-A′ indicates the area used for the cross-section plot shown in Figure 2. Geographical locations of the fault and the gaps are shown in the figure at the bottom.

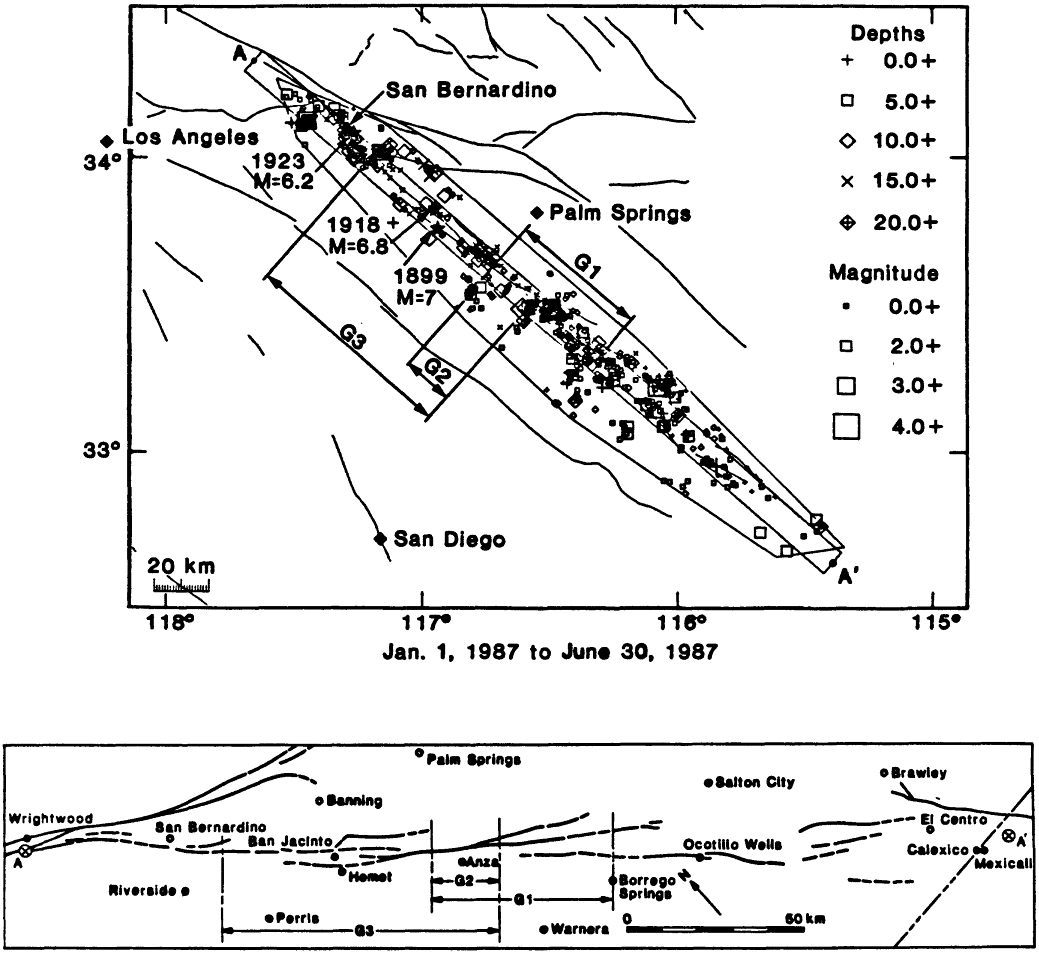

Figure 2. Seismicity cross section along the San Jacinto fault (lower figure). All the events in the box A–A′ in Figure 1 are shown. Three gaps, G1, G2 and G3 are indicated. The upper figure shows the variation of heat flow along the San Jacinto fault taken from Lachenbruch et al. (1985).

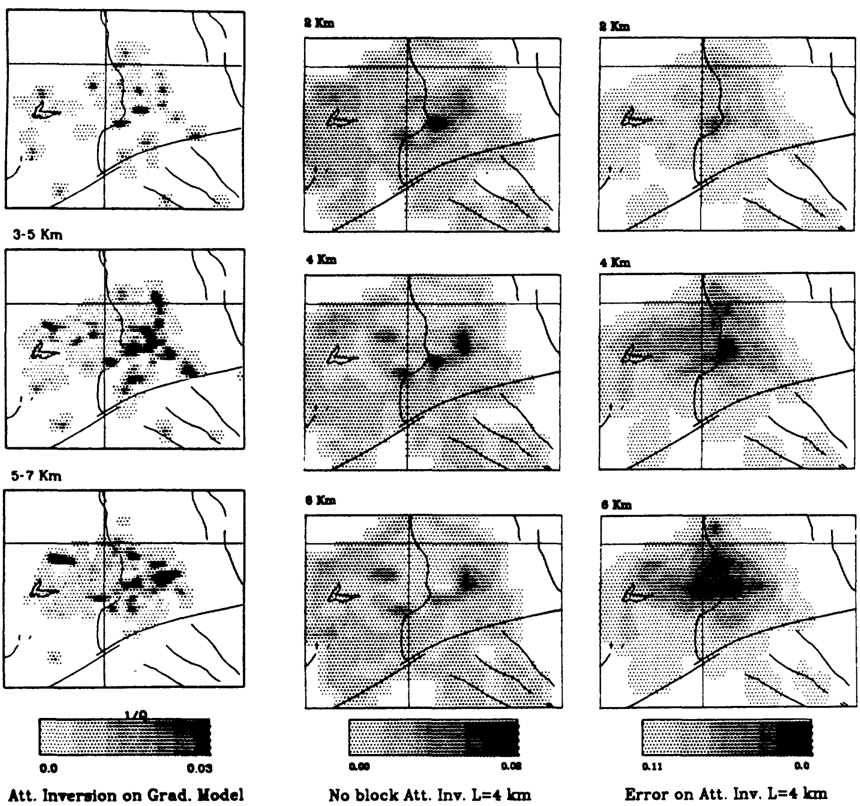

Figure 3. Comparison of iterative back-projection inversion (left) and no-block inversion (middle). The figures on the right show the errors for the no-block inversion.

GEODETIC STRAIN MONITORING

9960-02156

John Langbein
Branch of Tectonophysics
U.S. Geological Survey
345 Middlefield Road, MS/977
Menlo Park, California 94025
(415) 323-8111, ext. 2038

Investigations

Two-color geodimeters are used to survey, repeatedly, geodetic networks within selected regions of California that are tectonically active. This distance measuring instrument has a precision of 0.1 to 0.2 ppm of the baseline length. Currently, the crustal deformation is being monitored within the south moat of the Long Valley Caldera in eastern California, near Pearblossom, California on a section of the San Andreas fault that is within its Big Bend section and on Middle Mountain near Parkfield, California. Periodic comparisons with the prototype, two-color geodimeter are also conducted near Parkfield, California. These intercomparison measurements serve as a calibration experiment to monitor the relative stabilities of the portable and prototype geodimeters.

Results

1. Instrument Intercomparison

Since January 1986, we have completed six intercomparison experiments at Parkfield, California using both the portable and prototype two-color geodimeter. Each instrument is set up over an adjacent monument on Carr Hill and length measurements are made on 14 baselines which uniformly cover a 360° range in azimuth. Using the differences in observed baseline lengths, we have deduced both the relative stabilities of the geodimeters and the monuments to within 0.2 mm and 0.4 mm respectively.

Prior January 1986, we conducted this experiment on a reduced set of baselines using only a 150° range in azimuth. Data from these experiments, which go back to June 1984, indicate that both the geodimeters and monuments have changed relative to each other. For instance, the inferred instrument length scale has fluctuated as much as 0.4 ppm and fluctuations in monument displacements were on the order of 2 mm. However, the limited range in azimuthal control precluded us from resolving the ambiguity of change in instrument length scale and monument displacement.

Although January 1987 measurement of the length scale is higher than its previous measurements, the latter two observations are consistent with the data between January 1985 and October 1986. At this time we have no explanation for the discordant measurement of January 1987 although it should be noted that only the short baselines were measured in January 1987 because of intense fog.

2. Long Valley

We now have more than 4 years of line-length change data measured within the Long Valley Caldera. Within this 42-baseline network, measurements on about one-half of these baselines are made frequently; that is, from several times per week to once monthly. With this data set, it is possible to define a decrease in the rate of deformation within the caldera. We have modeled the line-length changes as a combination of inflation beneath the resurgent dome plus dextral slip within the south moat. The inflation is modeled as a combination of two sources, one at 10 km depth and the other at 5 km depth. Furthermore, as a result of geothermal production within 1-1/2 km of two of our monuments, we model the water withdrawal and its associated ground subsidence as a point source at 0.5 km depth. Production started in the spring of 1985.

A time-dependent function of each of the source terms is fit to the line-length changes. The result is shown in Figure 2. The additional data, which is not included in Langbein et al. (1987a), indicates that the caldera has been deforming at a fairly constant rate since early 1985. The rate before 1985 was roughly a factor of two faster than the current high rate.

In computing the time dependence of these four sources, we also had to account for the offset due to the Chalfant Valley earthquake. Although the position of the modeled fault plane is not a significant factor in modeling the offsets, we found that a source with a moment of 4.2×10^{25} dyne-cm or an equivalent earthquake of magnitude 6.4 is consistent with the two-color data.

3. Middle Mountain

Over the past year, four geodetic surveys have been conducted on a network that straddles Middle Mountain and near the source area of the 1966 main shock in Parkfield. The network uses two central stations. One station is located about 200 meters southeast of the Middle Mountain creepmeter. The second central station is roughly 2 km east of the fault.

To analyze these data, a model consisting of rigid block slip across the San Andreas fault plus uniform strain is proposed. Since a coordinate system used here is parallel and normal to the strike of the fault, N42°W, the resulting shear strain should be viewed as a residual. For instance, if the slip at depth is equal to the surface slip, that is, block translation, then the accumulated shear will be zero. However, if some weighted average of the slip at depth is greater than the average surface slip, then the shear strain will accumulate (positive).

The result of fitting this simple model of time-dependent slip and strain to the data is shown in Figure 3. The average slip rate for this area is computed to be 17 mm/a for the past year. The data over the past 2-1/2 months indicate that the average slip is greater by a factor of two than the preceding 10 months. The shear strain shows no appreciable accumulation within its expected error. The parallel and normal strains, however, show significant contraction. This areal contraction can be explained, in part, by adding more slip to the northwest of the Middle Mountain creepmeter. Because the network would be roughly centered in the compression lobe of the end of the hypothetical dislocation, the network should be measuring compression. However, various attempts to model a gradient in slip resulted in no apparent decrease in areal contraction assuming that the fault that is northwest of the network is slipping at 25 to 30 mm/yr.

4. Pinon Flat

Between March 1986 and July 1987, we have three surveys of a network near the Pinon Flat observatory. One of the seven baselines includes the VLBI site at the observatory. Based upon these data, we compute the following secular strain rates:

$$\dot{E}_{ee} = -\ 0.08 \pm 0.09 \text{ ppm/a}$$

$$\dot{E}_{en} = -0.27 \pm 0.06 \text{ ppm/a}$$

$$\dot{E}_{nn} = -0.26 \pm 0.05 \text{ ppm/a}$$

This pattern of deformation yields essentially uniaxial compression of 0.45 ± 0.08 ppm/a oriented N36 ± 5°E. The orthogonal extension rate is 0.11 ± 0.09 ppm/a. Since we will be measuring this network between three and four times per year, it will be interesting to compare the geodetic data with data from the laser strainmeter and the triaxial, borehole strainmeters.

Reports

Langbein, J., M. Linker, and D. Tupper, Analysis of two-color geodimeter measurements of deformation within the Long Valley caldera, June 1983 to October 1985, JGR, vol. 92, p. 9423-9492, 1987a.

Langbein, J.O., M.F. Linker, A.F. McGarr, and L.E. Slater, Precision of two-color geodimeter measurements: results from 15 months of observations, JGR, vol. 92, p. 11,644-11,656, 1987b.

Langbein, J., Geodetic monitoring of deformation within the Long Valley caldera, 1983.5-1987.1, data from the two-color geodimeter network, in Proceedings of the Symposium on the Long Valley Caldera, March 1987, LBL, U. of California.

Figure Captions

Figure 1. Results from instrument intercomparison at Parkfield. The top plot shows the inferred displacement of the monument used by the portable geodimeter relative to the monument used by the prototype instrument. The lower plot shows the inferred change in length scale of the portable instrument relative to the prototype.

Figure 2. The changes as a function of time of the size of hypothetical model sources for the Long Valley Caldera. The time variation is controlled chiefly by data from the two-color geodimeter network but is also constrained by three surveys of the Geodolite network between 1983 and 1985. Error bars represent one standard deviation for the estimation of the size of each source. The absolute size of the deep and shallow inflation sources is not well constrained because of the high statistical covariance between these two modeled sources.

Figure 3. The changes as a function of time of slip and strain inferred from geodetic data obtained near Middle Mountain, Parkfield, California. Since slip has been assumed to be block displacement, the resulting shear strain must be viewed as residual strain accumulation.

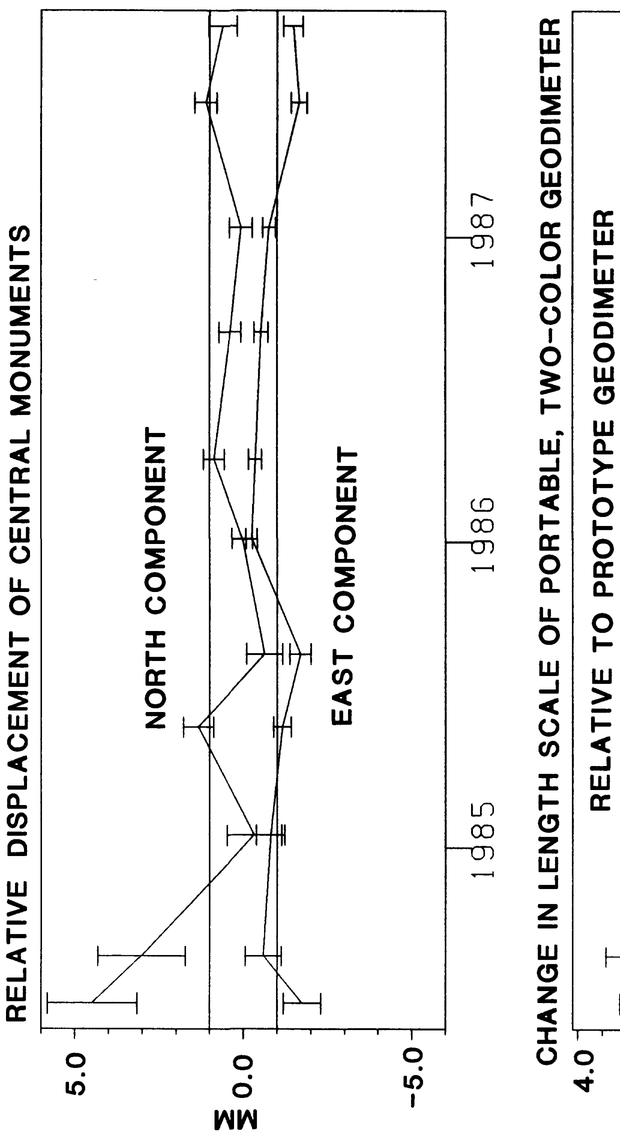
RELATIVE DISPLACEMENT OF CENTRAL MONUMENTS
NORTH COMPONENT
EAST COMPONENT
5.0
0.0
-5.0
MM
1985
1986
1987
CHANGE IN LENGTH SCALE OF PORTABLE, TWO-COLOR GEODIMETER
RELATIVE TO PROTOTYPE GEODIMETER
4.0
0.0
-4.0
MM
1985
1986
1987

FIG. 1

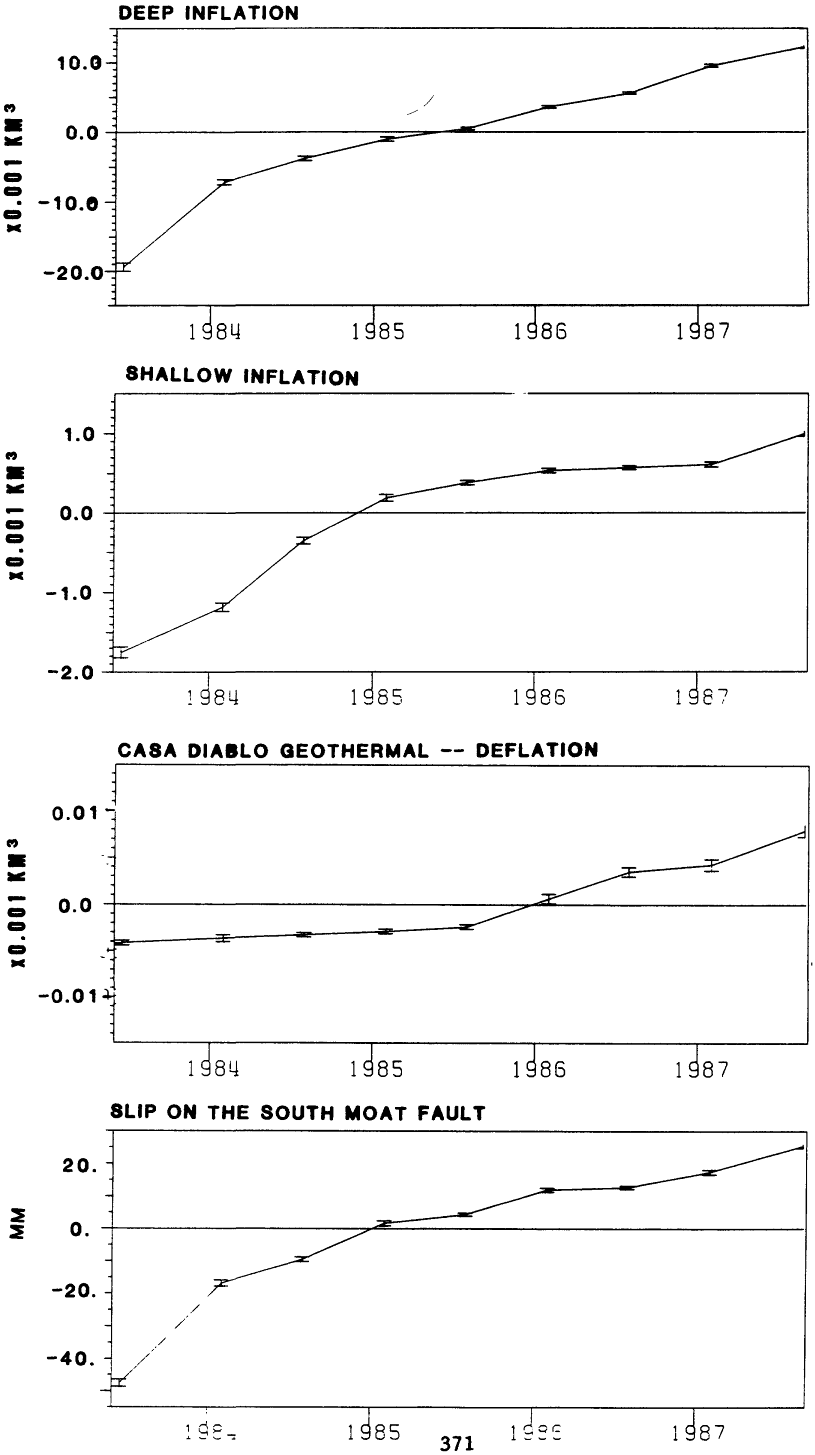
DEEP INFLATION
x0.001 KM³
10.0
0.0
-10.0
-20.0
1984
1985
1986
1987
SHALLOW INFLATION
x0.001 KM³
1.0
0.0
-1.0
-2.0
1984
1985
1986
1987
CASA DIABLO GEOTHERMAL -- DEFLATION
x0.001 KM³
0.01
0.0
-0.01
1984
1985
1986
1987
SLIP ON THE SOUTH MOAT FAULT
MM
20.
0.
-20.
-40.
1985
1987

FIG.2

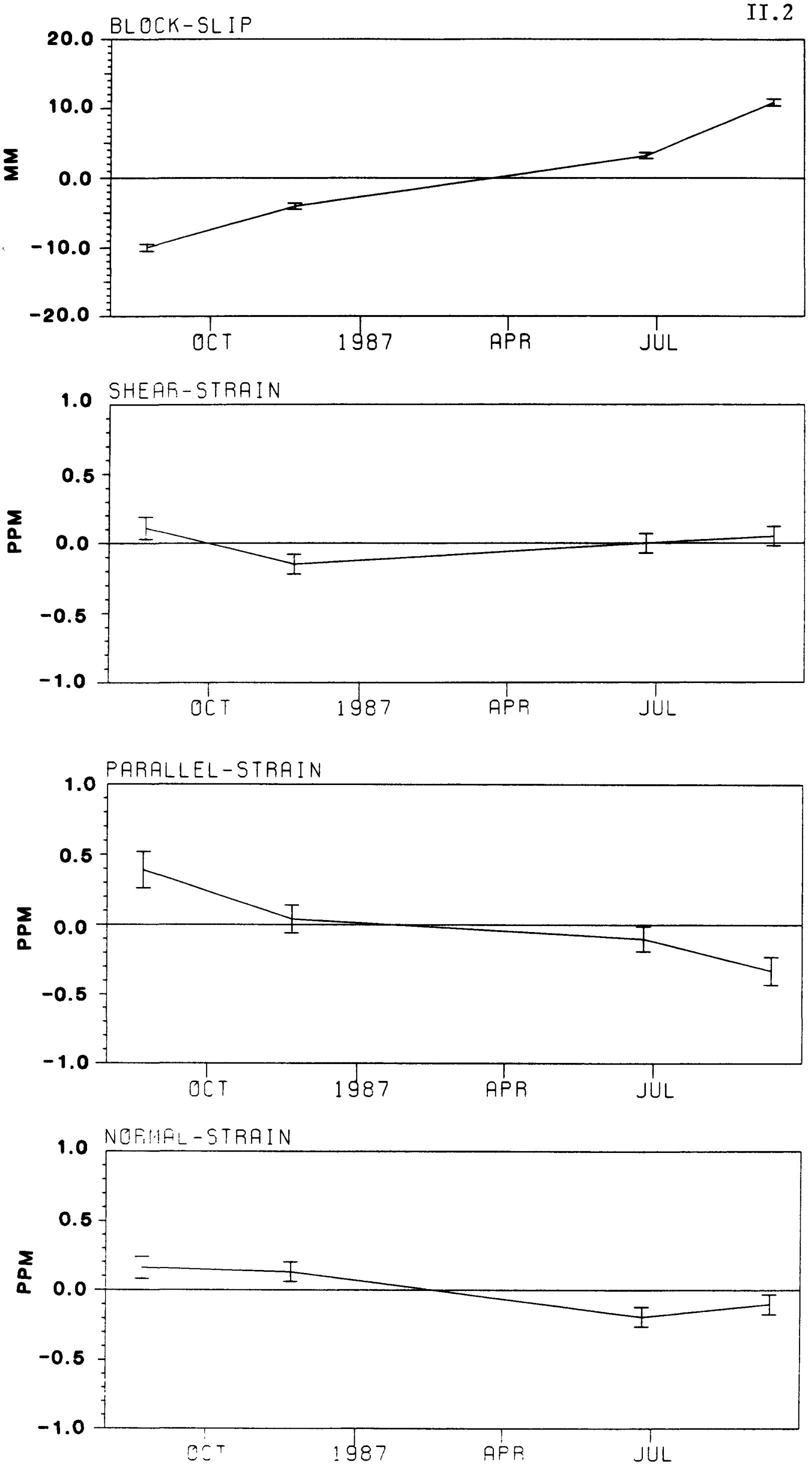
BLOCK-SLIP
MM
20.0
10.0
0.0
-10.0
-20.0
OCT
1987
APR
JUL
SHEAR-STRAIN
PPM
1.0
0.5
0.0
-0.5
-1.0
OCT
1987
APR
JUL
PARALLEL-STRAIN
PPM
1.0
0.5
0.0
-0.5
-1.0
OCT
1987
APR
JUL
NORMAL-STRAIN
PPM
1.0
0.5
0.0
-0.5
-1.0
OCT
1987
APR
JUL

FIG. 3

Microearthquake Data Analysis

9930-01173

W. H. K. Lee
U.S. Geological Survey
Branch of Seismology
345 Middlefield Road, Mail Stop 977
Menlo Park, California 94025
(415) 329-4781

Investigations

The primary focus of this project is the development of state-of-the-art computation methods for analysis of data from microearthquake networks. For the past six monthis I have been involved in:

(1) A project called "Investigation of signal characteristics of quarry blasts, nuclear explosions, and shallow earthquakes for regional discrimination purposes" for the Defense Advanced Research Projects Agency. The objective is to collect high-frequency seismic data generated by quarry blasts, controlled explosions, and shallow earthquakes, to study their signal characteristics, and to develop a method to discriminate between these three different sources.

(2). A collaborative project with Kei Aki and others on coda Q study in California. The objective is to use seismic coda waves recorded by Calnet for investigating the spatial and temporal variations of seismic attenuation.

Results

I was invited to the Centennial Symposium of the University of California Seismographic stations. A paper by Lee and Stewart, "Large scale processing and analysis of digital waveform data from the USGS Central California Micorearthquake Network" was presented. In this paper, we summarize the processing and analysis techniques and the current status of the coda Q study.

I was the convenor for a workshop on applications of personal computers at the IUGG General Assembly in Vancouver, Canada, August, 1987. A paper by Lee, Zirbes and Needham on "Two applications of personal computers for seismological studies at the U.S. Geological Survey" was presented.

Reports

Peng, J. Y., Aki, K., Chouet, B., Johnson, P., Lee, W. H. K., Marks, S., Newberry, J. T., Ryall, A. S., Stewart, S. W., and Tottingham, D. M., 1987, Temporal changes in coda Q associated with the Round Valley, California, earthquake of November 23, 1984, J. Geophyus. Res., v. 92, p. 3507-3526.

Phillips, W. S., W. H. K. Lee, and J. T. Newberry, 1986, Spatial variation of crustal coda Q in California, Pure and Appl. Geophys., in press.

Lee, W. H. K., Zirbes, M. D., and Needham, R. E., 1987. Two applications of personal computers for seismological studies at the U.S. Geological Survey. (Abstract), IUGG XIX General Assembly Abstracts, v. 1, p. 380.

Lee, W. H. K., and Stewart, S. W., 1987, Large scale processing and analysis of digital waveform data from the USGS central California Microearthquake Network; Proceedings of the Centennial Symposium of the Univ. of Calif. Seismographic Stations, in press.

Acquisition and Analysis of Data from Sacks-Evertson Borehole Strainmeters in California

1408001 G 1172

Alan T. Linde and I. Selwyn Sacks
Department of Terrestrial Magnetism
Carnegie Institution of Washington
5241 Broad Branch Rd. NW
Washington DC 20015
(202) 966 0863

This program is conducted in cooperation with the Geological Survey; in particular M. Johnston and D. Myren have been very active. Progress in detecting and interpreting strain changes associated with seismic activity has been hampered by the lack of an adequate array of instruments in any one area. This has recently improved significantly with the installation of several more instruments in the Parkfield area. The data acquisition capabilities now include 10 minute sampling with 16-bit satellite telemetry (the GS low frequency system) and, at many of the sites, high frequency triggered sampling with GEOS recorders.

Seismic Information

The wide frequency range of the instruments (zero frequency to several hertz) together with the high dynamic range (more than 120 dB) has allowed on-scale recording of many earthquakes, including all the larger ones. These data have been used in a number of earthquake source studies.

Long Term Strain Changes

The generally poor quality of rock in the vicinity of the San Andreas fault results in installations for which we must be cautious in interpreting long term (order of months to years) strain changes. Prior to the recent increase in the number of stations at Parkfield, our site separations have been too great too allow meaningful comparisons of long term effects (and we must wait for data to accumulate from the more recent installations at Parkfield). Coherence between data from one of our instruments and a nearby Gladwin three component borehole instrument has been noted however and a collaborative study is in progress.

Episodic Slow Strain Changes

We now have data from several different tectonic regions which suggest that stress buildup before an earthquake may be at least partially in the form of episodic slow slip on adjacent portions of the fault surface.

Before the Japan Sea (m=7.7) earthquake of 1983, approximately 100 slow strain events were recorded on the nearest Sacks-Evertson borehole instument (about 90 km from the epicenter). We have shown that these signals are consistent with slowly propagating slip on a deep extension of the main shock fault plane. The sense of this slip is such as to increase the stored strain energy in the region of the eventual earthquake. In Iceland, similar signals have also been recorded on the same type of instruments installed near the transform fault in the southern part of Iceland. In a study currently in progress, we have already seen that these signals are also consistent with slowly propagating slip on the transform. This area is currently denoted as a special study area for earthquake prediction because of an increased probability for a moderate sized event. There appears to be similarities between these areas and Parkfield. Earlier (1985) slow strain events were noticed on the borehole instruments at Gold Hill (and also there were corresponding changes in levels in a water well). More recently, with the expanded network of borehole instruments, episodic signals have been recorded over the network. We are now beginning a study to interpret these signals in terms of slow deformation at depth.

Our present main interest in this program is to examine as much data as possible which will bear upon the hypothesis that, at least in some cases, earthquakes are preceded by a non-uniform accumulation of strain energy in the source region through the mechanism of episodic slow slip events.

Parkfield Seismic Experiment

9930-02098

Allan G. Lindh, Catherine M. Poley
John Estrem, and Barry Hirshorn
Branch of Seismology
U.S. Geological Survey
345 Middlefield Road, MS-977
Menlo Park, California 94025
(415) 329-4778

Investigations

1. Real-time monitoring and analysis of Parkfield seismicity, as part of the Parkfield Prediction Experiment, with special attention given to seismicity near Middle Mountain.
2. Continued work on long-term earthquake probabilities along the San Andreas system.
3. Relocation and spatio-temporal analysis of central California coastal seismicity.
4. Coda-magnitude and "envelope magnitude" study.
5. Daily reprocessing and maintenance of RTP data, with an eye to seismicity changes. Bi-weekly review of station and network performance.
6. Continued work on incorporation of RTP and CUSP data into one database.
7. Monitoring of Parkfield leveling network and analysis of leveling data, as part of the Parkfield Prediction Experiment.

Results

1. Overall seismicity at Parkfield for the time period 1 April 1987 - 31 September 1987 was normal with 111 events. Activity near Middle Mtn. was slightly higher than normal with 38 events. Seven (7) of these events resulted in seismic alerts (see Figure 1). All (7) were level D; this exceeds the anticipated rate for level D alerts by 4 alerts (see Bakun, this volume).

   Events of interest include:
   (1) On Sunday morning August 15th, 1987 at 9:04 (PDT), a M=2.6 earthquake occurred near Simmler, 40 km south of Cholame (the southern end of the 1966 Parkfield earthquake rupture zone). Four (4) more events occurred there in the following two (2) hours, including a second M=2.6 and a M=2.0 event.
   (2) On September 18th a swarm of 5 M=1-2 earthquakes occurred in a 7 minute span at 6 km depth on the San Andreas fault just north of Parkfield. Four (4) events in 4 hours occurred in the same location on the 19th; single events occurred on the 20th, 21st, and 25th; there were 2 events within 1 minute of each other on the 26th. The swarm nature of seismicity is unprecedented in the detailed recordings of Middle Mtn. seismicity since 1971.

Catherine Poley, with Allan Lindh, Bill Bakun and Sandy Schulz, has completed work on analysing the effects of the 2 May 1983 M=6.7 Coalinga earthquake on the Middle Mtn. section of the San Andreas fault. A paper discussing this work has been published in NATURE.

Events from Parkfield are now being loaded into the VAX750 Parkfield disk for routine analysis of the seismograms.

2. Allan Lindh, using the different approaches used to calculate foreshock probability gains for Parkfield, has extended his study to determine the likelihood that the next characteristic Parkfield earthquake will be a foreshock to a larger earthquake on the southern section of the San Andreas. Efforts continue, to refine the probability estimates of the next characteristic Parkfield earthquake. A paper concerning these questions is in preparation.

3. Catherine Poley, with Allan Lindh and Jerry Eaton, has collected all the phase data from coastal California from San Francisco to the Transverse Ranges. Relocation and analysis of these data are underway and include systematic relocation, focal mechanism determination and stereo-plot projections of the seismicity.

   A subset of this coastal region is the seismicity which occurs in the San Ardo region. The November 24-25 1985 San Ardo earthquake sequence has been studied and is the subject of a paper by Catherine Poley, in press in BSSA.

4. Barry Hirshorn, with Allan Lindh, has developed a coda-magnitude relation by taking the RTP codas form the low-gain stations for all the M3+ events in the Coast Ranges, and regressing them against Berkeley's preliminary M_L estimates for the same events. Allan Lindh has used this formula, with station corrections determined by Caryl Michaelson, as the basis for a new computer program which allows rapid determination of magnitudes (M_Z) from low-gain station coda lengths using RTP and Prototype online phase data. For events between M3 and M6, M_Z appears to be a quite stable estimate of M_L (see Figure 3). An open-file report concerning this subject is in preparation.

5. Allan Lindh meets with John Van Schaak twice a week to review station performance. Barry Hirshorn, in conjunction with reprocessing of RTP data, runs weekly station quality meetings.

6. Successful efforts continue to incorporate RTP data in the CUSP database. RTP data is now reprocessed within the CUSP database.

7. John Estrem continues to keep the leveling network at Parkfield functional, and routine analysis of the leveling data continues. A fault-crossing leveling line has been installed at Gold Hill.

Reports

Poley, C.M., Lindh, A.G., Bakun, W.H. and Schulz, S.S., 1987, Temporal changes in microseismicity and creep near Parkfield, California, NATURE, v. 327, n. 6118, pp. 134-137.

Jones, L.M. and Lindh, A.G., 1986, Foreshocks and earthquake prediction at Parkfield, California (abs.), EOS Tran. AGU, 66, 982, 1985.

Bakun, W.H., et al., 1987, Parkfield Earthquake Prediction Scenarios and Response Plans, U.S. Geological Survey Open-File Report 87-192.

Poley, Catherine M., The San Ardo, California, earthquake of November 24, 1985, BSSA, in press.

Poley, C.M., Eaton, J.P., and Lindh, A.G., 1987, Recent seismicity of the central California region from San Francisco to the Transverse ranges (abs.): Cordilleran section Geol. Soc. Am. Abstracts with Programs, May 1987.

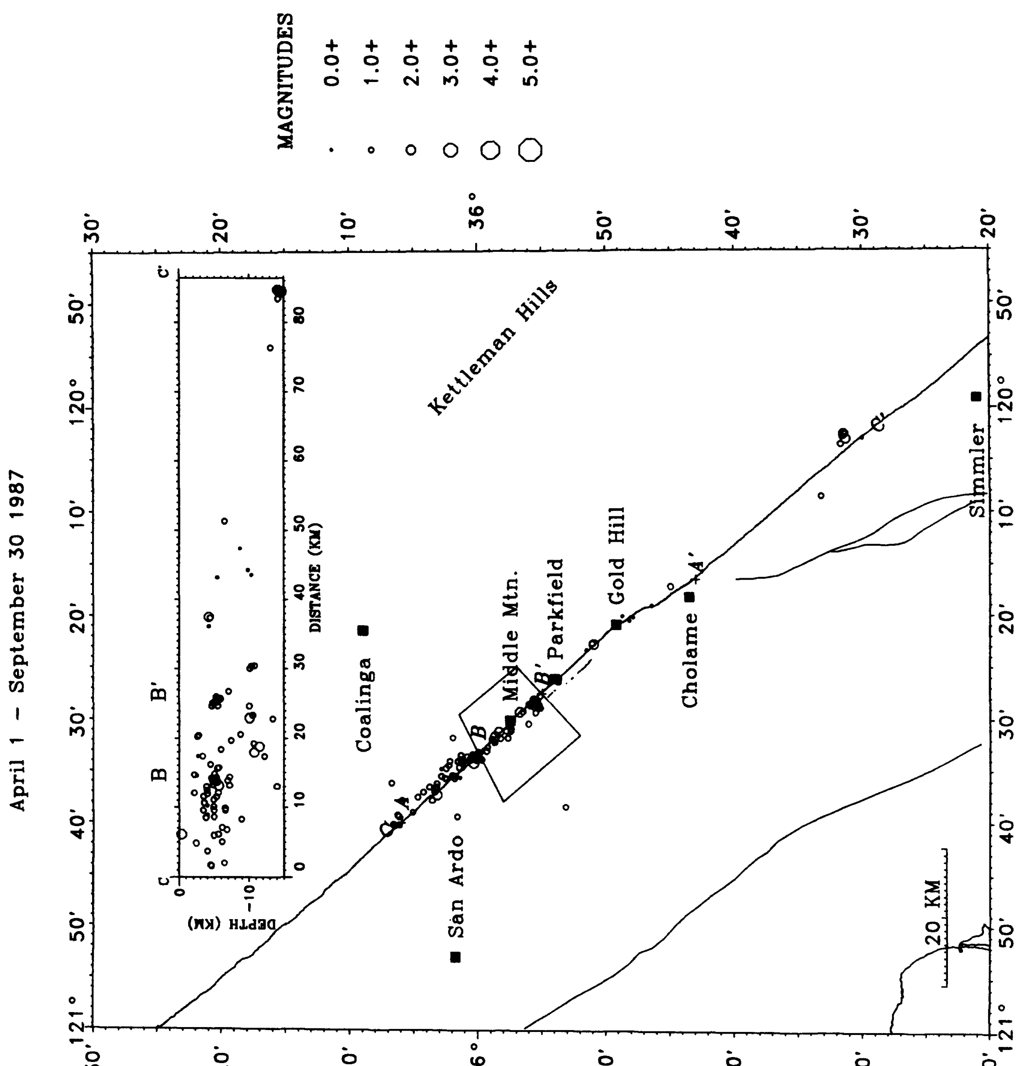

Figure 1. Map of epicentral locations, all magnitudes, from April 1, 1987 thru September 31, 1987. Inset is cross-section along A-A'. The Middle Mtn. region is indicated by the quadrilateral and by B-B' in the inset.

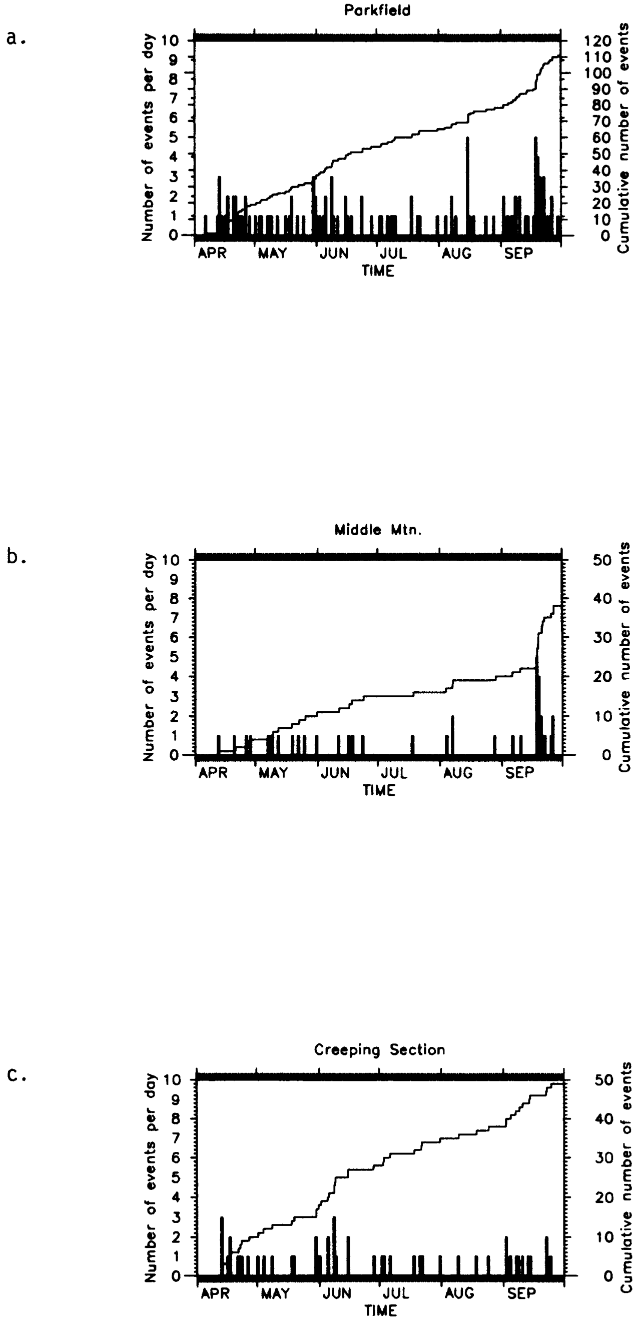

Figure 2. Histograms and cumulative number plots of seismicity, all magnitudes, from April 1, 1987 thru September 30, 1987. a) Parkfield seismicity. b) Middle Mtn. seismicity. c) Creeping section seismicity.

The Parkfield Cooperative Downhole Digital Seismic Network.

USGS #14-08-0001G1375

P.E. MALIN
Institute for Crustal Studies
University of California Santa Barbara
Santa Barbara, CA 93106

Network Status. (Alvarez et al., 1987) In cooperation with UC Berkeley and the US Geological Survey, we have established a 10 station network of 3-component downhole seismometers (Figure 1). The network serves two main purposes: (1) the detection and recording of microearthquakes in the magnitude range $-1<m<1$ and (2) the periodic recording of vibroseis monitoring signals. While parts of the network have been in operation since Aug 1985, the full network and its centralized recording system were complete this fall.

A typical station consists of a gimble leveled package of 5.5kΩ Mark Products L22E 2Hz seismometers cemented at the bottom of a 250m borehole (Figure 2). In a solar and battery powered hut at the well head, RefTek equipment gains the seismometer outputs by 80db, digitizes them to 16 bits at a rate of 500/sec, and transmits them to a central recording interface and computer. Earthquakes are detected by an algorithm combining both long-term to short-term ratios of ground motion and coincidence counting of stations exceeding the minimum trigger ratio. Triggered events are recorded in SEGY format on a 1/2" magnetic tape.

We are currently using the array to study the time, space, and magnitude statistics and source properties of very small earthquakes, the propagation of seismic waves in and around the San Andreas fault, the structure of the fault zone, site characteristic of each station, and the characteristics of coda waves. Data from the array is being included in the monitoring program of the Parkfield Earthquake Prediction Experiment. Below we summarize the results of our studies of site characteristics and coda waves.

Site Characteristics (Blakeslee and Malin, 1988). We have compared the S-wave spectra of microearthquakes recorded at the surface with their counterparts recorded at the bottom of the 200± meter boreholes. The degree to which the near surface affects the S-wave is of critical importance if spectra dependent parameters are to used for source parameter inversion. Our experience with the Parkfield data set leads us to infer that spectra recorded at the surface are dominated by two distinct factors. First, the high frequencies are not preserved in transit to the surface and are severely attenuated by demonstrably low values of Q. Second, simple first order reverberations due to heterogeneity in the near surface produce a marked interference effect in the spectra.

The ratio of an uphole-downhole pair of spectra should reflect only the transfer function of the path from the bottom of the borehole to the surface. This transfer function will be unaffected by the specifics of the source spectra, Greens's function or instrument response (same instuments). The transfer function for a wave traveling through a constant Q material is simply an exponential loss of high frequency that is scaled by the transit time of the wave in the material and the specific Q value of the material. When plotted on a lin-log basis constant Q attenuation will produce a linear roll off as a function of frequency. The best fit slope of that line is then inverted for a measure of average Q of the material between the seismometers. This procedure fail in those parts of the spectra that include the effects of interferring waves.

Spectral ratios from the Joaquin site have been stacked and exhibit a strong negative linear slope for high frequencies but becomes virtually flat at low frequencies (Figure 3). In the bandwidth between 12 and 40 Hz. Q is approximately 20. A Q calculated from the bandwidth between 0 and 12 Hz. yields value of about 300.

Spectral ratios from Vineyard Canyon have also been stacked (Figure 4). As was also seen at Joaquin, there is a relatively steep linear negative slope for high frequencies and a flat or even positive slope at low frequencies. From the bandwidth between 8 Hz. and 50 Hz. the slope is extremely linear and is well fit with a Q value of 16. Below 8 Hz. Q ranges from infinite to negative, which is clearly non-physical in terms of intrinsic attenuation. The frequency at which the roll-off changes from positive to negative appears to be a function of angle of incidence and azimuth.

To account for our observed spectral ratios, we have developed an combined first order dissipation and interfering upgoing-downgoing wave picture of our sites. With the simple model of a discontinuity near the surface and a constant Q throughout the medium two key aspects of the spectral ratios from Parkfield were successfully modeled. First, the high frequency roll off in the data is caused by a low Q material in the upper 200 meters. Second, the low frequency behavior in the ratio (including negative apparent Q) is dominated by the effect of reverberations in the near surface and does not reflect a bimodal behavior in intrinsic Q (Figure 5).

Coda Waves (Malin and Blakeslee, 1987). We have studied the S-wave codas of 21 digitally recorded microearthquakes from the Parkfield area in an effort to better understand their origin and value for earthquake prediction studies. The analysis was performed on the entire data set with no selective editing.

The uphole codas consistently differ from the downhole codas in their spectral content and their decay rate. The coda Q(f) was modeled as a power law $Q(f)=q_0 f^{ß} t^{\mu}$. Coda decay rates are transformed into log space and fit in the least squares sense with a plane which is parameterized by q_0, ß, and μ. Consistent differences emerge between uphole and downhole values of q_0, ß, and μ (Figure 6). The significance of various site effects was analyzed in an attempt to understand these differences in coda Q(f).

The high cut filtering of a low Q environment and the sinusoidal spectral modulation produced by reverberations do affect the appearance of the coda but appear to have little affect on the overall decay rate and do not seem to account for the observed difference in coda Q(f). Based on differences in uphole-downhole mean ellipticities, energy accumulation, and stacked amplitude ratios, the differences seem to stem from the inclusion of scattered surface wave energy which does not penetrate to depth.

The time sequential plots of q_0, ß, and μ show a trend which could be mistaken for source or propagation path changes, as has been postulated for precursory coda wave changes (Figure 6). By studying the various correlations of these parameters with source distance, we have concluded that the trend is not due to precursory changes. After removal of all the effects of source distance and character from our fitting method, it may be possible to use it as a tool for studies of precursory coda changes.

References.

Alvarez, M & UCSB Parkfield Group, T.McEvilly & UCB Parkfield Group, R. Dollar, T. Burdette & USGS Parkfield Group, 1987, The Parkfield Cooperative UCSB-UCB-USGS Downhole Digital Seismic Network, **EOS**, abstract for the 1987 Fall AGU meeting, San Franscisco, CA.

Blakeslee, Sam and Peter Malin, 1988, Near Surface Site Effects at Parkfield California from Direct Observation of S-waves Downhle, manuscript to be submitted to **BSSA**, 1988.

Malin, P.E. and Sam Blakeslee, 1987, A Comparison of Earthquake Coda Waves at Surface Versus Subsurface Seismometers, submitted to **JGR**, 11/1987.

FIG 1

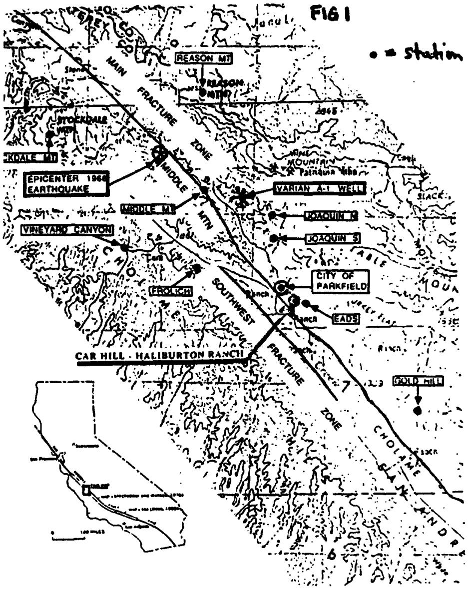

• = station

FIG 2

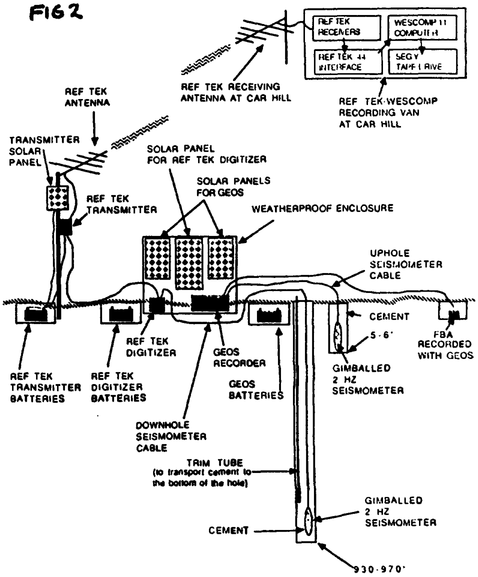

FIGURE BY A. MARTIN

FIG3

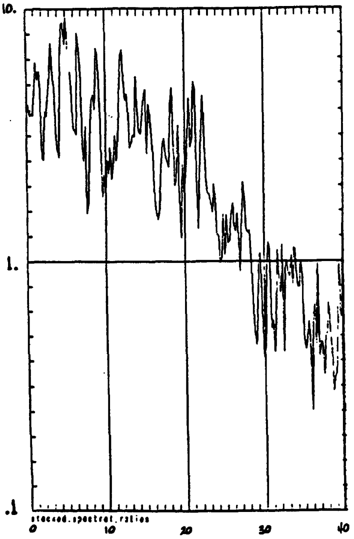

Stack of 8 S-phase spectral ratios from Joaquin site, no smoothing. Note: high frequency roll off, flattening of roll off for low frequencies.

FIG 4

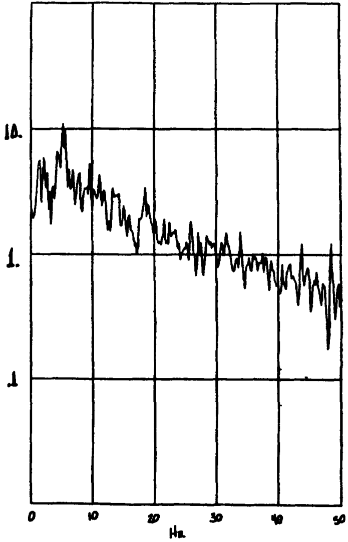

Stack of 15 S-phase spectral ratios from Vineyard, with no smoothing.
Note: high frequency roll off and flattening of roll off for low frequencies. Inversion of slope for Q gives Q=18.

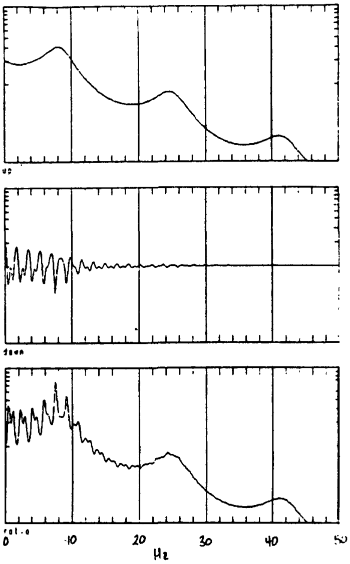

Figure 5:
Transfer function for signal with
1) free surface multiple
2) near surface reverberations
Top-scallop spacing now appropriate for discontinuity near surface
Middle-higher order interference patterns seen with small scallop spacing corresponding to large uphole downhole transit time.
Bottom-ratio give scalloping and anomalous negative Q for low frequency.

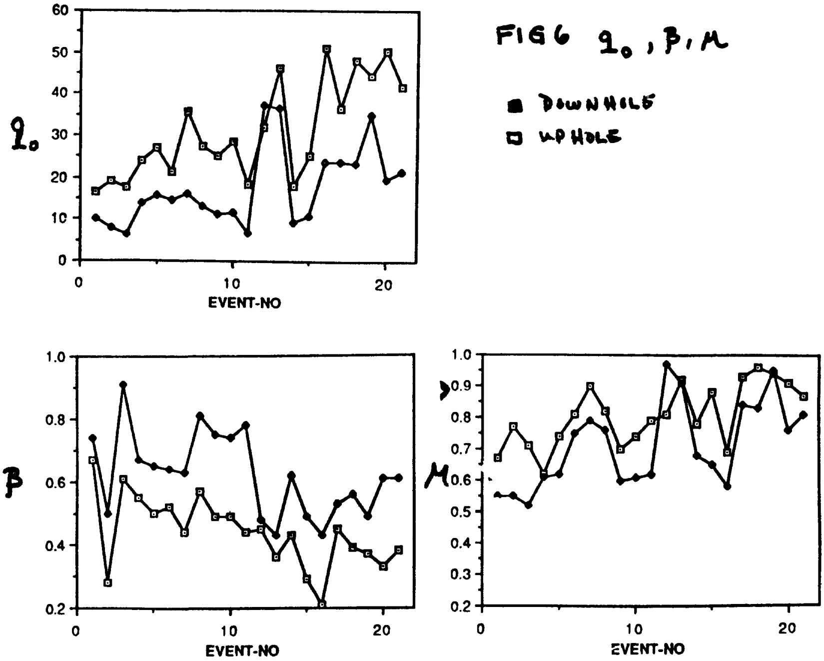

FIG 6 q_0, β, μ

Geomensor surveys in the Imperial Valley

Grant No. 14-08-0001-G1374

Ronald G. Mason
Geology Department, Imperial College
London SW7 2BP, England (011-441) 589 5111

Investigations

The purpose of this project, which was started in the early seventies, is to study movements on and around the Imperial fault in the neighborhood of El Centro. It involves the repeated measurement of a network of about 300 survey stations about 800 m apart, the most important part of which comprises a 10 km by 8 km block spanning the fault and including a 10 km length of the surface break associated with the 1979 earthquake. The instrument used is a Geomensor, with which standard errors of less than 1 mm (1ppm) are being achieved. The current grant is for remeasuring the main block, last measured in 1982, and for making certain extensions aimed at producing a better balance between coverage of the two sides of the fault, and better coverage of the junction of the Imperial and Brawley faults.

Results

During this reporting period ten weeks were spent in the field, during which more than 600 measurements were made, representing about half the field program. The results can not be fully evaluated until the survey is complete, when station coordinates can be computed for comparison with the 1982 results. However, comparison of the lengths of fault-crossing lines confirms that the fault is still creeping, but at a faster rate than had been predicted from earlier measurements. By contrast with the coseismic slip, which decreased generally from south to north, from about 600 mm at the southern end of the surface break to less than 400 mm at the northern boundary of our network, the fault has been creeping fastest near the middle of the surface break, near the Ross Road site of a Caltech creepmeter. There, the present rate of creep is greater than 13 mm/yr, and as of June 1987 the fault had crept about 400 mm since the earthquake, almost as much as the 413 mm it slipped during it.

EXPERIMENTAL TILT AND STRAIN INSTRUMENTATION

9960-01801

C.E. Mortensen
Branch of Tectonophysics
U.S. Geological Survey
345 Middlefield Road, MS/977
Menlo Park, California 94025
(415) 329-4856

Investigations

1. The satellite telemetry system has been brought to a state of relative reliability and stability. There are currently 108 Data Collection Platforms (DCPs) that transmit a variety of data through the GOES-6 spacecraft to the Direct Readout Ground Station (DRGS) in Menlo Park. Forty four of these DCPs transmit data at 10-minute intervals on an exclusively assigned random channel, which is being utilized under a special agreement with NESDIS. The remainder of the DCPs report at standard 3 or 4-hour intervals as assigned by NESDIS. This system transmits data from all types of low-frequency instruments including dilatometers, creepmeters, strainmeters, water-level meters, magnetometers, tiltmeters, and related measurements.

A sufficient number of DCP's to replace all of the existing telephone telemetry system is being procured. A system to back-up the satellite telemetry system with non-volatile, solid-state memory and dialup or dedicated telephonic communications path is under development.

2. A system to affect emergency communications and routine operational message traffic in the Parkfield area has been implemented. Seven wide-band, digitally-synthesized radios have been delivered and installed - six in field-service vehicles and one at the Car Hill laser observatory. These radios can communicate over the USGS repeater frequency, on commercial mobile radio-telephone frequencies, on the California Emergency Services Radio System, and through the USGS microwave link to the telephone system at Menlo Park. Additional capabilities are available with certain units including access to a large number of local emergency and operational radio nets. It is also planned to establish a capability to link directly to the telephone system locally by installing a phone-patch (already procured) at Car Hill. Equipment to establish a second radio network, with a separate repeater, in the Parkfield area is on order. The purpose of the second network will be to segregate the communications in

order to avert saturation of the circuits in the event of heavy operational activity in the area.

3. Networks of tiltmeters, creepmeters and shallow strainmeters have been maintained in various regions of interest in California. A network of 14 tiltmeters located at seven sites monitor crustal deformation within the Long Valley caldera. Other tiltmeters are located in the San Juan Bautista and Parkfield regions. Creepmeters located along the Hayward, Calaveras and San Andreas faults between Berkeley and the Parkfield area are maintained in cooperation with the Fault Zone Tectonics project. A shallow strainmeter is located near Parkfield, while observatory type tiltmeters and strainmeters are sited at the Presidio Vault in San Francisco, and a tiltmeter is installed in the Byerly Seismographic Vault at Berkeley. Data from all of these instruments are telemetered to Menlo Park via the GOES satellite, by phonelines and radio links, or both.

4. A short-haul telemetry system has been assembled from commercially available modules to acquire data from the tiltmeter that monitors rotational changes in the MIDE reflector pier of the two-color laser system at Parkfield.

5. In February, Carl Mortensen attended the Hawaii Symposium on "How Volcanoes Work", presenting a paper on the Long Valley tiltmeter array.

Dilatometer Operations

9960-03815

G. Douglas Myren
Branch of Tectonophysics
U.S. Geological Survey
345 Middlefield Road, MS/977
Menlo Park, California 94025
415-329-4858

Investigations and Results

Since April 1, 1987 the Dilatometer Operations project has been concerned with the routine maintenance of the dilatometers throughout California and the completion of the installations in Parkfield, California. As of the end of June 1987, the instrumentation of Parkfield dilatometers was completed.

In March 1987 the cable at the Searle Road dilatometer began to leak. Using a variation of a circuit developed by Doak/Poe of Carnegie Institute of Washington, we have been able to generate a signal from that instrument that satisfactorily represents the strain seen at depth at this location. This circuit has been applied at other locations experiencing similar problems with varying degrees of success. Eades, Echo Valley, and Adobe Mountain are the other locations with leaky cables.

In mid-July of 1987 we dismantled and "mothballed" the Eades dilatometer until it becomes possible to turn it on again with the permission of a new landowner.

Site	Instrument	Lat.	Long.	Depth(m)	
POPS	Postpile	37.6380	-119.0840	162.1	*
SRLS	Searle Rd.	36.8650	-121.5770	137.7	
EVSS	Echo Valley	36.8320	-121.6330	117.6	
DLDS	Donna Lee	35.9392	-120.4245	176.48	*
VCDS	Vineyard Cyn	35.9225	-120.5342	204.1	*
FRDS	Frohlich	35.9111	-120.4855	323.36	*
EADS	Eades Ranch	35.8942	-120.4212	267.2	
GH2S	Gold Hill 2	35.8345	-120.3438	177.7	*
GH1S	Gold Hill 1	35.8326	-120.3448	117.6	
JCDS	Jack Canyon	35.7125	-120.2025	169.13	*
RHDS	Red Hills	35.5411	-120.2535	229.16	*
BBSS	Black Butte	34.5690	-117.7300	170.4	
PUBS	Punchbowl	34.4340	-117.8740	176.2	*

The above sites are currently recording strain data on site, and via satellite in Menlo Park, California. GEOS 16 bit data recorders are collecting seismic data from the dilatometers with an asterisk. (The GEOS recorders are being operated by Tom Noche under Roger Borcherdts direction.) At VCDs and FRDS the Seismic Branch is collecting seismic information from the dilatometer for transmission over microwave to Menlo Park, California. This is also being done at the previously installed GH1 (Gold Hill) site.

Helium Monitoring for Earthquake Prediction

9570-01376

G. M. Reimer
U.S. Geological Survey, MS 963
Denver Federal Center
Denver, CO 80225
(303) 236-7886

INVESTIGATIONS

The variations of helium in soil-gas is being observed to see if a link can be established between variation in concentration and seismic activity. Several sample collecting stations have been established in central California along the San Andreas Fault and are being monitored to establish a data base. Stations had been in place for 7 years along a traverse from San Benito to Hollister and an interesting correlation between helium decreases and seismic activity was observed. Several of those stations have been moved to near Parkfield and now are the main focus of this monitoring program. Some stations are still maintained along the previous traverse but will not be maintained; as they become inoperative or vandalized, they will be withdrawn from the network.

RESULTS

The initial observations from the Parkfield stations indicate a similar pattern to the San Benito - Hollister network. The seasonal influence on the soil-gas concentrations is evident even after only 3 months of monitoring (Figure 1). The average concentration is higher at Parkfield by about 40 parts per billion. This is not unusual and is probably due to differences in soil type and the affinity to retain moisture. The figure shows the actual concentrations; they have not been averaged as have the data in previous reports for the San Benito - Hollister stations. As more data are collected, an averaging technique will be utilized and the same method of forecasting seismic activity that had been developed for the northern section of the network will be used for the Parkfield data. That method required an average helium decrease of at least 5 ppb to be observed for a minimum of 2 consecutive weeks. The comparison of the data base from the two areas will provide an excellent test of the validity of the forecasting model.

REPORTS

None in this semi-annual period.

FIGURE 1

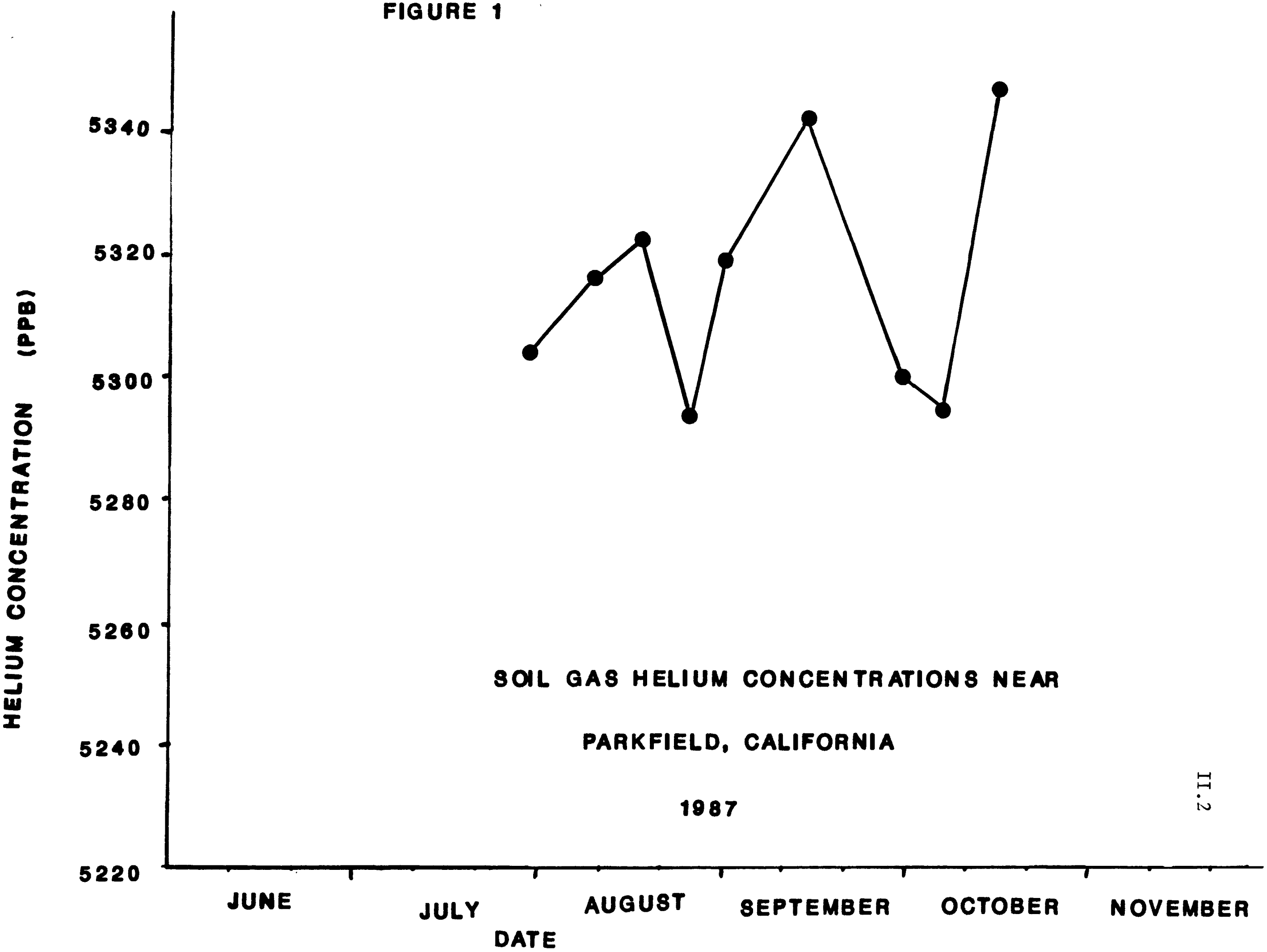

SOIL GAS HELIUM CONCENTRATIONS NEAR
PARKFIELD, CALIFORNIA
1987

Mechanics of Faulting and Fracturing

9960-02112

Paul Segall and M.V. Matthews
Branch of Tectonophysics
U.S. Geological Survey
345 Middlefield Road, MS/977
Menlo Park, California 94025
415-329-4861

Investigations

1. Analysis of crustal deformation and the earthquake slip cycle on the San Andreas fault near Parkfield, California.
2. Development of methods for assessing the adequacy of crustal deformation models.

Results

1. Since 1984 the U.S.G.S. and C.I.R.E.S. have jointly operated a two-wavelength geodimeter near Parkfield. While the average trends in the measurements are consistent with the deformation predicted by the Harris and Segall (1987) fault-slip model, the data exhibit large variations about the average trends. If tectonic, these signals can be inverted for time varying fault slip. However, the variations may reflect non-tectonic processes, such as local bench-mark instability. We have developed a general estimation method to search for temporally varying signals possibly contaminated by certain stochastic processes. Maximum likelihood estimates of the model parameters in the presence of Gaussian noise are obtained by casting the observation process for the network in a state space formulation, evaluating the likelihood function recursively using the Kalman filter, and employing a numerical optimization routine.

Initially we have considered a simple model in which baseline length changes include a linear trend, uncorrelated random errors, and Brownian random walk (assumed to model local benchmark motions). The maximum likelihood estimates of the uncorrelated (white noise) random errors contain a length independent (0.25 ± .11 mm) component and a length dependent component ($0.09 \pm 0.01 \times 10^{-6}$). These values are in good agreement with estimates obtained from data collected by Langbein et al. using the same instrument at Pearblossom in 1980-82. Our estimates for the Pearblossom data are: 0.28 ± 0.10 mm and $0.11 \pm 0.01 \times 10^{-6}$. We are thus able to conclude that the random instrumental errors have not changed since the instrument was moved to Parkfield.

2. Repeated geodetic measurements provide unique information on earthquake deformation processes. While researchers have devoted considerable attention to the inversion of geodetic data for fault slip and geometry, the problem of assessing the adequacy of the estimated models has been largely neglected. Since misfit from a 'true' model results solely from observational errors, it follows that a correct model will produce residuals that fail to exhibit coherent spatial patterns, and that are of size compatible with model independent measures of observation error. To test for systematic spatial patterns it is convenient to compare the predicted displacements from an estimated model with the observed displacements calculated from a 'model coordinate' solution. The 'model coordinate' displacements fit the data and are as close as possible to those predicted by the model. Thus, the comparison is not biased by indeterminate components of the displacement field.

The residuals from any deformation model can be separated into two orthogonal components, which we refer to as 'pure error' and 'lack of fit'. The pure errors measure the misclosure in the data, and are simply the residuals from the displacement calculation. The mean square pure error provides an unbiased, model-independent measure of the data variance. The lack of fit is the component of the residual potentially due to model inadequacy. If one assumes that the observational errors are normally distributed, then an appropriate F-statistic may be calculated to assess the significance of the lack of fit. In the absence of distributional assumptions non-parametric methods can be employed. These tests for residual patterns and lack of fit are conceptionally simple, easily implemented, and provide a reasonable basis for assessing general deformation models.

Reports

Harris, R. and P. Segall, Detection of a locked zone at depth on the Parkfield, California segment of the San Andreas fault, J. Geophys. Res., 92, 7945-7962, 1987.

Segall, P. and R. Harris, The earthquake deformation cycle on the San Andreas fault near Parkfield, Jour. Geophys. Res., 92, 10,511-10,525, 1987.

Pollard, D.D. and P. Segall, Theoretical displacements and stresses near fractures in rock: with application to faults, joints, veins, dikes, and solution surfaces, in Fracture Mechanics of Rock, D.K. Atkinson, ed., Academia Press, London, 1987.

Parkfield Area Tectonic Framework

9910-04101

John D. Sims
Branch of Engineering Seismology and Geology
U.S. Geological Survey
345 Middlefield Road, MS 977
Menlo Park, California 94025
(415) 329-5653

Investigations:

1. Field investigations of structural and stratigraphic relationships between late Cenozoic sedimentary units and underlying Franciscan and Late Cretaceous units in the Parkfield-Cholame area.

2. Field investigations of late Holocene and historic slip rates in the Parkfield to Carrizo Plain segment of the San Andreas fault.

3. Field investigations of the Tanlu fault zone, Peoples Republic of China and consultation with Chinese colleagues on methods of study and analysis.

Results:

1. Mapping in the Parkfield area was extended to the Red Hills just south of the hamlet of Cholame in order to investigate the stratigraphic and structural relationships of rocks exposed along the Red Hills fault. The mapping here reveals that existing geologic maps are in error regarding the stratigraphic relationships between late Miocene units. My mapping in the Red Hills shows that the white to buff fossiliferous marine sandstone of the Santa Margarita Formation is overlain with angular unconformity by red and maroon nonmarine conglomerate and sandstone of a formation I informally name the Red Hills formation. My mapping is at variance with that of Dibblee (1974). Dibblee (1974) maps the Santa Margarita as overlying red conglomerate and sandstone which he referred to as the Caliente Formation. However, the relationships are clearly exposed and the Red Hills formation is younger than the Santa Margarita Formation, which strongly suggests that the conglomerate and sandstone is not correlative with the Caliente Formation; thus I informally named the red conglomerate and sandstone the Red Hills formation. The Red Hills formation is in turn overlain by two younger conglomerate units. The lower of these two conglomerate units is unconformable on the Red Hills formation and the upper is unconformable on the lower conglomerate. Both conglomerates are probably referable to the Paso Robles Formation.

   My mapping also shows that the Pliocene and Pleistocene(?) Paso Robles Formation, that lies to the west of the Red Hills fault, is faulted against the Red Hills formation that lies to the east of the fault. To the southeast of the outcrops of the Santa Margarita and Red Hills formations the fault is overlapped by the Paso Robles Formation. Here, too, young geomorphic features suggest Pleistocene and Holocene fault movement. In the older rocks slickensides and fault geometry suggest high-angle reverse faulting. However, in the Paso Robles formation and drainages that cross the Red Hills fault, the motion appears to be in part right-lateral.

To the north of the bedrock outcrop belt in the Red Hills the Red Hill fault splays with one trace trending north-northwest and the other trending slightly east of north. Carl Wentworth has examined the Paso Robles and Holocene stream deposits near the southern end of the north-trending splay and reports that he found deformed and offset stream deposits. Photo reconnaissance of the area beyond the Red Hills suggests that the Red Hills fault crosses Cholame Creek about 2 miles east of Shandon and continues up just west of north canyon and eventually intersects the White Canyon fault in the Cholame Hills. The more north-trending splay, here called the Gillis Canyon fault, can be traced in photos to near Palo Prieto Canyon and the general area of the southernmost recognized extent of the White Canyon fault (fig. 1).

These new faults all appear to be active. The Gillis Canyon fault and the extension of the Red Hills fault to the northwest of the Red Hills are newly recognized. These faults, if correctly identified, show that deformation associated with the San Andreas fault or perhaps the basement thrust fault identified by Wentworth in the deep seismic line SJ-6.

2. Bob Sharp and I visited China in April and May, 1987. Our trip revealed to us the current Chinese view of the Quaternary history of movement on the Tanlu fault in Shandong Province. Geologic and geomorphic relationships are being comprehensively documented by the Shandong Seismological Bureau. They have an impressive amount of photographic, map, and cross-sectional documentation of the geomorphic and geologic features. We are impressed with the ambiguous nature of many of the claimed offset features. However, the historic seismicity and the record of major historic earthquakes on this fault proclaims that the Tanlu is an active and important fault. We reviewed the continuing field investigations by the Chinese geologists. Our discussions took place both in meetings in the Institute of Geology of the State Seismological Bureau (Beijing), the Shandong Seismological Bureau (Jinan), and in field trips along the Tanlu fault where evidence was directly viewed, discussed, and evaluated.

3. I collaborated with geophysicist colleagues from the USGS to plan a seismic reflection study of Cholame Valley. Four mini Sosie lines were shot in Cholame Valley in the area of the right stepover of the San Andreas. Three about equally spaced lines were shot perpendicular to the San Andreas and one line shot the length of the valley. Kay Shedlock (Denver) and Tom Brocher (Menlo Park) are processing the lines.

   Further collaboration with Bob Jachens, Bob Simpson, and Carl Wentworth on gravity and magnetic surveys in the Cholame Valley area is currently in progress. The gravity and magnetic data when fully integrated with the geologic mapping I have done in the area, will give a detailed regional picture of the Parkfield-Cholame area.

Reports:

Sims, J.D., submitted to Branch, Post late-Oligocene chronology of displacement on the San Andreas fault in central California: Evidence from displaced rock bodies, in Matti, J.C., and others, eds., Palinspastic reconstruction of the San Andreas fault: *Geological Society of America Memoirs*.

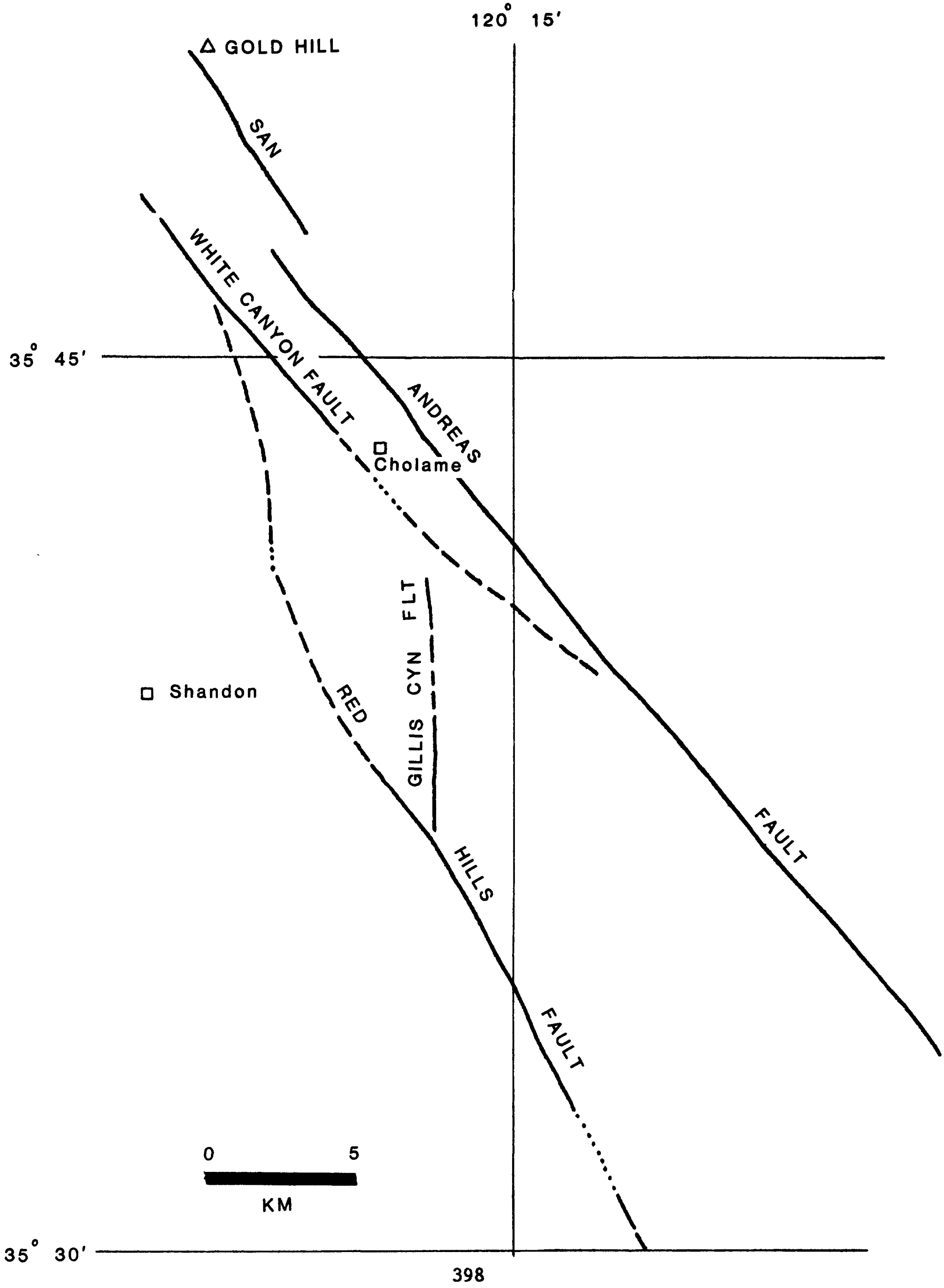
120° 15'
GOLD HILL
SAN
ANDREAS
FAULT
WHITE CANYON FAULT
35° 45'
Cholame
GILLIS CYN FLT
RED
HILLS
FAULT
Shandon
0
5
KM
35° 30'
398

Dense Seismograph Array at Parkfield, California

9910-03974

Paul Spudich
J.B. Fletcher
Branch of Engineering Seismology and Geology
U.S. Geological Survey
345 Middlefield Road, MS 977
Menlo Park, California 94025
(415) 329-5654 or (415) 329-5628

Investigations

1. Design of the EPRI-CSMIP dense seismic array at Parkfield, California.
2. Preliminary recording of microearthquakes at the EPRI-CSMIP array.
3. Site investigation for a USGS array to be installed at Hog Canyon on the west side of the San Andreas.

Results

During this period we performed calculations to aid in the design of the 10-element accelerograph array to be deployed by the California Strong Motion Instrumentation Program (CSMIP) around the Electric Power Research Institute (EPRI) array at Scobie Ranch (35°51.5' N, 120°17.0' W) near Parkfield. These calculations are still in progress. Nine portable DR-100 recorders having L-22 geophones were co-located with the EPRI surface accelerometers to record local microearthquakes, but the seismicity rate has been very low thus far, resulting in little usable data. We conducted site investigations for a separate dense array to be emplaced on the west side of the San Andreas near Hog Canyon. A suitable site has been found (35°19.0' N, 120°30.5' W), and landowner permission has been given verbally. The USGS array will use both accelerometers and geophones, enabling recording of all seismic signals above ground noise. Beamforming will be used to study the directional properties and temporal variation of coda-Q, in order to test the hypothesis that coda-Q fluctuates in some parts of the lithosphere before earthquakes.

Ten RT-72s from Ref-Tek (Dallas, Texas) have been ordered and we expect delivery in early winter. These are 6-channel, variable-gain systems that employ a 16-bit A/D. Seismic data and triggering information will be transmitted to a micro VAX using a local area network (LAN) called Arcnet. By using this LAN we will be able to add or drop stations at any time without upsetting the telemetry. Error detection and correction is done in hardware, which should result in high data integrity.

Reports

None.

10/87

10/23/87

Semi-Annual Technical Report XXV

Modeling and Monitoring Crustal Deformation
9960-01488

Ross S. Stein and Wayne Thatcher
Office of Earthquakes, Volcanoes, and Engineering
345 Middlefield Road, MS 977
Menlo Park, California 94025

415/329-4840

Investigations

1. Preliminary study of the 1987 Whittier Narrows Earthquake. Conducting releveling in the epicentral region of the 1 October 1987 M_L =6.1 thrust earthquake. The objectives of the geodetic measurements are to guage the fault geometry and slip together with seismic data, and deduce the relationship between the coseismic and long-term deformation at the site to estimate the earthquake repeat time there. The success of the project is dependent on a large magnitude of deformation relative to the non-tectonic subsidence (up to15 mm/yr) and measurement errors (Ross Stein, Jian Lin, and Wayne Thatcher).

2. Investigation of the growth of geologic structures by repeated earthquakes. (Ross Stein and Geoffrey King).

3. Study of the 1954 Fairview Peak-Dixie Valley Earthquakes. We have begun a reëxamination of the vertical and horizontal geodetic record to remove survey errors and study the fault slip, shape, and interactions at depth for this large multiple event (Jian Lin and Ross Stein).

Results

1. The growth of geologic structures by repeated earthquakes, 1: In many places, earthquakes with similar characteristics have been shown to recur. If this is common, then relatively small deformations associated with individual earthquake cycles should accumulate over time to produce geological structures. Following this paradigm, we show that existing models developed to describe levelling changes associated with the seismic cycle can be adapted to explain geological features associated with a fault. In this paper, the parameters that control the growth of a structure are identified. It is found that the flexural rigidity of the crust (or the apparent crustal thickness) provides the main control of the width of a structure. The loading due to erosion and deposition of sediment determines the ratio of uplift to subsidence between the two sides of the fault. The flexure due to sediment load is much more important in this respect than whether the fault is normal or reverse in character. We find that, in general, real structures are associated with apparent elastic thicknesses of 4 kilometers or less and consequently with very low flexural rigidities. This is in agreement with determinations of elastic thickness by some spectral comparisons of gravity with topography. The result suggests that the depth range of small earthquakes is not a correct measure of effective elastic thickness of the crust. Although, perhaps, surprising, the result is consistant with comparisons of geodetic slip rates with seismic moment release rates for parts of California (King, Stein, and Rundle).

2. The growth of geologic structures by repeated earthquakes, 2: A strong test of our understanding of the earthquake cycle is the ability to reproduce extant fault-bounded geologic structures, such as basins and ranges, which are built by repeated cycles of deformation. Along strike-slip faults, the coseismic and interseismic deformation are more nearly equal in magnitude and opposite in sign, resulting in little permanent deformation except for the fault offset. For dip-slip faults, portions of the crust are lifted and dropped, so buoyancy forces are exerted. The seismic and interseismic deformation do not balance, and structures grow and become subject to erosion and deposition. We consider three structures for which the structure and fault geometry are well-known: the White Wolf fault in California, site of the 1952 M7.3 Kern County earthquake, the Lost River normal fault in Idaho, site of the 1983 M7.0 Borah Peak earthquake, and the Cricket Mountain normal fault in Utah, site of Quaternary slip events. Basin stratigraphy, oil well correlations, and seismic reflection records are used to profile the structure, and coseismic deformation measured by leveling surveys is used to estimate the fault geometry. We add the deformation associated with the earthquake cycle (the coseismic slip and postseismic relaxation) to the flexure caused by the observed positive (sediment deposition) and negative (erosion) loads, to duplicate these structures, treating the crust as a thin elastic plate overlying a fluid substrate. The cumulative deformation is independent of the fluid viscosity for the 4-8 Ma structures, modestly dependent on the layer densities, and strongly dependent on the long-term elastic plate thickness. We deduce an elastic thickness of 2-4 km (equivalent to a flexural rigidity of $2\text{-}15 \times 10^{19}$ Nm). This is found where independent estimates of the elastic thickness from the admittance of surface topography with gravity yield values of about 5 km, and where coseismic fault slip extends to a depth of 10-15 km. Thus much of the seismogenic crust must weaken between large earthquakes. This causes the fault-bounded basins to narrow with time after each large earthquake. We also find that the interaction of postseismic relaxation and sediment loading causes normal and reverse faults to evolve differently: normal fault basins uplift and become shallower between earthquakes due to postearthquake relaxation, unless they are filled by sediments soon after each event. In contrast, the basin produced by a reverse fault subsides between earthquakes, and can thus accommodate a steady supply of sediments (Stein, King, and McCarthy).

Reports (excluding abstracts)

Stein, R.S., Reply to Reilinger, *J. Geophys. Res., 92,* 10,715-10,717, 1987.

Stein, R.S., Plate tectonic prediction fulfilled, *Physics Today, 40* (12), in press, 1987.

King, G.C.P., R.S. Stein, and J.B. Rundle, The growth of geological structures by repeated earthquakes: 1, Conceptual framework, submitted to *J. Geophys. Res.,* 1987.

Stein, R.S., G.C.P. King, and J. McCarthy, The growth of geological structures by repeated earthquakes: 2, Field examples of continental dip-slip structures, submitted to *J. Geophys. Res.,* 1987.

Fault Kinematics in the Imperial Valley, California: Implications for Earthquake Prediction on the Imperial, San Jacinto and Southern San Andreas Faults

14-08-0001-G1337

M.N. Toksoz and R.E. Reilinger
Earth Resources Laboratory
Dept. of Earth, Atmospheric, and Planetary Sciences
Massachusetts Institute of Technology
Cambridge, Massachusetts 02142
(617) 253-7852

INVESTIGATIONS

This project involves using available geodetic observations in conjunction with other geophysical and geological information to investigate contemporary tectonic processes along the southernmost segment of the San Andreas fault system. Specific studies include:

(1) Implications of the 1986 NGS GPS observations for seismic and aseismic faulting in the Imperial Valley,
(2) Geodetic deformation and paleoseismology,
(3) Interseismic deformation for normal fault earthquakes.

RESULTS

1. GPS Measurements in the Imperial Valley, California. During the summer of 1986, the National Geodetic Survey completed a dense GPS survey in the vicinity of the Imperial fault-Brawley Seismic Zone. Essentially all of the GPS observations were made at preexisting geodetic control points which were observed with conventional methods (trilateration and/or leveling) prior to and closely following the 1979 earthquake. The GPS observations have been processed at NGS and compared to the 1980 postearthquake trilateration measurements in the vicinity of the Imperial fault. Initial analysis indicates accelerated deformation following the 1979 earthquake. Current efforts are focused on using these new observations, together with the long history of conventional geodetic measurements in this area, to constrain models of strain accumulation and release along this segment of the Pacific-North America plate boundary. (This work is being done in cooperation with Richard Snay, NGS.)

2. Geodetic deformation and paleoseismology. Three examples from the Western U. S. are presented in which short-term geodetic deformation shows a close relationship to longer term deformation as revealed by topographic/structural relief. In the Imperial Valley of southern California, earthquake deformation (coseismic and postseismic) has a very similar spatial pattern to topographic relief within the complex transition zone between the Imperial and San Andreas faults. The relationship between long-term tectonic subsidence in this area and earthquake deformation suggests that currently active fault systems are very young relative to the age of the Imperial Valley or that activity has been episodic on these faults throughout this period. In the Pacific Northwest, considerable uncertainty persists as to the spatial and temporal character of ongoing deformation, although there appears to be some similarity between ongoing coastal tilting measured geodetically and tilting indicated by deformed marine terraces. While this similarity has been interpreted to indicate aseismic subduction, the question of a possible future large subduction earthquake in this area remains unresolved. Comparisons between earthquake deformation measured geodetically and structural relief in the Basin and Range province suggest that large interearthquake movements must occur in such normal-fault environments. These movements apparently involve broad regional uplift. Such uplift has been measured directly in the vicinity of the 1959 Hebgen Lake earthquake. Modeling suggests that postseismic viscoelastic relaxation and strain accumulation in an elastic lithosphere overlying a viscoelastic asthenosphere are possible physical mechanisms to generate these interseismic movements.

3. Interseismic deformation for normal fault earthquakes. Comparison between the coseismic vertical deformation associated with normal fault earthquakes and permanent deformation indicated by geologic structure indicates that large (i.e., comparable to coseismic) deformations must occur during the period between earthquakes. When sufficient geodetic and geologic information is available, it is possible to estimate the spatial character of this interseismic deformation. A case in point is the 1983 Borah Peak Idaho earthquake. This normal fault earthquake produced roughly 5 times as much basin subsidence as it did uplift of the adjacent mountain range. In contrast, geophysical and geological observations show that the basin is roughly as deep as the bounding range is high. Regional uplift of both the basin and range during the interseismic period can, in conjunction with the coseismic movements, produce this permanent structure. A similar normal fault event in the Basin and Range, the 1959 Hebgen Lake earthquake, was also accompanied by substantially larger subsidence than uplift (this is a direct consequence of normal slip on a dipping fault in an elastic half-space) although the basins and ranges have comparable relief. In this case postseismic geodetic measurements show broad regional uplift with a spatial pattern which is roughly consistent with that proposed for the Borah Peak event. Modeling suggests that postseismic viscoelastic relaxation and strain accumulation in an elastic lithosphere overlying a viscoelastic asthenosphere are possible physical mechanisms to generate interseismic uplift. These mechanisms may be the contemporary expression of those processes responsible for the high elevation of the Basin and Range Province.

PUBLICATIONS

Reilinger, R.E., Comment on "Saugus-Palmdale, California, field test for refraction error in historical leveling surveys, by Ross S. Stein, Charles T. Whalen, Sanford R. Holdahl, William E. Strange, and Wayne Thatcher," *J. Geophys. Res.*, *92*, 10,711-10,714, 1987.

Reilinger, R.E., R. Snay and H.C. Neugebauer, 1986 NGS GPS observations in the Imperial Valley, California: Implications for fault behavior, *EOS, Trans. Am. Geophys. Union*, *68*, 282-283, 1987.

Reilinger, R.E., Magmatic deformation from NGS measurements, *EOS, Trans. Am. Geophys. Union*, *68*, 287, 1987.

Reilinger, R.E., Interseismic deformation for normal fault earthquakes, *EOS, Trams. Am. Geophys. Union*, in press, 1987.

Reilinger, R.E., Geodetic deformation and paleoseismology, *in*, Crone, A.J., ed., *Proceedings of Workshop XXXIX-Directions in Paleoseismology, USGS Open File Rept.*, in press, 1988.

Earthquake Process

9930-03483

Robert L. Wesson
Branch of Seismology
U.S. Geological Survey
922 National Center
Reston, Virginia 22092
(703) 648-6785

INVESTIGATIONS

1. Analysis of theoretical and numerical models of the process active in fault zones leading to earthquakes.

2. Analysis of seismological and other geophysical data pertinent to understanding of the processes leading to large earthquakes.

3. Analysis of the potential for earthquakes induced by deep well injection.

RESULTS

1. The physical assumptions that 1) the fault zone is composed of stuck patches surrounded by areas of the fault zone that creep, and 2) the steady state creep rate at any point on the creeping portion is proportional to the steady state loading rate experienced at that point, provide strong constraints on the inversion of geodetically and instrumentally determined displacement rates. Under these assumptions, and for a given configuration of fault zone, stuck patches, and loading rate, the distribution of displacement rates on the creeping part of the fault is uniquely determined. For a fault zone modelled as a set of rectangular elements, the problem of inverting the geodetic data becomes a problem of finding that combination of elements on the fault surface, which when stuck, minimizes the difference between the observed, and calculated line-length changes and surface creep rates. This problem in combinatorial minimization can be approached by the method of "simulated annealing." Preliminary numerical experiments both with simulated data, and with the observed line length changes and creep rates at Parkfield, suggest that this method offers promise in resolving details of the geometry of the stuck patch expected to be responsible for the characteristic Parkfield earthquakes. An attractive feature of this method is that the rate of stress accumulation on the stuck patch can be easily calculated.

2. Analytic solutions for the displacements and stresses in an elastic plate containing an idealized creeping fault zone, developed by Tse et al. (1985), have been adapted to make predictions about the variation of stress orientation with depth at the Cajon Pass site, adjacent to the San Andreas fault. If the maximum regional principal stress is oriented at an angle greater than 45° to the strike of the

fault capable of creep, then on or close to the fault, the local maximum principal stress should be nearly normal to the fault. With increasing distance from the fault, the orientation of the local principal stresses should gradually approach those of the regional principal stresses. As depth increases near the fault, a much more interesting dependence is predicted. Near the surface, where the fault is weak and presumably creeps, the local maximum principal stress should be nearly normal to the fault, however, as depth increases and approaches the top of the locked zone, the local maximum principal stress orientation should rotate strongly toward the fault, to an even more acute angle than that made between the regional maximum stress and the strike of the fault. Below the locked zone, where ductile behavior is expected, the local maximum principal stress rotates back to nearly normal to the fault. Thus, these model calculations suggest that, as the Cajon Pass hole is deepened, the observed orientation of the maximum horizontal compression will rotate in a northwesterly direction toward the strike of the San Andreas fault.

3. Long-period surface waves recorded at DeBilt for the 1986 North Palm Springs earthquake (M_L=5.6) and the 1948 Desert Hot Springs earthquake (M_L=6.5) exhibit nearly identical wave forms, with amplitudes for 1948 about 20-30% larger. Peak amplitudes at Mt. Hamilton (MHC) are also about 30% larger for the 1948 event, although amplitudes of 3-6 sec surface waves are systematically smaller, suggesting a deeper rupture in 1948 than in 1986. The similarity of the wave forms at De Bilt, however, implies that the moments of the the two events are more similar than the disparity in their assigned M_L values would imply. Aftershock distributions for the two events derived from S - P times recorded on portable stations at distances less than 20 km, indicate that the two zones abut along the Banning strand of the southern San Andreas fault. Both aftershock zones are about 15 km long, 8-10 km wide, and dip to the northeast at 50°-60°, consistent with teleseismic first-motion focal mechanisms that exhibit right-slip motion on planes that strike northwest, and dip to the northeast, with as much as 20-30% thrust. Comparison of regional travel times indicate that the 1948 earthquake was southeast of the 1986 main shock.

REPORTS

Nicholson, C., H. Kanamori and C.R. Allen, Comparison of the 1948 and 1986 earthquakes along the southern San Andreas fault, Coachella valley, California, EOS Trans. AGU, in press.

Nicholson, C., Seismic slip on the southern San Andreas fault: 1948 and 1986, Seismol. Res. Lett. (Earthquake Notes), 58, p.14, 1987.

Nicholson, C., E. Roeloffs and R.L. Wesson, The northeastern Ohio earthquake of January 31, 1986: Was it induced?, Bull. Seismol. Soc. Am., 78, in press, 1988.

Wesson, R.L., Modelling aftershock migration and afterslip of the San Juan, California, earthquake of October 3, 1972, Tectonophysics, in press.

Wesson, R.L., and C. Nicholson, Intermediate-term, pre-earthquake phenomena in California, 1975-1986, and preliminary forecast of seismicity for the next decade, U.S. Geological Survey Redbook Conference and PAGEOPH, in press.

Wesson, R.L., and C. Nicholson, Earthquake hazard associated with deep well injection, U.S. Geological Survey Open-file Report 87-331, 108 p., 1987 (also U.S. Geological Survey Bulletin, in press).

Wesson, R.L., Dynamic modelling of propagating fault creep events, Seismol. Res. Lett. (Earthquake Notes), 58, p.8, 1987.

Wesson, R.L., Resolving details of the stuck patch on the San Andreas fault at Parkfield, California, EOS Trans. AGU, in press.

ROCK MECHANICS

9960-01179

James Byerlee
U.S. Geological Survey
Branch of Tectonophysics
345 Middlefield Road, MS/977
Menlo Park, California 94025
(415) 329-4841

Investigations

Laboratory experiments are being carried out to study the physical properties of rocks at elevated confining pressure, pore pressure and temperature. The goal is to obtain data that will help us to determine what causes earthquakes and whether we can predict or control them.

Results

A sample of Westerly granite was deformed under constant stress conditions: a pore pressure of 5 MPa, a confining pressure of 10 MPa, and an axial load of 170 MPa. Pore volume changes were determined by measuring the volume of pore fluid (0.01 M $KC1_{aq}$) injected into the sample. After 6 days of creep, characterized by accelerating volumetric strain, the sample failed along a macroscopic fault. Measurements of complex resistivity over the frequency range 0.001-300 Hz, taken at various times during creep, showed a gradual increase in both conductivity and permittivity. When analyzed in terms of standard induced polarization (IP) techniques, the changing complex resistivity resulted in systematic changes in such parameters as percent frequency effect and chargeability. These results suggest that it may be possible to monitor the development of dilatancy in the source region of an impending earthquake through standard IP techniques.

Reports

Lockner, D., Byerlee, J., 1986, Changes in complex resistivity during creep in granite, PAGEOPH, v. 124, nos. 54/55, p. 659-676.

PERMEABILITY OF FAULT ZONES

9960-02733

James Byerlee
Branch of Tectonophysics
U.S. Geological Survey
345 Middlefield Road, MS/977
Menlo Park, California 94025
(415) 329-4841

Investigations

Laboratory studies of the permeability of rocks and gouge are carried out to provide information that will assist us in evaluating whether in a given region fluid can migrate to a sufficient depth during the lifetime of a reservoir to trigger a destructive earthquake. The results of the studies also have application in the solution of problems that arise in nuclear waste disposal.

Results

Permeability was measured in rock samples from the DOSECC Cajon Pass drill hole at 15 different depths from 270 to 2,100 m. Samples 2.54 cm long and 2.54 cm in diameter were prepared in 3 orthogonal directions at each depth to test for permeability anisotropy. Confining and pore pressures were set to the lithostat and hydrostat for each depth. Room temperature steady-state flow measurements using deionized water were made over a period of 24 hours to determine each permeability value.

The first 500 m encountered in the drill hole were composed of sandstones with typically high permeability values of about $10^{-17} m^2$. The crystalline rocks between 500 and 2,100 m showed a systematic decrease in permeability with depth from 10^{-19} to $10^{-21} m^2$, regardless of composition. These values are particularly low compared to the applied effective stresses (10-30 MPa) because of the small grain sizes and healed cracks. Permeability was relatively isotropic in spite of pronounced foliation in some samples. These results imply that high fluid pressures may occur in sections of rock that are not fractured, leading to lower effective stresses acting at depth.

The Complexity of the Earthquake Sourcetime Function

14-08-0001-G-1389

Shamita Das
Lamont-Doherty Geological Observatory
of Columbia University
Palisades, New York 10964
(914) 359-2900

During the first six months of this project, Dr. B.V. Kostrov visited the U.S.A. for two months. The P.I. collaborated with him on two problems. First, the numerical BIE method was used to study more than thirty cases of spontaneous faulting. The models included faults with friction, barrens and asperities. The P and S wave sourcetime functions for the different models were obtained. A paper, whose abstract is attached resulted from this work. Second, work on improving the BIE method by developing analytical kernels for the integral equation was started and major progress was made. The initial results are very encouraging and promises drastic improvement in efficiency of the BIE method.

Abstract

By constructing more than thirty numerical spontaneous earthquake faulting models, the question of how and to what extent the asperity model can explain the complexity of the far-field pulse shapes (the source time function), i.e., the pulse consisting of several distinct subpulses, is investigated. The influence of multiple strength barriers and/or dry friction on the far-field waveforms has been studied using the simple model of a square fault with uniformly spaced square barriers. The central asperity is allowed to break to initiate the dynamic process. It is found that the pulse duration is shorter the greater the density of barriers (ratio of barrier size to barrier spacing).

The presence of friction has been found to have three different consequences. Firstly, the slipping area is reduced giving rise to a shorter pulse duration. Secondly, the rate of slip propagation is reduced which increases the pulse duration. Finally, the frictional stress drop, if present, increases the amplitude of the pulse. The interaction of these three effects together with the effect of the barriers results in different pulses depending on the relative role of these effects.

Breaking of multiple asperities with relatively short time delay between their fracturing produced a single pulse with steps in its rising portion, the pulse duration depending on the total time required for the asperities to break. Breaking of, say, two asperities with sufficient time delay between them produced a double pulse which is in accord with the asperity model of complex earthquakes. In the presence of friction, however, the pulse shape had a tendency to be more rough due to temporary arrests and restarts of slip on the fault. In one case of a fault with barriers and friction, an additional peak was observed in some directions from the source, the peak form and amplitude being essentially the same as those of the peaks due to breaking of asperities.

One may conclude that each subpulse observed on a complex far-field pulse is not necessarily interpretable as being due to the failure of an asperity on the fault. Furthermore, for the subpulses which can be related to asperity fracture, the duration is not determined by the size of the corresponding asperity but rather by the physical conditions on the fault.

The Physics and Mechanics of the Brittle-Ductile Transition

14-08-0001-G1340

Brian Evans and Joanne Fredrich
Dept. Earth Atmospheric and Planetary Sciences
Massachusetts Institute of Technology

14-08-0001-G1352

T.-F. Wong
Dept. Earth and Space Sciences
State University of New York, Stony Brook

Objectives: The physical mechanisms of semi-brittle rock failure in the Earth are poorly understood, but are important in understanding seismogenic faulting and aseismic fault creep. We are conducting an integrated laboratory and observational study to identify the deformation mechanisms which operate during the brittle-ductile transition, and to measure the effect of variations in pressure, temperature, porosity, and second-phase content on the strength of several rocks deformed in the semi-brittle regime. Current work is focusing on experimental deformation of marble and some theoretical investigations of fracture initiation.

Experimental Work to Date: We have performed an extensive series of triaxial experiments at room temperature and confining pressures up to 400 MPa on samples of Carrara Marble. Under these conditions the mechanical behavior ranges from brittle (failure localized on a single shear fault), to semi-brittle (non-localized, pressure-sensitive deformation), and at the highest pressures, to plastic (strength is insensitive to confining pressure). In the semi-brittle regime, samples were deformed to various strains and examined using optical and transmission electron microscopy (TEM). Microcrack density and anisotropy were characterized quantitatively using stereological techniques. We are now conducting a series of experiments which include measurements of volumetric strain. Some of our findings are summarized below.

1. Macroscopic stress-strain data indicate that the strength at 2.5% strain remains pressure dependent at confining pressures 100 MPa greater than that necessary to suppress macroscopic brittle faulting (30 MPa). However, the yield stress (i.e., the lowest stress at which the stress-strain curve is non-linear) is pressure independent after only 50 MPa of additional pressure.

2. Deformation mechanisms which operate in Carrara marble deformed in the semi-brittle regime are similar to those

observed in silicate rocks deformed at high temperature: twinning, microcracking, and dislocation glide (Figs. 1a and b). TEM observation suggests that dislocation flow can nucleate microcracks (Fig. 1b) as well as inhibit crack propagation. Twins are frequently associated with microcracks and voids.

3. In the semi-brittle regime, the density of twins and microcracks increases with strain at constant confining pressure. Microcracking occurs along grain boundaries and within grains, in directions subparallel to the applied stress.

4. Stereological measurements made on samples deformed in the semi-brittle regime indicate that both crack density at constant strain, and stress-induced crack anisotropy decrease with increasing confining pressure. The densities of cracks parallel and perpendicular to the applied stress increase linearly with strain at roughly the same rate (Fig 2). The stress-induced anisotropy is comparable to that previously found by other workers for samples of Westerly granite and San Marcos gabbro deformed almost to peak stress in the brittle field. However, normalized crack densities are significantly lower than those observed in the prefailure samples of the granite and diabase. If both the anisotropy and density of microcracking are critical to the localization process, then the factor which inhibits localization in the semi-brittle regime is the decreased density of microcracking.

Theoretical Calculations of Fracture Initiation: Both crack extension and crack nucleation may be affected by plastic processes. One model often cited in the interpretation of semi-brittle deformation involves the nucleation of a crack by dislocation pile-ups. However, most treatments of the dislocation pile-up, or Stroh crack problem have discussed the case of tensile loading. We have completed a preliminary analysis the pile-up problem under compressive loading using two different approaches. On the basis of energetic considerations, it appears that the nucleation process is pressure-independent and that, under compressive loads, the the propagation of a Stroh crack is stable for grain sizes less than a millimeter. Using the "weight function" technique of linear elastic fracture mechanics, some insight into the crack propagation geometry may be obtained. Beyond a certain length the Stroh crack is expected to take up a curved path to grow in a direction parallel to σ_1. We are in the process of analyzing the analogous problem of microcracking induced by mechanical twinning.

A second source for fracture initiation is the presence of fluid inclusions. Upon a change in temperature, or overburden pressure, these inclusions may become overpressured and crack via a process similar to hydrofracture. Observations of fluid inclusion decrepitation summarized by Roedder and others indicate that the diameter of a fluid inclusion and the maximum pressure difference which it will support appear to be inversely related. Once formed, any annular crack around the fluid inclusion will extend until the external and internal pressure are nearly equal.

Using linear elastic fracture mechanics, and assuming that fluid inclusions contain small initial flaws which scale with their diameter, the maximum pressure difference is predicted to depend directly on the critical stress intensity factor and indirectly on the square root of the inclusion radius, in qualitative agreement with decrepitation experiments done on San Carlos olivine. Once formed, the annular crack around the fluid inclusion will extend until the internal (gas) and external (mineral) pressure are nearly equal. The final radius of the annular crack is a function of the radius of the original fluid inclusion, and the internal and external pressures.

Bibliography:

Fredrich, J., B. Evans, and T.-F. Wong, The Mechanics of Semi-Brittle Deformation in Carrara Marble, *Fall Amer. Geophys. Un. Meeting,* Dec., 1987.

Wong, T.-F., Effect of pressure on propatation behavior of microcracks nucleated by Stroh's mechanism, *EOS, Trans. Amer. Geophys. Un., 68,* 404, 1987.

Wanamaker, B. J., B. Evans, and T.-F. Wong, Fluid Inclusion Decrepitation (Cracking) in San Carlos Olivine, *Fall Amer. Geophys. Un. Meeting,* Dec., 1987.

Figure 1. TEM bright-field micrographs of a sample deformed to (a) 2.4% axial strain at 50 MPa and (b) 5.4% axial strain at 120 MPa. In (a) dislocations lie along well developed slip planes and in (b) cracks are observed to emerge from either end of a slip band in a geometry suggestive of the Stroh crack mechanism (see text).

Figure 2. Stereological measurements of crack density per unit length were made on an optical microscope at a magnification of X320 on thick sections (2 mm) using reflected light. Sections were cut parallel to the applied stress and measurements were made in two perpendicular directions for each sample. The circles represent mean cracks per unit length in a direction parallel to the applied stress and the squares represent the mean cracks in a direction perpendicular to the stress axis. The open symbols are for a series of samples deformed at a confining pressure of 120 MPa and the closed symbols for a sample deformed at 85 MPa (closed symbols). Note that symbols are slightly offset from one another for clarity.

Bibliography:

Fredrich, J., B. Evans, and T.-F. Wong, The Mechanics of Semi-Brittle Deformation in Carrara Marble, *Fall Amer. Geophys. Un. Meeting,* Dec., 1987.

Wong, T.-F., Effect of pressure on propatation behavior of microcracks nucleated by Stroh's mechanism, *EOS, Trans. Amer. Geophys. Un., 68,* 404, 1987.

Wanamaker, B. J., B. Evans, and T.-F. Wong, Fluid Inclusion Decrepitation (Cracking) in San Carlos Olivine, *Fall Amer. Geophys. Un. Meeting,* Dec., 1987.

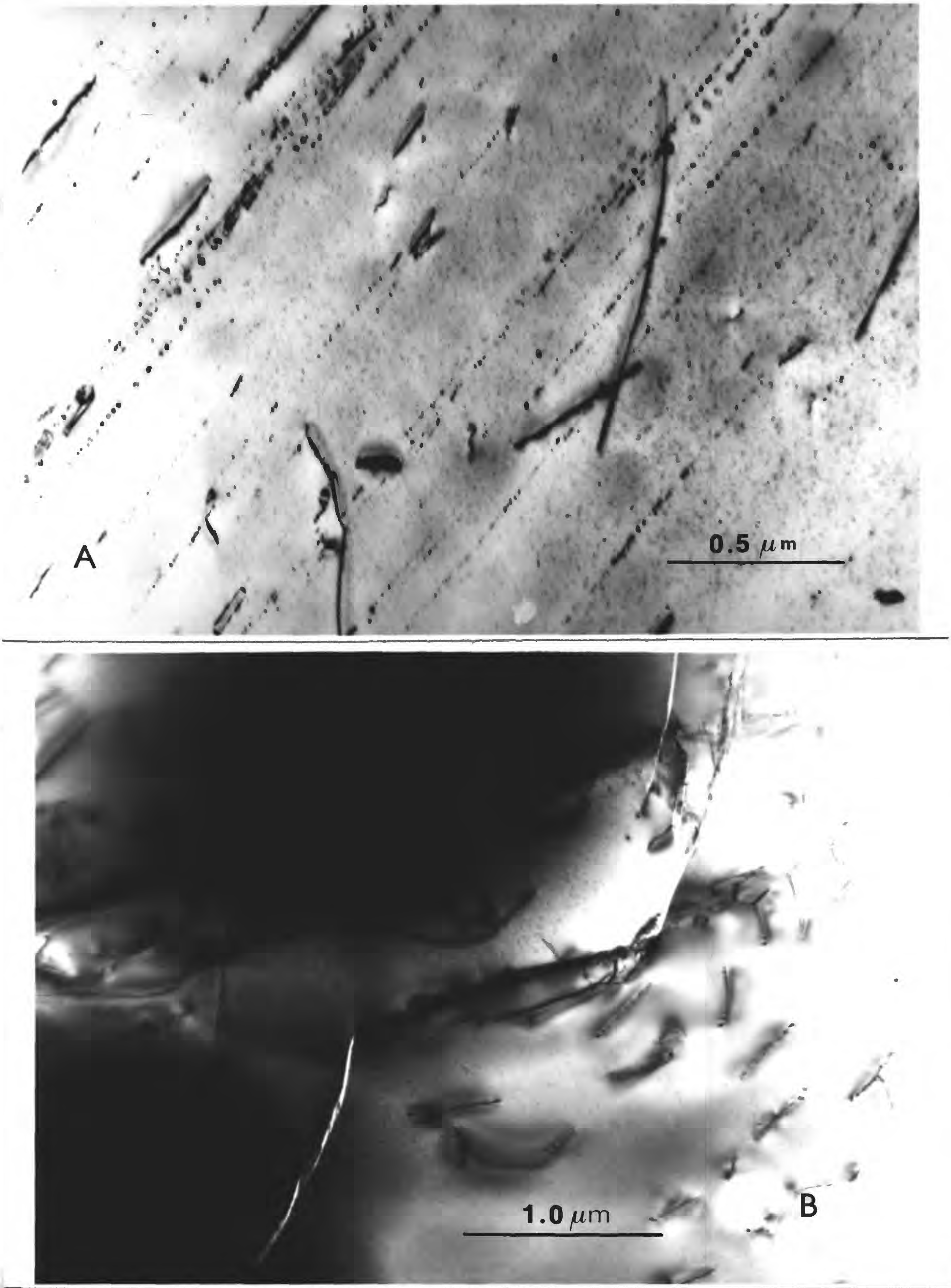

Figure 1. TEM bright-field micrographs of a sample deformed to (a) 2.4% axial strain at 50 MPa and (b) 5.4% axial strain at 120 MPa. In (a) dislocations lie along well developed slip planes and in (b) cracks are observed to emerge from either end of a slip band in a geometry suggestive of the Stroh crack mechanism.

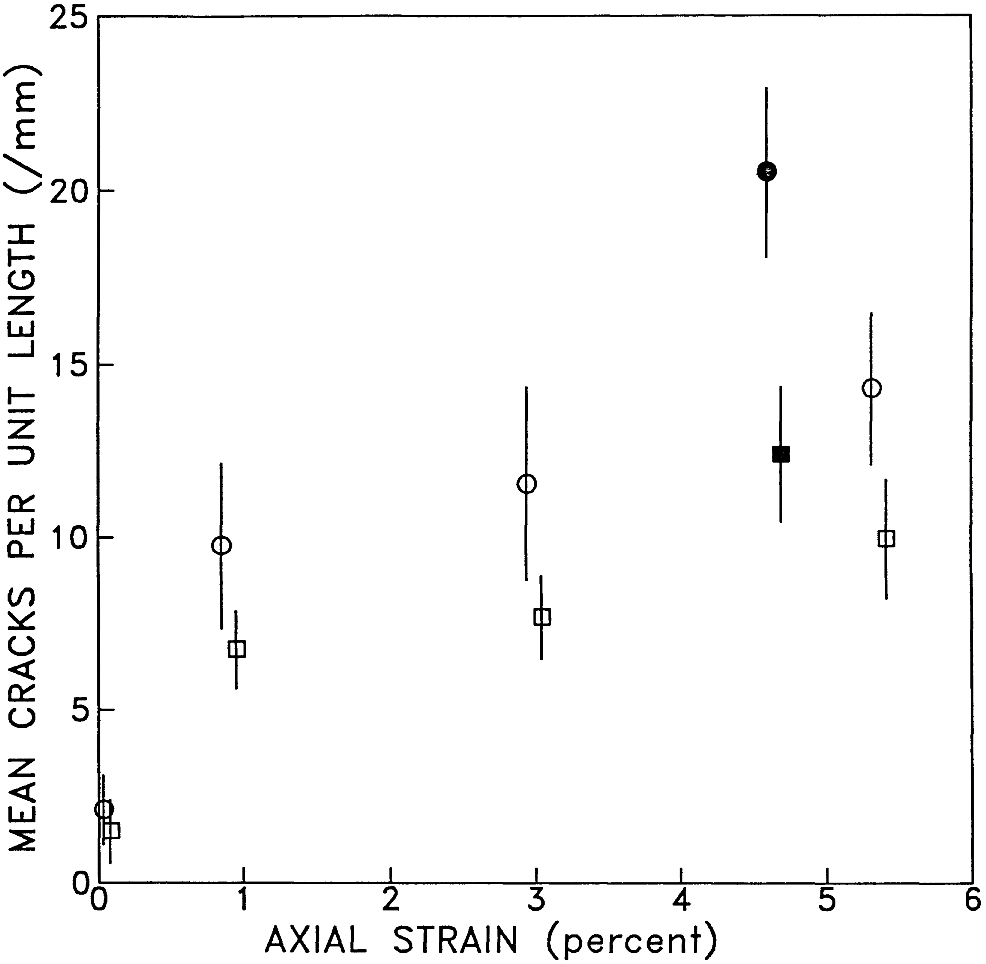

Figure 2. Stereological measurements of crack density per unit length were made on an optical microscope at a magnification of X320 on thick sections (2 mm) using reflected light. Sections were cut parallel to the applied stress and measurements were made in two perpendicular directions for each sample. The circles represent mean cracks per unit length in a direction parallel to the applied stress and the squares represent the mean cracks in a direction perpendicular to the stress axis. The open symbols are for a series of samples deformed at a confining pressure of 120 MPa and the closed symbols for a sample deformed at 85 MPa (closed symbols). Note that symbols are slighly offset from one another for clarity.

High Frequency Seismic and Intensity Data

9910-03973

Jack Evernden
Branch of Engineering Seismology and Geology
U.S. Geological Survey
345 Middlefield Road, MS 977
Menlo Park, California 94025
(415) 329-5627

Investigations:

1) Investigating via quantitative modeling of earthquake and explosion spectra the roles of elastic velocity structure, depth of focus and anelastic attenuation on the amplitude and spectral content of both compressional and shear phases (P_n, P_g, S_n, and S_g-L_g, etc.) as a function of distance.

2) Investigating via large data sets the P-wave spectral content of earthquakes and explosions, the intent being to place in the literature a definitive analysis of this relationship.

Results:

Both investigations in progress.

Reports:

None.

10/87

Earthquakes and the Statistics of Crustal Heterogeneity

9930-03008

Bruce R. Julian

Branch of Seismology
U.S. Geological Survey
345 Middlefield Road - MS77
Menlo Park, California 94025
(415) 323-8111 ext. 2931

Investigations

Both the initiation and the stopping of earthquake ruptures are controlled by spatial heterogeneity of the mechanical properties and stress within the earth. Ruptures begin at points where the stress exceeds the strength of the rocks, and propagate until an extended region (''asperity'') where the strength exceeds the pre-stress is able to stop rupture growth. The rupture termination process has the greater potential for earthquake prediction, because it controls earthquake size and because it involves a larger, and thus more easily studied, volume within the earth. Knowledge of the distribution of mechanical properties and the stress orientation and magnitude may enable one to anticipate conditions favoring extended rupture propagation. For instance, changes in the slope of the earthquake frequency-magnitude curve (''b-slope''), which have been suggested to be earthquake precursors and which often occur at the time of large earthquakes, are probably caused by an interaction between the stress field and the distribution of heterogeneities within the earth.

The purpose of this project is to develop techniques for determining the small-scale distributions of stress and mechanical properties in the earth. The distributions of elastic moduli and density are the easiest things to determine, using scattered seismic waves. Earthquake mechanisms can be used to infer stress orientation, but with a larger degree of non-uniqueness. Some important questions to be answered are:

** How strong are the heterogeneities as functions of length scale?

** How do the length scales vary with direction?

** What statistical correlations exist between heterogeneities of different parameters?

** How do the heterogeneities vary with depth and from region to region?

Scattered seismic waves provide the best data bearing on these questions. They can be used to determine the three-dimensional spatial power spectra and cross-spectra of heterogeneities in elastic moduli and density in regions from which scattering can be observed. The observations must, however, be made with seismometer arrays to enable propagation direction to be determined. Three-component observations would also be helpful for identifying and separating different wave types and modes of propagation.

The stress within the crust is more difficult to study. Direct observations require deep boreholes and are much too expensive to be practical for mapping small-scale variations. Earthquake mechanisms, on the other hand, are easily studied and reflect the stress orientation and, less directly, its magnitude, but are often not uniquely determined by available data.

This investigation uses earthquake mechanisms and the scattering of seismic waves as tools for studying crustal heterogeneity.

Results

Focal Mechanism Inversion

There are now enough strainmeters in California so that, for many earthquakes, static strain steps are detected at several sites. In addition, static offsets are frequently measurable by geodetic techniques. However, the only way to use these data to infer seismic moments and focal mechanisms has been by trial and error. The linear-programming algorithm of Julian [1986] is ideally suited to inverting static displacements, strains, and tilts, as well as seismic wave polarities and amplitudes. Consequently, we have extended the computer program based on this algorithm to handle static elevation differences, line-length changes, strain steps (dilatation or tensor components), and tilts. This program computes bounds on the set of mechanisms consistent with any data set, and is ideally suited to hypothesis testing and to automated focal mechanism determination. We plan to use this program to analyze the many recent earthquakes for which static offset data are available. In the long run, it may also be possible to incorporate static strain data into automatic real-time focal-mechanism determination.

Automatic real-time earthquake monitoring

Over the last several years, the USGS has developed a system for monitoring central and northern California earthquakes automatically in real time, using phase arrival information generated by the Real-Time Processor (RTP). The arrival data are processed by a separate computer system, which automatically computes earthquake hypocenters locations and magnitudes, maintains a data base of this information, and displays maps of current activity on interactive graphics terminals. This computer system includes an alarm facility, which detects large earthquakes and swarms and automatically notifies seismologists by means of a radio paging system, and a seismicity monitoring facility, which detects changes in regional rates of earthquake occurrence. The RTP and the associated computer system have become the main tool used by the USGS to monitor earthquakes in central and northern California, and in particular play a critical role in the current Parkfield earthquake prediciton.

During the last six months, several improvements have been made:

A second Integrated Solutions model V24 computer has been added, intended to replace the Digital Equipment corporation PDP-11/70, which is nearing the end of it expected life span. A redundant machine makes nearly continuous monitoring possible, even when hardware failures and routine maintenance occur. The new computers are much faster, and provide many other advantages, such as inter-machine communication through a local-area network.

Rex Allen's new Real-Time Processor, based on the Motorola 68020 microprocessor, is now operating, monitoring stations in the Parkfield area. At present, the data it generates are going into only one computer, however. This new machine is expected to expand to handle more stations, and to perform more extensive functions, as time goes along.

We have improved the facilities for monitoring seismicity changes and detecting unusual earthquakes and sequences. Now, the cumulative seismic moments in different geographic regions, in addition to the number earthquakes, are monitored. Also, it is now easier to update the data base of historical seismicity statistics, so the monitoring adapts more quickly to long-term changes such as ongoing aftershock sequences, and generates fewer false alarms.

Together with Andy Michael, we have added facilities to automatically compute fault-plane solutions for larger earthquakes. Routine operation began July 3, 1987, and has so far generated 993 fault-plane solutions.

Volcanic tremor and elastic-wave scattering

Two journal articles have been completed and submitted. One proposes a new mechanism for the generation of volcanic tremor by nonlinear flow-induced vibration of the walls of channels transporting magmatic fluids. The other article deals with the theory of weak scattering of elastic waves in a randomly heterogeneous medium. Another paper, using the scattering theory to predict coda shapes, is in preparation.

Reports

Julian, Bruce R., 1987, Scattering of elastic waves by random heterogeneities: J. Geophys. Res., submitted.

Julian, Bruce R., 1987, Nonlinear Flow-induced vibration: A possible mechanism for volcanic tremor: J. Geophys. Res., submitted.

Rupture Mechanics of Slip-Deficient Fault Zones

14-08-0001-G1167

J.R. Rice (P.I.), R. Dmowska, and N. Fares
Division of Applied Science and
Department of Earth and Planetary Sciences,
Harvard University
Cambridge, MA 02138
(617) 495-3445

(for period May 1, 1987 to October 30, 1987)

1. Investigations

1.1 Studies are underway on viscoelastic foundation models for an elastic crustal plate undergoing strike slip faulting. The aims are to see how sensitive are distributions of displacement along the Earth's surface and stress along the vertical fault cut to parameters of the viscoelastic layer and, also, to check the applicability of simple Elsasser modeling of foundation coupling.

1.2 The Savage and Burford (1973) model of a single buried line dislocation, of screw type, in an elastic half space is frequently used for interpreting geodetic data in a strike-slip environment. The interpretation of parameters of that model is being studied when it is used to fit a more elaborate, geodetically constrained model of crustal deformation for the San Andreas region (Li and Rice, 1987). In the latter model loading is by steady mantle flow, compatible with remote plate velocity, which transmits basal tractions to an elastic crustal plate through an underlying viscoelastic asthenospheric-like layer (lower crust).

1.3 Three dimensional elasticity analyses of shear fault (modeled as freely slipping crack) penetration into locked obstackes of variable strength continue to be pursued.

2. Results

2.1 Consider the geometry shown in figure 1. An elastic crustal plate overlies a Maxwellian viscoelastic layer which rests on an elastic halfspace. The elastic modulus μ for all three regions is assumed to be the same. A uniform dislocation slip b over depth z' is suddenly introduced in the upper crust. The immediate response (i.e. at t=0+) of this layered region is that of a uniform elastic halfspace. The "postseismic" changes of displacement along the earth's surface, and tractions on the vertical fault section, due to the relaxation of the viscoelastic layer have been calculated. The changes are from time 0+ to t.

We show results for three cases with times scaled by an appropriately defined relaxation time t_r (based on viscosity η) for each case:

(*i*) Viscoelastic layer, $W = H$, with $t_r = H \eta / W \mu = \eta / \mu$; dot-dash lines in figs. 2 and 3.

(*ii*) Viscous surface, $W \rightarrow 0$ and $\eta \rightarrow 0$ such that $t_r = H \eta / W \mu$ remains finite; solid lines in figs. 2, 3 and 4.

(*iii*) Viscoelastic half space, $W \rightarrow \infty$, with $t_r = \eta / \mu$; dashed lines in figs. 2 and 3.

The expressions for the postseismic displacements and tractions for the viscous surface and viscoelastic halfspace model can be interpreted in terms of an infinite series of displacements and tractions due to image dislocation sources. The temporal behavior of the first four images of the viscous surface model is such that the locations of the image dislocations move linearly away from the interfaces with increase in time, with the amplitude of the dislocations remaining constant. By contrast, the temporal behavior of the first four images of the viscoelastic halfspace model is such that the amplitudes of the contribution of those image dislocaitons decay exponentially with time, while their locaitons remain fixed. These remarks provide some understanding of how the postseismic displacements and tractions vary with time in the above limit cases.

The postseismic changes in fault shear tractions (normalized by $\mu b/H$) and surface displacements (normalized by b) caused by a suddenly introduced dislocation which ruptures the full thickness of the upper crust (i.e., $z' = H$) are shown in figures 2 and 3, respectively, for the three cases. The successive curves, sometimes overlapping for different cases, correspond to $t = 0.2\, t_r$, $2\, t_r$, $10\, t_r$ and $200\, t_r$.

The postseismic surface displacements, fig. 3, for the finite thickness viscoelastic layer (dot-dash) and for the viscous surface (solid line) are very similar. This suggests that post-seismic surface displacement data cannot be directly used to sensibly constrain a thickness value for a viscoelastic layer underlying the upper crust.

By contrast, the postseismic regains of shear traction on the fault (fig. 2) are somewhat sensitive to the viscoelastic layer thickness. During time values of the order of the characteristic relaxation time of the viscoelastic layer (referred to as short time response), the finite layer postseismic traction response is similar to that of the viscoelastic halfspace model. During time values much longer than the characteristic relaxation time of the viscoelastic layer (referred to as long time response), the finite layer postseismic traction is similar to that of the viscous surface model. This behavior may be explained as being due to the relative rigidity of the lower elastic halfspace being felt more with time. During the short time response, the viscoelastic layer has not relaxed sufficiently for the lower elastic halfspace to significantly influence the deformations near the slip region, whereas it has for the long time response. For the viscous surface model, the rigidity of the elastic halfspace affects response immediately.

In figure 4, the postseismic surface displacements of the viscous surface model (solid lines) are compared with the postseismic surface displacements of the generalized Elsasser model (dashed line) of Rice (1980) and Lehner et al. (1981), as used recently by Li and Rice (1987). In general, postseismic surface displacements of the two models tend to agree. The agreement is especially good in the short time response. However, the apparent diffusion rate of the Elsasser model seems to be somewhat slower than that of the viscous layer model. This slower apparent diffusion rate is evidenced by the long time response where the Elsasser postseismic displacements are higher closer to the fault and lower far from the fault than in the viscous layer model.

2.2 In work with V.C. Li and H.S. Lin of M.I.T. we are attempting to provide an improved basis for interpreting parameters inferred from the Savage-Burford (1973) model, when that model is used to approximately fit geodetic data in a strike slip environment. Surface displacement and strain rate have been deduced from geodetic measurements in networks located near the San Andreas Fault system in California. These surface deformation data have been used to estimate the locked depth along the fault zone and the aseismic creep velocity at greater depth by means of the classical buried screw dislocation model of Savage and Burford (1973). In present work we compare with that model the driving mechanism and stress accumulation process of a more elaborate model of a strike-slip plate margin, and the spatial variation of the associated surface deformation rate. The latter model (Li and Rice, 1987) effectively involves a continuous distribution of such dislocations in an elastic crustal plate due to free slip below a shallow locked zone. The tractions on the base of the plate are transmitted through a viscoelastic asthenospheric-like layer, in the lower crust, and originate from the drag of steady flow in the underlying mantle. Deformation rates predicted by the model are time dependent throughout the great earthquake cycle, and parameters have been constrained by geodetic data from the San Andreas system near Palmdale (McGarr et al., 1982); (Thatcher, 1983; King and Savage, 1984). The simpler single line dislocation model of Savage and Burford is then employed to provide a best mean-square fit to the surface deformation rate predicted by the more elaborate model over various distances from the fault trace. It is found that the 'best-fits' based on the single line dislocation model for both the locked depth and deep aseismic slip rate are significantly greater than the actual values used to generate the simulated "data", and become more so for sampling distances extending to increasing distances from the fault trace.

A manuscript is in preparation.

2.3 Linearized perturbation techniques within three-dimensional elasticity theory have been developed (Rice, 1985) to determine stress intensity factors along the tips of planar cracks whose fronts differs slightly in location from some simple reference geometry. Those techniques, developed originally for tensile cracks, were recently applied to shear mode cracks of half-plane type with crack front perturbed from a straight line (Gao and Rice, 1986). Recent studies have extended the techniques to shear mode cracks of shapes that are perturbed slightly from a circle (Gao, 1987a). Also, some new 3D elasticity solutions have been derived (Gao, 1987b), for point force loadings of normal and shear type acting along the freely sliding surfaces of two abutting half-spaces that are connected together over a circular patch. These solutions provide the starting point for applying the perturbation technique, so as to determine shear mode stress intensity factors along the borders of locked asperities, of shapes that can be regarded as slightly perturbed from a circle, on fault surfaces that are slipping elsewhere.

Current continuations of the work are using the new solutions to study how slip penetrates into a locked asperity of randomly variable fracture resistance. Present studies are directed to devising suitable sample functions of random resistance and to development of numerical methods to predict crack growth, including sudden jumps of the crack front to a new equilibrium positions before overall rupture of the asperity.

References

Gao, H., Nearly circular shear mode cracks, Int'l. J. Solids Struct., in press, 1987a.

Gao, H., Weight functions for external circular cracks, in review, 1987b.

Gao, H. and J.R. Rice, Shear stress intensity factors for a planar crack with slightly curved front, J. Appl. Mech., **53**, 774-778, 1986.

King, N.E. and J.C. Savage, Regional deformation near Palmdale, California, 1973-1983, J. Geophys. Res., **89**, 2471-2477, 1984.

Lehner, F.K., V.C. Li and J.R. Rice, Stress diffusion along rupturing plate boundaries, J. Geophys. Res., **86**, 6155-6169, 1981.

Li, V.C. and J.R. Rice, Crustal deformation in great California earthquake cycles, J. Geophys. Res., **92**, 11,533-11,551, 1987.

McGarr, A., M.D. Zoback, and T.C. Hanks, Implications of an elastic analysis of in-situ stress measurements near the San Andreas fault, J. Geophys. Res., 87, 7797-7896, 1982.

Rice, J.R., The Mechanics of earthquake rupture, in Physics of the Earth's Interior, edited by A.M. Dziewonski and E. Boschi, 555-649, Italian Physical Society/North Holland, Amsterdam, 1980.

Rice, J.R., First order variation in elastic fields due to variation in location of a planar crack front, J. Appl. Mech., **52**, 572-579, 1985.

Savage, J.C. and R.O. Burford, Geodetic determination of relative plate motion in central California, J. Geophys. Res., **78**, 832-845, 1973.

Thatcher, W., Nonlinear strain build-up and the earthquake cycle on the San Andreas fault, J. Geophys. Res., **88**, 5893-5902, 1983.

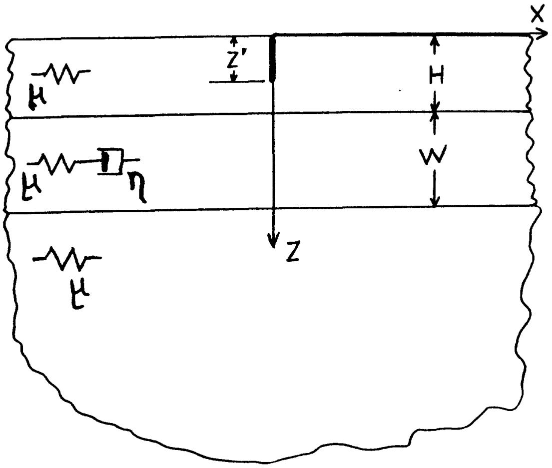
X
Z'
H
W
Z
μ
μ
η
μ

1

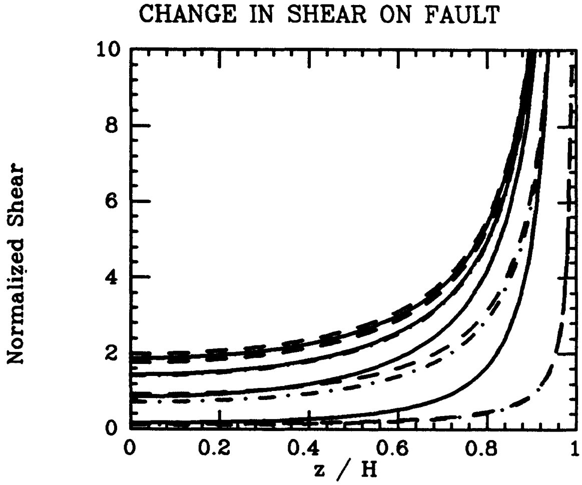
CHANGE IN SHEAR ON FAULT
Normalized Shear
z / H
0
2
4
6
8
10
0
0.2
0.4
0.6
0.8
1

2

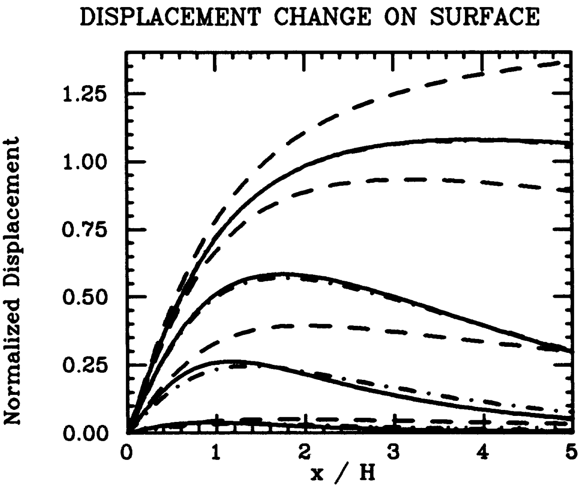
DISPLACEMENT CHANGE ON SURFACE
Normalized Displacement
1.25
1.00
0.75
0.50
0.25
0.00
0
1
2
3
4
5
x / H

3

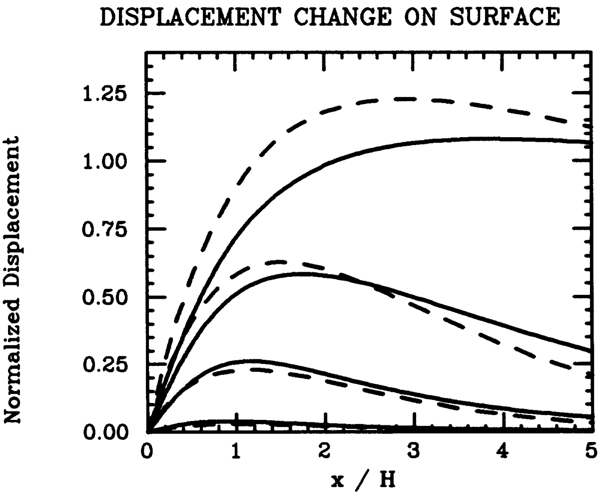
DISPLACEMENT CHANGE ON SURFACE
Normalized Displacement
1.25
1.00
0.75
0.50
0.25
0.00
0
1
2
3
4
5
x / H

4

ROCK DEFORMATION

9950-00409

Eugene C. Robertson
Branch of Geologic Risk Assessment
U.S. Geological Survey
MS 922, National Center
Reston, Virginia 22092
(703) 648-6792

Investigations

Cyclic loading tests in compression were made at strains to 10^{-3} at frequencies from 1 Hz to 0.002 Hz on samples of three common rocks. The purpose of the tests was to determine the effects of increasing strain and of fracturing on the anelastic properties of rocks in compression and to compare the results with those from similar tests on the same rocks in torsion.

Results

The following progress report on cyclic loading in uniaxial compression on rock samples includes data on compressive strength, elastic moduli, and attenuation, and compares the data with results from previous torsion tests. Applied stresses in both types of tests ranged between 5 and 65 percent of the strengths (0.05 and 0.65 S) of granite, basalt, and limestone; their average compressive strengths were observed to be 3.1, 3.3, and 2.0 kb, and their tensile (torsion test) strengths are 0.4, 0.3, and 0.2 kb, respectively.

The cyclic compression tests were driven at frequencies of 1.0, 0.1, 0.01, and 0.002 Hz and at axial strains between 0.05 and 0.3 percent. The oscillatory torsion tests were run at strains between 0.01 and 0.1 percent and at frequencies of 1 to 5 Hz. An important result in both types of experiments was the nearly full recoverability of original dimension after each of 6 to 12 successive tests despite large nonlinear deformation; there was no observable residual strain in the samples afterward. In both types of tests also, a small amount of strain hardening developed after successive runs at strains above 0.05 percent. Detailed variation of Young's modulus with strain and frequency was somewhat ambiguous; further more precise testing is needed.

The specific dissipation coefficient, Q^{-1}, was determined in the driven compression tests by the phase angle lag of strain behind applied stress; Q^{-1} in the torsion tests is measured by amplitude decay of oscillations of the pendulum. In basalt, in cyclic compression tests at frequencies of 1 to 0.002 Hz and at strains below 0.05 percent (about

0.1 S), the Q^{-1} is essentially constant at about 0.05; in torsion tests on basalt at 5 Hz, the Q^{-1} is constant at about 0.003, the difference may be due to differing absorption mechanisms, shear versus tensile fracturing. Under loading at strains above 0.1 percent (above 0.2 S), the values of Q^{-1} increase markedly to 0.3 for all frequencies from 1 to 0.002 Hz, with no apparent frequency effect at a given maximum loading amplitude. Similar results were found for Q^{-1} in granite and limestone tests. The energy density absorbed in one cycle in several compression tests of basalt samples at 1 Hz, at a strain of 0.1 percent, was about 2,000 J/m^3, and in torsion tests at 5 Hz, at about the same strain, the energy density for one cycle was about 100 J/m^3. Again the difference may be due to tensile versus shear absorption mechanisms.

It is expected that Q^{-1} will be even higher at larger strain, above 0.3 percent, and the transition to failure under cyclic loading in compression will provide information on criteria for strength and data on change of moduli and attenuation with increase of fracturing, and possibly be observable in the earth as precursory to an earthquake.

Heat Flow and Tectonic Studies

9960-01177

John H. Sass
Branch of Tectonophysics
U.S. Geological Survey
2255 North Gemini Drive
Flagstaff, AZ 86001
(602) 527-7226
FTS: 765-7226

Arthur H. Lachenbruch
Branch of Tectonophysics
U.S. Geological Survey
345 Middlefield Road
Menlo Park, CA 94025
(415) 329-4879
FTS: 459-4879

Investigations:

A preliminary interpretation of results from Phase 1 of the Cajon Pass drilling project has been completed.

Heat-flow studies from the southern California-Arizona Transect (PACE) are up-to-date, and a preliminary interpretation has been made.

Temperature measurements from the Salton Sea Scientific Drilling Project (SSSDP) have been completed, and an interpretive manuscript has been submitted for publication.

Heat flow has been calculated for research well VC-1 in the Valles Caldera and a preliminary model for the thermal regime of the caldera has been constructed.

New temperature data were obtained from the Alaskan North Slope near Prudhoe Bay as part of an attempt to characterize the stability field of gas hydrates in the region.

Results:

Cajon Pass. Over the past two decades, research on heat flow, rock mechanics, and the state of stress near the San Andreas fault has raised a basic question: Does the absence of a heat-flow anomaly over the San Andreas fault mean that there is little frictional heating (and low fault stress) or that abundant frictional heat (expected from high fault stress) is generated and then carried off by ground water or other sinks before it reaches the surface? To answer this question, direct measurements of heat flow, water movement, and stress are under way at the Cajon Pass borehole with a target at seismogenic depth. With the depth presently at 2.1 km, we can report the following. 1) The uncorrected near-surface heat flow is anomalously high; 30% to 40% greater than other measurements in this part of the fault zone. The anomaly can be accounted for by rapid local erosion for which there is geologic evidence. In this case, heat flow should be less by about 10% at the 2 km depth, and approach background values (70 mW/m^2) at the target depth (5 km) if frictional heating is unimportant. 2) Existing data are consistent with such a fall-off although thermal conductivity data are still inadequate to confirm it with confidence. Several hundred measurements by four different methods on core and drill cuttings have thoroughly characterized the thermal conductivity of the core (5% of the hole) but additional testing is needed to resolve a possible sampling bias in the cuttings. 3) In an alternate method under investigation, conductivity is estimated from mineral modes calculated from a suite of continuous geochemical well logs. 4) Ten precision temperature logs taken during and after drilling show that the temperature and its changes can be accounted for completely by heat-conduction theory; evidently heat transport by circulating ground water is not important.

PACE Studies. More than 200 values of heat flow are now available from the crystalline terranes of southern California, the Basin and Range province of Arizona, and Paleozoic sedimentary rocks of the southwestern Colorado Plateau (CP). Heat flow ranges from about 5 mWm^{-2} on the CP near Flagstaff, Arizona, to more than 150 mWm^{-2} in the crystalline rocks bordering the Salton Trough in SE California. The heat-flow pattern within this region is complex and appears to be controlled by regional physiographic and tectonic features.

Contemporary and Neogene tectonism appears to be responsible for the very high heat flow (>100 mWm^{-2}) associated with the Salton Trough and its neighboring ranges, the Death Valley fault zone and its southward extension, and zones of shallow (<10 km) Curie isotherms (as inferred from aeromagnetic data) in west-central and southern Arizona. Relatively low (<60 mWm^{-2}) heat flow in the Peninsular Ranges and eastern Transverse Ranges of California may be caused by thermal transients related to subduction and compressional tectonics. Hydrologic sinks may be associated with the low heat flows observed in these and other elevated blocks within the region.

No correlation is apparent between heat flow and near-surface radiogenic heat production. This absence of correlation is attributable to the complex tectonic history, involving lateral movement of basement terranes, and heat sources and sinks of different strengths, ages, and durations.

Salton Sea. At the conclusion of the active drilling phase of the Salton Sea Project, a series of logs was begun in an attempt to establish the equilibrium temperature profile. Initially, we were able to log to depths below 3 km, but, beginning in late May of 1986, we were unable to log below about 1.8 km because of damage to the liner. Our best estimates of formation temperature below 1.8 km are 305±5°C at 1,890 m and 355±10°C at 3,170 m. For the upper 1.8 km, the latest temperature log (October 24, 1986), using a digital "slickline" (heat-shielded downhole recording) device, appears to be within a few degrees Celsius of equilibrium. This was confirmed by a more recent log (July 31, 1987) to a depth of ~1 km. As in most other wells in the Salton Sea geothermal field, there is an impermeable, thermally conductive "cap" on the hydrothermal system; this cap extends to a depth of about 900 m at the Salton Sea well. Thermal gradients decrease from about 250 $mK\ m^{-1}$ (same as degrees Celsius per kilometer) in the upper few hundred meters to just below 200 $mK\ m^{-1}$ near the base of the conductive cap. Thermal conductivities of 19 samples of drill cuttings from this interval were measured at room temperature. The conductivity values were corrected for in situ porosity as determined from geophysical logs. Using one interpretation (no conductivity variation with temperature), thermal conductivities increase with depth (mainly because of decreasing porosity) resulting in component heat flows that agree reasonably well with the mean of about 450 mW m^{-2}. This value agrees well with heat flows measured in shallow wells within the Salton Sea geothermal field. A second interpretation, in which measured temperature-coefficients of quartz- and carbonate-rich rocks are used to correct thermal conductivities, results in constant, lower conductivities as a function of depth and consequently, systematically decreasing heat flux averaging about 350 mWm^{-2}. This interpretation is consistent with the inference (from fluid inclusion studies) that the rocks in this part of the field were once several tens of degrees Celsius hotter than they are presently. The age of this possible disturbance is estimated at a few thousand years.

Valles, VC-1. Over 5% of heat in the western U.S. is lost through Quaternary silicic volcanic centers, including the Valles caldera in north-central New Mexico. These centers are the sites of major hydrothermal activity and upper crustal metamorphism, metasomatism and mineralization, producing associated geothermal resources. We present new heat-flow data from Valles caldera corehole 1 (VC-1), drilled in the southwestern margin of the Valles caldera. Thermal conductivities were measured on 55 segments of core from VC-1, waxed and wrapped to preserve fluids. These values were combined with temperature gradient data to calculate heat flow. Above 335 m, which is probably unsaturated, heat flow is 247 ±16 mW m^{-2}. The only deep temperature information available is from an uncalibrated commercial log made 19 months after drilling. Gradients, derived from uncalibrated temperature logs, and conductivities are inversely correlated between 335 and 737 m, indicating a conductive thermal regime, and component heat fluxes over three depth intervals (335-539 m, 549-628 m and 628-737 m) are in excellent agreement with each other with an average of 504 ±15 mW m^{-2}. Temperature logs to 518 m depth with well-calibrated temperature sensors result in a revised heat flow of 463 ±15 mW m^{-2}. We use shallow thermal gradient data from 75 other sites in and around the caldera to interpret the thermal regime at the VC-1 site. A critical review of published thermal-conductivity data from the Valles caldera yields an average thermal conductivity of ≥1 W m^{-1} K^{-1} for the near-surface tuffaceous material, and we assume that shallow gradient values (°C km^{-1}) are approximately numerically equal to heat flow (mW m^{-2}). Heat loss from the caldera is asymmetrically distributed, with higher values (400 mW m^{-2} or higher) concentrated in the west-southwestern quadrant of the caldera. This quadrant also contains the main drainage from the caldera and the youngest volcanism associated with the caldera. We interpret the shallow thermal gradient data and the thermal regime at VC-1 to indicate a long-lived hydrothermal (and magmatic) system in the southwestern Valles caldera that has been maintained through the generation of shallow magma bodies during the long post-collapse history of the caldera. High heat flow at the VC-1 site is interpreted to result from hot water circulating below the base of the corehole, and we attribute the lower heat flow in the unsaturated zone to hydrologic recharge.

Gas hydrates. Natural gas occurs in an ice-like crystalline form (called "clathrate" or gas hydrate) under special conditions of high pressure and low temperature. Such conditions are common beneath the ocean basins but on the continents they occur only in and beneath very cold permafrost and adjacent submerged continental shelves. Equilibrium temperature measurements made by our project in the Alaskan Arctic over many years have provided the basis for recent mapping of the stability field for gas hydrate in response to a recent growth of interest in the subject.

There are several reasons why scientists and engineers have an interest in gas hydrates and offshore permafrost. Methane hydrate stores methane efficiently at low pressures; it may contain about 160 times as much methane as an equal volume of the free gas under standard conditions of temperature and pressure. Thus, relatively small volumes of methane hydrates may be potentially valuable energy resources if they can be exploited. Both methane hydrate and ice in permafrost can cause profound natural and engineering disruptions if they should be thawed; ice because of its loss of strength and gas hydrate because of its release of gas. Additionally, both methane hydrate and ice generally have much higher seismic velocity and electrical resistivity than water. Consequently, the distribution of both offshore permafrost and gas hydrate are important in the interpretation of geophysical surveys, for example, in petroleum exploration. Like carbon dioxide, methane is a "greenhouse" gas that affects the radiation balance of the atmosphere and, therefore, the climate. Thus, the possible role of methane hydrate as a source of atmospheric methane is a subject of great current interest. Additional scientific interest in methane hydrate stems from its use, when detected seismically beneath the sea floor, as an indicator of geothermal gradient and regional heat flow; and in offshore permafrost, as an indicator of shoreline history and oceanic transgression rates.

With support from the Department of Energy, we made precision temperature measurements in 10 idle oil-exploration wells at the Milne Point and Kaparuk oil fields on the Alaskan Arctic Coastal Plain. To make the measurements, our logging truck was driven to the Arctic and carried across the tundra to the sites by Rolligon, an off-road large-foot-print tractor-trailer. The information fills a gap in existing data between Prudhoe Bay and the western Arctic Coastal Plain in an area where gas hydrates are known to occur.

Reports:

De Rito, R. F., 1987, The effects of weak crust upon the strength of the continental lithosphere (extended abstract): U.S. Geological Survey Circular, in press.

Elders, W. A., and Sass, J. H., 1987, An overview of the SSSDP (abstract): EOS, v. 68, p. 438.

Lachenbruch, A. H., Sass, J. H., Lawver, L. A., Brewer, M. C., Marshall B. V., Munroe, R. J., Kennelly, J. P., Jr., Galanis, S. P., Jr., and Moses, T. H., Jr., Temperature and depth of permafrost on the Alaskan Arctic Slope: Pacific Section - SEPM Special Publication and U.S. Geological Survey Professional Paper 1399 (Branch approval, March 1986).

Lachenbruch, A. H., Sass, J. H., Saltus, R. W., Anderson, R. F., and Williams, C., 1987, Thermal regime at the Cajon Pass Research well (abstract): EOS, in press.

Langseth, M. G., Lachenbruch, A. H., and Marshall, B. V., 1987, Geothermal observations in the Arctic region: Decade of North American Geology volume, in press.

Munroe, R. J., and Sass, J. H., 1987, Thermal conductivity of samples from borehole VC-1, Valles Caldera, New Mexico: U.S. Geological Survey Open-File Report 87-184, 16 p.

Pollack, H. N., and Sass, J. H., 1987, Thermal regime of the lithosphere, in Haenel, R., Rybach, L., and Stegena, L., eds., Handbook of Terrestrial Heat-Flow Density Determination (Guidelines and Recommendations of the International Heat Flow Commission), in press.

Sass, J. H., 1987, Salton Sea Scientific Drilling Program: U.S. Geological Survey Yearbook, in press.

Sass, J. H., Hendricks, J. D., Priest, S. S., and Robison, L. C., 1987, Temperatures and heat flow in the State 2-14 well, Salton Sea Scientific Drilling Program (abstract): EOS, v. 68, p. 454.

Sass, J. H., and Lachenbruch, A. H., 1987, Heat-flow field of the California-Arizona crustal experiment and adjacent areas (abstract): Geological Society of America, Annual Meeting, Phoenix, Arizona, 1987, Abstracts with Programs, v. 19, no. 7, p. 829.

Sass, J. H., and Morgan, P., 1987, Conductive heat flux in VC-1 and the thermal regime of the Valles caldera, Jemez Mountains, New Mexico: Journal of Geophysical Research, in press.

Sass, J. H., Priest, S. S., Duda, L. E., Carson, C. C., Hendricks, J. D., and Robison, L. C., 1987, Thermal regime of the State 2-14 well, Salton Sea Scientific Drilling Project: Journal of Geophysical Research, in press.

Fractal Heterogeniety of Faults: Effect of Topography on Friction

14-08-0001-G1366

C.H. Scholz and N. Yoshioka
Lamont-Doherty Geological Observatory
of Columbia University
Palisades, New York 10964
(914) 359-2900

1. Elastic Shear Properties of Contacting Rough Surfaces

Investigations: Laboratory experiments have been carried out to investigate the elastic shear properties of rocks under various normal stress up to 33 MPa in a torsional configuration using cylindrical samples. Solid samples (without cut) of different length and saw-cut samples with different surface roughnesses have been examined. Topographies of the contact surfaces were measured for saw-cut samples and used to calculate the shear stiffness using a model which is modified from *Yamada et al.* [1987 a,b]. The calculated results were compared with the experimentally observed data.

Our goal is to develop a model for elastic shear behavior in rocks and to establish a shear constitutive law for cracked solids under compression.

(1) The shear stiffness of the contacting surfaces increases with the normal stress in a non-linear manner [Figure 1].

(2) The roughness of the contacting surfaces strongly affects the behavior mentioned in (1). The rougher the surfaces are, the smaller the stiffness. The increasing rate of the stiffness with the normal stress decreases with the increase of surface roughness.

(3) The shear stiffness and shear modulus of the solid samples is a strong function of the normal stress, which can be expressed as

$$k = A + B \log (p+1)$$

where k is the stiffness and p is the normal stress. The mimicry of the behavior of solid samples to the contacting surface suggests that the behavior of the micro-cracks inside the solid rock under compression is basically the same as that of the individual rough surface.

(4) The experimentally observed behavior of the contacting surfaces due to normal stress can be well described by a model calculation which uses topography data of the contact surfaces in the modified Yamada, et al. theory [Figure 2].

References

Yamada, K., N. Takeda, J. Kagami, and T. Naoi, Surface density of asperities and real distribution of asperity heights on rubbed surfaces, *Wear*, *47*, 5-20, 1978a.

Yamada, K., N. Takeda, J. Kagami, and T. Naoi, Mechanisms of elastic contact and friction between rough surfaces, *Wear*, *48*, 15-34, 1978b.

2. Wear and Gouge formation in brittle faulting

Results: The relationship between thickness of the gouge zone and total slip has been investigated with data collected by Robertson (1982) and others. A steady state wear law was developed and applied to this problem, and further compared with experimental data of Yoshioka (1986). This work has been published: Scholz, C.H., Wear and Gouge Development in Brittle Faulting, *Geology*, *15*, 493-495, 1987.

3. Brittle-Plastic transition and its effect on faulting.

A new analysis of the effect of the brittle-plastic transition of faulting and seismicity was made. This work will be presented at the 1987 Fall AGU and is in press: Scholz, C.H., The Brittle-Plastic transition and the depth of seismic faulting, *Geol. Runsch.*, in press, 1987.

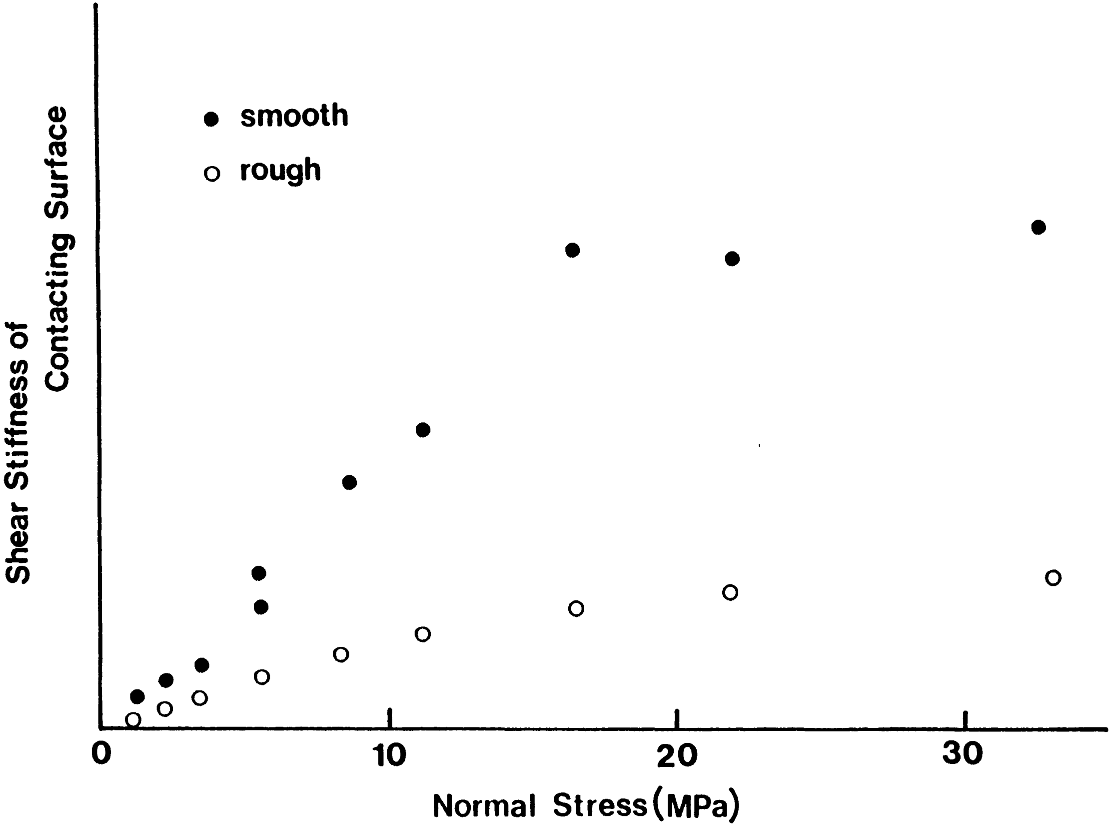

Fig. 1. Experimental measurements of the shear stiffness of rough surfaces in contact as a function of normal load. Measurements made of Westerly Granite surfaces of two different roughnesses.

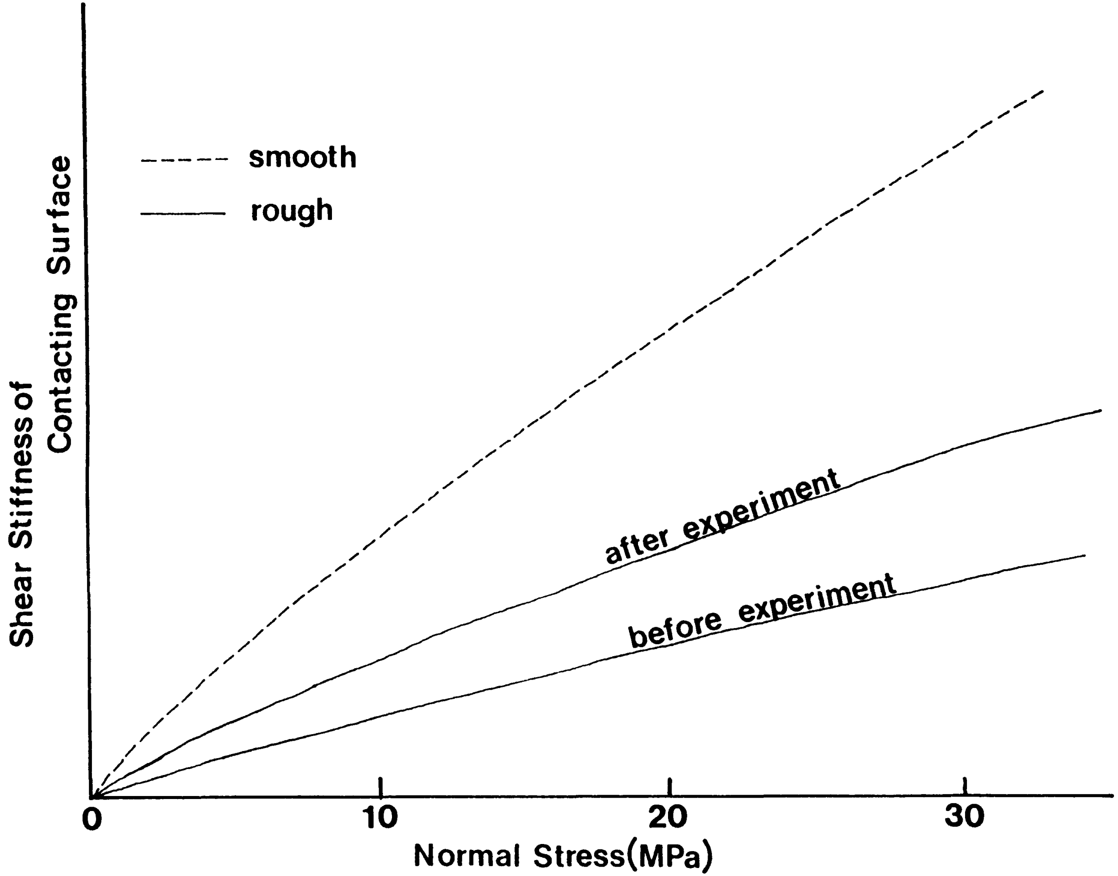

Fig. 2. Theoretical calculations of shear stiffness, based on the contact theory of Yamada et al., using topographic data from the tested surfaces. Before and after calculations reflect damage to the surface that occurs during the experiment.

Systems Analysis of Geologic Rate Processes

9980-02798

Herbert R. Shaw and Anne E. Gartner
Branch of Igneous and Geothermal Processes, U.S Geological Survey
MS 910, 345 Middlefield Road, Menlo Park, CA 94025
(415) 329-5245, 5209

Objective: The work on this project has the objective of summarizing multifractal sets of seismic and fault data for California as an approach to generalizing the patterns of seismic moment flux.

Results: In our summary of work for 1 October 1986 through 31 March 1987, we illustrated frequency-magnitude data in a form suggesting that they represent multifractal arrays. Although such arrays describe the geometry of inferred fracture systems, they are time-dependent in that each multifractal geometry reflects the seismic catalog used for its construction. Therefore, the fractal dimensions deduced from a given catalog may change or be added to with time and(or) with changing geographic locus. It is suggested that such dimensional sets may provide more sensitve indicators of impending earthquakes than the time-dependence of b-values because they indicate relative changes of 'topologic completeness' of the seismic data as functions of the chosen sizes and locations of geographic regions as well as the durations of the earthquake record. Such multifractal sets are subject to the usual uncertainties of frequency-magnitude data, but they can also be tested in terms of documented motions on specific faults using geologic data. We have found that data based on trenching studies and geologic estimates of slip rates (Wesnousky, 1986) reveal analogous multifractal arrays. However, these constructions represent longer recurrence times than are available in seismic catalogs and are weighted by the larger earthquakes, therefore the geologically inferred multifractal arrays are dimensionally skewed relative to those inferred from seismic data. Such dimensional contrasts may provide useful tests of both spatial and temporal models and may act to guide more detailed comparisons of geologic and seismic investigations.

We infer from these studies that seismic rupture of the crust in California takes place at many scales of length that are coordinated in space and time. According to this view, rupture is a diffuse process whereby a characteristic multifractal geometry is sampled progressively in time and space. There are many testable implications of such a model. For example, if the geometry of a 'complete' catalog were known, this knowledge would characterize a generalized earthquake cycle for all magnitudes. Because such a multifractal geometry reflects both spatial and temporal distributions, it would include information on such things as seismic gaps, 'Mogi doughnuts', and local seismic cycles of the Parkfield type. Although we cannot define a universal multifractal geometry (singularity spectrum) on the basis of present data, the process of testing coordinated fractal arrays in itself adds to the generalized concept and simultaneously provides interim predictions based on 'comparative completeness' of different regions throughout the state. In this way the multifractal concept could conceivably guide a statewide synthesis and monitoring technique at all energy scales ranging from microearthquakes to maximum events. Previous concepts that have subdivided earthquake mechanisms by magnitude, foreshock-aftershock styles, and so on, are considered to represent subsets of a multifractal geometry that is of universal dimensional character.

According to a multifractal model described in Shaw (1987), the flux of seismic moment diffuses through a system of fractures at all length scales from microfractures to the longest ruptures of the San Andreas fault. In this respect, both the motions associated with individual ruptures and the distributions of length scales resemble the diffusion of momentum in turbulent channel flow of a major river system, although the 'tributaries' of seismic flux are not visually delineated in the same sense. It is suggested that existing patterns of seismic energy flux throughout California are coordinated with waxing and waning activity emanating from three primary sources located in the vicinities of Plate Tectonic junctions rather than simply with slip rates measured along the San Andreas and related fault systems. These 'diffusive' sources are located geographically in the vicinities of Eureka, California, northwestern Nevada, and Baja California. They correlate, at least in part, with Plate Tectonic features described in studies by Suppe and others (1975), Herd (1978), and Wallace (1984).

References:

Herd, D. G., Intracontinental plate boundary east of Cape Mendocino, California, *Geology*, *6*, 721-725, 1978.

Shaw, H. R., A linguistic model of earthquake frequencies applied to the seismic history of California, *U.S. Geol. Surv. Open-File Rept. 87-296*, 1987.

Suppe, J., C. Powell, and R. Berry, Regional topography, seismicity, Quaternary volcanism, and the present-day tectonics of the western United States, *Am. Jour. Sci.*, *275-A*, 397-436, 1975.

Wallace, R. E., Patterns and timing of Late Quaternary faulting in the Great Basin province and relation to some regional tectonic features, *Jour. Geophys. Res.*, *89*, 5763-5769, 1984.

Wesnousky, S. G., Earthquakes, Quaternary faults, and seismic hazards in California, *Jour. Geophys. Res.*, *91*, 12587-12631, 1986.

EVALUATION OF DEFORMATION PROCESSES IN FAULT ZONES AT DEPTHS CORRESPONDING TO THE BRITTLE-DUCTILE TRANSITION

14-08-0001-G1341

CAROL SIMPSON
Department of Geological Sciences
Virginia Polytechnic Institute & State University
Blacksburg, VA 24061

now at
Department of Earth & Planetary Sciences
The Johns Hopkins University
Baltimore, MD 21218
(301) 338 8344

Investigations

Deformation in the Striped Rock Pluton, southwest Virginia, is associated with the formation of the nearby Fries Thrust Zone. Mapping on scales of 1:10 to 1:100 has documented the sequence and geometry of brittle and crystal plastic events that affect the plutonic rocks. Electron microprobe studies, scanning electron microscopy, transmission electron microscopy and optical microscopy are being used to determine the deformation conditions for the several deformation episodes that have occurred in this exhumed fault zone.

Results

The northwestern boundary of the Fries Thrust Zone, a km-scale, gently SE-dipping exhumed ductile fault, abuts the Striped Rock Pluton, a composite granite/syenite pluton of the Late Proterozoic Crossnore Plutonic-Volcanic suite of the southern Appalachians. Both the Striped Rock plutonic rocks and the country rock gneisses are cut by numerous ductile shear zones. Deformation associated with the FTZ has variably affected the Striped Rock Pluton. As far as 2km to the northwest of (i.e. structurally below) the FTZ, the plutonic rocks are cut by numerous cm-scale cataclasite zones and mm- to decimeter-scale mylonite zones. This deformation is heterogeneously distributed, becoming less well developed with distance from the FTZ. Preliminary field and microstructural investigations indicate that four significant deformation events are recorded in the plutonic rocks, at least the first two of which are directly related, geometrically, and spatially with deformation along the FTZ.

Deformation commenced with a brittle transgranular cracking event that produced ENE-trending Mode I dilatant cracks. Fracture density is highly variable throughout the pluton. Where fracturing is intense, mm-wide mineralized cracks are mm to cm apart and up to several cms in length. Distributed unstable crack arrays with extremely regular geometry formed preferentially in porphyritic lithologies and allowed bulk ductile deformation with significant volume increase of the rock. Cataclasite zones up to a meter wide formed preferentially in areas of uniform original grainsize. Bulk rock mineralogy (host granite + fracture fill) in fractured areas is significantly changed. The fractured rock is enriched in Si, Fe and K with respect to the host rock. Almost all feldspar grains contain abundant intergranular fractures that are usually dilatant and oriented along (001) or (010) cleavage planes. These fractures are either sealed or filled with mineral precipitate. Healed intragranular cracks in original quartz grains are defined by CO_2-rich fluid inclusion arrays.

The brittle deformation was followed by a mylonite-forming event that produced conjugate shear zones of opposite movement sense: Northwest-directed thrust zones and southeast-directed extensional zones. Deformation conditions for both sets belong to lower greenschist facies. Localization of crystal plastic flow occurred in preference on mineralized veins, especially quartz veins, and in mica-rich phases of plutonic rocks; reaction softening is concentrated in altered vein wall rock. The resultant mylonite zones are often richer in silica than their protolith and contain quartz ribbons with rather uniform crystallographic orientation of component grains. Estimation of the contribution of vein quartz to bulk chemical analyses of both protolith and mylonite shows that apparent silica enrichment in many mylonite zones may be due in large part to pre-existing quartz veins.

Adjacent to the FTZ, both the Striped Rock Pluton and the surrounding Cranberry Gneiss country rock are deformed into mylonitic augen gneisses. The majority of the ductile deformation zones have a foliation with trend 040° to 080°, a moderate dip to the SE, and exhibit a well-developed mineral elongation lineation that plunges at 40° to 60° towards 158°; these fabrics are subparallel to those in the adjacent portion of the Fries Thrust Zone. Geometrical evidence suggests that all early brittle and subsequent ductile deformation occurred during a single deformation event as the crystalline thrust sheet was emplaced. Strain localization is common where "flaws" are present, such as inclusions of country rock, micaceous or porphyritic phases of the pluton, mineralized veins, or fractures. The nature of the "flaws" appears to govern whether the subsequent deformation mode is brittle, ductile, or a combination of the two.

Reports

Simpson, C. and Kalaghan, T. 1987. Deformation in the Striped Rock Pluton, N.W. margin of the Fries Thrust Zone, S.W. Virginia. *Geol. Soc. Am. Abstracts with Programs* 19 (2): 129.

Simpson, C. 1987. Exhumed Fault Zones: The Role of Fractures in Ductile Deformation. *AGU Fall Mtg.*, submitted.

Fault Patterns and Strain Budgets

9960-02178

Robert W. Simpson
U.S. Geological Survey
Branch of Tectonophysics
345 Middlefield Road, MS/977
Menlo Park, California 94025
415-329-4865

Investigations

Purpose is to understand the interactions of faults and fault segments through time using very simple elastic dislocation models. Latest investigations have been in collaboration with David Oppenheimer and Paul Reasenberg to attempt to understand the distribution of aftershocks to the Morgan Hill earthquake and the nature of their focal mechanisms.

Results

Oppenheimer and Reasenberg have shown that the pattern of aftershocks to the 1984 Morgan Hill, California earthquake is quite distinctive. Aftershocks falling close to the plane of the Calaveras fault showed right-lateral focal mechanisms with one plane striking NW-SE, aftershocks to the northeast side of the Calaveras showed right-lateral solutions with one plane oriented N-S, whereas aftershocks to the southwest of the Calaveras showed thrust mechanisms with nodal planes striking parallel to the fault. We used a dislocation model based on the mainshock slip distribution inferred by Hartzell and Heaton (1986, BSSA, v. 76, p. 649-674) to calculate the changes in static stress field that accompanied the Morgan Hill rupture. Although we do not know much about the pre-earthquake stress field onto which these changes were superposed, the observed pattern of aftershocks and their focal mechanisms agree poorly with results predicted by a model in which the pre-earthquake stress field was dominantly right-lateral shear oriented parallel to the Calaveras fault. Much better agreement is obtained if the volumes experiencing aftershocks were subjected to a dominantly compressive pre-earthquake stress field oriented nearly perpendicular to the strike of the Calaveras fault. It is difficult to rule out the possibility that such a compressive field might arise purely from local complications such as changes in strike of the Calaveras fault. However, a regional compressive field of considerable lateral extent in the vicinity of the San Andreas plate boundary has recently been proposed by Springer (1987, Tectonics, v. 6, p. 667-676) and by Zoback and others (1987, in press). In either case it appears that aftershock studies in conjunction with dislocation modelling may offer interesting constraints upon the orientations and magnitudes of regional stress field.

Earthquake Forecast Models

9960-03419

William D. Stuart
Branch of Tectonophysics
U. S. Geological Survey
Pasadena, California 91106
(818) 405-7816

INVESTIGATIONS

Theoretical Fault Models Applied to Earthquake Prediction

1. Additional analysis of a recently constructed instability model for great earthquakes at the Nankai Trough subduction zone to determine the effect of normal stress and fault shape.

2. Construct model for seismic quiescence and creep retardation before moderate earthquakes on the San Andreas fault in central California.

3. Calculate precursory and coseismic piezomagnetic anomalies associated with earthquake instability.

Mesozoic and Cenozoic Motions of Lithosphere Plates

1. Study causes of motion and motion changes of plates in Pacific basin during geologic time.

RESULTS

Theoretical Fault Models Applied to Earthquake Prediction

1. In instability models for dip-slip faults, time-dependent normal stresses occur due to the free surface and changes of fault dip. When the fault law in a recently developed model is modified to allow for changing normal stress, the effect is small for both a flat and curved fault. However, when the model fault has a bend (dip increase) similar to the one thought to exist near the Nankai Trough, the computed pre-instability slip history differs from that for a flat fault. The main difference is that slip is largely confined below the brittle section of the fault, with fault slip pentrating upward with time. In contrast, simulations with a flat fault give more complicated pre-instability slip, with much of the slip often occuring within the brittle section.

2. A preliminary model for seismic quiescence and creep retardation involving spacial variation of fault and crustal properties is under study.

3. A procedure for computing the piezomagnetic field change before moderate earthquakes near Parkfield was completed some time ago. The procedure combined an earthquake instability model with analytic solutions by Sasai. However, after further thought it appears that certain of his results may be unphysical; this problem is under study.

Mesozoic and Cenozoic Motions of Lithosphere Plates

1. No reportable results.

REPORTS

Stuart, W. D., Studies of San Andreas fault, Nature, 327, 99-100, 1987.

______________, Review of Earthquake Source Mechanics, Edited by Das, Scholz, and Boatwright, Pure and Applied Geophysics, 125, 853-855, 1987.

______________, Nonlinear constitutive laws, dislocations, and earthquake forecast models (abs.), Annual Meeting Amer. Soc. Mech. Eng., Appl. Mech. Div., June, 1987, Cincinnati.

______________, Forecast model for great earthquakes at the Nankai Trough subduction zone, Pure and Applied Geophysics, 126 (2-4), 1988, in press; also in USGS Open-File Report 87-000, Aki and Stuart, eds., 1987, in press.

Stuart, W. D., and K. Aki, eds., Intermediate-Term Earthquake Prediction, Pure and Applied Geophysics, 126 (2-4), 1988, in press.

Aki, K., and W. D. Stuart, eds., Physical and Observational Basis for Intermediate-Term Earthquake Prediction, Proceedings Workshop XXXVII, USGS Open-File Report 87-000, Vols. I and II, 1987, in press.

Rupture Geometry of Pseudotachylyte-bearing Brittle Seismic Fault Structures

14-08-0001-G1395

Mark T. Swanson
Department of Geosciences
University of Southern Maine
Gorham, Maine, 04038
(207) 780-5350

Investigations:

Detailed photomosaic mapping was conducted on a variety of scales at exposures of three fault structures along the southern Maine coast as examples of duplexing in the strike-slip environment. Pseudotachylyte associated with some of these fault structures suggests rapid slip rates characteristic of earthquakes in a paleoseismogenic zone. The interactive duplex structures studied in these exposures are interpreted as the actual mechanism of rupture associated with earthquake generation. The fault exposures were selected in order to study the variations in kinematic patterns due to changes in depth of formation and the controlling effects of a prominent planar anisotropy in the host rocks. The mapped fault structures include the following:

a.) The breccia and minor pseudotachylyte-bearing Two Lights fault structure within the Cape Elizabeth Formation at Cape Elizabeth (horizontal planar anisotropy, phyllitic quartzite host rocks, Carboniferous age, intermediate crustal levels, 2-5 km., dextral strike-slip, 8m. total displacement, 1:30 scale mapping).

b.) The breccia-bearing York Cliffs fault structure within the Kittery Formation at York, Maine (vertical planar anisotropy, interbedded metapelite and quartzite host rocks, Mesozoic age, shallow crustal levels, 1-2 km., sinistral strike-slip, 1m. total displacement, 1:6, 1:30 and 1:120 scale mapping).

c.) The pseudotachylyte-bearing faults of the Fort Foster Brittle Zone within the mylonitic Rye Formation of Gerrish Island (vertical planar anisotropy, mylonitic host rocks, Precambrian to Carboniferous (?) age, deeper crustal levels, 5-10 km., dextral strike-slip, 100 m. (?) total displacement, 1m. increments, 1:15 and 1:60 scale mapping).

Results:

Strike-slip faulting in all three locations was found to involve duplexing in accommodating displacements. The style of structural duplexing and the internal kinematic patterns were found to vary with depth of formation as well as with the effects of a controlling planar anisotropy.

Two Lights fault structure:

Numerous fault structures within the Cape Elizabeth Formation are developed along coastal exposures in the vicinity of Two Lights State Park in Cape Elizabeth, Maine. The faults are typically dextral strike slip and were found to develop minor pseudotachylyte, breccia and fine-grained cataclasites. The mapped structure is exposed with over 100 meters of outcrop length and accommodates nearly 8 meters of right-lateral displacement measured from offset steeply-dipping boudined quartz veins. The overall structure consists of 4-5 left-stepping en echelon strike-slip segments. The host rocks for these structures have a dominant horizontal planar anisotropy as S_0 and S_1 surfaces related to F_1 recumbent fold structures. A weak second S_2 cleavage surface is sporadically developed but with little influence on the developed fault structures. A prominent S_3 dextral strike-slip shear fabric resulting in asymmetric foliation and quartz vein boudinage appears to be related to the dextral shear expressed within these fault structures.

The dominant kinematic pattern developed in these fault structures involves P-shear type linkages between the dominant left-stepping dextral shear segments, doubly-tapered lens-duplexing, and extensional "horsetail" relays and terminations. Contractional lens duplexes are typically doubly-tapered with leading P-type lateral ramp structures and trailing R-type shear structures or extensional "horsetail" relays. Composite lens duplex structures show stacking or pileup of individual duplex lenses. Internal duplex deformation may involve ramping P-type dextral shears and/or small-scale high-angle reverse kink structures. R-type dextral shears may also develop during extension segmenting the original duplex lens. Minor extensional lens duplex structures are also developed as "horsetail" relays between local right-stepping en echelon fault segments. Some duplex development appears to begin by the initiation of pairs of leading low-angle P-type ramps and trailing extensional "horsetail" fracture arrays producing an asymmetric scallop-shaped decoupled duplex lens.

York Cliffs fault structure:

A single sinistral strike-slip fault structure is developed in coastal exposures of the Kittery Formation just north of Neddick Harbor in York, Maine. This fault structure is generally developed parallel to the prominent near-vertical S_0 bedding anisotropy as limbs to upright isoclinal F_2 fold structures. The mapped fault structure is exposed with nearly 130 meters of outcrop length and accommodates approximately 0.8 meters of sinistral displacement. Quartz-cemented breccias and gouge are the dominant fault products; pseudotachylyte is noticeably absent. The fault also cross-cuts and is cut by individual Mesozoic-age mafic dikes and depth of development is inferred to be shallow, on the order of 1-2 kilometers.

The dominant kinematic pattern developed in this fault structure involves the formation of distinctive slab-duplexes where the decoupled fault slabs are controlled by the thicker upright quartzite beds within the Kittery Formation. Extensional "horsetail" fracture arrays are also prominently developed as termination structures at either end of this sinistral fault zone.

Extensional slab duplexes typically develop as long layer-parallel zones of shear and extensional fracturing and brecciation. A single distinctive duplex slab, 10 meters in length and .25 meters in width, has deformed internally into discrete doubly-tapered lenses by low-angle R-shear structures. These individual R-shear lenses show evidence of significant internal extension by high-angle X-X′ shear fracture sets. R′ shear fractures are relatively rare but are clearly developed in association with the R-shear lens boundaries. Several areas show cross-cutting relationships where early R-R′ shears have been cut by later X-X′ shear fractures during layer-parallel extension subsequent to decoupling.

Minor contractional slab-duplexes are also developed with a distinctive internal R′ shear fracture set developed behind leading P-shear ramps. The two examples of contractional slab-duplexes found in these exposures are paired with extensional slab-duplexes distributed on opposite sides of the dominant shear surface particularly near the southwestern fault termination. Counterclockwise rotation of the decoupled internal blocks may lead to the formation of "crush breccias" and gouge. Other quartz-cemented breccias develop as small-scale pull-aparts at releasing bends and dilational jogs along the generally layer-parallel sinistral shear surfaces.

Fort Foster brittle zone:

Faults of the Fort Foster brittle zone consist of a complex array of dextral strike-slip structures developed parallel to the prominent near-vertical mylonitic layering within the Rye Formation along the southeastern shoreline of Gerrish Island, Maine. Pseudotachylyte (and minor breccia) is abundantly developed associated with distinctive coupled layer-parallel fault structures, originally termed pseudotachylyte generation zones and now interpreted as slab-duplex structures. These structures form a complex duplex-mosaic where the bounding layer-parallel slip surfaces are the sites of pseudotachylyte generation. The fault structures are exposed with 400 meters of outcrop length representing a slightly oblique section through a 60 meter wide fault complex. Total displacement across the brittle fault complex may reach 100′s of meters with individual slip increments of approximately a meter or less. The association of the brittle structures with kinematically similar Rye Formation mylonites and the general level of erosion suggests that these structures developed at depths approximating the brittle-ductile transition and the base of the seismogenic zone.

The dominant kinematic pattern within the Fort Foster brittle zone is the distinctive layer-parallel slab-duplex. Slab-duplexes may reach over 100 meters in length and a meter or less in width. Internal deformation within individual slab-duplexes involves assemblages of contractional P-P′ shears, kinks and asymmetric folds and extensional X-X′ shears and minor extensional fractures. Low-angle interactive ramp structures in R and P orientations serve as the leading and trailing structures for the development of the individual slab duplexes. Many of the distinctive contractional and extensional structures within the individual slab-duplexes are linked or coupled together to form (flat-bottomed or topped) scallop-shaped lens duplexes within the larger slab-duplexes similar to those described from the Two Lights fault structure. Extensional "horsetail" fracture arrays as observed in both of the more shallow structures are conspicuously absent in the pseudotachylyte-bearing Fort Foster brittle zone.

Preliminary Conclusions:

The presence of a prominent vertical planar anisotropy was found to strongly influence the style of interactive strike-slip faulting regardless of depth of development. The prominent planar anisotropy enhances the development of the distinctive slab-duplexes of the Fort Foster and York Cliffs fault structures. Extensional "horsetail" fracture arrays as relays or termination structures are uneffected by a controlling planar anisotropy but appear to be suppressed at depths approaching the brittle-ductile transition. The likely presence of strongly mylonitic host rocks near the base of the seismogenic zone (as a vertical planar anisotropy for strike-slip fault structures) suggests that the pseudotachylyte-bearing slab-duplex structures would be a likely kinematic pattern for rupture during earthquake generation. The en echelon surface geometry of active strike-slip fault zones may converge at depth to overlapping zone-parallel slab-duplex configurations upon reactivation of the ductile fault fabrics. Current earthquake source zone models as segmented colinear slip zones would be more accurately described in terms of an en echelon slip zone model modified for significant overlap.

References:

Swanson, M.T., 1987, Strike-slip duplex structures in vertical anisotropic rocks, Geol. Soc. Amer., Abstr. with Prog., V. 19, p.

Swanson, M.T., 1986, Shear fracture geometry of pseudotachylyte generation zones and the internal structure of brittle seismic fault structures, U.S. Geol. Surv., Open-File Report, 86-31, p.450-454.

Swanson, M.T., 1986, The internal structure of the Fort Foster Brittle Zone: Rupture geometry of an earthquake focus at Gerrish Island, Maine, Geol. Soc. Amer., Abstr. with Prog., V. 18, p. 767.

EXPERIMENTS ON ROCK FRICTION CONSTITUTIVE LAWS APPLIED TO EARTHQUAKE INSTABILITY ANALYSIS

USGS Contract 14-08-0001-G-1364

Terry E. Tullis
John D. Weeks
Department of Geological Sciences
Brown University
Providence, Rhode Island 02912
(401) 863-3829

Investigations

1. We have discovered that the magnitudes of the constitutive parameters measured to date in our rotary shear machine need to be corrected somewhat because our current sliding jacket assembly shows a small, but significant, positive velocity dependence.

2. We have measured constitutive parameters of artificial layers of granite gouge and find that even after correcting for the positive depencence of the jacket assembly, the steady-state velocity dependence of the gouge is positive (velocity strengthening) at most velocities studied.

3. We have extended our numerical study of temporal and spatial variations in strain and displacement associated with the model earthquake cycle of Tse and Rice (1986) to include more cases and find that the magnitude of predicted premonitory signals that might be used in a field program of earthquake prediction depends sensitively on the constitutive paramcters used.

Results

1. We are conducting a series of calibration tests to measure the contribution of the high pressure sliding jackets to the frictional strength measured in our high gas-pressure rotary shear apparatus. Our gas-tight jackets are made of Teflon and steel rings and greased O-rings (Fig. 1); resistance to slip on the various jacket interfaces contributes to the apparent sliding resistance of the rock sample, and to the velocity dependence of that resistance. Calibration tests are performed with polished steel samples separated by a thin layer of Teflon, both with and without jackets, and at a variety of confining pressures and normal stresses. Subtracting the contribution from the steel/Teflon sample gives values for the jacket alone (Fig. 2). This data can then be used to correct our data for the friction of rocks (see below). Our preliminary results show that without confining pressure, the jackets have an unmeasureably low strength, but that in the range of 20 to 60 MPa confining pressure, at which most of our rock experiments have been performed, the jacket strength is small but significant, measuring 1.0 to 1.5 MPa (referred to the area of the sample) in the velocity range of 0.1 to 32. mm/sec.; this strength is nearly independent of confining pressure in this pressure range. The velocity dependence of the jacket resistance is positive, and is in the range 0.07 to 0.13 MPa per e-fold increase in slip rate. We are exploring ways of reducing the magnitude of the jacket resistance.

2. We have used these preliminary results on jacket strength to correct friction data for experiments on Westerly granite both with and without a layer of crushed "gouge." For the confining pressures used in those experiments (20 to 75 MPa) the correction for jacket strength amounts to only a 2 to 3% reduction in the measured resistance; however, the correction for the velocity dependence of friction is large. Figure 3a shows uncorrected data for the velocity dependence for sliding of granite separated by a 1 mm layer of "gouge," including the contribution from the jacket friction. The values of **a-b** (the change in coefficient of friction per e-fold change in slip rate) were measured by stepping between the velocities indicated; here, **a-b** depends upon velocity, such that the gouge is more velocity strengthening at higher velocity. Figure 3b shows the same gouge data corrected for the jacket friction. The correction has reduced the values of **a-b**, and has reduced the dependence of **a-b** upon velocity. However, it has not changed the conclusions to be drawn from the data: the velocity dependence of the gouge friction is positive, and lessens with large slip displacement. Data for the velocity dependence of initially bare granite surfaces was published by Tullis and Weeks (1986) without cor-

rection for the jacket resistence. They reported values of **a-b** in the range −0.0015 to −0.003 (velocity weakening) for slip velocities of from 0.01 to 10 mm/sec. Eliminating the contribution from the jacket friction changes the range of values of **a-b** to −0.002 to −0.005.

3. We have continued our study of the temporal variation in the strains and displacements that occur in realistic fault models, paying particular attention to how such information might be useful to earthquake prediction programs, such as showing the best locations for deployment of instruments to monitor precursory geodetic signals. We have based our work on the model by Tse and Rice (1986) of the mechanical behavior of a crustal strike-slip fault undergoing an earthquake cycle. This model is particularly useful because it employs a rate- and state- dependent friction constitutive law that describes laboratory friction results very well, and it reproduces many features of the slip behavior of the San Andreas fault. We have studied the sensitivity of the geodetic predictions of this model to changes in the values of the friction constitutive parameters L and **a**−**b** and in the amount of dynamic overshoot during the earthquake. Simulations of the earthquake cycle were examined with several values of L, ranging from 5 to 80 mm, with near-surface values of **a**−**b** of −0.0015 and −0.003, and with either zero or 30% dynamic overshoot. Previously, Tullis (1987a, 1988) studied the case with L=40 mm, **a**−**b** = −0.003, and no dynamic overshoot. We find that the model predictions are strongly affected by changes in L and **a**−**b**, and only slightly affected by the amount of dynamic overshoot. Generally, measurements made near the focal depth are more informative than those made at the surface and, for surface measurements, those made 3-5 km away from the fault are more useful than those made 1-500 m away from the fault. Keeping **a**−**b** constant (−0.003) and varying L, we find that for surface measurements 3-5 km from the fault, sharp increases in velocity that would be detectable with a two-color laser occur 1 week to 1 month before the earthquake for all values of L≥20 mm. The time interval of warning depends on the value of L; the velocity begins to increase sharply much earlier for the larger values of L than for the smaller values. This trend is illustrated in Fig. 4, which shows velocity at the surface, 500 m away from the fault plotted versus log time until the next earthquake for a range of values of L. The sharp increase in velocity would be detectable 1 m from the fault using a creepmeter if L≥60 mm; it would occur about 1 month before the earthquake if L = 80 mm, and about 6 days before the earthquake if L = 60 mm. In addition, near-field surface and depth measurements of velocity appear to be equally useful if L≥60 mm, and far-field surface measurements are as good as near-field depth measurements, for L≥20 mm. This observation is encouraging for earthquake prediction, because of the great difficulty associated with measuring displacement at depth (compared to the surface), but it is only true for sufficiently large ratios of L/(**b**−**a**). Strain changes at the surface are smaller than at depth and are at or below ambient noise levels except possibly for L≥60 mm. These conclusions are only valid for a fault with no along-strike variation in its behavior. For the more realistic situation in which the instability initiates over a laterally and vertically limited patch, rather than a vertically limited strip, we expect the signals at the surface to be smaller if all other parameters are held constant. The sensitivity of the model predictions to the values of L and **a**−**b** places strong emphasis on the necessity of accurately determining the value of these parameters for natural faults.

Reports

Blanpied, M.L., T.E. Tullis, and J.D. Weeks (1987), *Frictional behavior of granite at low and high sliding velocities*, Geophys. Res. Lett., *14*, 554–557.

Lorenzetti, E. A., M. L. Blanpied, J. D. Weeks, and T. E. Tullis, *Velocity dependence of quartz frictional behavior*, Eos, Trans. AGU, *68*, 405.

Tullis, T. E. (1987a) *Rock friction constitutive behavior from laboratory experiments and its implications for an earthquake prediction field monitoring program*, in *Proceedings of USGS Conference on Physical and Observational Basis for Intermediate-Term Earthquake Prediction*, Open-File Report (U.S. Geol. Surv. National Earthquake Hazards Reduction Program) (in press).

Tullis, T.E. (1987b), *Micromechanics of frictional resistance of calcite*, Eos, Trans. AGU *68*, 405.

Tullis, T. E. (1988) *Rock friction constitutive behavior from laboratory experiments and its implications for an earthquake prediction field monitoring program*, Pure Appl. Geophys., *126*, no. 2–4 (Special Issue on Intermediate-Term Earthquake Prediction) (in press).

Yund, R. A., T. E. Tullis, J. D. Weeks, and M. L. Blanpied, *Microstructures in experimental fault gouges*, Eos Trans. AGU, *68*, 405.

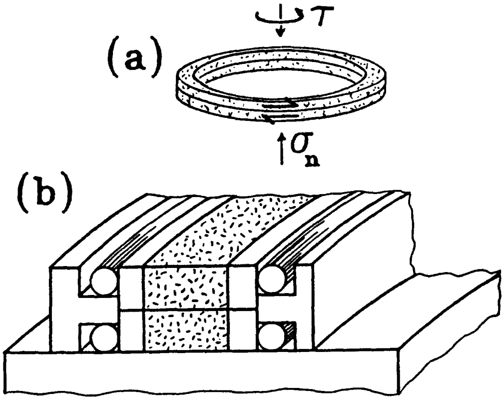

Figure 1. Sample and one of two jacketing geometries used in the high pressure rotary apparatus.
a) the samples alone (for the calibration tests, rock is replaced by steel and teflon).
b) a cutaway of a high pressure jacket, made of teflon rings, O–rings, and steel retainer rings. Friction on sliding interfaces in the jacket contributes to the measured resistance.

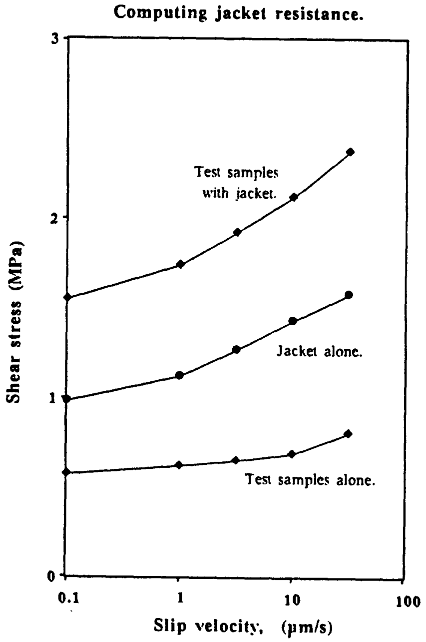

Figure 2. Method of determining the jacket resistance. It is found by subtracting the resistance of the steel/teflon samples measured alone from the total resistance of the samples and jacket. The jacket resistance, and the velocity dependence of that resistance, varies with slip velocity.

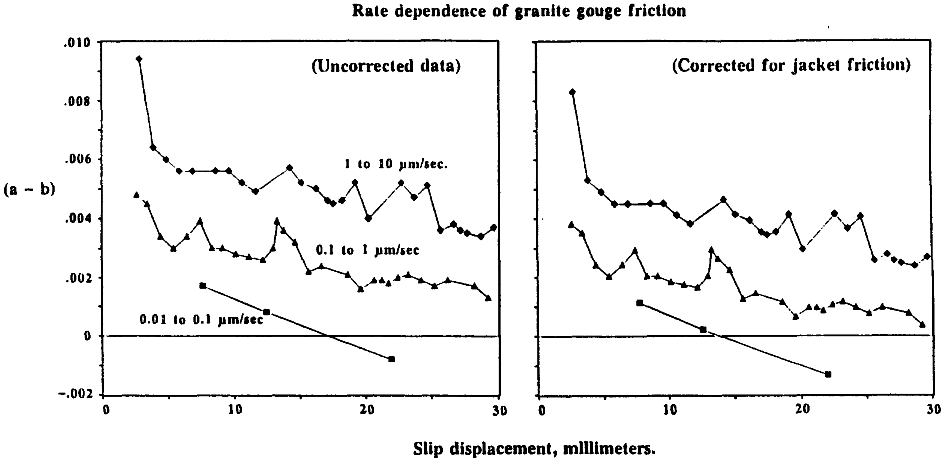

Figure 3. Rate dependence of friction of granite gouge, before and after correction for jacket resistance, for the first portion of a sliding experiment at 75 MPa normal stress. a) the data before jacket correction. b) the data after jacket correction. The correction does not change the two conclusions: first, that the gouge is velocity strengthening, with higher velocity dependence, **a** - **b**, at higher slip velocity; and second, that the velocity dependence becomes less positive with large slip displacement.

Fig. 4. Velocities at the surface 500 m away from the fault, plotted versus log time until the next earthquake, for several values of L. Detectability limit is calculated for a two-color laser, 1.4 km long line (45° angle to fault, 500 m from fault trace on both sides); velocities above this limit will be detectable. Note that the velocity begins to increase sharply much sooner for large values of L than for small values of L.

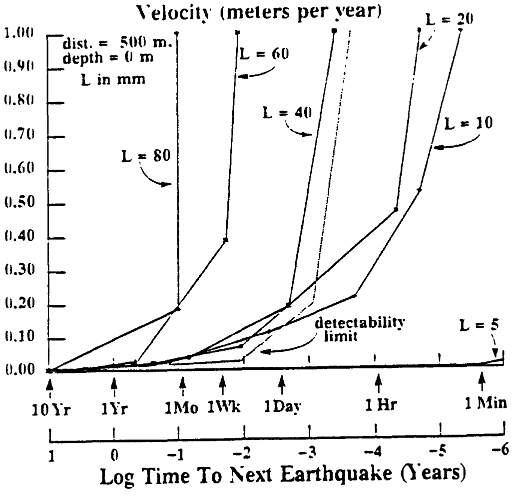

Earthquake Fault Shape and Slip Pattern from Inversion of Geodetic Data

14-08-0001-G1383

Steven N. Ward and Sergio E. Barrientos

C. F. Richter Seismological Laboratory
Earth Sciences Board
University of California
Santa Cruz, CA 95064
(408) 429-2480

INTRODUCTION. The great Chilean earthquake of May 22, 1960 is one of the largest events ever recorded [*Kanamori*, 1977]. Vertical and horizontal tectonic deformation was observed over an area 200 km wide and about 1000 km long, from the city of Concepción in the north to the trench-rise-trench triple junction nearby Taitao Peninsula in the south (Figure 1) [*Plafker* and *Savage*, 1970]. Previous large earthquakes in the northern end (Concepción) of the region occurred in 1570, 1575, 1751, and 1835. In the central-southern (Valdivia–Chiloé) segment, events with magnitude greater than 7.5 occurred in 1575, 1737, and 1837 [*Lomnitz*, 1970]. For the 1835–1837 sequence there is evidence of significant vertical displacements. According to Darwin [1851, p.29-30], uplift between 2.4–2.7 m were observed at Isla Mocha, Concepción, and Isla Lemus. It is clear that uplifting has been occurring over long periods of time. Terraces developed in the Quaternary can be observed in Hueicolla, Mehuín, Corral [*Fuenzalida et al.*, 1965], Arauco Peninsula and Isla Santa María [*Kaizuka et al.*, 1973]. Uplifts are apparently occurring in the present day as well. Tide gage measurements recorded from 1965 to 1970 indicate that Puerto Montt is elevating at a rate of 30 mm/yr [*Wyss*, 1978].

This information suggests that the region affected by the 1960 earthquake is subjected to continuous significant vertical displacements. In this context, our goal is to determine the slip pattern on the fault associated with the 1960 event and incorporate our results into the deformation cycle associated with subduction.

DATA. Figure 1 shows aftershocks with magnitude greater than 6 (hexagons) and minor aftershocks (triangles) determined by ISC during eight years after the main event. Seismicity is concentrated in the Mocha Block at the northern end of the 1960 rupture. The epicenter of the main shock is not precisely located because a large foreshock occurred few minutes before the main event. *Kanamori* and *Cipar*, [1974] estimated the seismic moment of the 1960 event to be 2.7×10^{30} dyne cm with an average dislocation of 24 m using a Pasadena long-period strain seismogram. *Kanamori* [1977] estimated the moment to be 2.0×10^{30} dyne cm.

Plafker and *Savage* [1970] provided detailed descriptions of the sea level changes at more than 150 localities in the region affected by the 1960 earthquake. These measurements, which were observed eight years after the event, range from 5.7 m of uplift in Guamblin Island to 2.7 m of subsidence in the city of Valdivia. The sea level data is augmented by a leveling line that runs from the city of Los Angeles to Puerto Montt (north–south orientation) which was surveyed prior to (1959) and after (1963-1964) the 1960 event. The data distribution is shown in Figure 2. In addition to the data collection, *Plafker* and *Savage* [1970] analyzed the static deformation of the 1960 event and presented some teleseismic evidence to support their preferred uniform slip solution that involves between 20 and 40 m of dip slip on a fault 1000 km long and at least 60 km wide.

VARIABLE SLIP MODEL. The method to be used to recover the slip distribution of the 1960 event has been previously described in detail by *Ward* and *Barrientos*, [1986]. This technique is based on the construction of spatially finite dislocations by superposition of elemental point sources uniformly distributed over the fault plane. In the searching procedure, we provide the dip and slip (rake) angles, location of the plane, and the strike of the fault trace, and then invert for the slip that best satisfies the observations. Since the surface trace of the fault cannot be recognized, we assume that the Peru–Chile trench corresponds to the updip projection of the rupture plane. This assumption fixes the strike of the fault plane to N7°E. The rake was assumed to be consistent with the long term slip direction (100° $\sim$ 105°)of the Nazca plate relative to the South American plate predicted by the RM2 plate model of *Minster* and *Jordan* [1978]. Imposing a planar dislocation with variable slip over an area much larger than the expected region of faulting, we searched values of dip angle from 5° to 35° and selected the one which minimized the sum square of residuals.

The variable slip model (Figure 3) indicates that most of the moment release was concentrated in a 800 km long narrow band parallel to the coast located offshore east of the trench. The region of maximum slip (> 15 m) varies in width from 100 km in the north to 50 km in the southern extreme. At the northern end of the rupture (36°S– 38°S) there appears to be an independent patch of slip weakly connected to the main region of moment release. The total moment of this model is 1.0×10^{30} dyne cm, one half of the estimated seismic moment. The down–dip region of slip (> 5 m) between 42°S and 44°S is responsible for the observed inland uplift at those latitudes.

The model fit can be observed in Figure 4*a* along four profiles perpendicular to the trench and in Figure 4*b* two profiles parallel to the trench.

Figure 5 compares two models, with and without the down–dip region of slip (> 5 m) between 42°S and 44°S. This experiment suggests that if the down–dip patch of slip is postseismic (0 to 8 years after the event), it would have caused an uplift at the tide gage of Puerto Montt of the order of 70 cm, and propagated at velocity of 25 km/yr (minimum bound). Independent estimates of uplift during 1965 and 1970 [*Wyss*, 1976] indicate a nearly constant uplift rate of 3 cm/yr for the tide gage at Puerto Montt. Future examination of the uplift beyond 1970 (up to 1986) will determine if the rate is decreasing with time. If so, we believe this would make an excellent case for down–dip postseismic creep or slip growing in place.

Another interesting aspect of the slip distribution is the close association of regions of maximum slip with the segmentation of the Nazca plate. Figure 6 shows the slip distribution projected on the map containing the fracture zones. The Valdivia and Guafo fractures are two major tectonic elements in the subducting Nazca plate. The four fracture zones seem to act as boundaries between areas of concentrated coseismic slip. This implies that more interseismic slip occurs close to fracture zones during the interseismic period, if we accept uniform subduction rates averaged over the earthquake cycle for the plate as a whole.

References

Kelleher, J., Rupture zones of large Southamerican earthquakes and some predictions. *J. Geophys. Res., 77*; 2087–2103, 1972.

Lay, T., H. Kanamori, and L. Ruff, The asperity model and the nature of large subduction zone earthquakes. *Earthquake Pred. Res., 1*; 3–71, 1982.

Lomnitz, C. Major earthquakes and tsunamis in Chile during the period 1535 to 1953. *Geolog. Rundschau, 59*, 938–960, 1970.

Minster, J. B., and T. H. Jordan, Present–day plate motions. *J. Geophys. Res., 83*; 5331-5334, 1978.

Nishenko, S., Seismic potential for large and great interplate earthquakes along the Chilean and Southern Peruvian margins of South America: A quantitative reappraisal. *J. Geophys. Res., 90*; 3589–3615, 1985.

Plafker, G. and J. C. Savage, Mechanism of the Chilean earthquakes of May 21 and 22, 1960. *Geol. Soc. Am. Bull., 81*, 1001–1030, 1970.

Ruff, L. J., Fault asperities inferred from seismic body waves. In H. Kanamori and E. Boschi (Editors). Earthquakes: Observation, Theory and Interpretation. *Proc. of the International School of Physiscs "Enrico Fermi"* , Varenna, Italy, 1982.

Ward, S. N., and S. E. Barrientos, An inversion for slip distribution and fault shape from geodetic observations of the 1983, Borah Peak, Idaho, earthquake. *J. Gephys. Res., 91*; 4909–4919, 1986.

Wyss, M., Local changes of sea level before large earthquakes in South America. *Bull. Seis. Soc. Am., 66*, 903–914, 1976.

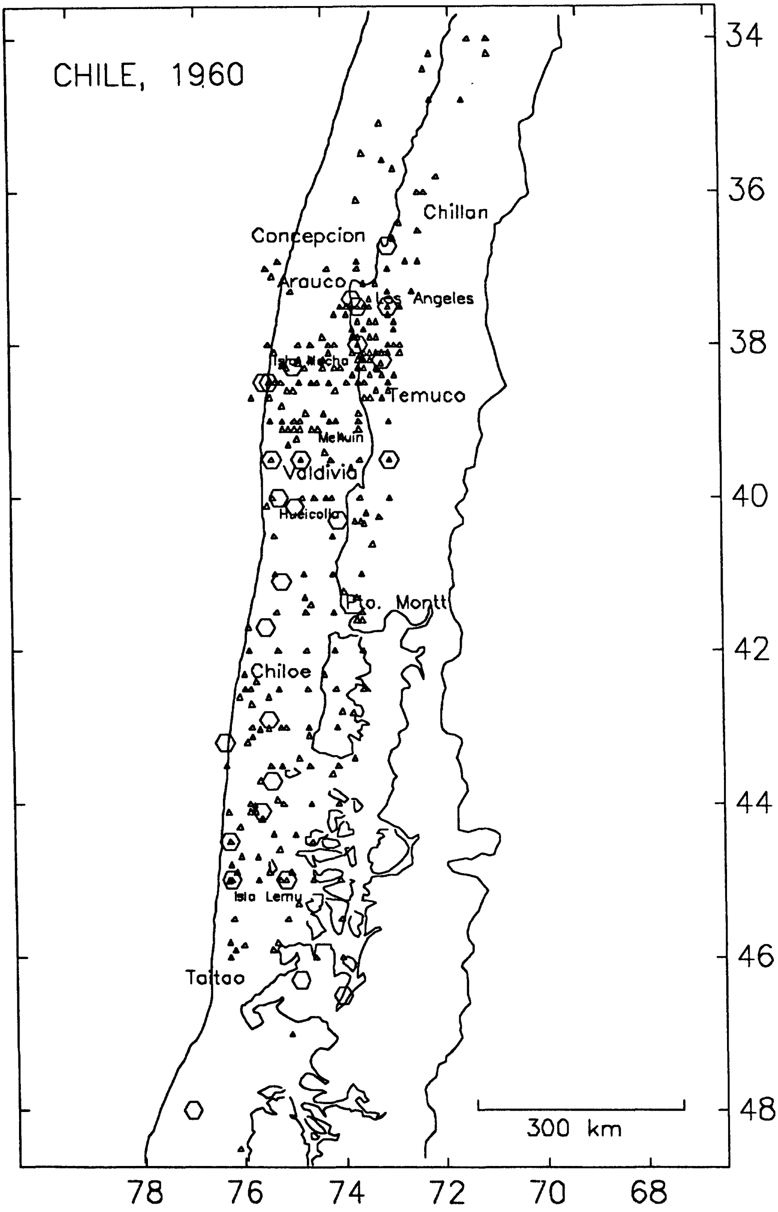

Fig. 1. Site of the 1960 great southern Chile earthquake. Vertical deformation extended from the city of Concepción in the north to the Taitao Peninsula in the south. The hexagons and triangles correspond to aftershocks with magnitudes greater and less than 6.0 respectively. Epicenters and magnitudes taken from the ISC catalog. Aftershock activity is almost completely restricted to the region offshore east of the trench.

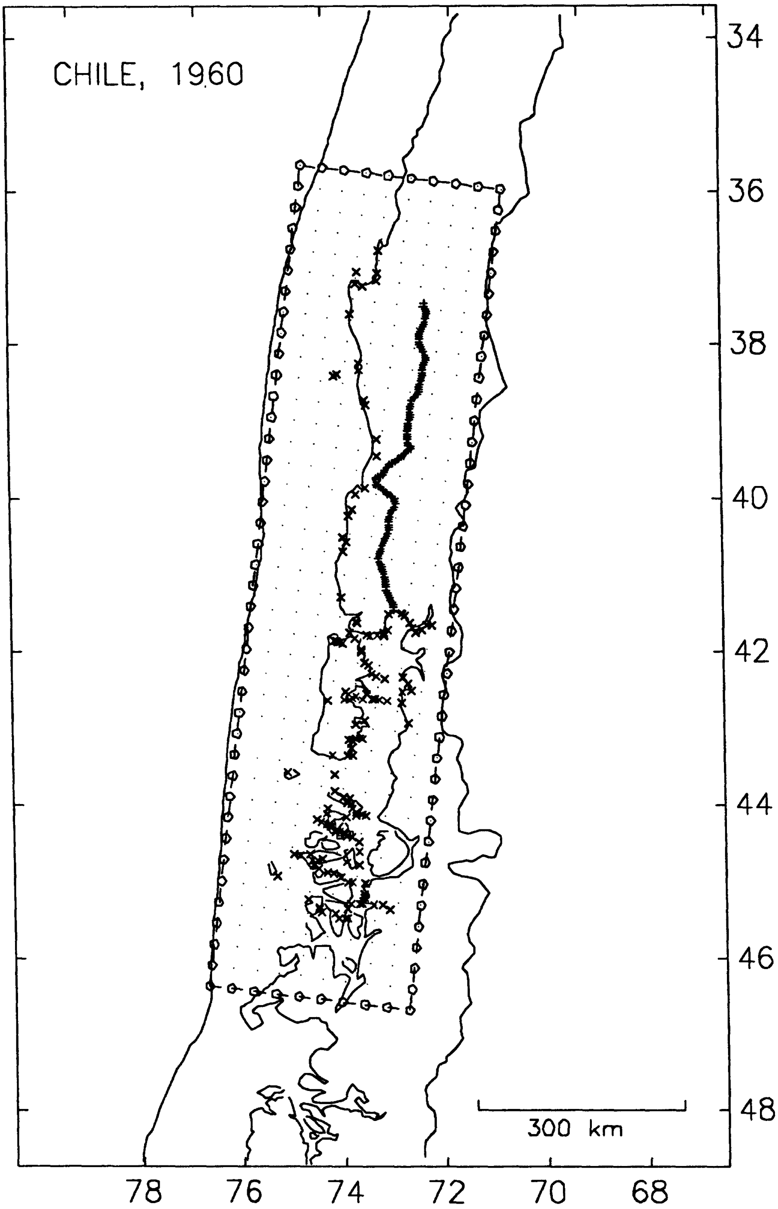

Fig. 2. Observations of vertical elevation change. Vertical crosses are leveling line obervations surveyed in 1959 and in 1963-1964. Diagonal crosses are estimated sea level changes observed in 1968. The rectangle shows the distribution of point sources used in the slip inversion.

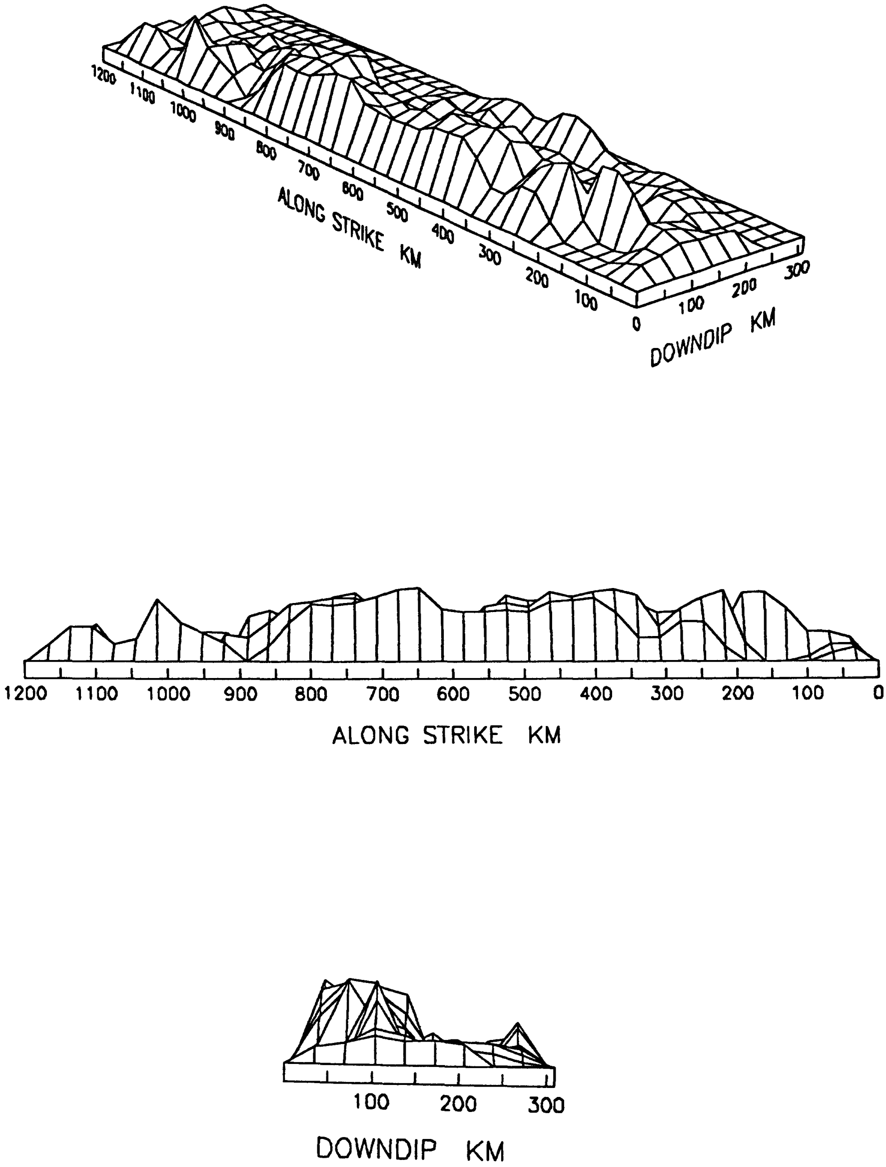

Fig. 3. Three different views of the slip distribution of the 1960 event in southern Chile. The maximum slip is 24 m. Most of the slip is concentrated from the trench down–dip up to 150 km. In the northern segment (900 km to 1200 in the along strike panel) there seems to be independent patches of slip. The same situation occurs in the down–dip figure (250–300 km).

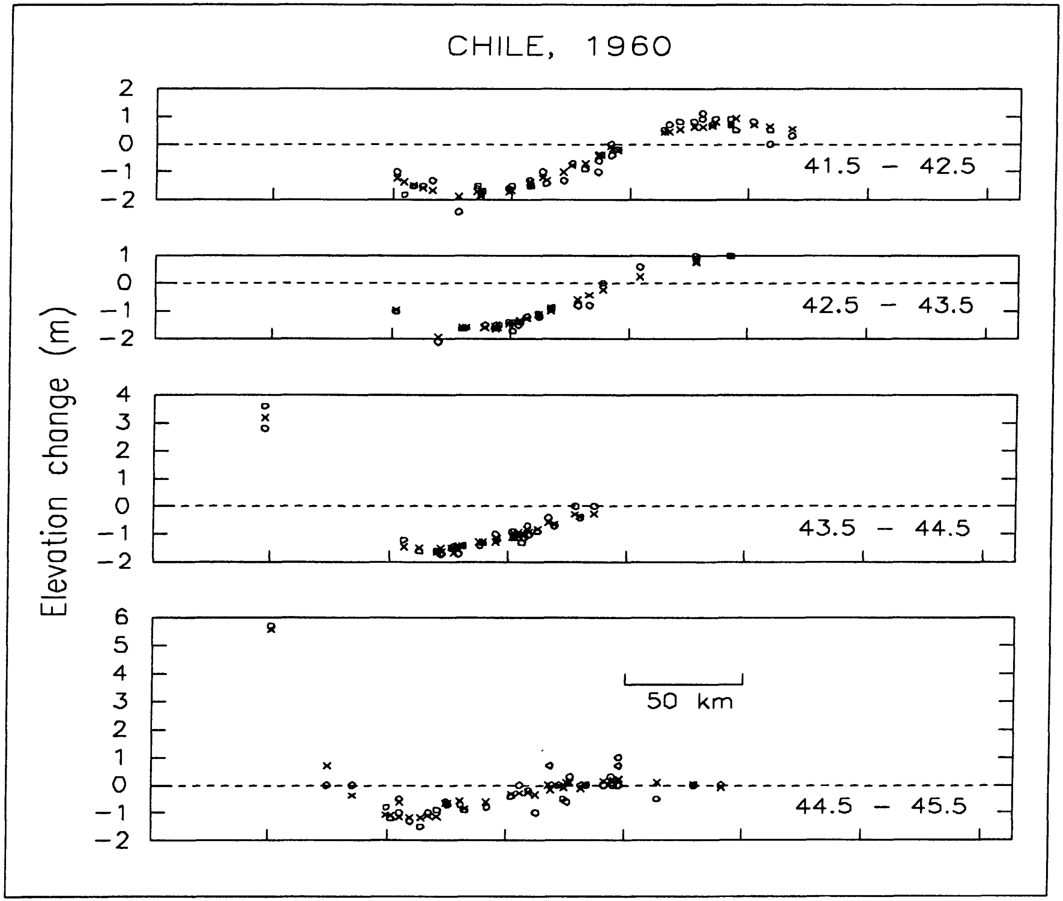

Fig. 4. Model fit. *4a* shows four profiles perpendicular to the trench. Circles are observations and crosses are elevation changes predicted by the model. *4b* shows two profiles parallel to the trench, along the coast and along the leveling line.

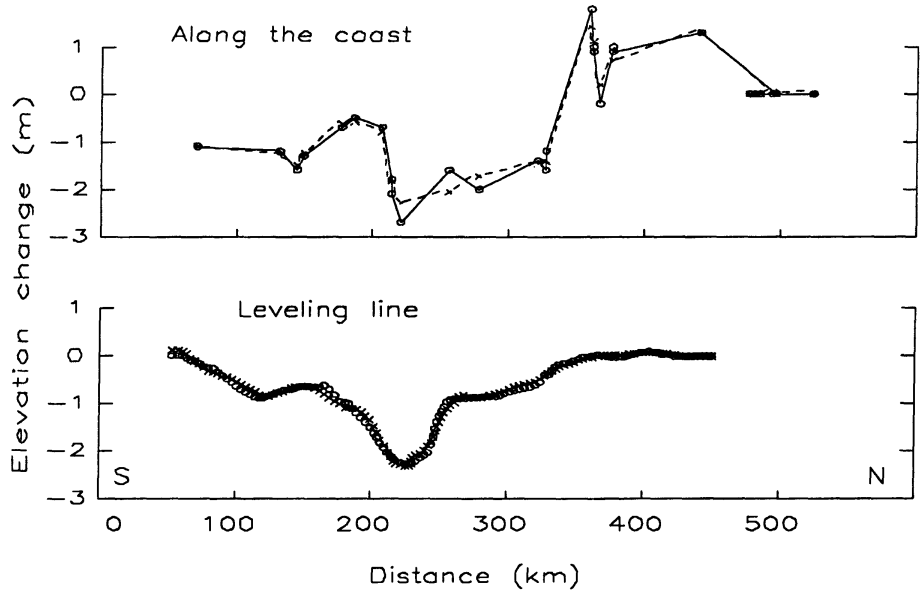
Along the coast
Leveling line
Elevation change (m)
1
0
−1
−2
−3
S
N
0
100
200
300
400
500
Distance (km)

Fig. 4b

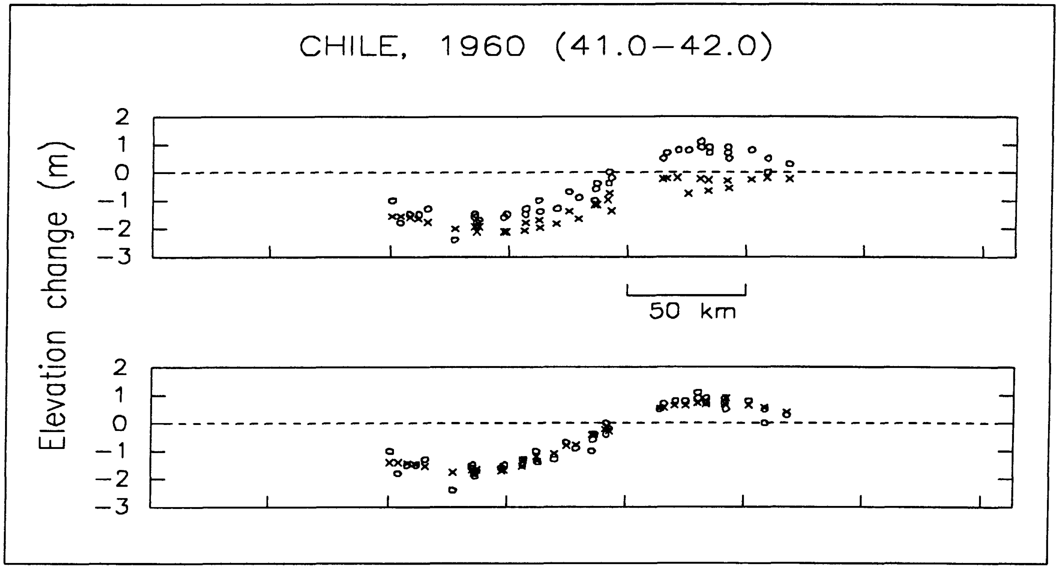

Fig. 5. Comparison of two models. Bottom represents the model fit for those observations between 41° – 41°S (circles are observations and crosses are predicted values). The top panel shows the effect of removing the down–dip slip patch between 41° – 43°S. An arrow marks the expected value at the tide gage in Puerto Montt.

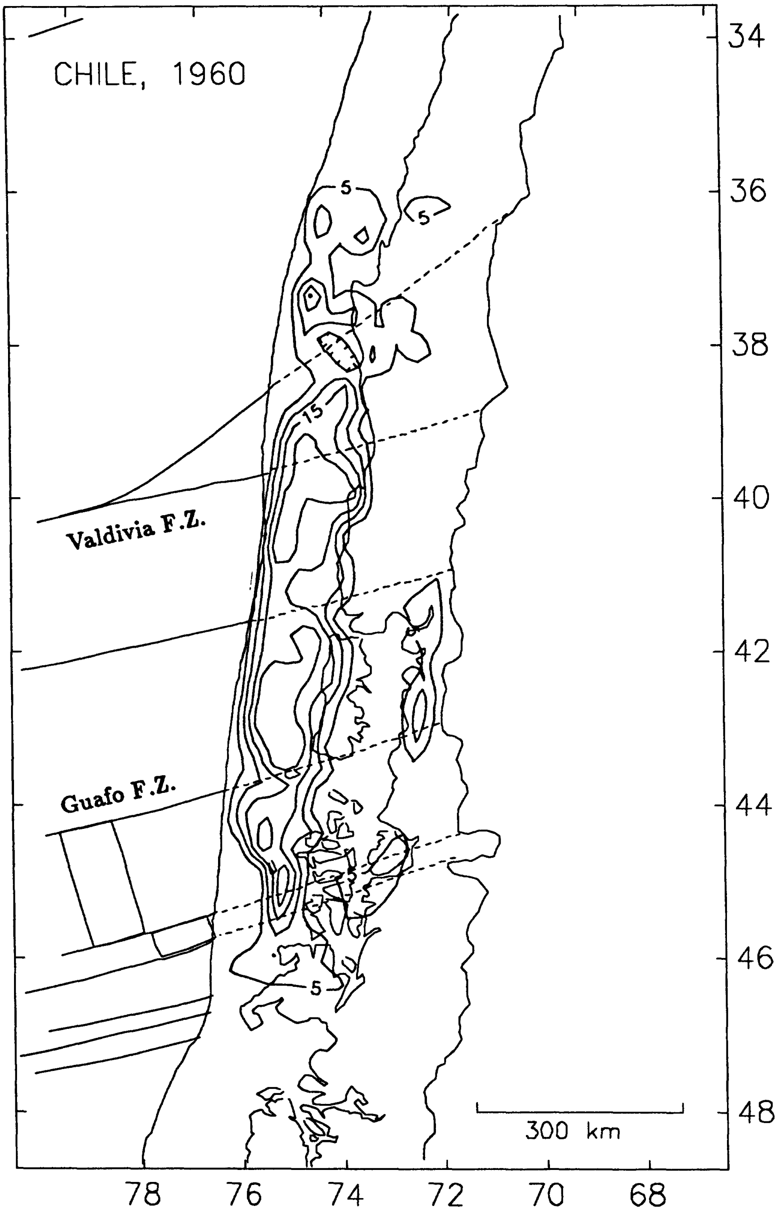

Fig. 6. Slip distribution of the 1960 event projected on a map view with the fracture zones. Most of the slip is located offshore east of the trench. All fracture zones except for the Valdivia F.Z. seem to act as regions of relative low slip.

Deep Hole Desalinization of the Dolores River

9920-03464

William Spence
National Earthquake Information Center
U.S. Geological Survey
Denver Federal Center
Box 25046, Mail Stop 967
Denver, Colorado 80225
(303) 236-1506

Investigations

This project relates to monitoring the seismicity of the region of the intersection of the Delores River and Paradox Valley, southwest Colorado. The project is a component of the Paradox Valley Unit of the Colorado River Basin Salinity Control Project and is being performed for the U.S. Bureau of Reclamation with support from the Induced Seismicity Program of the U.S. Geological Survey. In this desalinization project, it is proposed to pump approximately 30,000 barrels/day from brine-saturated rocks beneath the Dolores River through a now completed borehole to the Madison-Leadville limestone formation of Mississippian age, some 15,000 feet below the surface. There is a possibility of seismicity being induced by this desalinization procedure, especially in the long term. The project objectives are to establish a pre-pumping seismicity baseline and, during the pumping phase, to closely monitor the discharge zone for possible induced seismicity. If induced seismicity does occur, it should be possible to relate it to formation characteristics and to the pumping pressure and discharge rates.

Results

A 10-station seismograph network is centered at the location of the proposed injection well. This high-gain network has a diameter of about 80 kilometers, and has been in operation since September 1983. Seismic data are brought to Golden, Colorado, via microwave and phone line transmission. These data are fed through an A/D converter and then through an event detection algorithm. The network has operated at high quality, except for two periods when it was decommissioned by lighting strikes. Analysis procedures have been considerably complicated by a high rate of blasting activity in the region, but means have been developed to distinguish the occurrence of natural earthquakes to good reliability.

Notable regional earthquake activity are a swarm of shallow events (maximum magnitude 3.2) near Carbondale, Colorado, a similar swarm near Crested Butte, Colorado, a magnitude 3.4 shallow earthquake near Blue Mesa Reservoir, Colorado, and a magnitude 2.8 earthquake that was preceded by three events and followed by four events all located about 25 km SE of Grand Junction, Colorado. In the vicinity of the network, the earthquake catalog is complete to about magnitude 2.0, but very few earthquakes have occurred in the immediate vicinity of the proposed injection well. Most of the seismicity in the area of the network is in the shallow crust. However, of the 222 earthquakes located for the period January 1, 1984-June 30, 1987, 46 are in the depth range 10-20 km and 16 earthquakes are deeper than 20 km, with several events in the depth range 30-55 km. These results, shown in figure 1, indicate that microearthquakes are distributed throughout the crust of the Colorado Plateau, with occasional events in the upper mantle. The shallow and deeper earthquakes follow a diffuse north-south trend, parallel to the eastern boundary of the Colorado Plateau. These results, combined with a lack of historical seismicity at the zone of the Paradox Valley seismic network, indicate that any seismicity induced by deep-well injection near Paradox Valley should be identifiable as such.

Report

Spence, W., and Chang, P-S., 1987, Seismic monitoring in the region of the Paradox Valley, Colorado--Annual Report, July 1986-June 1987: U.S. Bureau of Reclamation, Deep Well Injection Site, Paradox Valley Unit, Colorado River Basin Salinity Control Project, 14 p.

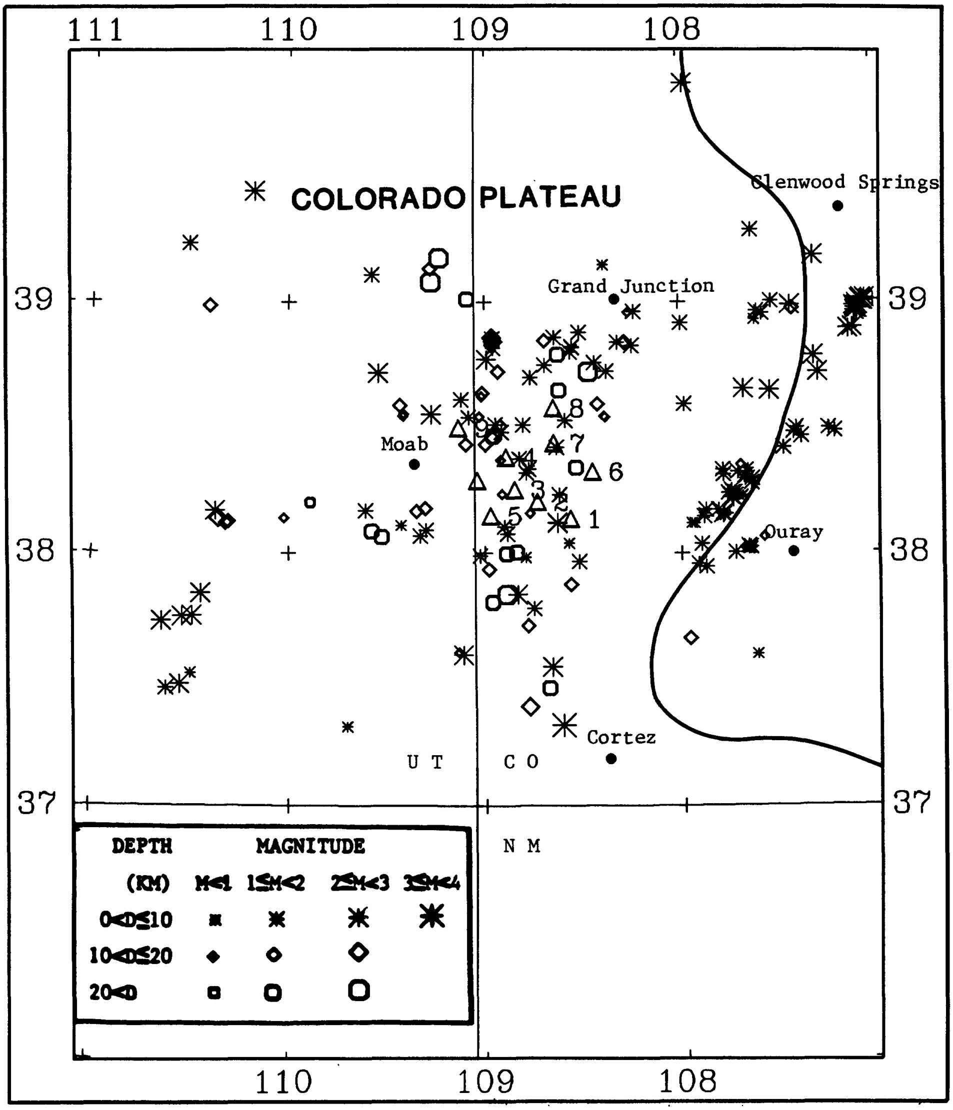

Figure 1.--Hypocenters of earthquakes located using data of the Dolores River/Paradox Valley seismographic network, January 1, 1984-June 30, 1987. There is a concentration of shallow earthquakes that spans the eastern boundary of the Colorado Plateau, whereas many earthquakes deeper than 20 km are within the Colorado Plateau. Seismograph locations are indicated by numbered triangles.

Regional and National Seismic Hazard and Risk Assessment

9950-01207

S. T. Algermissen
Branch of Geologic Risk Assessment
U.S. Geological Survey
Denver Federal Center, MS 966
Denver, CO 80225
(303) 236-1611

Investigations

1. Investigations of the regional attenuation of Modified Mercalli intensity with distance for historical earthquakes of Utah continued and a prliminary attenuation relation applied to the hypothetical occurrence of a magnitude 7.5 earthquake at six different locations along the Wasatch Front. Preliminary maps of expected MMI effects in the cities of Salt Lake City, Ogden, and Provo have been prepared.

2. Assessment of Modified Mercalli intensities in Seattle, Washington resulting from the April 29, 1965 and the April 13, 1949 earthquakes on a block-by-block basis is continuing.

3. Mark-sense forms for a portable, microcomputer-based system for rapid field collection and evaluation of post-earthquake damage data have been completed. Questions regarding earthquake damage on the mark-sense forms are keyed specifically to building classifications 1 through 5 of the Insurance Services Office structural classification system. The field system was fully tested following the October 1, 1987 Whittier Narrows, California earthquake. The system will make possible rapid estimation of percent damage and loss to structures within a building classification framework.

4. Revisions and updating of the main computer program for seismic hazard analysis, Seisrisk II, have been completed and documented in USGS Bulletin 1772. The revisions formally introduce the third generation, Seisrisk III, of computer processing for USGS ground-motion and regional liquifaction hazard mapping efforts. Enhancement of seismotectonic modeling capabilities is continuing.

5. Research is continuing on a variety of aspects of probabilistic ground motion hazard estimation. Effects of observational errors in relating magnitude scales and fitting the Gutenberg-Richter parameter β have been analyzed and results summarized in a paper in the BSSA. Effects of minimum magnitude and attenuation uncertainty on seismic hazard calculations are also being investigated. Consequences of alternative source zone configurations on ground motion values having a 1 in 500 annual excedance probability for the east coast have been investigated and the re-

sults published in Earthquake Spectra.

6. Maps of probabilistic estimates of maximum acceleration and velocity in rock in the contiguous United States having a 90 percent probability of not being exceeded in 50 and 250 years (Open-File Report 82-1033) have been updated using variability $log_e\sigma = 0.62$ for attenuation and $log_{10}\sigma = 0.52$ in fault length-magnitude for the ground motion estimates. The maps are being submitted to the Building Seismic Safety Council under the National Earthquake Hazards Reduction Program to aid the development of new national seismic resistant design proceedures for buildings and will be released as a set of Miscellanious Field Investigations maps.

Results

1. The best statistical fit to Modified Mercalli intensity vs distance for historical earthquake data of Utah is given by the equation $x = 17.76(I_o + 1)^{1.46}$. Although data from 10 historical earthquakes was used to derive the relationship, the large amount of intensity information from the 1934, Hansel Valley earthquake dominates the data set. A conversion from M_L magnitude to intensity is give by $I_o = 0.61 + 1.09M_L$ as determined from all I_o, M_L pairs in the Utah earthquake catalog. Applying these relations to hypothetical locations of an $M_L = 7.5$ earthquake along the Wasatch Front near the cities of Provo, Salt Lake City, and Ogden results in intensities of IX+ in the epicentral areas with the the distant cities experiencing intensity effects of VI+.

2. Detailed assessment of the Modified Mercalli intensity in the cities of Seattle and Olympia, Washington will allow assessment of the correlation between observed earthquake damage and measured, instrumental site-response from field studies that are to be completed in the near future. The relation between ground failure effects from the 1965 and 1949 earthquakes and intensity level has been summarized in a USGS Bulletin that is currently under revision following internal review.

3. The microcomputer-based damage survey system permits damage data to be rapidly entered from standardized forms using an optical scanner. Following the Insurance Services Office (ISO) structural classification system, mark-sense forms for standardized field collection of damage data have been completed for wood frame buildings (Class 1), All-Metal Buildings (Class 2), Steel Frame Buildings (Class 3), Reinforced Concrete Buildings (Class 4), and Concrete, Brick or Block Buildings (Class 5). Structural subdivisions of the primary building types within the ISO classification system are also accomodated by the mark-sense forms. The field system was fully implemented following the October 1, 1987 Whittier Narrows, California earthquake to assess planned proceedures and field operations. Field proceedures fit well with the routine of conducting a post-earthquake Modified Mercalli intensity (MMI) survey, although considerably more attention is required to the details and age of building construction. Within the relatively small area of greatest damage (MMI=VIII, northwest Whittier), the systematic documentation of building damage was organized by census tract so as to fully utilize Bureau of Census data in future loss estimates. Throughout a large area of relatively lower damage (generally MMI=VI through MMI=VII), a random sample of census tracts were documented, as well as the locations of maximum damage for the MMI assignment. A

detailed analysis of the collected damage data is currently underway.

4. Seisrisk III is a revision of Seisrisk II that was described previously in Open-File Report 82-293. Seisrisk II and Seisrisk III were designed to compute maximum ground-motion levels that have a specified probability of not being exceeded during fixed time periods at each of a set of sites uniformly spaced on a two-dimensional grid. Seisrisk II assumes that seismicity within a seismic source zone is uniform; that is, each point within a source zone has the same probability of being the epicenter of a future earthquake. This assumption means that the projected rate of earthquakes changes abruptly at a source zone boundary; an effect of such a change in seismicity is that calculated probabilistic ground-motion levels may differ substantially at sites a few kilometers apart near a boundary. Seisrisk III allows earthquakes within a source zone to be normally rather than uniformily distributed. The result is that calculated acceleration levels vary more smoothly at sites near zone boundaries. In modeling fault ruptures, Seisrisk III treats the closest-distance ruptures as occurring over a range of magnitudes (rather than at only a descrete set of magnitudes as in Seisrisk II) resulting in smoother acceleration densities from fault ruptures. In both Seisrisk II and Seisrisk III, artificial parallel faults may be modeled to fill area source zones when specific earthquake causal faults cannot be identified through geological investigations, or when areas of similar faulting can be identified but no individual fault is favored for near-future rupture. If a series of equidistant parallel faults are input to the program, Seisrisk III performs a partial distance-smoothing to simulate a finer spacing between faults in order to better approximate a uniform distribution. Both Seisrisk II and Seisrisk III calculate probabilistic ground motions at all sites resulting from earthquakes in a single source before proceeding to the next source. This requires retaining intermediate calculations for each site to accumulate ground-motions from successive sources. Seisrisk II wrote these intermediate results onto a disk; Seisrisk III saves the results in two-dimensional arrays in memory thus increasing program effficiency. Seismotectonic modeling capabilities of Seisrisk III are continuing to be enhanced which will eventually result in the next generation of probabilistic ground-motion mapping computer code. Most recently, the capability to model dipping, planar fault ruptures has been coded and verified and is an integral part of the current on-line program.

5. Determination of a minimum magnitude to include in a hazard analysis is a nontrivial problem, and should be based on engineering criteia. For any given value of minimum magnitude (m_{min}), the calculated frequency of exceeding various levels of ground motion depends on assumptions regarding the range of accelerations that can result from various earthquakes of a given magnitude and distance from the site. Minimum magnitude has an increasing effect on hazard calculations as the assumed range of ground motion increases. If ground motions resulting from earthquakes are lognormally distributed, a small fraction of the earthquakes will produce ground motions that differ by several σ (the standard deviation, which is independent of magnitude and distance) from the median values. As σ increases, the range of ground motions for earthquakes of a given magnitude and distance increases. Earthquakes are usually assumed to occur within seismically homogeneous source zones, that is within a specific source zone, earthquakes in the range, $m_{min} \leq m \leq m_{max}$, occur randomly in space and time in accordance with a Gutenberg-Richter magnitude-

frequency relationship. Thus, the expected number of earthquakes in an interval of width Δm increases exponentially with decreasing magnitude. This means that although only a small fraction of the smaller earthquakes produce ground motions several σ greater than median values, the absolute number of such ground motion occurrences may be significant.

To account for this effect, a proceedure tapering the minimum magnitude is introduced. The proceedure includes a fraction of the earthquakes with magnitudes less than m_{min} in the calculations, such that the fraction decreases to zero as the magnitude decreases below m_{min} to some magnitude m_0. In this case, the frequency of earthquakes with magnitudes m_0 or greater would still be in accordance with a Gutenber-Richter relationship, and as before, all earthquakes with magnitudes $m_{min} \leq m \leq m_{max}$ would be included. However, now included is a fraction, f, of the earthquakes in the range $m_0 \leq m \leq m_{min}$ such that the fraction decreases from $f = 1$ at m_{min} to $f = 0$ at m_0. Although the same results can be obtained by using a probabilistic minimum magnitude, conceptually, the two approaches differ. In the probabilistic minimum magnitude, we postulate the existance of a true minimum damaging magnitude and model our uncertainty regarding what value that magnitude should assume. In the tapered minimum magnitude, we assert our belief that some, but not all, of the earthquakes at lower magnitudes could potentially be damaging and that damaging earthquakes do not terminate abruptly at some magnitude, but rather, that a decreasing fraction of the lower magnitude earthquakes is potentially damaging.

6. Incorporating statistical variability in attenuation and fault-rupture length generally increases estimated acceleration and velocity values in areas of modeled faults and areas of moderate-to-high seismic activity rates above those shown in Open-File Report 82-1033. For example, acceleration values having a 90 percent nonexceedance probability in 50 years for the New Madrid earthquake region, Charleston earthquake region of South Carolina, and the Puget Sound area of Washington, are increased 38, 10, and 20 percent, respectively, above values estimated in OF 82-1033.

Reports

Bender, Bernice, 1987, Effects of magnitude and attenuation uncertainty on seismic hazard calculations: Bulletin of the Seismological Society of America, (submitted).

Bender, Bernice, 1987, Effects of observational errors in relating magnitude scales and fitting the Gutenberg-Richter parameter β: Bulletin of the Seismological Society of America, v.77, p. 1400--1428.

Bender, Bernice, and Perkins, D.M., 1987, Seisrisk III: A computer program for seismic hazard estimation: U.S. Geological Survey Bulletin 1772, 48 p.

Thenhaus,P.C., Perkins, D.M., Algermissen, S.T., and Hanson, S.L., 1987, Earthquake hazard in the eastern United States: Consequences of alternative seismic source zones: Earthquake Spectra, v. 3, p. 227--261

Regional and Local Hazards Mapping in the Eastern Great Basin

9950-01738

R. Ernest Anderson
Branch of Geologic Risk Assessment
U.S. Geological Survey
Box 25046, MS 966, Denver Federal center
Denver, CO 80225
(303) 236-1584

Investigations

1. Completed preliminary compilation of known and suspected late Quaternary scarps in (a) alluvium, (b) Quaternary basalt, (c) pre-Quaternary bedrock in the eastern two thirds of the Cedar City 1° X 2° quadrangle, Utah. This compilation also shows locations of Quaternary basaltic eruptive centers (mainly cinder cones). All data, together with an earlier compilation of scarps in alluvium in the western third of the quadrangle, were digitized and work was started on a text to accompany the map.

2. Fault-slip studies and structural mapping continued in the vicinity of the 1966 Clover Mountains earthquake, Nevada, and the results are compared and contrasted with results of fault-slip studies in the Caliente and Mesquite areas, Nevada, done in cooperation with geologists from the University of Paris.

Results

1. The inclusion of known and suspected late Quaternary fault scarps in basalt and bedrock in the Cedar City quadrangle greatly increases the area inventoried for young faulting by including the portion of the quadrangle in the High Plateaus underlain mostly by bedrock. Though age-of-faulting uncertainties arise in combining such a compilation with one showing only scarps in alluvium, the combined compilation suggests a dramatic southward decrease in frequency of late Quaternary surface faulting in the quadrangle. Only the major long plateau-bounding faults such as the Hurricane and Sevier appear to have had late Quaternary surface displacements in the southern part of the quadrangle, whereas many faults with trace lengths of 10 km or less have been active in the northern part. The strong preference for northeast strikes seen in the compilation of scarps in alluvium (Anderson, 1980) is even more dramatic in the combined compilation. The compilation of basaltic volcanic centers of Quaternary age shows several northeast alinements and one northwest alinement. None are situated on mapped faults, thus introducing the possibility that structures that control magma eruption (presumably tensile in nature) penetrate deeper than the mapped faults.

2. Fault-slip studies and structural mapping in the vicinity of and in the area northwest of the 1966 Clover Mountains earthquake have failed to identify a significant number of north-northeast-striking dextral faults as analogs to the preferred nodal plane indicated by the earthquake data (Rogers and others, 1983). North- and north-northeast-striking fractures

and joints are widespread. Over large areas they have controlled drainage-pattern development, suggesting that they are remarkably long and straight structures. They postdate the main phase of Neogene extension which occurred in response to northeast-southwest least compressive stress. Apparently the north- and north-northeast-trending structures formed as steep joints that contained σ_1 and σ_2. Small offsets are apparent on some, suggesting that they evolved into faults, but evidence for strike-slip displacement is generally lacking. Extensive fault-slip studies in the Caliente area 35 km northwest of the epicenter suggest a paleostress orientation for the youngest deformation (possibly the same event that formed the joints) that is inconsistent with dextral slip on a north-northeast-striking fault. Also, abundant fault-slip evidence was found for sinistral slip on north- and north-northeast-striking steep faults 30-40 km southeast of the epicenter. Thus, dextral slip on a north-northeast-trending fault associated with the 1966 earthquake is a paradox in terms of recently acquired geologic evidence.

Our cooperative studies with geoscientists from the University of Paris, France, of the distribution, magnitude, and style of faulting and of the paleostress history of a transect across the southern Nevada seismic belt has yielded important results. Strata have strikes approximately parallel to the faults but dip in the opporite direction with bedding-to-fault angles averaging 90°. Fault-slip studies of 1,100 fault surfaces in the remarkably well-exposed northern part of Rainbow Canyon south of Caliente, Nev.., shows fault-strike preference between 120° and 155° and a dip-direction preference to the southwest. Synfaulting sediments form growth-fault assemblages that contain an exceptional record of deformation. Dip-slip and strike-slip faulting predominates, resulting in a strongly bimodal distribution of rake angles. The average values for two consecutive extension directions determined by inversion of the fault-slip data are 55° and 110°. These represent separate tectonic events that are in good agreement with clockwise paleostress rotations determined elsewhere in the Basin and Range. Each is represented by strike-slip and dip-slip displacements with the magnitude of dip slip far exceeding that of strike slip , and the magnitude of the early (55°) event far exceeding that of the late (110°) event. Total extension is about 90 percent and is partitioned between block-boundary faulting (70 percent) and block interior faulting (20 percent). The age of the shift from early to late extension direction cannot be constrained more closely than post 13 m.y. for the Caliente area, but our studies in the Mesquite Basin to the south indicate a late Pliocene age for a similar clockwise rotation of computed paleostress. There are no data that we are aware of that would preclude such a young age for the Caliente area.

References

Anderson, R.E., 1980, Factors that complicate determination of the neotectonic stress field in southwestern Utah: Geological Society of America Abstracts with Programs, v. 12, n o. 6, p. 265-266.

Rogers, A.M., Harmsen, S.C., Carr, W.J., and Spence, William, 1983, Southern Great Basin seismological data report for 1981 and preliminary data analysis: U.S. Geological Survey Open-File Report 83-669, 240 p.

Reports

Anderson, R.E., 1987, Neogene geologic history of the Nevada-Utah border area of and near latitude 37°30' N.: Geological Society of America Abstracts with Programs, v. 19, no. 7, p. 572.

Depth to Bedrock Map in the Greater Tacoma Area, Washington

9950-04073

Jane M. Buchanan-Banks
Branch of Geologic Risk Assessment
U. S. Geological Survey
David A. Johnston Cascades Volcano Observatory
5400 MacArthur Boulevard
Vancouver, Washington 98661
(206) 696-7996 FTS 422-7996

Investigations

Visits were made to the Department of Natural Resources, Division of Geology and Earth Resources, Olympia, to obtain data from their files on thickness of unconsolidated material within the Tacoma and Centralia 30 by 60' quadrangles. Materials on deep well logs throughout the project area were ordered from Survey, state, and public libraries and copies of texts and maps were made.

Results

Drilling logs for deep oil wells were examined to determine depths and units penetrated. Several wells provided information on unconsolidated material in the eastern part of the study area. Theses and other publications available only in Olympia were examined and ordered where appropriate.

Geologic maps showing bedrock units outcropping at the surface were collected and reduced to appropriate scale for transference to the Tacoma and Centralia sheets.

Because travel was hampered by lack of funds, numerous telephone inquiries were made: (1) to persons involved in various aspects of Washington geology to advise them of the project, and to solicit their input, and (2) to explore the possibility of obtaining marine seismic refraction data needed to determine thickness of unconsolidated material beneath Puget Sound.

Holocene and Quaternary Geologic Studies

9540-03787

Robert O. Castle
Branch of Western Regional Geology
345 Middlefield Road, MS 975
Menlo Park, CA 94025
(415) 329-4941

Investigations

1. Began supplementary investigations of anomalous vertical displacements in the Los Angeles/Long Beach Harbor area. These studies are intended to enlarge on the earlier work of Leypoldt, Nason, and Wyss.

2. Completed revisions of earlier report on short-wavelength oscillatory vertical displacements astride the San Andreas fault in southern California.

Results

1. Continuing investigations of the historic geodetic record show that at least parts of the San Andreas fault in the central Transverse Ranges sustained short-wavelength oscillatory displacements that accompanied the long-wavelength tilting associated with the early evolution of the southern California uplift.

2. Service as acting chief of the branch of Western Regional Geology precluded substantive project accomplishments during the period June-September 1987.

Reports:

Mark, R.K., Gilmore, T.D., and Castle, R.O., 1987, Evidence of suppression of the unequal refraction error in geodetic leveling: Journal of Geophysical Research, v. 92, no. B3, p. 2767-2790.

Castle, R.O., Elliott, M.R., and Gilmore, T.D., 1987, An early-20th-century uplift in southern California: U.S. Geological Survey Professional Paper 1362, 70 p.

Engineering Behavior Study of Sites Affected by Past Seismic Activity in the Charleston, S.C. Area

14-0800001-G1348

G. W. Clough
Department of Civil Engineering
Virginia Polytechnic Institute and State University
Blacksburg, Virginia 24061
(703) 961-6637

Investigations

Recent investigations by geologists and geophysicists in the vicinity of Charleston, S.C. have led to new information regarding the seismic history of the area. This work has derived largely from the study of exposures of artifact liquefaction features. These exposures are in many cases found in drainage ditches that are excavated by farmers and developers to lower the ground water table. Through the use of dating of organic materials found in the features, it has been established that the Charleston area has been subjected to a series of major earthquakes, all but one of which predate the recorded history of this location.

To date, much effort in the investigations has been expended in the process of simply locating many of the liquefaction features, and mapping the sites and dating of the soils involved. Because of the scope of the work thus far, little time has been allotted to detailed engineering type testing. Work of this nature can usefully supplement that done so far, providing quantitive information which can be used to allow for:

1.) A capabilty to compare the behavior of the soils to those elsewhere in the US and the world. This will allow one to determine if the soils involved in the Charleston sites are more or less susceptible to liquefaction than elsewhere.

2.) The possibility of quantifying acceleration levels that could have led to the liquefaction events. Such information, if developed systematically and at enough sites can assist in the definition of the seismic regime.

3.) Determination of the lateral extent of the soil conditions that presumably led to the liquefaction features.

4.) Sorting out of the meaning of the range of unusual liquefaction features identified at the field sites.

5.) Definition of the reasons why the liquefaction features are located in certain areas and not others.

Results

The project was funded in March of 1987. Since this time, work has focused on collection of documents and reading background material, developing the necessary field equipment, undertaking field work, and preparing for the laboratory testing phase. The documents of interest concern historical accounts of the 1886 Charleston earthquake, and recent studies by personnel who have worked in identifying the pre-history liquefaction features. This phase the work is largely complete.

Preparations for the field testing involved equipment development and two visits to the Charleston area to identify prime test sites and establish geometric controls to define test probe locations. The field testing is to mainly be done by augering and cone penetration testing. A supplemental program of work is to be conducted using a commercial drill rig which will obtain soil samples at depth, and perform standard penetration tests. The basic apparatus for the field work is a small drill rig which has been adapted to allow the researchers to perform cone penetration testing using a specially designed electric small-scale cone penetrometer. Developments for the drill rig-cone testing scheme involved: (1) Establishing a means of controlling the rate of cone penetration; (2) Devising a system to allow higher reaction forces than could be obtained by gravity alone; (3) Adding a structural element which constrains the tendency for buckling of the cone rods; (4) Modifications to a previously existing small-scale cone to insure minimal drift in the electronics of the cone; (5) Development of a PC based automated data aquisition system for continuous monitoring of the cone depth, tip resistance, and sleeve friction.

The field work is now underway, and approximately 15 cone penetrometer holes and 12 auger holes have been completed. With the completion of the first phase of the testing, the data will be digested, and a second phase of testing will be undertaken. The data to date from the first phase of the field work shows that the soil profiles at the liquefaction sites are remarkably uniform. The soils which are most susceptible to liquefaction lie at depths of 10 to 20 feet below the ground surface. These materials are relatively uniform sands. There are indications of some differences in fines contents in the sands, and this will by studied further as samples are brought into the laboratory.

The laboratory effort has involved developing a new cyclic testing system which allows for strain controlled testing of soil samples. Strain controlled testing will be useful in determining the response of the stiff marls that underlie the sandy soils at the test sites. The results from the tests will be used in the ground response studies to determine levels of acceleration that would be required to cause liquefaction features that are observed at the test sites.

Earthquake Hazard Investigations in the Pacific Northwest

14-08-0001-G1390

R.S. Crosson
Geophysics Program
University of Washington
Seattle, WA 98195
(202) 543-8020

Investigations

The objectives of this research are to provide fundamental data and interpretations for earthquake hazard investigations. Currently, we are focusing on seismicity, structure, and tectonic questions related to the possibility of a major subduction earthquake on the Juan de Fuca - North American plate boundary. Specific tasks which we have worked on in this contract period are:

1. Structure of the subducted Juan de Fuca plate beneath western Washington.

2. Tomographic inversion of travel times to determine three-dimensional earth structure in the Puget Sound and Mt. St. Helens region.

3. Locations, focal mechanisms and occurrence characteristics of crustal and subcrustal earthquakes beneath western Washington and their relationship to regional tectonic stresses and subduction processes.

4. A comprehensive review of historical and instrumentally located earthquakes in Washington and Oregon.

Results

1. We have recently developed a preliminary model for the structure of the subducted Juan de Fuca plate beneath western Washington based on earthquake locations and broadband seismograph data (supported under other funding). This model features an arch in the plate which plunges eastward beneath the Puget Sound region. This arch in the subducting plate may explain both the localization of slab seismicity beneath Puget Sound and structural features of the coastal margin region. Deformation of the subducting plate may influence coupling between the North American and JDF plates, an important consideration in earthquake hazard studies.

2. We are using full three-dimensional tomographic inversion of travel time data to study lateral variation of crustal velocity in western Washington. The study area is divided into a grid of blocks, and travel times from the U. W. network data base are compared to travel-times computed from a starting velocity model. An appropriate velocity perturbation to each of the blocks in the grid is determined through tomographic inversion.

The tomographic inversion technique has been used to study the three-dimensional velocity structure in the immediate area surrounding Mt. St. Helens. This is an area of interest due to the recent and ongoing eruptive activity, with abundant data provided by extensive associated seismicity. The inversion results indicate a low velocity zone beneath the crater of the volcano, perhaps due to a magma chamber.

3. We are studying focal mechanisms in western Washington with the objective of determining the most probable direction of regional tectonic stress. Focal mechanisms determined manually for several hundred earthquakes in western Washington are being used as a data base. input to a program developed by Gephart and Forsythe (1984). This program computes how well an input set of mechanisms fits a specified set of orthogonal stress axes. By testing many sets of possible stress orientations, the best fitting stress axes can be determined.

For shallow crustal earthquakes, preliminary results indicate that N-S horizontal compression predominates in western Washington, and that seismicity in southwestern Washington is compatible with a pre-existing fault plane being activated by N-S horizontal compression. In the deeper suite of earthquakes which lie within the subducting Juan de Fuca slab, our preliminary analysis indicates that compression is approximately vertical, and the 90% confidence interval area of the tensional axis covers a crescent shaped area stretching from the northwest to southeast quadrants.

The shallow seismicity of the Puget Sound area is being investigated to determine whether it is possible to define active faults by using focal mechanisms combined with study of the distribution of well-located earthquakes. Although previous studies have not defined active faults in the shallow suite, more data has been acquired, and the subject deserves review.

4. In cooperation with the USGS, we have prepared a revised catalog of earthquake times, locations, and magnitudes. We are writing a a review article on seismicity of Washington and Oregon to accompany the catalog. Seismologists from both the USGS and the U.W. have contributed to both the catalog and the overview article, which will be published in the multi-volume "Decade of North American Geology", which will include a national map of seismicity plus articles on regional seismicity.

Articles

R. S. Crosson and T. J. Owens, 1987, Slab geometry of the Cascadia subduction zone beneath Washington from earthquake hypocenters and teleseismic converted waves, Geoph. Res. Letts., Vol. 14, No. 8, p. 824.

Ludwin, R. S., S.D. Malone, R.S. Crosson, 1987 (in press), Washington Earthquakes 1983, National Earthquake Information Service.

Ludwin, R. S., S.D. Malone, R.S. Crosson, 1987 (in press), Washington Earthquakes 1984, National Earthquake Information Service.

Ludwin, R. S., S.D. Malone, R.S. Crosson, 1987 (in press), Washington Earthquakes 1985, National Earthquake Information Service.

Ludwin, R. S., C.S. Weaver, L.L. Noson, A.I. Qamar, R.S. Crosson, S.D. Malone, W.C. Grant, T.S. Yelin, J.E. Zollweg ,1987 (in preparation), Seismicity in the Pacific Northwest, in Decade of North American Geology, published by Geol. Soc. Am.

Reports

Qamar, Anthony, Anne Rathbun, Ruth Ludwin, Linda Noson, Robert S. Crosson, and Stephen D. Malone, 1987, Earthquake Hypocenters in Washington and Northern Oregon - 1981; Washington State Department of Natural Resources, Division of Geology and Earth Resources, Information Circular 83.

Qamar, Anthony, Ruth Ludwin, Robert S. Crosson, and Stephen D. Malone, 1987, Earthquake Hypocenters in Washington and Northern Oregon; 1982-1986; Washington State

Department of Natural Resources, Division of Geology and Earth Resources, Information Circular 84.

Univ. of Wash. Geophysics Program, 1987, Quarterly Network Report 87-A on Seismicity of Washington and Northern Oregon

Univ. of Wash. Geophysics Program, 1987, Quarterly Network Report 87-B on Seismicity of Washington and Northern Oregon

Univ. of Wash. Geophysics Program, 1987, Quarterly Network Report 87-C on Seismicity of Washington and Northern Oregon

Abstracts

R. S. Crosson and T. J. Owens, 1987, Slab geometry of the Cascadia subduction zone from earthquake hypocenters and teleseismic converted waves, Seis. Res. Letts., Vol. 58, p. 27.

VanDecar, J.C. and R. S. Crosson, 1987 (in press), Automated Determination of Teleseismic Relative Phase Arrival Times using multi-channel cross-correlation and least squares, EOS.

Lees, J.M., 1987 (in press), Tomographic inversion of local earthquake travel time data for lateral velocity variation in western Washington, EOS.

Investigations of Intraplate Seismic-Source Zones

9950-01504

W. H. Diment
Branch of Geologic Risk Assessment
U.S. Geological Survey
Box 25046, MS 966, Denver Federal Center
Denver, CO 80225
(303) 236-1574

Investigations

1. Reprocessing and interpretation of seismic-reflection data in upper Mississippi Embayment to investigate deep structure.

2. Quantitative geomorphic study of stream profiles in the southeastern part of the Ozark Mountains.

3. Interpretation of seismic-reflection data recorded on the Mississippi River.

4. Analysis of level line data in the upper Mississippi Embayment and environs.

5. Continued geologic and geophysical investigations of the Meers fault in Comanche County, Okla.

6. Convened USGS-sponsored workshop on "Directions in Paleoseismology" in Albuquerque, New Mexico, April 22-25, 1987, and organized publication of proceedings volume from the workshop.

7. Effects of earthquakes on high temperature wells in the Long Valley caldera, Mono County, Calif.

8. Analyses of seismological data from China.

9. Regional studies.

10. Analysis of stream profile data in an area of active faulting immediately west of Pierre, South Dakota, and in the vicinity of the super conducting super collider site in eastern Colorado.

Results

1. The data from interpretation of seismic-reflection profiles for the seismic-reflection lines in the north part of the New Madrid seismic zone have been submitted to CTR for publication as an MF map. The final interpretation for seismic-reflection lines across the Reelfoot Rift has been completed and manuscript in being reviewed.

2. A draft report entitled "Analysis of stream-profile data for the eastern Ozark Mountains region and their geologic implications," by F.A. McKeown, M.J. Cecil, B.L. Askew, and M.B. McGrath, has been returned to BCTR after making editorial corrections. Publication as a USGS Bulletin has been requested.

3. Major reflectors are being correlated for the entire length of the Mississippi River survey. Detailed processing of approximately 20 km, covering most of the loop above New Madrid, is underway.

4. Compilation and analysis of level line data for the upper Mississippi Embayment and vicinity was completed by Richard Dart and an open-file report is ready for technical review. Completion of this report has been delayed temporarily by other activities (Dart, 1987a, b; Dart and Zoback, 1987a, b).

5. Newly acquired radiocarbon ages from three recently studied sites indicate a late Holocene age for the last movement of the Meers fault. Where the scarp is formed in resistant Post Oak Conglomerate, movement on the fault has locally dammed several small gullies and ponded fine-grained alluvium upslope from the scarp. Excavations in the ponded alluvium at two sites exposed 1.4-2.3 m of organic-rich silt overlying red sandy gravel interpreted to be bedrock alluvium. The onset of deposition of the silt is thought to mark the time the scarp formed. Soil humus from the basal part of the silt at the two sites has radiocarbon ages of 1,865±25 and 1,690±45 yrs B.P.

   An excavation on the downthrown (south) side of a 3.35-m-high bedrock scarp in the Post Oak Conglomerate exposed a 45-cm-thick pod of organic-rich material, interpreted as a soil pressure ridge, resting on bedrock residuum. Soil humus from the pod has a radiocarbon age of 1,325±45 yrs B.P. The stratigraphy of the deposits overlying this pod permits an interpretation of a second faulting event. Orange gravelly colluvium buries the organic-rich pod and a weak, organic-rich horizon that may be an incipient A horizon is locally presented on the colluvium. This weak organic-rich horizon is abruptly truncated against fault gouge, implying that it is faulted, and it has a radiocarbon age of 1,165±45 yrs B.P. Similar studies at several other sites are needed to support or refute this interpretation.

   Geophysical studies of the Meers fault are directed toward a better understanding the relationship between the fault scarp and deep structures that extend to hypocentral depths. Seismic-reflection profiles, combined with aeromagnetic and gravity data will help define regional and local structural relationships between the Wichita uplift and the Anadarko Basin.

   Correlated field tapes of pertinent COCORP data across the Meers fault have been purchased; reprocessing and reinterpretation of these data will involve the cooperative efforts of Crone, Cecil, and personnel in the Branch of Petroleum Geology .

   Five 512-fold, industry seismic-reflection lines across the fault have been recently released for purchase. Cecil, Crone, and Shedlock have reviewed these data and identified parts that are pertinent to project goals. If sufficient funding is available, about 47.3 km of the data set will be purchased, reprocessed, and reinterpreted.

As part of the overall geophysical analysis, Cecil is using gravity and magnetic data to model the basin-uplift transition. Detailed aeromagnetic data are currently being digitized and samples of several exposed rock types have been collected to measure their magnetic susceptibility. Cecil has obtained gravity data from published and unpublished sources. To supplement these gravity data, Cecil and S. Robbins (Branch of Petroleum Geology) have made more than 350 additional measurements in areas of poor regional coverage and along two detailed traverses across the fault scarp.

6. The workshop on "Directions in Paleoseismology" was held in Albuquerque, N. Mex., on April 22-25, 1987. Seventy senior scientists, researchers, and program managers gathered to review the achievements and discuss future goals of studies related to paleoseismology. The novel format of the program for the workshop was unanimously regarded as an outstanding success. The attendees included scientists from Canada, New Zealand, Japan, and France. The proceedings of the workshop will be published as a USGS open-file report, edited by A.J. Crone.

   The open-file report will include a series of review papers on topics pertinent to paleoseismology in addition to summaries of the group discussion sessions. About 40 reviewed manuscripts for the proceedings volume have been edited and returned to the authors for preparation of the final camera-ready copies. Publication of the report is anticipated to be in the spring 1988.

7. Temperature logs obtained in Chance No. 1 (south moat of the Long Valley caldera, Mono County, Calif.) in 1976, 1982, 1983, 1985, 1986, and 1987 show a progressive cooling in the uncased part of the hole. Examination of the rate of change suggests that the cooling began to accelerate about the time of the strong earthquakes of May 1980 (Diment and Urban, 1985). The cooling is attributed to the enlargment of the Hot Bubbling Pool which is an evaporator for cooling subsurface waters that circulate to the surface and return to depth. Temperature logs from Mammoth No. 1 (near Casa Diablo Hot Springs, 3 km west of Chance No. 1) obtained in 1979, 1982, and 1983 are also being processed and examined for seismically induced phenomena (Urban and Diment, 1984; 1985).

   More recently, precision temperature logs and gamma-ray logs were also obtained in two other hot wells (PLV-1 and RDO8) in the southwest moat of the caldera 6-11 days before and 3-4 days, and 61-64 days after the Chalfant (50 km ESE of well) earthquake (M_S=6.2 PDE, M_L=6.4 BRK) of July 21, 1986. Temperatures in RDO8 are within 10 °C of boiling at 1,100 ft in RDO8 (Urban and others, 1987a, b, c). RDO8 is close to the western terminous of South Moat fault which experienced unusually high seismicity following the 1980 earthquakes. The work in RDO8 was partially supported by participants in the Continental Scientific Drilling Program.

8. Under the Chinese-American Cooperative Earth Sciences Program, K.A. Shedlock and her colleagues from universities and The Peoples Republic of China have conducted extensive studies of the structure and tectonics of the North China basin (Shedlock and others, 1987; Shedlock and Roecker, 1987). These studies are applicable to the better understanding of similar regimes in the United States.

9. L.C. Pakiser and W.D. Mooney perceived the need for the summary/review volume: "Geophysical framework of the Continental United States." A conference was held in Golden between March 17 and 20, 1986 and 24 papers were presented. A total of 31 chapters has been submitted. GSA has agreed to publish the product in their Memoir series. All manuscripts have been reviewed and two-thirds have been revised and accepted. Estimated date of submission to GSA is December 1987. The Memoir is estimated to be at least 650 printed pages.

10. In cooperation with T.C. Nichols and D.S. Collins (Project 9950-02478, Rock deformation induced by subsurface excavation and use), Meridee Jones-Cecil has continued to analyze 25 digitized streams west of Pierre, S.D. Greater rejuvenation (uplift?) of the eastern portion of the study area, once covered by Pleistocene glaciers, is evident from quantitative examination of the stream profiles. Sinuosity along larger streams and local changes in stream gradient are currently being examined in order to help define smaller block movements.

    Reconnaissance field checking of the most marked anomalies in 15 stream profiles digitized by Meridee Jones-Cecil in the area of the proposed superconducting supercollider site in eastern Colorado showed no evidence for active tectonics. In at least one locality, the anomalies appeared to be caused by manmade changes. An ancient paleodrainage system may have been the cause of a marked alignment of anomalies and stream-course changes.

Reports

Crone, A.J., 1987, Stop 3--Evidence of lateral slip on the Meers fault, in Ferring, C.R., compiler, Late Quaternary stratigraphy, neotectonics, and geoarchaeology of southwestern Oklahoma: Denton, Texas, Institute of Applied Sciences, North Texas State University, Guidebook for the 5th Annual Field Trip, Friends of the Pleistocene, South-central Cell, p. 24-30.

______1987, The Meers Fault, SW Oklahoma--Evidence of multiple episodes of Quaternary surface faulting [abs.]: Geological Society of America Abstracts with Programs, v. 19, no. 7, p. 630.

Dart, R.L., 1987, Horizontal stress orientations from well-bore breakouts in the south-central United States [abs.]: Geological Society of America Abstracts with Programs, v. 19, no. 5, p. 269.

______1987, South-central United States well-bore breakout data catalog: U.S. Geological Survey Open-File Report 87-405, 95 p.

Dart, R.L., and Zoback, M.L., 1987, Principal stress directions on the Atlantic continental shelf inferred from the orientations of borehole elongations: U.S. Geological Survey Open-File Report 87-283, 40 p.

______1987, Application of well-bore breakout stress method to areas within the continental United States, *in* Abstracts of Papers, Second International Symposium on Borehole Geophysics for Minerals, Geotechnical, and Ground Water Applications [abs.]: Minerals and Geotechnical Logging Society, A Chapter at Large of the Society of Professional Well Log Analysts.

______1987, Application of well-bore breakout stress method to areas within the continental United States: Proceedings of The Minerals and Geotechnical Logging Society, 2nd International Symposium on Borehole Geophysics (in review).

Diment, W.H., and Urban, T.C., 1985, Temperature variations with time in a perennially boiling well in the Long Valley caldera, Mono County, California: Observations in Change No. 1 (1976-83): Geothermal Resources Council Transactions, v. 9, part 1, p. 417-422.

Harding, S.T., and Dwyer, Ruth-Ann, 1987, A large fault determined from seismic-reflection data in the New Madrid seismic zone and its relationships to seismicity: Tectonics (Submitted.)

Shedlock, K.M., Baranowski, J., Xiao, W., and Ju, X., 1987, The Tangshan aftershock sequence: Journal of Geophysical Research, v. 92, p. 2791-2803.

Shedlock, K.M., and Roecker, S.W., 1987, Elastic wave velocity structure of the crust and upper mantle beneath the North China basin: Journal of Geophysical Research, v. 92, p. 9327-9350.

Urban, T.C., and Diment, W.H., 1984, Precision temperature measurements in a deep geothermal well in the Long Valley caldera, Mono County, California: EOS [Transactions of the American Geophysical Union], v. 65, p. 1084-1085.

Urban, T.C., and Diment, W.H., 1985, Convection in boreholes: limits on interpretation of temperature logs and methods for determining anomalous fluid flow, *in* Proceedings National Water Well Association Conference on Surface and Borehole Geophysical Methods in Ground-Water Investigations: National Water Well Association, Worthington, Ohio, p. 399-414.

______1987, Repeated precise temperature logs in hot boreholes--one key to understanding the evolution of geothermal systems, *in* Abstracts of Papers, Second International Symposium on Borehole Geophysics for Minerals, Geotechnical, and Ground Water Applications [abs.]: Minerals and Geotechnical Logging Society, A Chapter at Large of the Society of Professional Well Log Analysts, p. I.2.

Urban, T.C., Diment, W.H., and Sorey, M.L., 1987, Temperature and natural gamma-ray logs obtained in 1986 for drill hole RDO8 (Shady Rest), Mammoth Lakes, Mono County, California: U.S. Geological Survey Open-File Report 87-291, 102 p.

______1987, Hydrothermal regime of the south moat of the Long Valley caldera, Mono County, California and its relation to seismicity--New Evidence from the Shady Rest borehole (RDO8): Geothermal Resources Council Transactions, v. 11 (Director's approval 7/9/87).

Urban, T.C., Nathenson, Manuel, and Diment, W.H., 1987, BPE and BPD-BASIC programs for microcomputers to calculate the local boiling point and boiling-point depth curve for "pure" water: U.S. Geological Survey Open-File Report 87-17, 58 p.

A LIQUEFACTION POTENTIAL MAP FOR CHARLESTON, SC

USGS Grant Award 14-08-0001-G1435

Dr. David Elton
Auburn University
Civil Engineering Department
Auburn University, AL 36849
(205) 826-4321

Dr. Tarik Hadj-Hamou
Civil Engineering Department
Tulane University
New Orleans, LA
(504) 865-5778

Liquefaction of soils during earthquakes can cause great damage. History is replete with examples of extensive damage caused by liquefaction. The public must have a quantitative evaluation of the possibility of liquefaction in order to be adequately protected from this earthquake-induced hazard. Liquefaction potential mapping provides a powerful and effective way to provide this protection. These maps show contours of the probability (risk) of occurrence of liquefaction for different magnitude earthquakes and return periods. This proposal develops a new method of liquefaction potential mapping, and then applies it to Charleston, SC.

Charleston, SC, was chosen for a test of the new method because it is susceptible to liquefaction. Recent geologic discoveries indicate that there have been several very large earthquakes accompanied by liquefaction in the Charleston area. From these conditions, Charleston obviously has a liquefaction risk. The high population density of Charleston makes evaluation of the threat imperative.

The objectives of this proposal are to develop -

1. a new methodology for creating liquefaction potential maps,
2. a liquefaction susceptibility map for peninsular Charleston, SC. This map will give the annual probabilities of exceedance for peninsular Charleston.
3. an understanding of the nature of the ground conditions in Charleston, SC, an area of seismic risk. The soil types, locations, variability, and properties will be studied. This information will be very useful in many other hazard mitigation studies.

The approach used in this study is based on the liquefaction evaluation method of Seed and his co-workers (1971, 1983, 1985). It relies on the use of Standard Penetration Test (SPT) data to evaluate how susceptible the soil is to liquefaction. A knowledge of seismic conditions is also needed in order to evaluate the probability of certain ground accelerations occurring. These two factors are combined to produce a liquefaction potential map.

Work completed to date includes:

1. completion of the geotechnical and geological information about the area of interest,
2. Conversion of the values of penetration resistance into threshold accelerations, and mapping of threshold accelerations for liquefaction potential.
3. Perform a seismic risk analysis of the area to evaluate the probability of exceedance of different ground acceleration for all possible earthquake magnitudes.

Work to be completed includes:

1. Combination of the the data from step 2 and 3 to develop the map of probability of exceedance of threshold accelerations for liquefaction.
2. Draw contours or zones of equal risk for liquefaction by joining locations on the map that present same probability of exceedance of the threshold acceleration for liquefaction.

The method outlined in this proposal has some distinct advantages over current techniques. One advantage is the use of the simplified Seed and Idriss method (1981), which is very easy to implement. Others are the separation between the geotechnical and seismological analyses, and the development of a map of quantitative probability of occurrences of threshold accelerations, rather than a relative description.

Seismic Hazard Studies, Anchorage, Alaska

9950-03643

A.F. Espinosa
Branch of Geologic Risk Assessment
U.S. Geological Survey
Box 25046, MS 966, Denver Federal Center
Denver, Colorado 80225
(303) 236-1597

Investigations

1. Work leading to public release and distribution of the Anchorage B-7 NE surficial geologic map is nearly complete.

2. Fifteen earthquakes recorded in the seismological field experiment conducted in Anchorage, Alaska, have been edited and are being analyzed. This topic on "Ground amplification studies in areas damaged by the Alaskan earthquake" will be jointly used in the site-response study obtained on different geologic environments with the damage evaluation along 15th and DeBarr Avenues.

3. In cooperation with the Office of Mineral Resources, Denver, Colo., field investigation of paleoseismicity of the region is continuing, based on detailed analyses of emergent tidal sediments and intercalated organic materials. Some radiocarbon dates from previous field seasons have been received and are being analyzed for similarities of chronology with time of cyles of major seismic activity elsewhere in southern Alaska.

4. Samples at a depth of 155 m from the Anchorage Tikishla Park drill hole (USGS Open-File Report 86-293) have been provided for geochemical analyses in cooperation with the Coal Geology Branch and most data reduction is completed. Previous paleontological work indicates that this drill hole penetrates Tertiary rocks that are substantially deeper than previously thought, and further paleontological analyses have been requested from the Branch of Paleontology and Stratigraphy.

Results

1. Field observations in cooperation with the State of Alaska, Division of Geology and Geological Surveys were completed for the Anchorage B-7 NE and SE quadrangle areas in sectors previously not investigated because of inclement weather. Thick vegetation and lack of exposures hampered work along the lower margins of major valleys.

2. A preliminary version of the surficial geologic map of the Anchorage B-7 SE quadrangle area has been completed, including map-unit boundaries, most of the map-unit designations, and initial typescript of text, and map is now ready for coauthor contribution.

3. In cooperation with the Alaskan Geology Branch, helicopter-supported field investigations were undertaken in the Gulkana A-1 quadrangle area, with

incidental field observations in the Gulkana B-1, B-3, and Nabesna B-6 quadrangle areas. A long-sought source for the Sanford volcanic mudflow has been identified.

4. An intensity catalog covering the period 1786-1981 for the State of Alaska and the Aleutian Islands is being released as a USGS bulletin.

5. Flying was completed by the Branch of Geophysics for side-looking airborne radar imagery covering much of the project area. Studies of its applicability for interpretation of the distribution of sediments and structures in the Anchorage Lowland are underway.

Reports

Bartsch-Winkler, Susan, and Schmoll, H.R., 1987, Earthquake-caused sedimentary couplets int eh upper Cook Inlet region, Alaska, in Hamilton, T.D., and Galloway, J.P., eds., Geologic studies in "Alaska by the U.S. Geological Survey during 1986: U.S. Geological Survey Ciurcular 998, p. 92-95.

Brockman, S.R., Espinosa, A.F., and Michael, J.A., 1987, Catalogue of intensities and magnitudes for earthquakes in Alaska and the Aleutian Islands--1786-1981: U.S. Geological Survey Bulletin, 205 p. (in press).

Espinosa, A.F., and Rukstales, K.S., 1988, Geometry of the Benioff zone and mode of subduction beneath southwestern Alaska and the Aleutian Islands: U.S. Geological Survey Investigations Map I-1945 (1 sheet).

Espinosa, A.F., Rukstales, K.S., and Michael, J.A., 1987, Digital seismicity catalog of Alaska and the Aleutian Islands, 1797-1981: U.S. Geological Survey Open-File Report 87- , 25 p.

Herraiz, M., and Espinosa, A.F., 1987, Coda Waves--A review: Pure and Applied Geophysics (PAGEOPH), v. 125, no. 4, p. 499-577.

Lade, P.V., Updike, R.G., and Cole, D.A., 1987, Cyclic triaxial tests of the Bootlegger Cove Formation, Anchorage, Alaska: U.S. Geological Survey Bulletin 1825, 147 p.

Odum, J.K., 1987, Point-load index and laboratory unconfined compressive strengths of some units of the coal-bearing Tyonek Formation, Beluga coal resource area, upper Cook Inlet region, Alaska, in Rao, P.D., ed., Focus on Alaska's coal '86: Proceedings of the Conference held at Anchorage Alaska, Alaska, October 27-30, 2986, University of Alaska-Mineral Industry Research Laboratory MIRL Report Number 72, p. 150-156.

Odum, J.K., 1987, Yehle, L.A., Schmoll, H.R., Gardner, C.A., and Dearborn, L.L., Lithological, geotechnical properties analysis, and geophysical log interpretation fo U.S. Geological Survey drill holes 1C-79, 2C-80, CW 81-2, and CE-82-1, Tyonek Formation, upper Cook Inlet region, Alaska: U.S. Geological Survey Bulletin (Branch approval)

Schmoll, H.R., and Yehle, L.A., 1987, Surficial geologic map of the northwestern quarter of the Tyonek A-4 quadrangle, south-central Alaska: U.S. Geological Survey Miscellaneous Field Studies Map MF-1934, scale 1:31,680.

Yehle, L.A., and Schmoll, H.R., 1987, Surficial geologic map of the Anchorage B-7 NW quadrangle, Alaska: U.S. Geological Survey Open-Fiel Repoort 87-168, 11 p., scale 1:25,000.

Updike, R.G., Olsen, H.W., Schmoll, H.R., Kharaka, Y.K., and Stokoe, K.H., 1987, Geologic and geotechnical conditions adjacent to the Turnagain Heights landslide, Anchorage, Alaska: U.S. Geological Survey Bulletin 1817 (in press).

Updike, R.G., and Ulery, C.A., 1988, Bedrock geology of the Anchorage (B-7 SE) quadrangle, Alaska: U.S. Geological Survey Map (1 sheet)

Yehle, L.A., and Schmoll, H.R., 1987, Surficial geologic map fo the Anchorage B-7 NE quadrangle, Alaska: U.S. Geological Survey Open-File Report 87-416, 20 p., scale 1:25,000.

Soil Development as a Time-Stratigraphic Tool

9540-03852

Jennifer W. Harden
Branch of Western Regional Geology
U.S. Geological Survey
345 Middlefield Road, MS 975
Menlo Park, California 94025
(415) 329-4949

Investigations

1. Slip-rate studies along the Calaveras Fault near San Felipe Creek: Jennifer Harden, Kathy Harms, Malcolm Clark. See also M.M. Clark, this volume.

Results

1. Soils are being used to date Quaternary surfaces along San Felipe Creek (Table 1). Time of offset of erosional scarps along the creek can be estimated by ages of the terraces set into the scarps. In addition, the stream appears to have been diverted from a more northwesterly course, and the diversion may be related to fault displacement. Radiometric dates are in agreement with soil ages and will contribute to improved calibration of soils to dates for further studies in the S.F. Bay region.

Reports

Switzer, P., Harden, J.W. and Mark, R.M., 1987, A statistical method for estimating rates of soil development and ages of geologic deposits: a design for soil-chronosequence studies. Mathematical Geology vol. 20, no. 1, p. 49-61.

Table 1. Soil properties and ages estimates of terraces of San Felipe at Calaveras fault.

Terrace	Soil horizons present	Munsell Maximum color	Thickness of Bt cm	Texture[1] Bt/parent mat.	Soil Development index[2]	Age of Correlative soil at Merced, CA[3] ka	^{14}C age of charcoal ka
West of fault							
E (youngest)	A/AC/C	10YR6/4	0	---	10		---
D	$A/Bt/Bt_b$	7.5YR5/6	150	SCL/SL	70	20 130	38.4±1.8 (probably infinite)
C	$A/Bt/Bt_b$	5-7.5YR5/8	200-300	SCL/L-SL	100	130	---
B (oldest)	$A/Bt/Bt_b$	5-7/5YR5/8	160-300	CL/L	100-140	130-250	---
East of fault							
T (youngest)	A/AC/C	10YR5/4	---	---	25	10	8.4±.2
Q	$A/Bt/Bt_b$	7.5YR4/6	200-300	CL/L	100	130-250	---

---

[1] S, sandy; C, clay; L, loam

[2] Using rubification, texture, clay films, dry consistence on only one soil. More data pending.

[3] Correlations to dated soils at Merced are based on soil development indices.

Seismic Slope Stability

9950-03391

Edwin L. Harp
U.S. Geological Survey
Branch of Geologic Risk Assessment
345 Middlefield Road, Mail Stop 998
Menlo Park, California 94025
(415) 329-4891

Investigations

As part of a research fellowship supported by the Japanese Sociecy for the Promotion of Science, the project was directed to establishing a correlation between the distributions of landslides and the distribution of strong ground shaking from the Izu-Oshima-Kinkai and Nagano-Ken-Seibu earthquakes. On the basis of the strong motion records and landslide maps produced from both of these earthaukes, effort was focused on developing a relation between calculated landslide intensities (concentrations) and values of an instrumental seismic intensity called Arias Intensity.

Results

Landslide maps from both the Izu-Oshima-Kinkai and Nagano-Ken-Seibu earthquakes were used to prepare landslide intensities for areas equidistant from the earthquake source zones at 1-km intervals. Seismic strong-motion acceleration records were used to calculate Arias intensities. Both the landslide intensities and Arias intensities were plotted against distance from the seismic sources and intensity-distance regressions were calculated. Using this data regressions were then calculated for Arias intensity versus landslide intensity for each of the earthquakes.

At present calculations are complete for the Izu-Oshima-Kinkai data. Regression relations were developed for two different source models; one for a fault rupture of 17 km and another of a 29 km source length. The former source model yields the relation $I_L=4.68I_A + 0.36$ while the latter model requires that $I_L=6.55I_A + 0.69$.

Similar calculations for the Nagano-Ken-Seibu data are not yet complete. Because of the lack of near-field strong motion records, a near-field main shock record is being synthesized to provide an acceleration-time record from which to calculate Arias intensity.

The Arias intensity-distance relations for the threshold of landslides for the Izu-Oshima-Kinkai earthquake gives values of Arias intensities of 0.14 m/s for the 17 km source model and 0.18 m/s for the 29 km source . These values are in good agreement with a threshold value of 0.15 m/s estimated by Wilson and Keefer (1986) from a comparison of a probabilisitic distribution of Arias intensity versus distance for a magnitude 6.5 earthquake in southern California and the farthest distances to landslides from

40 worldwide earthquakes. The Arias intensity threshold for the Nagano-Ken Seibu earthquake may well be significantly higher than 0.15 m/s due to the extremely short distance from the source zone to the limit of landsliding, 11 km.

References

Wilson, R.C., and Keefer, D.K., 1985, Predicting areal limits of earthquake-induced landsliding in Ziony, J.I. ed., Evaluating Earthquake Hazards In The Los Angeles Region: U.S. Geological Survey Professional Paper 1360, p. 317-345.

ANALYSIS OF SEISMIC RISK FROM FOCUSING AND RESONANCE IN SALT LAKE VALLEY BY NUMERICAL SIMULATION OF THE WAVE EQUATION

Contract Number: 14-08-0001-G1344

Julie Hill
Harley Benz
Gerard Schuster (P.I.)
Geology and Geophysics Department
University of Utah
Salt Lake City, Utah 84112

OBJECTIVES

Focusing and resonance of seismic waves in alluvial-filled basins play a major role in determining which valley locations are most susceptible to severe ground shaking. From an accurate knowledge of the valley's P- and S-wave velocity structure, attenuation and geometry it may be possible to predict the ground shaking potential of a basin by numerical simulation of the wave equation.

The objective of this research is to roughly predict the amplification (resonance and focusing) of seismic waves for various sites within the Salt Lake Valley. Seismic wave propagation in a Salt Lake Valley model is simulated using a finite difference solution to the wave equation.

RESULTS

Four results of significance have been obtained thus far:

1). There are three reflectors in the Salt Lake basin which appear to play a major role in the resonance of low frequency waves. Figure (2a) depicts the three reflectors interpreted from the CDP seismic data; the seismic data were obtained by Mountain Fuel Co. (loaned to us by Robert Smith) along the R-11 line shown in Figure (1a). The lithology of the three layers is provided by well log data, of which sonic log #1 is depicted in Figure (2b). The three reflectors define the base of the unconsolidated sediments (R1), the base of the semi-consolidated sediments (R2), and the contact between the consolidated sediments and basement (R3). A cross-sectional diagram of these reflectors is given in Figure (1b). This model appears to be roughly consistent with the refraction model of Bashore (1982).

2). Modeling the response of symmetrical basins (Bard and Bouchon, 1980) is inadequate to predict the ground shaking potential of the Salt Lake basin. The plane SH-wave response of the symmetrical basin in Figure (3a) is compared to that of the Salt Lake Basin in Figure (3b). These simulations show that asymmetrical basin structure tends to diminish the multiple reflections from the basin's western wall.

3). Layered structure is shown to be an essential factor in controlling the surface distribution of resonance energy. In particular, the R1 and R2 reflectors appear to play a major role in controlling the surface response for source frequencies between .2 and 1.5 Hz. Figure (4) shows the effect of incorporating layers into the Salt Lake basin model. Figure (4a) shows the weak response of the unconsolidated layer (reflector R1) to an impinging plane SH-wave. A much greater response is excited when both the unconsolidated (R1) and semi-consolidated (R2) contacts are included in Figure 4b; resonance effects take the form of lateral reflections from the east and west walls of the basin. Comparing Figure (3b) to Figure (4b) shows that the combination of both reflectors R1 and R2 play an important role in the resonance process. The effect of incorporating the consolidated sediment-bedrock contact (R3) into the model in Figure (4c) is relatively unimportant in changing the character of the events in Figure (4b); however, it does appear to slightly increase the amplitude of events compared to the resonance excited by the R2 and R1 contacts in Figure (4b). These and other simulations show that the strong impedance contrast at reflector R2 coupled with reflector R1 are the dominating influences on resonance for frequencies between .5 and 1.5 Hz.

A summary of the instantaneous energy of the seismic traces integrated from 0.0 to 20.0 seconds is given in Figure (5). The seismograms in Figures (3b), (4b) and (4c) are squared, integrated in time, and divided by the energy of the incident wavelet to give the total normalized energy curves in Figure (5). Note that the rapid oscillatory shape of the curve is primarily controlled by the combination of reflectors R1 and R2 while the slower variation appears to be controlled by the R2 reflector. Evidently, the R3 reflector appears to play only a minor role in determining the curve's shape. The R2 and R3 reflectors act as efficient traps for energy. This is not too surprising since the R2 reflector is characterized by well over a 150 percent contrast in impedance.

4). Some correlation is observed between our theoretical predictions and the site responses measured from NTS blasts (Hays and King, 1984). Figure (1) shows the locations of sites in which the valley's response to NTS blasts was measured by Hays and King (1984). SH recordings were normalized to bedrock recordings and their frequency responses are depicted by the dashed lines in Figure (6). Overlaid are solid lines which represent the predictions from computer simulations of a plane SH-wave normally incident on the Salt Lake basin model in Figure (1). The basin's subsurface structure is unknown at USGS sites 3, 6, 8, and 9 in Figure (1a); however, gravity data suggests that the structure underlying sites 3, 6, 8 and 9 is similar to that underlying the arrow in Figure (1b). All of the measured responses (dashed lines) in Figure (6) are characterized by peaks at around 0.4 Hz and 0.8 Hz. This is similar to the predicted response (solid lines in Figure 6) over the deep part of the basin depicted by the arrow in Figure (1b). Unfortunately, the dominant incident energy for the USGS recordings resulted primarily from L_g waves in the crust; in contrast, the incident energy for our computer simulations was only a plane SH body wave normally incident on the basin. This mismatch of incident fields is a topic of future research. However, preliminary results show that even obliquely incident plane SH-waves provide spectra similar to that shown in Figure (6).

The computer simulations were limited in source bandwidth to frequencies between .5 and 1.7 Hz because, at these frequencies, the basin response is most sensitive to the intermediate and deep portions of the basin. This frequency range was significant for the September 19, 1985 Mexico City earthquake because it spans the resonance frequencies of intermediate height buildings. Moreover, higher source frequencies require a detailed knowledge of the basin geometry while our knowledge of the Salt Lake Valley Basin was limited to the coarser features such as R1, R2, and R3.

SUMMARY

Assuming a uniform soil distribution over the Salt Lake Valley floor, computer simulations show that the .2 to 1.5 Hz seismic response at the R-11 line in Salt Lake Valley is mainly influenced by the unconsolidated (R1) and semi-consolidated (R2) reflectors. The deep easternmost portion of the basin is affected more strongly than the shallow western part of the basin. This may mean that the 5- to 30- story (downtown) buildings may be more strongly affected by low-frequency resonance than if these buildings were located (on the same soil) in the far western part of the basin.

These results must be considered preliminary because our study did not take into account the lateral variability of the top-soil or the L_g nature of the incident energy. Moreover, the NTS site data were located too far from the R-11 line to truely verify our predictions. Unfortunately, deep seismic data do not appear to exist anywhere else in the valley to provide structural information. Deep well log data, however, do exist throughout the valley (Arnow and Mattick, 1968, and Mattick, 1970), and can possibly define the R1 reflector depth; gravity data may be able to define the depth of the R2 reflector. This data will be used in the second year of our study to model both the SH and P-SV responses throughout the valley, including the valley locations where the NTS data are available. We will also initiate three-dimensional modeling of basin models by a scalar Boundary Integral Equation method.

REFERENCES

Arnow, T. and Mattick, R.E., 1968, Thickness of valley fill in the Jordan Valley east of the Great Salt lake: Utah, U.S.G.S. Prof. Paper, 600-B, B79-B82.

Bard, P.Y., and Bouchon, M., 1980, The seismic response of sediment filled valleys. Part I. The case of incident SH-waves: BSSA, 70, 1263-1286.

Bashore, W.M., 1982, Salt Lake Valley and Wasatch Fault crustal structure: University of Utah MS thesis.

Benz, H., 1986, Elastic wave propagation in heterogeneous media from normal faulting earthquakes, in preparation.

Hays, W., and King, K., 1984, The ground shaking hazard along the Wasatch Fault Zone, Utah: USGS Proceedings of Conference XXVI, 133-147.

Mattick, R.E., 1979, Thickness of unconsolidated to semi-consolidated sediments in Jordan Valley, Utah: USGS Prof. Paper, 700-C, C119-124, 1970. 600-B, B79-B82.

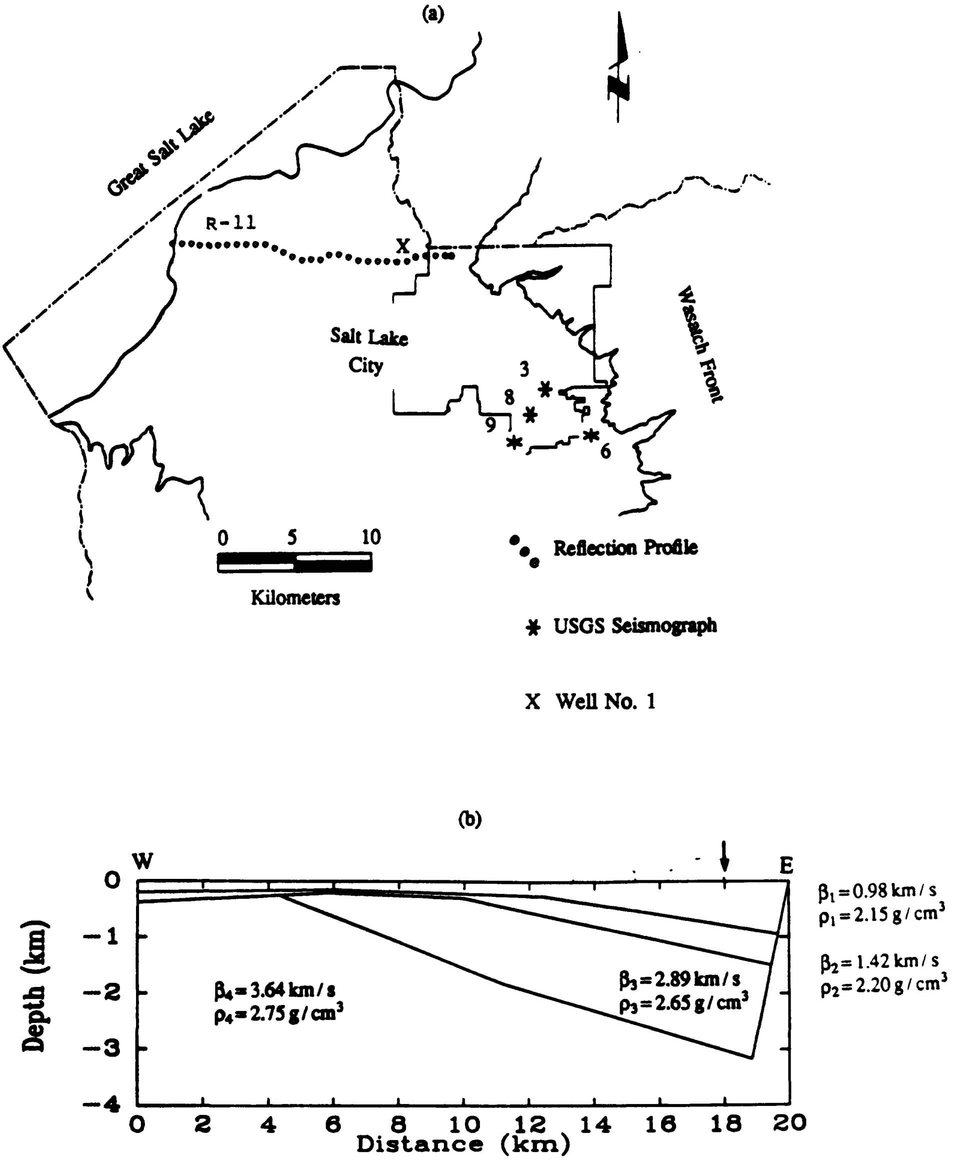

Figure 1. The Salt Lake Valley is depicted in (1a) and the basin's cross-section interpreted from the R-11 CDP profile is depicted in (1b). This alluvial-filled valley trends 35 km from north to south from the Salt Lake to the Traverse Mountains. It is bounded on the east by the Wasatch Fault and on the west by the Oquirrh Mountains.

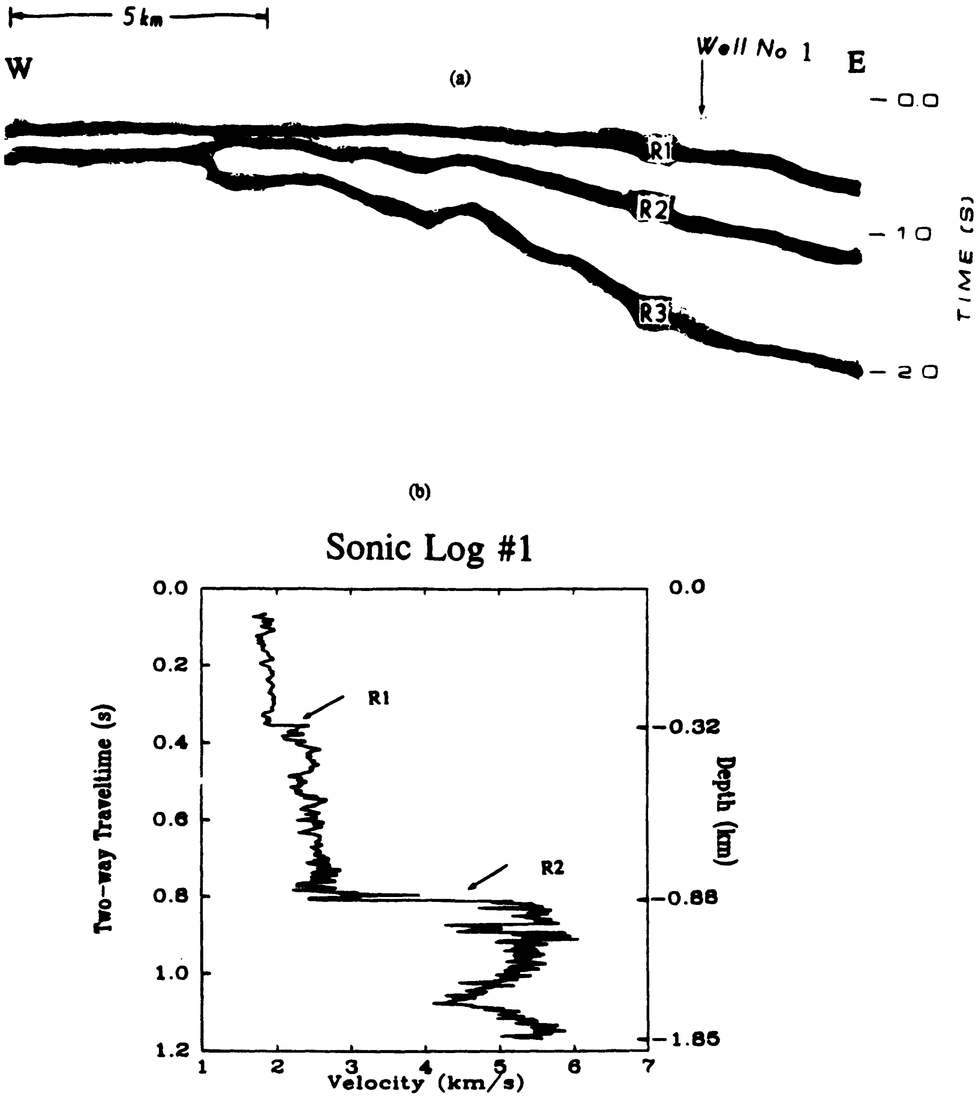

Figure 2. Figure (2a) depicts the interpreted CDP profile from the R-11 seismic line in Figure (1a). Figure (2b) shows the sonic log obtained from the #1 well on the eastern most part of the R-11 line.

(3a)

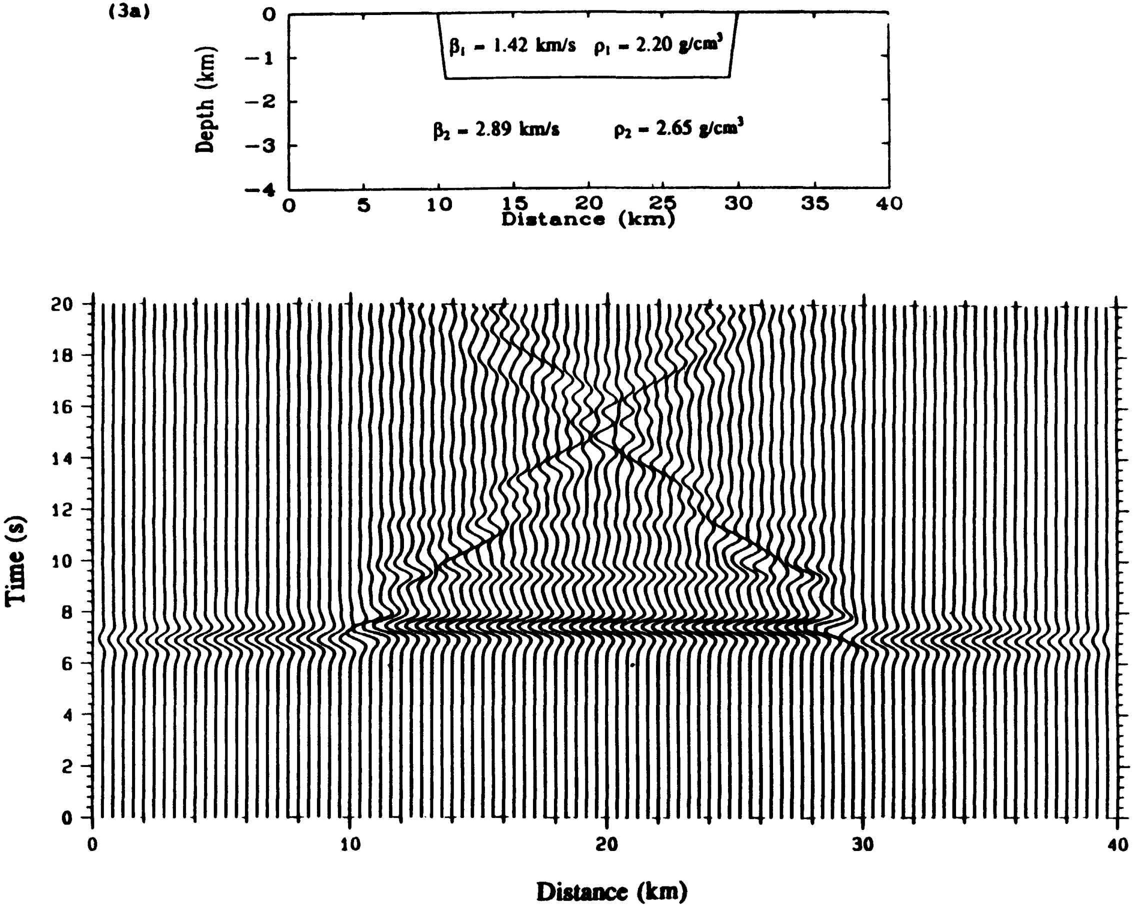

Figure 3. Figures (3a) and (3b) depict the plane SH-wave response of the, respectively, symmetrical and asymmetrical basin models. The plane wave is normally incident from below and the response is measured at the free surface. These source and receiver parameters are the same for Figures (4) and (5). The scaling factor for both sets of seismograms is the same.

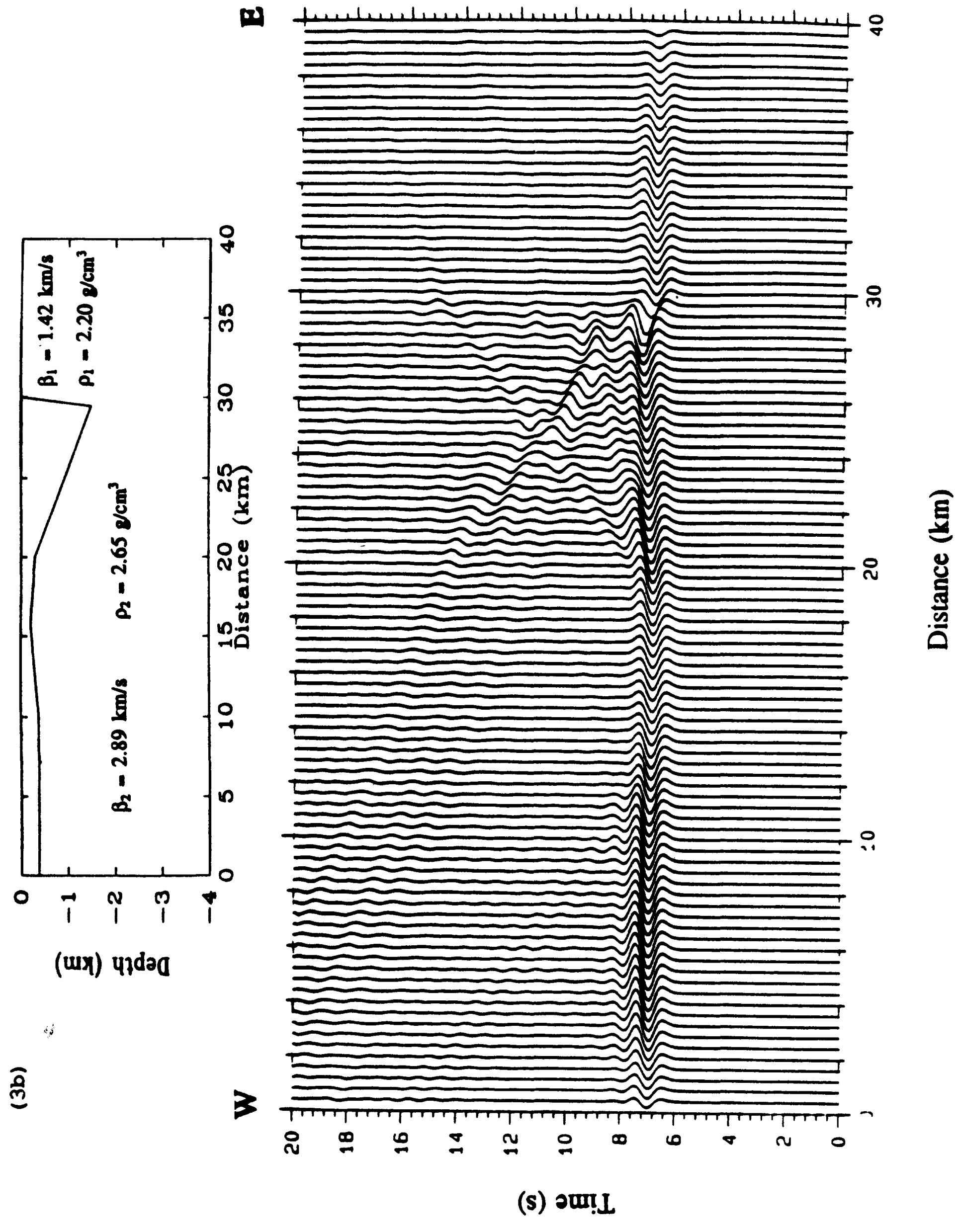
(3b)
W
E
Depth (km)
0
−1
−2
−3
−4
0
5
10
15
20
25
30
35
40
Distance (km)
β₁ = 1.42 km/s
ρ₁ = 2.20 g/cm³
β₂ = 2.89 km/s
ρ₂ = 2.65 g/cm³
Time (s)
20
18
16
14
12
10
8
6
4
2
0
0
10
20
30
40
Distance (km)

(4a)

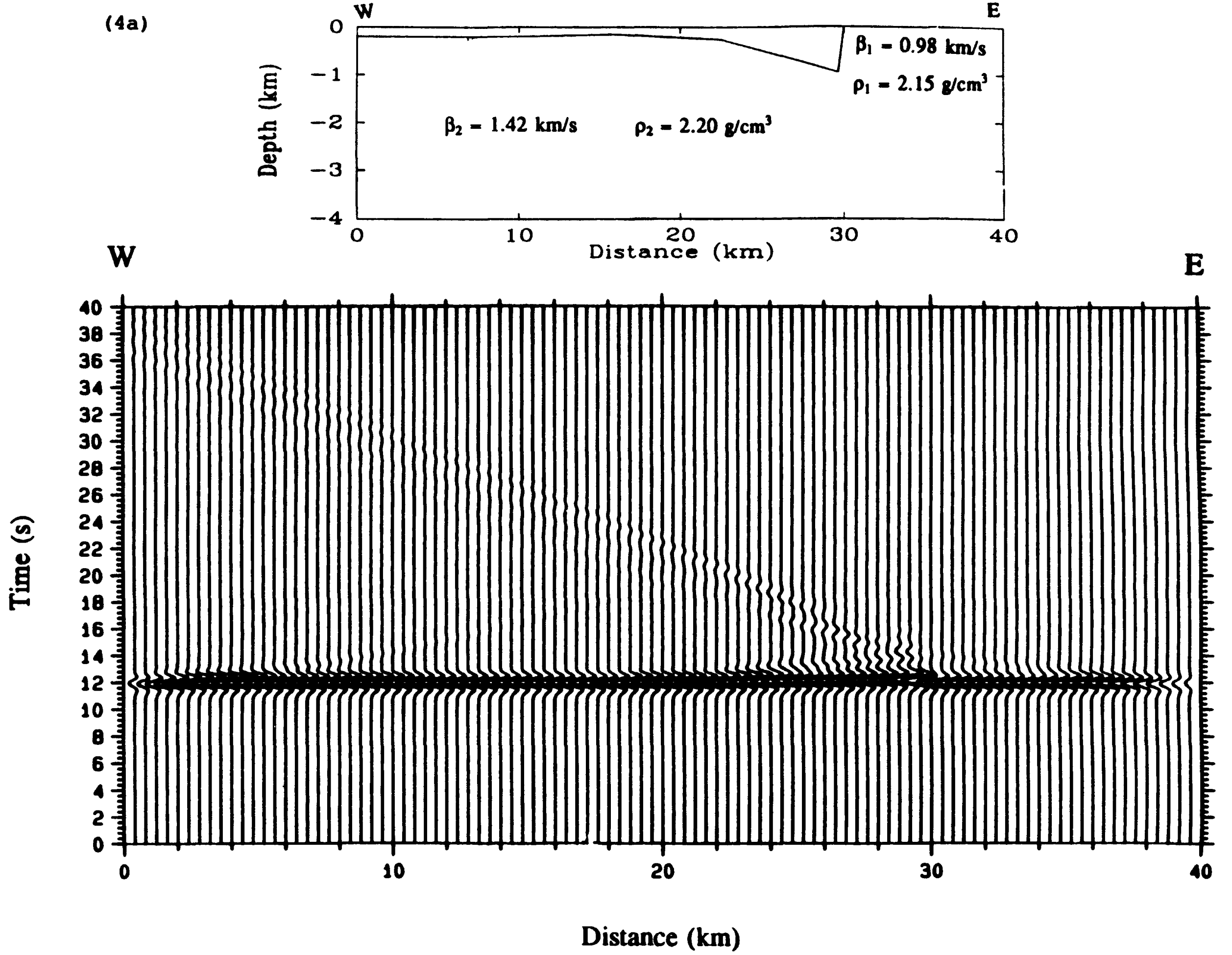

Figure 4. Plane wave SH responses for basin models of varying complexity. All seismograms are normalized to their maximum amplitude.

(4b)

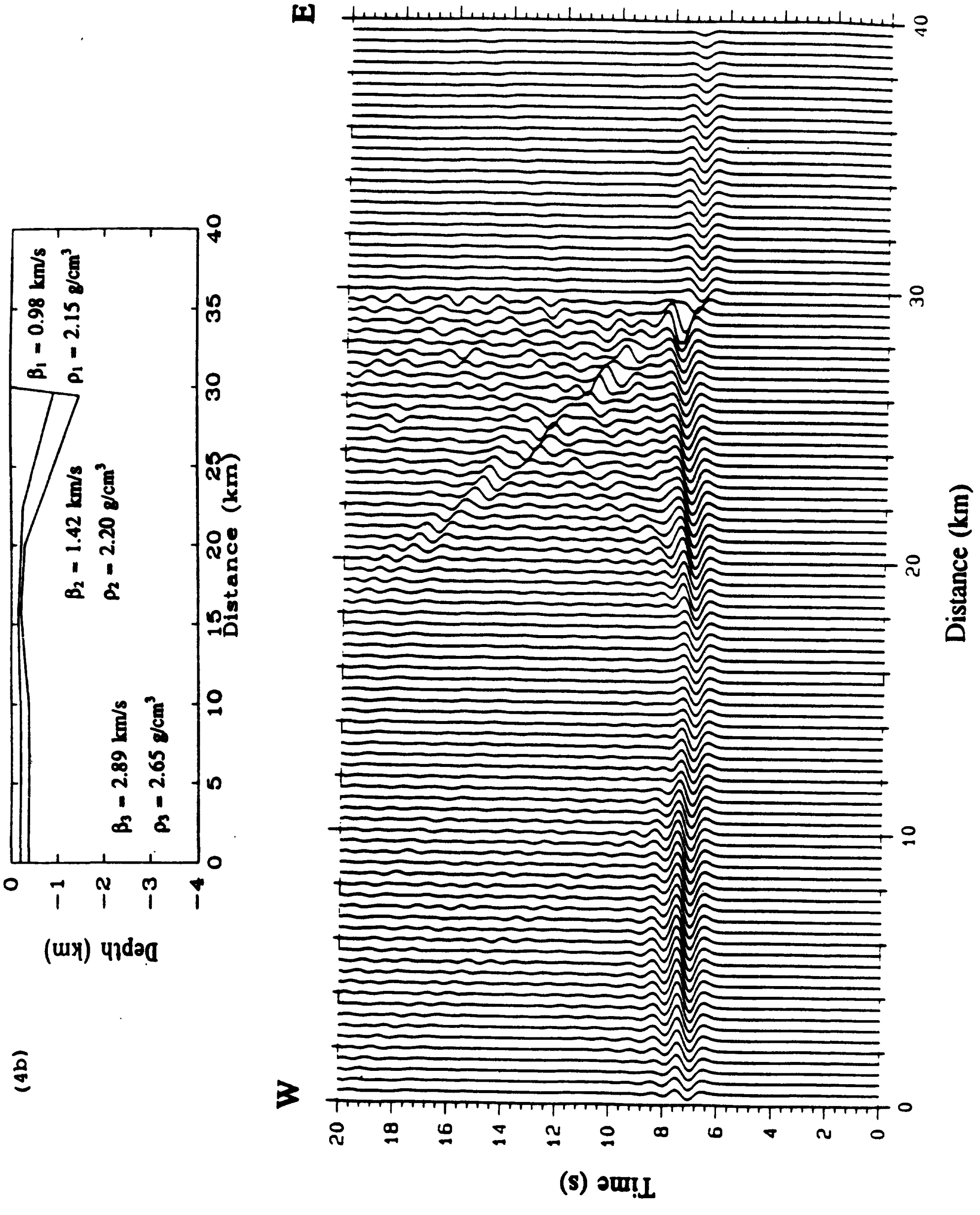
Depth (km)
0
−1
−2
−3
−4
0
5
10
15
20
25
30
35
40
Distance (km)
β₁ = 0.98 km/s
ρ₁ = 2.15 g/cm³
β₂ = 1.42 km/s
ρ₂ = 2.20 g/cm³
β₃ = 2.89 km/s
ρ₃ = 2.65 g/cm³
W
E
Time (s)
20
18
16
14
12
10
8
6
4
2
0
0
10
20
30
40
Distance (km)

(4c)

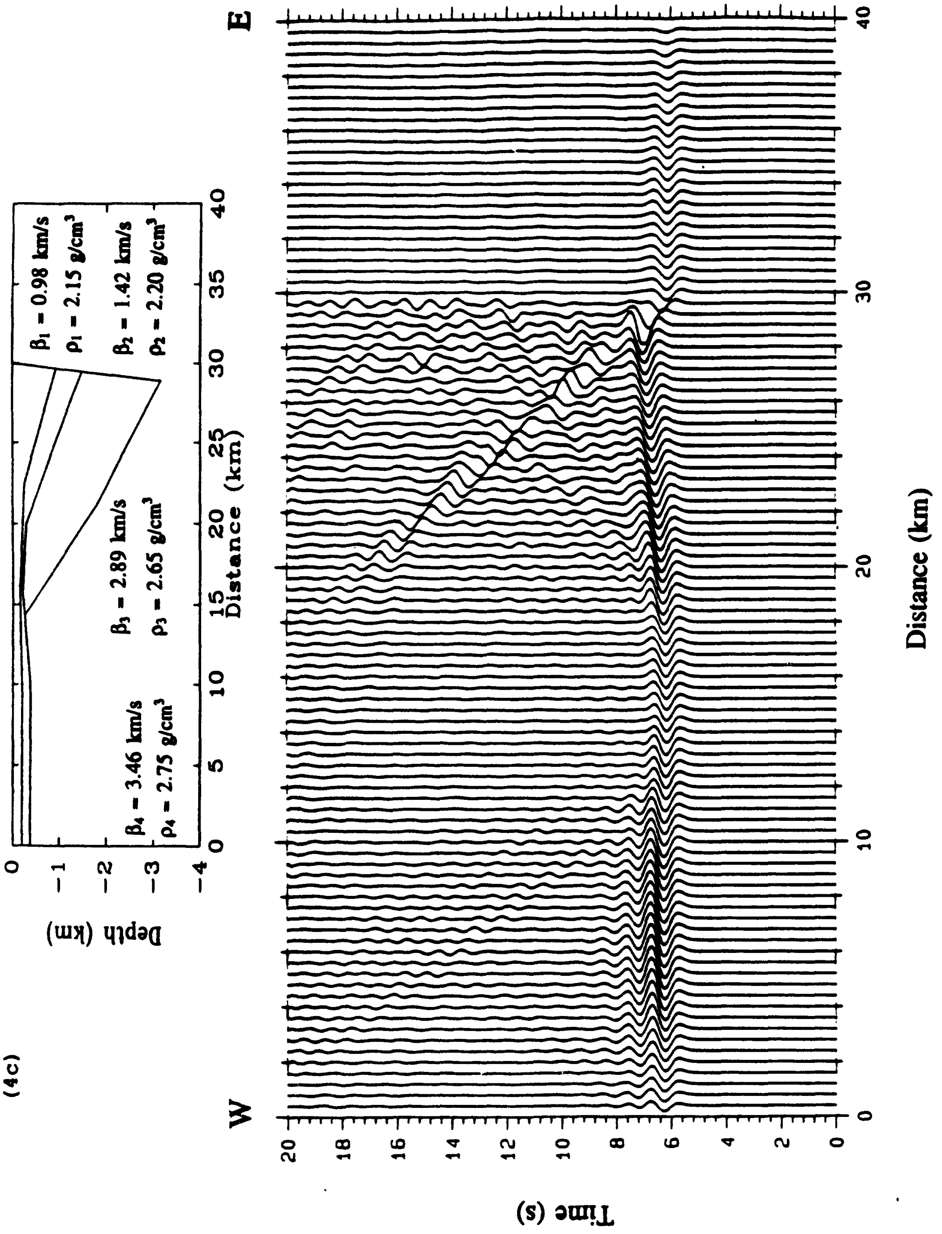
β₁ = 0.98 km/s
ρ₁ = 2.15 g/cm³
β₂ = 1.42 km/s
ρ₂ = 2.20 g/cm³
β₃ = 2.89 km/s
ρ₃ = 2.65 g/cm³
β₄ = 3.46 km/s
ρ₄ = 2.75 g/cm³
Depth (km)
0
−1
−2
−3
−4
0
5
10
15
20
25
30
35
40
Distance (km)
W
E
Time (s)
20
18
16
14
12
10
8
6
4
2
0
0
10
20
30
40
Distance (km)

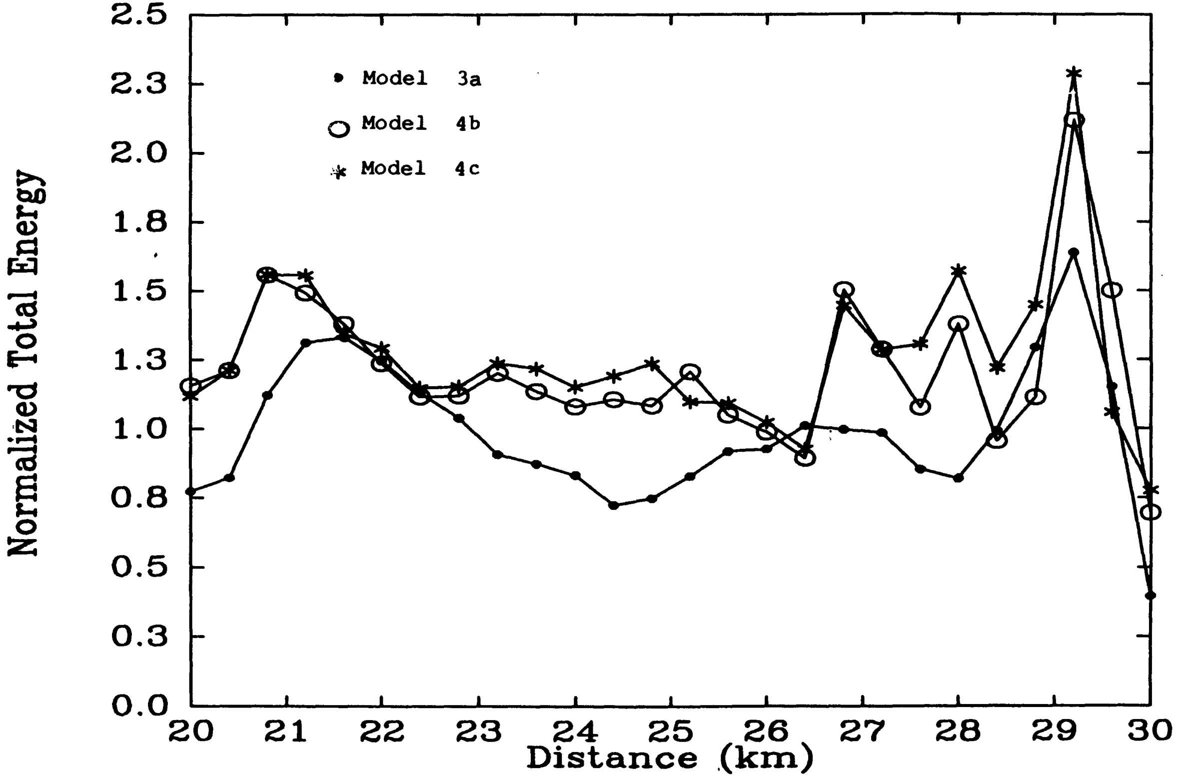

Figure 5. The integrated normalized energy from the seismic traces in Figures (3b), (4b) and (4c) is shown above.

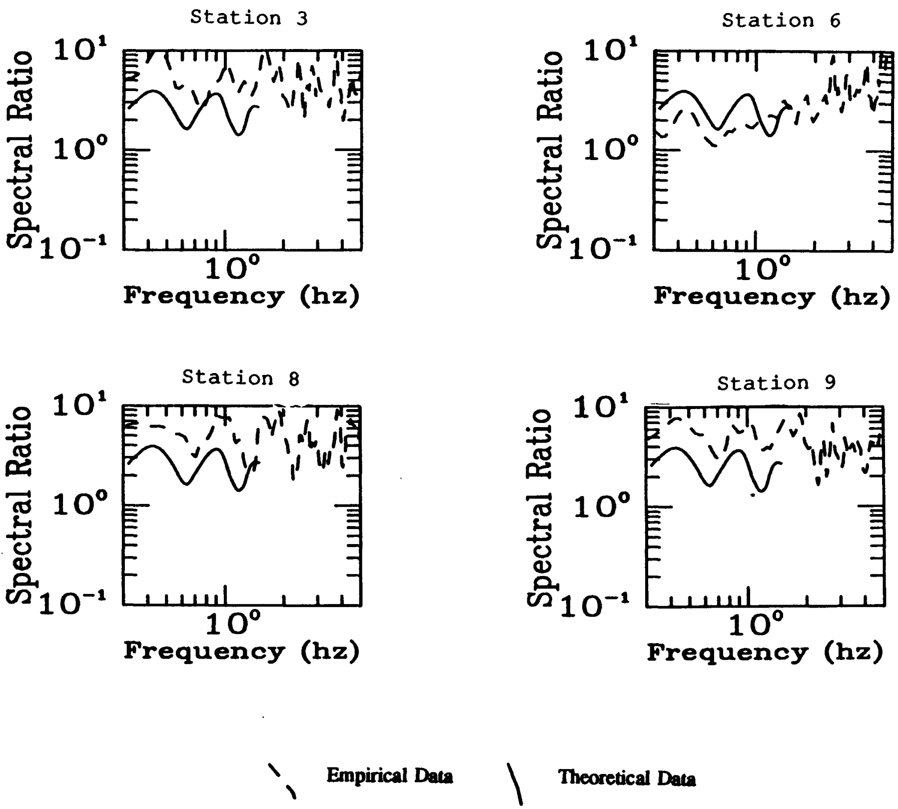

Figure 6. The USGS site responses (dashed lines) recorded from NTS blasts are shown above and their site locations are given in Figure (1a). The solid lines correspond to predictions from computer simulations using the Salt Lake Valley model in Figure (1a) and the site location is given by the arrow in Figure (1b). In this case, the simulations assumed a normally incident plane SH-wave banded between .1 and 2 Hz.

EARTHQUAKE HAZARD EVALUATION OF THE WEST VALLEY FAULT ZONE IN THE SALT LAKE CITY URBAN AREA

14-08-0001-G1397

Jeffrey R. Keaton

Dames & Moore, 250 E. Broadway, Suite 200
Salt Lake City, UT 84111 (801-521-9255)

INVESTIGATIONS

Existing shallow subsurface data from geotechnical investigations are being collected for systematic analysis using a stratigraphic model developed during research on a related project (No. 14-08-0001-22048). Drilling and trenching will be planned on the basis of the interpretations of the subsurface data and examination of stereoscopic aerial photographs. The goal of the present research is location of traces of the West Valley fault zone in the northern part of Salt Lake County.

RESULTS

The stratigraphic model appears to be useful in conjunction with geomorphic expression of faulting visible on aerial photographs for selecting sites for specific subsurface exploration.

Urban Hazards Seismic Field Investigations and the Study of the Effects of Site Geology on Ground Shaking

9950-01919

K. W. King and A. C. Tarr
Branch of Geologic Risk Assessment
U.S. Geological Survey
Denver Federal Center, MS 966
Denver, CO 80225
(303) 236-1591

Investigations

The objectives of this project are: (a) to improve the understanding of how shallow underlying geology affects ground motion, (b) to develop integrated techniques and methodologies for efficiently and effectively obtaining and processing digital seismic response data, seismic reflection and refraction data, seismic and geological borehole data, and building response data, and (c) to produce relative ground response maps for urban study areas. Specific goals for this reporting period were: (1) conclude seismic response measurements in the Wasatch Front urban area, (2) conclude the first phase of seismic response and shallow seismic geophysics studies in the Puget Sound-Portland urban areas, (3) complete shallow seismic studies of subsurface toxic waste sites near Farmington, New Mexico and a site on the Hanford Reservation in Washington, (4) test the feasibility of using a microcomputer in the field to examine Mini-sosie seismic data, (5) establish the design for a geotechnical data base which would link all data sets needed in the projection of a relative ground response map, and (6) begin the implementation of geographical information systems (GIS) technology for seismic hazards map production in the Pacific Northwest study area. Details of the field effort are:

(1) Wasatch Front

Ground response data were recorded at four sites on the Salt Lake Inter-island Dike locations and at five sites in the Ogden area. The Inter-island data have been analyzed. The results will be presented at the December Wasatch Front workshop. Down-hole compressional and shear wave profiles were obtained from 11 shallow bore holes in the Wasatch area. The down-hole data will be added to the existing data set for a final bore hole/shallow reflection report in the near future. Six additional high-resolution shallow reflection profiles were obtained in the west Salt Lake area.

(2) Puget Sound

Three field studies were conducted in the Pacific Northwest during the reporting period. Two studies concentrated on recording ground motions from nuclear tests at the Nevada Test

Site, chemical explosions at a coal strip mine in west-central Washington, and ambient seismic background vibrations. The third study used high-resolution shallow reflection means to obtain shallow (20'-300') subsurface velocity and structure profiles at 16 selected sites in the Seattle, 12 sites in Olympia and 3 sites in Portland urban areas. The sites were selected according to past earthquake intensity studies, surficial geology, and urban locations. A test of a prototype microcomputer system was completed during the reflection study (item 4). A six-station, semi-permanent, radio-telemetered seismic network was installed in the West Seattle area. A major structure at each of three of the site response locations was tested for basic engineering parameters (natural-period, damping, mode shapes).

(3) Waste Site Studies

High-resolution shallow reflection methods (HRSR) were used to map shallow subsurface structures at the Hanford site. The purpose of the experiement at the Hanford site was to see if the HRSR method could map structure on the top of and/or in a buried basalt stratum. The Farmington, New Mexico study used the HRSR method to map the buried liquid waste reservoir size and shape. Approximately 3 miles of HRSR profile were run and analyzed on the two projects.

(4) Field Computer

The use of a microcomputer in the recording truck of the field reflection system has been proposed as a cost-effective way to perform necessary preliminary data analysis in the field so as to fine tune the parameters for the HRSR methods. A test of a prototype microcomputer system was completed during the Pacific Northwest field study.

(5) Geotechnical Data Base

Production of a relative ground response map for a large urban area requires the acquisition and analysis of many hundreds of pieces of seismic, geological, and geotechnical data. The rational organization and manipulation of so much data requires a data base management system (DBMS) and a data base structure which permits linking many types of data. Portability of the DBMS and data sets to several kinds of computers and ability to access the data base in the field suggest implementation on a microcomputer system. A prototype design and implementation was completed during the reporting period; a report describing the implementation is now in review.

(6) GIS

Production of a seismic hazards map for an urban area requires integrating results of research (such as relative site response, landslide susceptibility, lifeline vulnerability) in a map format. GIS technology has shown promise in recent years as a powerful tool for spatial analysis and manipulation of data with geographical attributes. Because a seismic hazards map is multidisciplinary, an interdivisional investigation was established to use GIS technology in production of preliminary seismic hazards maps; this project took the lead in the investigation.

Results

Wasatch Front: Analysis of the site response data show that areas adjacent to the south edge of the Great Salt Lake have site response in the 0.5-5 Hz frequency band similar to the areas in the West Valley City area. The HRSR data and the down-hole data are being reduced and will be correlated with the site response data in the near future.

Puget Sound: The analysis of ths site response data in Olympia and Seattle correlates well with the intensity values obtained in the 1949 and 1965 earthquakes. Analysis of the HRSR data from West Seattle and Portland have very good profiles in the glacial sediments; however, the data from Olympia were of poor quality due to the extremely low velocities in the outwash tills and have not resulted (to date) in acceptable profiles. All data are being analyzed further.

Waste Site Study: The HRSR methods were able to map structure on the buried basalt layers (approximately 200-500 feet deep) at the Hanford area. The HRSR method was successful in mapping a shallow buried liquid waste zone (approximately 50-90 feet deep) in the Farmington, New Mexico area. The HRSR method is not a Mini-sosie reflection method; it is a shallow reflection method developed by USGS/KGS joint research effort.

Field Computer: The method has shown some success, but considerable more work is to be done in the software development and the data exchange methods.

Geotechnical Data Base: A prototype geotechnical DBMS was completed during the reporting period; and Open-file Report describing the DBMS has been completed by A. Tarr and is currently in technical review. The DBMS employs relational data base techniques and is implemented using dBase III Plus software on an IBM PC/XT microcomputer and VAX 11/750 minicomputer. The geotechnical data base consists of thirteen relations which contain various sets such as site response measurements, reflection and refraction profile data, intensity values, velocity models, and bore hole geology. The data base is implemented on two computers so that data analysis is possible using software only available on the VAX while data entry and retrieval operations are possible in the field using a portable microcomputer.

GIS: An interdivisional proposal entitled "Applications of Geographical Information Systems Technology for Pacific Northwest

Hazards Studies" was submitted to the GIS Task Force for support under the Director's GIS fund. The USGS participants are: A. Tarr (GD), M. Crane (NMD), and W. McFarland (WRD). Under the proposal, a GIS project would be established to integrate expertise and data sets from the respective Divisions to produce seismic hazards maps expected from the Regional Earthquake Hazards Assessment of the Pacific Northwest.

Reports

Brewer, W.A. and King, K.W., (abs.) Nuclear waste site characterization using shallow seismic profiling: 1987 Phoenix Oct. 26.

King, K.W., Algermissen, S.T., Carver, D., (abs.) Seismic ground response study in the Puget Sound Urban Areas: AGU Pacific Northwest Meeting, 1987.

Williams, R.A., King, K.W., Tarr, A.C., Carver, D.L., (abs.) High resolution shallow reflection study of glacial deposits, West Seattle Urban Area: AGU Pacific Northwest Meeting, 1987.

King, K.W. and Algermissen, S.T., (abs.), Seismic and vibration hazards investigation of Chaco Culture Historic Park: IAEG International Symposium, Athens, Greece, Sept. 19-23, 1988.

Algermissen, S.T. and King, K.W., (abs.), Seismic and vibration hazards investigation of Hovenweep National Park: IAEG International Symposium, Athens, Greece, Sept. 19-23, 1988.

Tarr, A.C. and King, K.W., 1987, USGS begins seismic ground response experiments in Washington: Washington Geologic Newsletter, Vol. 15, No. 2, p. 11-18.

Quaternary Geology Along the Wasatch Fault Zone, Utah

9950-04182

Michael N. Machette
Branch of Geologic Risk Assessment
U.S. Geological Survey
Box 25046, MS 966, Denver Federal Center
Denver, Colorado 80225
(303) 236-1243

Project members: M.N. Machette, A.R. Nelson, S.F. Personius, R.L. Wheeler, and K.A. Haller.

Investigations

1. Completed field investigations (mainly checked mapping and reviewed new trenches) along the Wasatch fault zone. Preliminary results from our 1986 trenches were presented in three poster sessions at the Rocky Mountain section of GSA.

2. Map compilation of Wasatch fault zone, 1:50,000 scale. Personius completed compilation of the Brigham City segment, and Nelson and Personius continued compilaton of the Weber segment. Machette completed compilation of the Utah Valley part of the Wasatch fault zone (American Fork, Provo, and Spanish Fork segments), although the description of units and explanation are not complete.

3. Scott and Shroba's 1:24,000-scale map of the Salt Lake City segment has been reformatted to fit our series, and is being recompiled at 1:50,000 scale by Personius, Haller, and Machette.

4. Radiocarbon dating. Personius prepared and submitted 4 samples of organic matter for ^{14}C dating by Steve Robinson (USGS-Menlo Park). Nelson prepared and submitted 19 samples of organic matter for ^{14}C dating by Robert Stuckenrath (University of Pittsburg). All of the samples collected from our Fall-1986 trenches have been submitted.

5. Nelson, Machette, and Wheeler participated in a USGS-sponsored workshop on "Directions in Paleoseismology" held April 23-24, 1987 at Albuquerque, N. Mex.

6. Reconnaissance of the Lemhi and Beaverhead faults (Idaho) and the Red Rock fault (Montana) was completed by Haller during the summer. Field investigations included scarp profiling at 45 locations, evaluating soil development at 18 critical sites, and checking mapping completed earlier in the year from aerial photo reconnaissance. These data will be the basis for evaluating the seismotectonic history of the region.

7. Wheeler completed routing his manuscripts on segmentation of the Wasatch fault zone. Two USGS Bulletins describe statistical and simulation methodology, and analysis and interpretation of evidence. A chapter for the Wasatch Professional Paper describes results, with applications to other historic Basin-Range normal faults (the reviewed drafts of chapters of this professional paper have been published together as an open-file report).

Results

1. Completion of our cooperative trenching effort with the Utah Geological and Mineral Survey has given us an expanded data base for analyzing recency and recurrence intervals of surface rupturing along the Wasatch fault zone. We now have at least one major trench site on the seven most active segments and will be able to test our hypothesis that the Wasatch fault zone has more segments (12) than the six originally proposed by Schwartz and Coppersmith (1984). In addition, the results of radiocarbon analyses will permit us to place tighter constraints on the times of most recent movement along the critical, urbanized parts of the fault zone.

2. The 1:50,000-scale map of the Brigham City segment has been through technical review and received branch approval. These maps will provide a comprehensive base for further evaluations of earthquake-hazards potential. We will publish the maps initially in the MF series (black and white, limited distribution) for early release (FY88-FY89) and later in the I series (color, wide distribution).

3. Cooperative research with S.L. Forman and James McCalpin (USGS contract work) on thermoluminescence (TL) dating of fault-scarp colluvium is proceeding with favorable results after a substantial amount of experimental work on bleaching and dose-rate determinations. Samples have been collected from new trenches along the Wasatch fault zone at Mapleton, Water Canyon, Nephi, Levan, American Fork, and East Odgen.

4. Although dating is incomplete, the American Fork Canyon trench site has yielded interesting results concerning the recency and possible recurrence intervals of large-magnitude earthquakes and associated surface ruptures along the American Fork segment of the Wasatch fault zone. Radiocarbon analyses of charcoal and organic matter (buried A horizons) from the trench reveal younger faulting than previously considered. Figure 1 and the associated table show the current control for timing of events at the trench site.

   The trenches at American Fork Canyon exposed Holocene alluvial fans, which we consider to have been stabilized 4,500-5,000 yrs ago on the basis of a ^{14}C date of 4,740 yrs B.P. These deposits commonly are displaced 7-8 m where the fault zone has a simple geometry of parallel normal faults. A preliminary TL age estimate from trench AF-1 suggests that the most recent faulting occurred before 400-550 yrs ago (sample ITL-U23; S.L. Forman, written commun., 1987), but after 980 ^{14}C yrs B.P. (A ^{14}C date from the youngest fault scarp colluvium is 140±120 ^{14}C yrs B.P., which we consider to be too young and thus erroneous.) In view of the fault scarp's degraded morphology, we previously thought the youngest event was <2,000 yrs. Thus, we are surprised by the young ages for the most recent event.

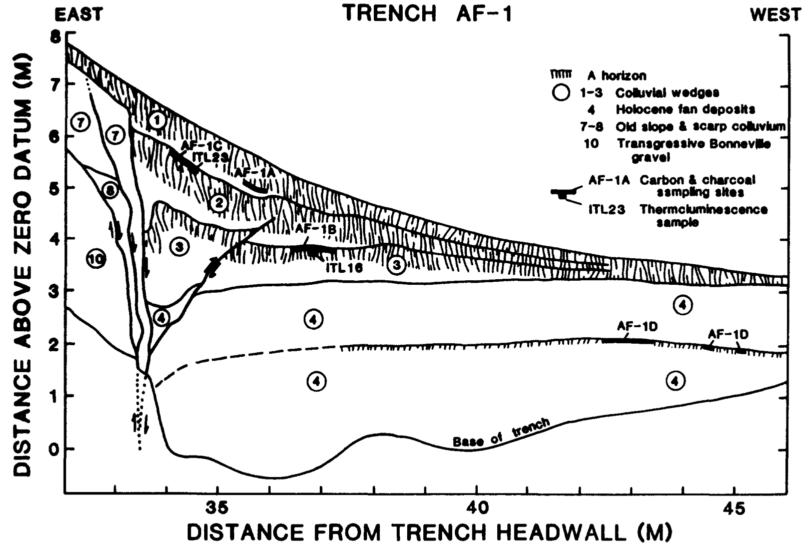

Samples listed from young (unit 1) to old (unit 4). Symbols: ^{14}C, radiocarbon date; TLB, TL age estimate by the total bleach method; TLR, TL age estimate by the regeneration method. TL data from S.L. Forman, written commun., 1987.

Sample No.	Geologic unit, remarks	Type of material; type of age control (and date)
AF-1A	1, near base of upper fault-scarp colluvium.	Charcoal; postdates last event. (^{14}C=140±120 yrs B.P. TAMS; erroneous)
ITL-23	2, top of middle fault scarp colluvium.	Silty A horizon; time of last event. (TLB=400±50 yrs B.P.) (TLR=500±50 and 550±50 yrs B.P.)
AF-1C	2, ...do...............	Organic matter in A horizon; maximum age of last event. (preliminary ^{14}C=980 yrs B.P., USGS)
ITL-16	3, top of lower fault scarp colluvium.	Silty A horizon; time of second event. (TLB=3,200±300 yrs B.P.) (TLR=2,400±300, 2,600±300 yrs B.P.)
AF-1B	3, ...do...............	Organic matter in A horizon; maximum age of second event. (preliminary ^{14}C=2,620 yrs B.P., USGS)
AF-1D	4, middle Holocene debris-flow deposit.	Charcoal; predates third event, maximum age of unit 4. (^{14}C=4,740±90 yrs B.P., TAMS)

FIGURE 1. Part of the log of trench AF-1, American Fork segment of the WFZ. Diagram shows three colluvial wedges (units 1-3) on the upthrown and downdropped fault blocks. Sample numbers refer to age control in table.

appear to yield younger ages than those on gentle scarps. Thus, because a scarp broken by repeated Holocene movement becomes higher and steeper with each succeeding event, an A horizon buried during the first fault event at a site would generally yield an older MRT age immediately after burial than would an A horizon developed on the steep scarp formed after the third or more event.

Using the above assumptions, there appears to have been at least three, and probably four, fault events recorded in the trenches across the two main scarps at the East Ogden site (table 1) since the debris-flow units were deposited 4,200 yrs ago. Both of the main faults probably ruptured the ground surface during the three largest events (a, b, and c on table 1). Displacement during event c seems to have been only about half that during events a and b. Mixing of near-surface stratigraphic units by burrowing and the problems with interpreting MRT ages on these units make it difficult to prove that the westernmost scarp at the site has been displaced by a small event within the past 500-600 yrs; if so, the displacement was probably <0.8 m. These conclusions raise questions about the minimum size of displacement that can be recognized in trenches, about whether large later events destroy evidence of small earlier events, and about the limits of MRT ages in resolving fault events spaced 500-1,000 yrs apart.

TABLE 1.--Estimates of fault-event displacements and ages for five trenches at the East Ogden site on the northern part of the Weber segment of the Wasatch fault zone.

Trench	Fault event	Maximum wedge(s) thickness (m)	Estimated displacement (m)		Estimated age (yrs B.P.)
			Stratigraphic	NVT	
EO-1	a	>1.6	2.8	2.2	<4.2
	b	2.0	2.6	2.1	[1]≈3.5
	c	0.8	0.9	0.9	<1.0
EO-2	a	<3.0	2.5	2.5	3.0-4.2
	b	1.9	3.5	3.5	1.0-3.0
	c	1.2	2.2	2.2	<1.0
EO-3	c	>1.2 (2)	2.0	1.2	<1.0
	d	<0.9	1.2	0.8	<0.6
EO-4	c or d	0.7	1.4	1.2	<0.5-1.0
EO-5	c	0.8	1.8	1.2	<0.8

[1] Preliminary TL age estimate (standard deviation at least a few hundred years) for the oldest distal colluvial sediment deposited following this event based on analyses by Steve Forman (INSTARR, University of Colorado, oral commun., 1987).

The TL regeneration age-estimate from sample ITL-U16 places the second-most-recent fault event at about 2,400-2,600 yrs B.P. (S.L. Forman, written commun., 1987), which is close to a preliminary radiocarbon age of 2,620 ^{14}C yrs B.P. from the buried soil. The third and oldest fault event in trench AF-1 must have occurred after 4,740±90 ^{14}C yrs B.P. (sample AF-1D), which is the age determined from debris-flow deposits under the third and lowest colluvial wedge. We estimate that the youngest part of the debris flow is about 4,500 ^{14}C yrs on the basis of the position of the radiocarbon sample and lack of buried soils (the oldest colluvial wedge buried fresh debris-flow material).

Trenching of the fault scarps on Holocene deposits shows that three surface faulting events contributed subequal amounts to the 7-8 m of net displacement recorded since about 4,500 ^{14}C yrs B.P. The three Holocene events produced discrete colluvial wedges that were exposed in all the trenches, although only two events are indicated in the third trench (AF-3). Although some of our radiocarbon analyses are still pending, preliminary radiocarbon dates, TL age estimates, and stratigraphic relations constrain the three Holocene fault events between about 500(?) yrs and 4,500 ^{14}C yrs ago. Faulting must have occurred over intervals longer than several hundreds of years (probably 1,000-2,000 yrs) in order to develop the moderately thick A horizons we found on each of the wedges in AF-1.

5. A total of 32 samples of organic carbon (organic matter or charcoal) have been prepared for radiocarbon analysis, and as of Oct. 1 we had received the results for 23. Nineteen of the age determinations were performed by Stuckenrath at the Univ. of Pittsburg (see table 1). Most of these samples are from Nelson's trenches at East Odgen.

Radiocarbon analyses of 3 charcoal samples and 16 concentrated A-horizon samples from five trenches at the East Ogden site on the Weber segment of the Wasatch fault have been completed. The results highlight many of the problems with using soil A-horizon MRT (mean residence time) ages to estimate the timing of faulting events on normal faults. Of the 10 samples collected within 1 m of the present surface, two pairs of sample ages were inverted (lower sample younger than a stratigraphically higher sample) and four samples yielded >112 percent modern carbon. These anomalous results are probably due to incorporation of modern "bomb" carbon into the A-horizon samples by mixing of surface sediment into the lower part of the A-horizon (burrows) and possibly by rapid migration of humic acids in near-surface ground water of coarse-grained materials. Several MRT ages may also reflect reworking of old A-horizon sediment exposed in fault scarps into new A horizons that develop on colluvial debris wedges adjacent to the scarps. Thus, fault events recorded by near-surface units (<1-m depth) are difficult to accurately date using MRT ages, at least at sites where most units are sandy to gravelly.

Ages for deeply buried horizons appear more consistent than shallow-samples, but only a single age is available for each event in each trench (table 1). Based on our limited data for shallow-samples, A-horizon sediment from the center of a 20- to 40-cm-thick modern A horizon on a typical scarp along the Wasatch fault would yield an age of 100-400 yrs B.P. if no bomb carbon were present. On steep scarps, A horizons

Unpublished results of FY86 investigations (Nelson) suggest events a, b, c, and possibly an earlier event are recorded at Garner Canyon, 6 km north of East Odgen. Displacements at Garner Canyon are less than half the size of displacements at East Ogden for the same events, as would be expected for a site only 5 km from the end of a major fault segment. Less dating control is available at the Kaysville site (Swan and others, 1980), 22 km south of East Ogden near the center of the Weber segment. Their maximum age for the two youngest events at Kaysville suggests events c and d (East Ogden site) were recorded there. If so, displacements during event c were comparable at the two sites, but displacement during event d was greater at Kaysville than at East Ogden and not recognized at Garner Canyon. Possibly, event d is the result of an earthquake that ruptured only the central part of the Weber segment in the past 500-600 yrs.

6. Preliminary evaluation of data gathered by Haller indicates that the Lemhi, Beaverhead, and Red Rock faults are all segmented and surface faulting has occurred on at least one segment of each fault in the past 15,000 yrs. The morphology and distribution of the fault scarps on alluvium show striking similarity to the Lost River fault, west of this study area.

7. Wheeler's work on the Wasatch fault zone led to the conclusion that persistent segment boundaries have controlled large rupture zones throughout much or all of the evolution of the fault zone at the Pleasant View, Salt Lake, Traverse Mountains, and Payson salients. He also concluded that persistent segment boundaries should exist on other normal-fault zones in the Basin and Range Province where exposed or shallowly buried transverse bedrock ridges (some with salients) indicate accumulated slip deficits, and where two or more individual large rupture zones have started or stopped. Testing this model against five historic earthquake sequences in the Basin and Range indicates the existence of two persistent boundaries on the Lost River fault zone of Idaho (which ruptured in 1983), one persistent boundary between the Dixie Valley and Fairview faults of Nevada (December 1954), and one persistent and one nonpersistent boundary in the Pleasant View, Nevada, rupture zone (1915). The north end of the Dixie Valley fault is not a segment boundary, persistent or otherwise. There is too little information available to test the model for both ends of the Rainbow Mountain, Nevada, rupture zone (July-August 1954), the south end of the Fairview Peak rupture zone, and the north end of the Pleasant Valley rupture zone. The Hebgen Lake, Montana, earthquake (1959) occurred on a fault zone that is too young for the model to apply: it appears that the fault-zone geometry is still evolving. Boundary names and locations for fault zones other than the Wasatch are as follows.

Fault zone	Boundary name	Type	Location
Lost River, Idaho.	Willow Creek Hills.	Persistent...	Between Warm Spring and Thousand Springs segments.
Do.	Elkhorn Creek	....do.......	Between Thousand Springs and Mackay segments.
Dixie Valley, Nev.	Pirouette Mountain.	....do.......	Between Dixie and Fairview Valleys.
Various, at Pleasant Valley, Nev.	Sou Hills.....	....do.......	Sou Hills scarp of 1915.
	(Unnamed).....	Nonpersistent	Gap between Tobin and Pearce scarps of 1915.

Related results are reported under project 9950-01207 (S.T. Algermissen, project chief).

Reports

Hawley, J.W., and Machette, M.N., 1987, Late Cenozoic evolution of basins and valleys in the southern Rio Grande rift: Geological Society of America, Abstracts with Programs, v. 19, no. 7, p. 697.

Machette, M.N., 1987, Neotectonics of the Rio Grande rift, New Mexico: Geological Society of America, Abstracts with Programs, v. 19, no. 7, p. 754.

Machette, M.N., 1987, Preliminary assessment of paleoseismicity at White Sands Missile Range, southern New Mexico--Evidence for recency of faulting, fault segmentation, and repeat intervals for major earthquakes in the region: U.S. Geological Survey Open-File Report 87-444, 40 p.

Machette, M.N., Personius, S.F., and Nelson, A.R., 1987, Quaternary geology along the Wasatch fault zone--Segmentation, recent investigations, and preliminary conclusions,Chapter A in Hays, W.W., and Gori, Paula, eds., Assessment of Regional Earthquake Hazards and Risk along the Wasatch Front, Utah; U.S. Geological Survey Open-File Report 87-585, v. I, p. 1-72.

Wheeler, R.L., and Krystinik, K.B., 1987, Evaluating coinciding anomalies along a fault trace or other traverse--Simulations and statistical procedures: U.S. Geological Survey Bulletin 1802 (in press).

______1987, Persistent and nonpersistent segmentation of the Wasatch fault zone, Utah--Statistical analysis for evaluation of seismic hazard, in Hays, W.W., and Gori, Paula, eds., Assessment of regional earthquake hazards and risk along the Wasatch Front, Utah: U.S. Geological Survey Open-File Report 87-585. (Also submitted as Professional Paper).

______1988, Segmentation of the Wasatch fault zone, Utah--Summaries, analyses, and interpretations of geological and geophysical data: U.S. Geological Survey Bulletin 1827 (in press).

Determining Landslide Ages and Recurrence Intervals

9950-03789

Richard F. Madole
Branch of Geologic Risk Assessment
U.S. Geological Survey
P. O. Box 25046, MS 966
Denver, Colorado 80225
(303) 236-1617

Investigations

1. Earthquake-induced landslides and liquefaction in western Washington.

2. Landslide recurrence intervals, Wasatch Plateau, Utah.

Results

1. Western Washington

Earthquake-induced landslides

Data from a reconnaissance study of the Ribbon Cliff landslide near Entiat, Washington (a possible earthquake-induced landslide), suggests that this slide is considerably older than previously thought. Opinion differs as to the age and origin of the slide. Several publications list it as having been caused by the 1872 earthquake, and use the slide to estimate the position of the earthquake epicenter. However, Kienle and others (1978), in a report prepared by Shannon and Wilson, Inc., Geotechnical Consultants, use dendrochronological data to show that the main body of slide debris has not moved significantly in the past 215 years. I concur with this conclusion. On the basis of the percentage of lichen cover on the main body of slide debris and the presence of a weakly developed soil locally, I estimate that the age of the majority of slide debris may be on the order of millennia rather than centuries.

Liquefaction

The areas in the Puget Lowland most susceptible to liquefaction are on valley floors within and near the estuaries of the major rivers that drain into the Puget Sound from the Cascade Range to the east. These areas are underlain by sections of predominantly fine sand and sandy silt, commonly 20-30 m thick, and water table is usually at a depth of less than 3 m. Although Holocene alluvium is widespread on the floors of these valleys over much of the Puget Lowland, the alluvium is generally gravelly (therefore less susceptible to liquefaction than sandy sediment), except within 5-10 km of the Puget Sound. The interstream areas of the Puget Lowland are covered almost entirely by late Pleistocene glacial drift, most of which has a low susceptibility to liquefaction.

Although areas highly susceptible to liquefaction are apparently extensive, severe constraints exist with respect to identifying paleoliquefaction features. The greatest constraint is the exceptionally limited amount of exposed Holocene stratigraphy, and liquefaction features are generally too large to be identified solely by coring. Much of the area most susceptible to liquefaction is within 0-2 m of sea level and/or water table, which is one of the conditions that promotes liquefaction; hence, natural stratigraphic exposures are few and shallow. Also, urbanization and modification of the landscape is extensive in and near the large estuaries; several estuaries are major ports (for example, Seattle, Tacoma, and Olympia). Lastly, cutbank exposures along the lower reaches of the rivers are uncommon because of extensive construction of levees for flood protection and use of rip-rap to prevent erosion of the levees and river banks.

The Skagit River deltaic plain, possibly including the adjoining deltaic plain of the Stillaguamish River, was selected as the best area in which to search for paleoliquefaction features using aerial photography and trenching because of the size of the plain, the character of the sediment, lack of urbanization, and the great extent to which agriculture maintains large tracts of bare ground and low or cropped vegetation. The lower Chehalis River valley will serve as a secondary area for study, because it contains a thick section of chiefly sandy sediment derived mainly from areas south of the limit reached by glacier ice of the Puget lobe. The rivers in the vicinity of Seattle, Tacoma, and Olympia are less suitable because of extensive modification and urbanization of valley floors. The Nisqually River deltaic plain, near Olympia, is an exception, but conversion to a wildlife refuge ended farming there, and allowed dense stands of tall grass and other vegetation to become reestablished, reducing the potential for locating liquefaction features in this area with aerial photography.

Study to date indicates that two, possibly three, fluvial deposits of Holocene age are widespread on the valley floors of the Puget Lowland. Although little work has been done previously on these deposits, their Holocene age is well established by many ^{14}C ages obtained for Pleistocene units present along the valley sides and on the adjoining uplands. The ages of these stratigraphic units can be used to date liquefaction in much the same manner as the ages of displaced stratigraphic units are used to date movement on faults.

2. Wasatch Plateau, Utah

Three ^{14}C ages obtained during 1987 of charcoal from landslide-dammed lake deposits in Manti Canyon, Utah, show that stratigraphic relations of lake deposits and alluvium deposited in response to landslide damming of valleys must be interpreted carefully. What may appear superficially to be a single alluvial fill or lake deposit may, in fact, be a nested set of deposits of different ages that filled the valley to about the same level during each interval of damming.

The three ^{14}C ages show that (1) a major episode of slope movement, which produced lateral ridges on Manti slide about 2,000 years ago (reported on previously), also temporarily dammed Manti Creek about 2,130 ± 55 yr B.P. (PITT-15), (2) the last major movement of the Manti slide prior to the 1970s occurred after 1,345 ± 65 yr B.P. (PITT-13), probably about 1,000 B.P. based on the degree of soil development in pond deposits translocated by the movement, and (3) the last episode of landslide damming of Manti Creek near the toe of the Manti slide occurred about 1,515 ± 50 yr B.P. (PITT-14), but was caused by the failure of North slide on the opposite side of the canyon from the Manti slide.

An estimated 10,000 mollusks were identified in samples collected on or near the Manti slide from translocated pond deposits, soils buried by lateral ridges, and landslide-dammed lake deposits and alluvium. The specimens represent 32 taxa, 29 of which are gastropods and 3 are pelecypods. The diversity of the fauna and the relative proportions of terrestrial, aquatic pulmonate, and aquatic gill-bearing gastropod species appears to distinguish environments of deposition. This finding should prove useful in subsequent studies that consider the record of landslide recurrence as recorded in fissures and other depressions caused and maintained by repeated slope movements.

Chronology of Paleoearthquakes on the Wasatch Fault Zone by Thermoluminescence (TL) Dating

Contract #:14-08-0001-G1396

James McCalpin
Dept. of Geology
Utah State University,
Logan, Utah 84322,
(801) 750-1220

Steven L. Forman
Center for Geochronological Research
Univ. of Colorado,
Boulder CO. 80309-450
(303) 492-6072

Objectives: This study focuses on developing and applying the relatively new thermoluminescence (TL) technique to date Holocene and Pleistocene surface-faulting events on the Wasatch fault zone. For the TL technique to be useful sediment must have been exposed to light for a sufficient time during sedimentation to reduce previously acquired TL. After deposition, the TL signal accumulates in the mineral grains by exposure to ionizing radiation from the decay of radioactive elements. The TL technique directly dates mineral grains, reflecting the time since deposition of the sediment.

In conjunction with U.S. Geological Survey the Ogden, Provo, Salt Lake and other segments of Wasatch fault zone have been sampled for thermoluminescence dating. Targeted samples for analyses are faulted loess and pond silts and fault derived colluvial-wedge sediments. The accuracy of the TL method is tested by dating modern and radiocarbon dated sites. These analyses are providing better constraints for defining the timing and re-occurrence of faulting events as well as ascertaining the extent of fault segments.

Data Acquisition and Analysis: The first six months of this project have been devoted to sample collection and TL analysis. Ninty-five TL samples were collected from 11 trench sites along the Wasatch fault zone (Fig. 1); analyses are complete or in progress for 20 of those samples.

1. Initial efforts concentrated on defining the TL properties of sediments commonly encountered in the depositional environments near the Wasatch fault zone. The most common sediments are scarp-derived colluvium (proximal and distal), debris flow-alluvium, sag-pond muds and loess. In addition, buried A horizons are found developed on any of the above sediment types. Progress in defining the suitability of each sediment type or soil for TL dating is briefly summarized below.

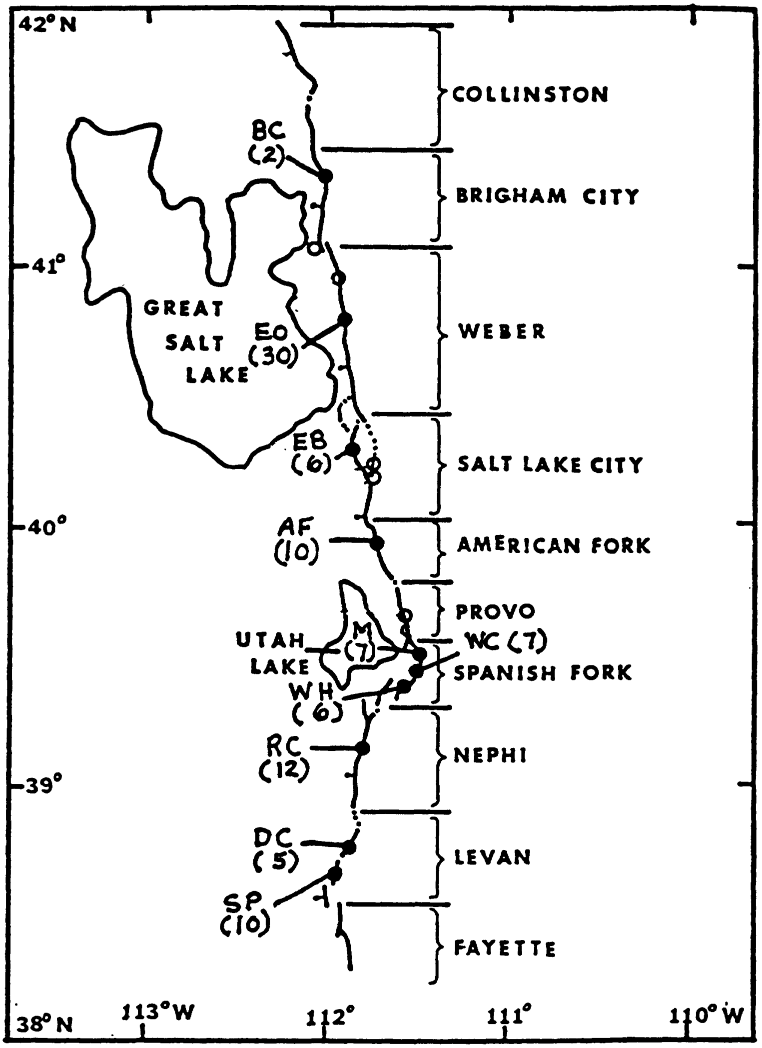

Figure 1: Map of the 10 Wasatch fault zone segments showing locations of and number of TL samples collected at each trench site. BC = Brigham City, EO = East Ogden, EB = East Bench Fault, Dresden Lane, AF = American Fork, M = Mapleton, WC = Water Canyon, WH = Woodland Hills, RC = Red Canyon, DC = Deep Creek (natural exposure), SP = Skinner Peaks. Number in parentheses indicates total number of TL samples collected at each site.

a. Proximal colluvium: Stony proximal colluvium shed from fault scarp free face has not yet been tested for TL properties. Depositional models (A.R. Nelson, pers. commm.) suggest the TL signal of these sediments is not adequately reduced by light prior to deposition and would yield TL dates closer to the age of the derived material than the tectonic event that deposited the colluvium. TL analysis of proximal colluvium from modern (1983, Borah Peak earthquake) and pre-historic wedges will be preformed in the next 6 months.

b. Distal colluvium: Sandy and silty distal colluvium is believed to accumulate from slopewash deposition and should be well light bleached prior to deposition, however to date no modern samples have been sampled to confirm this assumption. Two samples of distal colluvium from trench EO-1 at East Odgen have been dated. The lower sample yielded a TL age-estimate of 2.8 ± 0.3 ka, while a sample 1.2 m above and 0.4 m below the modern surface yielded an age estimate of 0.9 ± 0.1 ka. These dates are consistent with radiocarbon chronology for this site (A.R. Nelson, personnal communication).

c. Debris flow alluvium: TL properties of a buried debris flow from Deep Creek site indicate that this sediment type is poorly light bleached. This sediment type can not be accurately dated by TL.

d. Sag pond sediments: A modern sag pond mud shows complete initial light bleaching and yields a TL age estimate of <300 years. A buried sag pond from trench 2 at American Fork gave the TL age estimate of 0.5 ± 0.1 ka, which is in agreement with radiocarbon date on a subjacent soil of 800 ± 70 yr B.P. (M.N. Machette, pers. comm.).

e. Loess: Loess is one of the sediment types most amenable to TL dating. Unfortunately special depositional conditions must prevail to allow the trapping and preservation of loess in the normal fault-scarp environment. A buried loess from trench 1 and trench 3, American Fork, yielded TL age estimates of 6.7 ± 3.0 ka and 7.2 ± 1.0 ka which are in agreement with the radiocarbon date on charcoal of 7290 ± 100 yr B.P. (AA-2268; M.N. Machette, pers. comm.)

f. Buried A horizons: Previous studies (Wintle and Catt, 1985; Forman et al, in press) have demonstrated that A horizons of soils are well light bleached and amenable to TL dating. Buried A horizons commonly occur in Wasatch fault zone excavations developed on either faulted alluvial fan surface or fault derived colluvium. The lower and upper A horizons from tench 1 at American Fork gave TL age estimates of 2.7 ± 0.3 ka and 0.5 ± 0.1 ka which are in good agreement with the corresponding radiocarbon dates of 2620 ± 70 yr B.P.

(USGS-2531) and 980 ± 70 yr B.P. (USGS-2532; Machette, et al, pers. comm.). Preliminary TL age estimates on buried A horizons from South Mapleton (5.5 ± 0.5 ka), Deep Creek (1.0 ± 0.2 ka) and Red Canyon (15 ± 2 ka) are consistent with geologic and radiocarbon age constraints. The TL dating of buried A horizons is a focus of this project, because of it's closely limiting nature for constraining fault timing and because of the potential independent radiocarbon control from adjacent samples.

2. TL age constraints on paleoseismic events on the Wasatch fault zone: This aspect of the project is in the developing stages. TL age estimates from the American Fork segment suggest that the earliest faulting event was post 7 ka years ago. The penultimate faulting event occurred ca. 2.6 ka ago followed by the latest seismic event 500-1000 years ago. Additional laboratory analysis will provide similar chronologic control for paleoearthquake events on other segments of the Wasatch fault zone.

Acknowledgments

Much of laboratory analyses were completed by M.E. Jackson and P. Maat. Jackson was also responsible for excavations on the Levan and Nephi Segments. We proffer sincere appreciation to M.N. Machette, A.R. Nelson, A.J. Crone and W. Lund for collaboration in the field and the laboratory.

Publications

Forman, S. L., Jackson, M.J. and McCalpin, J., 1987: Thermoluminescence (TL) dating studies of colluvial and alluvial sediments from Utah and Colorado: preliminary results. Geological Society of America Abstracts with Programs, Rocky Mountain Section, v. 19(5): 275.

Jackson, M.J., Forman, S.L. and Machette, M.N. 1987: Dating paleoseismic events using the thermoluminescence (TL) dating method: Preliminary results. EOS Transactions, American Geophysical Union, 68(44): 1287.

Forman, S.L. (in press): Application and limitation of thermoluminescence to date Quaternary sediments: In "INQUA Volume on Quaternary Dating Methods" Quaternary Science Reviews

Forman, S.L., Jackson, M.E., J. McCalpin and Maat, P., (in press): The potential of using thermoluminescence to date buried soils in colluvial and fluvial sediments from Utah and Colorado, U.S.A: preliminary results. Quaternary Science Reviews

Forman, S.L., Maat, P. and Jackson, M.E. (in press): The Thermoluminescence dating of paleoearthquakes: recent results and future prospects. Geol. Soc. of Amer. Abstracts with

Programs, Cordileran Section.

References Cited

Forman, S.L., Jackson, M.E., J. McCalpin and *Maat, P., (in press): The potential of using thermoluminescence to date buried soils in colluvial and fluvial sediments from Utah and Colorado, U.S.A: preliminary results. Quaternary Science Reviews

Wintle, A.G. and Catt, J. (1985). Thermoluminescence dating of soils developed in late Devensian Loess at Pegwell Bay, Kent. Journal of Soil Science, 36, 293-298.

Database Management

9910-03975

Charles S. Mueller
Branch of Engineering Seismology and Geology
U.S. Geological Survey
345 Middlefield Road, MS 977
Menlo Park, California 94025
(415) 329-5646

Investigations

1. Development of techniques for data playback, processing, management, and export with emphasis on large datasets collected with portable digital event-recording seismographs (e.g., GEOS).

2. Design and implement relational databases for strong-motion (ESM) and aftershock/special-experiment data (ESGDB). The goal of the databases is to enhance researcher access to diverse Branch datasets.

Results

1a. No new datasets.

1b. The following datasets were exported to other research institutions:

Coalinga aftershock data: Stanford University

Imperial Valley Differential Array data: Woodward-Clyde Consultants, Pasadena, CA.

1c. A new block-binary seismogram file header standard was developed and incorporated into existing seismic analysis programs.

2. ESGDB: Design and update of seismic trace table was completed.

Reports

None.

10/87

Earthquake Recurrence and Quaternary Deformation in the Cascadia Subduction Zone, Coastal Oregon

9950-04180

Alan R. Nelson and Stephen F. Personius
Branch of Geologic Risk Assessment
U.S. Geological Survey
Box 25046, MS 966, Denver Federal Center
Denver, Colorado 80225
(303) 236-1596; FTS 776-1596

Investigations

A fundamental question in earthquake hazards research in the Pacific Northwest is whether great earthquakes will occur on the Cascadia subduction zone in western Washington and Oregon. The present seismic quiescence in the region may reflect (1) aseismic subduction of the Juan de Fuca plate, (2) a locked plate interface where accumulating stress results in a great earthquake, or (3) possibly a locked interface due to rapidly slowing subduction during the Quaternary. If seismic subduction is continuing in the Washington portion of the zone, slip along the plate interface in Oregon may have ceased. To resolve these issues, both the Holocene and the late Quaternary geologic records in the Cascadia zone in Oregon must be examined for evidence of coseismic and interseismic deformation.

If great earthquakes have occurred in the Cascadia subduction zone, there should be a record of coseismic uplift, submergence, or liquefaction in the Holocene sediments along the Pacific Northwest coast. Nelson is studying the character of middle and late Holocene (0-5 ka) sea-level rise along the central Oregon coast, chiefly by studying outcrops and cores in carefully selected estuarine marshes. These deposits have the advantages that (1) coring can provide a record of submergence as well as uplift, (2) independent types of faunas sensitive to sea-level changes (marsh plants, foraminifera, diatoms) can be studied separately, and (3) small amounts of organic material in cores can be ^{14}C dated by accelerator techniques. Rocky headlands are also being examined for evidence of raised intertidal fossils indicative of Holocene uplift. Emphasis will be placed on identifying episodes of sudden uplift or subsidence (probably 0.5-2 m/event) and distinguishing those that may be coseismic from those produced by other processes. If great earthquakes have occurred in the region, recurrence is probably in the 500- to 2,000-year range.

Long-term (late and middle Quaternary) deformation of the Oregon Coast Range is being investigated by Personius. This study will attempt to determine rates and styles of deformation by using fluvial terrace sequences, which trend perpendicular to the coast, as datums. Fieldwork in July and August was concentrated on the Umpqua, Smith, and Siuslaw Rivers in the central Oregon Coast Range. Over 40 exposures of terrace sediments ranging in height from 1 to >100 m were examined. Numerous samples of wood, charcoal, and peat will allow radiocarbon dating and correlation of the lower terraces. Samples taken in the silty overbank facies will be dated using thermoluminescence analysis (TL); the TL-dated terraces, and three different volcanic ashes discovered in other terrace sediments will be used to correlate the older remnants. These correlations will be used to construct longitudinal terrace profiles from which rates and styles of deformation will be derived.

Results

There appear to be striking differences in the history of late Holocene relative sea level along the south-central Oregon coast. Detailed work will be required to determine if these differences are due to regional or local tectonic effects or other processes.

Nelson took cores and examined outcrops at 18, tidally-dominated, estuarine marsh sites in six estuaries between Bandon and Florence. Most sites yield cores with, at most, one buried mud-peat couplet similar to those in southwestern Washington suggested by Atwater to be coseismic. Thus, most sites show a stratigraphy characteristic of slowly submerging coasts with no abrupt changes in sedimentation. An alternate possibility is that coseismic jerks of subsidence have occurred, but that rapid sea level rise and low sedimentation rates have not allowed marsh surfaces to develop between submergence events.

In contrast, in the South Slough arm of Coos Bay, 10 cores show four to eight abruptly buried marsh surfaces that are 0.5-1.6 m apart. The fourth buried surface below the present marsh in one core dates from 2.5 ka. This site is near the axis of a syncline, and tilted marine terraces on the west limb of the syncline document continued late Pleistocene folding of this structure. Thus, the South Slough buried surfaces may record local Holocene coseismic faulting or folding rather than regional deformation of the central Oregon coast during great subduction earthquakes.

Rooted spruce stumps that are now in the intertidal zone at three localities were sampled for ^{14}C analyses. Marsh surfaces buried by overbank deposits were studied in outcrop along the Coos and Coquille Rivers.

Samples of modern foraminifera faunas were collected along seven elevational transects in four marshes to determine if the faunas can be used to accurately identify the position of mean higher high water in cores. Micropaleontology analyses of pilot samples from (1) a core taken in a marsh along the Salmon River and (2) a core from northern Coos Bay shows that common salt marsh foraminifera are present at most levels in the cores. Based on marsh studies in other parts of the world, we should be able to use these marsh foraminifera faunas to relocate former sea levels more accurately than can be done with marsh plant or diatom fossils.

Exposures of fluvial sediments along the Umpqua, Smith, and Siuslaw Rivers were more numerous than expected. The sequence of fluvial sediments associated with the terrace remnants was remarkably uniform, regardless of the height above modern river level. These deposits typically consist of 1-2 m of sandy pebble and cobble gravel overlying bedrock, with 2-5 m of silt and silty sand overlying the sandy gravel. The degree of soil development increases with height above the modern river level.

Radiocarbon dates from two 8- to 9-m-high terraces on the Umpqua River and one of its tributaries have been obtained; an 8-m-high terrace 125 km upriver was dated at about 10 ka, whereas a 9-m-high terrace only 25 km upriver on

Scholfield Slough was dated at >26.5 ka. Many more dates and construction of longitudinal profiles will be required to determine if this relationship is caused by a decrease in uplift near the coast, or is simply the result of decreasing stream gradient as the river nears the coast.

Reports

Nelson, A. R., Atwater, B. F., and Grant, W. C., 1987, Estuarine record of Holocene subduction earthquakes in coastal Oregon and Washington, USA [abs.]: International Union for Quaternary Research, 12th International Congress, Ottawa, Canada, July 31-August 9, 1987, Programme with Abstracts, p. 231.

Nelson, A. R., 1987, Apparent gradual rise in relative sea level on the south-central Oregon coast during the late Holocene--Implications for the great earthquake hypothesis [abs.]: EOS [Transactions of the American Geophysical Union], abstract for AGU fall meeting (submitted).

Determination of the Subduction Geometry beneath Western Washington using Teleseismic Body Waveforms

Contract No. 14-08-001-G1343

Thomas J. Owens
Department of Geology
University of Missouri-Columbia
Columbia, MO 65211
(314) 882-3231

Investigation

This summary covers the period from January 20, 1987 to October 20, 1987. The project is designed to constrain the dip of the subducting Juan de Fuca plate beneath western Washington using broadband teleseismic receiver function analysis on data recorded on a linear east-west profile of digital event recorders located at about 46.8°N. The array was installed by R.S. Crosson of the University of Washington and has been operating since the fall of 1986. The instrumentation for the sites consists of Sprengnether DR-200 digital event recorders and Kinemetrics SV-1/SH-1 intermediate period seismometers. The profile consists of 4 stations extending from the site of a recent study by Owens *et al.* (1987) near Satsop, WA eastward toward Mt. Rainier (Figure 1). The portable instruments are spaced at 20 to 30 km intervals. Data from the intermediate period passband of DWWSSN station LON (Longmire, WA) are also being analyzed for comparison with our data.

Results

We have begun to assemble and analyze the data set. Progress includes:

1. Collection and processing of about 60 teleseismic events at the portable sites. Site 1 has been analyzed by Owens *et al.* (1987) and preliminary work at site 7 was done by Lapp (1987). The results for these studies and our continuing analysis of sites 6, 7, and 8 will be presented by Lapp *et al.* (1987). The most important conclusion to date is that the converted phases observed by Owens *et al.* (1987) at site 1 are clearly visible at site 7 and appear to exist at site 8 as well. Amplitude and timing variations at site 1 were modeled to infer a slab dip of about 20° in the direction 110°. This observation is in agreement with a model proposed by Crosson and Owens (1987) that predicts an arch in the Juan de Fuca plate beneath Puget Sound. Our location south of this region is on the flank of this arch in a region where local dip of the slab would be somewhat south of east. Figure 2 plots radial receiver functions from three of the sites in our profile. The important observation is that the slab Ps phase identified at site 1 is definitely delayed in time as we move eastward, an observation consistent with its association with the subducting Juan de Fuca plate. Lapp (1987) estimated the dip based only on this delay to be about 17°. This value is quite consistent with the value predicted by Owens *et al.* (1987) at site 1 based on timing and amplitude considerations. The moveout of the slab phase is more striking when compared to the relatively constant timing of the Ps converted phase from the continental Moho. Continuing analysis is focusing on the large amplitude variations that the slab Ps exhibits as we move across the array. The decreased amplitude at site 8 may be related to heating of the slab, but the variation relative to the large amplitudes observed at site 7 seems extreme considering the stations are only offset by 30 km. Owens *et al.* (1987) point out that the amplitudes of the slab Ps phase is also influenced by the velocity of the shallow surface layers. More analysis will be required to integrate the amplitude variations into our interpretation. Analysis of site 6, which appears to be influenced

by shallow structural complexities, should also help constrain the nature of the amplitude variations in the observed slab phases.

2. Collection and processing of 46 teleseismic events from LON. Our original event list consisted of 164 events, Mb ≥ 6.0 known to be well-recorded in North America. Of these, only 46 actually triggered the intermediate-period passband at LON, due to the low sensitivity of the triggering algorithm. The 46 events that were available are good quality and have been processed to isolate the receiver structure response. These receiver functions tend to have slightly increased noise level near about 1 Hz, possibly due to a peak in the intermediate period instrument response at this frequency. It is immediately obvious that the LON receiver functions are more complex than the receiver functions from the rest of the array. The shallow complexities in structure observed by Langston (1979) in his analysis of LON long-period data clearly dominate the intermediate period response as well. LON completes our east-west profile. It appears that the shallow structure complications (due to the proximity of Mt. Rainier) known to exist at this site are pervasive enough to prevent a straight forward analysis of the deep slab structure. We have tested a number of "end member" slab models and have not modeled the data well with any model to date. If the velocity contrast remains large as the slab descends, then our tests indicate that its response should be observable at LON. Therefore, we suspect that the velocity contrast of the subducting oceanic Moho has been reduced by re-heating enough that it no longer produces large converted arrivals. Although of secondary interest to this project, if this is the case, the additional analysis we plan for site 8 will allow us to evaluate how rapidly this change in the subducting plate occurs.

Acknowledgements

We are indebted to John Hoffman, USGS Albuquerque Seismological Laboratory, for assistance in identifying events which triggered the intermediate passband at LON.

References

Crosson, R.S. and T.J. Owens, Slab geometry of the Cascadia subduction zone beneath Washington from earthquake hypocenters and teleseismic converted waves, Geophys. Res. Let., 14, 824-827, 1987,

Langston, C. A. (1979). Structure under Mount Rainier, Washington, inferred from teleseismic body waves, J. Geophys. Res., 84, 4749-4762.

Lapp, D.B., The subduction geometry beneath western Washington from deconvolved teleseismic P-waveforms, M.S. Thesis, Univ. of Washington, 70 pages, 1987.

Lapp, D.B., R.S. Crosson, T.J. Owens, The subduction geometry beneath westem Washington from deconvolve teleseismic P-waveforms, EOS, Fall AGU Meeting, 1987.

Owens, T.J., R.S. Crosson, and M.A. Hendrickson (1987). Constraints on the subduction geometry beneath western Washington from broadband teleseismic waveform modeling, submitted to BSSA, June 1987.

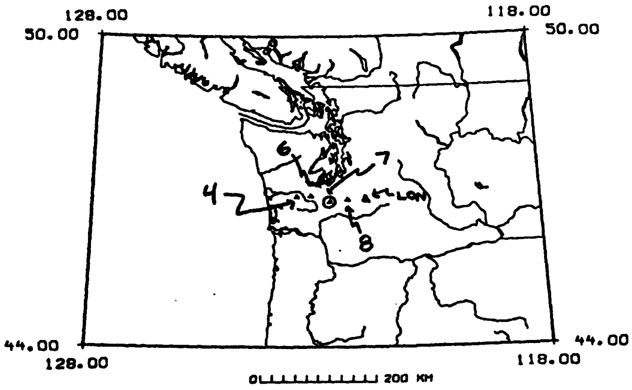

Fig. 1 Broadband array configuration for this study. Sites are identified by number. Circled site (7) was studied by Lapp (1987, MS Thesis, Univ. of Washington). LON is a DWWSSN station.

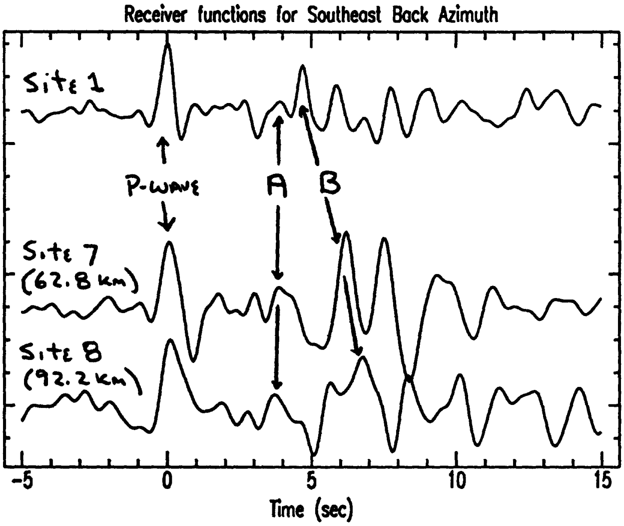

Fig. 2 Deconvolved receiver functions for the southeast back azimuth at array sites 1 (8 km southwest of site 4) site 7, and site 8. Distances from sites 7 and 8 to site 1 are given in parentheses at the right of each of these traces. Traces are offset along the vertical axis amounts corresponding to these distances. The two label phases correspond to the Ps converted phases from the continental Moho (phase A) and the oceanic Moho of the subducted Juan de Fuca plate (phase B). The moveout of phase B suggests a slab dip of 17° (Lapp *et al.*, 1987).

Data Processing, Golden

9950-02088

Robert B. Park
Branch of Geologic Risk Assessment
U.S. Geological Survey
Box 25046, MS 966, Denver Federal Center
Denver, CO 80225
(303) 236-1638

Investigations

The purpose of this project is to provide the day-to-day management and systems maintenance and development for the Golden Data Processing Center. The center supports Branch of Geologic Risk Assessment with a variety of computer services. The systems include a PDP 11/70, a VAX/750, a VAX/780, a MicroVAX, and two PDP 11/34's. Total memory is 14 mbytes and disk space is approximately 4 G bytes. Peripherals include four plotters, ten mag-tape units, an analog tape unit, two line printers, 5 CRT terminals with graphics, and a Summagraphic digitizing table. Dial-up is available on all the major systems and hardwire lines are available for user terminals on the upper floors of the building. Users may access any of the systems through a Gandalf terminal switch. Operating systems used are RSX11 (11/34's), Unix (11/70), RT11 (LSI's) and VMS (VAX's).

Results

Computation performed is primarily related to the Hazards program; however, work is also done for the Induced Seismicity and Prediction programs as well as for DARPA, ACDA, and U.S. Bureau of Reclamation, among others.

The data center supports research in assessing seismic risk and the construction of national risk maps. It also provides capability for digitizing analog chart recordings and maps as well as analog tape. Also, most, if not all, of the research computing related to the hazards program are supported by the data center.

The data center also supports equipment for online digital monitoring of Nevada and Colorado Western Slope seismicity. Also, it provides capability for processing seismic data recorded on field analog and digital cassette tape in various formats.

Analysis of Liquefaction Susceptibility in San Jose, California

14-08-0001-G1359

M.S. Power, R.R. Youngs, and F.H. Swan III
Geomatrix Consultants
One Market Plaza, Spear Street Tower, Suite 717
San Francisco, California 94105
(415) 957-9557

and

R.W. Mearns
City of San Jose
801 North First Street
San Jose, California 95110
(408) 277-4693

Investigations

Liquefaction susceptibility is being evaluated primarily by means of examination and analysis of the data base on the subsurface conditions in San Jose available in the files of the City. The data base consists of logs of several thousand borings contained in more than 1800 reports of geotechnical investigations conducted in San Jose during the period 1975 to 1987. We have completed the compilation of blow count data in cohesionless soil layers having potential susceptibility to liquefaction as well as ground water level data contained in these reports. We are also compiling other available data that are useful in evaluating liquefaction potential, including shear wave velocity data and cone penetrometer test data. Following completion of a preliminary analysis of the compiled data, we will be conducting a limited program of borings with standard penetration test blow count measurements and cone penetrometer tests at selected locations to supplement the existing data.

Geologic mapping has been conducted to aid in interpreting the subsurface data and define boundaries between soil units having different liquefaction susceptibilities. For this task, we have used the subsurface data base and previous geologic mapping by others (Helley and others, 1979), evidence for historic liquefaction (Lawson, 1908; Youd and Hoose, 1978), and examination of aerial photographs.

Results

Liquefaction susceptibility will be quantified primarily on the basis of statistical analysis of the blow count data, ground water level data, and use of liquefaction potential correlations by Seed and others (1983, 1985). Available cone penetrometer test data and shear wave velocity data will be used with appropriate existing correlations such as that by Dobry and others (1982). Liquefaction susceptibility will also be correlated to geologic age and depositional environment using relationships developed by Youd and Perkins (1978). The potential consequences of liquefaction (lateral movements and settlements) will be considered in describing and mapping liquefaction susceptibility.

Overall results of the investigations will be displayed on standard U.S.G.S. quad sheet map bases (scale 1 : 24,000) and a series of cross sections. These will be maintained in the Department of Public Works of the City of San Jose for use by city officials and the general public.

References

Dobry, R., Ladd, R.S., Yokel, F.Y., Chung, R.M., and Powell, D., 1982, Prediction of pore water pressure buildup and liquefaction of sands during earthquakes by the cycle strain methods: Building Science Series 138, National Bureau of Standards, U.S. Department of Commerce, U.S. Government Printing Office, Washington, D.C.

Helley, E.J., Lajoie, K.R., Spangle, W.E., and Blair, M.L., 1979, Flatland deposits of the San Francisco Bay region, California -- their geology and engineering properties and their importance to comprehensive planning: U.S. Geological Professional Paper 943.

Lawson, A.C., 1908, The California earthquakes of April 18, 1906, Report of the State Earthquake Investigation Commission, Carnegie Institute of Washington.

Seed, H.B., Idriss, I.M., and Arango, I., 1983, Evaluation of liquefaction potential using field performance data: Journal of Geotechnical Engineering, ASCE, v. 109, no. 3, p. 458-482.

Seed, H.B., Tokimatsu, K., Harder, L.F., and Chung, R.M., 1985, Influence of SPT procedures in soil liquefaction resistence evaluations: Journal of Geotechnical Engineering, ASCE, v. 111, no. 12, p. 1425-1445.

Youd, T.L., and Hoose, S.N., 1978, Historic ground failures in northern California triggered by earthquakes: U.S. Geological Survey Professional Paper 993.

Youd, T.L., and Perkins, D.M., 1978, Mapping liquefaction-induced ground failure potential: Journal of the Geotechnical Engineering Division, ASCE, v. 104, no. GT4, p. 433-446.

Quaternary Framework for Earthquake Studies
Los Angeles, California

9540-01611

John C. Tinsley
Branch of Western Regional Geology
U.S. Geological Survey
345 Middlefield Road, MS 975
Menlo Park, California 94025
(415) 329-4928

Investigations

1. Geology and relative ground motion, Wasatch Region: Analysis of logs of boreholes and samples obtained during the drilling operations conducted in the Salt Lake City area during FY 86 continued during FY 87. A second and final phase of drilling investigations at 15 sites in the Wasatch region has been completed (9/87) and laboratory samples are being analyzed. Downhole shear-wave and P-wave studies and shallow-reflection profiles were completed at most of the sites and drilled in 1987 (J. Tinsley, D. Trumm, K. King, and D. Carver).

2. Holocene stratigraphy and fold deformation rates near Coalinga, CA: Recent field studies have emphasized detailed mapping and interpretations of selected exposures of Holocene sediments along Los Gatos Creek from the Pleasant Valley syncline across the Coalinga anticline into the San Joaquin Valley. These studies of surficial geology have been augmented by mapping the upper contact of the underlying Tulare Formation in the subsurface along Los Gatos Creek, using shallow seismic refraction techniques and drillers' descriptions contained in water well records. The mapping of a 5000-year old isochron from the vicinity of the anticlinal fold axis westward into the Pleasant Valley syncline has been frustrated owing to extensive and laterally persistent cut- and-fill relations involving chiefly channel deposits within this critical reach (D. Trumm, R. Stein, and J. Tinsley).

3. Geology of ground motion stations and regional aspects of site-response in the Puget Sound area, Washington:

   Ground-motion recordings have been made by K.W. King, (USGS, Golden, Colorado) at about 20 sites in the Tacoma-Olympia area and at about 10 sites in the Seattle, Washington area in order to estimate site-dependent attributes of earthquake ground motion spectra relative to bedrock sites in this Washington area. Geologic studies of the near surface stratigraphy and the influence of the strata on site response will commence at these sites in FY 88.

Results

1. Lithologic logs, 3-inch Shelby-tube-type samples, down-hole shear wave and compressional wave velocity profiles, and soil parameters including bulk density, dry density, consolidation tests, particle size analyses and unconfined compressive strength studies comprise a suite of geologic data used to characterize ground-motion recording stations in the Provo and Ogden areas, Utah. Fifteen sites were drilled during August and September, 1987. Approximately 70 sites now exist at which ground motion emanating from the Nevada Test Site has been recorded on different site geologies; we have explored 35 of these sites by drilling. The thickness of various semiconsolidated and unconsolidated key strata and the wave-propagation characteristics of the deposits will enable sites to be classed in terms of (1) the site periods most likely to be amplified or to resonate during earthquake shaking and (2) the sets of geologic characteristics most useful for predicting site response in the Wasatch Region.

2. The Holocene history of Los Gatos Creek near Coalinga, CA has been characterized by a series of at least 4 aggradational episodes during the past 5500 radiocarbon years before present. Detailed mapping of outcrops recently exposed the erosional effects of winter discharge along Los Gatos Creek indicates that the oldest Holocene sediments may be exposed near locality C84-101. Fine-grained silt containing 4-inch diameter sections of trees up to 4 ft. in length were mapped and sampled for radiocarbon analyses. Mapping of the Tulare Formation beneath the Holocene and late Pleistocene (?) deposits bridging and flanking the Coalinga Anticline has been accomplished using shallow seismic refraction techniques. The seismic stratigraphy indicated by profiles at 12 localities along Los Gatos Creek is shown in table 1. Detailed analyses and construction of detailed cross-sections using these relations and relations gleaned from lithologic logs of water wells is in progress at this writing.

3. The initial results of the Puget Sound study are sparse. Initial contacts have been made in the Portland, OR, area, and contacts have also being made in the Seattle-Tacoma-Port Townsend areas. Nine instrument stations have been deployed in the Seattle area; the geologic setting of these stations is being evaluated using a database assembled by James C. Yount (USGS, Menlo Park).

Worldwide Standardized Seismograph Network (WWSSN)

9920-01201

Russ Wilson
WWSSN Project Chief
Branch of Global Seismology and Geomagnetism
U.S. Geological Survey
Albuquerque Seismological Laboratory
Building 10002, Kirtland AFB-East
Albuquerque, New Mexico 87115-5000
(505) 844-4637

Investigations

1. Technical and operational support was provided to each station in the Worldwide Standardized Seismograph Network (WWSSN) as needed and required.

2. One hundred and fifteen (115) modules and components were repaired, and one hundred and forty-three (143) separate items were shipped to eighty-six (86) separate locations to support the WWSSN network during this period.

Results

1. A continuous flow of high-quality seismic data from the cooperating WWSSN stations within the network was provided to the users in the seismological community.

WWSSN Maintenance and Calibration Visits:

1. Galapagos Islands, Ecuador (GIE) - Status not known.

2. Ponta Delgada, Azores (PDA) - May 1987, sent new Nicad batteries; August 1987, sent new frequency standard; station should be fully operational.

3. All other WWSSN stations are fully operational.

4. Bogota, Colombia (BOG) - May 1987, field engineer, Mr. Leo Sandoval, while working at the BOCO SRO station, Bogota Columbia, visited the BOG WWSSN station to correct a minor problem.

Heated Stylus System for WWSSN Seismograph Networks:

1. April 1987, six heated-stylus conversion kits were received from Kinemetrics Systems and installed at the ALQ WWSSN station for a 30-day evaluation and found to meet all specifications.

2. Due to continuing budget restrictions, we are requesting that each WWSSN station make the conversion from photographic recording to heated-stylus recording.

3. A detailed set of installation instructions with drawings and photographs is being provided to each WWSSN station. A detailed set of WWSSN daily operation and record changing instructions with photographs is also being provided each WWSSN station.

4. The first production of heated-stylus conversion kits (six channels) were received from Kinemetrics Systems on July 22, 1987. They were tested and found to meet all specifications. They were shipped to Toledo, Spain (TOL) and are now being installed by field engineer Mr. Juan Nieto.

During the month of August 1987, heated-stylus conversion kits were tested and sent to the following WWSSN stations to be installed by station personnel:

1.	Bermuda (BEC)	Three-LP, One-SP
2.	Guam (GUA)	Three-LP, One-SP
3.	Anpu, Taiwan (ANP)	Three-LP, One-SP
4.	Trieste, Italy (TRI)	One-LP, Three-SP
5.	Honiara, Soloman Islands (HNR)	Three-LP, One -SP
6.	Stuttgart, Federal Republic of Germany (STU)	Three-LP, One-SP
7.	Malaga, Spain (MAL)	Two-LP, Two-SP
8.	Tasmania, Australia (TAU)--This is a DWWSSN station	
9.	Charters Towers, Australia (CTA)--This stations has Streckeisen seismometers and is being installed by field engineer, Mr. Gary Gyure	
10.	Helwan, Arab Republic of Egypt (HLW)	One-LP, Three-SP
11.	Bulawayo, Zimbawe (BUL)	Three-LP, One-SP
12.	New Delhi, India (NDI)	Three-LP, One-SP
13.	Adelaide, Australia (ADE)	Three-LP, One-SP

During the month of September 1987, heated-stylus conversion kits were tested and sent to the following WWSSN stations to be installed by station personnel:

1.	La Plata, Argentina (LPA)	Three-LP, One-SP
2.	Hong Kong (HKC)	Three-LP, One-SP
3.	Istanbul, Turkey (IST)	Three-LP, One-SP
4.	Valentia, Ireland (VAL)	Three-LP, One-SP
5.	Addis Ababa, Ethiopia (AAE)	Three-LP, One-SP
6.	Lapaz (Zongo Valley), Bolivia (LPB)	Three-LP, One-SP
7.	Matsushiro, Japan (MAT)	Three-LP, Three-SP
8.	Rabul, East New Britain (RAB)	Three-LP, One-SP

Geophysical and Tectonic Investigations of the Intermountain Seismic Belt

9930-02669
Mary Lou Zoback
U.S. Geological Survey
Branch of Seismology
345 Middlefield Road, Mail Stop 977
Menlo Park, California 94025
(415) 329-4760

Investigations

1) The state of stress in Western California along the San Andreas fault system.

2) Preliminary analysis of the global pattern of intraplate stress.

3) Analysis of feasibility of deepening an existing 4 km deep petroleum exploration well in the Sevier Desert, Utah. This well is located in the hanging wall block of the Sevier Desert detachment fault, a low angle normal fault which extends through the upper crust and has probable late Quaternary movement along it. The well will probably need to be deepened 1.5 to 2.0 km to intersect and sample the detachment.

Results

1) About 200 quality-ranked horizontal stress orientation indicators are now available for California (Figure 1). The data include stress-induced well bore breakouts, earthquake focal mechanisms, hydraulic fracturing in-situ stress measurements, and young (< 2 m.y.) volcanic alignments. Right-lateral strike-slip focal mechanisms along the San Andreas fault or the other major sub-parallel strike-slip faults (e.g., the Hayward, Calaveras, and San jacinto faults) are not plotted in Figure 1, instead arrows indicate the sense of lateral offset on these faults. An important contribution to this map (which accounts for about half the data points in west-central California) is a wellbore breakout study by Mount and Suppe (GEOLOGY, in press).

   These contemporary in-situ tectonic stress indicators generally show northeast-directed horizontal compresion, nearly perpendicular to the strike of the fault, particularly in central California. Such compression explains recent uplift of the Coast Ranges and the numerous active reverse faults and folds that trend nearly parallel to the San Andreas and are otherwise unexplainable in terms of strike-slip deformation. We propose that fault-normal crustal compression in central California is the result of extremely low shear strength of the San Andreas and slightly convergent relative motion between the Pacific and North American plates. Preliminary in-situ stress data from the Cajon Pass scientific drill hole (located 3.6 km northeast of the San Andreas in southern California near San Bernadino) are also consistent with a weak fault as they show no right-lateral shear stress at 2km depth on planes parallel to the San Andreas fault.

2) A global database of modern tectonic stress orientations is currently being compiled with the cooperation of numerous investigators world-wide. Four main categories of stress data are included in the database: earthquake focal mechanisms, in-situ stress measurements, wellbore elongations (breakouts), and recent geologic data including volcanic alignments and fault slip analysis (Figure 2).

A preliminary analysis of available data indicates that throughout portions of many intraplate regions the stress regime is compressive (thurst or strike slip faulting) and the maximum horizontal compressive stress direction (S_{Hmax}) is in the direction of absolute motion of that plate (relative to a hot spot reference frame). The strong positive correlation between S_{Hmax} orientation and absolute plate motion could be interpreted as indicating that basal (resistive) drag is responsible for the intraplate stress field. Alternatively, both the stress field and the absolute velocity vector may have a common origin in one of the major plate tectonic forces, i.e. net slab pull or ridge push.

Exceptions to the correlation between S_{Hmax} orientation and absolute plate motion can be found in broad regions on nearly every plate, including the central portion of northern South America, southeastern China, southernmost Africa, southern and southwestern Australia, and southern Fennoscandia, However, the most notable exceptions to this general correlation occur in regions of extensional tectonism. These include thermally elevated intraplate rift zones such as the East African rift and the western Cordillera of North America (where abundant data indicate several distinct stress provinces), and uplifted areas within convergent plate boundary zones (such as the Himalayas and the Andes). The direction of extension within the highly uplifted portions of convergent terrains is generally in the direction of convergence (relative motion) which is also generally the absolute plate motion direction.

3) The Cominco American Beaver River Unit #2 well was drilled through Precambrian sedimentary rocks thrust over Lower Paleozoic carbonates and quartzites. Total depth of the abandoned well is 13,192 feet (4.022 km). Seismic reflection data near the hole indicate that a prominent reflector interpreted as the Sevier Desert detachment fault is probably only 1.5-2.0 km deeper than bottom of the hole. A group of us (George Thompson and Mark Zoback, Stanford; Paul Morgan, N. Arizona Univ.; Bob Smith, Univ. of Utah) are investigating the possibility of proposing to DOSECC to deepen this well in order to sample the Sevier Desert detachment at a locality in which the fault seperates Lower Paleozoic carbonates and quartzites from Precambiran crystalline rock. Preliminary analysis of the drilling record of the existing well indicates that the well is in good shape and very close to vertical. Planned experiments include stress, physical property, and strain fabric studies within the active low-angle normal fault-zone, analysis of metamorphic grade in rocks adjacent to the fault, and seismic studies of the fault zone to determine the source of the prominent reflector asscociated with it. A workshop intended to produce a pre-proposal to DOSECC is being planned for January of February of 1988.

Reports

Zoback, M. L., 1987, Global pattern of tectonic intraplate stresses: IUGG/UGGI XIX General Assembly, Vancouver, Canada, v.2, p. 456.

Zoback, M. D., Scotti, O., Zoback, M. L., Eaton, J. P., Healy, J. H., Oppenheimer, D., Reasenberg, P., Wentworth, C., Mount, V. S., Suppe, J., Jones, L., Raleigh, C. B., and Wong, I. G., 1987, New evidence on the state of stress of the San Andreas fault, Science, in press.

FIGURE CAPTIONS

Figure 1 - Generalized geologic map of California with data points showing the direction of maximum horizontal compression in the crust. The length of the bars attached to each data point is a measure of its quality (A,B, or C). The symbol associated with each data point indicates the type of stress indicator. Stress directions inferred from focal mechanisms of earthquakes directly on the San Andreas, or major, righ-lateral strike-slip subsidiary faults are not included.

Figure 2 - Maximum horizontal stress orientations compiled for the World Stress Map Project as of 9/1/87.

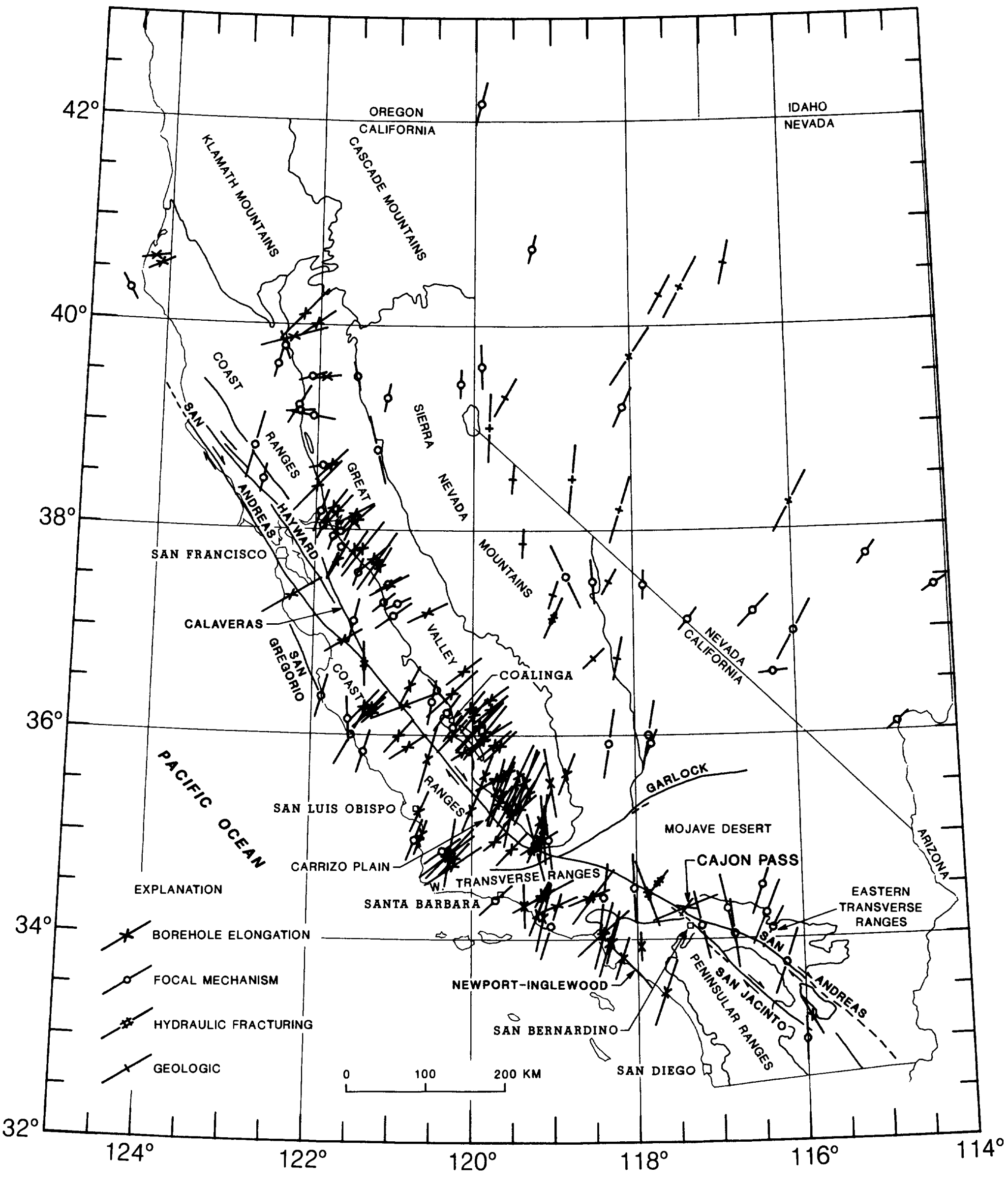
42°
40°
38°
36°
34°
32°
124°
122°
120°
118°
116°
114°
OREGON
CALIFORNIA
IDAHO
NEVADA
KLAMATH MOUNTAINS
CASCADE MOUNTAINS
COAST RANGES
SAN ANDREAS
HAYWARD
GREAT VALLEY
SIERRA NEVADA MOUNTAINS
SAN FRANCISCO
CALAVERAS
SAN GREGORIO
COAST RANGES
COALINGA
NEVADA
CALIFORNIA
PACIFIC OCEAN
SAN LUIS OBISPO
GARLOCK
MOJAVE DESERT
CARRIZO PLAIN
W. TRANSVERSE RANGES
CAJON PASS
ARIZONA
SANTA BARBARA
EASTERN TRANSVERSE RANGES
EXPLANATION
BOREHOLE ELONGATION
FOCAL MECHANISM
HYDRAULIC FRACTURING
GEOLOGIC
NEWPORT-INGLEWOOD
SAN ANDREAS
SAN JACINTO
PENINSULAR RANGES
SAN BERNARDINO
SAN DIEGO
0
100
200 KM

WORLD STRESS MAP - S_{Hmax} ORIENTATIONS

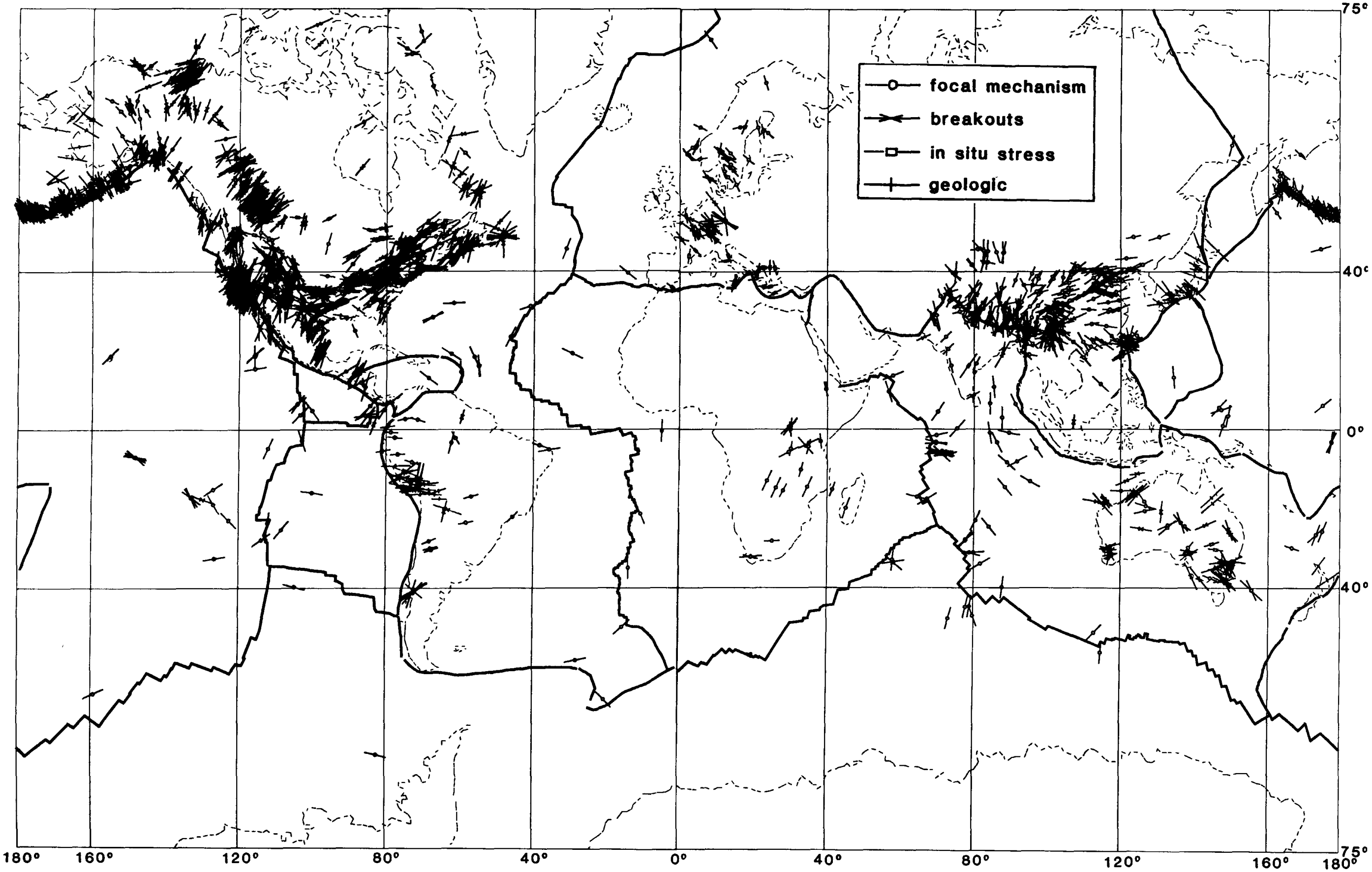

Title: Tsunami Threat Analysis for the Pacific Northwest
Number: 14-08-0001-G1346
Investigator: Gerald T. Hebenstreit
Institution: Science Applications International Corporation
Address: 1710 Goodridge Drive McLean, VA 22102
Phone: 703-827-4975

Numerous investigations in recent years of the seismicity of the Juan de Fuca Plate area of the eastern Pacific have led to the hypothesis that a major subduction-type earthquake in the Plate is a real possibility, despite the absence of historical records of such earthquakes. If this hypothesis is indeed true, then the northwestern regions of the United States and Canada are at risk. If such an earthquake or series of earthquakes were to occur off the western coast of North America, the threat would not only be from ground motions, but also from tsunamis generated by the motion of the sea floor in the outer shelf and slope area. The purpose of this study is to examine the nature of this tsunami risk by conducting numerical simulations of tsunami generation and propagation in the nearshore environment of the Juan de Fuca Plate region.

The first step in this study was to define possible source areas within which thrust earthquakes (the most common tsunami-producing type) could reasonably occur. Examination of recent literature on this subject lead to the identification of three broad areas of concern. These are delineated in the Figure 1. Details of each area will be discussed in a succeeding paragraph.

A simple picture of tsunamigenesis during a thrust earthquake can be gained by picturing a large piston at the bottom of a pool of water. If the piston is suddenly pushed upward, it displaces a volume of water and deforms the surface of the pool. The process of returning the free surface to an equilibrium state is accompanied by the generation of surface waves radiating away from the site of the disturbance. This analogy can be applied to tsunamigenesis in the ocean to provide a relatively simple tool for making estimates of tsunami threat. If a thrust earthquake is postulated for an area, and if an estimate can be made of the vertical motion of the "piston" (i.e., of the sea floor) as a result of the earthquake, then a deformation pattern can be imposed on the sea surface and the nature of the resulting surface waves can be calculated.

A source displacement model such as that of Mansinha and Smylie (1971) can be used to estimate the sea floor deformation, but several key pieces of information must be specified before this model can be used. We must have reasonable estimates of the length and width of the fault, the dip angle of the fault, the probable depth of the upper edge of the fault plane, and the average vertical displacement over the area of the fault. Some of these parameters, such as the length of potential fault planes and a representative dip angle for the region, can be gleaned from examination of the geologic setting of the Cascadia subduction zone. The other values can be obtained by close reading of existing literature. The lack of historical seismicity in the region makes it difficult to place any confidence levels on the numbers obtained in this manner, but the fact that they are reasonable implies that they are sufficient for this study. Prime sources for this type of information are papers by Rogers (1987) and Heaton and Hartzell (1986a,b). The values being used in the simulations in this study will be discussed in terms of each of the potential source zones (see Figure 1.)

Area A covers the region of the Gorda South Plate, which is bounded at its southern end by the Mendocino Fault Zone. Although it is possible that rupture in this block would occur in conjunction with the sections to the north, it seems more likely that rupture would be local. The region is between 150 and 250 km long. Rogers estimates the rupture width in this area to be approximately 100 km, a value tentatively suggested by Heaton and Hartzell (1986a.) Scholz (1982) provides an empirical relationship which indicates that the average displacement during a maximum size earthquake in this block would be roughly 3 m.

Area B includes the entire Juan de Fuca Plate, from the Gorda South Plate to the northern end of the Explorer Plate. Although a rupture which would include the entire 1000-plus km length of this area is not without historical precedent, it is more likely that the block would rupture in two or three segments. Each of these possibilities are being explored by the simulations. Rogers estimates the rupture width in the area to be 100 km. Depending on the rupture length chosen for study, displacement could be as much as 18 m. Four basic cases will be examined for this study. In the first case, the entire block ruptures. The other three involve the block rupturing in one of three segments which divide the block into roughly equal lengths.

Area C includes the Explorer Plate, located along the northern half of Vancouver Island. This block is between 100 and 300 km long, depending on whether or not the Winona block (which adjoins the Explorer Plate to the north) is included for consideration. Since the two blocks have different downdip lengths (Rogers, 1987), it is likely that they would not be coupled in a major earthquake. Rogers estimates the width of the block to be 200 km, with a resulting displacement estimate of 2 m.

Although the Winona Block is a candidate for rupture on its own, it will not be included in this study in order to restrict the geographical extent of the numerical grid and reduce the required computational resources.

Heaton and Hartzell (1986b) used a dip angle of 10 degrees for their study of hypothetical earthquakes in the Cascadia subduction zone. Historical seismicity in the area lends creedence to this value, and so it has been adopted for use in this study. The depth of the upper edge of the fault plane is rarely estimated in the literature. However, a value can be arbitrarily chosen for each separate case to ensure that the displacement pattern reaches a maximum along the edge of the outer slope. Although this choice is subjective in each case, it will provide usable values for this type of "worst case" study.

An example of the type of sea floor displacement pattern that can be produced by the Mansinha-Smylie model is shown in Figure 2. Note that the pattern is a dipole, with areas of both uplift and subsidence. In all cases, given the shallow dip angle, sudsidence will occur on land. Because the tsunami model being used in not capable of simulating runup on shore, any land-centered subsidence can be ignored. The uplift pattern in Figure 2 is based on the values for the Explorer Plate.

As of October, 1987, the bathymetry for the study has been assembled and filtered to meet the needs of the study and hypothetical source motions have been nearly all tested. Full model runs only began in October, due to several intransigent computer problems. Analysis of the initial runs was not completed in time for this summary. Final runs will be completed by the end of 1987 or early 1988.

References

Heaton, T.H. and S.H.Hartzell, 1986a: Source characteristics of hypothetical subduction earthquakes in the northwestern United States. Bulletin of the Seismological Society of America, 76(3), 675-708.

Heaton, T.H. and S.H.Hartzell, 1986b: Estimation of strong ground motions from hypothetical earthquakes on the Cascadia subduction zone, Pacific northwest. Open-File Report 86-328, U.S. Geological Survey, Pasadena, CA.

Mansinha, L. and D. E. Smylie, 1971: The displacement fields of inclined faults. Bulletin of the Seismological Society of America, 61, 1433-1440.

Rogers, G.C., 1987: Megathrust potential of the Cascadia subduction zone. Pacific Geoscience Centre, Sidney, British Columbia. (Submitted to Canadian Journal of earth Sciences)

Scholz, C.H., 1982: Scaling laws for large earthquakes: consequences for physical models. Bulletin of the Seismological Society of America, 72, 1-14.

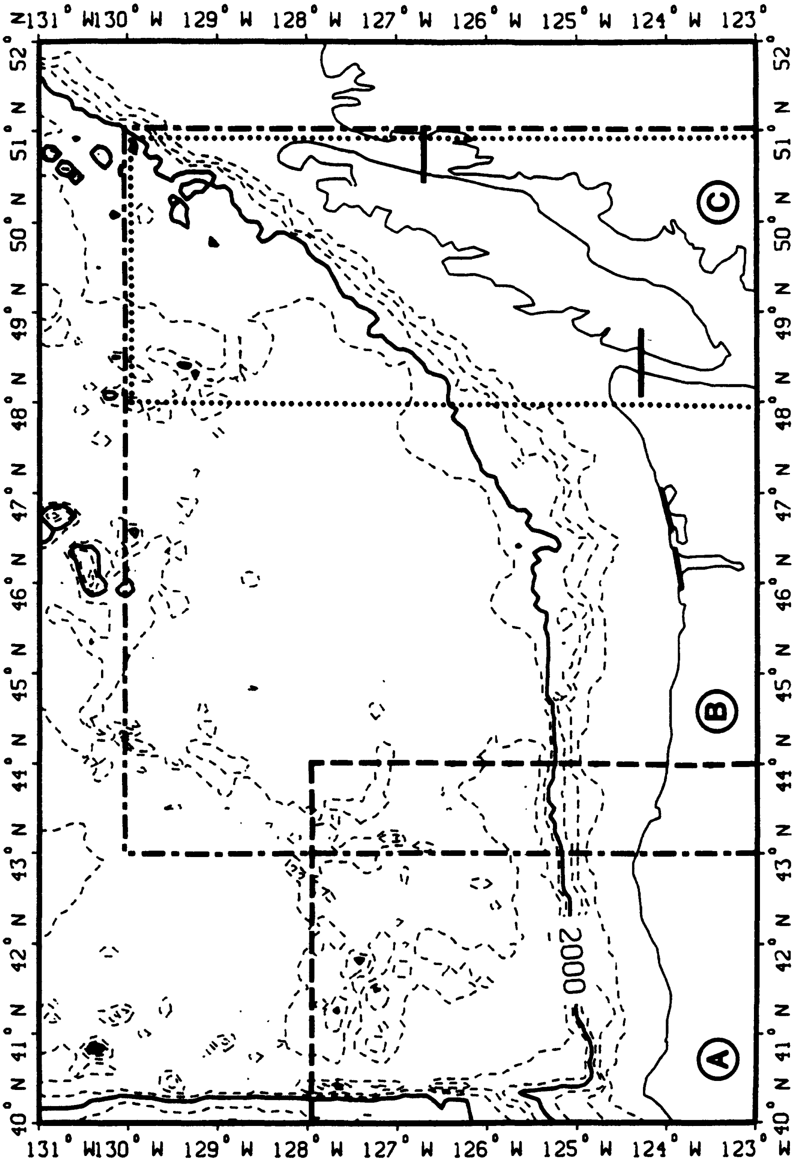

Bathymetry (meters) of the study area and the three major source areas to be examined

Figure 1

GORDA SOUTH UPLIFT

Length 200 km
Width 100 km
Depth 20 km
Dip 10 deg

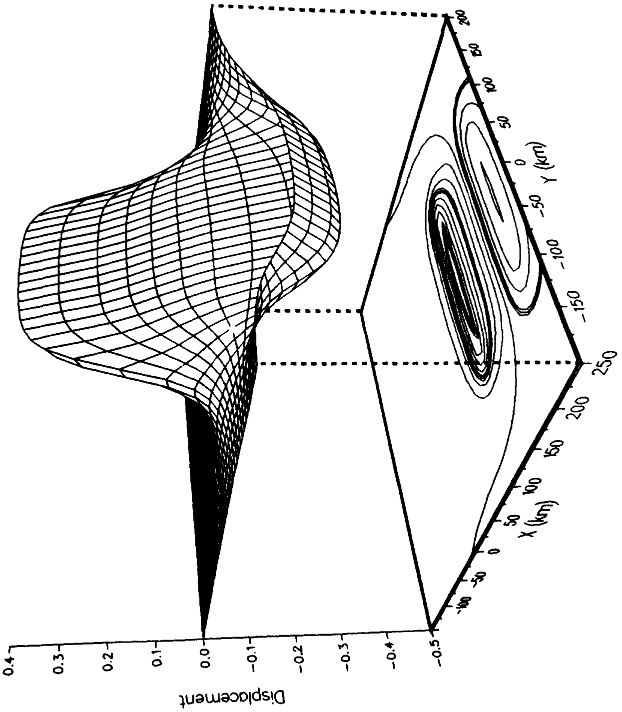

Figure 2

Earthquake-Resistant Design and Structure Vulnerability

9950-04181

Edgar V. Leyendecker
Branch of Geologic Risk Assessment
U.S. Geological Survey
Denver Federal Center, M.S. 966
Denver, CO 80225
(303) 236-1601

Investigations

1. A program has been initiated to examine, evaluate, and improve the estimation of casualties and aggregate monetary losses associated with the occurrence of earthquakes in the United States.

2. An investigation is underway to develop improved measures of vulnerability of structures to damage, including the refinement of our understanding of earthquake damage and the applicability of the existing data base on earthquake damage.

3. Investigations continue for development/identification of cost-effective techniques for determining inventory at risk.

Results

1. Plans are being made for development of an improved and consistent loss-estimation methodology that can be applied in a uniform way on a regional basis for the estimation of losses throughout the United States. As a first step in this new project, planning for a USGS Workshop on earthquake losses to be held in mid-FY 88 has started. Participants will include both USGS and non-USGS researchers and users. Results of this workshop will be used in defining approaches or guidelines that should be used in conducting loss-estimation studies.

An evaluation of risk (losses) for the Seattle urban area is anticipated as part of the initial application of preliminary results of this project.

2. Examination of current vulnerability relationships is underway with a review of existing earthquake damage data bases. Plans for the collection of earthquake damage data following selected earthquakes are being made, including development of data collection techniques. Improvement of vulnerability relationships, including parameter variability, depends heavily on the collection of earthquake damage data. These techniques will be used and refined following a significant (one with at least moderate damage) future earthquake.

Analysis of vulnerability relationships appropriate for the Seattle area is underway as part of this project.

3. Development of inventory at risk is costly and is a major impediment to accurate loss estimates. Methods are being developed to identify and obtain the critical elements of inventory needed for loss assessment in urban areas, including field inventory techniques. A preliminary field inventory procedure is being developed. Plans for preparation of inventory training procedures are underway. Both the survey and training procedures will be evaluated and revised following a trial use.

A plan for an inventory in the Seattle urban area is being developed for initial application of some of the techniques.

GEOLOGIC AND ENGINEERING STUDIES-SOUTH CAROLINA

9950-03868

Stephen F. Obermeier
Branch of Geologic Risk Assessment
U.S. Geological Survey
MS 926, National Center
Reston, Virginia 22092
(703) 648-6791

Investigations

Continued study of regional development of earthquake-induced sand blows in coastal South Carolina and southeastern North Carolina. Wood (limb material) and charcoal clasts have been collected from five craters far from the 1886 meizoseismal zone, and carbon^{-14} data from these clasts have be used to place limits on earthquake dates.

A draft copy of a manuscript has been completed which describes characteristics of earthquake-induced liquefaction features in different geologic settings.

Results

Features interpreted to be earthquake-induced sand blows of Holocene age have been discovered throughout much of the coastal region in South Carolina and in the southeastern extremity of North Carolina. Nearly all these sand blows presently are manifested as filled craters.

Interpretation of an earthquake origin for the craters is based on independent lines of evidence: (1) the filled craters have a morphology consistent with historical descriptions and photographs of sand blows produced by the Charleston, South Carolina earthquake 1886; (2) the filled craters occur near or along the crests of Pleistocene beach ridges, which is a setting that corresponds with the geologic-topographic setting of the most abundant craters produced by the 1886 earthquake; (3) filled craters are especially abundant at sites reported in 1886; and (4) the filled craters have sedimentary relations that are consistent only with a suddenly applied, strong, short-lived, upward-directed hydraulic force which, on the topographically high beach ridge crests could reasonably have been produced only by earthquake-induced liquefaction.

The craters generally formed in episodes long-separated in time. Radiocarbon ages show that at least three prehistoric, liquefaction-inducing earthquakes have taken place within the past 7200 years near Charleston. Ages of some craters far from Charleston differ from ages near Charleston. Insufficient data have been collected to determine if all crater ages far from Charleston differ from ages near Charleston.

Both the diameter and relative abundance of pre-1886 craters are greater in the vicinity of Charleston (particularly in the 1886 meisoseismal zone) than elsewhere along the coastal regions of South Carolina and southeastern North Carolina, although the susceptibility of the widespread beach deposit sites to earthquake-induced liquefaction is approximately the same throughout this area. These data indicate that, in this coastal region, the strongest earthquake shaking during the Holocene has taken place repeatedly near Charleston.

Reports

Obermeier, S. F., Weems, R. E., and Jacobson, R. B., 1987, Earthquake-induced liquefaction features in the coastal South Carolina region: U.S. Geological Survey Open-File Report 87-504, 17 p.

Late Quaternary Faulting, Southern San Andreas Fault Zone

9910-04098

Michael J. Rymer
Branch of Engineering Seismology and Geology
U.S. Geological Survey
345 Middlefield Road, MS 977
Menlo Park, California 94025
(415) 323-8111, ext. 2081

Investigations:

1. Paleomagnetic investigation of tectonic rotation in the Indio Hills, Riverside Co., Calif.
2. Late Quaternary history of the Banning and Mission Creek segments of the San Andreas fault zone in the Indio Hills, Riverside County.

Results:

1. Paleomagnetic samples were collected in three sections in the Indio Hills: (1) in the Palm Spring Formation, between the San Andreas and Indio Hills faults and 5-1/2 km SE of where the Banning and Mission Creek faults split from the San Andreas; (2) in the Ocotillo Formation, between the Banning and Mission Creek faults and 6-1/2 km NW of the split; and (3) in the Ocotillo Formation, between the Banning and Mission Creek faults and 13 km NW of the split. Paleomagnetic data from these sections indicate minor clockwise and conterclockwise rotations. The three sections respectively consist of 13 three-sample sites in 370 stratigraphic meters, 16 sites in 55 m, and 54 sites in 383 m. Each sample was progressively demagnetized using alternating-field and thermal (max 700° C)-demagnetization steps. Principal-component analysis was used to find the directions of best least-squares fit to the demagnetization data. Samples with normal and reverse polarities were found and the data set passed the fold test. Magnetic reversals, fossil vertebrates (see 2, below), and the Bishop tuff (see 2, below) indicate early to middle Pleistocene ages for the sampled sections. The paleomagnetic data indicate counterclockwise rotation of 14±6° in the Palm Spring section and clockwise rotations of 5±8° and 14±8°, respectively, in the Ocotillo sections. Differences in sense of rotation are due to the different structural settings and not to formation type or age. Although large block rotations of as much as 40° have been proposed in the region, documented rotations along the San Andreas fault indicate little to no rotation. More paleomagnetic samples are being analysed from each of the three sections and additional sampling is planned in the Ocotillo Formation at Edom Hill, south of the Banning fault.

2. Study of the Quaternary history of the Indio Hills is progressing through geologic mapping, soils chronologic mapping, with Tom Rockwell (SDSU), and paleomagnetic analyses, above. Contributions during this report period to understanding age control in the Indio Hills include finding the Bishop tuff and a fossil horse skull. The Bishop tuff was found in the Ocotillo Formation in informally named member 3. The tuff was chemically identified by Andrei Sarna-Wojcicki and paleomagnetically constrained to be the 730,000 yr old deposit from the Long Valley caldera. A fossil horse skull also found in the Ocotillo Formation was identified by C.A. Repenning (USGS) as a form that is variously assigned as *Equus occidentalis* or *Equus bautistensis*. These species are both described from the Bautista beds of Frick (1921), where the Bishop tuff has also been found (Sarna-Wojcicki and others, 1984). Taken together, these data suggest a middle Pleistocene age for the sampled part of the Ocotillo Formation.

Reports:

Rymer, M.J., Boley, Janet, and Weldon, Ray, 1987, Nonuniform rotation (Pleistocene) along the San Andreas fault in the Indio Hills, southern California [abs.]: EOS, Transactions American Geophysical Union, v. 68.

Rymer, M.J., 1987, Geologic aspects of the San Salvador, El Salvador earthquake of Ocotober 10, 1986, Earthquake Spectra, v. 3, in press.

Harlow, D.H., White, R.A., Rymer, M.J., Alvarez, S., and Martinez, C., i prep., The San Salvador earthquake of 10 October 1986 and its historica contextL: [submitted to Science].

10/87

San Andreas Segmentation: Cajon Pass to Wallace Creek

9910-03983

David P. Schwartz, Robert V. Sharp, and Ray J. Weldon
Branch of Engineering Seismology and Geology
U.S. Geological Survey
345 Middlefield Road, MS 977
Menlo Park, California 94025
(415) 329-5651, 5652, 5658

Investigations

The project goal is to refine existing and/or develop new segmentation and fault behavior models for the San Andreas fault between Wallace Creek and Cajon Pass.

1. Develop new slip rate and recurrence data from Wallace Creek to south of Cajon Creek.

2. Critically review published and unpublished data and, where possible, existing field relationships to define and quantify uncertainties in: a) timing, displacement, and lateral extent of individual past earthquakes; and b) location-specific slip rate estimates.

3. Map and characterize the style of secondary faulting along the San Andreas, particularly near the junction with the San Jacinto fault on the south and near Liebre Mountain on the north.

Results

1. 96 St. (Littlerock) site. Shallow seismic refraction profiling was tried and appears to be a useful technique for defining buried channel geometries in bedrock below the offset alluvial fill sequence at this locality. Extensive profiling will be undertaken in Fall 1987 in preparation for final trenching at this site planned for Winter/Spring 1988. (Schwartz, Weldon, Fumal)

2. Wrightwood site. Seven radiocarbon samples were dated from the two trenches excavated during 1986. These seven samples were chosen from about 30 datable horizons that were collected to establish the range of time represented by the stratigraphic section at this site and to guide this year's excavation. They were not chosen to actually date earthquakes or critical units for slip rate determination; that will be done this year when new excavations are completed and there is a better understanding of the stratigraphic position of the critical units.

   In trench 1, the southeastern trench excavated across the entire fault zone (about 170 meters) in 1986, we dated charcoal from a burn in the unfaulted fill terrace that extended at least 30 meters north of the fault zone. The age is between 643 and 847 AD (all dates are C-13 and dendro corrected). This demonstrates that no fault activity has occurred north of the main zone in at least the last 1140 years. The main zone in this trench consists of three faults associated with a broad pressure ridge or anticline, above which the section has been clearly eroded. The youngest peat preserved in the main zone was dated at 652 to 847 AD, so the most recent history of the fault is not present here. This unit (peat 100) was traced south of the main zone and is the lowest unit exposed in trench 1 at its south end. Approximately 3-1/2 meters of section, including at least 20 datable units, exist above peat 100 and are involved in faulting and folding across three subsidiary fault zones. Two samples were dated (peat and wood) from about 1 meter below the top of this section and yielded dates of 1436 to 1658 AD and 1495 to 1658 AD, respectively. In the upper meter there is evidence for one faulting event; however, four new trenches across the secondary fault zones are currently being examined, so additional events may be found in other exposures. There are an as yet undetermined number of events preserved above peat 100 in the secondary fault zones. Hopefully, the new trenches will help establish the exact stratigraphic horizon of each event. When this is accomplished the section will be dated in greater detail to obtain the timing of individual events.

Three samples from the northwestern trench excavated last year were also dated. Two peats involved in the faulting, one about 50 cm below the surface and another about 1 meter down, yielded dates of 1478 to 1661 AD and 1290 to 1412 AD, respectively. At least one and possibly two deformational events post-date both of these peats. It is interesting to note that the upper 1-1/2 to 2 meters of section (including the dated peats) has been deformed about the same degree. Below this package sediments are much more severely deformed. Either a significant hiatus exists (which seems doubtful from the conformity of the sediments away from the fault zone) or there has been a substantial period of time without earthquakes prior to the deformation that occurred in the upper part of the section. This will hopefully be resolved by dating some of the older peats that were collected from this trench last year.

This Fall investigations are focusing on three-dimensional trenching of the three secondary faults south of the main zone in trench 1 with the goal of determining the number of events and style of deformation during the past 1100 to 1300 years on the secondary zones. (Weldon, Fumal, Schwartz)

Reports

Alexander, J., and Weldon, R., 1987, Comparison of structural style of the Liebre Mountain and Squaw Peak thrust systems, offset across the San Andreas fault, southern California [abs.]: *Geological Society of America, Abstracts with Programs,* Cordilleran Section, v. 19, no. 6, p. 353.

Schwartz, D.P., and Weldon, R.J., 1987, San Andreas slip rates: preliminary results from the 96th Street site near Littlerock, California [abs.]: *Geological Society of America, Abstracts with Programs,* Cordilleran Section, v. 19, no. 6, p. 448.

Weldon, R.D., and Humphreys, E., 1987, Plate model constraints on the deformation of coastal southern California north of the Transverse Ranges [abs.]: *Geological Society of America, Abstracts with Programs,* Cordilleran Section, v. 19, no. 6, p. 452.

10/87

Historical Normal Fault Scarps -- Wasatch Front and Vicinity

9910-04102

David P. Schwartz
Branch of Engineering Seismology and Geology
U.S. Geological Survey
345 Middlefield Road, MS 977
Menlo Park, California 94025
(415) 329-5651, FTS 459-5651

Anthony J. Crone
Branch of Geologic Risk Assessment
MS 966, Box 25046
Denver Federal Center
Denver, Colorado 80225
(303) 236-1595

Investigations:

The project goal is to study historical and recent normal fault scarps in the Great Basin in order to calibrate geological techniques used to identify individual past earthquakes and the amount of displacement during each, quantify earthquake recurrence intervals, and evaluate earthquake recurrence models and fault segmentation models. Investigations have concentrated on 1) recurrence and segmentation along the 1983 Borah Peak, Idaho surface rupture and associated scarps of the Lost River fault zone, and 2) recurrence and paleo-displacements on the Wasatch fault zone at the Dry Creek site near the southern end of the Salt Lake segment and at the Mapleton site on the Provo segment.

Results:

1. Lost River fault zone (Schwartz, Crone, Hanks).

A) Warm Springs segment. Investigations continued at two trench sites. At Rattlesnake Canyon, a drainage located 2.3 km north of Gooseberry Creek, 10 cm of vertical displacement occurred in 1983. Trenches across a scarp and filled graben in an alluvial fan indicate only one pre-1983 event. Net vertical displacement during this event was 1.1 to 1.2 m. Carbonate soil development is comparable to the carbonate soil developed on 12-15 ka Pinedale outwash fans to the south, suggesting a similar age for this fan. Charcoal from an *in situ* burn within the colluvial wedge 90cm above the bottom of the pre-1983 graben has a radiocarbon age of 4940 ± 200 14 yr BP (dendro corrected to 5655 or 5715 cal BP). Because the basal facies of a colluvial wedge is generally deposited within a few years to a few hundred years following scarp formation, the proximity of the burn layer to the base of the wedge suggests the event is reasonably close in time to the radiocarbon date. Detrital charcoal from colluvium below the burn has been collected and submitted for dating.

At 25 km Creek, a drainage located 5.2 km south of Gooseberry Creek, trenches show two events displacing a pre-Pinedale(?) alluvial fan. There was no displacement at this location in 1983. The net vertical tectonic displacement across the two-event scarp is 2.75 to 2.8 m. The most recent of the two events displaces a stream terrace inset into the alluvial fan. Charcoal from a burn layer in colluvium derived from the most recent event scarp across the terrace yielded an age of 5280 ± 240 14 C yr BP (dendro corrected to 6030 or 6160 cal BP), which is comparable to the date obtained at Rattlesnake Canyon.

B) Thousand Springs segment. Profiles of the reconstructed pre-1983 scarp at Doublespring Pass yielded a diffusion age of 6000 to 8000 years years ago for the timing of the pre-1983 event along this segment of the fault.

C) Mackay segment. A trench at Lone Cedar Creek at the north end of the segment crossed a single-event scarp in fan deposits. This event displaced volcanic ash identified as Mazama (6700 years) (A. Sarna-Wojcicki, personal communication, 1987). At Lower Cedar Creek, 20 km to the south, trenches and profiles show two or three events in an alluvial fan with a stage III carbonate soil that had been previously mapped by Scott (1984) as middle Pleistocene. Preliminary interpretation of these trenches suggests that only one event has occurred since deposition of an ash identified as Glacier Peak (11,300 years) (A. Sarna-Wojcicki, personal communication, 1987). The initial interpretation is that the post-Mazama event at Lone Cedar Creek and post-Glacier Peak event at Lower Cedar Creek are the same event.

Evidence of timing of past events based on new radiocarbon dates, identification of volcanic ashes, and diffusion modeling of fault scarps suggests the late Pleistocene-Holocene behavior of the north half of the Lost River fault zone is characterized by space-time clustering of large magnitude, scarp-forming earthquakes during the mid-Holocene. This appears to have occurred between about 5500 and 8000 years ago, although events could have been much more closely spaced in time. Prior to this, there appears to have been no surface faulting along this part of the zone since at least 12,000 years ago.

Surface faulting along the proposed Warm Springs segment in 1983 was discontinuous, with displacements significantly smaller than the pre-1983 scarps. A still unresolved question is whether the pre-1983 Warm Springs and pre-1983 Thousand Springs events were actually the same earthquake that completely ruptured through the Willow Creek Summit barrier, or whether both sections of the fault behave as independent rupture segments.

2. Wasatch Fault Zone, Utah (Schwartz, Budding, and W. Lund of the Utah Geological and Mineral Survey).

A) Dry Creek Site. New radiocarbon dates have been obtained from soils buried by colluvium from the two most recent events. In trench DC-1A, two samples from the A-horizon that represented the ground surface at the time of the older event yielded dates of 5230 ± 80 and 4910 ± 100 ^{14}C BP (dendro corrected to 5975 and 5650 cal BP, respectively); the same soil in adjacent trench DC-1B gave an age of 4710 ± 90 ^{14}C yr BP (dendro corrected to 5455 cal BP). In DC-1A the soil that formed the ground surface at the time of the most recent event gave an age of 1830 ± 80 ^{14}C yr BP but the same soil from DC-1B gave 1170 ± 60 ^{14}C yr BP. The new radiocarbon dates suggest the older event occurred shortly after 5500 to 6000 years ago. The timing of the most recent event remains poorly constrained by radiocarbon and additional samples have been submitted to try and resolve differences in dates from the two trenches.

B) Mapleton site. Five trenches were excavated at two locations near Mapleton, Utah. At the Mapleton North site two trenches exposed charcoal-bearing graben-fill deposits. Charcoal from a debris flow deposited just prior to the most recent event gave an age of 770 ± 100 ^{14}C yr BP; charcoal from an in site burn on deposits that immediately overlies faulted units gave an age of 445 ± 70 ^{14}C BP. This yields a dendro-corrected age range of 1170 AD to 1480 AD with a preferred range of 1265 AD to 1440 AD for the timing of the most recent event at this point on the Wasatch fault.

At the Mapleton South location, 0.8 km to the south, three trenches exposed evidence for the two most recent events. This site may yield information on the timing of the older event. Small amounts of detrital charcoal from a unit near the top of the fan initially faulted during the older event has been submitted for accelerator dating. Preliminary TL dates of silts near the upper part of the fan (M. Jackon, University of Colorado, personal communication) are 5000 ± 1000 years.

The new dates for timing of the most recent event, and published dates, indicate the Wasatch fault zone from Ogden to Levan has failed in a sequence of large magnitude earthquakes during the period from about 300 to 1500 years ago. Preliminary dates for older events from Dry Creek and Mapleton, and published dates from North Creek, suggest a similar period of activity may have ended about 4000 years ago.

Reports:

Hanks, T.C., and Schwartz, D.P. (1987), Morphologic dating of the pre-1983 fault scarp on the Lost River fault at Doublesprings Pass road, Custer County, Idaho: *Seismological Society of America Bulletin*, v. 77, p. 837-846.

Lund, W.R., and Schwartz, D.P., 1987, Fault behavior and earthquake recurrence at the Dry Creek site, Salt Lake segment, Wasatch fault zone, Utah [abs.]: *Geological Society of America Abstracts with Programs*, Rocky Mountain Section, v. 19, no. 5, p. 317.

Schwartz, D.P., (1988) Earthquake recurrence intervals and paleoseismicity along the Cordillera Blanca fault zone, northern Peruvian Andes: *Journal of Geophysical Research*, in press.

10/87

CONTINUING INVESTIGATIONS OF EARTHQUAKE RISKS TO UTAH WATER AND GAS SYSTEMS

14-08-0001-G1394

Craig Taylor
NTS Engineering
6695 East Pacific Coast Highway
Long Beach, CA 90803
(231) 493-6651

Objectives

This project develops seismic risk estimates for culinary water and natural gas facilities along the Wasatch Front, Utah, with an emphasis on Weber and Utah County facilities. Assisted by recent advances in the geosciences and in seismic vulnerability modeling, these risk estimates are intended for use by local utility representatives to identify facilities or components to be upgraded and system limitations to be overcome. Specific project objectives include:

1. Collecting detailed data on culinary water and natural gas systems and on new and improved estimates for geologic hazards;

2. Developing the theoretical framework: defining pertinent seismic source zones, updating attenuation functions, incorporating relative site response factors, enhancing methods for estimating ground displacement probabilities, upgrading seismic pipe vulnerability modes, and developing seismic fragility models for wells and other key types of nodes.

3. Developing findings and presenting them: constructing isoseismal maps and damage estimates for the large suite of earthquakes modeled, examining the sensitivity of these estimates to such input parameters as soft surficial soil dynamic amplification factors, and conveying relevant information to utility representatives to help initiate or else to advance seismic risk reduction programs.

Results

Trips to Utah and to Golden, Colorado have been made to gather data and to gain further insights on how recent geoscience advances assist in analyzing seismic risk to Utah facilities. Detailed data have been gathered and complied on natural gas system facilities in Utah and Weber Counties and on culinary water systems for the cities of South Ogden, Ogden, Provo, and Orem. To assist in assessing the seismic resistance of electrical, mechanical, and structural elements within these systems, R. Campbell and M. Salmon have made engineering sites inspections for culinary water facilities in the Ogden City Water Department, the South Ogden Water Department, the Salt Lake County Conservancy District, the Salt Lake Department of Public Utilities, the Orem City Department of Public Works and the Provo City Department Water and Wastewater Department. Utah State University has provided raw liquefaction data for Utah and Weber Counties, Dames and Moore has provided a study of the West Valley fault systems, and the Utah County geologist has provided a thesis on the Hansel Valley fault system.

For this study, seismic source zones are defined along the Taylorsville, Granger-Hunter, Hansel Valley,Cache Valley, and the Wasatch fault systems. Following R. Wheeler, the simplifying assumption is used that the Wasatch fault has four "persistent" segment boundaries and so five principal segments: the northernmost, the Weber, the Salt Lake, the Provo, and the southernmost segments. In addition, earthquakes from a random source zone are modeled by assuming that their fault ruptures and/or epicenters occur on lines drawn parallel to the Wasatch fault zone. Attenuation functions from K. Campbell are being used. These, however, permit several options for the Wasatch fault region and sensitivity analyses will be developed to indicate how significantly various assumptions concerning attenuation and amplification affect expect pipe break estimates for earthquake scenarios evaluated. One major factor affecting expected pipe breakage, the probability of liquefaction occurring along the pipelength, will not likely be resolved in the project time frame. For the 2304 microzones (township sections) used in this project to cover exposures from Utah County north through Weber County, crude liquefaction probability estimation procedures have been developed which incorporate earthquake duration, approximated cyclic shear ratios, critical blow counts, and the assumption that probabilities of liquefaction within a microzone increase with estimated cyclic shear ratio. To assist in resolving one other major factor affecting previous pipe breakage at higher (Modified Mercalli intensities IX and X) earthquake intensities, R. Eguchi has revised previous models for estimating pipe breakage resulting from ground vibration.

Preliminary pipe breakage and regulator station "housing" failure probability estimates for various earthquake scenarios have recently been developed for Weber County natural gas facilities and these are under review by the natural gas company for their use as a basis in developing system performance analyses. One preliminary conclusion of the engineering site inspections is that--among structural elements, and mechanical and electrical equipment surveyed in filtration plants, wells, and booster stations--retrofit of electrical equipment is clearly needed and is likely to be very cost-effective.

References

Campbell, Kenneth W., "Predicting Strong Ground Motion in Utah," in press to Hays, W.W. and P.L. Gori, eds., Evaluation of Regional and Urban Earthquake Hazards and Risk in Utah, forthcoming U.S. Geological Survey Paper.

Keaton, Jeffrey R., Donald R. Currey, and Susan J. Olig, Paleoseismicity and Earthquake Hazards Evaluation of the West Valley Fault Zone, Salt Lake City Urban Area, Utah. Salt Lake City, Utah: Dames & Moore and Department of Geography, University of Utah, U.S. Geological Survey Contract No. 14-08-0001-22048, March 6, 1987.

Robison, Robert M., "The Surficial Geology and Neotectonics of Hansel Valley, Box Elder County, Utah," M.S. thesis, Utah State University, Logan, Utah, 1986.

Earthquake Hazards Studies, Metropolitan Los Angeles-Western Transverse Ranges Region

9540-02907

R.F. Yerkes
Branch of Western Regional Geology
345 Middlefield Road, MS 975
Menlo Park, California 94025
(415) 329-4946

Investigations and results

1. Historic earthquakes (Yerkes and Paia Levine, with W.H.K. Lee). The south boundary of the Transverse Ranges between Santa Barbara Channel and Cajon Pass was mapped by combining geologic evidence of fault activity, relocated epicenters for 1974-85 (with some gaps), and fault-plane solutions. The indicated tectonic regime is consistent with that shown by convergence combining reverse displacement on east-trending faults and strike slip or lateral slip on northwest- or northeast-trending faults.

   CIT-USGS and USC P-wave arrivals were used with the HYPO71 program of Lee and Lahr (1975), revised for the IBM PC AT, to relocate 2300 M_L 0-5 events, yielding more than 400 useful single- event solutions in the 40- by 175-km area.

   Prominent seismic activity for the period was concentrated around the 1973 Point Mugu earthquake, and numerous reverse solutions are associated with the Anacapa fault. Similar solutions are concentrated around the 1979 M_L 5 Malibu earthquake 8 km south of Malibu Beach, perhaps associated with the Anacapa-Santa Monica or San Pedro Escarpment zones. A broad patch of activity south of the Santa Monica fault zone between the Newport-Inglewood zone and Pasadena is characterized by strike slip and reverse solutions associated with northwest- and west-northwest-trending faults such as the Whittier fault zone (on which the 10/1/87 M_L 6.1 reverse (or thrust) earthquake may have occurred). Several patches of seismicity in the Puente Hills include strike-slip or reverse events along the northeast-trending San Jose and Walnut Creek faults, and scattered reverse events along the Whittier and Cucumonga faults. Two prominent bands of strike-slip events are associated with northeast-trending faults in the northern Chino basin. The Santa Monica and Sierra Madre zones were not clearly associated with seismic activity. Projection of the fault-plane solutions on geologic sections suggests the presence of seismically-active blind thrusts in basement rocks below 6 km along the northern margin of the basin (as proposed by T.L. Davis, 1987).

2. Quaternary stratigraphy, chronology, and tectonics, southern California region (Sarna-Wojcicki, BWRG). This investigation is presently concentrating on improvement of age control for Quaternary deposits, and on providing age control for studies of neotectonics.

   a. Continued investigations reported in vol. XXIV, p. 621-623, USGS OFR 87-374.

b. Conducted several short-term studies to provide tephrochronologic age control in support of active-fault and tectonic studies: (1) A tuff (IHO23A; table 1) collected by Mike Rymer (BESG) from an area near the Indio Hills, southern California, in alluvium mapped previously as the Imperial Formation, was suspected by Rymer of being younger. Electron-microprobe analysis of the glass shards from this tuff by Charlie Meyer (BWRG) indicates that the tuff is most similar to a tuff in the Modelo Formation in Balcom Canyon near Ventura, California, suggesting an old age of about 8 to 9 Ma on the basis of diatom zonation at the latter locality (J. A. Barron, BPAS, written commun., 1986), and favors the initial age call. The degree of hydration of the glass also suggests an older age for the tuff. Another tephra layer (IHO51A; table 1) collected by Rymer, an ash from faulted fan alluvium in the younger Ocatillo Formation of the Indio Hills, matches well with the Bishop ash bed. A normal magnetic polarity on this unit and a magnetic reversal a short stratigraphic distance beneath the ash bed obtained by Rymer confirm the identity of this tephra layer as the Bishop ash bed (0.74 Ma), and the identity of the magnetic reversal as the Brunhes/Matuyama. (2) A tuff (DR 87-12; table 1) collected by J. Alan Bartow (BWRG) near the top of the non-marine Pliocene alluvium, just below the base of the non-marine Tulare Formation in the Lillis Ranch area north of the Coalinga anticline in the east-central Coast Ranges, matches on the basis of its shard composition with the Ishi Tuff, the age of which is about 2.5 Ma, based on both K-Ar and fission-track dates. The same tuff bed occurs to the south near the top of the marine San Joaquin Formation, just below the base of the Tulare Formation at North Dome of the Kettleman Hills, California. This tuff is an important reference datum for studies of tectonic deformation in this area. (3) Trenches across the active Mackay segment of the Lost River fault zone, in Idaho, exposed an ash layer (DS-LCC-1; table 1) sampled by Dave Schwartz (BESG). We identify this layer as the Mazama ash bed erupted about 6850 yrs b.p., as based on numerous radiocarbon determinations by others. Another ash bed from near this locality is tentatively identified as one of the Glacier Peak ash beds, about 11,000 yrs in age. (4) A tephra layer (CMT-3; table 1) exposed in deformed fan alluvium in a trench across the 1932 trace of the Cedar Mountain fault in central Nevada was collected by John Bell of the Nevada Bureau of Mines and Geology. The tephra layer matches best with the Glass Mountain G ash bed, estimated to be about 1.0 Ma, although the identification on the basis of electron probe is not definitive.

Reports

Sarna-Wojcicki, A.M., 1987, Quaternary tephrochronologic datums. Extended abstract in Directions in Paleoseismology, USGS Workshop, Albuquerque, N.M., Apr. 22-25, p. 41-44.

Sarna-Wojcicki, A.M., Meyer, C.E., Brown, F.H., Slate, J.L., and Roth, P.H., 1987, Correlation of widespread upper Neogene tephra layers among continental, onshore marine, and deep-ocean sediments, Pacific Ocean margin of North America and Indian Ocean margin of East Africa. In Barron, J.A., and Blueford, J.R., Fourth International Congress on Pacific Neogene Stratigraphy, IGCP Project 246 - Pacific Neogene events in time and space, Berkeley, California, July 29-31, p. 95-96.

Sarna-Wojcicki, A.M., Morrison, S.D., Meyer, C.E., and Hillhouse, J.W., 1987, Correlation of upper Cenozoic tephra layers between sediments of the western United States and eastern Pacific Ocean and comparison with biostratigraphic and magnetostratigraphic age data. Geological Society of America Bulletin, v. 98, p. 207-223.

R.F. Yerkes, Levine, Paia, and Lee, W.H.K., Contemporary tectonics along south boundary of central and western Transverse Ranges, southern California (abs): prepared for AGU Fall Meeting, approved 8/20/87.

Table 1. Electron-microprobe analysis of volcanic glass shards from several tephra layers in the western U.S. that provide age control to neotectonic studies. C.E. Meyer (BWRG, Menlo Park), analyst. Values given are concentrations in weight percent, recalculated to 100 percent on a fluid-free basis.

Sample	IH023A	MOD-1	IH051A	BT-11C1	DR87-12	KT-11A	DSLCC-2	CRL-5	CMT-3	BT-1A
SiO_2	76.99	75.00	77.84	77.71	78.15	78.47	73.68	73.10	77.55	77.53
Al_2O_3	12.70	12.63	12.60	12.59	12.37	12.16	13.82	14.38	12.62	12.65
Fe_2O_3	2.85	2.88	0.72	0.72	0.83	0.86	2.14	2.15	0.75	0.75
MgO	0.12	0.12	0.05	0.03	0.14	0.14	0.47	0.48	0.05	0.04
MnO	0.04	0.04	0.04	0.04	0.04	0.04	0.06	0.06	0.05	0.04
CaO	0.99	0.98	0.43	0.42	0.76	0.77	1.59	1.60	0.41	0.42
TiO_2	0.33	0.37	0.08	0.06	0.14	0.16	0.42	0.39	0.06	0.06
Na_2O	3.55	3.22	3.62	3.67	3.75	3.59	5.05	5.03	3.67	3.71
K_2O[1]	2.44[1]	4.76[1]	4.62	4.76	3.82	3.81	2.76	2.82	4.86	4.81
Total[2]	91.18	92.12	94.45	93.89	94.16	93.48	99.87	97.81	94.34	95.44

---

[1] K_2O, and to a lesser extent, Na_2O, are subject to post-depositional leaching or enrichment, depending on the nature of the depositional and storage environment. This is particularly true for older tehra layers (>ca. 4 Ma).

[2] Original total, before recalculation to 100 percent.

IH023A - Tuff in the Imperial Formation, near the Indio Hills, southern Calif.
MOD-1 - Tuff in the Modelo Formation, Balcom Canyon, Ventura, Calif.
IH051A - Ash in the Ocatillo Formation, Indio Hills, southern Calif.
BT-11C1 - Bishop ash, airfall beneath the Bishop Tuff, north of Bishop, Calif.
BR87-12 - Tuff from unnamed non-marine Pliocene Formation, east-central Coast Ranges, Calif.
KT-11A - Ishi Tuff from the uppermost marine San Joaquin Formation, beneath contact with Tulare Formation, Kettleman Hills.

DSLCC-2 - Ash in trench across Lost River fault zone, Idaho.
CRL-5 - Climactic Mazama airfall pumice, Crater Lake, Oregon
CMT-3 - Tephra layer in trench across Cedar Mountain fault, central Nevada.
BT-1A - Glass Mountain G ash bed, north of Bishop, Calif.

A Demonstration Project on Seismic Risk Assessment and Hazard Mitigation through Land Use Planning

USGS Grant No. 14-08-0001-G1386

Philip C. Emmi
Department of Geography
University of Utah
Salt Lake City, Utah 84112
(801) 581-5562

Research Objectives

A serious earthquake affecting lives and property is a real possibility along the Wasatch Front. Counties and municipalities are well advised to assess the risks and take appropriate action. The goal of this study is to compile and translate research on seismic and related geologic hazards in Salt Lake County into a form which has meaning for public decision makers. Objectives include integration of hazards maps into a computer-based geographic information system, compilation of mapped data on cultural features, loss estimation, seismic risk assessment, and evaluation of mitigation policy options. The project began in February, 1986, and will continue barring extension until February, 1988.

Accomplishments and Results

To date, over sixty-two data and digital map files have been collected. These include boundary files, digital maps on seismic and related geologic hazards, digital maps and data files on current and projected (2005) population and land use, and digital map and data files on various cultural features. These are maintained on a geographic information system with digital cartographic overlay and analysis capabilities.

Our most significant results to date rely on earlier studies of probabalistic estimates of maximum bedrock velocities and bedrock-to-soil transfer functions to derive estimates of the intensity and spatial distribution of seismically induced ground shaking. The result are presented as a set of maps describing Modified Mercalli Intensities with a 10% chance of exceedence over 10, 50 and 250 year periods (Emmi, 1987a).

Areas of recent progress include an opinion survey of seismic risk perception, a review and evaluation of literature on seismic damage functions, a review of literature on local hazard mitigation policy options, continued management of inventory data, development of computer programs for loss estimation, and continued meetings with local planning officials.

Our opinion survey explored four aspects of risk perception – relative perception of risk from different natural and man-made hazards, degree of concern about risk of damage to home and injury to self and family members, degree of concern about emergency response capabilities, and degree of support for land use controls and building codes to protect against earthquake loss. The University of Utah Survey Research Center administered the survey to 706 randomly choosen adults living in four Wasatch Front

Counties. Results are accurate to within ± 3.7% of reported results.

Results indicate that respondents feel more at risk from earthquakes than from other hazards. They are especially concerned about injury to self and family members and about the capacity of hospitals to extend timely medical attention. Two-thirds felt earthquake risk was "serious enough to justify regulation" of land use and building construction. Support for fault tract set-back regulations and stringent building code requirements was also high. Support increased with education and income. It did not vary with political outlook: both liberals and conservatives were equally likely to support seismically oriented regulations (Emmi, 1987b and c).

Survey results were reported by three local newspapers and two radio stations. In each the author noted that survey results were clear — local residents are aware of the hazard, concerned about the risk and demand public measures to reduce exposure.

Our review and evaluation of literature on seismic damage functions had two purposes — to collect references and to assess the inferential validity of the research. Our review found that, though researchers employed a generally similar methodology, there was suffient variation with respect to unit of analysis, measure of seismic intensity, definition of damage, specification of functional form, measurement of co-variance, and use of control variables as to exacerbate comparisons among results (Ying, 1987). The Applied Technology Council's (Rojahn, 1985) use of the Delphi technique to filter noisy results is very helpful. Yet we remain uncertain about the reliability and generalizability of the damage functions they present.

Evaluation of inferential validity focused on the concept validity of intensity measures and on error in the specification of functional form (Emmi and Kay, 1987). The MMI measure of seismic intensity — based on the measurement of structural damage — was found to be partially tautological in its definition. Partial tautology guarantees strong covariation between damage to a class of buildings and the MMI measure of seismic intensity. This, in turn, muddles accurate specification of the underlying relationship between damage and the site-specific articulation of seismic energy.

With respect to the mathematical form of the damage relationship, researchers generally chose the double-log form. This form has the desired S-shape, but it also admits to the extrapolation of loss to more than 100% of the inventory's value — a logical impossibility. We re-calibrated a double-log model using instead a logit transform. Results were neatly bounded between zero and 100% loss, and the fit was slightly better. We find the logit model superior to the double-log model.

The purposes of a review of literature on local mitigation options were to classify strategic options and to screen for local applicability (Carr, 1987). Several classification schemes were identified and a combination of two were used. Options were classified accordingly and screened using reviewer judgement. The shorter list was prepared for presentation to a policy advisory panel. Their choices will be assessed for relative effectiveness.

The continued management of inventory data has presented several problems on which progress has been made. Errors in data location codes on computer tapes containing assessor data files made these tapes unuseable until the errors were located and corrected.

Data on building frame-type is essential for seismic loss estimation. While assessor data files contain entries on building frame-type for commerial buildings, the residential data files contain no such data items. Other data items had to be used as a basis of classification among frame-type categories. Branching algorithms were developed to categorize each residential unit by frame-type. The algorithms employed as classification criteria data on the age and the major and minor exterior wall-types of each dwelling. The result was a classification of residential units into one of four frame-types — unreinforced masonry, reinforced masonry, wood frame, and brick veneer over wood frame.

Frame-types for commerial buildings in county assessor files include steel, reinforced concrete, and masonry structures with load bearing walls; steel and reinforced concrete with non-load bearing walls; and wood frame strctures. These categories do not correspond to the categories for which ATC-13 provides damage functions (Rojahn, 1985). Other data had to be used to go from the assessor's system of categorization to the ATC-13 system. Again branching algorithms were used to re-categorize buildings into ATC-13 categories. These algorithms used data on frame-type, age and height. The result was a re-classification into one of eleven commercial building categories for which ATC-13 provides damage functions.

Assessor records on residential units are in digital form, but records on commercial structures are only partially in digital form. Our data on such structures is a stratified random sample of the assessor's paper records. However, our sample design has proven to be problemmatic. We have succeeded in drawing a 10 to 25 percent sample of commercial records from each quarter-sections in our study area. In many quarter-sections, either the population of records is too small to be reliably sampled, or the sample is too small to reliably represent characteristics of its population. While trying to sample at the quarter-section level, we have rudely encountered the limitations in the law of large numbers. We are now exploring solutions to this problem, including aggregation to a coarser level of spatial delineation and the acquisition of more sample data.

We have also made progress on the development of computer programs to facilitate loss estimation. Inputs to loss estimation are threefold — large tabular data files on structural characteristics (location, value, height, frame-type), mapped data files on Modified Mercalli Intensities (with 10% exceedence probabilities for 10, 50 and 250 years), and sets of damage functions (by frame-type and height). The programming problem is to asssign MMI values to each parcel, read structure frame-type, height and value data, apply the appropriate damage function, compute expected loss, and compile the results for subsequent digital mapping. The key to solving this problem is a conversion table between the Sidwell parcel addressing system and the UTM coordinate system with which seismic intensities are mapped. The conversion table has been developed and is now being applied to the problem of loss estimation for residential structures.

Since last report, we have held three meetings with local planning officials to keep them informed of our progress and to be informed of their information needs. Two of these meetings were at the University Campus, while a third was hosted by the Utah Geological and Mineral Survey.

References Cited

Carr, Eugene E. 1987. Seismic hazard mitigation policy options. USGS Grant No. 14-08-0001-G1386 Working Paper 10-22-87. Center for Public Affairs & Administration, University of Utah.

Emmi, Philip C. 1987a. Seismic risk and mitigation policies: An assessment of problems and possibilities in Salt Lake County, Utah, Wasatch Front Forum, Vol. III, No. 3/4 (Spring/Summer).

_______ . 1987b. Survey results on seismic risk perception, emergency response capability, and local hazard mitigation measures: Wasatch Front Counties, Utah. USGS Grant No. 14-08-0001-G1386 Working Paper 9-1-87. Department of Geography, University of Utah.

_______ . 1987c. Utahns nervous about earthquake risk: Survey show support for regulations, Wasatch Front Forum, Vol. III, No. 3/4 (Spring/Summer).

Emmi, Philip C. and Paul A. Kay. 1987. Problems of specification error and concept validity in research on seismic damage functions. USGS Grant No. 14-08-0001-G1386 Working Paper 10-19-87. Department of Geography, University of Utah.

Fan, Ying. 1987. Review of literature on seismic damage functions. USGS Grant No. 14-08-0001-G1386 Working Paper 9-20-87. Department of Geography, University of Utah.

Rojahn, C., et al. 1985. *Earthquake Damage Evaluation Data for California,* ATC-13 Report. Redwood City, CA: Applied Technology Council, 492p.

Near-Surface Lithologic and Seismic Properties

9910-01168

J.F. Gibbs
W.B. Joyner

Branch of Engineering Seismology and Geology
U.S. Geological Survey
345 Middlefield Road, MS 977
Menlo Park, California 94025
(415) 329-5631 or (415) 329-5640

Investigations

Measurement of seismic velocity and attenuation to determine the effect of local geology on strong ground motion and to aid in the interpretation of seismic source parameters.

Results

Analysis of downhole data from the Vinyard Canyon site near Parkfield indicates that the shear-wave Q is approximately 4 in the interval from 57.5 to 102.5 m (fig. 1). Shear velocity anisotropy of about 20 percent is found, confirming the preliminary results previously reported.

Reports

Joyner, W.B., 1987, Strong-motion seismology: *Reviews of Geophysics*, v.25, p. 1149-1160.

Joyner, W.B., 1987, Ground-motion parameters for seismic design: Course on Recent Advances in Earthquake-Resistant Design, University of California, Berkeley, July 20-24, 1987.

10/87

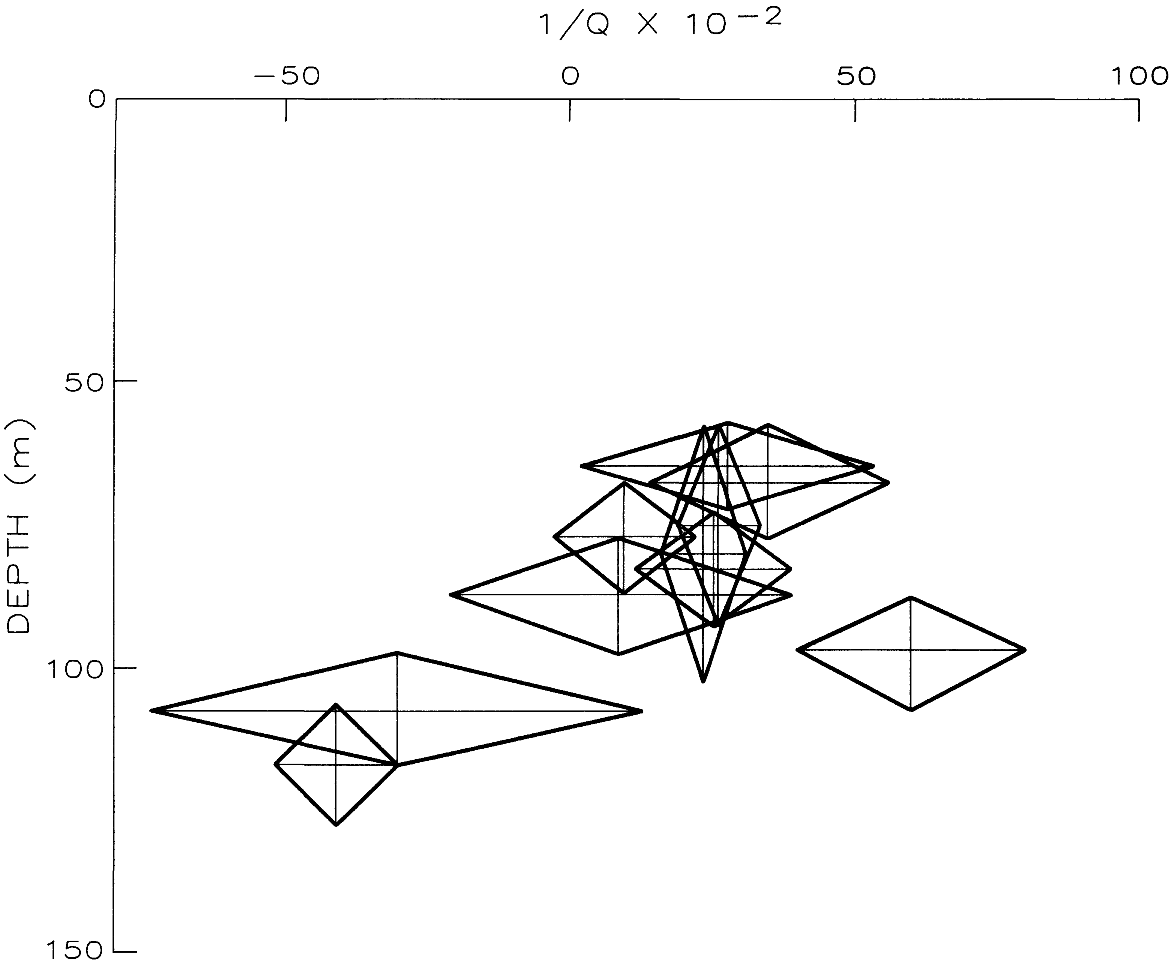

Near surface attenuation coefficient 1/Q from borehole data near Parkfield, CA. Horizontal width of diamond indicates error range and vertical height indicates depth range of Q measurements. The better estimated values ($Q \approx 4$) are the tall-narrow diamonds near center of figure. Gibbs & Joyner, 9910-01168

Spirit Lake Hazard Evaluation

9910-03590

Thomas L. Holzer
Branch of Engineering Seismology and Geology
U.S. Geological Survey
345 Middlefield Road, MS 977
Menlo Park, California 94025
(415) 329-5637

Investigation

Evaluation of liquefaction resistance of debris blockages impounding Spirit, Castle Creek, and Cold Water lakes north of Mount St. Helens, Washington, by field monitoring.

Results

Two instrumentation arrays consisting of accelerometers and pore-pressure transducers were removed in September owing to instrumentation failures and reduced seismic hazard.

Reports

None.

10/87

Experimental Investigation of Liquefaction Potential

9910-01629

Thomas L. Holzer
Branch of Engineering Seismology and Geology
U.S. Geological Survey
345 Middlefield Road, MS 977
Menlo Park, California 94025
(415) 329-5637

Investigations

1. Establishment of an instrumented site in Parkfield, California, to monitor both pore-pressure build-up in sands and strong ground motion during the predicted Parkfield earthquake.

2. Evaluation of ground settlements during earthquakes and the effect of densification on liquefaction resistance during future earthquakes.

3. Analysis of potential for subsidence-induced fault offset across fault-line scarps in Las Vegas Valley, Nevada.

Results

1. Failure of at least 6 of the 8 original pore-pressure transducers installed in June 1986 at the Parkfield liquefaction array prompted abandonment of the original transducer array and establishment of a new nearby array with different transducers. Three different types of transducers have been selected and plans call for a total of 16 transducers to be in place by December 1987. In June 1987, cone penetration testing was conducted at the site of the new array, electrical conduit for 16 transducers was buried, and 6 transducers were installed to restore the functionality of the array. In addition, the inclinometer casing at the array was resurveyed.

2. Empirical and analytical approaches for estimating seismically induced pore-pressure build-ups and settlements were compared. Both approaches were found to consistently predict the occurrence of liquefaction, but disagreed in their predictions of settlement. The analytical approach fails to model adequately the post-liquefaction behavior of sands, which results in lower estimates of settlement than the empirical approach. On the other hand, the empirical approach is largely based on the field performance of many sites and consequently provides only upper-bound estimates of settlement.

3. Results from repeated surveys of nine 2- to 4-km-long leveling lines established in Las Vegas Valley, Nevada, in 1978 were analyzed. Monitoring confirms that differential displacements are occurring across preexisting faults. The differential displacements consist of flexures that range in width from 0.08 to 1.5 m. The maximum rate of differential displacement, 46 mm/yr, is across a 0.38-km-wide zone on the Eglington scarp in northwest Las Vegas Valley. Displacement fields at most of the

monitoring lines do not appear to be precursory to discrete fault slip. Surface deformation along these lines probably will continue as a smooth flexuring. Differential displacements in two places occur over a narrow zone and are in the same sense as preexisting fault displacements. The deformation may be precursory to fault slip if subsidence continues.

Reports

Bennett, M.J., 1987, Liquefaction analysis of the 1971 ground failure at the San Fernando Valley Juvenile Hall, California: 28 p., 12 figs., 3 tables (Approved by Director, June 17, 1987).

Holzer, T.L., and Gabrysch, R.K., 1987, Effect of water-level recoveries on fault creep, Houston, Texas: *Ground Water*, v. 25, no. 4, p. 392-397.

Holzer, T.L., 1987, Modern surface deformation across fault scarps in Las Vegas Valley, Nevada [abs.] in *Geological Society of America Abstracts with Programs*, v. 19, no. 7, p. 706.

Holzer, T.L., and Lluria, M.R., 1987, Selected hydrogeological problems in central Arizona, in Field-Trip Guidebook for 1987 Geological Society of America Annual Meeting, *Arizona Bureau of Geology and Mineral Technology Special Paper No. 5*, p. 205-211.

Holzer, T.L., Youd, T.L., Bennett, M.J., and Stepp, J.C., 1987, Parkfield liquefaction and ground motion experiment [abs.]: *American Geophysical Union Fall Meeting* (Approved by Director, August 24, 1987).

WEST VALLEY CITY
EARTHQUAKE HAZARDS REDUCTION PROGRAM
PHASE II

14-08-0001-G1-398

Joseph L. Moore, AICP
West Valley City Community Development Department
2470 So. Redwood Rd.
West Valley City, Utah 84119
801-974-5501

SCOPE:

To compile and analyze existing geologic/seismic data as part of a citywide effort to understand and hopefully mitigate some of the consequences of a significant seismic event in the West Valley City, Utah area. This study of a potentially catastrophic earthquake event will be utilized in the planning and emergency management functions within City government.

SPECIFIC OBJECTIVES:

1. **Define the Study Area** - Phase II covers the entire jurisdiction of West Valley City, from about 7200 West to the Jordan River and from 2100 South to about 4700 South, encompassing 26 square miles.

2. **Inventory and Digitally Map Study Area Attributes** - Initially a base map at 1" = 1000' scale has been produced showing streets and lot lines. At this time overlays of the available geologic/seismologic data are being digitized utilizing a Computer aided mapping (Cam) system. These overlays will include liquefaction (Anderson), faults (USGS), fault zone (Nelsen) ground shaking (Hays & King), soil types (SCS), water table (SCS), landslides, tectonic subsidence (Anderson & Keaton). In addition, overlays of critical facilities are to be digitally produced.

3. **The Digital Overlay Mapping of Study Area Attributes** - Once the information for the maps identified in step 2 is completed they will be overlayed upon each other with the intent of delineating high risk multi-hazard areas.

4. **Target High Risk Seismic Zones** - This information will help lead to defined areas of greater seismic risk. A separate map will be developed displaying the high risk areas for West Valley City.

5. **Damage and Loss Potential** - Critical facilities and lifelines that were considered structurally marginal will be identified for their importance in the urban environment and the consequences of their failure.

FINDINGS:

Our intent is not to generate new information but to compile and synthesize the existing geologic/seismic data produced by other researchers. The question that has always concerned the researcher has been whether such information was readily available and usable by local officials. On the whole adequate information exists except in the area of ground shaking and reaction of various soil types at various depths. Some gross information was compiled but it seems quite vague for our effort. It is hoped that during 1988 there will be a new more detailed study of the ground shaking and soil reaction issue which can be incorporated into this report.

A consultant, Bruce Kaliser, has been added to our staff. The emphasis of his work will be to further refine available information concerning the ground shaking issue and to assess the accuracy/validity of other subject areas to enhance the final product of this report. There are still questions surrounding the adequacy of the data, especially in terms of supporting legally justifiable ordinances in the implementation phase of the grant. Kaliser will assure that the best information has been made available and is accurately interpreted within the grant.

The final section of the report will include an implementation strategy. Much research has been completed utilizing examples from California and other states. Ordinances, building code modifications, Master Plan elements and other information has been compiled for our purposes.

Brabb, E. E., ed. Progress on Seismic Zonation in the San Francisco Bay Region, Circular 807. Arlington, Virginia: U.S. Geological Survey, 1979.

Governor's Conference on Geologic Hazards. Utah Geological and Mineral Survey Circular 74, Atwood, Genevieve, Director. Salt Lake City, Utah: Utah Geological and Mineral Survey, December, 1983.

Richins, William D., et al. Earthquake Data for the Utah Region July 1, 1978 to Dec. 31, 1980. Salt Lake City Utah: University of Utah Seismograph Stations, Department of Geology and Geophysics, University of Utah, October 1981.

Mabey, Don R., and Atwood, Genevieve. "Fluctuations of the Level of Great Salt Lake." Survey Notes Vol. 18, No.1. Salt Lake City, Utah: Utah Geological and Mineral Survey, Spring 1984, pp. 3-8.

Mabey, Don R. "Earthquake Hazards in Utah." Survey Notes Vol. 18, No. 4. Salt Lake City, Utah: Utah Geological and Mineral Survey, Winter 1985.

Marine, Wendell and Price, Don. "Geology and Ground-Water Resources of the Jordan Valley, Utah." Water Resources Bulletin #7, Salt Lake City, Utah: Utah Geological and Mineral Survey, (Dec. 1964(, pp. 7-10, 22-27.

Ringholz, Raye C. "The Inevitability of Earthquake." Utah Holiday, January 1981, pp. 54-58.

Anderson, Loren R., et al. Liquefaction Potential map for Davis County, Utah. Eight plates, scale 1:48,000. Logan, Utah: Department of Civil and Environmental Engineering, University of Utah. U.S. Geological Survey, Professional paper, contract: 14-08-001-19127, February, 1982.

Anderson, Loren R., et al. Liquefaction Potential map, Salt lake County, Utah. Eight Plates, scale 1:48,000. Logan, Utah: Department of Civil and Environmental Engineering, Utah State University, and Dames and Moore Consulting Engineers, Salt lake City, Utah. U.S. Geological Survey, Professional paper, 1982.

Bruhn,R.L., et al. Structure of the Salt Lake Segment, Wasatch Normal Fault Zone; Implications for Rupture Propagation during Large Earthquakes. Salt Lake City, Utah: Department of Geology and Geophysics, University of Utah, 1985.

Currey, Donald R. Paleolake History in Reconstructing Neotechtonic History and Assessing Earthquake Hazards: The Special Case of Lake Bonneville and the Wasatch Front. Salt Lake City, Utah: Department of Geography, University of Utah, March, 1986.

Hays, Walter W. Evaluation of Local Site Amplification of Earthquake Ground Motion, An Important Consideration In Earthquake-Resistant Design In Utah. Reston, Virginia: U.S. Geological Survey, 1986.

Keaton, Jeffery R., Currey, Donald R., and Olig, Susan J. Paleoseismicity and Earthquake Hazards Evaluation Salt Lake City, Utah of the West Valley Fault Zone, Salt Lake Urban Area. Salt Lake City, Utah: Department of Geography and Department of Geology and Geophysics, University of Utah, 1985.

King, Kenneth W. Efforts on Site Geology on the Level of Ground Shaking Along the Wasatch Front. Denver, Colorado: U.S. Geological Survey, 1986.

Tingey, James L. and Findlay, Ralph F. Emergency Management in Utah for Earthquakes. Salt Lake City, Utah: Utah Division of Comprehensive Emergency Management, 1986.

Earthquake Hazards Research Applications

9900-90022

Walter W. Hays, Paula L. Gori, and William J. Kockelman
Office of Earthquakes, Volcanoes, and Engineering
905 National Center
Reston, Virginia 22092
(703) 648-6711; (FTS) 959-6711

Investigations

Since fiscal year 1978, the U.S. Geological Survey's (USGS) Earthquake Hazards Reduction Program has sponsored a program to foster implementation of research results at all levels of government and in the private sector. The objectives of the program are to:

- Establish "good neighbor" partnerships with Federal, State, and local government agencies and private organizations in the United States to encourage implementation of the National Earthquake Hazards Reduction Program (NEHRP).
- Strengthen local expertise throughout the Nation, stimulate interested persons to accelerate their research about earthquake hazards, and foster implementation of seismic safety policies.
- Disseminate research results and information produced by the USGS to all users, including Federal, State, and local government agencies, engineers and scientists, professional organizations, model building code groups, and others who can incorporate and utilize them in their programs.

Results

In FY 1987, this program supported many diverse activities throughout the United States to meet the above objectives. The principal activities which this program supported are summarized below.

Workshops

Research implementation in Fiscal Year 1987 was highlighted by workshops to evaluate the earthquake hazards research application process during the period 1977-1987. Each year since 1978, regional workshops have been held in cooperation with other Federal agencies throughout the United States to foster State and local implementation of measures to reduce earthquake hazards. During 1987, these workshops concentrated on understanding, evaluating, and improving the research implementation process itself.

The first workshop, sponsored by USGS, concentrated on the communication of hazard and risk information. The second set of three regional workshops, sponsored by all the principal agencies of the National Earthquake Hazards Reduction Program, concentrated on the process of applying earthquake hazards research by States and local jurisdictions.

1) Workshop on "The U.S. Geological Survey's Role in Hazards Warnings," February 2-3, 1987.

Thirty-one physical scientists and social scientists participated in a 2-day USGS sponsored workshop on "The U.S. Geological Survey's Role in Hazards Warnings," in Golden, Colorado, on February 2-3, 1987.

The idea for the workshop evolved from a recommendation at a 1986 meeting of the National Research Council's Subcommittee on Earthquake Research for the USGS to consider reviewing the way it performs its roles in public warning and dissemination of hazards and risk information. At the meeting, social scientists and physical scientists had an opportunity to learn lessons from social science research as well as from the experiences of scientific colleagues in order to understand, evaluate, and improve the communication of hazards and risk information. The workshop participants' recommendations for more effective communication are contained in USGS Open-File Report 87-269, "The U.S. Geological Survey's role in hazards warnings."

2) Workshops on "Research Applications of the National Earthquake Hazards Reduction Program," in California, June 23-25, 1987; in the West Exclusive of California, September 9-11, 1987; and in the East, October 20-22, 1987."

The USGS, National Science Foundation (NSF), Federal Emergency Management Agency (FEMA), and National Bureau of Standards (NBS) joined together to sponsor 3 regional workshops on research applications. The goals of the 3 regional workshops were to:

1) Evaluate some of the applications that have been made during the past decade in the National Earthquake Hazards Reduction Program and to determine why these applications came to fruition.

2) Motivate workshop participants to seek ways to accelerate and improve future application of research.

3) Develop recommendations to improve the current process that links researchers and research applications through programs and policies of USGS, NSF, FEMA, and NBS.

During the three workshops, which were held in San Diego, California; Denver, Colorado; and Knoxville, Tennessee; workshop participants grappled with the questions of why specific research applications were or were not successful in their region and how the process of research, translation, dissemination, and implementation could be improved. A broad mix of applications were reviewed including:

1) Public information and education programs
2) Seismic safety organizations
3) Building design requirements and codes
4) Land-use regulations
5) Building retrofit ordinances
6) Earthquake insurance
7) Earthquake response planning
8) New design and construction practices

At each workshop, 30 to 40 individuals representing local, State, and Federal government, building professions, academia, and private industry found that certain factors increased the likelihood that research would be incorporated into hazard reduction policies and programs. These general findings and the specific assessments of each application discussed at the workshops are contained in the proceedings of the workshops which are being published as USGS open-file reports. All 3 groups of participants identified factors that facilitate ultimate use of the research by policy makers at all levels of government and in private industry and by the public.

Other activities to foster application of research

In addition to convening regional workshops, this program sponsored activities of State organizations and other groups to increase the application of earthquake hazards research. These activities included:

- Support for the seimic safety activities of Utah, Oregon, Washington, and South Carolina State Geological Surveys.
- Support for the 2nd International Earthquake Conference in Los Angeles, California.

Reports

Gori, P. L., and Hays, W. W., eds., 1987, Proceedings of Conference XL, a workshop on "The U.S. Geological Survey's role in hazards warnings," U.S. Geological Survey Open-File Report 87-269, 120 p. plus appendices.

Hays, W. W., and Gori, P. L., eds. 1986, Proceedings of Conference XXXV, a workshop on "Earth science considerations for earthquake hazards reduction in the Central United States," U.S. Geological Survey Open-File Report 86, 172 p.

Hays, W. W., and Gori, P. L., eds., 1987, Proceedings of Conference XXVI, a workshop on "Assessment of geologic hazards and risk in Puerto Rico," U.S. Geological Survey Open-File Report 87-008, 385 p.

Hays, W. W., and Gori, P. L., eds., 1987, Proceedings of Conference XXVIII, a workshop on "Earthquake hazards along the Wasatch Front, Utah," U.S. Geological Survey Open-File Report 87-154, 146 p.

Global Digital Network Operations

9920-02398

Howell M. Butler
Branch of Global Seismology and Geomagnetism
U.S. Geological Survey
Albuquerque Seismological Laboratory
Building 10002, Kirtland AFB-East
Albuquerque, New Mexico 87115-5000
(505) 844-4637

Investigations

The Global Digital Network Operations presently consists of 15 SRO/ASRO and 14 DWWSSN stations. The primary objective of the project is to provide technical and operational support to keep these stations operating at the highest percentage of recording time possible to provide high-quality digital seismic data to the seismic research community. This support includes operational supplies, replacement parts, repair service, modification of existing equipment, installation of systems and on-site maintenance, training and calibration. A service contract provides technicians to perform on-site maintenance and installations, as well as to perform repair-and-test of seismometers and all replaceable units that comprise the various network systems. Contract technicians are also provided for special projects such as on-site noise surveys, special telemetered system installations, system renovations, and evaluation and testing of seismological and related instrumentation.

The following on-site station maintenance activity was accomplished:

KBS - Kingsbay, Spitsbergen - DWWSSN - One maintenance visit
AFI - Afiamalu, Samoa - DWWSSN - Three maintenance visits
ANMO - Albuquerque, New Mexico - SRO - Two maintenance visits
ANTO - Ankara, Turkey - SRO - One maintenance visits
BGIO - Bar Giyora, Israel - SRO - One maintenance visit
LEM - Lembang, Indonesia - DWWSSN - Two maintenance visits
CHTO - Chaing Mai, Thailand - SRO - Two maintenance visits
BOCO - Bogota, Colombia - SRO - One maintenance visit
HON - Honolulu, Hawaii - DWWSSN - One maintenance visit
ZOBO - La Paz, Bolivia - ASRO - One maintenance visit
TOL - Toledo, Spain - DWWSSN - One maintenance visit
BCAO - Banqui, Central African Republic - SRO - One maintenance visit
CTAO - Charters Towers, Australia - ASRO - One maintenance visit

Special Activity

One programmer worked in the Data Processing Center primarily on the VAX system and the Chinese (CDSN) operating system.

One field engineer was in China full time during this period assisting in maintenance and training of CDSN personnel.

Streckeisen Seismometer Systems were installed at Afiamalu, Samoa; Toledo, Spain; and Charters Towers, Australia. At the same time, TOL and CTA WWSSN station recorders were converted to heated pen.

During this period, one field engineer was assigned full time to the WWSSN heated-pen program for testing and check out of the production units.

Results

The Global Digital Network continues with a combined total of 29 SRO/ASRO/DWWSSN stations. The main effort of this project is to furnish the types of support at a level needed to keep the GSN at the highest percentage of operational time in order to provide the highest quality digital data for the world-wide digital data base.

U.S. Seismic Network

9920-01899

Marvin A. Carlson
Branch of Global Seismology and Geomagnetism
U.S. Geological Survey
Denver Federal Center
Box 25046, Mail Stop 967
Denver, Colorado 80225
(303) 236-1506

Investigations

U.S. Seismicity. Data from the U.S. Seismic Network (USSN) are used to obtain preliminary locations and magnitudes of significant earthquakes throughout the United States and the world.

Results

As an operational program, the USSN operated normally throughout the report period. Data were recorded continuously in real time at the National Earthquake Information Center's (NEIC) main office in Golden, Colorado. At the present time, 120 channels of SPZ data are being recorded at Golden on develocorder film. This includes data telemetered to Golden via satellite from both the Alaska Tsunami Warning Center, Palmer, Alaska, and the Pacific Tsunami Warning Center, Ewa Beach, Hawaii. A representative number of SPZ channels are also recorded on Helicorders to give NEIC real-time monitoring capability of the more active seismic areas of the United States. In addition, 15 channels of LPZ data are recorded in real time on multiple pen Helicorders.

Data from the USSN are interpreted by record analysts and the seismic readings are entered into the NEIS data base. The data are also used by NEIS standby personnel to monitor seismic activity in the United States and world wide on a real time basis. Additionally, the data are used to support the Alaska Tsunami Warning Center and the Pacific Tsunami Warning Service. At the present time, all earthquakes large enough to be recorded on several stations are worked up using the "Quick Quake" program to obtain a provisional solution as rapidly as possible. Finally, the data are used in such NEIS publications as the "Preliminary Determination of Epicenters" and the "Earthquake Data Report."

Development is continuing on an Event Detect and Earthquake Location System to process data generated by the USSN. We expect the new system to be ready for routine operational use by spring of 1988. At that time, the use of develocorders for data storage will be discontinued. Ray Buland and David Ketchum have been doing most of the developmental programming for the new system. A Micro Vax II will be used as the primary computer of the Event Detect and Earthquake Location System. PDP 11/23's and PDP 11/73's are being used as front ends to off load the real-time data collection from the

Micro Vax II. A second Micro Vax II has been procured to serve as a backup to the primary system. The two Micro Vaxs share 1.3 gigabytes of disk storage.

During FY 1987, four stations of a pilot VSAT Network were installed. Three of the stations were former RSTN sites at McMinnville, Tennessee, St. Regis Falls, New York, and Black Hills, South Dakota, which are now operated by the Branch of Global Seismology and Geomagnetism. The fourth site is the first prototype National Seismic Network Station at Bergen Park, Colorado. The data is transmitted via satellite to a shared Master Earth Station and on to the NEIC at Golden, Colorado.

Earth Structure and its Effects upon Seismic Wave Propagation

9920-01736

George L. Choy
Branch of Global Seismology and Geomagnetism
U.S. Geological Survey
Denver Federal Center
Box 25046, Mail Stop 967
Denver, Colorado 80225
(303) 236-1506

Investigations

1. Enhancement of NEIC reporting services. We are incorporating techniques of analyzing broadband data into the data flow of the NEIC. However, the accuracy of source parameters extracted from digitally recorded data depends on the correct application of propagation corrections to waveforms. Broadband data can then be used on a routine basis to increase the accuracy of some reported parameters such as depth and to compute additional parameters such as radiated energy.

2. Use of body wave pulse shapes to infer attenuation in the Earth. We are developing techniques to determine the depth- and frequency-dependence of attenuation in the Earth. Resolution of this frequency dependence requires analysis of a continuous frequency band from several Hz to tens of seconds. It also requires consideration of the contributions of scattering and slab diffraction to apparent broadening of a pulse.

3. Use of differential travel-time anomalies to infer lateral heterogeneity. We are investigating lateral heterogeneity in the Earth by analyzing differential travel times of phases that differ in ray path only in very narrow regions of the earth. Because such phases often are associated with complications near a cusp or caustic, their arrival times can not be accurately read without special consideration of the effects of propagation in the earth as well as additional processing to enhance arrivals.

Results

1. A computer package has been implemented that routinely processes digital data received by the NEIC into broadband records using the method of Choy and Boatwright (1981) and Harvey and Choy (1982). The broadband data are now routinely used by the NEIC to determine with greater accuracy the depths of earthquakes. Techniques for determining depths of earthquakes using broadband data are described in Choy and Engdahl (1987). A semi-automated version of the algorithm of Boatwright and Choy (1986) has been implemented to compute the radiated energies of earthquakes with $m_b > 5.8$. The frequency-dependent Q model of Choy and Cormier (1987) has been incorporated into the energy algorithm.

2. We are attempting to separate intrinsic attenuation from scattering in waveforms. We synthesize waveforms using a method that simultaneously models causal attenuation and source finiteness. Under the assumption that intrinsic attenuation can be described by minimum phase operators, we can attribute discrepancies in the waveforms to scattering.

3. We have developed a source-deconvolution technique that resolves differential travel times of body waves near cusps and caustics. Application of this algorithm to PKP waves sampling the inner core suggests that regional velocity variations exist within the upper 200 km of the inner core. The regional variations are consistent with those obtained from global inversions of absolute PKP times. We are reading high quality arrival times of PcP and branches of PKP, corrected for propagation effects. This accumulation of data can be used to determine if propagation phenomena have biased the catalog data which have been used to derive models of lateral heterogeneity.

Reports

Choy, G. L., and Engdahl, E. R., 1987, Analysis of broadband seismograms from selected IASPEI events: Physics of the Earth and Planetary Interiors, v. 47, p. 80-92.

Systems Engineering

9920-01262

Harold E. Clark, Jr.
Branch of Global Seismology and Geomagnetism
U.S. Geological Survey
Albuquerque Seismological Laboratory
Building 10002, Kirtland AFB-East
Albuquerque, New Mexico 87115-5000
(505) 844-4637

Investigations

Continued the development and support of the China Digital Seismograph Network (CDSN).

Results

CDSN System No. 12 construction and assembly is nearly complete. CDSN System No. 12 will provide the same data recording techniques as the other 11 CDSN systems and will also provide a satellite telemetry channel for data transmission. Work is continuing on a special satellite data receiving station to record and analyze the CDSN data. The initial satellite link will be tested using parts and equipment from the Sandia RSTN satellite network.

During the past year, major repair requirements and operational testing of CDSN units that were returned from the CDSN Maintenance Facility at Beijing, China, were handled by the Albuquerque Seismological Laboratory (ASL) Engineering Section. Additional units that had a higher than expected failure rate or took longer due to the shipping time between China and the United States were purchased and tested at ASL before shipping to the CDSN Maintenance Center. The CDSN Maintenance Center is gradually gaining expertise to repair and maintain the CDSN systems and individual units and replacement boards.

Reanalysis of Instrumentally Recorded United States Earthquakes

9920-01901

J. W. Dewey
Branch of Global Seismology and Geomagnetism
U.S. Geological Survey
Denver Federal Center
Box 25046, Mail Stop 967
Denver, Colorado 80225
(303) 236-1506

Investigations

1. Relocate instrumentally recorded U.S. earthquakes using the method of joint hypocenter determination (JHD) or the master event method, using subsidiary phases (Pg, S, Lg) in addition to first arriving P-waves, using regional travel-time tables, and expressing the uncertainty of the computed hypocenter in terms of confidence ellipsoids on the hypocentral coordinates.

2. Evaluate the implications of the revised hypocenters on regional tectonics and seismic risk.

Results

Jim Dewey has written a paper on the role of seismotectonic paradigms in the design and interpretation of seismicity studies. Paradigms are "universally recognized scientific achievements that for a time provide model problems and solutions to a community of users" (Kuhn, 1970, p. viii). A paradigm is a framework within which the community identifies and solves the puzzles of its discipline.

Seismicity studies are usually motivated by one or both of two paradigms--an earthquake-source paradigm in which displacement along preexisting faults is the cause of earthquakes and a regional-tectonics paradigm based on plate tectonics. Although the fault paradigm is about a century old and the plate-tectonics paradigm more than two decades old, both paradigms seem as susceptible as ever to being extended to cover still more seismotectonic phenomena. The earthquake/fault paradigm is being extended to incorporate examples of segmented faults, of active faults that are quiescent for long periods between major earthquakes, of second-order seismogenic faults that are subsidiary to major regional faults, and of seismogenic faults that do not outcrop at the ground surface. The earthquake/plate-tectonics paradigm is being extended to predict the percentage of slip on plate-boundary faults that is released aseismically, to account for high rates of deformation that extend far into the interior of some continental plates, and to predict the orientations of midplate stresses. Midplate earthquakes continue to pose problems for both paradigms. It is noteworthy, nevertheless, that some of the most significant recent observational advances in midplate seismicity are consistent with the plate-tectonics and faulting paradigms.

References Cited

Kuhn, T. S., 1970, The structure of scientific revolutions (2nd ed.): University of Chicago Press, Chicago, 212 p.

Reports

Dewey, J. W., 1987, Instrumental seismicity of central Idaho: Bulletin Seismological Society America, v. 77, p. 819-836.

Dewey, J. W., Hill, D. P., Ellsworth, W. L., and Engdahl, E. R., Earthquakes, faults, and the seismotectonic framework of the contiguous United States, in L. C. Pakiser and W. D. Mooney (eds.), Geophysical framework of the continental United States: Memoir of the Geological Society of America (in press).

Dewey, J. W., Hypocenter mapping and the extensibility of seismotectonic paradigms, in J. J. Litehiser (ed.), Proceedings, symposium on the centennial anniversary of the Mount Hamilton seismographic station, Berkeley, California, 28-30 May, 1987: University of California Press (in press).

Global Seismology

9920-03684

E. R. Engdahl
and
J. W. Dewey

Branch of Global Seismology and Geomagnetism
U.S. Geological Survey
Denver Federal Center
Box 25046, Mail Stop 967
Denver, Colorado 80225
(303) 236-1506

Investigations

1. Depth Phases. Develop procedures for the global analyses of earthquake depth phases and source characteristics using broadband seismograms of body waves.

2. Earthquake Location in Island Arcs. Develop practical methods to accurately locate earthquakes in island arcs.

3. Subduction Zone Structure. Develop techniques to invert seismic travel times simultaneously for earthquake locations and subduction zone structure.

4. Global Synthesis. Synthesize recent observational results on the seismicity of the earth and analyze this seismicity in light of current models of global tectonic processes.

Results

1. Depth Phases. Source parameters have been systematically determined for all earthquakes $M_w \geq 5$ that occurred between 172° and 179° W. longitude in the Adak Island region of the central Aleutians during 1977-1986. Centroid-moment tensor (CMT) solutions yield stable results for 76 events. We relocate the events using a plate model developed for the region and use two alternative methods of depth determination. The first method uses broadband P-wave displacement seismograms and the long-period CMT data set in an inversion for the mechanism, depth, and time function of the source. The second method uses arrival times of direct and prominent reflected phases, primarily pwP, from short-period and broadband digital seismograms.

Systematic analysis of these events provides an unusually well-constrained data set for the study of stress release along an active subduction zone. Three earthquakes, which occurred seaward of the trench axis, are located just below the crust-mantle interface and show extension nearly perpendicular to the trench axis. Sixty-four events are located in the active thrust zone 50-130 km north of the trench axis, and, except for 5 unusual events, are characterized by thrust mechanisms with one nodal plane dipping north at a shallow angle. In map view, the projection of the P axis of the moment tensors for these events agrees well with the direction of relative plate motion for the region. In cross section, the thrust zone appears as a thin (thickness < 15 km) interplate region; the dip angle of the shallow dipping plane gently steepens with depth. Five earthquakes, which occurred as aftershocks of the May 7, 1986, earthquake ($M_w = 8$) in the crust of the overriding plate, are characterized by strike-slip mechanisms. Six events at depths greater that 50 km have null axes nearly parallel to the strike of the slab.

2. Earthquake Location in Island Arcs. Nothing new to report.

3. Subduction Zone Structure. Early work with body waveforms for slab modeling used ray trajectories and densities to estimate ray theoretical amplitudes and to identify multipathing, but could not calculate the frequency dependent effects of head waves and diffraction along slab boundaries and radiation having wavelengths on the order of or larger than slab width. Recently, however, the techniques of forward modeling of body waves in two- and three-dimensional structures have been systematically advanced to show these effects to be highly sensitive to slab width and its variations with depth. Application of these new techniques to the central Aleutian and Kurile subduction zones demonstrate that waveforms of P and S waves can provide important new constraints on slab structure that are independent of the information provided by their arrival times.

Some general features of wave propagation in subducted slabs are highlighted. The anomalous features are of three kinds: (1) faster material in the slab advances the arrivals that leave the source region in the plane of the slab; (2) faster material in the slab tends to defocus energy leaving the source region in the plane of the slab; (3) the waveforms of energy that leave the source region in the plane of the slab can be distorted, with emergent first arrivals and a long-period, late-diffracted arrival, which can make the full waveform appear as a broadened pulse. Slab diffraction is akin to a head wave traveling along the underside of the slab. It arrives late in the waveform because it is sensitive to the slower velocity structure that surrounds the higher velocity slab. In general, thinner slabs of a given length produce more waveform broadening and smaller amplitudes for signals that leave the source in the plane of the slab. It is also predicted that slab diffraction will be observed at all azimuths on the downdip side of a steeply dipping slab, strongest in a direction oblique to the normal to the strike of the slab, evolving into a prominent secondary phase along strike, and rapidly decaying on the side opposite to the dip. Slab diffraction effects have been demonstrated for both P and S waves, but are more pronounced in the case of S waves. However, attenuation affects S waves more than P waves, so that both types of body waves are needed to study waveform distortions due to slabs.

There seems to be strong evidence for slab diffraction effects in P waves from central Aleutian earthquakes. The observations reported by Vidale and Garcia-Gonzalez (1987) and Engdahl and Kind (1986), and the modeling reported by Vidale and Helmberger (1986) suggest that the central Aleutian slab is relatively thin, probably no more than 40-50 km thick. Further development of the inversion techniques of Engdahl and Gubbins (1987) and more investigation of broadband data and modeling is needed to confirm this result.

Thus far, the primary source of information on penetration of the Kurile slab beyond 670 km has been travel-time anomalies. However, slab length will still have some tradeoff with lateral variations in slab shape and velocity, and the magnitude of velocity perturbation within the slab. A priori constraints of thermal models and phase changes can reduce, but not eliminate these tradeoffs. The possibility of using amplitudes and waveforms as additional constraints on the modeling of slab structure has been demonstrated. Vidale and Helmberger (1986) presented evidence for slab diffraction effects along an azimuth perpendicular to the strike of the slab for a 135 km deep Kurile event, but not for an event at 540 km depth. Silver and Chan (1986) showed that a zone of multipathed arrivals can exist for S waves from deep focus Kurile earthquakes observed along azimuths parallel to the strike of the slab. The duration of the predicted multipathing, however, is too small to account for the duration of the tail in broadband waveforms of the S wave. Cormier (1987), based on modeling studies, suggests that the mechanism of slab diffraction is sufficient to explain the duration of observed S pulses in many azimuths without additional ray theoretical arrivals. Multipathing along strike, however, is consistent with the observations of high variability in S waveform widths and complexity for azimuths close to the strike of the slab (e.g., Silver and Chan, 1986; Beck and Lay, 1986). Thus, there is conflicting evidence in amplitude and waveform data on the geometry of the Kurile slab near and below the 670 km discontinuity and the data may require independent lower mantle lateral heterogeneity as well.

4. Global Synthesis. A highlight of the Decade of North American Geology (DNAG) program is four new continent-scale tectonic maps (geothermal, stress, seismicity, and geologic) on a common base. The maps are in color, at a scale of 1:5,000,000, and use a Transverse Mercator projection. Construction of the seismicity map has required the rationalization of more than one-half million earthquake epicenters from global, national, regional, and local catalogs. Duplicate entries were removed regionally based on a comparison of reported origin times, epicentral locations, and magnitudes. The reduced data base spans an interval from A.D. 1500 to 1985. Only those data that exceed the magnitude-completeness threshold for each region and time period were plotted. In all parts of the map, earthquakes of magnitudes less than 4 are represented by small dots, larger earthquakes by filled circles of various sizes in proportion to magnitude, and great earthquakes ($M \geq 7$) by large rings. Different colors are used to distinguish modern from historic data and to show deep ($h \geq 50$ km), intraplate earthquakes in subduction zones. The modern data are more useful than historic data for resolving seismotectonic features, as they have more accurate locations and lower magnitude-completeness thresholds. This scheme of symbols and colors reveals details of the seismotectonic fabric of North America yet preserves a perspective of historical earthquake occurrence.

Construction of the DNAG Seismicity Map of North America has revealed important facets about earthquake monitoring in the western United States.

For the most part, the western United States, including the Rocky Mountain region, is reasonably well monitored by present day networks. Areas monitored to only about the magnitude 3.5 level include Oregon, large parts of Idaho, and Arizona. These are regions of low seismicity in which funding agencies have not been inclined to support the installation of permanent networks (although some short-term studies have been made). The offshore regions, especially west of about 126° near Cape Mendicino, obviously pose a special problem and are complete only to relatively high teleseismic magnitude thresholds.

There is considerable overlap in network coverage over large areas of the western United States. Networks in California and Nevada apparently share phase data and, in some cases, the actual data stream, but individual catalogs often extend beyond their network boundaries, and there is considerable uncertainty in the choice of preferred hypocenters. To some extent, there is a duplication of effort, but this is probably desirable to insure continuity in the overall catalog. Somewhat better coordination between the United States and Canada exists in the Pacific northwest and with Mexico in the Baja California region.

The users of regional network data in the western United States could certainly benefit through improved usage of magnitudes and better regional recurrence estimates. The types of magnitudes commonly used vary, and relationships between them are not well known. Some standardization seems essential. In most cases, network magnitude thresholds with time are only subjective estimates. It is possible and necessary to perform a more careful analysis over well-defined regions.

Finally, there needs to be a coordinated effort to correct and update the DNAG database for the western United States. This will require better definition of network coverages with time, determination of more accurate regional magnitude completeness thresholds, and some attempt to rationalize the differences between reported magnitudes.

Reports

Choy, G., and Dewey, J. W., 1987, Rupture process of an extended earthquake sequence--Teleseismic analysis of the Chilean earthquake of 3 March 1985: Journal of Geophysical Research (submitted).

Ekström, G., and Engdahl, E. R., 1987, Earthquake source parameters and stress distribution in the Adak Island region of the central Aleutian Islands, EOS (American Geophysical Union, Transactions) (in press).

Engdahl, E. R., Vidale, J. E., and Cormier, V. F., Wave propagation in subducted lithospheric slabs, Proceedings of the 6th Course: Digital Seismology and Fine Modeling of the Lithosphere, Marjorana Center, Sicily (submitted).

Engdahl, E. R., and Rinehart, W. A., 1987, Seismicity map of North America: Proceedings of the Berkeley Centennial Symposium (submitted).

Global Seismograph Network Evaluation and Development

9920-02384

Jon Peterson
Branch of Global Seismology and Geomagnetism
U.S. Geological Survey
Albuquerque Seismological Laboratory
Building 10002, Kirtland AFB-East
Albuquerque, New Mexico 87115-5000
(505) 844-4637

Investigations

1. China Digital Seismograph Network (CDSN).

2. Incorporated Research Institutions for Seismology (IRIS) global seismograph network (GSN).

Results

1. The CDSN has fully operational during the report period, and CDSN data are being distributed on the Albuquerque Seismological Laboratory (ASL) network-day tapes. An ASL representative, on site for most of the period, has assisted in servicing the stations and organizing the network maintenance center. Preparations are underway for an acceptance test to be held in China in October. A joint report on the network has been prepared.

2. The establishment of the IRIS/USGS data collection center at the ASL is progressing very well. A Micro Vax II cluster is in operation with VMS operating system; software development for data review and network-volume assembly is well underway; and an additional processor and large-capacity disk were ordered in late September. Current plans are to convert to the new format for distribution of the January 1, 1988, network-day tape. The ASL staff has supported IRIS in monitoring development of the IRIS II system, is preparing for prototype testing in early 1988, and has continued to test and evaluate both borehole and surface-type broadband seismometers that may be used in the GSN.

Digital Data Analysis

9920-01788

Stuart A. Sipkin
Branch of Global Seismology and Geomagnetism
U.S. Geological Survey
Denver Federal Center
Box 25046, Mail Stop 967
Denver, Colorado 80225
(303) 236-1506

Investigations

1. Moment Tensor Inversion. Apply methods for inverting body phase waveforms for the best point-source description to research problems.

2. Other Source Parameter Studies. Apply methods for inverting body phase waveforms for distributed kinematic and dynamic source properties.

3. Broadband Body-Wave Studies. Use broadband body phases to study lateral heterogeneity, attenuation, and scattering in the crust and mantle.

4. Earthquake Recurrence Statistics. Use earthquake recurrence statistics and related parameters to better understand the earthquake cycle and study how they can be used for prediction and forecasting purposes.

5. Real-Time Earthquake Location. Experiment with real-time signal detection, arrival-time estimation, and event location for regional earthquakes.

6. Data Collection Center. Develop a state-of-the-art data collection center to handle digital waveform data collection for the next decade.

7. NEIC Monthly Listing. Contribute both fault-plane solutions (using first-motion polarity) and moment tensors (using long-period body-phase waveforms) for all events of magnitude 5.8 or greater when sufficient data exists. Contribute waveform/focal-sphere figures of selected events.

Results

1. Moment Tensor Inversion. A paper assessing the large number of non-double-couple earthquakes occurring in the Nazca plate subduction zone has been published. We find that these earthquakes are caused by slip on non-planar fault surfaces which is, in turn, due to the extreme structural complexity in this region. An anomalous seismic event which occurred off the coast of Japan has been analyzed. The resulting mechanism is consistent with the hypothesis that this event was caused by fluid injection.

2. Other Source Parameter Studies. A journal article on the inversion of teleseismic P waveforms for the distribution of fault slip has been submitted for publication. The long-period data constrain the duration and seismic moment of an earthquake, while the short-period waveforms are necessary to resolve the variation of slip on the fault. Results for moderate-to-large earthquakes imply a stress and/or strength heterogeneity along the fault surface.

3. Broadband Body-Wave Studies. High-quality digitally recorded broadband data sets from the Gräfenberg Array in West Germany and the Regional Seismic Test Network in North America have been collected. Multiple-ScS differential travel times have been computed by waveform cross-correlation. Estimates of the multiple-ScS attenuation operator have been obtained using a phase-equalization and stacking technique. For the tectonic Eurasia and North America paths, we obtain Q_{ScS} of 136±27 and 182±21, respectively, over the frequency band 0.015-0.125 Hz. In this band, there is no apparent frequency dependence.

4. Earthquake Recurrence Statistics. A paper describing a new earthquake forecasting algorithm has been published. Work is underway on applying the algorithm to cases where only one recurrence interval is available, where the recurrence interval must be estimated from other information, and where only paleoseismic information is available.

5. Real-Time Earthquake Location. The network processor software for the National Seismic Network (NSN) has been up for testing. The new version has been debugged and some performance enhancements made. New work on obtaining real-time starting solutions has been initiated. The first NSN prototype station has been installed in Bergen Park, Colorado, and some good event recordings obtained. Procurements for the NSN seismometers, telemetry, network processing system, mass storage, and field processing systems are being prepared.

6. Data Collection Center. Software conversion is well along. Additional hardware needed to become fully operational will be delivered in early December 1987. A new data distribution format has been proposed and awaits final adoption by international organizations.

7. NEIC Monthly Listing. Since January 1981, fault-plane solutions for all events of magnitude 5.8 or greater have been contributed to the Monthly Listings. Since July 1982, moment tensor solutions and waveform/focal-sphere plots have also been contributed. Fault-plane solutions for the period 1981-1985, and moment tensor solutions for the period 1981-1983, have been compiled and published. In the last 6 months, solutions for approximately 66 events have been published. Detailed regional seismicity maps, covering the time period from 1971 to 1986, for 16 seismogenic areas worldwide, have been prepared and presented at various international and domestic meetings.

Reports

Buland, R. P., 1987, Can the regional seismic networks benefit from national seismic network technology? [abs.]: Seismological Research Letters, v. 58 (in press).

Buland, R. P., 1987, A national system of seismic networks [abs.]: EOS (American Geophysical Union, Transactions), v. 68 (in press).

Buland, R. P., and Nishenko, S. P., 1987, Earthquake forecasting along simple plate boundaries [abs.]: Abstracts, 19th IUGG General Assembly, Vancouver, Canada, p. 261.

Kubas, A., and Sipkin, S. A., 1987, Non-double-couple earthquake mechanisms in the Nazca plate subduction zone [abs.]: EOS (American Geophysical Union, Transactions), v. 68, no. 16, p. 359.

Kubas, A., and Sipkin, S. A., 1987, Non-double-couple earthquake mechanisms in the Nazca plate subduction zone: Geophysical Research Letters, v. 14, no. 4, p. 339-342.

Lee, W.H.K., Zirbes, M. D., and Needham, R. E., 1987, Two applications of personal computers for seismological studies at the U.S. Geological Survey [abs.]: Abstracts, 19th IUGG General Assembly, Vancouver, Canada, p. 380.

Mendoza, C., and Hartzell, S. H., 1987, Slip distribution during the 1985 Michoacan earthquake from teleseismic P waves [abs.]: Abstracts, Mexican Geophysical Union Annual Meeting, Ensenada, Mexico (in press).

Mendoza, C., and Hartzell, S. H., 1987, Inversion for slip distribution using GDSN P waves: North Palm Springs, Borah Peak, and Michoacan earthquakes: Bulletin Seismological Society of America (submitted).

Nishenko, S. P., and Buland, R. P., 1987, A generic recurrence interval distribution for earthquake forecasting: Bulletin Seismological Society of America, v. 77, no. 4, p. 1382-1399.

Sipkin, S. A., 1987, Body wave analysis of the anomalous seismic event near Tori Shima, Japan [abs.]: EOS (American Geophysical Union, Transactions), v. 68, no. 16, p. 358-359.

Sipkin, S. A., 1987, Moment tensor solutions estimated using optimal filter theory for 51 selected earthquakes, 1980-1984: Physics of the Earth and Planetary Interiors, v. 47, p. 67-79.

Sipkin, S. A., 1987, A comparison of the USGS moment tensor solutions, USGS first-motion focal mechanisms, and Harvard CMT solutions [abs.]: Abstracts, 19th IUGG General Assembly, Vancouver, Canada, p. 280.

Sipkin, S. A., 1987, Observation and analysis of broadband multiple-ScS phases [abs.]: EOS (American Geophysical Union, Transactions), v. 68 (in press).

Seismicity and Tectonics

9920-01206

William Spence
Branch of Global Seismology and Geomagnetism
U.S. Geological Survey
Denver Federal Center
Box 25046, Mail Stop 967
Denver, Colorado 80225
(303) 236-1506

Investigations

Studies carried out under this project focus on detailed investigations of large earthquakes, aftershock series, tectonic problems, and Earth structure. Studies in progress have the following objectives:

1. Use earthquake focal mechanisms and integrative tectonics to infer the origins of present-day stresses acting at the proposed Cascadia subduction zone (W. Spence).

2. Explore the consequences of the slab pull force acting at the zone of plate bending that is downdip of the lower end of an interface thrust zone (W. Spence and W. Z. Savage).

3. Provide tectonic setting for and analysis of the 1974 Peru gap-filling earthquake (W. Spence and C. J. Langer).

4. Examine the seismicity and tectonics of the Isthmus of Panama using earthquake relocation methods and modern techniques of focal-mechanism determination.

5. Determine the maximum depth and degree of velocity anomaly beneath the Rio Grande Rift and Jemez Lineament by use of a 3-D, seismic ray-tracing methodology (W. Spence and R. S. Gross).

Results

1. Earthquakes in the Juan de Fuca plate that is subducted beneath the State of Washington generally exhibit extensional stresses. These stresses are due to the slab pull force, the primary driving force for subduction and for shallow, subduction earthquakes. However, the 60 percent slowing of Cascadian subduction over the interval 6.5-0.5 m.y.B.P. (Riddihough, Journal of Geophysical Research, 1984) suggests that the local slab pull force is diminishing in its capability to lead to great subduction earthquakes. Magnetic anomaly lineations cannot resolve plate motions for the last 500,000 years; thus, present-day details of subduction of the Juan de Fuca plate must be inferred from recent geologic, tectonic, and seismic data.

The seismicity of the Cascadia subduction zone is anomalous when compared to other subduction zones. A synthesis of 19 focal mechanisms for the zone from Cape Mendocino to the Queen Charlotte fault shows that most of the offshore earthquakes are associated with maximum compressive stress axes that trend about N-S (fig. 1). The locations of these earthquakes indicate that much of the offshore plate system is being compressed by the northwestward motion of the Pacific plate. Similarly, there is considerable evidence for N-S compression in the shallow crust of the overriding North American plate, from Cape Mendocino northwards to Vancouver (see fig. 1). The fact that the South Gorda block is not subducting but is being driven northward suggests that a N-S shear traction is being transmitted into the overriding plate, consistent with the observed landward focal mechanism data. The slowing of Cascadian subduction and the Pacific plate's motion leading to pervasive N-S compression in the Cascadian plate system suggest that the in-plate driving forces of the Juan de Fuca plate no longer dominate the Juan de Fuca plate's motion and that the cessation of subduction at Cascadia is in progress. This unusual subduction environment will complicate estimates of the timing and size of future subduction earthquakes at Cascadia.

2. Interface thrust zones typically have dips in the range 8-15°, whereas lithospheres that are subducted into the mantle typically have dips in the range 40-70°, giving an average dip increase in the mantle of about 45°. These dip increases often occur within 40-60 km of plate length. These zones of sharp dip increases (slab bends) have not been given much attention because generally they lack large earthquakes. This is in sharp contrast to the well-studied zones of bending beneath oceanic trenches where there are frequent normal-faulting earthquakes. It has been noted by Ruff and Kanamori (1983) that great, interface thrust earthquakes terminate their downdip ruptures at the updip part of mantle slab bends. Spence (1987) showed that the slab pull force is the primary force that causes shallow, subduction earthquakes (see fig. 2). He also interpreted the mantle slab bends as a pivot for the summed slab pull force of the more deeply subducted plate. In this study, we model the stress distribution in the mantle slab bend, acting under a slab pull load. We find that the observed lack of earthquakes in the mantle slab bend is due to ductility there. However, the strength of the work-hardened ductile portion of the slab bend is more than sufficient to transmit the slab pull load into the shallow subduction zone.

3. The great 1974 Peru thrust earthquake (M_S 7.8, M_W 8.1) occurred in a documented seismic gap, between two earthquakes each with magnitude of about 8, occurring in 1940 and 1942. Additional major earthquakes occurred in this region in 1966 and in 1970; all but the 1970 shock represent thrust faulting. The stress release of the October 3, 1974, main shock and aftershocks occurred in a spatially and temporally irregular pattern. The multiple-rupture main shock produced a tsunami with wave heights of 0.6 ft at Hawaii and which was observed, for example, at Truk Island and at Crescent City. The aftershock series essentially was ended with the occurrence of a M_S 7.1 aftershock on November 9, 1974. The several years of preseismicity data to this earthquake include an unusually clear example of the "Mogi donut" pattern.

4. Earthquakes occurring in the Costa Rica-Panama-Colombia region provide important information on the tectonic framework of the Panamanian Isthmus in Central America. Earthquake epicenters generally define the boundaries between the Cocos, Nazca, and Caribbean plates; focal mechanisms for these earthquakes reflect the relative motion of the plates. However, the boundary between the Caribbean and Nazca plates presently is not well defined by seismicity. A more detailed examination of the seismicity pattern is currently being conducted to obtain a more complete understanding of the seismotectonic characteristics of the Panama segment. Earthquake locations for events with $m_b \geq 5.0$ are being recomputed with the method of joint hypocenter determination (JHD). Also, focal mechanisms for many of these earthquakes are being recompiled from the published literature or are being determined using modern surface-wave techniques.

5. To a depth of about 160 km, the upper mantle P-wave velocity beneath the Rio Grande rift and Jemez lineament is 4-6 percent lower than beneath the High Plains Province. A 3-D, P-wave velocity inversion shows scant evidence for pronounced low P-wave velocity beneath the 240-km-long section of the Rio Grande rift covered by our array. However, the inversion shows a primary trend of 1-2 percent lower P-wave velocity underlying the northeast-trending Jemez lineament, down to a depth of about 160 km. The Jemez lineament is defined by extensive Pliocene-Pleistocene volcanics and late Quaternary faults. The upper mantle low-velocity segment beneath the Jemez lineament is at most 100 km wide and at least 150-200 km long, extending in our inversion from Mt. Taylor through the Jemez volcanic center and through the Rio Grande rift. A Backus-Gilbert resolution calculation indicates that these results are well-resolved.

Reports

Mendoza, Carlos, 1986, Source mechaisms of Colombia aftershocks using surface-wave data: Bulletin of the Seismological Society of America, v. 76, 1597-1613.

Mendoza, Carlos and Hartzell, S. H., Inversion for slip distribution using GDSN P-waves--North Palm Springs, Borah Peak, and Michoacan earthquakes: Bulletin of the Seismological Society of America (submitted).

Spence, William, 1987, Slab pull and the seismotectonics of subducting lithosphere: Reviews of Geophysics, v. 25, p. 55-70.

Spence, William, 1987, Implications of the slowing of subduction at Cascadia [abs.]: EOS (American Geophysical Union, Transactions) (in press).

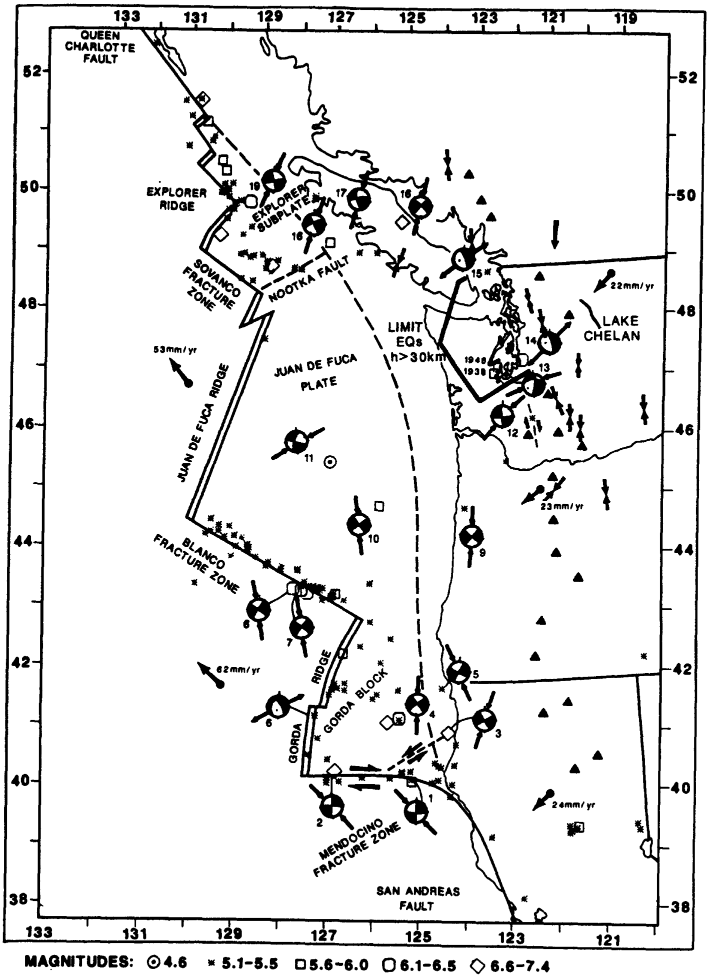

Figure 1. Cascadia seismicity, 1964-June 1986, for earthquakes of magnitude ≥ 5.1. Additional key earthquakes are shown by dates or are indicated by focal mechanism solutions. Volcanoes indicated by triangles. For earthquake focal mechanisms, directions of greatest compressional stress indicated by convergent arrows for strike-slip earthquakes; directions of least compressional stress indicated by divergent arrows for normal-faulting earthquakes. Additional focal mechanism data indicating N-S compression in central Washington and east of Vancouver are shown by arrows that meet. Most earthquakes deeper than 30 km are within the bracketed zone. Geometry of ridges and fracture zones, and absolute plate motions for time frame ending 0.5 m.y. ago are from Riddihough (1984).

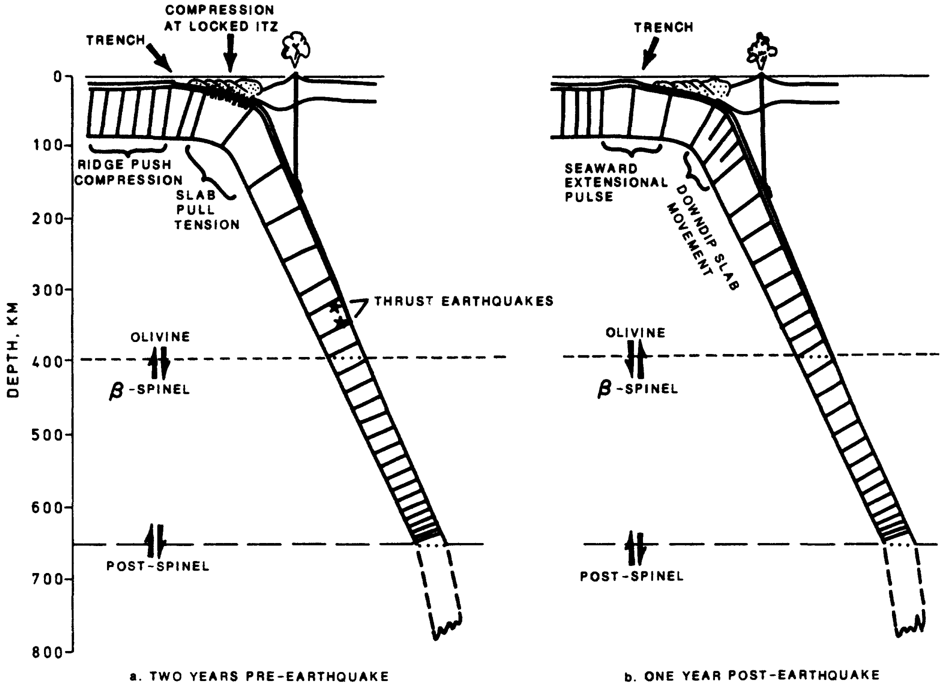

Figure 2. Schematic diagram of stresses in a subducting plate (a) two years before a great subduction zone earthquake and (b) one year after a great subduction zone earthquake. The slab pull force, which causes plate sinking, dominates greatly over the ridge push force, which leads to horizontal motions of the surface plates. This figure illustrates how the sinking of subducted plate is resisted at a locked subduction zone, ultimately causing high stress and great earthquakes there (Spence, 1987). After a great subduction earthquake, continued plate sinking perpetuates the earthquake cycle. This sinking provides the primary physical basis for the recurrence of great subduction earthquakes.

United States Earthquakes

9920-01222

Carl W. Stover
Branch of Global Seismology and Geomagnetism
U.S. Geological Survey
Denver Federal Center
Box 25046, Mail Stop 967
Denver, Colorado 80225
(303) 236-1500

Investigations

1. One hundred and forty-five earthquakes in 19 states were canvassed by a mail questionnaire for felt and damage data. Both Alaska and California were canvassed for 46 earthquakes. The largest magnitude event occurred on April 6, 1987, in the Andreanof Islands, Aleutian Islands, Alaska, at 51.164° N., 179.880° W., normal depth, magnitude 6.3 m_b and 6.4 M_s; felt on Adak Island. An earthquake near Eureka, California, on July 31, 1987, at 40.415° N., 124.407° W., magnitudes 5.6 m_b and 6.0 M_s, caused minor damage at Eureka and Petrolia, California. The most significant event was the June 10, 1987, earthquake in southern Illinois. It was located at 38.713° N., 87.954° W., magnitude 4.9 m_b, 4.4 M_s, 5.1 m_{blg}, causing only minor damage.

2. Hypocenters for earthquakes in the United States for the period April 1, 1987, to September 30, 1987, have been computed and published in the Preliminary Determination of Epicenters (PDE) Weekly and Monthly Listings.

Results

A preliminary maximum intensity of VI has been assigned to both the June 10, Illinois, and the July 31, California earthquakes. Most of the intensity VI effects for the Illinois event were located in the vicinity of the epicenter. The damage consisted of old chimney cracked or broken at the roofline, cracks in exterior brick walls and interior plaster or sheetrock walls, cracks in streets and sidewalks, and cracked concrete and cinderblock foundations. This earthquake was felt over a contiguous area of 433,000 km^2 in nine states with isolated felt reports from seven other states. The California earthquake caused the same type of damage.

State seismicity maps for Indiana (MF-1974), North Carolina (MF-1988), Ohio (MF-1975), and Vermont (MF-1987) have been updated through 1983 and reprinted.

A new color seismicity map of the conterminous United States and adjacent areas, 1975-1984, has been published at a scale of 1:5,000,000 showing the seismicity and tectonics of the 48 states.

Reports

Reagor, Glen, 1987, Preliminary isoseismal map and intensity distribution for the southeastern Illinois earthquake of June 10, 1987: U.S. Geological Survey Open-File Report 87-578, 3 p.

Stover, C. W., 1987, United States earthquakes, 1983: U.S. Geological Survey Bulletin 1698, 197 p.

Stover, C. W., Seismicity map of the conterminous United States and adjacent areas, 1975-1984: U.S. Geological Survey Geophysical Investigations Map GP-984.

Data Processing Section

9920-02217

John Hoffman
Branch of Global Seismology and Geomagnetism
U.S. Geological Survey
Albuquerque Seismological Laboratory
Building 10002, Kirtland AFB-East
Albuquerque, New Mexico 87115-5000
(505) 844-4637

Investigations

1. IRIS/USGS Data Collection Center. The Incorporated Research Institutions for Seismology (IRIS) have designated the Albuquerque Seismological Laboratory (ASL) to be the data collection center (DCC) for a new global network of digitally recording seismograph stations. Most of a new computer system has been purchased and installed, a new format has been developed, and approximately half of the data processing software has been written.

2. Data Management System for the China Digital Seismograph Network. The Data Management System in Beijing is completely installed and fully operational. A number of modifications and upgrades have been made to the software, and further training is scheduled in Albuquerque for two data management system personnel.

3. Data Processing for the Global Digital Seismograph Network. All of the data received from the Global Network and other contributing stations are reviewed and checked for quality.

4. Network-Day Tape Program. Data from the Global Network stations are assembled into network-day tapes which are distributed to regional data centers and other government agencies.

Results

1. IRIS/USGS Data Collection Center. IRIS is planning to install a network of 50 or more digital recording seismograph stations around the world during the next 5 years. All of the data from this network will be forwarded to the DCC located at the ASL. As part of this program, IRIS is funding much of the new hardware required by the DCC to process the large amount of data. In FY86, two MicroVax II computer systems, complete with disk memory and Ethernet communications, were purchased and installed at the ASL. During FY87, a third MicroVax and more disk memory were purchased. The new MicroVax hardware uses the VMS operating system, and new software will be required for processing this data. A new format has been developed at the ASL which will be used both to record data in the field and also to distribute this data in the form of network-day tapes to interested users. During FY88, an optical/laser jukebox memory system will be purchased for use for on-line storage and also to archive the seismic data.

2. Data Management System for the China Digital Seismograph Network. The Data Management System, located in Beijing, China, is now processing all of the data received from the China Digital Seismograph Network (CDSN). The Chinese are now producing network-day tapes which contain all of the data recorded by the CDSN for a specific calendar day on one digital tape. During the past 6 months, several upgrades and modifications have been made to the system software. A continuing maintenance problem has been the RA60 disk drives which have experienced several head crashes. A new Winchester Disk Memory System, Model RA81, will be installed in December 1987, and will be replace the troublesome RA60 disk drives. A final training session will be held in Albuquerque in early 1988 for two personnel from the Data Management System. Copies of digital tapes from five of the DCSN stations are regularly forwarded to the ASK and the data incorporated into the network-day tape program.

3. Data Processing for the Global Digital Seismograph Network. During the past 6 months, 623 digital tapes (208 SRO/ASRO, 297 DWWSSN, and 118 CDSN) from the Global Network and other contributing stations were edited, checked for quality, corrected when feasible, and temporarily archived at the ASL. The Global Network is presently comprised of 11 SRO stations, 4 ASRO stations, and 14 DWWSSN stations. In addition, there are six contributing stations which include Glen Almond, Canada, plus the five stations from the China Network.

4. Network-Day Tape Program. The network-day tape program is a continuing program which assembles all of the data recorded by the Global Digital Seismograph Network plus the contributing stations for a specific calendar day onto one magnetic tape. This tape includes all the necessary station parameters, calibration data, frequency response, and time-correction information for each station in the network. Copies of these tapes are distributed to several university and government research groups for detailed analysis. The network-day tape archive at the ASL contains tapes for each day beginning January 1, 1980, up to the present.

National Earthquake Information Center

9920-01194

Waverly J. Person
Branch of Global Seismology and Geomagnetism
U.S. Geological Survey
Denver Federal Center
Box 25046, Mail Stop 967
Denver, Colorado 80225
(303) 236-1500

Investigations and Results

The Quick Epicenter Determinations (QED) continues to be available to individuals and groups having access to a 300-baud terminal with dial-up capabilities to a toll-free watts number or a commercial telephone number in Golden, Colorado. The time period of data available in the QED is approximately 3 weeks (from about 2 days behind real time to the current PDE in production). The QED program is available on a 24-hour basis, 7 days a week. From April 1, 1987 through September 30, 1987, we have had approximately 2505 log-ins.

The weekly publication, Preliminary Determination of Epicenters (PDE) continues to be published, averaging about 100 earthquakes per issue. The QED, PDE Monthly Listing and Earthquake Data Report (EDR) continue to be prepared on the VAX/1180 with very little down time encountered.

Telegraphic data are not being received from the USSR on magnitude 6.5 or greater earthquakes at this time. We had discussions with Aleksei Gvishiani during his visit with us in February of 1987, but to date we are not receiving data.

Data from the People's Republic of China via the American Embassy are being received in a very timely manner and in time for the PDE publication. We continue to receive four stations on a weekly basis from the State Seismological Bureau of the People's Republic of China. The Bulletins with additional data are not being received in time for the Monthly. We have rapid data exchange (alarm quakes) with Centre Seismologique European-Mediterranean (CSEM), Strasbourg, France, and Instituto Nazionale de Geofisica, Rome, Italy, and Sicily, and data by telephone from Mundaring Geophysical Observatory, Mundaring, Western Australia and Japan Meteorological Agency (JMA).

The Monthly Listing of Earthquakes is up to date. As of September 30, 1987, the Monthly Listing and Earthquake Data Report (EDR) were completed through May 1987. A total of 5,351 events was published for the 6-month period. Total number of events published for 1986 were 12,709. Solutions continue to be determined when possible and published in the Monthly Listing and EDR for any earthquake having an m_b magnitude ≥ 5.8. Centroid moment tensor solutions from Harvard University continue to be published in the Monthly Listing and EDR. Moment tensor solutions are being computed by the U.S.

Geological Survey and are also published in the above publications. Waveform plots are being published for selected events having m_b magnitudes $\geq$ 5.8. Beginning with the month of October 1985, depths for selected events were obtained from broadband displacement seismograms and waveform plots published in the Monthly.

The Earthquake Early Alerting Service (EEAS) continues to provide information on recent earthquakes on a 24-hour basis to the Office of Earthquakes, Volcanoes, and Engineering, scientists, news media, other government agencies, foreign countries, and the general public. Forty-two releases were made from April 1, 1987 through September 30, 1987. The most significant earthquake released in the United States during this reporting period was a magnitude 5.0 on June 10, 1987, in southern Illinois. Foreign earthquakes: a magnitude 5.9 in Luzon, Philippine Islands; a magnitude 7.1 in the Vanuatu Islands on August 2; and a magnitude 7.0 in northern Chile on August 8.

Reports

Monthly Listing of Earthquakes and Earthquake Data Reports (EDR); six publications from December 1986 through May 1987. Compilers: W. Jacobs, L. Kerry, J. Minsch, R. Needham, W. Person, B. Presgrave, W. Schmieder.

Person, Waverly J., Seismological Notes: Bulletin of the Seismological Society of America, v. 77, no. 2, May-June 1986; v. 77, no. 3, July-August 1986; v. 77, no. 4, September-October 1986; v. 77, no. 5, November-December 1986.

Preliminary Determination of Epicenters (PDE); 26 weekly publications from April 3, 1987 through October 2, 1987, numbers 11-87 through 36-87.

Quick Epicenter Determination (QED) (daily): Distributed only by electronic media.

Person, Waverly J., "Seismological Research Letters," v. 58, no. 2, Significant earthquakes of the world 1986.

Monthly Listing of Earthquakes--April, May, June (Microfiche): Seismological Research Letters. Compilers: W. Jacobs, L. Kerry, J. Minsch, R. Needham, W. Person, B. Presgrave, W. Schmieder.

Person, Waverly J., Earthquake Information Bulletin "Earthquakes," v. 18, no. 6, January-February 1986; v. 18, no. 6, March-April 1986. "Earthquakes," v. 19, no. 1, May-June 1986; v. 19, no. 1, July-August 1986.

Seismic Review and Data Services

9920-01204

James N. Taggart
Branch of Global Seismology and Geomagnetism
U.S. Geological Survey
Denver Federal Center
Box 25046, Mail Stop 969
Denver, Colorado 80225
(303) 236-1506

Investigations and Results

Technical review and quality control were carried out on 402 station-months of seismograms from the Worldwide Standardized Seismograph Network (WWSSN). During this reporting period, 674 station-months were photographed by the contractor, who had finally caught up with the review process at the end of the fiscal year. In addition to the original silver halide microfiches, the contractor provides one set of silver halide copies for the WWSSN archives and diazo copies for the standing orders. The Geological Survey of Canada furnishes high-quality filmed seismograms each month from 15 or 16 stations of the Canadian Standard Network (CSN). This project is responsible for the duplication and distribution of CSN films which are formatted one station-month on a 35mm reel.

Filmed seismograms were purchased at cost by 72 requesters during Fiscal Year 1987, including eight standing orders for WWSSN microfiches and two standing orders for CSN 35mm microfilm. Altogether, 1,700,000 filmed seismograms were supplied to these requesters on 1,430 reels and 68,670 microfiches of various kinds.

The branch was designated World Data Center A for Seismology (WDC-A) on October 1, 1986. Many functions of the project, especially those dealing with the world wide distribution of filmed historical seismograms, fall under the aegis of WDC-A. The historical archives now contain about 600,000 films of pre-1963 seismograms on 16mm and 35mm reels. A report discussing problems and recommendations was presented to the Historical Seismograms Working Group, International Union of Geodesy and Geophysics, Quadrennial Meeting, Vancouver, British, in August of 1987.

National Strong-Motion Network: Data Processing

9910-02757

A.G. Brady
Branch of Engineering Seismology and Geology
U.S. Geological Survey
345 Middlefield Road, MS 977
Menlo Park, California 94025
(415) 329-5664

Investigations

Routine Processing. The last of the records from the Chile earthquake and aftershocks, as obtained from Chile, has been processed and the Open-File report containing all the processed data has been published.

The local commercial digitizing company in use for more than ten years has undergone major ownership and managerial changes during the last year but recently restarted with effectively the same technical and scientific personnel. The records from the North Palm Springs earthquake (M 5.9, 8 July 1986) have been digitized, and processing continues at USGS.

A set of records from two of the Coalinga aftershocks (September 9 and 11, 1983) has been selected in a study of topographical amplification--whether records at the crest of Anticline Ridge are significantly larger, and at which frequencies, than those of the surrounding flat ground. The routine processing of these records is complete, and comparison of Fourier spectra shows that amplification occurs in some frequency ranges and not in others. An approach to a theoretical analysis of the transfer function at the site has been investigated.

A workshop was organized in Menlo Park, August 3-7, 1987, on record digitization and the various uses to which processed records are put. Attendees from outside the USGS included representatives from EPRI, Santa Clara University, and two government agencies in Japan. A Proceedings is in preparation.

A one-day workshop was attended in Vancouver, August 8, 1987, on routine processing of digitized strong-motion accelerograms. This workshop was well attended by research personnel from around the world. It was timed to be just prior to the IUGG General Assembly.

Simplification of the routine processing programs is underway, with a view to making better use of the capabilities of the in-house VAX computers. Portability to other facilities is a prime consideration.

Results

Routing processing, including digitizing (D), computer processing (P), and report preparation (R) of strong-motion accelerograms continues: 5 records (D), additional durations of Chile mainshock and aftershock records, March 3, and subsequent dates, 1985; 8 records (P), two Coalinga aftershocks September 9 and 11, 1983; 17 records (P) North Palm Springs earthquake, July 8, 1986.

Reports

Celebi, M. (compiler), 1987, Processed Chile earthquake records of 3 March 1985 and aftershocks: *U.S. Geological Survey Open-File Report 87-195.*

National Strong-Motion Network: Engineering Data Analysis

9910-02760

A.G. Brady and G.N. Bycroft
Branch of Engineering Seismology and Geology
U.S. Geological Survey
345 Middlefield Road, MS 977
Menlo Park, California 94025
(415) 329-5665 or (415) 329-5664

Investigations

Soil Structure Interaction

1. Previously obtained results for the transfer functions of a gravity dam should be applicable to the case of a ridge in hilly country, provided the ridge is sufficiently separated from other hilly features by flat land. An investigation is proceeding to determine the assumptions necessary to be applied to a particular ridge in the Coalinga Anticline Ridge area in order that the theoretical results may be valid.

2. The only structural records from the USGS permanent network of strong-motion accelerographs recording the North Palm Springs earthquake of July 8, 1986 were obtained from the I10/15 interchange bridge in Colton, California, epicentral distance 62 km. Horizontal displacements in the vault and within a bridge cell are of the order of 1 cm. An investigation is proceeding to determine amplitudes and frequencies of the bridge deck motion with respect to the vault. The most prominent ground motion has an amplitude of 0.9 cm at a period of 4 sec. The bridge follows this motion closely. The most prominent relative motion has an amplitude of 0.2 cm with period 0.44 sec.

Reports

None.

10/87

National Strong Motion Data Center

9910-02085

Howard Bundock
Branch of Engineering Seismology and Geology
U.S. Geological Survey
345 Middlefield Road, MS 977
Menlo Park, California 94025
(415) 329-5621, FTS. 459-5621

Investigations:

The objectives of the National Strong Motion Data Center are to:

Maintain a strong capability for the processing, analysis, and dissemination of all strong motion data collected on the National Strong Motion Network and data collected on portable arrays;

Support research projects in the Branch of Engineering Seismology and Geology by providing programming and computer support including digitizing, graphics, processing and plotting capabilities as an aid to earthquake investigations;

Manage and maintain computer hardware and software so that it is ready to process data rapidly in the event of an earthquake.

The Center's facilities include a VAX 11/750 computer operating under VMS Version 4.5, a PDP 11/70 running RSX-11M+ and two PDP 11/73 computers. The Center's computers are part of a local area network with other branch, OEVE, Geologic Division, and ISD computers, and we have access to computers Survey-wide over Geonet. Project personnel joined other office branches in the support of the OEVE VAX 11/785.

Investigations during the last six months of FY87 included analysis of various laser printer technologies for use with presently used plotting and word processing packages. Project personnel have further developed and documented a complete procedure for digitizing and plotting map features such as fault lines, etc. The project has planned and helped accomplish setting up computer communications in temporary quarters while asbestos fireproofing is removed from Buildings 7 and 8. The project has also protected and kept computer systems on line while this work was done in the computer room itself. The project has studied newer computers, compatible with present communications configurations and has put together an entry level system that will increase CPU capacity for the Branch. The project also conducted further research into VAX/VMS compatible laser optical disk technology. The project continues its support of the OEVE VAX 11/785 project. As an ongoing policy, the project has kept its hardware up to current revision levels, and operating system, network, and other software at the most recent versions.

Results:

As a result of these and previous investigations, the project has:

Installed laser printer hardware and software for Branch and Office computer systems.

Instructed Branch and Office scientists in the use of our graphics/digitizing system for plotting surface topography, faults and hypocenters.

Successfully insured that Branch and Office computers remained up and running during asbestos removal from Building 7 and part of Building 8.

Purchased and planned installation of a VAX 8250 BI computer for the Branch.

Tested another demo optical disk drive on the branch VAX 11/750. The project is following the progress of both 12" and 5 1/4" disk technology so that we will be ready to purchase wisely when these systems have been fully developed. Compatibility and standardizing problems must be resolved before a purchase can be justified.

Managed the OEVE VAX 11/785 and have joined with representatives from other Branches in managing the project.

Managed, maintained, updated Branch computer system hardware and software.

Reports:

None.

Instrumentation of Structures

9910-04099

Mehmet Celebi
Branch of Engineering Seismology and Geology
U.S. Geological Survey
345 Middlefield Road, MS 977
Menlo Park, California 94025
(415) 329-5623 or 329-5930

Investigations:

1. The process of selection of structures to be recommended for strong-motion instrumentation has continued in Los Angeles, Orange County, northeastern United States (Boston), Alaska, Hawaii, and Puget Sound (Seattle). This effort is being extended to Puerto Rico and Salt Lake City.

2. The process to design instrumentation schemes for selected structures has continued. Applicable permits for two structures, one in San Bernardino and the other in Anchorage in Alaska, have been obtained.

3. The process of actual instrumentation of structures has continued in Los Angeles (1100 Wilshire Finance Building) and in Charleston, SC (the Charleston Place). The strong-motion recording systems in these two buildings are now operational. Non-destructive testing of 1100 Wilshire Finance Building will take place soon. Agreements have been made to instrument Salt Lake City and County Building in cooperation with the City of Salt Lake City. The building is the first building being retrofitted by base isolation. Non-destructive dynamic testing of the building is being carried out progressively to evaluate the dynamic characteristics of the building before and after being rehabilitated by base isolation.

4. The minimal instrumentation in a building in Alhambra, southern California, is being upgraded to contain extensive instrumentation.

5. Agreements have been made with UCLA to convert the wind-monitoring system in the Theme Buildings in Los Angeles (previously financed by NSF) into a strong-motion monitoring system. Plans are being made to implement the conversion.

6. Studies of records obtained from instrumented structures are carried out.

Results:

1. A draft of the report of the Alaska advisory committee for strong motion instrumentation of structures has been prepared. This report is now being reviewed by the committee members.

2. A draft of the report of the Los Angeles advisory committee for strong motion instrumentation of structures has been prepared. This report is now being reviewed by the committee members.

3. A USGS Circular (947) that summarizes the program has been published.

4. A draft of the report of the Boston area advisory committee for strong motion instrumentation of structures has been prepared. This report is now being finalized and will be issued shortly.

5. The Hawaii committee on strong motion instrumentation of structures has completed its deliberations and a draft report is being prepared.

6. Papers resulting from study of records obtained from structures are prepared.

<u>Reports</u>:

Celebi, M., Safak, E., Brady, G., Maley, R., and Sotoudeh, V., 1987, Integrated instrumentation plan for assessing the seismic response of structures--A review of the current USGS program: *U.S. Geological Survey Circular 947*, 38 p.

Celebi, M., Bongiovanni, G., Safak, E., and Brady, G., 1987, Seismic response of a large-span roof diaphragm (paper submitted to SPECTRA).

Celebi, M., and Safak, E., 1987, Earthquake response of a unique building in Vina Del Mar, Chile: Society for Experimental mechanics Conference, Houston, Texas, Proceedings, June 1987.

General Earthquake Observation System (GEOS)
GEOS Analysis and Playback Systems (GAPS)

9910-03009

Gary L. Maxwell and Roger D. Borcherdt
Branch of Engineering Seismology and Geology
U.S. Geological Survey
345 Middlefield Road, MS 977
Menlo Park, California 94025
(415) 329-5618 or (415) 329-5619

Investigations

1. Development and construction of a portable, broad band, high-resolution digital data acquisition capability for seismology and engineering (GEOS).
2. Development of mini- and micro-computer systems (hardware and software) for retrieval, processing, and archival of large volumes of digital data (GAPS).
3. Development of hardware and software components to improve functionality, versatility, and reliability of digital data acquisition and retrieval systems.

Results

Design features and modifications to the General Earthquake Observation System (GEOS) incorporated or being investigated during this report period with assistance from M. Kennedy, J. Sena, C. Dietel, E.G. Jensen, and J. VanSchaack include:

1. Award of RFP for construction of 330 channels of recording capability through the fabrication and assembly of fifty-five six-channel GEOS recording units. Development of first unit under award is to begin during the first months of the next reporting period.
2. Development of a prototype low-power semiconductor buffer memory capable of storing over one million digital data samples. Memory units were undergoing final evaluation and test at end of this report period.
3. Enhancement of existing 270 channel recording capability to include additional memory for use by recorder software and hardware arithmetic assist module to implement complex real-time event triggering algorithms.
4. Completion of software package to allow for remote interrogation of recorder units *via* standard RS232C protocol implemented over phone lines or satellite telemetry. Integration of this package with remainder of GEOS runtime software was underway at the end of this reporting period.

Reports Utilizing Data Recorded by GEOS and Processed by GAPS

Borcherdt, R.D., Johnston, M.J.S.., and Glassmoyer, G.M., 1987, On the use of volumetric strain meters to infer additional characteristics of seismic wave fields: *Seismological Research Letters*, v. 58, p. 24.

Celebi, M., Prince, J., Dietel, C., Onate, M., and Chavez, G., 1987, The culprit in Mexico City -- amplification of motions: *Earthquake Spectra*, v. 3, p. 315-328.

Celebi, M., 1987, Topographical and geological amplifications determined from strong-motion and aftershock records of the 3 March 1985 Chile earthquake: *Seismological Society of America Bulletin*, v. 77, p. 1147-1167.

Dietel, Christopher, and Borcherdt, Roger D., eds., 1987, GEOS data summary for active and passive seismic experiments conducted in support of Northern Nevada lithospheric experiments - PASSCAL: *U.S. Geological Survey Open-File Report 87-326*.

Johnston, M.J.S., Borcherdt, R.D., and Glassmoyer, G.M., 1987, Static and dynamic strain during the July 21, 1986, Chalfant earthquake near Long Valley Caldera, California: *Seismological Research Letters*, v. 58, p. 20.

Johnston, M.J.S., Linde, A.T., Gladwin, M.T., and Borcherdt, R.D., 198_, Fault failure with moderate earthquakes: accepted by *Tectonophysics*.

Structural Response in Support of National Strong Motion Program

9910-02759

Erdal Safak, Mehmet Celebi, A. Gerald Brady, and Richard Maley
Branch of Engineering Seismology and Geology
U.S. Geological Survey
345 Middlefield Road, MS 977
Menlo Park, California 94025
(415) 329-5648, FTS 459-5648

Investigations

1. Implementation of structural instrumentation and design of instrumentation schemes for structures selected by instrumentation advisory committees.

2. Develop methodologies and computer software to analyze ground motion and structural vibration recordings.

3. Continue on site response studies and structural damage correlation during the 3 March 1985 Chile earthquake.

4. Continue on structural characteristic evaluation during the 19 September 1985 Mexico earthquake.

5. Testing of the Salt Lake City and County building, which is the first building in the world to be retrofitted by base isolation.

Results

1. As part of structural response study efforts through strong-motion instrumentation, and in accordance with recommendations of committees, two new structures are now instrumented. These are the 1100 Wilshire Building (33 stories) in Los Angeles and the Charleston Place Building (8 stories) in Charleston, South Carolina. Instrumentation schemes for these two buildings were designed.

2. A computer program is being developed to identify source and site amplification of earthquake motions from ground motion recordings, and frequency, damping, and mode shapes of buildings from the ambient and earthquake vibration recordings.

3. After the 3 March 1985 Chile earthquake ($M_s=7.8$), and as a result of observation of damages on ridges, as well as alluvial and sandy sites, site response studies were conducted. The results showed that there were topographical and geological amplification and these two factors contributed to the patterns of responses observed during post-earthquake surveys. In addition, data obtained from structures are being studied.

4. Approximately 15 structures in Mexico City were tested in January 1986. Some of these structures were tested in 1962 also. Studies are being finalized on the changes of dynamic characteristics of these structures.

5. Prior to installation of base isolaters, a set of vibration data from the building was obtained in September 1987 during a nuclear explosion test at the Nevada test site. Another set will be obtained after the base isolaters are installed.

Reports

Celebi, M., and Safak, E., 1987, Earthquake response of an unique building in Vina del Mar, Chile (invited paper): Spring Conference, Society of Experimental Mechanics, Houston, Texas, June 14-19, 1987, Proceedings.

Safak. E., and Celebi, M., 1987, On identification of site amplification from earthquake records (invited paper): Spring Conference, Society of Experimental Mechanics, Houston, Texas, June 14-19, 1987, Proceedings.

Safak, E., 1987, A band-limited, windowed, white-noise process for modeling earthquake motions, International Conference on Soil Dynamics and Earthquake Engineering, Third, Princeton, New Jersey, June 22-24, 1987, Proceedings.

Celebi, M., Dietel, C., Prince, J., Onate, M., and Chavez, G., Site amplification in Mexico City (Determined from 19 September 1985 Strong-Motion 1Records and from Recordings of Weak Motions): International Conference on Soil Dynamics and Earthquake Engineering, Third, Princeton, New Jersey, June 22-24, 1978, Proceedings.

Safak, E., 1987, Discrete-time domain models for site amplification (invited paper), 13th Regional Conference on Earthquake Engineering, Istanbul, Turkey, Sep 14-24, 1987, Proceedings.

Celebi, M., 1987, Topographical and Geological amplifications determined from strong-motion and aftershock records of the 3 March 1985 Chile earthquake, *Bulletin of the Seismological Society of America*, v.77, no. 4, pp. 1147-1167.

Celebi, M., Safak, E., Brady, A.G., Maley, R., and Sotoudeh, V., 1987, Integrated instrumentation plan for assessing the seismic response of structures - A review of the current USGS program: *U.S. Geological Survey Circular 947*.

Celebi, M., Prince, J., Dietel, C., Onate, M., and Chavez, G., 1987, The culprit in Mexico City -- Amplification of Motions, *Earthquake Spectra*, v. 3, no. 2, p. 315-328.

Physical Constraints on Source of Ground Motion

9910-01915

D.J. Andrews
Branch of Engineering Seismology and Geology
U.S. Geological Survey
345 Middlefield Road, MS 977
Menlo Park, California 94025
(415) 329-5606

Investigations

Application of the diffusion equation to scarp degradation.

Implications of fault geometry for earthquake mechanics.

Results

The manuscript with R.C. Bucknam on nonlinear diffusion of scarps was revised considerably. Data not previously considered at small scarp slopes require that a linear term be added to the nonlinear transport model. This revision reduces scatter in model ages between scarps on different ambient slopes.

Tom Hanks and I wrote a paper reconciling our views on the importance of ambient slope and on the nonlinear slope dependence of the transport law.

Work has started to model the interaction of many fault segments with arbitrary orientations. A boundary integral method in two-dimensional plane strain is being used to model interacting frictional surfaces in quasistatic equilibrium.

Reports

Andrews, D.J., and Bucknam, R.C., 1987, Fitting scarp degradation by a model with nonlinear diffusion (to appear *Journal for Geophysical Research*).

Hanks, T.C., and Andrews, D.J., 1987, Far-field slopes and the nature of general diffusion models of scarplike landforms in weakly consolidated terrains in *Proceedings of Conference XXXIX -- Workshop on Directions in Paleoseismology: U.S. Geologial Survey Open-File Report 87-___.*

10/87

Estimation of High Frequency Ground Motion

9910-03833

D.M. Boore

Branch of Engineering Seismology and Geology
U.S. Geological Survey
345 Middlefield Road, MS 977
Menlo Park, California 94025
(415) 329-5616

Investigations:

Work was started on analyzing two different data sets not previously examined. These are the recordings of the Nahanni, Northwest Territories, Canada earthquakes of October, November, and December 1985, and aftershocks of the Tangshan, China earthquake.

Results:

1. We have collected recordings of 9 events in the Nahanni region, ranging in size from M_s 4.9 to 6.9. The data include western Canada digital network (WCTN), global digital network (GDSN), and strong-motion accelerograph records (the latter for three events in December, 1985). We are in the process of computing spectral ratios of the events at WCTN stations, the purpose being to remove path effects and thereby illuminate the source scaling of the spectra. We also compared, observed, and predicted response spectra computed from records obtained at 2 sites within 10 km of the M_s F_1 6.9 earthquake of 23 December 1985. The response spectra for both sites have been computed for the first 7 secs of the record, in order to exclude the contribution from a large but inexplicable burst of energy late in the record from site 1 (this energy is not present at site 2, which is situated 11 km from site 1 and, like site 1, is situated at the northern end of the rupture zone of the earthquake). The predictions have been made from the empirical results, largely using California strong-motion records (Joyner and Boore, 1982), and from the theoretically based predictions of Boore and Atkinson (1987) for ground motions in eastern North America, who used the theoretical method outline in this paper. The intraplate scaling laws of Boatwright and Choy have also been considered. For the latter predictions, two distances have been used: the distance to the closest point of the rupture surface and the distance to the approximate center of the rupture surface. Both of the distances rely on my estimate of the location of the rupture surface, which I have based on aftershock locations F_2 (*e.g.*, Weichert *et al.*, 1986). The predictions are in reasonable accord with the observations, especially in view of the fact that the predictions are intended to be predictions of mean motions; any one observation can be more than a factor of 2 from the mean (the standard deviation of individual observations is close to a factor of 1.8).

Reports

A report on the work being done on this project was presented at a workshop on ground motion estimation in eastern North America, organized by the Electric Power Research Institute, and held in Palo Alto, California in April, 1987.

Atkinson, G.M. and Boore, D.M., *in press,* On the m_N, M relation for eastern North American earthquakes: *Seismological Research Letters*.

Boore, D.M., and Atkinson, G.M., 1987, Stochastic prediction of ground motion and spectral response parameters at hard-rock sites in eastern North America: *Seismological Society of America Bulletin,* v. 77, p. 440-467.

Ground Motion Prediction for Critical Structures

9910-01913

David M. Boore
William B. Joyner
Branch of Engineering Seismology and Geology
U.S. Geological Survey
345 Middlefield Road, MS 977
Menlo Park, California 94025
(415) 329-5616 or (415) 329-5640

Investigations:

1. Study the investigation of amplitudes from Wood-Anderson instruments in southern California.

2. Estimate ground motions and response spectra in eastern North America.

3. Estimate ground shaking close to large faults.

Results:

1. Studies of almost 10,000 amplitude readings taken from Wood-Anderson instruments from over 900 earthquakes demonstrates that Richter's distance correction used in the computation of local magnitudes (M_L) leads to values that are too high for large earthquakes and too small for small earthquakes. The bias is generally less than 0.25 units, however. New station corrections have been determined. There is no indication that the attenuation correction is a function of magnitude.

2. A stochastic model with constant stress parameter of 100 bars produces a reasonable fit to the sparse strong motion data from earthquakes in eastern North America; predictions based on the scaling law proposed by Nuttli in 1985 are much lower than the observations, while those based on a 1987 modification of the Nuttli scaling relation give estimates similar to those from the 100 bar scaling model. With this validation of the basic model, theoretical attenuation models as a function of magnitude have been derived for response spectra.

Reports:

Hutton, L.K., and Boore, D.M., *in press*, The M_L scale in southern California: *Seismological Society of America Bulletin*, v. 79.

Joyner, W.B., and Boore, D.M., Ground-motion parameters for seismic design: Notes for a short course on earthquake engineering, University of California, Berkeley, 1987.

Boore, D.M., 1987, The estimation of ground shaking caused by earthquakes: Fifth Canadian Conference on Earthquake Engineering, Proceedings, A.A. Bakema, Rotterdam, p. 27-38.

10/87

Anelastic Wave Propagation

9910-02689

Roger D. Borcherdt
Branch of Engineering Seismology and Geology
U.S. Geological Survey
345 Middlefield Road, MS 977
Menlo Park, California 94025
(415) 329-5619

Investigations:

1. Volumetric strain measurements for inference of additional characteristics of anelastic seismic wave fields.

2. Characteristics of higher frequency (20-130 Hz) radiation near seismic sources.

Results:

1. Volumetric strain--Theoretical descriptions of volumetric strain and displacement fields for radiated seismic energy predict that simultaneous observations of each on colocated sensors permits inferences regarding the radiated fields that cannot be inferred from either sensor alone. Theoretically, volumetric strain meters respond to P waves but not S waves. Volumetric strain is not dependent on angle of incidence nor azimuth and shows amplitude and phase modulation dependent on intrinsic material absorption. S energy converted to P energy at the free surface is detectable on a strain meter. It is predicted to be largest for angles of incidence beyond critical, for which the inhomogeneous P energy is reflected with wave field characteristics distinct from those for homogeneous waves in low-loss anelastic solids. As a result, simultaneous observations on colocated sensors should allow, 1) the resolution of superimposed P and S radiation fields, and in particular superimposed P and S waves reflected from the free surface, 2) angle of incidence and apparent phase velocity based on amplitude ratios and, 3) intrinsic material absorption and characteristics of low-loss inhomogeneous wave fields.

2. High-frequency seismic radiation--In cooperation with G. Glassmoyer, data from the ten-station array of portable digital instrumentation (GEOS) deployed to record the aftershock sequence of the moderate (m_b 4.9) earthquake that occurred on January 31, 1986 near Painesville, Ohio is continuing to be analyzed. High-resolution (16-bit; 96 dB), broadband (400 sps; 200 Hz) recordings of two of the larger aftershocks (m_b 2.2; 2.5) show that seismic signals as high as 130 Hz were resolvable above background noise levels at hypocentral distances up to 18 km. Spectral ratios suggest strong site resonances near 20 Hz and other resonances at frequencies exceeding 60 Hz. Modeling of the soil response based on two-dimensional anelastic wave propagation suggests that the exaggerated levels of shaking near 20 Hz could be due in part to response of near-surface soil layers to S energy incident at angles of incidence near 30 degrees. Source parameters determined by minimizing the influence of local site conditions

from the high resolution date for 9 events extend estimates of moments down to 10^{17} dyne-cm. The estimates of moment as a function of source radius are consistent with Mof^4 scaling.

Reports

Borcherdt, R.D., 1987, Volumetric strain in relation to particle displacements for body and surface waves in a general viscoelastic half-space, accepted *Geophysical Journal, Royal Astronomical Society*.

Borcherdt, R.D., and Glassmoyer, G., 1987, On the aftershock sequence of the earthquake of January 31, 1986 in northeastern Ohio: effects of bandwidth and local geology on observed high-frequency ground motion: Proceedings, Workshop on Earthquake Ground Motion Estimation in Eastern North America, Los Altos, California.

Johnston, M.J.S., Lindh, A.T., Gladwin, M., and Borcherdt, R.D., 1986, Fault failure for moderate earthquakes (Japan and California): accepted *Tectonophysics*.

Borcherdt, R.D., Johnston, M.J.S., and Glassmoyer, G.M., 1987, On the use of volumetric strain meters to infer additional characteristics of seismic wave fields, Seismic Res. Letters, v.58, p. 24.

Johnston, M.J.S., Borcherdt, R.D., and Glassmoyer, G.M., 1987, Static and dynamic strain during the July 21, 1986, Chalfant earthquake near Long Valley Caldera, California, Seism. Res. Letters, v. 58, p. 20.

Seismic Waveform Analysis Project

8-9930-03790

Thomas H. Heaton
Branch of Seismology
525 S. Wilson Ave.
Pasadena, CA 91106

Investigations

1. Waveform inversion studies of the 1986 North Palm Springs earthquake. Different waveform data sets including teleseismic P-waves and local strong motion records are used to invert for the earthquake rupture history assuming a three-dimensional fault model. Different inversion techniques are also investigated; linear inversion for just fault slip and iterative linearized inversion for both rupture time and fault slip.

2. Calibration studies of the Southern California Short Period Network. Calibration signals from the 250 station USGS southern California network are being recorded and compared with theoretical calculations for the complete system response.

Results

1. Results from the inversion of teleseisic P-waves for the North Palm Springs earthquake are given in the preceding summary of technical reports (Vol. XXIV, U.S.G.S. Open File 87-374). We have now completed the inversion of the local strong motion records.

   Photographic enlargements were made of copies of the USGS strong ground motion records for the North Palm Springs earthquake. These enlargements were then digitized at Caltech and merged with the digitzed strong motion records previously obtained from the state of California and Southern California Edison. The records were all processed in an identical manner: integrated to velocity, bandpass Butterworth filtered from 0.2 Hz to 3 Hz, and given a final time step of 0.05 sec. These parameters were chosen to limit the frequency bandwidth and the number of time domain points in the inversions, but yet still preserve all the important features of the velocity records. The 9 stations (27 components) comprising the strong motion data set are listed in Table 1.

   The parameterization of the fault plane (Strike = 287°, dip = 46°) used in the inversions is shown in Figure 1. The hypocenter is indicated by a solid dot. The fault plane is divided up into 88 subfaults for which the inversion finds the strike-slip and dip-slip dislocations which best fit, in a least squares sense, the strong motion velocity records. Since there was no surface rupture and since the aftershocks were deeper thean 4 km, the rupture was assumed to be restricted to depths between 4 and 15 km.

The rupture front is assumed to advance outward from the hypocenter, located at a depth of 11 km, with a constant rupture velocity of 3.0 km/sec. This velocity is 80% of our estimate of the local shear-wave velocity in the source region. The rupture fills the entire fault plane after 5 seconds.

Synthetic full-wave Green's functions were calculated for the structure in Table 2. The velocities vary smoothly between the point values given in Table 2. After conducting several preliminary inversions to adjust stabilization parameters, model MS8 in Figure 2 was obtained. Figure 2 shows contours of dislocation in centimeters for strike-slip motion, dip-slip motion, and the vector sum. The maximum dislocation is 43 cm and the moment is 1.9×10^{25} dyne-cm.

2. Calibration pulses from the southern California network that are captured within earthquake triggers are being saved in their own archival files. This practice has continued for the past 6 months resulting in calibration pulses for 1/3 of the network. Using a program supplied by Mary Allen, theoretical calibration pulses have been calculated and compared with the observations. This procedure allows us to evaluate our ability to predict the system response as well as to follow and evaluate station deterioration.

   A systematic, continuous, analog recording of all southern California network stations was made on strip chart paper using a compressed time scale to determine the calibration pulse times. Some stations were found to have large drift rates and even discontinuous jumps in the times of the calibration pulses. This behavior makes recording of the calibration pulses by the digital on line system difficult.

Reports

Mendoza, C. and S. Hartzell (1987). Inversion for slip distribution using GDSN P waves: North Palm Springs, Borah Peak, and Michoacan earthquakes, Bull. seism. Soc. Am., (submitted).

Heaton, T.H. and S.H. Hartzell (1987). Earthquake ground motions, Annual Reviews, in press.

Table 1

Strong Motion Stations

Station	Latitude	Longitude	Institution	Components
DHS Desert Hot Springs	33.962	116.509	CDMG	90°,Up,0°
PSA Palm Springs Airport	33.829	116.501	CDMG	90°,Up,0°
POF Poppet Flat	33.851	116.852	CDMG	90°,Up,0°
DHL Devers Hill	33.930	116.580	SCE	90°,Up,0°
NPS North Palm Springs	33.924	116.543	USGS	300°,Up,210°
WWT Whitewater Trout	33.989	116.655	USGS	270°,Up180°
MVF Morongo Valley	34.048	116.577	USGS	135°,Up,45°
CAB Cabazon	33.918	116.782	USGS	270°,Up,180°
FVR Fun Valley	33.925	116.389	USGS	135°,Up,45°

Table 2

Velocity Structure (Smooth gradients)

Depth	(km/sec)	(km/sec)	(gm/cm^3)
0.	3.0	1.5	2.2
5.5	6.3	3.64	2.75
16.	6.7	3.87	2.82

TH(9):lr

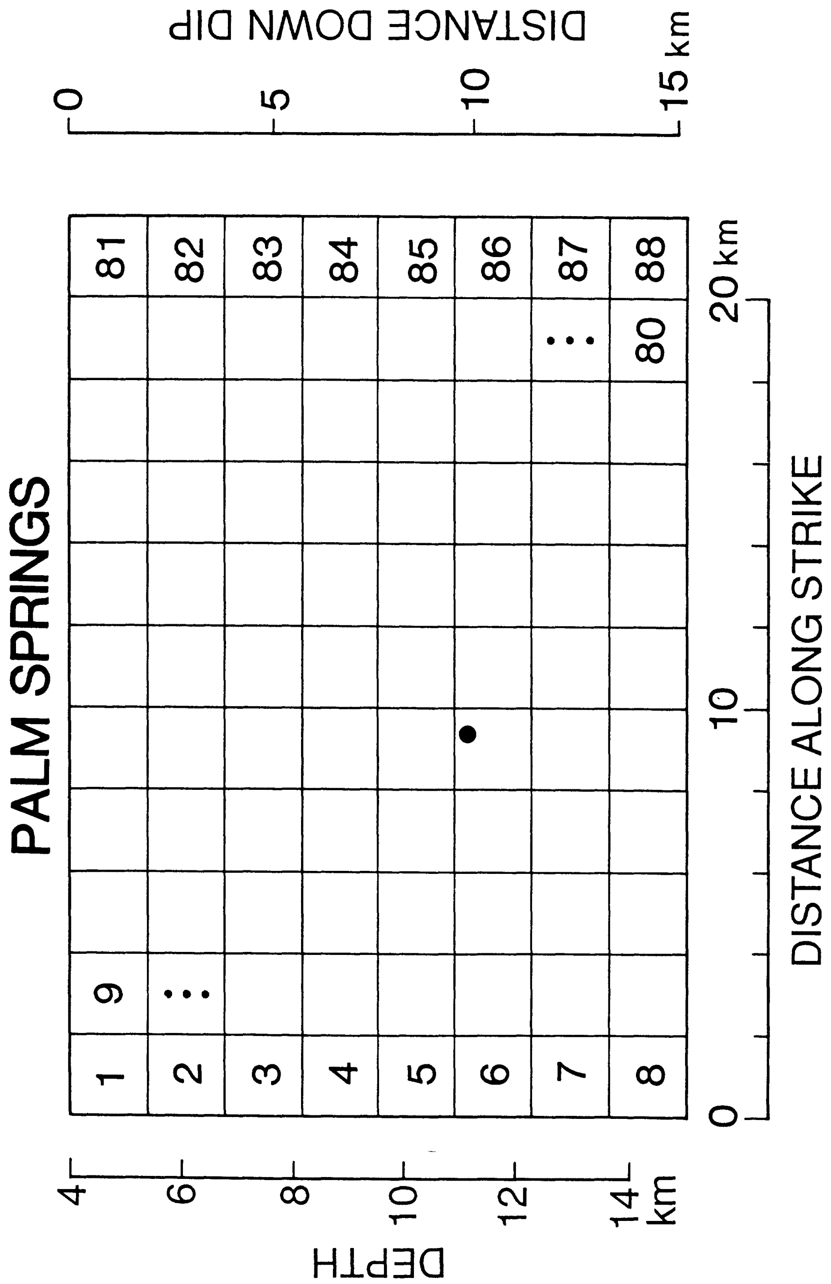
PALM SPRINGS
DISTANCE DOWN DIP
0
5
10
15 km
DEPTH
4
6
8
10
12
14 km
1
2
3
4
5
6
7
8
9
. . .
. . .
80
81
82
83
84
85
86
87
88
DISTANCE ALONG STRIKE
0
10
20 km

North Palm Springs

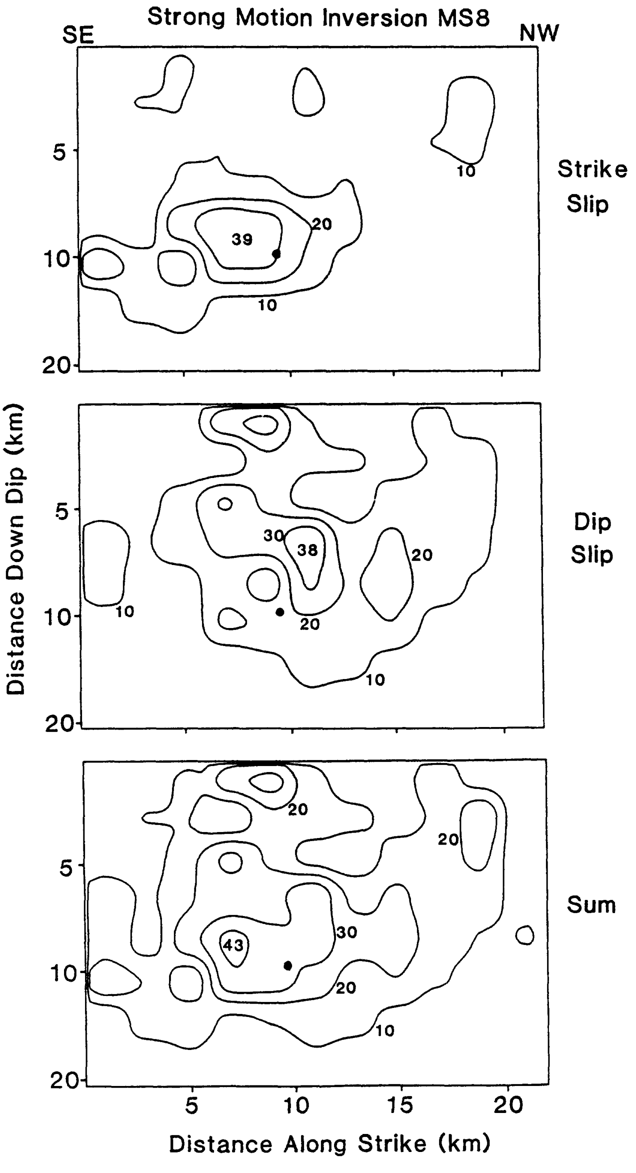

Velocity and Attenuation Measurements in Engineering Seismology

9910-02413

Hsi-Ping Liu
Branch of Engineering Seismology and Geology
U.S. Geological Survey
345 Middlefield Road, MS 977
Menlo Park, California 94025
(415) 329-5643

Investigations

1. Seismic attenuation measurements using the pulse-broadening method. Three methods are generally being used for field measurement of seismic anelastic attenuation: amplitude-decay, spectral-ratio, and pulse-broadening. The pulse-broadening method is more accurate than the amplitude-decay method because pulse-broadening is unaffected by far-field geometric spreading. The pulse-broadening method is simpler than the spectral-ratio method because of the very short length of seismogram required; the segment from the first break to the first extremum is all that is needed for the pulse rise-time calculation. However, with the notable exception of Blair and Spathis (1984), the effects of source spectrum have been neglected in the applications of the pulse-broadening method. Numerical calculations of one-dimensional wave propagation using realistic source-time functions have been carried out in order to investigate the effects of source spectrum on the dependence of initial rise-time and pulse-width on internal friction and distance.

2. *In-situ* measurement of seismic velocity and attenuation in the San Francisco bay mud. Seismic properties of near-surface earth materials such as the San Francisco bay mud have a significant effect on earthquake ground motions. Field work using a hammer source and a vertical geophone string embedded in the bay mud for the measurement of compressional wave velocity and attenuation has been completed at an undeveloped site in Foster City, California.

3. Installation of 2-Hz, 3-component borehole seismometers near the San Jacinto fault zone at the Pinon Flat Observatory. Several recent studies (*e.g.* Anderson, 1986) have suggested that spectra of small earthquakes can be strongly influenced by attenuation in the shallow crustal layer near the receiver. Following the installation of two borehole seismometers in the San Jacinto fault zone at Keenwild in the last report period, we have manufactured and installed two borehole seismometers at the Pinon Flat Observatory in order to study the effect of topography on earthquake spectra by comparing seismograms obtained at Keenwild with those obtained at Pinon Flat. Each borehole seismometer contains three orthogonal geophones having natural period of 0.5 s. The horizontal geophones are leveled to 0.1 degrees, which is necessary to avoid nonlinear response and asymmetrical clipping. The boreholes were drilled to depths of 150 and 300 meters in granite and the instruments were emplaced at the bottom of each hole. Co-sited with the boreholes is one surface instrument which uses the same sensors as the borehole seismometers.

Results

1. Numerical examples of one-dimensional wave propagation using realistic source time-fucntions in an anelastic material characterized by frequency-independent internal friction demonstrate that (a) the source time-function has a strong influence on the dependence of initial rise-time τ and pulse-width w on internal friction Q^{-1} and distance x, (b) in general τ and w have different functional dependence on Q^{-1} and x, and (c) the slope $\partial\tau / \partial x$ for particle displacement computed for a band-limited source time-function can be either greater or less than the corresponding value computed for a delta-function displacement source time-function. Result (a) corroborates the result for τ given by Blair and Spathis which implies that the commonly used linear rise-time and distance relation $\tau = \tau_0 + CT/Q$ where T is the travel time and C a source-independent constant, is an oversimplification of one-dimensional anelastic wave-propagation; source spectrum must be considered when inferring seismic attenuation from changes in rise-time. Result (c) demonstrates that the assertion made by Blair and Spathis, that $\partial\tau / \partial x$ of wave-trains generated by band-limited source time-function is always less than the corresponding value generated by a delta-function source time-function, is incorrect. A procedure for applying the plane-wave propagation in an anelastic medium to field determination of seismic attenuation is also given.

2. Playback of data recorded on the USGS GEOS digital recorder have been completed for data collected on June 16 and July 10, 1987. Data analysis is held up pending the evaluation of the effect of near-field terms on the determination of seismic anelastic attenuation using the pulse-broadening technique.

3. The two borehole seismometers installed at Pinon Flat have been calibrated *in-situ* using the release test and the phase-ellipse test. Routine recording and analysis of earthquakes are carried out under the project: "Analysis of Natural Seismicity at Anza" (9910-03982).

References Cited

Anderson, J.G., 1986, Implication of attenuation for studies of the earthquake source: *Geophysics Monograph*, v. 37 (Maurice Ewing v. 6), p. 311-318.

Blair, D.P., Spathis, A.T., 1984, Seismic source influence in pulse attenuation studies: *Journal of Geophysical Research*, v. 89, p. 9253-9258.

Reports

Liu, H.-P., 1987, Effects of source-spectrum on seismic-attenuation measurements using the pulse-broadening method: submitted for Branch review.

Seismic Properties of the Carbonate Accumulation Layer in Quaternary Fans: Potential for Macroscopic Dating Technique

9910-04193

Hsi-Ping Liu
Branch of Engineering Seismology and Geology
U.S. Geological Survey
345 Middlefield Road, MS 977
Menlo Park, California 94025
(415) 329-5643

Investigations

Calcareous soils found in alluvial fans cut by normal faults have been used to determine the ages and amounts of Quaternary faulting (*e.g.*, Machette, 1978). "Soil ages, and hence fault ages, can be calculated by measuring the total pedogenic calcium carbonate content in a section of buried paleosols and by using an independently established maximum soil formation rate." Carbonate cementation also increases the shear rigidity of the soil; the product of shear rigidity and thickness of a paleosol is likely proportional to the length of period of tectonic stability during which the soil layer was exposed at the surface. The research objective of this project is to determine the shear rigidity of calcareous soils of known age by seismic methods using the shear-wave generator developed by Liu *et al.* (1987). The shear rigidity determined by the seismic methods will be correlated with the thickness and the known age of the paleosols.

Results

Since project approval in August, 1987, sites for the first field measurements have been located on an alluvial fan on the Lost River fault near Mackay, Idaho. The calcareous soils range from upper Pleistocene, middle to lower Pleistocene, and Pliocene in age.

Reference Cited

Liu, H.-P., Warrick, R.E., Westerlund, R.E., Fletcher, J.B., and Maxwell, G.L., 1987, An air-powered impulsive shear-wave source with repeatable signals: *Seismological Society of America Bulletin, in press.*

Machette, M.N., 1978, Dating Quaternary faults in the southwestern United States by using buried calcic paleosols: *Journal of Research U.S. Geological Survey*, v. 6, no. 3, p. 369-381.

10/87

Analysis of Large Tremors Associated with Gold Mining Operations in South Africa or, Rockbursts in South Africa

9901-04100

Art McGarr
Branch of Engineering Seismology and Geology
U.S. Geological Survey
345 Middlefield Road, MS 977
Menlo Park, California 94025
(415) 329-5645

Investigations:

1. Mine tremors of magnitude 3 and greater are recorded locally and regionally with a view to improving our understanding of the high-frequency nature of small- to medium-sized earthquakes.

Results:

1. During March 1986, four local and three regional and four seismic stations were installed in and around the four gold mining districts of South Africa that account for most of the mining-induced seismicity. This research is supported by the Defense Advance Projects Research Agency. Since installation, typically 20 events per month of $M \geq 3$ are recorded and analyzed, the largest to date being of $M = 4.6$. These data have already provided novel insights regarding (1) the nature of seismic source processes of both earthquakes and explosions, (2) some essential difficulties in discriminating between earthquakes and explosions, and (3) a more exact understanding of strong ground motion in both the near- and far-field of earthquakes.

Reports:

McGarr, A., Bicknell, J., Sembera, E., and Green, R., 1987, Analysis of exceptionally large tremors in two gold mining districts of South Africa *in* R.P. Young, ed., Proceedings, Fred Leighton Memorial Workshop on Mining Induced Seismicity, Montreal, August 30, 1987, p. 23-38.

10/87

Strong Ground Motion Prediction in Realistic Earth Structures

9910-03010

P. Spudich
Branch of Engineering Seismology and Geology
U.S. Geological Survey
345 Middlefield Road, MS 977
Menlo Park, California 94025
(415) 329-5654

Investigations

1. Development of an automated iterative procedure for determining earthquake rupture behavior based on near-source ground motion records.

2. Studies of the S wave coda of aftershocks of the 1984 Morgan Hill earthquake.

Results

1. In collaboration with G. Beroza of MIT, we have developed an iterative procedure for modeling strong motion records and finding rupture mechanisms. Ground motions are linearly related to the amount of slip on the fault but are nonlinearly related to rupture time. Consequently, to invert for rupture time, an iterative procedure is employed. Using the isochrone formalism, it is computationally rapid to calculate the partial derivatives of seismograms with respect to rupture time and slip amplitude on the fault. The inverse of this partial derivative matrix is multiplied by 'residual' seismograms to obtain a perturbation to the current slip and rupture time model. We usually obtain convergence in 5-10 iterations. The inversion is stabilized by applying smoothness and positivity constraints to the slip perturbation. The positivity constraint is implemented using a penalty function method. We have applied this inversion method to data from the 1984 Morgan Hill, California, earthquake. The results indicate that slip amplitude on the fault plane was extremely variable, and that the rupture front did not propagate uniformly away from the hypocenter. In particular, rupture was delayed on a 12 km^2 section of the fault 14 km to the southeast of the hypocenter. The rupture front surrounded the region, which subsequently failed with a component of rupture propagation back toward the hypocenter. Similar behavior has been observed in dynamic rupture models with stress or strength inhomogeneities. This segment of the fault ruptured with a large slip amplitude, releasing 12% of the total seismic moment from 4% of the total area of the aftershock zone. The surface trace of this section of the fault is characterized by a complex left-step that could act to increase the normal stress acting across the fault. However, the distribution of aftershocks indicates that the fault at depth may be simpler and that it bends to the right. In either case, our rupture model suggests that this segment of the fault represents an asperity, which initially resisted rupture, but eventually ruptured massively. We estimate the shear fracture energy for this earthquake to be $2 \times 10^6 J/m^2$.

2. Using an array analysis technique reported on previously, T. Bostwick and I have examined the composition of waves comprising the S wave coda in aftershocks of the 1984 Morgan Hill earthquake. Our data were digital recordings of the aftershocks made using the GEOS instrument. Because of the short recording duration for each event, and because each GEOS recorded only a small number of events, we were able to examine only the early coda, which is the part of the seismogram between the direct S wave arrival time and twice the S wave arrival time, at three seismic stations on considerably different site geologies. At all stations the early coda is dominated by waves that reverberate in a shallow region beneath the station. Coda-Q, however, is unaffected by the large station-to-station variations in geology, further substantiating the hypothesized deep lithospheric origin for codas waves.

   We are attempting to apply our analysis procedure to seismograms of longer duration in order to determine directly the composition of the late coda. We are using recordings of the same Morgan Hill aftershocks recorded at regional Calnet stations. These records have much longer duration, giving us an ample data set from the late coda.

Reports

Beroza, G., and Spudich, P., 1987, Linearized inversion for fault rupture behavior: Application to the 1984 Morgan Hill, California, earthquake: submitted, *Journal of Geophysical Research*.

Spudich, P., and Bostwick, T., 1987, Studies of the seismic coda using an earthquake cluster as a deeply buried seismograph array: *Journal of Geophysical Research*, v. 92, p. 10526-10546.

Deep Continental Studies Potpourri in Engineering Seismology and Geology

9910-04189

Ray Weldon
Branch of Engineering Seismology and Geology
U.S. Geological Survey
345 Middlefield Road, MS 977
Menlo Park, California 94025
(415) 329-5658

Investigations

1) North Branch of the San Andreas fault, Santa Ana Canyon. The project is funded by the Army Corps of Engineers to determine the activity of the North Branch, which passes a few 100 meters from their proposed Seven Oaks Dam across the upper Santa Ana River.

2) Geologic setting of the DOSECC Cajon Pass hole. The project is jointly funded by NSF and the Survey to better characterize the geologic setting of the Cajon Pass well by mapping, core characterization, paleontology, and integration of the geological and geophysical observations.

Results

1) Army Corps Project: Several exposures were excavated across the fault where it is crossed by the Santa Ana River Valley. In one exposure, two strands of the fault were found to offset a Pleistocene strath terrace, overlying fluvial gravel and a colluvial cap. This was a surprise because previous studies had inferred that the strath was not displaced, based on its constant height above the active wash across the fault zone. The combined displacement of the two faults yields little net vertical separation, whereas each fault has several meters of vertical separation and obvious facies differences across it. It is therefore tentatively inferred, pending more study, that the sense of displacement across the zone is strike slip.

   Ten soil pits have been described and collected on the offset terrace and the terraces immediately above and below it by Les McFadden and Bruce Harrison of the University of New Mexico. Laboratory work is being carried out. The field descriptions suggest that the offset terrace is on the order of 50,000 years old; which is basically consistent with its geomorphic position and other estimates of the age of similar terraces in the Transverse Ranges. The soils are somewhat unusual in that their development is heavily influenced by colluvium shed off the very steep hillslopes. To determine the effect of this process on the inferred ages of the surfaces, Bruce Harrison is also describing soils on terraces close to steep slopes in Cajon Pass, where the age and soil development are better understood.

2) DOSECC Project: Mapping near the well has demonstrated that the local structure is more complex than previously believed. In particular, a tight anticline-syncline pair that trends north to northwest parallel to the nearby Squaw Peak fault passes right through the drill site. It probably overlies a basement reverse fault, related to the Squaw Peak thrust, that is responsible for the difference in depth of various sedimentary and plutonic units recognized in both the DOSECC and earlier ARKOMA wells. Ongoing mapping in the area will lead to a better understanding of the late Miocene compressional deformation that is principally responsible for the complexity in structure near the well and should eventually lead to better cross-sections through the area.

Preliminary analysis of core and cuttings from the DOSECC hole suggest that the lowest sedimentary unit (referred to as a "mystery unit") encountered in the well is not the Miocene Crowder Formation as had been speculated from the cuttings and geophysical logs from the ARKOMA well. The leading candidate for this unit is the top of member 3 of the Miocene Cajon Formation, which would suggest that the fault between it and the overlying Cajon Formation is quite minor. However, the mystery unit bears some similarities with continental facies of the Oligocene Vaqueros Formation, which outcrops in the area. Microvertebrate fossils recovered from cuttings of the mystery unit are being examined by Bob Reynolds of the San Bernardino County Museum (the local microvertebrate expert) and his identification of key species should help resolve the problem.

Work is also underway to integrate the geophysical observations with the local geology. In particular, we are assisting Art Lachenbruch's group in developing an uplift and erosion history of the well site to correct the heat flow observations for these surficial effects. Efforts are underway with Jack Healy's and Mark Zoback's groups to understand the unusual stress orientation in the context of the active faulting. One of the most interesting results so far from the project is that the stress orientation in the well is most consistent with the Cleghorn fault, the closest active fault to the well, and not the San Andreas fault, which is 4 km away, suggestive of a highly variable stress field near the San Andreas fault.

Reports

None.

INDEX 1

INDEX ALPHABETIZED BY PRINCIPAL INVESTIGATOR

INDEX 2

INDEX ALPHABETIZED BY INSTITUTION

☆U.S. GOVERNMENT PRINTING OFFICE: 1988-586-636/99066